Institut für Verbrennungskraftmaschinen und Thermodynamik
Institute of Internal Combustion Engines and Thermodynamics

Technische Universität Graz
Graz University of Technology

9th International Conference

TUNNEL SAFETY AND VENTILATION

- New Developments in Tunnel Safety -

12. - 14. June 2018

Graz University of Technology

Redaktion / Editor:
P. Sturm / S. Minarik

I m p r e s s u m:

Verlag der Technischen Universität Graz
www.ub.tugraz.at/Verlag

Reports of the Institute of Internal Combustion Engines and Thermodynamics,
Graz University of Technology, Vol. 102

Herausgeber/Publisher: Univ.-Prof. Dr. H. Eichlseder

ISBN: 978-3-85125-606-2

ORGANISATION

A.Univ.-Prof. Dr. Peter STURM
Mrs. Sabine MINARIK
Graz University of Technology
Institute of Internal Combustion
Engines and Thermodynamics
A-8010 Graz, Inffeldgasse 25B/V Austria

Tel.: +43/316-873 30200
Tel.: +43/316-873 30231
Fax.: +43/316-873 10 30231
E-Mail: minarik@tugraz.at
Homepage: www.ivt.tugraz.at

PREFACE

Ladies and Gentlemen, Dear Participants,

This conference series started in 2002 in order to provide a forum for information exchange among operators, users, technicians, scientists and companies involved in the design, construction and equipping of road and rail tunnels. The success of the 2002 conference led to the organization of biennial follow up meetings.

While the first conferences were strongly influenced by the tunnel incidents of the late 1990's and related safety issues, the focus today is more on questions concerning tunnel operation, and the potential for conflict between the need to comply with regulatory requirements and the need for tunnel upgrades.

Road traffic is increasing, at both a national as well as an international level. Thus, while in densely populated areas there is much greater demand for sub-surface transportation, in rural areas there is an increasing need to upgrade the road infrastructure. The upgrading process constitutes a big challenge in practice, as – in contrast to new tunnel construction – several prevailing structures and systems act as constraints and have to be taken into consideration in planning. There is also the additional need to ensure that traffic flow can be maintained throughout the construction period.

Investments in rail traffic in Austria are now booming. Three major rail tunnel projects are currently under construction in Austria. The Semmering Base tunnel with a length of 27 km, and the Koralmtunnel with a length of 33 km, are core parts of the Baltic - Adriatic corridor. The Brenner Base tunnel, with a length of 55 km, connects Austria and Italy. These projects, as a result of their history and complexity, place enormous demands on, and represent major challenges for, all parties involved in construction and operation.

The question of tunnel safety is a highly controversial field. It is often claimed that several new techniques are now on the market and that these can help to improve safety due to quicker and more reliable detection, more efficient installations and/or additional equipment. However, such 'improvements' often result in significant increases in complexity, as well as in the cost of operation and maintenance of the new safety equipment. We are thus left with plenty to discuss in the next few days.

This conference wouldn't be the "Graz" conference without the related exhibition. Many companies have put a lot of effort into presenting their latest developments and technologies. Conference participants now have the chance to make contact with leading companies in the electro-mechanical tunnel business, to establish new contacts, and also to strengthen existing ones.

Another exciting and distinguishing aspect of the "Graz" conference is the accompanying technical tour. After many years of negotiations concerning financing and legal aspects, the research center Research@ZaB - Zentrum am Berg is currently in the process of realisation. This unique research facility is now under construction in a specially dedicated part of the Styrian Erzberg (an open-pit iron mine in operation since the 11th century). The test center comprises two parallel tubes for road traffic and another two for rail traffic, each of about 400 m in length. These tubes lead into an existing tunnel, which has been suitably equipped up to a length of about one kilometre. The five tubes meet in a central cavern, forming a huge tunnel complex offering numerous possibilities for research, operation and training.
The tour of the Res@ZaB contains a visit to the new tunnel tubes currently under construction, followed by a fire test at the construction site.

Last but not least, I would like to extend a special thank you to our scientific committee for its valuable work in defining the objectives of this conference, and in selecting the presentations.

We also extend our professional thanks to all the authors for their hard work in preparing abstracts, papers, posters, and of course, for their presentations.

And finally, we wish to offer our sincere thanks to all the people in the background who have been working to ensure that this will be a smooth, enjoyable and effective conference for us all.

It is my pleasure to welcome you all on behalf of the conference scientific committee and to wish you all a successful meeting and a sound basis for fertile networking in the future.

Peter J. Sturm

Graz, June 2018

CONTENTS

"TUNNEL SAFETY AND VENTILATION"
Graz, 12. - 14. June 2018

THE KORALM RAILWAY LINE - THE CHALLENGES OF AN INFRASTRUCTURE PROJECT

Klaus Schneider

ÖBB Infrastructure AG, Austria

INTRODUCTION

The Koralm Line is a newly built, double track, electrified railway line running between Graz and Klagenfurt that will allow a maximum train speed of 250 km/h. The total length of the line is almost 130 kilometres. The core element of the Koralm Line is the 32.9 kilometre Koralm Tunnel. A new intercity train station is being built at each of the two entrances to this tunnel; these are the stations Weststeiermark and Lavanttal. In the course of the project 23 stations or stops are being newly erected or rebuilt – not including the initial stations Graz and Klagenfurt – 12 of them directly on the new line. All in all the Koralm Line includes about 50 kilometres of tunnels, more than 100 bridges, 108 kilometres of railway, around 290 kilometres of overhead lines and more than 150 points.

Koralm Line Fact Box
130 km total length
Up to 256 trains every day
Two track, electrified, high performance line
250 km/h possible maximum speed
2 hours and 40 minutes travel time from Vienna to Klagenfurt
45 minutes travel time from Graz to Klagenfurt
Projected start of operation 12/2025

This project is among the most important transportation infrastructure projects in Austria and Europe. The Koralm Railway Line forms an important section of the Baltic–Adriatic Corridor (Danzig – Ravenna) and is also a part of the TEN core network. This north-south axis that crosses the eastern Alps connects the ports and regions in the north (Scandinavia, the Baltic, Poland) with Central Europe and with the ports and regions of the north Italian economic area. From the Austrian viewpoint the Koralm Line represents a decisive structural improvement for the southern Austrian region. Together with the Main Station Vienna and the Semmering Base Tunnel the Koralm Line will make an important contribution to modernising and improving the capacity of the southern railway line.

Building the Koralm Line as a flat railway line will enable an efficient and competitive freight transport service to be operated, while for passenger transport attractive journey times can be achieved. In accordance with the density of settlement along the southern line transport capacities of a competitive quality can be reached. Travel time between Graz and Klagenfurt will be reduced from almost three hours at present to just 45 minutes. Due to to the Koralm Line and in conjunction with the full development of the southern line, including the completion of the Semmering Base Tunnel, it will be possible to reduce travel time between Vienna and Klagenfurt from 3 hours and 50 minutes at present to just under 2 hours and 40 minutes.

A series of new or adapted train stations ensure regional connections between high-priority supra-regional rail traffic with the regional public feeder and local transport and due to park&ride facilities with the private motorised traffic. As a result the regions western Styria and Lavanttal and the Bleiburg area will be better connected to the central areas Graz and Klagenfurt.

1. CURRENT WORKS

On the Styrian approach to the Koralm Tunnel tender specifications planning for the section Graz-Weitendorf is proceeding at full speed. In the area Weitendorf –Wettmannstätten services have been running on part of the line since 2010 and the remaining works in western Styria on bridges and subgrade for the Koralm Tunnel have been concluded. At present, work is being carried out on the permanent way and on the Weststeiermark train station building.

In the Koralm tunnel from the Styrian side (building lot KAT 2) a length of more than 21.5 km has been driven in both tubes, of which approx. 17.1 and 16.3 km were made using tunnel boring machines. In the northern tube tunnelling work was completed at the beginning of the year, at present the TBM is being dismounted before starting work on fitting-out the structural shell.

From the Carinthian side (building lot KAT 3) tunnelling work for the southern tube has been completed. In the northern tube the difficulties caused by the Lavanttal main fault zone have been overcome and, following the conversion of the TBM from an earth pressure to a hard rock machine, driving work in the crystalline mountain section will soon begin again. Alongside the structural works the main focus of attention is on the technical equipping of the line and on the challenging logistics involved in fitting this equipment.

In Carinthia building work is on schedule. Driving work for the Granitztal tunnel chain, for the tunnel sections in the St. Kanzian area, where the geology presented particular challenges in the form of fine sands and lacustrine deposits, and for the Stein and Lind tunnels has been completed. At present work on fitting out these tunnels is underway. On the open stretch bridges and the subgrade are being constructed. The section immediately before Klagenfurt was completed two years ago, apart from the superstructure.

To summarise: around 90 per cent of the Koralm Line is either under construction or partly completed.

2. TUNNEL BUILDING

In building the tunnels along the Koralm Line a number of different construction and tunnel driving methods were used, depending on the specific geological and local conditions. Alongside the open building method the closed building method was used for the most part. It can be said that all the usual tunnel building methods (cyclical drive – dissolution method by excavating or blasting and providing support by means of sprayed concrete/anchor construction as well as continuous driving – TBM followed by lining with segments) were used in constructing the Koralm Line. In total about half of the total tunnel driving is being carried out by tunnel bore machines.

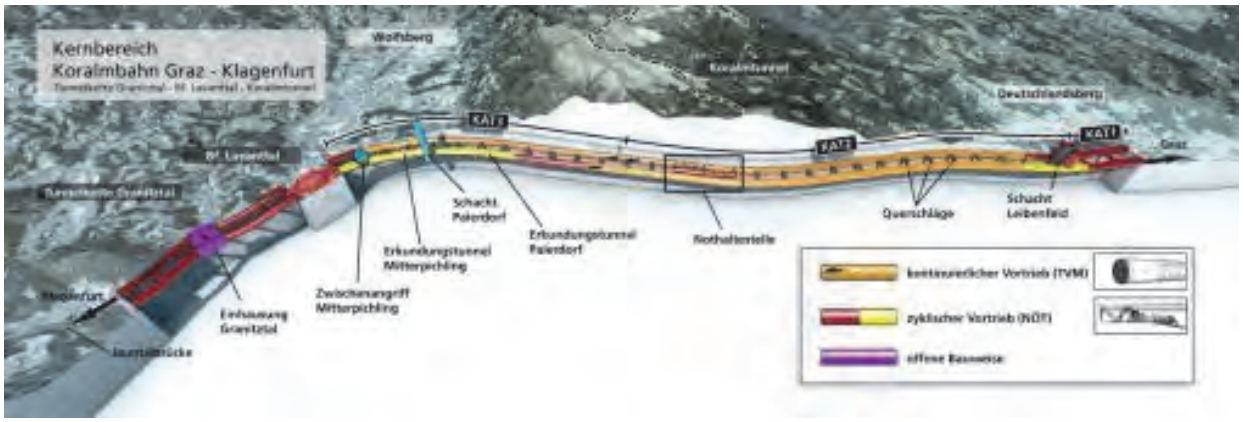

Figure 1: Overview Koralm Tunnel and Granitztal tunnel chain l (ÖBB/3D-Schmiede)

In order to select the appropriate tunnelling method, extensive explorations of the geology were made. Special importance was attached to the exploratory work on the Koralm Tunnel and the associated planning of the route. All the standard exploration methods - augmented by a variety of innovative measures – were used at different stages in the framework of the overall exploration program in order to obtain a broad understanding of the geological composition of the Koralpe mountain. A total of around 21 000 linear metres of core drilling was carried out – the most spectacular to depths of up to 1 200 metres. In addition from both tunnel entrance areas a 10 km-long system of exploration tunnels and shafts was built which provided important information about the geological, hydro-geological and geothermal conditions inside the mountain. These results provided a basis for the detailed description of the building ground used in the construction work tender documents.

SEMMERING BASE TUNNEL: CONSTRUCTION, DEEP INTERMEDIATE ACCESS SHAFTS, TBM- AND DRILL AND BLAST TUNNELING

Gerhard Gobiet
ÖBB-Infrastruktur AG, Projektleitung Semmering, Austria

ABSTRACT

For the successful realization of major infrastructure project not only technical issues but also numerous legal problems have to be solved and intense processes of communication have to be conducted. The responsible project team of the ÖBB-Infrastruktur AG has been working intensely on the implementation of the Semmering Base Tunnel since 13 years. The project exhibits, based on its history and its complexity, very high requirements and challenges all parties concerned in new ways. [1]

The 27.3 km long Semmering Base Tunnel (SBT) consist of two single-track running tunnels for railway and is being driven from the portal at Gloggnitz and from three intermediate access points in Göstritz, Fröschnitzgraben and Grautschenhof. It passes geologically extremely challenging rock mass with an overburden up to 800 m.

For organizational, scheduling and topographical reasons, the tunnel is divided into three construction contracts. The eastern contract section SBT1.1 “Tunnel Gloggnitz” has been under construction since mid 2015. Construction started on the middle part, contract section SBT2.1 “Tunnel Fröschnitzgraben” at the start of 2014. The western contract section SBT3.1 “Tunnel Grautschenhof” has been under construction since May 2016. [2]

Keywords: Semmering Base Tunnel

1. THE SÜDBAHN ACROSS THE SEMMERING

The 41 km long mountain route across the Semmering, opened in 1854, is an important part of the European railway connections. Despite the brilliant engineering achievements of its builder Karl Ritter von Ghega, it increasingly proves to be a technical bottleneck for a future-oriented railway operation of the 21st century.

In the spring of 2005, a political consensus was reached between the Austrian Federal Government and the states of Lower Austria and Styria to provide a uniformly efficient railway infrastructure along the Südbahn as a nationally and internationally important transport axis for Austria as an economic location.

The two running tunnels of the Semmering Base Tunnel, designed with a low gradient according to the specifications is, in addition to the Koralm Railway and the Vienna Central Station, an essential component for the realization of this goal. In the future, it will ensure an economical and contemporary rail freight traffic and it will increase travel comfort by reducing travel time between Vienna and Graz by 50 minutes.

2. COMMUNICATION, COMPETENCE, COORDINATION - THE THREE PILLARS TO SUCCESS

After the project was commissioned in March 2005, an area for planning and evaluation of approx. 300 km² was specified between the starting point Gloggnitz and the intersection point with the existing route in Mürzzuschlag/Langenwang. Subsequently the development of the project was started.

In addition to the actual evaluation and planning, an active involvement of the public for a dialog between the project management, the responsible decision makers and the stakeholder groups of the region was established.

In addition to the project-specific Steering Committee (ÖBB, BMVIT, SCHIG, Lower Austria, Styria), project-accompanying local and regional committees (working forum) were set up to publicize this important project in the region and to actively integrate suggestions and ideas from the region into the planning process.

In 50 working sessions with an intensive exchange with the 170 members of the forum, the development of a stable and locally accepted tunnel route was possible.

In addition to this process, the project was presented through an offensive information policy in numerous regional, national and international lectures, conferences, papers and information evenings. [1]

3. AUTHORITIES PROCESS

On May 31, 2010, the project was submitted to the Federal Ministry of Transport, Innovation and Technology (BMVIT) to obtain the permits relating to the environment as well as the approval of the railway authorities. This included more than 10.000 pages of report and 700 m² of plans.

At the same time, the necessary submissions on the supplementary permit procedures for water law, monument protection, aviation and waste management in the federal states of Lower Austria and Styria were made, and the two nature conservation procedures at the administrative authorities of the federal states were submitted. In the meantime, all procedures have been completed in a positive manner, and all decisions for the construction of the Semmering Base Tunnel have been obtained. [3]

4. THE PROJECT SEMMERING BASE TUNNEL

The 27.3 km long Semmering Base Tunnel will provide improved travel quality for passengers and considerably increase the capacity for rail freight transport. The main components of the entire tunnel system are two single-track running tunnels, cross passages at a maximum spacing of 500 m and an emergency station in the middle section of the tunnel with two shafts about 400 m deep for ventilation an extraction in case of an incident.

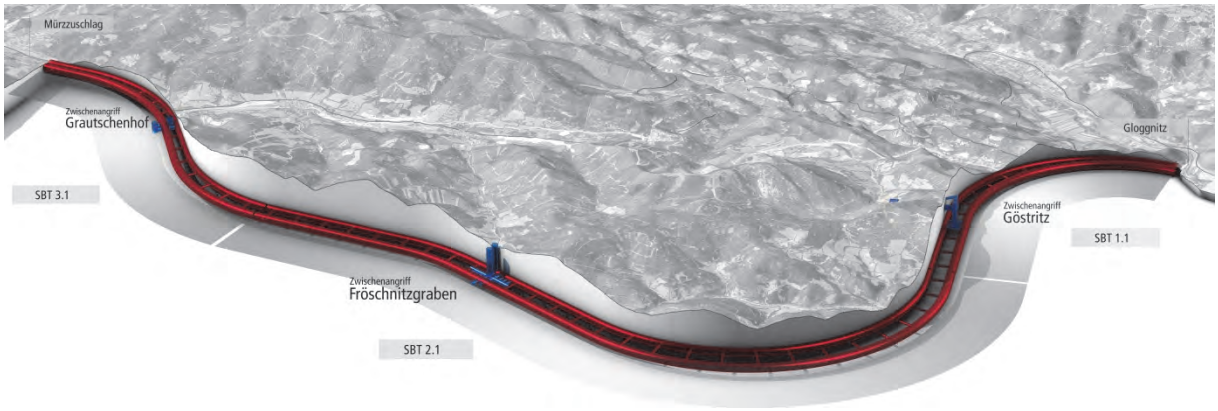

Figure 1: Semmering Base Tunnel: Overview and construction sections (ÖBB, 3DSchmiede)

The rail tunnel is for reasons of scheduling, logistics and geology being driven from several construction sites and access points, managed through three tunnel section contracts (Figure 1). In addition to the logistical challenges, complex geological and hydrogeological situations (Figure 2) have to be overcome.

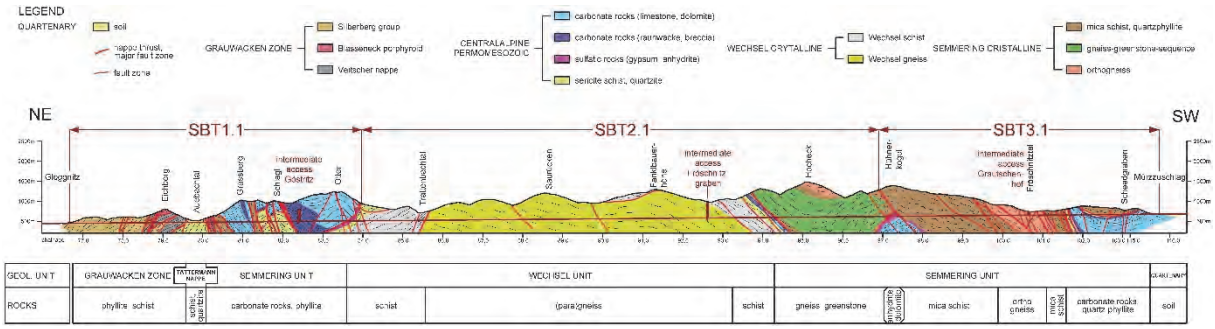

Figure 2: Semmering Base Tunnel, simplified geological longitudinal section (ÖBB, 3G)

The contract section "Tunnel Gloggnitz" (SBT1.1) is being undertaken conventionally with excavator and blasting starting from two sites. The first driving starts from the tunnel portal in Gloggnitz in direction towards Mürzzuschlag. The intermediate access point in Göstritz consists of a 1,000 m long access tunnel and two 250 m deep shafts, from the bottom of which the running tunnels are being driven towards both directions.

The construction logistics are similarly complex on the contract "Tunnel Fröschnitzgraben" (SBT2.1): two tunnel boring machines are working from the intermediate access point at Fröschnitzgraben in the direction of Gloggnitz and blast and excavator heading is underway towards Mürzzuschlag. In Order that tunneling was able to start from the Fröschnitzgraben, two 400 m deep shafts were sunken since 2014. At the moment, large caverns are being constructed for the later emergency station and the conventional driving towards Mürzzuschlag has started. In 2018 the two tunnel boring machines will start operating towards Gloggnitz.

On the third contract "Tunnel Grautschenhof" (SBT3.1), two 100 m deep shafts were sunken since September 2016. At the moment the caverns for logistics are being finished and the drivings of both running tunnels have started towards Mürzzuschlag as well as towards Gloggnitz.

5. CONTRACT SBT1.1 – GLOGGNITZ TUNNEL SECTION

Starting from the portal in Gloggnitz (Figure 3), the first 4.7 km of tunnel pass through a sequence of schists, phyllites and graphitic phyllites using conventional tunneling methods whereof about half has been driven so far.

Figure 3: Contract SBT1.1 – Tunnel Gloggnitz: Portal Gloggnitz, Crossing Schwarza (ÖBB-Infrastruktur AG, Ebner)

The rocks tend to high convergence and are thus unsuitable for the use of tunnel boring machines. After crossing a valley with quartzite rocks and sericitic phyllites, the tunnel passes through the aquiferous carbonate stock of the Grasberg and into the Schlagl faultzone.

To control the hydrological conditions (up to 300 l/s and up to 26 bar) in the karstified carbonates, directed boreholes are drilled successively for advanced grouting. For this reason caverns will be built in a suitable distance to the grouted areas. From there 300 m long directed boreholes will be drilled around and in the tunnel section from which the rock will be grouted.

From the intermediate access point in Göstritz, which consists of an access tunnel about 1 km long and two blind shafts about 250 m deep, at the head and bottom of which complex caverns are needed for the logistics, two distinctive rock formations are encountered simultaneously:

- In the drive to the east, the approx. 1 km long Grasberg Schlagl fault complex with about 500 m overburden, with mica schist, slate and sericite phyllite, which are the product of a lateral displacement of about 10 km.
- In the drive about 1.5 km long to the west, the karstified dolomite/marble stock of the Mitterotter where the rock mass is to be pre-treated with advance grouting on the same principle as the drive from Gloggnitz.

The access tunnel and the caverns at the shaft head area have already been completed. At the moment the two shafts are being sunken, the bottom will be reached mid 2018 (Figure 4).

Figure 4: Contract SBT1.1 – Tunnel Gloggnitz: junction at the shaft head area in Göstritz (ÖBB-Infrastruktur AG, Ebner)

6. CONTRACT SBT2.1 – TUNNEL SECTION / INTERMEDIATE ACCESS POINT FRÖSCHNITZGRABEN

For the intermediate access point Fröschnitzgraben, two shafts more than 400 m deep and with a diameter of about 10 m were sunken down to tunnel level. At the bottom of the shafts, a longitudinal cavern about 400 m long and cross caverns are currently being excavated to house the necessary equipment for tunneling such as workshop, concrete plant and areas for materials handling (Figure 5). In the complete state, this will be used as part of the emergency station.

Figure 5: Contract SBT2.1 – Tunnel Fröschnitzgraben: Caverns for construction equipment and the later emergency station

In the approx. 8.6 km long east drive, predominantly gneisses and schists with minor localized faults and little water ingress are expected. This tunnel section is thus the only part of the entire project where tunnel boring machines can be used due to the competent rock mass conditions.

The requirements for the tunneling system derived from the geotechnical planning resulted in the specification and suitability of a tunnel boring machine (OD 10.1 m) with single shield (TBM-S) or one with double shield (TBM-DS). It also requires provision for the carrying out of appropriate additional and special measures in the cutter head and shield areas. The frequency and assignment of these are described as part of the geotechnical forecast in the contract documents, with the specific requirements being described in detail in the technical conditions of contract. The contractor has selected a TBM-S.

The need for a ring segment lining (30 cm) in combination with an in-situ concrete inner lining (25 cm) with pressure-relieved waterproofing between was derived from the forecasted ground conditions and the requirements concerning the future operation. A segmental lining system without waterproofing has therefore been chosen.

The 4.3 km long conventional drive to the west is essentially characterized by the boundary between the Wechsel unit (gneisses) and the Semmering unit (gneisses and greenstones). The thick fault zone of this boundary consist of quartzites, fractured phyllites and flaked aquiferous carbonates.

In this area, a zone with a length of about 200 to 300 m with heavy water ingress and high initial water pressures is expected and fractured rocks could tend to flowing conditions. As the critical zone is approached, it will be investigated and if necessary measures for waterproofing and improvement of the rock mass will be carried out trough up to 250 m long directed boreholes.

A significant part of this contract is the landfill site in Longsgraben, which is planned with an area of about 20 ha and a capacity of about 5 million m³ for the landfill compartments “excavated material” and “construction residues” (Figure 6). In this landfill material excavated from all three intermediate access points of the Semmering Base Tunnel will be deposited.

Material with more serious geogenic contamination such as gypsum, anhydrite and mineralized rock has to be disposed of separately.

Figure 6: Contract SBT2.1 – Tunnel Fröschnitzgraben: Landfill Longsgraben with the compartment “excavated material” in the foreground and “construction residues” in the background (ÖBB-Infrastruktur AG, Ebner)

Prior to landfill operation extensive preparatory measures were necessary (diversion stream to valley flanks, construction of site access road). After completion of construction, the landfill area will be recultivated and reforested.

The deposition of the material excavated from the tunnel at this landfill site near the tunnel will make a significant contribution to relieving the region from transport nuisance during the construction works. The material excavated from the drive in Gloggnitz will be carted away by rail.

7. CONTRACT SBT3.1 – TUNNEL SECTION / INTERMEDIATE ACCESS POINT GRAUTSCHENHOF

This tunnel section, almost 7 km long, is geologically dominated by the Semmering crystalline, consisting of mica schists, gneisses and carbonate units, with the Semmering main fault passing through as well. The intermediate access is down two shafts about 100 m (Figure 7).

Figure 7: Contract SBT3.1 – Tunnel Grautschenhof: Shaft Sommerau 1, muck removal through shaft (ÖBB-Infrastruktur AG, Ebner)

Three transverse caverns will be constructed at the shaft bottoms for construction logistics.

At the end of the east drive (approx. 3.8 km), a fault system of anhydrite and dolomite will be reached, which has a high swelling potential. In the west drive, long sections will pass through the Semmering main fault where heavily fractured areas with mica schists, coarse gneiss and friable gneiss will be encountered. The aquiferous carbonates that have to be passed through may be encountered as relatively dry since the dewatering in the pilot tunnel of the previous tunnel project is still active. The west drive will continue until shortly before the station at Mürzzuschlag where it will meet the cut-and-cover slope cut.

In order to verify and determine the exact location and extend of the fault zones and the aquiferous carbonates from the tunnel, extensive advance investigation measures will be carried out (with backflow preventer up to 50 bar).

Grouting is planned in the karstified carbonate rocks at the eastern end of the contract section, where water inflows of up to 300 l/s with pressure of about 23 bar are forecast. For this purpose, grouting caverns will be constructed in the geotechnically most favorable section at an appropriate distance from the area to be grouted. From these, 250 m long directed boreholes will be drilled around the excavated section and the rock mass grouted. The objective is to produce an improved ring around the excavated section to protect the tunnel drive from high water ingress.

Most of the grouting will however be necessary in the area of the shaft bottom and the adjacent running tunnels, where the Fröschnitztal valley is crossed. According to the forecast heavily fractured and softened coarse gneisses will be encountered, sometimes with components that are susceptible to erosion, tending to flow out under the corresponding water pressure. In

contrast to the grouting work on carbonate rocks, the main objective of the grouting work here is not to reduce the permeability of the rock mass but to improve the bonding of the rock mass. First experiences were gained in the course of the sinking of the second construction shaft.

8. OUTLOOK

The construction period for the contracts described above will extend into the year 2024, with tunneling continuing until 2023. From 2023, the installation of the railway equipment will follow, partly simultaneously, until the tunnel opens at the end of 2026. In order to achieve this target, great challenges with the geological and geotechnical conditions will have to be overcome during the construction phase, in order that rail service can start after opening.

9. LITERATURE

[1] Gobiet, G., Wagner, O. K. (2013). *Das Projekt Semmering-Basistunnel neu*. Geomechanics and Tunnelling 6 No. 5, S. 551–558, Ernst & Sohn: Berlin

[2] Gobiet, G., Nipitsch, G., Wagner, O. K. (2017). *Der Semmering-Basistunnel – Besondere Herausforderungen beim Bau*, Geomechanics and Tunnelling 10 (2017), No. 3, S. 291-297, Ernst & Sohn: Berlin

[3] Gobiet, G. (2013) *Der Semmering-Basistunnel neu – das Projekt im Überblick*, Geomechanics and Tunnelling 6 (2013), No. 6, S. 680-687, Ernst & Sohn: Berlin

EU-DIRECTIVE 2004/54/EG - IMPLEMENTATION – STATUS REPORT AUSTRIA

S. Wiesholzer
BMVIT Federal Ministry for Transport, Innovation and Technology, Vienna, Austria

ABSTRACT

This report gives a status of the application of the EU Directive 2004/54/EC in Austria under the Road Tunnel Safety Law for the year 2018.

Since 2006 nearly 260 procedures for the approval of the design of the refurbishment and for new tunnels and commissioning were successful fulfilled. Since 2014 amendments of the RVS regulations were stopped for legal certainty.

The deadline for the refurbishment 30 April 2019 can be nearly reached for the existing tunnels on the trans-European road network. For those tunnels, which don´t meet this deadline temporally limited derogations with alternative risk-reduction measures are required.

Keywords: Tunnel safety management

1. INTRODUCTION

The Austrian Road Tunnel Safety Law STSG BGBl. I Nr. 54/2006 has been in force since May 2006 and represents the basis for the planning, construction and maintenance of the Austrian motorway and expressway tunnels. The implementation of this law was mainly based on the EU Directive 2004/54/EG issued by the European Parliament and the Council on 29 April 2004. The Austrian Road Tunnel Safety Law was revised in 2010 and 2013 to reduce golden platting and to implement the new Austrian administrative tribunals. Because of economic reasons the deadline for the refurbishment of tunnels outside the trans-European road network (TERN) was extended to the year 2029.

2. STATUS OF COMPLIANCE OF EXISTING TUNNELS

In April 2006, 71 Austrian motorway and expressway tunnels longer than 500 m were in operation. For these tunnels the Austrian administrative authority carried out the first report with the review of safety documentations and inspections of each tunnel. In April 2007, only three tunnels fulfilled the minimum standards of the STSG.

In June 2018, 85 tunnels longer than 500 m are in operation. 52 of them comply with the minimum standards of the STSG, on the TERN 40 of 67.

In Austria the implementation of safety requirements focuses especially on the construction of about 77 km second tunnel tubes. Only the second tunnel tubes of the tunnel Perjen (about 3 km) and the Karawanken (about 8 km) are still under construction, all other tunnel tubes are already under operation. Five existing STSG-Tunnels in the western Austrian region will remain as bi-directional tunnels.

Furthermore, main measures of the implementation work are the construction of emergency exits at a maximum distance of about 350 m in accordance with a treaty with the Austrian fire brigades and emergency stations at a maximum distance of 250 m and the implementation of measures for the fire resistance. As after more than 20 years in operation most electric equipment in the existing tunnels has normally reached its maximum functional lifespan, the corrective maintenance and upgrading to the technical state-of-the-art leads to significant extra costs. To reach the minimum standards the Tunnel-Manager ASFINAG invests approximately 5.5 billon euros from 2000 till April 2019.

On 30 April 2019 only the cross border tunnel Karawanken can´t comply with the minimum requirements on the trans-European road network, so temporally limited derogations from the minimum requirements according ANNEX I Point 1.2.1 of the EU Directive 2004/54/EG are envisaged by the member states Slovenia and Austria. The risk analyses show that an equivalent level of safety can be ensured by the already installed risk reducing measures:

- Thermo-scanner at each portal
- Dosing system for heavy goods vehicles at each portal

For the tunnels outside the TERN the deadline was extended to the year 2029, but already 8 of the 12 existing tunnels will comply with the minimum standards of the STSG on April 2019. Only the tunnels Semmering, Steinhaus, Spital on the S6 Semmering expressway and the tunnel Landeck on the A12 Inntal highway need to be refurbished till 2029.

3. APPROVAL PROCEDURES

Due to the STSG a lot of approval and inspection procedures in a time with restricted human resources in the authorities have to be carried out to reach the minimum safety requirements till April 2019 on the TERN. For legal certainty the amendments of the RVS regulations were stopped since 2014. ASFINAG and the bmvit are now evaluating the end of this stop.

Figure 1 shows the trend the approval procedures till 2019.

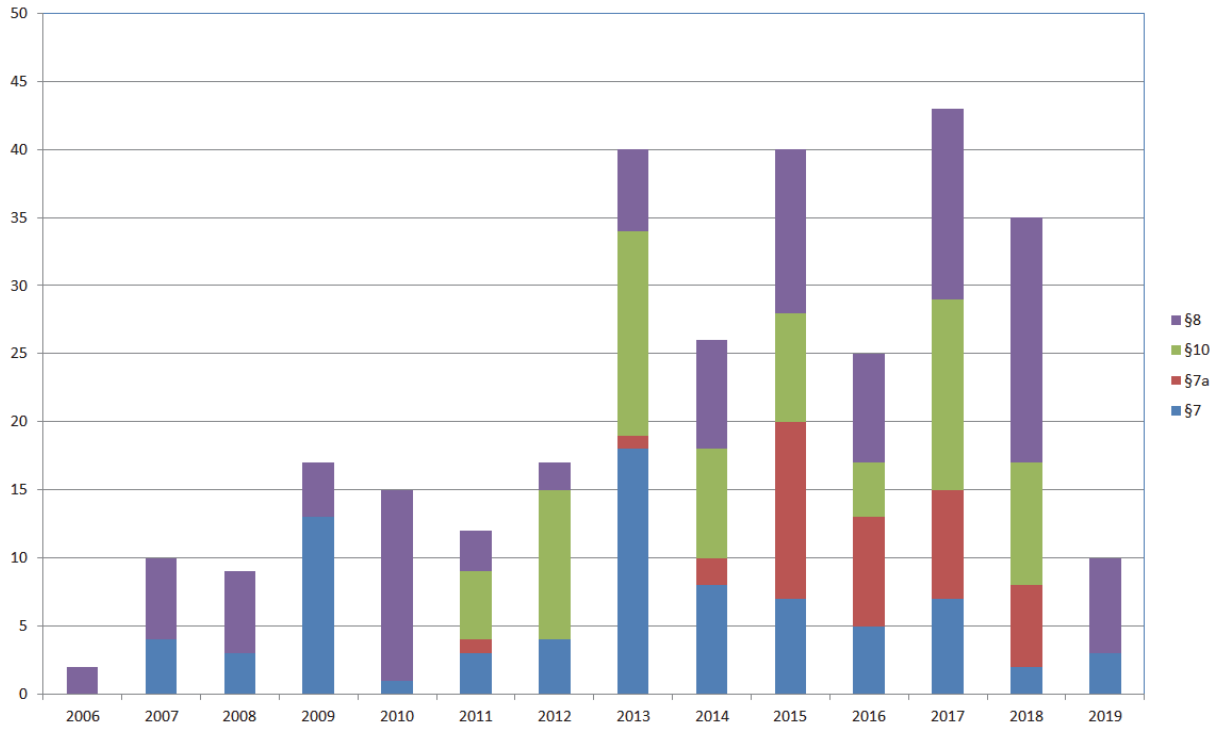

Figure 1: Approval procedures 2006 till 2019 in Austria

But the decline of the approval procedures does not mean that the ASFINAG does not longer invest in tunnel safety. There are new tunnels, that have to be built, like the tunnel Donau-Lobau on the S1 expressway or the tunnels Speltenbach, Rudersdorf, Königsdorf on the S7 expressway and two tunnels on the A 26 highway. Also the refurbishment of the tunnels does not end. During the current six-year programme from 2018 to 2023 7.8 billion euros will be invested in infrastructure by the ASFINAG, about 100 milllion euros will be spent for the refurbishment of the tunnels each year.

4. COLLECTION AND ANALYSIS OF INCIDENTS

The EU Directive 2004/54/EC requires reports on fires in tunnels after accidents, which clearly affect the safety of road users in tunnels, and on the frequency and causes of such incidents.

Figure 2 shows the trend of the accident casualties from 1999 till 2015 in Austria prepared by the Austrian Road safety board KFV [1] (The red line shows the deaths, the blue line the casualties, the grey line the accidents with casualties).

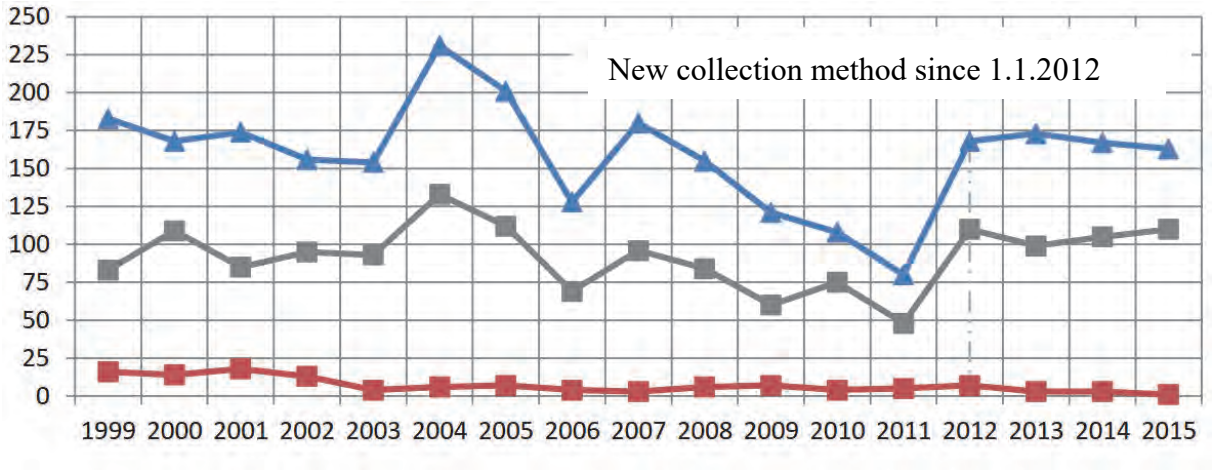

Figure 2: Trend of the accident victims 1999 till 2015 in Austria

Between 1999 and 2015 there were on average 92 tunnel accidents involving personal injury every year on motorway and expressway tunnels longer 200 m. In an average year 7 road users were killed, 20 severely injured and 118 slightly injured. In 2017 only 2 road users were killed in a tunnel accident.

5. CONCLUSIONS

After more than 12 years of experience with the application of the EU Directive 2004/54/EC in Austria the number of casualties decreases. The Tunnel safety management is now well developed. The deadline for the refurbishment 30 April 2019 can be nearly reached for the existing tunnels on the trans-European road network.

6. BIBLIOGRAPHY / REFERENCES

[1] KFV *"Sicherheit von Straßentunnels, Verkehrssicherheit in Tunnels in Autobahnen und Schnellstraßen"* (1999-2015), 2016

TODAY IS TOMORROW´S YESTERDAY – TUNNEL SECURITY THROUGH THE AGES

Günter Rattei, Ulrike Stiefvater
ASFINAG Service GmbH, Austria

ABSTRACT

Both tunnel safety and tunnel engineering have been subject to enormous changes over the last few decades, from simple single-tube tunnel structures to high-tech twin-tube multi-lane tunnels. The expansion of new tunnel technologies has, for example, led to changes in tunnel control systems used in ASFINAG traffic management centres, which were called control centres in the past. In the early stages of tunnel oversight the focus was on video surveillance systems, while today the focus is more on traffic control and incident management.

Tunnel accident statistics prove that the overall danger in highway tunnels and other roadway tunnels has been minimised by means of the measures that have been taken over the past few years. At the same time, the technological advances have led to an increase in the need for maintenance support aimed at guaranteeing the maximum lifespan of the technical equipment.

1. TUNNEL SAFETY: DATA, FIGURES AND FACTS

The current EU-wide mandate focusing on increasing the safety of tunnels is due to the fire incidents that occurred in 1999 in the Mont Blanc Tunnel (France/Italy) and in the Tauern Tunnel (Austria).

These tragic events demonstrated quite plainly the potential extent of existing risks, especially those of fires involving large transport vehicles, while at the same time showing that there were both deficiencies in terms of incident management and a potential to improve safety. In the first stage of the safety improvement process that took place early in the 2000s, laws, regulations and guidelines were prepared in order to both harmonise and improve the standards in terms of safety and risk minimisation. Before this time, no unified safety standards were available. At the end of the 2000s the Austrian highway and expressway network included 110 tunnel structures (over 80 metres in length), of which 28 were single-tube structures with bidirectional traffic. Today there are 166 tunnel structures on Austrian highways and expressways, of which ten are bidirectional tunnels.

Since 2006 ASFINAG has collected the data related to both fires and accidents occurring in tunnel structures and compiled them into a tunnel incident database, which is available for internal use. The results are used as a basis for tunnel risk analysis according to the RVS 09.03.11 guidelines.

In the observation period between 2001 and 2016, tunnel kilometres increased by 130% (currently 2018: 166 tunnel structures including a total of 401 kilometres) while at the same time the number of traffic fatalities decreased by 72%.

Table 1: Tunnel safety 2001 to 2016, ASFINAG.

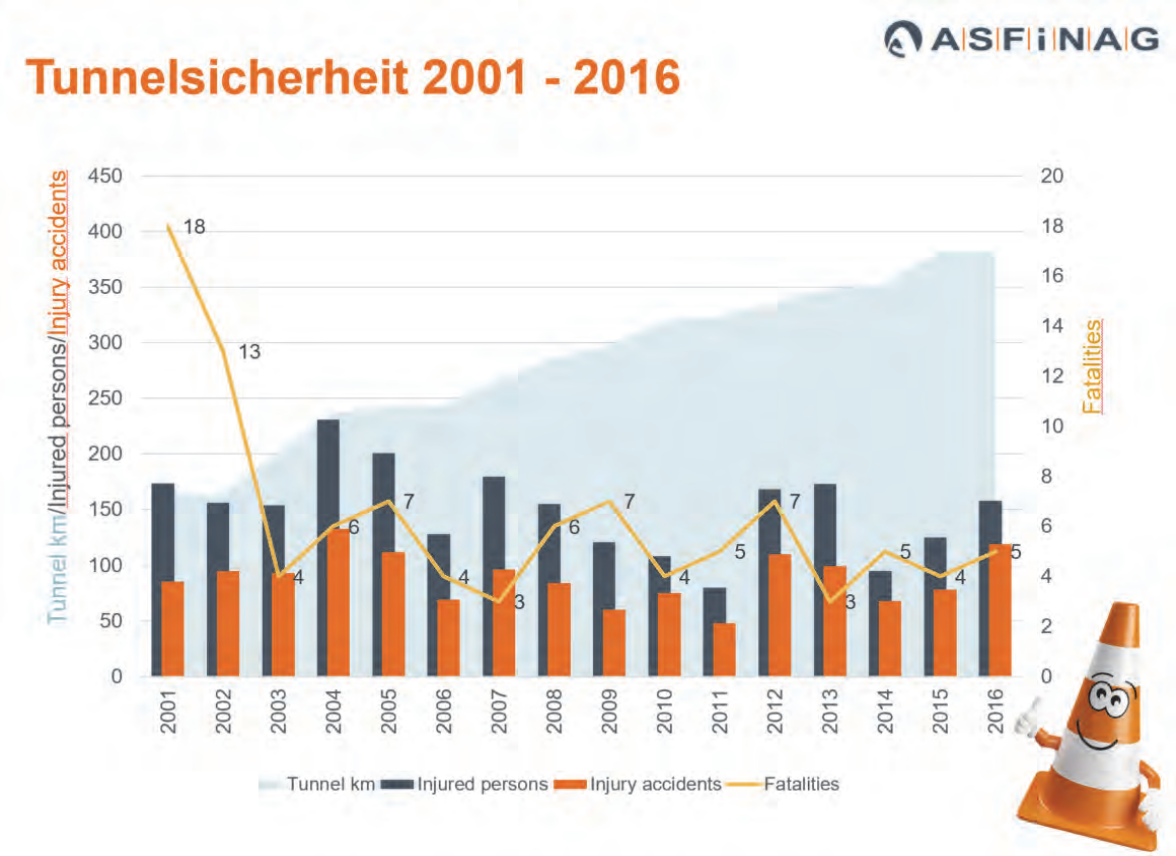

2. ADVANCES IN TUNNEL TECHNOLOGIES – YESTERDAY AND TODAY

With the implementation of the road tunnel safety law (STSG) in Austria in 2006, a means to regulate tunnel structures longer than 500 metres (currently 86 tunnel structures) was made available, which aims for project realisation by 2019. In addition to the legal framework, RVS guidelines guarantee standardisation in tunnel safety equipment. In order to comply with the related requirements in Austria, investments in both structural facilities and technical facilities as listed below have been made and are being made:

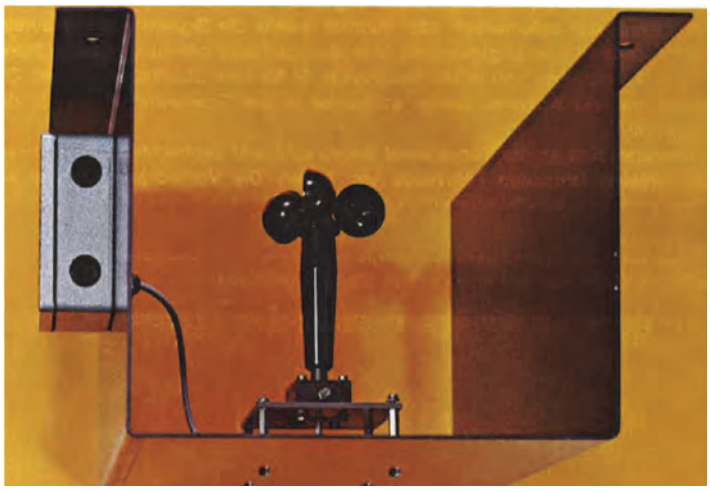

Figure 1:
Anemometer; *airflow measurement device,* 1975.

Construction of a second tunnel tube: Tunnel structures with an AADT exceeding 20,000 vehicles have to be designed as unidirectional tunnels.

Ventilation systems: Tunnel structures with lengths greater than 700 metres must be equipped with a ventilation system (including both longitudinal ventilation and transverse ventilation). The flow conditions have to be regularly measured by putting the data through a plausibility check, while at the same time taking into consideration thermal effects due to differences in temperature.

Control centres/traffic management centres: Unifying control centres and transforming them into traffic management centres (24/7 surveillance).

Figure 2:
Tunnel control centre room Katschberg-Nord, overall view, 1975.

Figure 3:
Emergency breakdown bay, Katschberg tunnel, 1975.

Detection systems: Tunnels must be equipped with both video surveillance systems and fire detection systems as well as with acoustic monitoring systems (AKUT)

Traffic route guidance and traffic control: Both LED information panels and self-illuminating LEDs as well as escape route signs have to be installed in order to help people to better orient themselves. The installation of sensors allows for both the carrying out of traffic volume monitoring and detection of vehicles parked in breakdown bays (occupancy detection loops)

Optimisation of lighting systems: Increasing luminance and utilisation of white light and LEDs.

Emergency call facilities: These are facilities that should help tunnel users to report events more rapidly and to contact the traffic management centre. Emergency call facilities include both emergency phones and manual emergency call buttons, which are installed in emergency call niches and at emergency call points.

Design outside the tunnel portals: Visual indicator facilities including both traffic signals and LED information boards as well as specification of speed limits.

Reduction of intervals between escape routes: The distances between escape routes have been set in collaboration with the emergency services, defining distance lengths of 250 metres to maximally 500 metres.

Drainage systems: 100 litres per second over a length of 200 metres.

Improving safety of portals and breakdown bays: In unidirectional tunnels concrete crash barriers have been installed at the portals and in the breakdown bays, whereas in bidirectional tunnels crash absorbers have been put in place to make critical points more safe.

Structural fire protection: Structural fire protection components must be installed in certain tunnel areas in compliance with the required protection level as specified in the related fire protection report.

An Example

The 5.5 kilometre long Bosruck Tunnel on the A9 Pyhrn Autobahn was opened in 1983. At that time the following facilities were installed: 27 video cameras, 8 carbon monoxide/visibility measuring devices, several traffic lights and variable traffic signs in the form of trivision signs. Only a working computer and an operator were then required to guarantee appropriate traffic control. [Autobahnen- und Schnellstraßen-Finanzierungs-Aktiengesellschaft, 2012].
In 2013 the second tunnel tube with a length of 5.4 kilometres was opened. Today this tunnel structure is equipped with the following facilities: 68 video cameras in the original tube, 70 cameras in the newly built tube (including the pre-portal area), 7 carbon monoxide/visibility measuring devices for each tube and in total 35 illuminated lane markers and digitally variable traffic signs. Two operators are required to guarantee appropriate surveillance and traffic control.
The surveillance and the control of the tunnel structure are no longer carried out in the vicinity of the tunnel structure itself; this is now handled centrally from one of the nine traffic management centres.

3. OUTLOOK: TUNNEL SAFETY AND TUNNEL ENGINEERING OF TOMORROW

The fast-paced growth in technology definitely generates an increasing demand for maintenance support. After 30 years, tunnel structures built in the 70s and 80s, which make up the majority of Austrian tunnel structures, needed refurbishment in the 2000s. Due to the continuous need for adaptations in order to adhere to the latest state of the art, refurbishments are already required after only ten years. The peak level of this development seems to have not yet been reached; we must thus start from the assumption that in the future, the intervals between required refurbishments will continue to decrease.

This is accompanied by a simultaneous increase in both personnel and costs as well as by the need to frequently close tunnels. Now the question is whether such a vast array of technical equipment is really necessary when it comes to improving tunnel safety.

4. SUMMARY

The experiences collected so far in Austria in the field of traffic and tunnel safety show that structural expansion measures together with modifications carried out to adhere to the most recent state of the art as well as further advancements have significantly contributed to risk minimisation.

Along with this development, a rise in the need for refurbishment and maintenance work has been noted. The future question is to what extent is technical equipment required in order to guarantee optimal safety in tunnels. New innovations such as autonomous driving and augmented reality as well as advances in terms of systems engineering will represent some future challenges for agencies that manage high-speed roadways.

5. SOURCES

Autobahnen- und Schnellstraßen-Finanzierungs-Aktiengesellschaft (2012). *Das Autobahnnetz in Österreich. 30 Jahre Österreich, Österreich: Pinix Druckerei GmbH.*

FIGURES

Tauernautobahn Aktiengesellschaft (1976). *Tauernautobahn Scheitelstrecke. Eine Baudokumentation bis zur Verkehrsfreigabe am 21. Juni 1975, Österreich: Verlagsanstalt Tyrolia.*

REQUIREMENTS FOR ESCAPE DOORS IN THE TUNNELS OF THE KORALM RAILWAY LINE – SPECIAL FOCUS ON THERMAL LOADS DURING FIRE

[1]Helmut Steiner, [2]Michael Beyer, [2]Peter-Johann Sturm
[1]ÖBB PNA – PLK 1, Austria
[2]Graz University of Technology, Austria

ABSTRACT

As escape ways are an integral part of rail tunnel safety, the escape doors themselves require particular attention. The doors must be solid enough to withstand the high pressure fluctuations caused by high-speed rail traffic, and must also be capable of withstanding high temperatures.

This paper focuses on the defined temperature requirement for escape doors in the Koralmtunnel. Various regulations define the temperature requirements, e.g. for concrete surfaces. These requirements define temperature levels and exposure times in the form of time-temperature curves. As there is no uniform international standard, the requirements imposed depend more or less on national policy. Well-known temperature curves are the HC curve, the HC-increased curve, and the 'standard fire time-temperature curve', in accordance with EN 13501-2. All of these differ in terms of maximum temperature value, time dependent increase in temperature, and duration of temperature exposure.

In order to define a credible temperature requirement for tunnel doors, numerical investigations were performed taking an incident with a maximum heat release rate of 100 MW as a thermal boundary condition. These investigations resulted in a time-temperature curve which could be used in testing the fire resistance of escape doors. The results from an analysis of temperature and heat release data from full-scale fire tests up to 200 MW peak heat release confirmed the validity of the newly-defined test conditions. It turns out that the 'standard fire time-temperature curve', as defined in EN 13501-2, represents reliable test conditions.

Keywords: Emergency doors, thermal resistance, tunnel safety, CFD calculations

1. INTRODUCTION

The so called 'southern corridor', with the Koralm railroad and the Koralmtunnel, is part of the some 1,800 km long Baltic – Adriatic rail corridor of the Trans European Network – Transport (TEN-T) [2], [3].

The Koralm railroad connects the Austrian federal regions Styria and Carinthia, and their capital cities, Graz and Klagenfurt. This new, high-performance track is characterized by very low track gradients. It reduces the travel distance between the two capital cities by 100 km and the travel time by more than 2 hours.

The core part of this new route is the Koralmtunnel with a length of 32.9 km, and is currently the 6th longest railway tunnel in the world. The maximum rock overburden is some 1200 m.

An emergency stop station with a length of 900 m is situated between the two tubes roughly in the middle of the tunnel. Cross passages are located every 500 m. These serve as escape routes and also house the necessary equipment required for tunnel operation and maintenance.

2. REQUIREMENTS FOR ESCAPE DOORS

2.1. General

Upon operation, the Koralm railroad will constitute an important part of the TEN-T. A high level of safety and reliability/availability are thus of the utmost importance. In the event of a fire, it is essential that passengers can be evacuated to so-called safe areas. The use of appropriate escape doors in the safe areas is thus a key element of any safety plan. These doors must comply with multiple (sometimes conflicting) requirements. For example, while the need for doors to withstand high pressure fluctuations and high temperatures implies the use of heavy doors, this may also make it more difficult for passengers to open the doors. An overview of the various requirements for escape doors can be found in [4].

2.2. Pressure fluctuations

All equipment within the tunnel is exposed to high pressure fluctuations resulting from rail traffic. Pressure waves caused by trains entering the tunnel, and reflected at the exit portal, can amount to some thousands of Pa, depending on type of the train, train speed, drag coefficients, and tunnel cross-section. These shock waves result in additional loads on doors, and exceed those resulting from static forces. Door durability and maintenance requirements are also important considerations ([5], [6]).

2.3. Fire resistance and time-temperature curves

In the case of a tunnel fire, train users must be evacuated into a safe area via escape doors. These doors must withstand the fire and provide sufficient shelter from the fire over a predefined time period (TSI-SRT survivable conditions). Standards such as DIN EN 13501 define the necessary level of fire resistance of escape doors.

Combustion is a process where heat and smoke are released. In practice, the release rate depends on many parameters and is largely unpredictable. After ignition the development of the fire depends on parameters relating to fuel, temperature, oxygen content, humidity etc. In order to have clear and replicable testing conditions, time-temperature curves are used to define subject exposure. All of these have a certain initial phase, where the temperature rises from ambient to maximum values. These curves are intended to idealize the characteristics of a design-fire. The maximum temperature to be achieved varies according to the different application ranges. For road and rail tunnels various time-temperature curves are in use, but no one has yet defined an internationally valid standard.

Viewed historically, the ‘standard fire time-temperature curve’ in accordance with EN 1363-1:2012/ISO 834 was the first attempt at standardization in Europe (around 1920). Other curves such as the HC-curve (1970’s), the RABT-curve (1985), the ZTV-ING curve (1995), the RWS-curve, and the HC_inc (for fuel fires in road tunnels) were then subsequently established. Research projects such as EUREKA 499 (FIRETUN), tests at the Runehamar test site, and others, aimed to verify the validity of these curves with respect to different fire sources, such as road and rail vehicles. In Austria, the so-called EBM/HC1200 curve was established for application in rail tunnels.

However, as seen in Figure 1, the majority of these curves has more or less the same shape and differs largely only in terms of maximum temperature level. Most of the curves are mainly applied to structural fire protection, while the ETK curve (standard temperature curve according to ISO 834) is often used for installations such as escape doors.

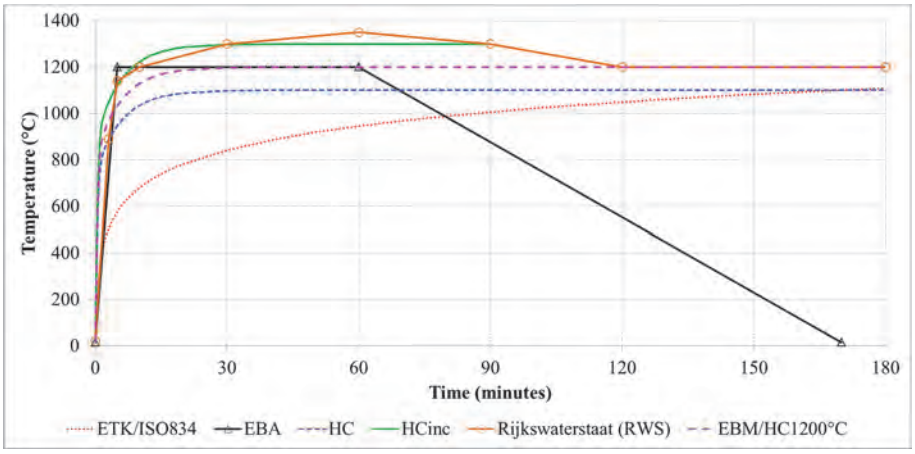

Figure 1: Comparison of existing time-temperature curves for fire-proofing [1]

Which time-temperature curve best meets tunnel requirements is often the subject of debate and curve definitions normally represent a practical compromise between basic necessity and feasibility. However, due to the differences concerning the objectives of structural fire safety and escape way safety for tunnel users, the temperature requirements for the structure need not be identical to that for escape:

- Tunnel users require escape possibilities for a certain timespan related to the self-evacuation period
- Structural fire protection must guarantee the self-support of the tunnel and the escape ways

3. NUMERICAL SIMULATIONS

The objective of the investigations was to determine the temperature loads in the case of a fire acting on mechanical equipment (dampers, escape doors etc.) mounted in the area of the cross passages. For this study a cross passage with an escape door (sliding door including frame and guidance elements) mounted outside of the cross passage (this means towards the rails), was examined. While such door installations are required where there is a lack of space inside the cross passage they also result in the smallest distance to a potential fire source (worst case). Such a situation was analysed for a fire with a peak heat release rate of 100 MW and 75 MW. An additional case with a heat release rate of 75 MW and an escape door mounted inside the cross passage (affects approx. 90% of all cross passages of the Koralmtunnel) was also examined.

In order to minimize the requisite computational effort, only a tunnel segment of 290 m in the proximity of the fire location, and the cross passage under analysis, were considered. The fire source (a low floor carriage with a lorry) is located 180 m downstream of the inlet in order to provide enough space to avoid any adverse influences on the inlet boundary conditions, e.g. by a possible back layering of the hot smoke gases. Standard quality assurance procedures were applied in the CFD calculation (e.g. grid independency).

The highest gas temperatures normally appear some meters downstream of the fire source (see [8]). Based on this experience, the fire source with the dimension of 4.5 m x 3 m x 20 m (height x width x length) was situated approximately 3 m upstream of the centreline of the emergency door. Figure 2 shows the computational domain of the Koralmtunnel.

The tunnel segment considered has a cross section of 45.6 m² and a slope of 0.3%, and a concrete lining with a depth of 0.4 m. The concrete lining was taken into consideration when calculating the convective heat transfer. The physical properties used were: specific heat capacity of 1000 J/kgK, a density of 2400 kg/m³, heat conductivity of 2.0 W/mK and an initial rock temperature of 15°C.

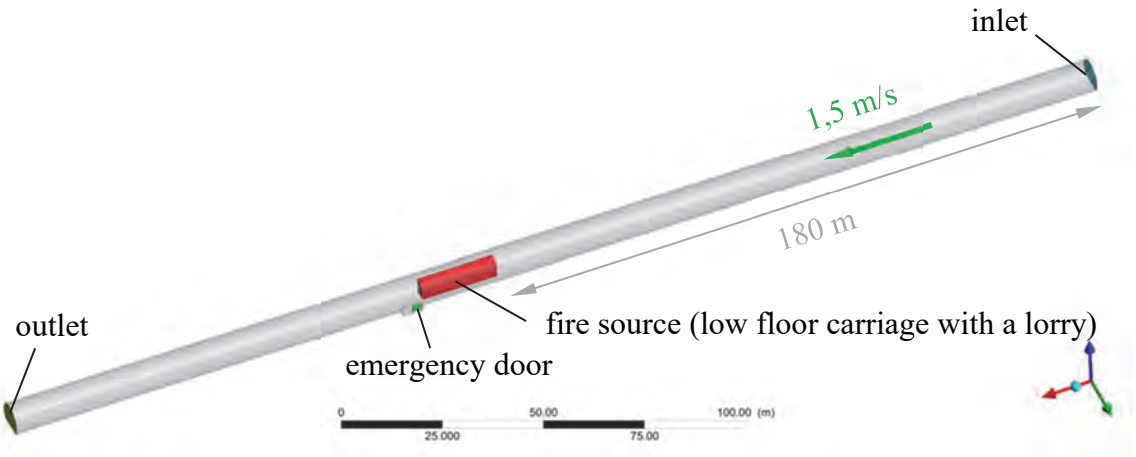

Figure 2: Computational domain (Koralmtunnel)

3.1. Numerical Model

ANSYS Fluent software was used for the numerical study. Turbulence was modelled using the realizable k-e model [7] and the enhanced wall function. A hybrid mesh comprising a few million elements was applied for the discretization of the 3D geometry analysed and a method with second order accuracy was selected for the numerical computation of the conservation equation.

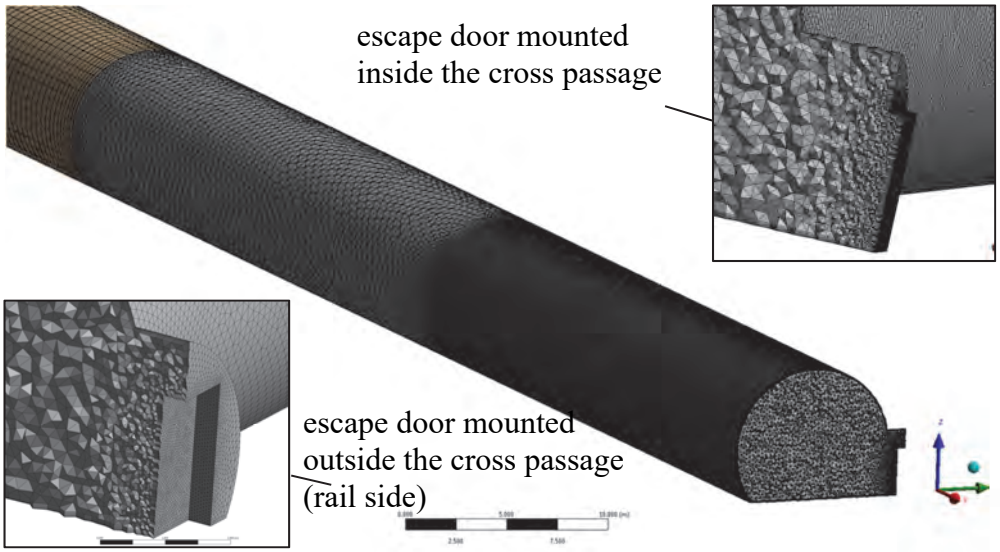

Figure 3: Computational mesh of the Koralmtunnel with an escape door mounted inside and outside the cross passage

In the case of fire, the ventilation system provides a volume flow rate upstream of the fire location of approx. 70 m³/s. This results in an air velocity of approx. 1.5 m/s (inlet boundary condition). An air temperature of 15°C at the inlet was assumed. For the outlet, an outlet pressure boundary condition with an average gauge pressure of 0 Pa was chosen.

The surface of the escape door was defined to be adiabatic. This means that the temperature at the surface of the escape door is equal to the gas temperature adjacent to the escape door and that the escape door does not influence the surface temperature due to the heat transfer (depending on heat conductivity and specific heat capacity of the escape door). This makes it possible to compare the calculated gas temperature at the escape door with the fire time-temperature curves (see Figure 1).

The fire is represented by a volumetric heat and mass source as suggested in [10]. Thus the numerical model does not simulate the combustion process and requires information on the heat release rate (HRR), the mass source, the time course and so on. For this, it was assumed that the fire exhibits a linear increase in heat to the maximum HRR within 5 minutes (which represents a strongly conservative approach), followed by a constant HRR for the remaining simulation time. Both, the increase of the HRR and the retention of the peak value represent an extreme fire scenario and are therefore a strongly conservative approach. Real fire tests e.g. the Runehamar fire tests, showed that the time to peak for such heat release rates (100 MW and 75 MW) was consistently >10 minutes and the peak value was retained only for some minutes [9]. Nevertheless, these characteristics of the heat source were chosen in order to consider a worst case scenario. As heat source, fossil fuel with a calorific value of 42.6 MJ/kg was used. This results in a fuel mass flow of 2.35 kg/s for the 100 MW case, and 1.76 kg/s for the 75 MW case.

Owing to the expected high soot proportion of the combustion gases and their insulating properties, the effects of thermal radiation were neglected. Hence, it is assumed that all heat release is captured in convection.

Simulations were carried out until steady state flow conditions were obtained. Longer simulation times would only result in an increase of the wall temperatures, which can be assumed would only have an insignificant effect on the temperature load on the escape door.

3.2. Results

In all simulation cases, steady state flow conditions were recorded after 10 minutes simulation time. Figure 4 depicts the temperature distribution after 10 minutes at the surface of the escape door (right) and in the tunnel cross sections at the heat source (left) as well as in a plane parallel to the floor (at half the height of the escape door). It can be observed, that in addition to the longitudinal air flow, a secondary flow with two counter-rotating vortices is formed. Due to these vortices hot smoke gases move from the tunnel ceiling to the bottom along the tunnel profile, resulting in a relatively high temperature gradient between the traffic room and the cross passage (see Figure 4). Because of this flow pattern the gas temperature in the cross passage region, as well as at the escape door, is noticeably lower than in the traffic room.

Figure 5 (100 MW case) and Figure 6 (75 MW case) depict the temperatures at the surface of the escape door (maximum local temperature and the area-averaged temperature) and compare them with commonly used time-temperature curves. After reaching steady state flow conditions the temperature values were extrapolated for the considered time period of 90 minutes.

For the 100 MW fire case maximum local temperature amounted to 1095°C and the area-averaged temperature to 860°C for the installation case “outside”. For the same installation, but a fire size of 75 MW, the temperature values are lower by about 20%. Considering the installation case “inside”, the maximum local temperatures are lower by about 10%. However, although the escape door is in this case less exposed to hot smoke gases, the area-averaged temperatures are almost the same. Owing to the strong increase of the heat release rate (time to peak of 5 minutes), a strong increase of the temperature values at the escape door can be observed. This leads to the situation that for this period (the first 30 minutes) the area-averaged temperatures overshoot the values of the standard fire time-temperature curve (ETK/ISO834). For the remaining time they remain below the ETK/ISO834 values.

100 MW after 10 minutes (escape door outside)

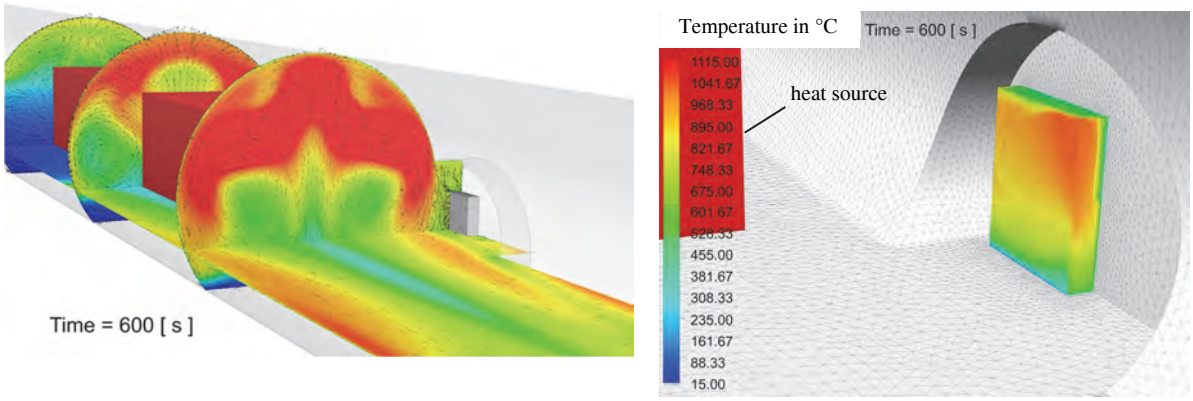

75 MW after 10 minutes (escape door outside)

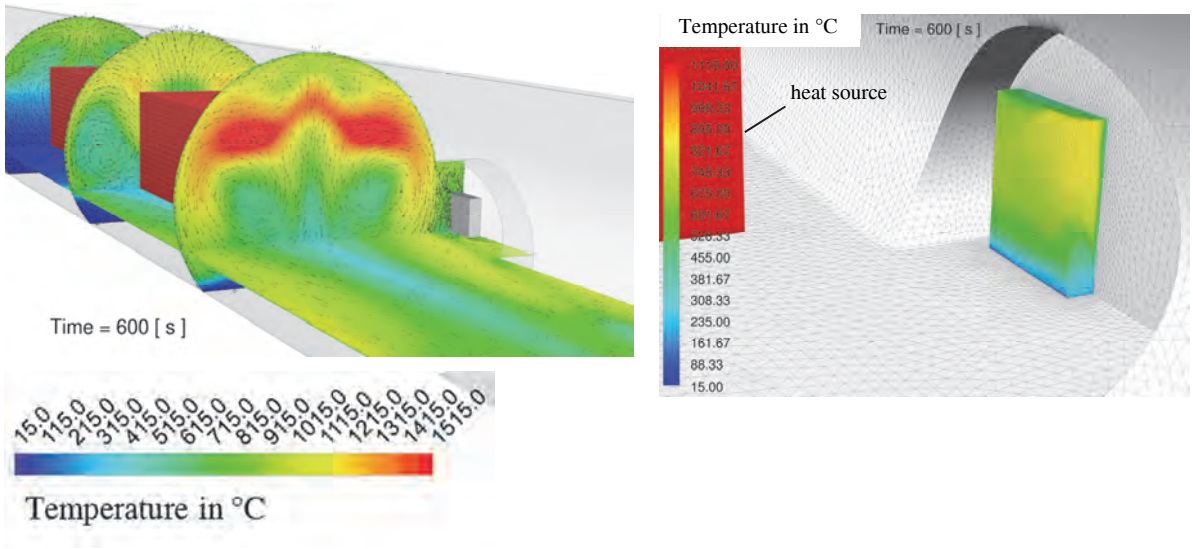

75 MW after 10 minutes (escape door inside)

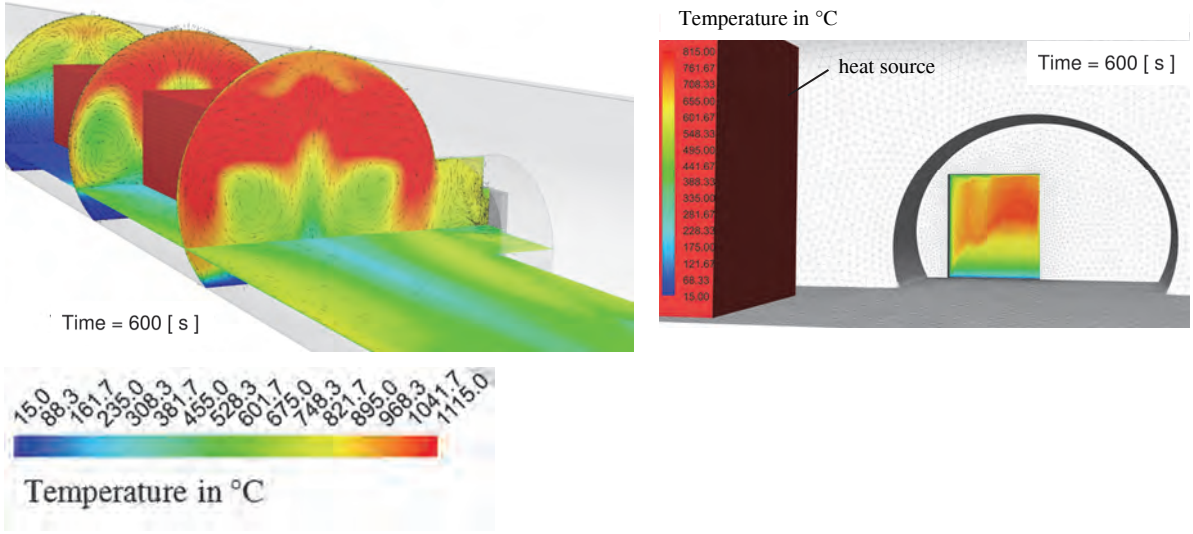

Figure 4: Temperature distribution and velocity vectors in the traffic room and on the escape door for all simulation cases after a simulation time of 10 minutes

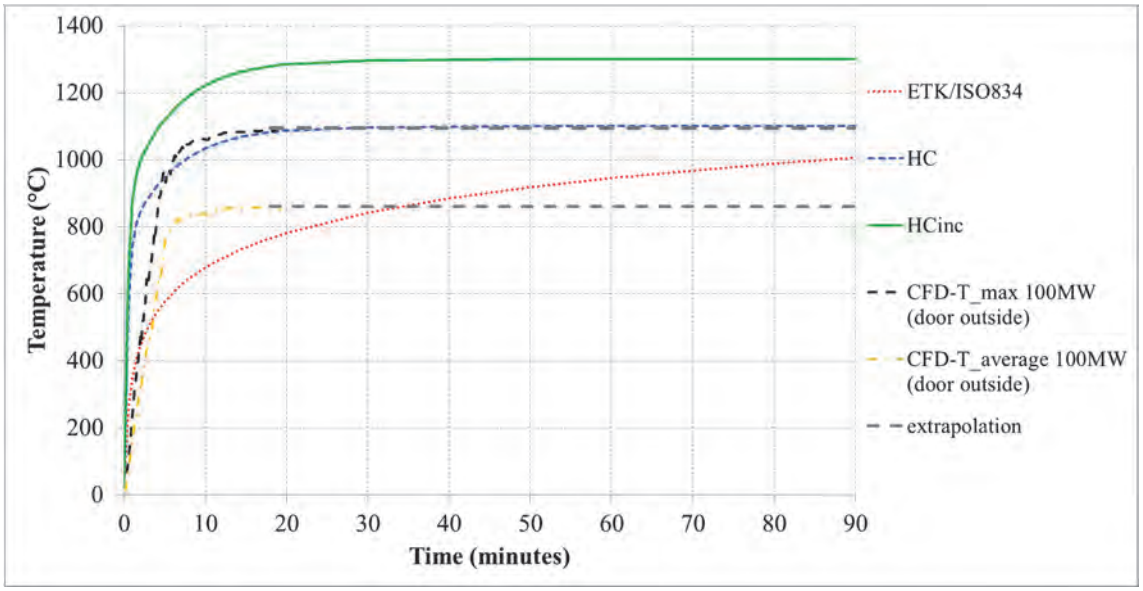

Figure 5: Comparison of typical fire time-temperature curve with the time-dependent gas temperature at the escape door obtained from the simulation for a 100 MW fire

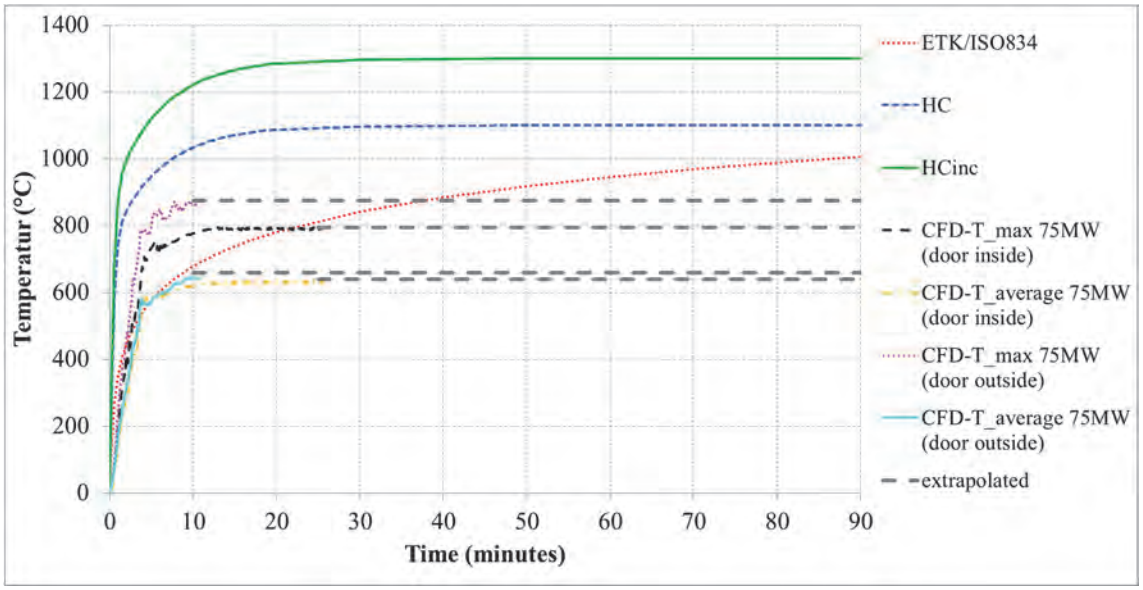

Figure 6: Comparison of typical fire time-temperature curve with the time-dependent gas temperature at the escape door obtained from the simulation for a 75 MW fire

An evaluation of the total energy input (area under the curve and calculated according to eq. 1) results in the fact that for all simulated cases the energy input is below the energy input resulting according to the standard fire time-temperature curve (ETK/ISO834). When defining the specific energy input (which can also be considered as time-average temperature) it was assumed that the heat transfer coefficient h, and the area of the escape door A, are constant for all calculated cases.

$$\frac{\dot{Q}_{90}}{A \cdot h} = \frac{\int_0^{90min} \Delta T(t) \cdot dt}{90min} \qquad \text{eq. 1}$$

Figure **7** depicts the specific energy input, the maximum area-averaged and maximum local temperature at the escape door for all simulated cases compared to the values related to the standard fire time-temperature curve (ETK/ISO834). In all cases the ETK/ISO834 scenario reflects the worst case, except for the maximum local temperature in the 100 MW fire.

However, a HRR of 100 MW at a volume flow rate of 70 m³/s is a theoretically attainable value. Real fire tests in tunnels have shown that the heat release rate is restricted by the effective calorific value and the required amount of air/oxygen (see chapter 3.3). Hence, in the case of real combustion, the HRR at an air-volume flow rate of 70 m³/s is lower (by about 90 MW, see Figure 9). A 90 MW fire case would result in a maximum temperature of some 1000°C and would be in the range of the ETK/ISO834 values.

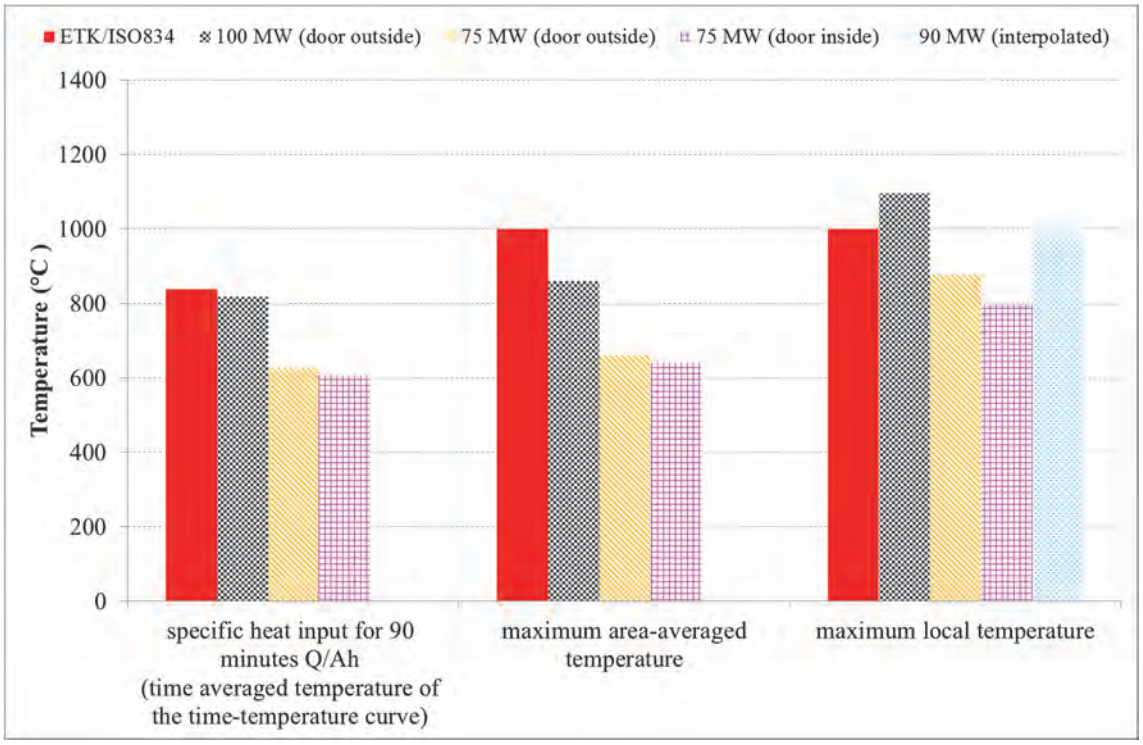

Figure 7: Temperature load on the escape door in all simulation cases compared with the values of the standard fire time-temperature curve (ETK/ISO834)

3.3. Discussion of the results

The simulations were performed for a specific tunnel geometry. In order to test the validity of the results with respect to other combinations of heat source, tunnel geometry and air volume flows, comparisons with results from full-scale tests were performed.

In order to do this the fire characteristics (calorific value H_W, minimum air requirement L_{min} etc.) for two of the Runehamar fire tests (with a peak heat release rate of about 200 MW and 120 MW, see Figure 8) were analyzed and the minimum air requirement derived. The data used for this process are summarized in Table 1 and were obtained from [9] and [11].

At a given air mass flow rate $\dot{m}_L$ the peak HRR $\dot{Q}$ mainly depends on the fire load (type of fuel), the efficiency of the combustion and the interaction between the fuel and the passing air (how much air/oxygen reaches the surface of the fuel). When comparing the two selected tests (T1 and T3), it can be seen that the mass flow rate of the air was the same for both cases (same amount of oxygen). However, T1 resulted in a HRR maximum that was twice as high, due to a higher calorific value of the fuel and the fact that oxygen (air) could penetrate the combustibles (wooden pallets) in a uniform way.

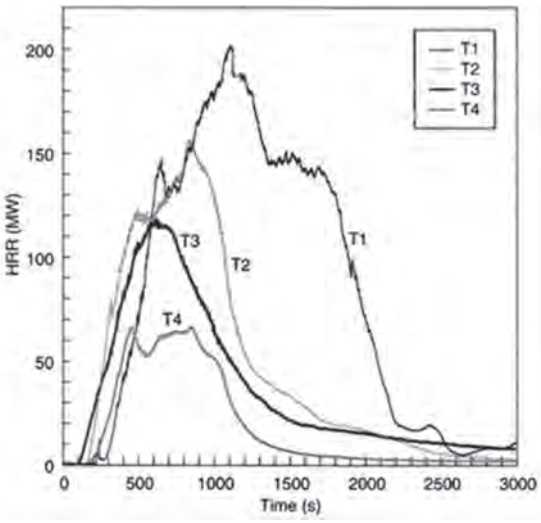

Figure 8: HRR as determined in Runehamar fire tests [11]

Table 1: Parameters of real fire tests derived from the Runehamar fire test acc. to [9] and [11]

	T1	T3
Load	380 wood pallets. 74 polyethylene pallets	Mixed goods. comprising plastic and wood furniture. fixtures. and toys; also 10 large tires
Total mass	11010 kg	8550 kg
Peak heat release rate $\dot{Q}$	201.90 MW	118.60 MW
Total heat release	242000 MJ	131000 MJ
Caloric value H_W	21.98 MJ/kg	15.32 MJ/kg
Air velocity during the test	3.00 m/s	3.00 m/s
Cross section area of the tunnel	50.00 m²	50.00 m²
Air temperature upstream the fire	12.00 °C	9.50 °C
Air density upstream the fire	1.24 kg/m³	1.25 kg/m³
Volume flow rate upstream the fire during the test	150.00 m³/s	150.00 m³/s
Mass flow rate during the test $\dot{m}_L$	185.82 kg/s	187.46 kg/s
Max. messured temperature during the test	1365.00 °C	1281.00 °C
Mass flow rate of the fuel (Peak) $\dot{m}_B$	9.19 kg/s	7.74 kg/s
Minimum air requirement L_{min}	20.23 kg air/kg fuel	24.22 kg air/kg fuel
Air density upstream the fire (Koralmtunnel)	1.17 kg/m³	1.17 kg/m³

Based on the calorific value and the minimum air demand of both tests, the maximum HHR - as a function of the volume flow rate upstream of the fire - was determined, and is shown in Figure 9 (left). The diagram also includes the results from the simulation cases 100 MW and 75 MW at an air volume flow rate of 70 m³/s. As can be seen, in the simulation for 100 MW, HRR exceeds the values found in the real fire tests. For a volume flow rate of 70 m³/s, it is supposed (based on T1 data) that the achievable maximum HRR is lower (~90 MW), due to oxygen limitations).

As shown in Figure 9 (left), the HRR increases linearly with volume flow rate. On the other hand, when keeping the HRR constant the mean temperature at the location of the fire T_B decreases linearly with the increasing volume flow rate. The right side of Figure 9 depicts temperature vs. volume flow rate. It can be seen, that the mean temperature remains constant with increasing volume flow rate even as the HRR increases and only depends on the calorific value and the minimum air demand.

Figure 9 (right) depicts the mean temperature at the location of the fire depending on the volume flow rate. Data was derived from the Runehamar fire test (T1 and T3) and the numerical simulations. The maximum value of the air temperature recorded during the fire test T1 was 1365°C (202 MW). This also indicates that the temperature level of the simulated 100 MW fire

(at a volume flow rate of 70 m³/s) is too high. Hence, it can be concluded that the simulation reflects more of a theoretical case than reality.

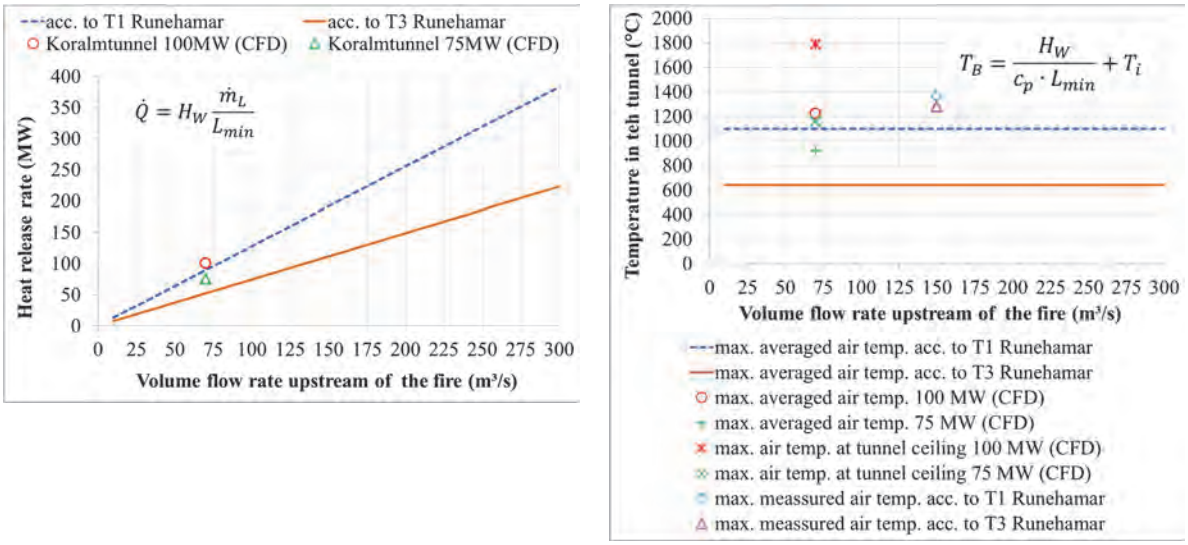

Figure 9: Heat release rate and mean temperature at location of fire, depending on the volume flow rate derived from the Runehamar fire tests acc. to [9] and [11] and obtained from the simulations

4. SUMMARY AND CONCLUSIONS

The aim of this study was to determine the temperature load on the escape doors for the tunnels of the Koralm railway line in order to derive a representative fire time-temperature curve when testing the fire resistance of the escape doors. For this a CFD-model based on the Koralmtunnel geometry was created and the temperature load of the escape door for a fire with a heat release rate (HRR) of 100 MW and 75 MW was evaluated. The results of this CFD study were then compared to data from full-scale fire tests.

An evaluation of the full-scale fire test showed that the HRR increases almost linearly with the air mass/volume flow rate in the tunnel (owing to an increase of oxygen) but the mean temperature at the location of the fire remains constant as the mass/volume flow rate increases (assuming the same fuel/calorific value and minimum air requirement).

Based on data from the CFD study, together with data from the full-scale tunnel tests, a maximum temperature of 1000°C and an area-averaged temperature of about 860°C at the escape door was derived. These results are valid for tunnels with a similar shape and flow characteristics (secondary flow with two vorticities as presented in Figure **4**) and are then independent of the mass/volume flow rate in the tunnel.

This study leads to the conclusion that escape door fire resistance may be adequately tested using the standard fire-temperature curve, as defined in DIN EN 1363 or ISO 834.

5. REFERENCES

[1] Blosfeld Jürgen; Brandkurven für den baulichen Brandschutz von Straßentunnel; Bericht der Bundesanstalt für Straßenwesen; Brücken- und Ingenieurbau; Heft B 67; August 2009

[2] ÖBB-Infrastruktur AG; The Koralm Railway, A part of the new Southern Railway Line; 2012

[3] Baltic Adriatic; Second Work Plan of the European Coordinator Kurt Bodewig; December 2016; European Commission – Directorate General for Mobility and Transport, Brussels, Belgium

[4] Lierau Michael, Römer Marcus, De Candido Luigi; Tunnel-Fluchttüren – Erfahrungen und Erkenntnisse aus 20 Jahren Tunnelbau; Proc. Swiss Tunnel Congress 2016; S. 182

[5] Steiner Helmut, Hannes Kari, Michael Reiterer; Erste Schritte zur Entwicklung von "neuen" ÖBB-Tunneltüren; Vortrag - Dynamik Tage Wien 2016, Austria

[6] Steiner Helmut, Hannes Kari, Michael Reiterer; Baudynamische Analysen bei der Entwicklung von Tunneltüren für die ÖBB: Simulationsberechnungen der Druck- und Sogbelastungen, Stoßspektren, Eigenfrequenzen, Ermüdungsbemessung; STUVA Conference 2017; Forschung + Praxis 49; S. 393

[7] T.-H. Shih, W. W. Liou, A. Shabbir, Z. Yang, and J. Zhu. A New k-Eddy-Viscosity Model for High Reynolds Number Turbulent Flows - Model Development and Validation. Computers Fluids, 24(3):227{238, 1995.

[8] Sturm P., Bacher M., Beyer M., Höpperger B., Croll J., Fire loads and their influence on ventilation design – A simple model for use in regulations, BHR Group ISAVT14, Dundee, Scotland, 11–13 May, 2011, pp. 293–307.

[9] Ingason H., Li Y. Z., Lönnermark A.: Tunnel Fire Dynamics, Springer Science+Business Media New York, 2015, ISBN 978-1-4939-2198-0

[10] Karki, K. C., Patankar, S. V., Rosenbluth, E. M., & Levy, S. S. (2000). CFD Modeler for Jet Fan Ventilation Systems. BHR Group 10th ISAVVT, Boston.

[11] NFPA: SFPE-Handbook of Fire Protection Engineering, 4th Edition, Massachusetts, 2008, ISBN-10: 0-87765-821-8

CHANGE IN THERMAL CONDITIONS DURING CONSTRUCTION AND OPERATION OF A LONG RAILWAY TUNNEL – TAKING THE KORALMTUNNEL AS AN EXAMPLE

[1]Daniel Fruhwirt, [1]Michael Bacher, [1]Peter-Johann Sturm, [2]Helmut Steiner
[1]Graz University of Technology, Austria
[2]ÖBB PNA – PLK 1, Austria

ABSTRACT

The requirements for the thermal conditions inside the tunnel differ between the construction phase and tunnel operation. During the construction phase, the main constraint is the maximum allowable air temperature in the working areas, since this must not be exceeded. In contrast, during railway operation, the thermal conditions in the tunnel itself are important because tunnel air is often used for cooling technical equipment, which is usually located in special rooms or zones within the cross-passages between the two tubes of the tunnel.

Thermal conditions in a tunnel depend on a variety of parameters and these vary as one proceeds from the construction to the operation phase. To give a brief overview of the impact of such parameters, the Koralmtunnel, which is still under construction, is taken as an example. The Koralmtunnel (KAT) is an approximately 32.9 km long twin-tube railway tunnel located in the south of Austria, connecting the federal states of Carinthia and Styria. It forms, together with the Semmering base tunnel, the core part of the Austrian section of the Baltic-Adriatic axis within the Trans-European railway network. The KAT has about 70 cross-passages containing utility rooms for the electrical and IT equipment. To guarantee that the acceptable temperature limits for the single rooms are maintained, tunnel air is required for a cooling process. For reasons of cost efficiency, a simple mechanical ventilation system is to be installed in as many cross-passages as possible. Where this simple cooling process is not sufficient, air conditioning is required. Simulations were performed in order to identify those tunnel regions where tunnel air is cool enough to ensure compliance with thermal requirements.

Keywords: tunnel climate, construction-operation requirements, thermal parameters

1. INTRODUCTION

1.1. Koralmtunnel

Figure 1-1 shows the Baltic – Adriatic corridor of the Trans-European Network – Transport (TENT-T) [1], [2], as well as the Austrian section, the so called southern corridor. The core of this southern corridor is formed by the Semmering Base Tunnel (SBT) with a length of 27.3 km, and the Koralmtunnel (KAT), with a length of 32.9 km. Both tunnels are currently under construction and the whole line will be operated as high-performance track, connecting Vienna with Klagenfurt via Graz. The Koralm stretch will reduce the travel distance between Graz and Klagenfurt from 230 km to 130 km and the travel time from 3 hours to less than one hour [3], [4].

Today the KAT is the sixth longest railway tunnel in the world. To meet the safety requirements as given in TSI, an emergency stop station with a length of about 900 m has been constructed in the middle of the tunnel. A ventilation system maintains smoke free areas within the emergency stop station and manages smoke propagation through the tunnel [5]. As the overburden at the location of the emergency stop is more than 900 m (maximum 1200 m), ventilation is carried out by two ventilation stations, each located about 3.5 km from the portal.

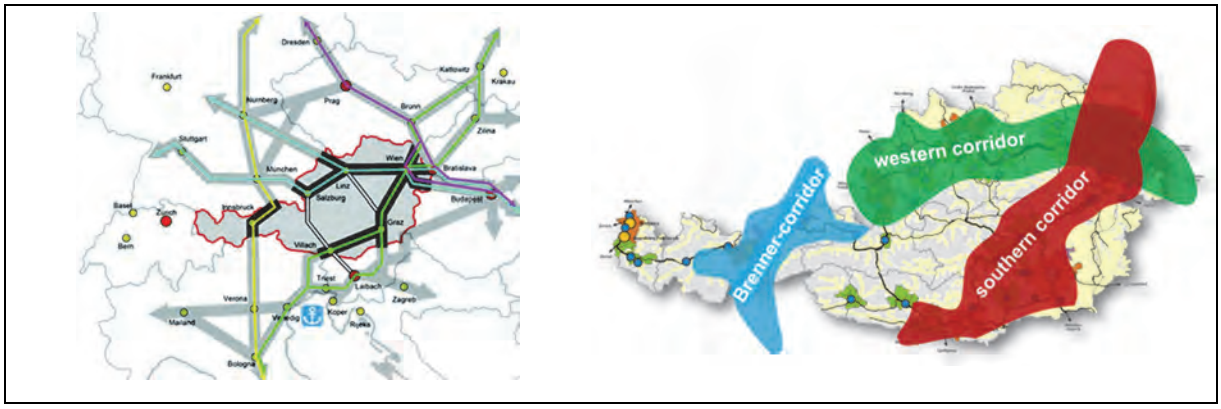

Figure 1-1: Railway corridors in Austria and its neighboring countries (Source: ÖBB INFRA)

Figure 1-2 shows a sketch of the tunnel with the emergency stop station roughly in the middle and the two ventilation stations in the east and west.

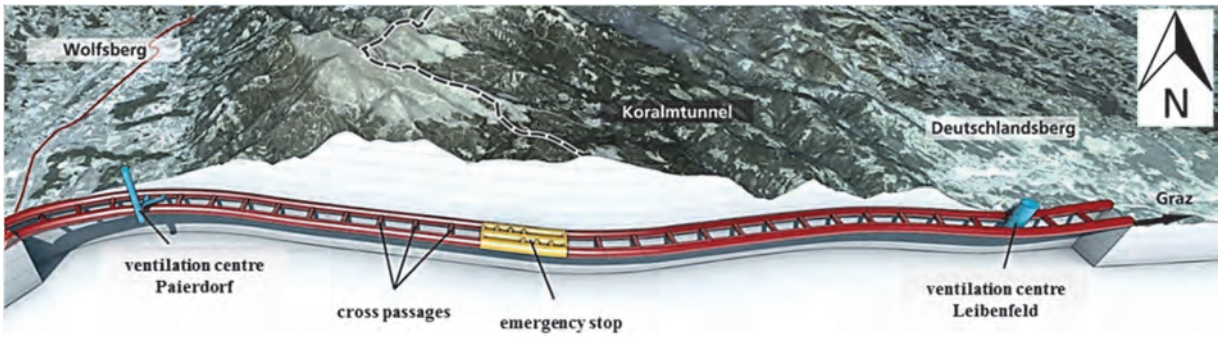

Figure 1-2: Schematic of the Koralm rail tunnel (Source: ÖBB INFRA)

The cross-section of both tubes varies between 42.5 m² and 51.8 m². It was optimized in terms of construction costs, traction power consumption, with a focus on the attainable maximum speed, and the impact of the pressure on and in the train.

Every 500 m there are cross-passages (see Figure 1-3), which serve as escape ways from the incident tube into the safe areas (unaffected tube). Within these cross-passages are also utility rooms which contain the technical equipment needed for operation (electricity, IT, etc).

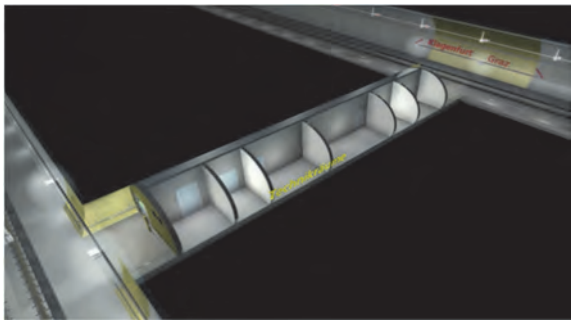

Utility rooms

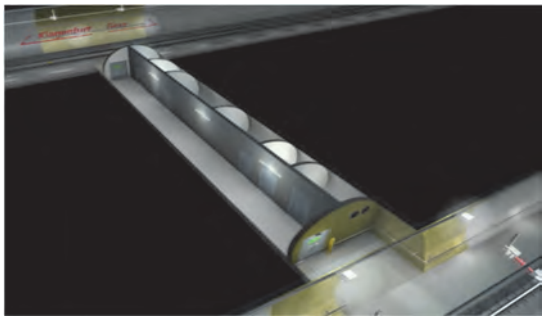

Escape-passageway

Figure 1-3: Schematic of a cross passage with utility rooms and escape passageway (Source: ÖBB INFRA)

1.2. Construction phase

Currently the Koralmtunnel is still under construction. Once tunneling is finished, the installation of the rail tracks and the technical equipment is to begin. This installation and implementation phase is split into two phases. While the first phase is concerned with completion of construction work (finalization of the slab track surface, installation of curbs, etc., i.e. mainly work concerning concreting), the installation of technical equipment in both tubes and the cross-passages is to be dealt with during the second phase.

The excavation work in the tunnel was divided into three lots, each with a different schedule. This has resulted in the unpleasant situation that while the final installation work has already begun in the first lots, in the remaining lot excavation is still ongoing. The western part of the tunnel will be finished some months later. Thus, implementation of different ventilation systems is required over time, one for an east and one for a west section, with brattices to separate the different lots in each tunnel tube.

The decisive parameter during construction is the maximum acceptable air temperature (dry and wet bulb temperature). The restrictions in this case are given in guidelines, such as the SUVA-Pro [7]. The guidelines mostly define maximum air temperatures in consideration of the relative humidity. For the construction phase of the Koralmtunnel, a temperature of 30°C (dry bulb temperature), is defined as maximum acceptable air temperature in the working areas. Additionally, the minimum (0.2 m/s) and maximum (6 m/s) air velocities in the working areas are also defined.

1.3. Operation phase

During operation, tunnel air is used for cooling the technical equipment in the cross-passages [6]. To ensure cost efficiency, two different cooling systems are employed. A simple ventilation system with axial-fans and ducts where tunnel air is filtered and blown into the utility rooms, and an air conditioning system which uses tunnel air for re-cooling. Dependent on the tunnel air temperature along the tunnel tubes, the cross-passages will be equipped with one of these systems. In tunnel sections with lower air temperature, the ventilation system will be installed and in tunnel sections with higher air temperatures or cross-passages with higher heat release from technical equipment, the air conditioning system will be used.

2. BOUNDARY CONDITIONS

2.1. Meteorology

2.1.1. Outside air temperature

As soon as outside air gains access to a tunnel, the outside air temperature becomes a parameter in managing tunnel air temperature. The importance of the outside temperature is normally higher for short tunnels, or for long tunnels, in sections close to the portals.

For the current simulations the weather data (outside air temperature) from the region for the years 2010-2016 [8] was processed. It turned out, that in 2013 summer short-term outside air temperatures, which represent the worst case in terms of achieving compliance with the temperature specifications, were at a maximum. In order to take these peak values at least partly into account, the average of the hourly values for 2012 and 2013 (Figure 2-1) was used as input.

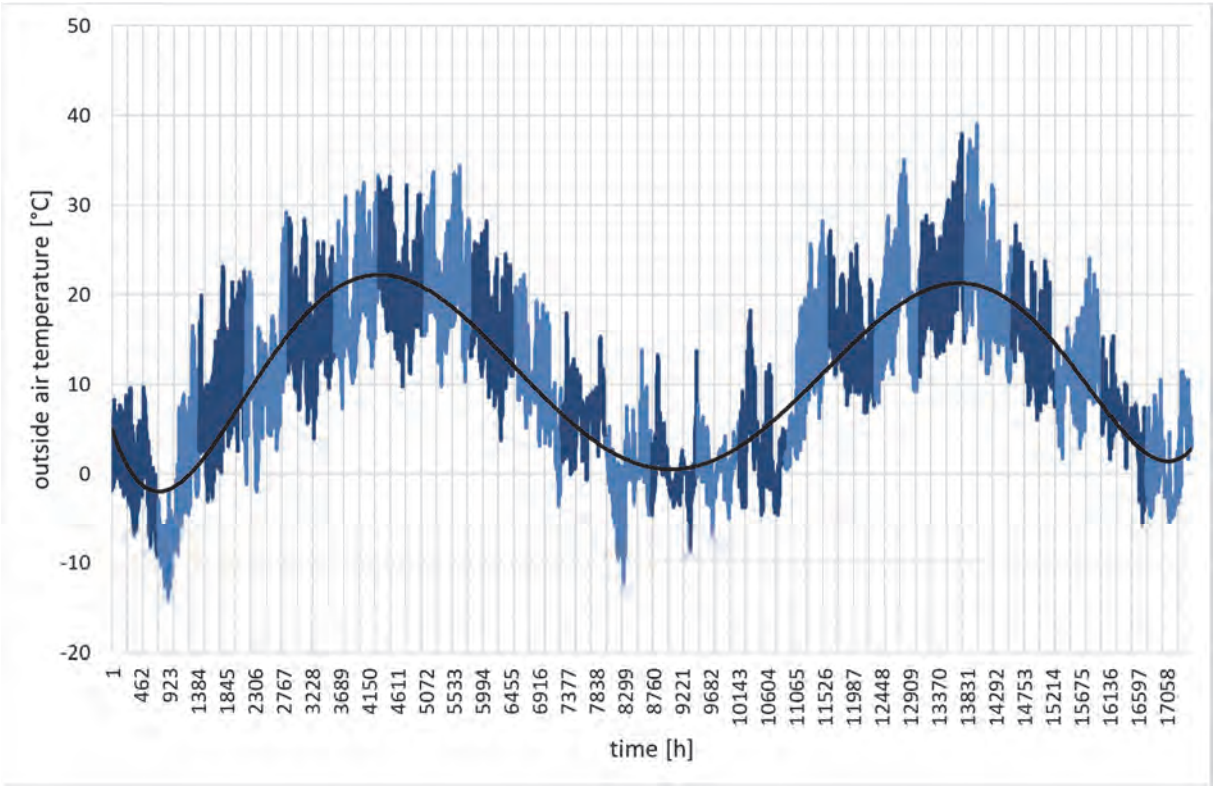

Figure 2-1: Outside air temperature curve - Deutschlandsberg, January 2012-December 2013

2.1.2. Pressure differences between portals

The Koralm tunnel passes through a mountain range which acts as meteorological divide. This results in a quite noticeable barometrical pressure difference between the portals. In the design of the ventilation system of the KAT, the 98 percentile values of the pressure differences between the portals were used. They amounted to 106 Pa at the east portal and 230 Pa at the west portal. During the implementation/equipment phase, ventilation will be carried out by two independent ventilation systems, applying supply-return air methodology (U-ventilation system) via both tubes. Hence, the acting pressure difference is marginal. In the final part of the installation phase, the brattices will be removed and the meteorological pressure difference between both portals will in general provide a sufficient airflow through the individual tubes.

During the tunnel operation the pressure differences between both portals are of course decisive in any incident case, as well as during maintenance and phases where no trains are in the tunnel. As soon as trains run through the tunnel, the piston effect is much more important for the air flow than the pressure difference arising due to the meteorology.

2.2. Rock temperature

The rock temperature is one of the major parameters for the tunnel air temperature during construction and operation. Figure 2-2 shows rock temperature and the overburden curve of the KAT. The dependence of the rock temperature on the overburden is clearly visible. The highest rock temperature is about 32°C. The rock temperature curve was measured and monitored during the excavation phase and represents the starting condition for the simulation of the time dependent evolution of tunnel-wall temperatures along the tunnel.

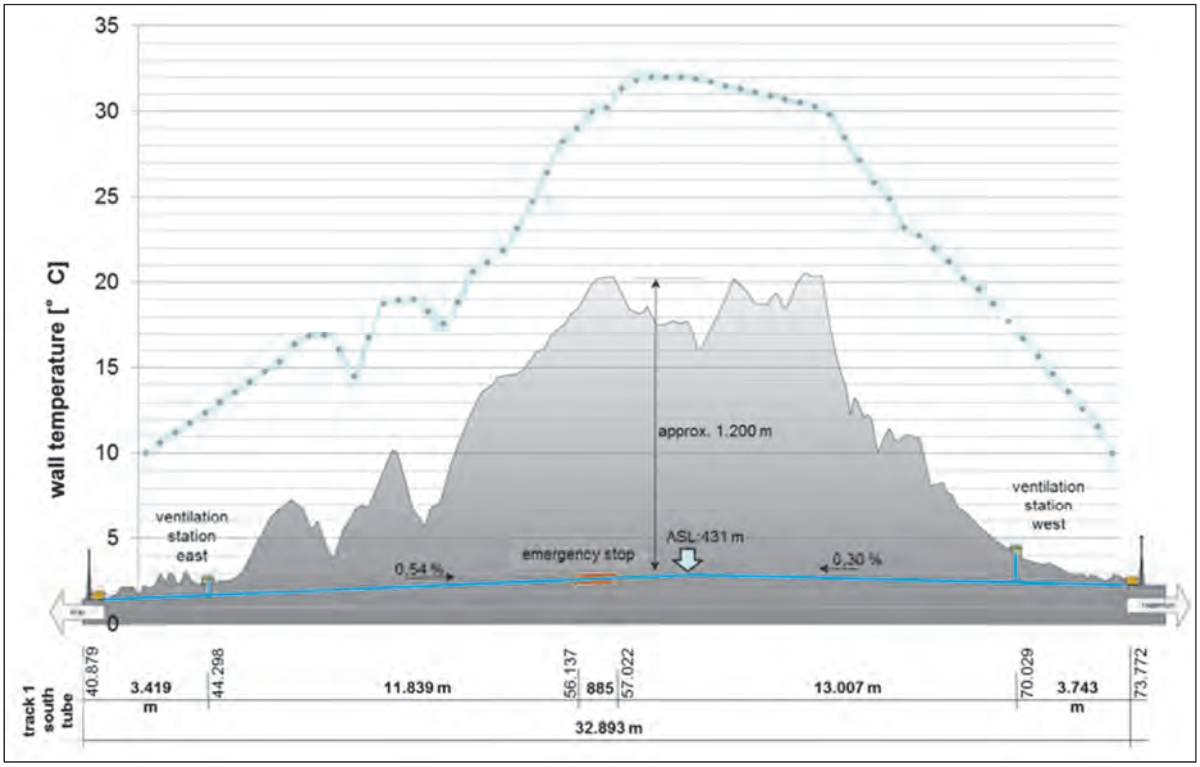

Figure 2-2: Koralm tunnel –rock temperature and overburden
(Source: ÖBB INFRA, ACTES)

2.3. Construction and equipment phase

The different stages of the construction process in a long tunnel pose several problems when designing work place ventilation. In the current case, installation in the east will start even while excavation work in the west is still ongoing. Hence, the logistics for installation, transport of materials etc. are quite complex and are subject to continuous change. This has a clear impact on ventilation possibilities.

2.3.1. Fresh air requirement

In general, the fresh air requirement is the major parameter for tunnel air conditions. It varies during the individual construction and equipment phases. The power requirement for diesel driven machinery is the driving parameter. The highest demand is needed for trains and cranes while concreting. According to the SIA 196 [9] 4 m³/min/kW and 2 m³/min/person is required. The machinery in the KAT requires some 70 m³/s at maximum. The higher the fresh air volume flow the bigger the influence of the outside air temperature.

2.3.2. Heat release from machinery and concrete works

The main heat sources are operating machinery and the drying process of the concrete. The latter source is considerable in the present case, as the slab track and the walkways require huge amounts of concrete. Per day sections with a length of 240 m are concreted alternately in both tubes (current assumption). This results in a relatively high release.

2.4. Tunnel in operation

2.4.1. Trains

The most important heat sources during operation are the trains themselves. The impact of trains depends on their speed, and on the geometry of both the trains and the tubes. The piston effect of the trains generates an air flow in the tubes, which is essential for the thermal conditions along the tunnel. Hence, the time interval between the trains, as well as their driving direction,

are essential parameters. Owing to operational or maintenance factors, driving direction in a tube may sometimes change during the day, i.e. one hour east to west, next hour west to east. There are several operating scenarios for the Koralm railways, varying from 2 to 6 trains per hour in one direction.

Trains also represent thermal masses, so the convective heat released by the trains can lead to considerable changes in thermal conditions. Depending on the slope, the convective heat released by breaking also has to be considered. The highpoint of the KAT is a few kilometers west of the emergency stop station. A regular train station is located on both sides of the tunnel. Thus, stopping at these stations entails the release of breaking energy within the tunnel.

2.4.2. Technical equipment

Since tunnel air is used for cooling the utility rooms inside the cross-passages, the released heat from technical equipment, such as from the telecommunication units or the power supply units, has to be considered. Technical equipment has been installed in all of the 70 cross-passages. The released heat varies between 3 kW and 25 kW, depending of the type of equipment installed. A single cross-passage would not have a big impact on the thermal conditions, but the sum of transported heat can lead to noticeable changes in thermal conditions within the tunnel. Due to redundancy reasons, both cooling systems (ventilation, or air conditioning) are capable of re-cooling in both tubes. Depending on the tunnel air temperature in front of the cross-passages, re-cooling takes place in the tube with the lower air temperature. Hence, roughly 50% of the cross passages will be cooled from one side, and the other 50% from the other side.

2.4.3. Maintenance

In the KAT, one tube is to be closed for 5 hours every day for maintenance (current assumption). The maintenance plan has to be taken into consideration during the design of the cooling and ventilation systems. The main parameters here are the maintenance intervals, duration of maintenance, machinery used, etc. If one tube is closed for maintenance, the second one is still in operation, and due to the movement of the trains, air flow, and therefore heat transport, is given. In the tube undergoing maintenance, airflow depends on meteorology, and where required, on the maintenance ventilation.

3. SIMULATIONS

3.1. Software

For calculating the thermal conditions inside the KAT, the software package “IDA-Tunnel” [11] was used. IDA Tunnel is a flow simulator, developed for aerodynamic application in rail and road tunnel systems. It solves continuity, momentum and energy equations in a 1D approach. “IDA-Tunnel” is capable of calculating heat conduction in solid layers, convective heat at the solid-fluid border, as well as radiation due to fire-incidents or similar events.

3.2. Simulation-model

The simulation model contains the geometry of the tunnel, as well as the boundary and starting conditions. To create the geometry, the tubes were divided into 500 m long sections, corresponding to the distance between the cross-passages. The emergency stop station, located in the middle of the tunnel between the two tubes, was neglected in the model geometry as it has no noticeable influence on the thermal conditions. Each section was further split into 100 m long subsections in order to facilitate calculations.

With increasing simulation time, rock temperature changes noticeably with penetration depths. Figure 3-1 depicts the structure of the tube, the insulation, and the different concrete layers. Heat conduction was calculated for these layers until a constant rock temperature was reached (remark: the constant rock temperature differs along the longitudinal axis of the tunnel). Penetration depth varied with simulation time automatically.

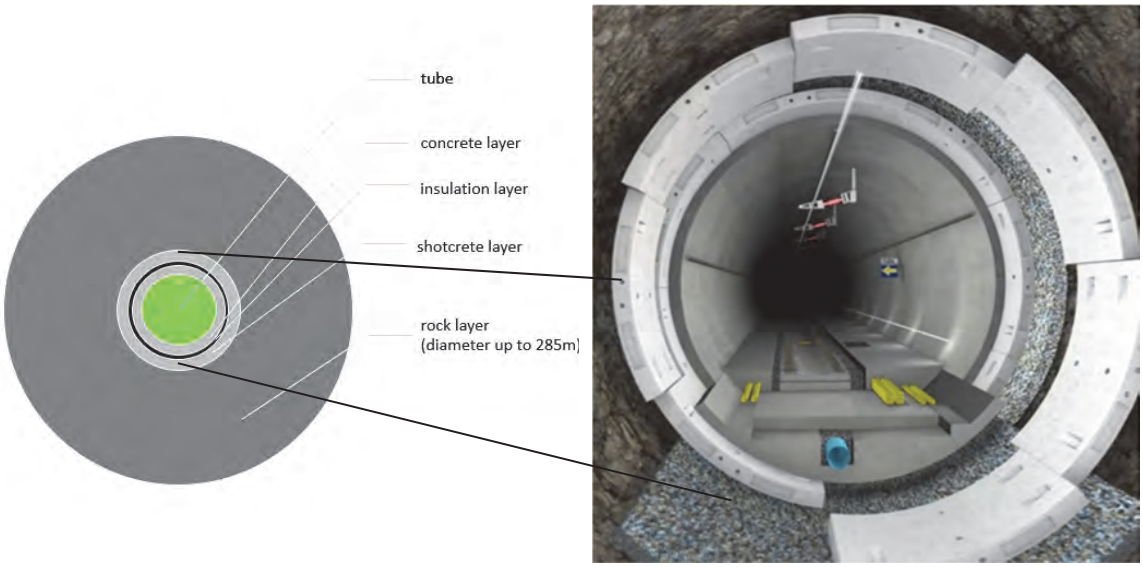

Figure 3-1: left: IDA model of radial wall layers; right: Scheme of the tube (Source: ÖBB INFRA)

3.3. Results

3.3.1. Thermal conditions – construction phase

The rock temperature in each tunnel section, according to Figure 2-2, were implemented as a starting condition. Considering the chosen supply/return or U-ventilation systems (east and west section) for construction ventilation, brattices at the corresponding locations in the tube were implemented in the model as area changes with small leakage rates. The required fresh air amount is provided by fans located at the east portal. It is assumed that this part of the construction phase will last for two years with ventilation being permanently active.

In order to achieve air temperatures below 30°C, air coolers with all their advantages and disadvantages are needed. The impact of an air cooler depends on the ratio between cooled and total air mass flow. Since re-cooling is done by a separate water circuit, the temperature and the mass-flow of the water is also an important parameter. Nevertheless, the cooling power must be high enough to compensate for the heat released from concreting, from the machines, and from the rock. The cooling system was modelled as a thermal sink with a total cooling power of 800kW, which corresponds to the cooling power of two air coolers.

To demonstrate the impact of those two air coolers a separate simulation was done. Figure 3-2 shows the temperature evolution as a function of tunnel position and operation time. At the inlet portal (right side Figure 3-2) the dependency of the tunnel air temperature on the outside conditions is clearly visible. In the first few meters, tunnel air temperature follows strictly the curve of the outside air temperature. This influence is visible - with decreasing impact – up to 5 to 6 km into the tunnel. At tunnel center, where the highest rock temperatures occur, the air coolers reduce the tunnel air temperatures to about 20°C. At the area near the outlet-portal, the tunnel air temperature is nearly constant over the whole period.

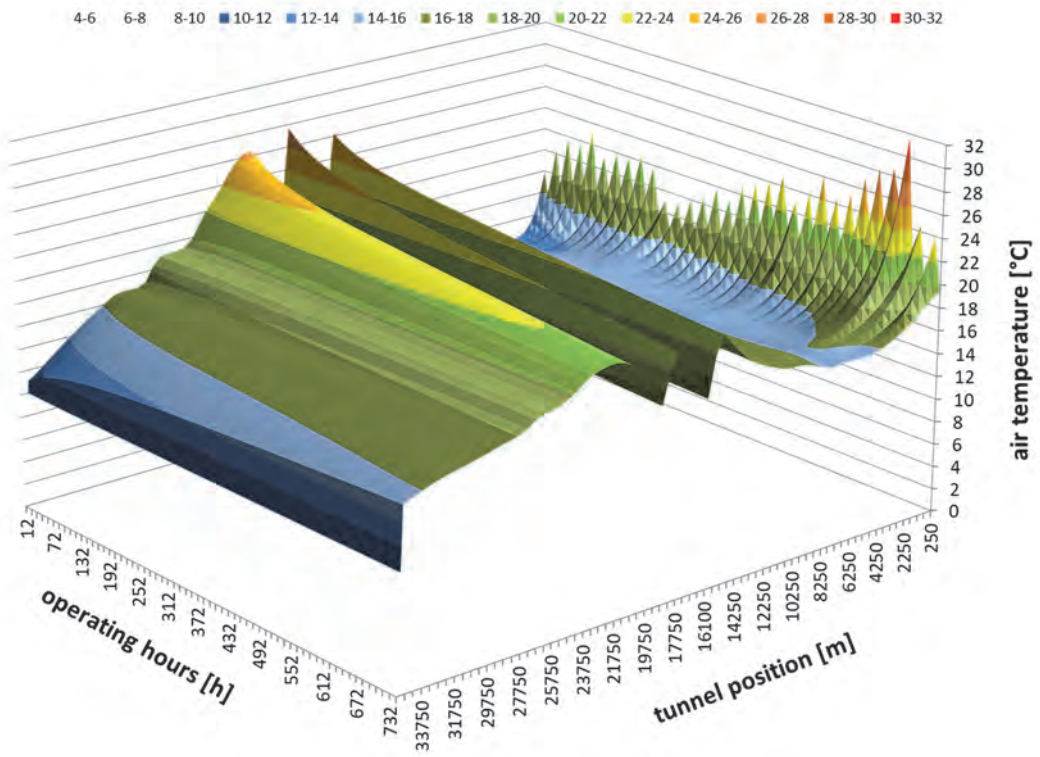

Figure 3-2: Impact of ambient air and air coolers on the thermal conditions in KAT - ventilation section east

As the air coolers move with the construction activities they operate only for short limited periods at the same locations. Hence, they can be neglected in long-term simulations, where the focus was on the evolution of tunnel air temperature and thus on rock temperature and wall surface temperature. The air volume flow was set at 50 m³/s in both ventilation sections, which represents the time-weighted average value during the implementation/equipment phase (min. 25 m³/s – max. 70 m³/s).

Figure 3-3 shows the wall temperature curve of the south tube (supply air tube) at representative times during the KAT implementation/equipment phase. The starting condition was given by the measured rock temperature along the tunnel. The simulation results show the large influence of the outside conditions on the wall temperature in areas close to the portals. In the tunnel center, construction ventilation as a stand-alone system for cooling applications is able to reduce the wall surface temperature by 5°C in the ventilation section east, and by about 2°C in ventilation section west. This difference is due to the high rock temperatures at the beginning and the fact that the high rock-temperature regions are mainly located in ventilation section west. This leads to higher tunnel air temperatures at the tunnel center in section west and therefore a lower capability of transporting heat from the wall and from the rock.

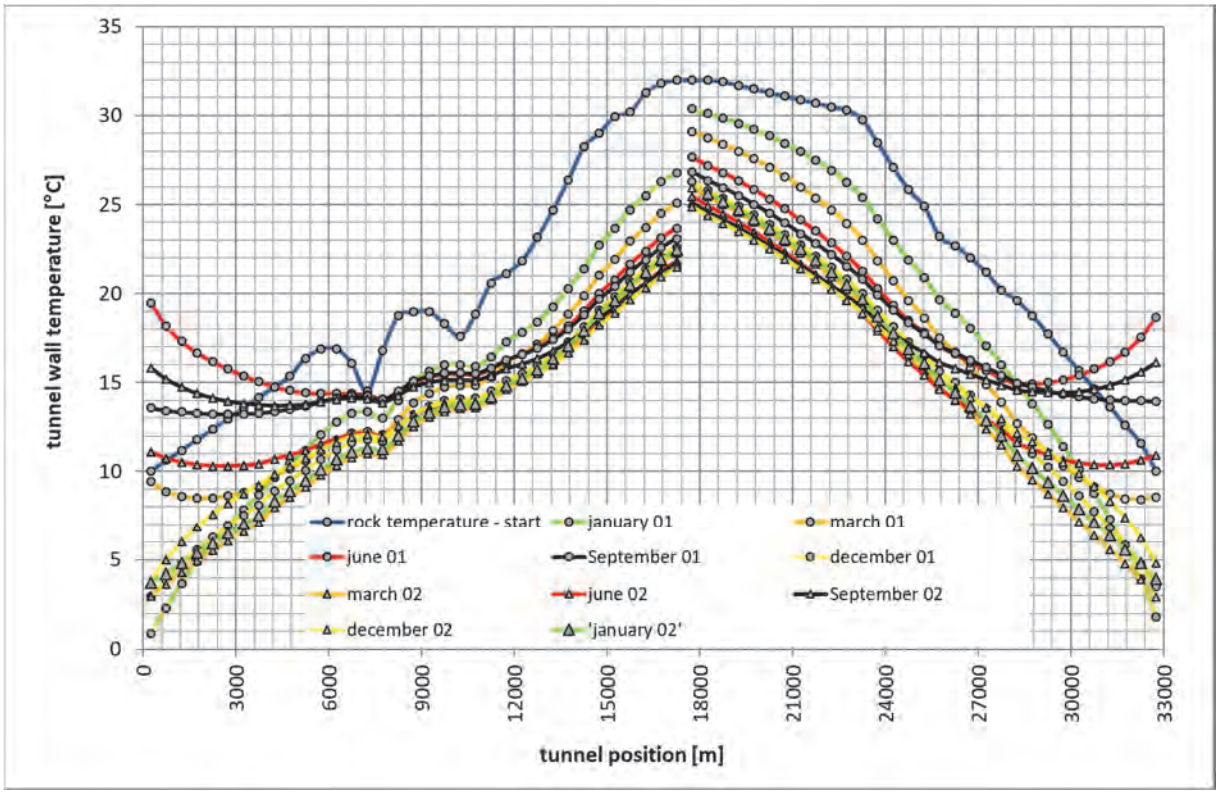

Figure 3-3: KAT – tunnel wall temperature curves for the south-tube at representative times during implementation/equipment phase (01 – 1st year, 02 – 2nd year)

Figure 3-4 depicts similar situations, but for the north tube (exhaust air tube). As here the air flows from tunnel center towards the portals in order to be expelled, the warm air from the tunnel center leads to a rise in tunnel wall temperatures close to the exit/outlet portals. The difference between the wall temperature curves at different times is smaller here as there is no noticeable influence of outside conditions.

As a result of these simulations air coolers are to be integrated into the trains transporting concrete and other materials in order to not to exceed the permissible 30°C threshold value for air temperature in working areas.

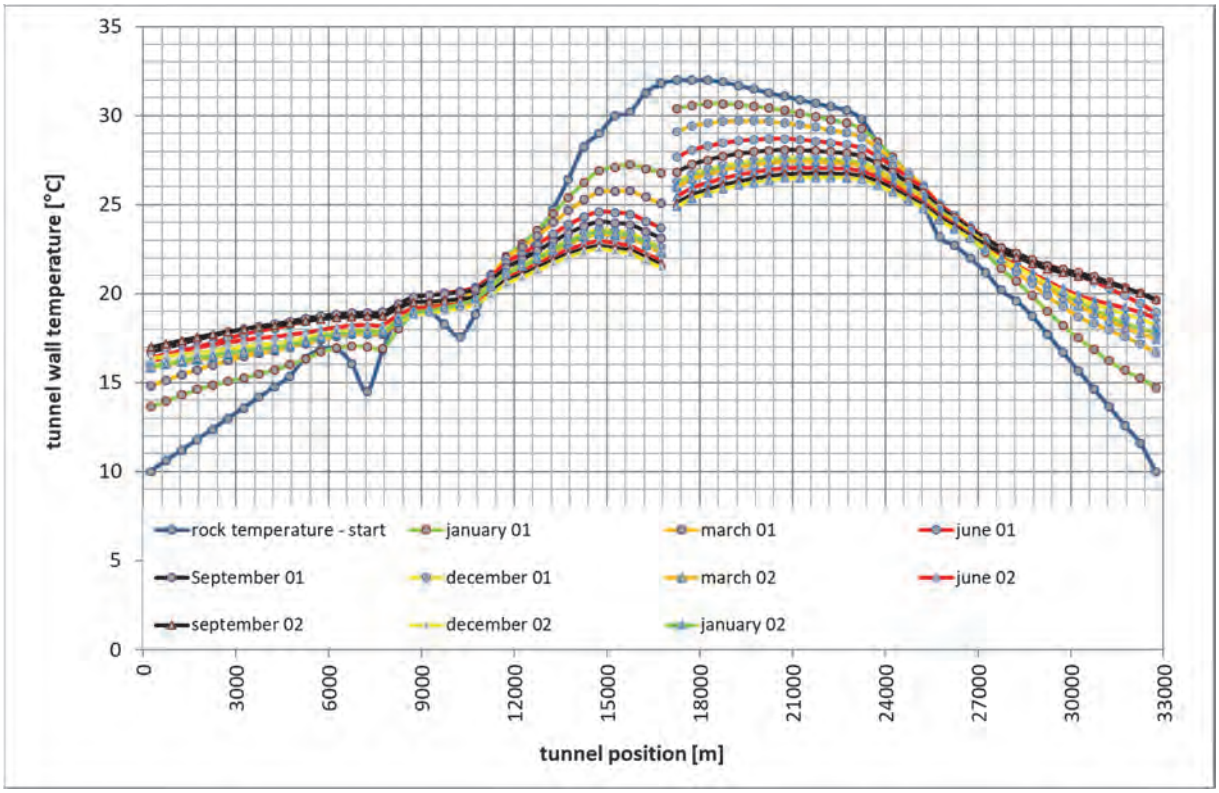

Figure 3-4: KAT - tunnel wall temperature curves for the north-tube at representative times during implementation/equipment phase (01 – 1st year, 02 – 2nd year)

3.3.2. Thermal conditions – railway operation phase

For the simulations during the operation phase the two tubes were assumed to be separate in terms of heat transfer. The rock temperatures from the results gained for the end of the construction phase were used as the starting condition.

Two scenarios were simulated. The first concerned a low traffic volume with two trains (1 passenger and 1 freight train) per hour in a driving regime corresponding to Table 3-1. The second scenario involved high traffic with 6 trains (1 passenger and 5 freight trains) per hour in the same driving regime. For simplification, the heat release of technical equipment in the cross-passages was considered to be linear over each 500m grid cell.

Table 3-1: Main driving direction of the trains as a function of the days of a week (current assumption)

Tube	1. day	2. day	3. day	4. day	5. day	6. day	7. day
South	west	east	east	east	west	east	east
North	east	west	west	west	east	west	west

In order to take rising ambient air temperatures over the next few decades into account (i.e. climate change), results from a local meteorological expert assessment were used [10]. A scenario concerning business as usual (no/little GHG reduction) was taken as a point of reference.

Table 3-2: Shows the current values (no. 1) and expected values (no.2) of the monthly average temperatures at the east portal of the Koralmtunnel. The delta value (no. 3) was added as a constant value (per month) to the outside temperature curve (hourly average) from Figure 2-1

No.	Years	January	February	March	April	May	June	July	August	September	October	November	December
1	T [°C] 1971-2000	-3.12	-0.52	4.18	8.48	13.78	16.88	18.58	18.08	13.68	8.38	2.28	-1.82
2	T [°C] 2021-2050 expected value	-0.62	1.87	6.46	10.66	15.91	18.97	20.63	20.19	15.85	10.62	4.60	0.59
3	T [°C] Delta 1-2	2.50	2,39	2.28	2.18	2.13	2.09	2.05	2.11	2.17	2.24	2.32	2.41

When calculating humidity, the influence of water brought into the tunnel by the train (rain, snow), as well as that of seepage, was neglected, as the quantification of the amounts remains rather uncertain, and also because evaporation would in any case lead to lower air temperatures.

By way of example, the calculated temperature profile in both tubes at the location of cross-passage 10 is shown in Figure 3-5. This cross-passage is located some 5 km from the east portal and 28 km from the west portal. Hence, the north tube experiences the influence of ambient temperature much more as the train traffic in this tube is mostly east to west (see Table 3-1).

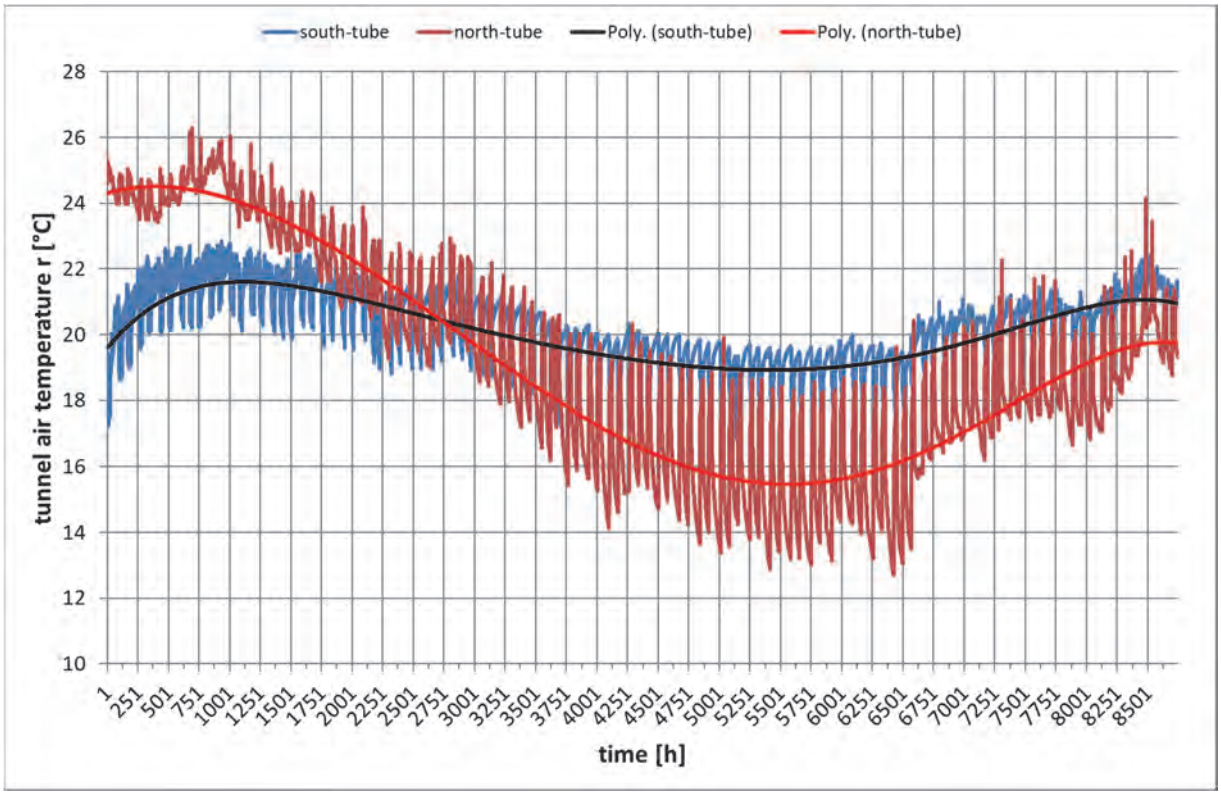

Figure 3-5: Tunnel air temperature curve at cross-passage 10 - south and north tube, January - December of the first year of operation

The main goal of the in-tunnel climate simulations, was the identification of tunnel regions where the cooling of the utility rooms can be achieved by simple mechanical ventilation and of regions where air conditioning is required. The most stringent conditions concerning the air temperature result from the telecommunication units. According to the technical requirements air temperature must not exceed 22°C in this room. In order not to exceed this value, tunnel-air temperature needs to be lower by some 2°C at minimum (i.e. <20°C) –depending on the thermal loads from the installed equipment. The simulation analysis was performed for all cross-passages in the tunnel.

As an example, the results achieved for the cross-passages QS01, QS05, QS10 and QS20 (location see Table 3-3) are shown in Figure 3-6 for the first year of operation, considering the low traffic scenario as worst case. The calculated temperature fields were further categorized into slabs of 1°C.

Table 3-3: Cross-passages and their distance from portals

	Distance from east portal	Distance from east portal
Cross-passage	[km]	[km]
QS01	0.5	32.5
QS05	2.5	30.5
QS10	5.0	28.0
QS20	10.0	23.0

Air temperature at cross-passage 1 (QS01) is strongly influenced by outside conditions. This results in a wide range of temperatures (hours per year in the corresponding temperature interval). At cross-passage 5 (QS05) the temperature range is nearly the same, but the number of hours with an air temperature lower than 11°C is strongly reduced. The further the cross-passage is inside the tunnel, the smaller is the frequency of low temperature events (see the histogram part of Figure 3-6).

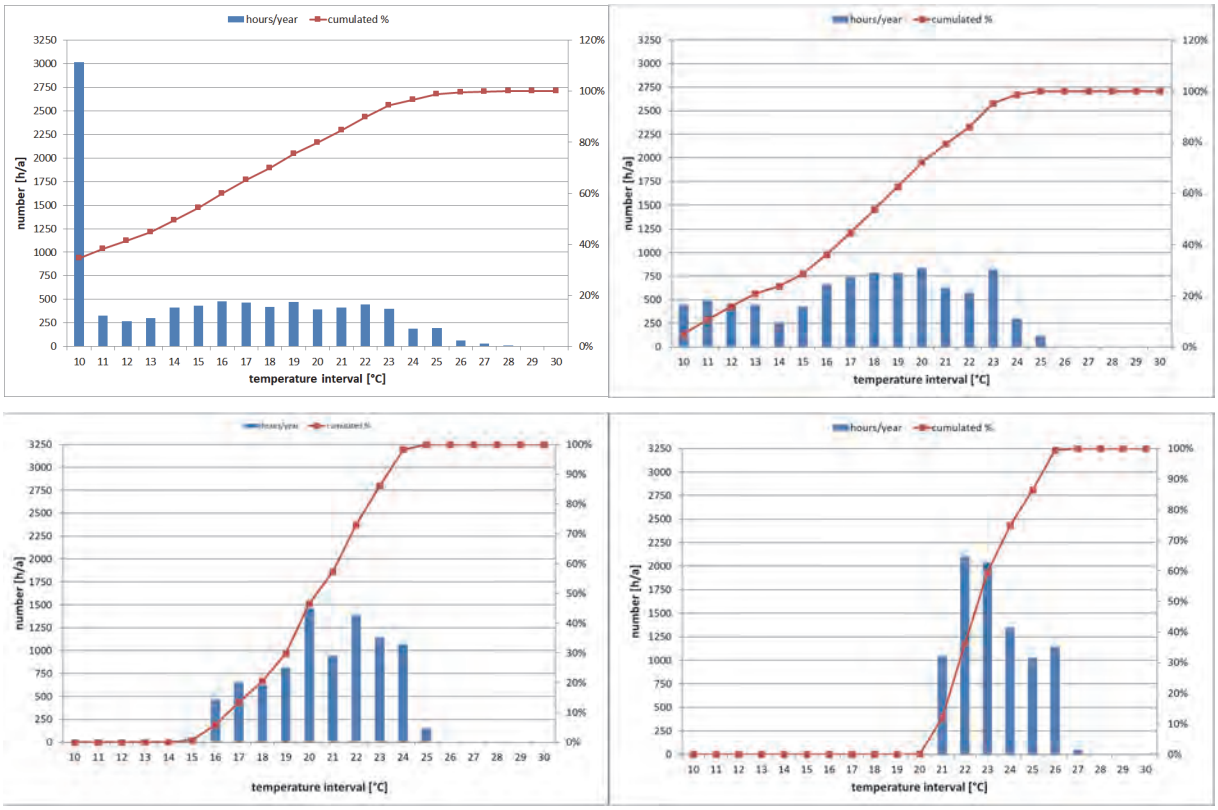

Figure 3-6: Histogram of air temperatures in telecommunication room, low traffic scenario, first year of operation (top left/QS01, top right/QS05, bottom left/QS10 and bottom right/QS20)

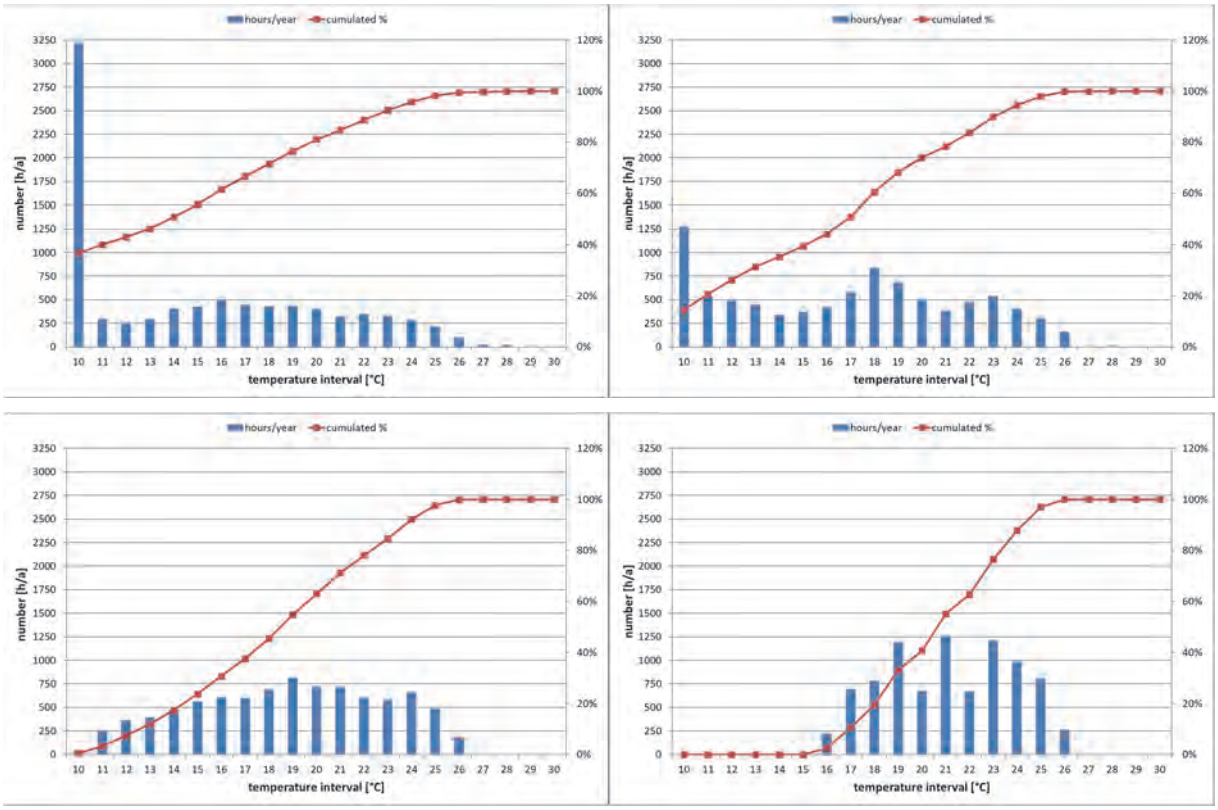

Figure 3-7 shows the results for the simulations based on the high traffic scenario for the first year of operation. Owing to the increased traffic volume and the increased air-flow from the piston effect, the influence of the outside air is more pronounced.

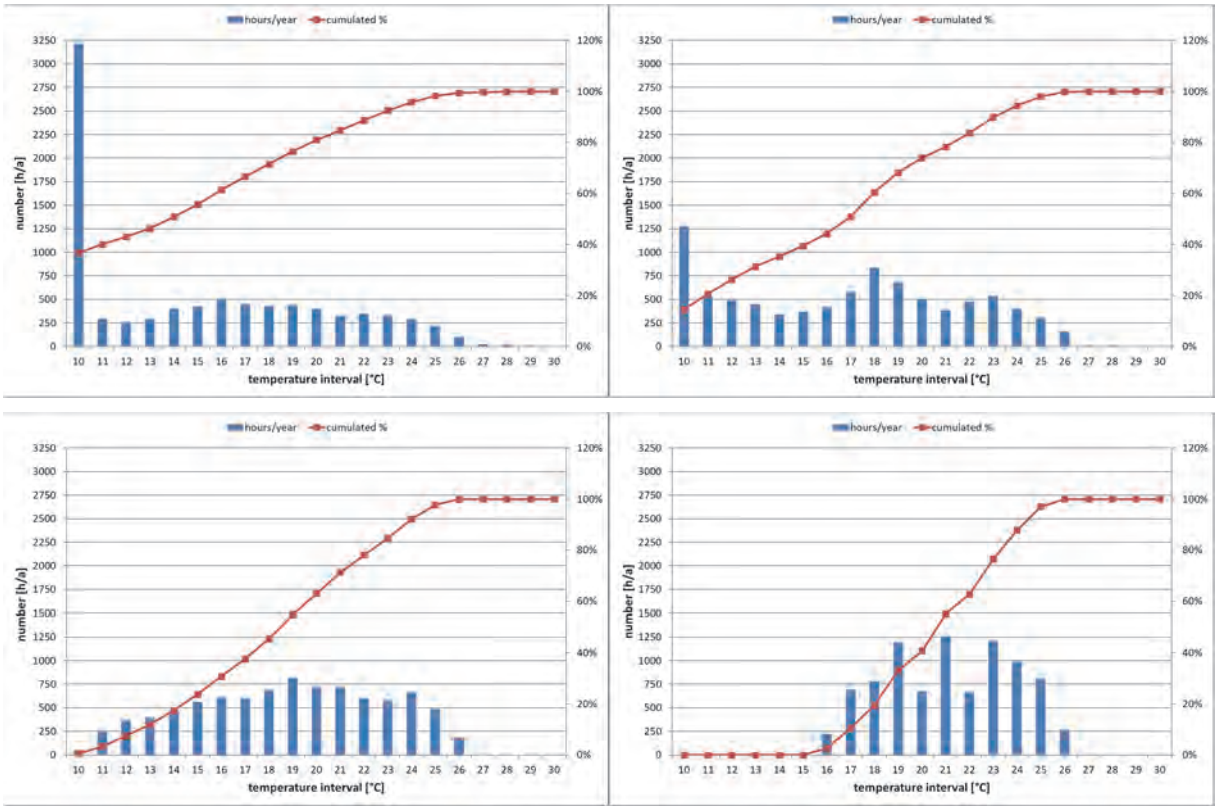

Figure 3-7: Histogram of air temperatures in telecommunication room - high traffic scenario, first year of operation (top left/ QS01, top right/QS05, bottom left/ QS10 and bottom right/ QS20)

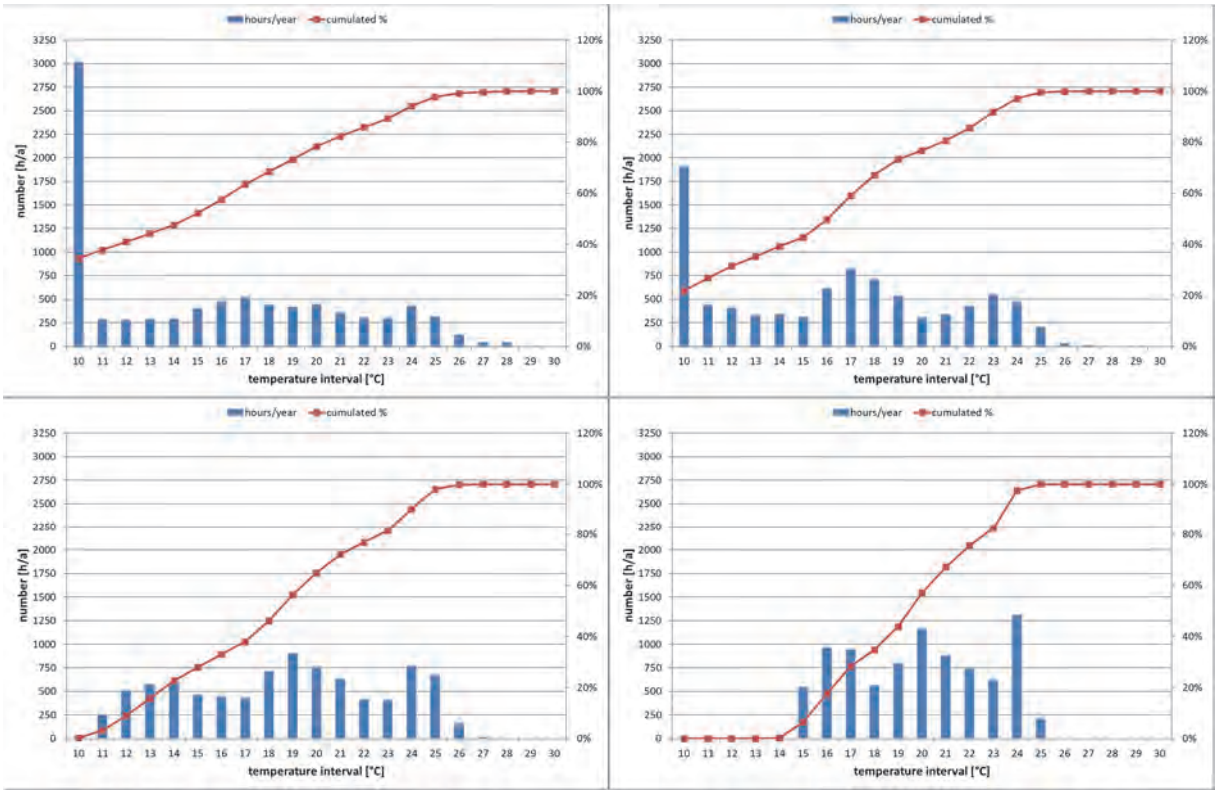

Figure 3-8: Histogram of air temperatures in telecommunication room, high traffic scenario, second year of operation (top left: QS01, top right: QS05, bottom left: QS10, bottom right: QS20)

Since the trains lead to a change of tunnel air conditions, it is expected that tunnel climate will also change in the following years of operation. To get an idea of the extent of this change, a further simulation for operation year two was also carried out. Figure 3-8 shows the results of this simulation for the high traffic scenario and selected cross-passages.

Figure 3-9 contains a direct comparison of the results for almost all cross-passages between operation year 1 and 2. The diagram shows number of hours per year where the 22°C criterion for the telecommunication rooms is violated. Remark: The cross-passages in tunnel center (cross-passage 28 - 41) are neglected, as the wall/rock temperatures are already above this limit. Within the first half of the tunnel (15 km) in most regions the number of hours of exceedance decreases. This is not true for some cross-passages near the portal due to an assumed increase of outside temperature for these years. Interestingly the number of exceedances decreases rapidly for the cross passages 13 to 27. In the second half of the tunnel – from QS 44 onwards – the changes are minor, due to the assumed driving regime in the tunnel and the specific location of the telecommunication room within the cross passage.

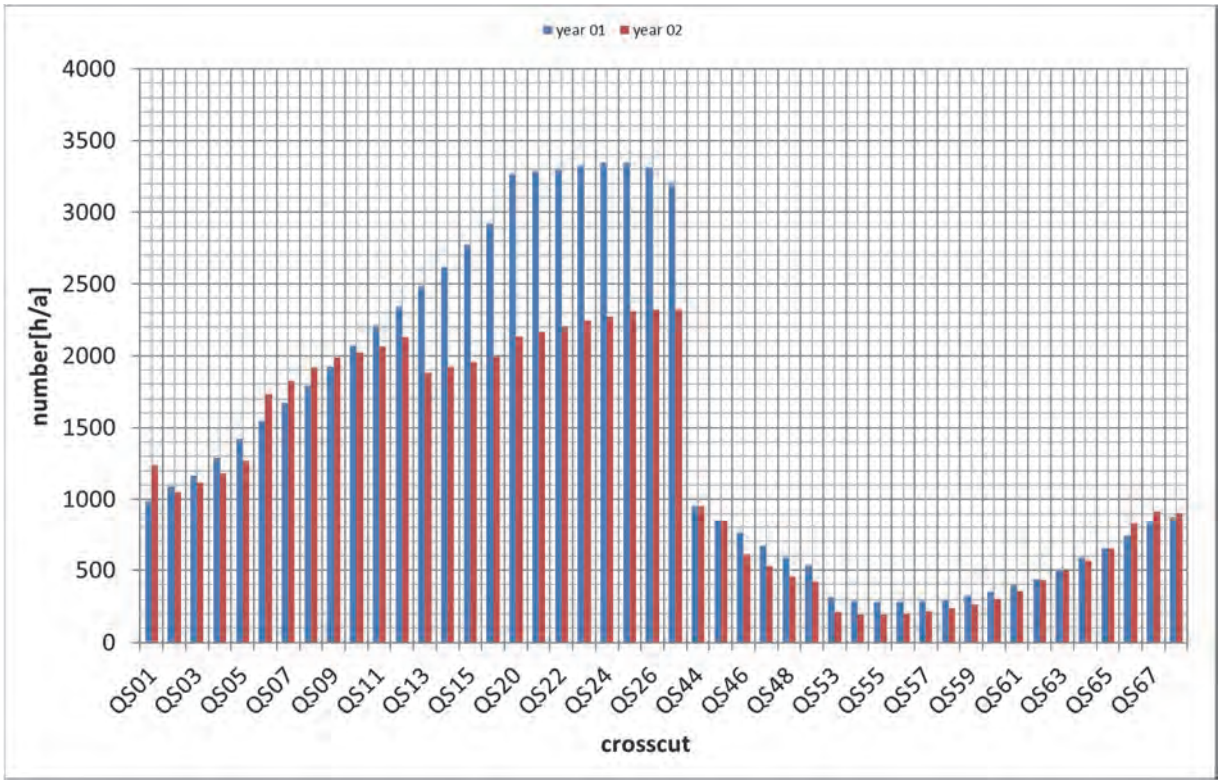

Figure 3-9: Comparison of temperature criterion (<22°C) violation in telecommunication rooms in operation year 1 and 2

4. SUMMARY AND CONCLUSIONS

The aim of this study was to forecast the thermal conditions in the Koralmtunnel during the implementation/equipment and the operation phase. Tunnel climate requirements differ between these two phases. While in the former phase workplace conditions dominate, the latter phase is characterized by the need to maintain a specific temperature level in the utility rooms for telecommunication and tunnel operation.

While the rock temperature is mainly responsible for the general level of tunnel air temperature, the heat released as a result of concreting (hydration) and from the machines used, defines the actual value for local tunnel air temperature. The simulations show that in order to maintain the required workplace conditions the temperature criterion can only be met by employing a sophisticated cooling system, including air coolers. Owing to the continuous change in the location of excess heat generation, and the required flexibility in power supply, the air-cooler is integrated into the supply trains. At a later stage, as soon as the main concreting work is finished, the ventilation and cooling systems will be fixed at specific locations inside the tunnel.

In order to meet the temperature requirements in the utility rooms during operation, air-cooling is required in most of the cross-passages within the tunnel. For reasons of cost efficiency and maintenance, simple mechanical ventilation systems are preferred. However, due to the fact that very high rock temperatures prevail over long distances within the tunnel, and due to the very stringent temperature criterion established for the telecommunication room, air conditioning is required at many cross passages. The simulation tool was employed in defining which cooling system is appropriate for the various cross passages. It turned out that the operation regime, i.e. which and how many trains are running inside the tunnel, together with rock temperatures and ambient air temperature, are the most decisive parameters. The more traffic there is in the tunnel, the more pronounced is the influence of ambient temperatures. On the other hand, the longer the tunnel is in operation, the more the wall temperature will decrease.

In the end, it turned out that in regions close to the portals (high influence of ambient temperatures) as well as in those with high rock temperatures air cooling systems are required, while in the remaining regions a simple mechanical ventilation system is sufficient.

5. REFERENCES

[1] ÖBB-Infrastruktur AG; The Koralm Railway, A part of the new Southern Railway Line; 2012

[2] Daniel Suter, Christoph Rudin, Peter Luginbühl; Erfahrung und Erkenntnisse aus der Instandhaltung und der Störungsbewältigung aus fast zehn Jahren Betrieb des Lötschberg-Basistunnels; STUVA-Tagung 2015, Dortmund; Forschung + Praxis 49; S. 335

[3] bmvit; The Baltic Adriatic Axis, Element of the future European TEN-T Core Network; 2010

[4] ÖBB-Infrastruktur AG; Durchbruch in die Zukunft - Der Koralmtunnel; 2012

[5] Michael Bacher, Peter Sturm, Daniel Fruhwirt, Johannes Rodler, Helmut Steiner, Johannes Sampl; Ventilation and Safety Concept of the Emergency Stop Station and the Cross Passages of the 33 km long Koralm Rail Tunnel; ISAVFT Lyon, France; S. 335

[6] Helmut Steiner, Peter Sturm, Michael Bacher, Daniel Fruhwirt; Kühlung von technischen Räumen in Eisenbahntunnel zur Erhöhung der Standzeiten und Minimierung der Wartung: Möglichkeiten der Optimierung am Beispiel Koralmtunnel; STUVA-Tagung 2017, Stuttgart; Forschung + Praxis 49; Forschung + Praxis 49; S. 335

[7] SUVA Pro; Arbeitsmedizinische Prophylaxe bei Arbeiten im Untertagebau im feucht-warmen Klima; Schweizerische Unfallversicherung Luzern CH; 2003

[8] Amt der Steiermärkischen Landesregierung; meteorological data for the Koralm region, http://www.umwelt.steiermark.at/cms/ziel/2060750/DE/, accessed 10/12/2017

[9] SIA 196; Baulüftung im Untertagebau; SIA Zürich CH; 1998

[10] ZAMG; temperature rise due to climate change; Zentralanstalt für Meteorologie und geodynamic, Austria, internal document 2017/GR/002543, 08/11/2017

[11] IDA-Tunnel; Version 4.5 build 1; EQUA Simulation AB

A VALIDATION OF THE FIRE DYNAMICS SIMULATOR FOR SMOKE DISPERSION FROM METRO STATIONS

[1]Conor Fleming, [2]Norman Rhodes
[1]SNC-Lavalin, Vancouver, Canada
[2]Independent consultant, Washington DC, USA

ABSTRACT

In the event of a fire in a metro system, exhausted smoke should be prevented from recirculating into the underground space or entering neighbouring buildings. This can be achieved through judicious positioning of smoke exhaust vents and air intakes, and the design performance can be verified through numerical modelling.

The modelling method should capture the underlying flow physics at the relevant length and time scales, so that smoke transport can be predicted to a practical degree of accuracy. In the context of metro station smoke recirculation, the region of interest encompasses local air intakes and is likely limited to one or two street canyons. The flow field at this scale is highly unsteady, comprising freestream turbulence associated with the atmospheric boundary layer as well as eddies generated by vortex-shedding from buildings.

Fire Dynamics Simulator (FDS) is expected to be a suitable modelling tool due to its large-eddy simulation formulation. The dominant eddies at building scales are simulated directly, and a simple turbulence model is applied to capture the effect of the smallest eddies. FDS has been comprehensively validated for buoyancy-driven flow and mass transport problems, and is widely used in the design and analysis of tunnel ventilation systems. In this study we use FDS version 6.5.3 to predict the flow around rectangular buildings at model scale and show that it compares favourably with experimental results and more established numerical tools (e.g. commercial RANS and LES software packages).

Keywords: Fire Dynamics Simulator, urban dispersion, metro station smoke dispersion

1. INTRODUCTION

The work described in this paper was prompted by a requirement in the design of Toronto's Eglinton Crosstown Light Rail Transit (ECLRT) line to check that smoke emitted from ventilation shafts in the event of a fire does not recirculate to an extent that compromises station entrances.

The ECLRT line will carry passengers along Eglinton Avenue from Weston Road in the west to the Kennedy TTC subway station in the east. The new rapid transit line will include a 10-kilometre underground portion between Keele Street and Laird Drive, running on dedicated right-of-way transit lanes that will be separated from regular traffic for the rest of the route to ensure reliable, fast travel times for customers.

Figure 1: The Eglinton Crosstown LRT route

There are fifteen underground stations including three interchange stations at Cedarvale Station, Eglinton Station and Kennedy Station and two terminal stations at Mount Dennis Station and Kennedy Station. The above-ground section runs between Laird Drive and Kennedy Station, there are 10 LRT at-grade stops and three underground stations in this section.

In the design of tunnel ventilation systems the emission of exhaust gases from the system into the atmosphere is always an important design consideration. In road tunnels, for example, limitations on the concentration of exhaust gases around portals and exhaust shafts can significantly increase the design requirements, such as discharging at high level to achieve sufficient dilution of emissions into the atmosphere before reaching ground level, and some jurisdictions require a net inward flow at portals. In subway systems the general principle is to exhaust smoke through vent shafts and draw outside air into the station through entrances, providing an unobstructed egress route for patrons. Thus, it is necessary to check that smoke is not present in high concentrations at the entrances.

In the present study the requirement for low concentrations of smoke at station entrances and HVAC intakes has been demonstrated using CFD simulations. Such studies have often been done using wind tunnels to resolve atmospheric dispersion problems and to establish guidelines for particular situations. More recently, numerical methods have also been used. To the authors' knowledge, the first example of the first use of CFD methods for this purpose was the Heathrow Express rail link to London – wind tunnel experiments were carried out for one design situation and this data was compared with a CFD solution using a Reynolds Average Navier-Stokes (RANS) method and found to give good agreement. It was noted however, that some care had to be given to ensure that the atmospheric turbulence was correctly prescribed. Having established this validation of the method, subsequent station designs, and the performance of the ventilation systems with respect to potential re-entrainment of exhaust, were carried out using CFD.

The ECLRT design work utilized the Fire Dynamics Simulator (FDS) code to simulate the atmospheric dispersion of smoke for each underground station, taking into account station vents, local buildings, entrances and HVAC inlets. To verify the approach and develop a methodology for the setting of physical boundary conditions, experimental cases for wind flow over buildings were simulated with FDS and also with the more established RANS simulation method for comparison. This paper summarizes the verification studies.

2. METHODS

The simplest dispersion predictions employ Gaussian plume methods. They are widely used and highly developed for specific applications, but are generally more applicable to large scale problems. The unsteady, three-dimensional nature of flow in the near field of buildings is not compatible with these methods, and so the more sophisticated (and more expensive) CFD approach is adopted.

Two different CFD codes have been used in this study, one using a RANS method with a k-ε turbulence model and the other using FDS with its large-eddy simulation (LES) turbulence model. The RANS method may have the advantage of economy since a steady-state solution can be obtained. However, unsteady periodic fluctuations can occur around obstacles and this may invalidate the steady state assumption. LES is inherently unsteady, and should be capable of predicting such fluctuations as long as the dominant eddy scales are resolved adequately.

The boundary conditions for a RANS simulation are fairly straightforward to implement. Vertical profiles of velocity, turbulence kinetic energy and dissipation rate can be prescribed at the inlet boundary. In an LES simulation, the process is more complex.

A fundamental challenge in LES modelling is the prescription of an unsteady, turbulent velocity profile at the upstream boundary. The conventional method for channel flows is to generate and record a suitable inflow profile via a precursor simulation which is periodic in the streamwise direction. To avoid the computational effort associated with the precursor simulation, Jarrin (2008) developed a synthetic eddy method, where eddies are generated during the simulation by flow perturbations near the inflow boundary and convected into the domain. In this model, available in FDS, the magnitudes and frequencies of these perturbations are set automatically to reflect the user-defined turbulence length scale, l, eddy density (or 'number of eddies'), N, and root-mean-square of velocity fluctuations, u_{RMS}.

Ideally, the dominant turbulence length scale could be determined from high-frequency velocity measurements. In the absence of such data, we have chosen the building height as the input eddy length scale so that freestream turbulence has a similar length scale to building-generated turbulence.

Jarrin (2008) derives a formula for estimating the eddy density, $N = V_{\mathrm{B}}/l^3$, where V_B is the volume of a three-dimensional, virtual 'box' enveloping the inlet boundary, within which the eddies are generated. The volume of this box is $V_{\mathrm{B}} = (w + 2l)(h + 2l)(2l)$, where w and h are the width and height of the inlet boundary respectively.

The RMS velocity can be calculated from turbulence intensity, I, as $u_{\mathrm{RMS}} = \bar{u}I$, where $\bar{u}$ is the time-averaged velocity, or from turbulence kinetic energy, k, as $u_{\mathrm{RMS}} = \sqrt{2k/3}$.

Note that FDS can only accommodate piecewise-constant profiles of turbulence parameters at the inlet.

3. VALIDATION CASES

Two cases have been studied to assess FDS and the more common RANS approach to dispersion simulation, and to establish a correct methodology for this type of problem. Both cases consider the flow over rectangular buildings at small scale. The first is a single building, taken from the Architectural Institute of Japan Guidebook for Practical Applications of CFD to Pedestrian Wind Environment around Buildings (AIJ, 2016; see also Tominaga et al, 2008). Figure 2 shows the geometry and the location of measurements of velocity and turbulence.

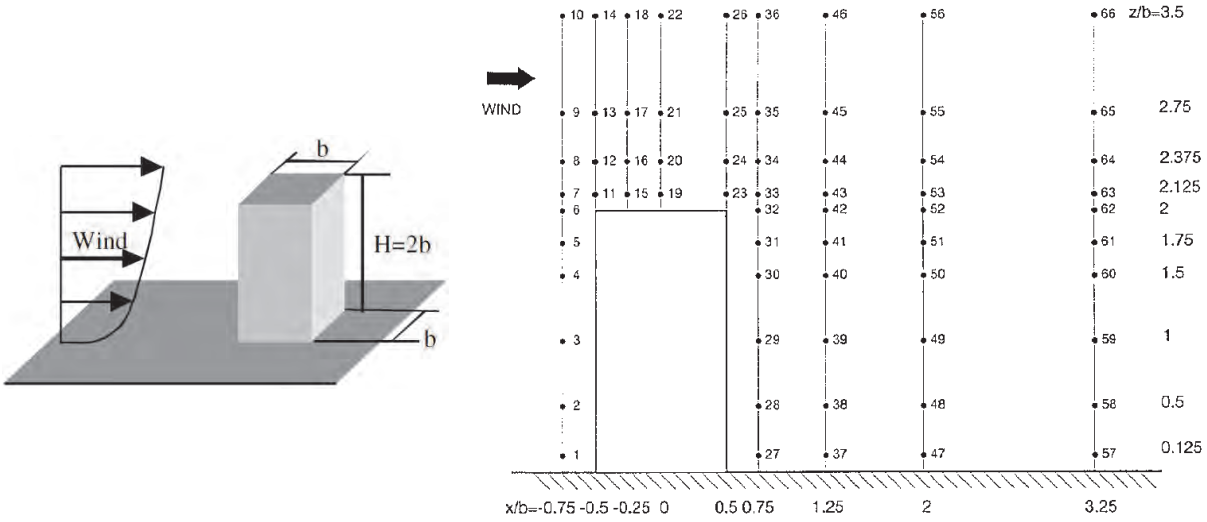

(a) (b)

Figure 2: Illustrations of (a) geometry and (b) measurement locations in the vertical mid-plane for case 1: flow past an isolated building (AIJ, 2016).

In the second case, Chang & Meroney (2003; see also Chang, 2006) considered arrays of up to twelve buildings as shown in Figure 2. In these experiments, several ratios of building height, *H,* to spacing, *B,* were considered, as well as the number of upstream building rows, *N*. A tracer gas (ethane) was introduced from a point source in the centre of the array and species concentration measurements were made along the lines shown in Figure 3. The present paper considers the case $B/H = 1$ and $N = 1$. It should be noted that the inlet boundary conditions for this case were not well defined by Chang & Meroney.

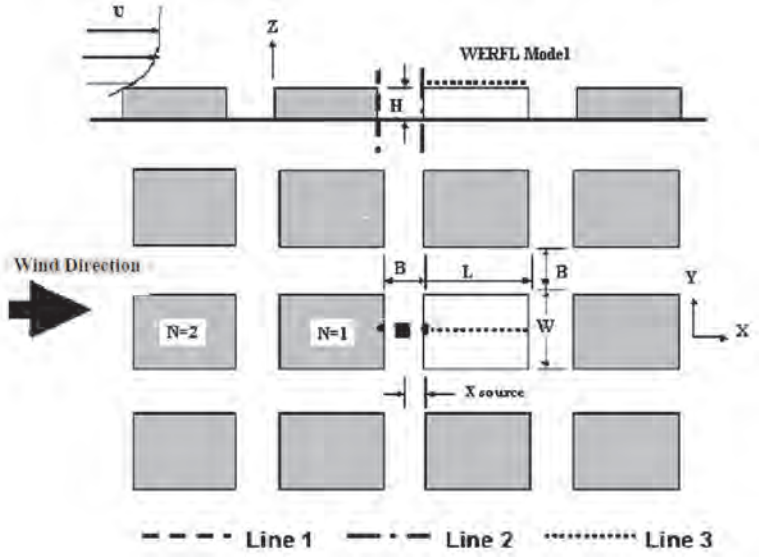

Figure 3: Illustration of geometry and measurement locations for case 2: dispersion in a street canyon (Chang, 2003). Note that the $N = 1$ case is simulated here, i.e. only a single row of buildings upstream of the source.

The geometry for both problems reflects the wind tunnel dimensions of the experiments. In both cases orthogonal grids were used and the general computational setup is similar to Gousseau et al (2013) for Case 1 and Chang & Meroney (2003) and Chang (2006) for Case 2. Velocity and approximate turbulence profiles were prescribed at the inlet boundary (the left side in Figures 2 and 3) and appropriate wall and pressure boundaries were prescribed on the other faces of the solution domain. The FDS model for Case 1 featured a uniform grid (rather

than stretched) of cubic elements with edge length $\Delta x = H/20$ in the near field, and a near-field element edge length of $\Delta x = H/16$ for Case 2. The FDS timestep was adjusted automatically to maintain a maximum Courant number of $C = ut/\Delta x_{\min} < 0.9$, where t is time.

Typical results for Case 1 are shown in Figures 4 (a) and (b) which present normalized velocity and turbulence kinetic energy profiles respectively. Three sets of results are presented, FDS and RANS simulations carried out by the authors, and for turbulence, an additional LES prediction from Gousseau et al (2013) is included. These results are for profiles on the vertical mid-plane of the building, $y/b = 0$, at the downstream location $x/b = 1.25$, where b is the building dimension in the streamwise direction and x is measured from the centre of the building.

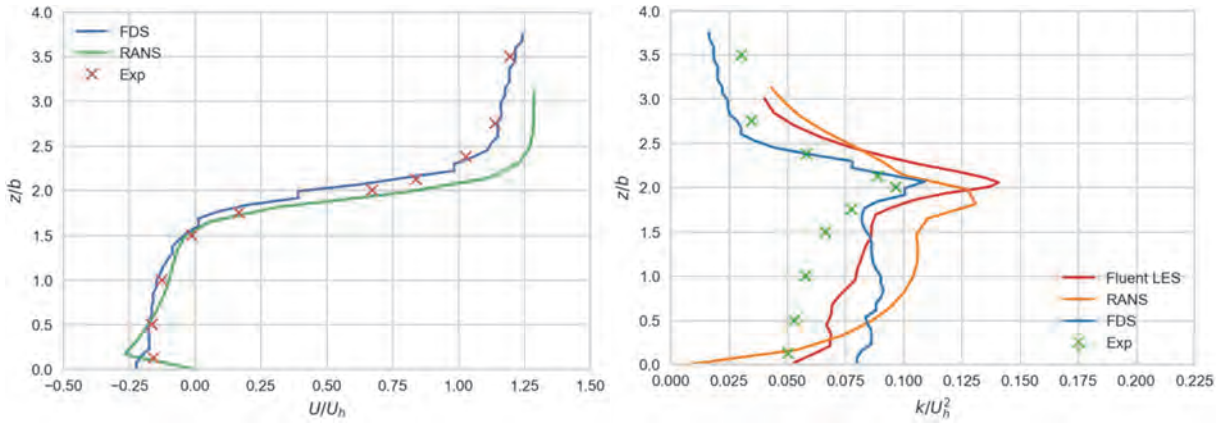

(a) (b)

Figure 4: Normalized profiles of (a) velocity and (b) turbulence kinetic energy along a vertical line at $y/b = 0$ and $x/b = 1.25$.

It can be seen that the velocity profile at this position is well predicted by both CFD codes. All the codes somewhat over predict the turbulence kinetic energy, both the peak, which occurs at the building height ($z/b = 2$) and in the wake of the building below $z/b = 2$. In practice this over-prediction might result in greater dispersion of a scalar quantity, yielding slightly lower values of peak concentration, suggesting that the prediction of ground-level concentration might be non-conservative. Rigorous grid studies have not been carried out by the authors and so it is possible that these results might be improved by finer resolution. However, Gousseau et al reported deterioration in their LES prediction with finer grids – a rather alarming conclusion which is discussed by the authors.

The second test case proved to be more challenging, as the boundary conditions were not adequately defined – although profiles of velocity, kinetic energy and dissipation were given, the normalising velocity was not. Had the experiment been independent of Reynolds number, this would not have been important, but studies showed a strong sensitivity to the velocity magnitude.

The RANS simulations that were carried out in a steady-state mode gave results that were of the correct order, but were greatly influenced by the inlet turbulence properties. It was felt that the flow in the experiment was probably unsteady, and further work is required to elaborate this potential effect.

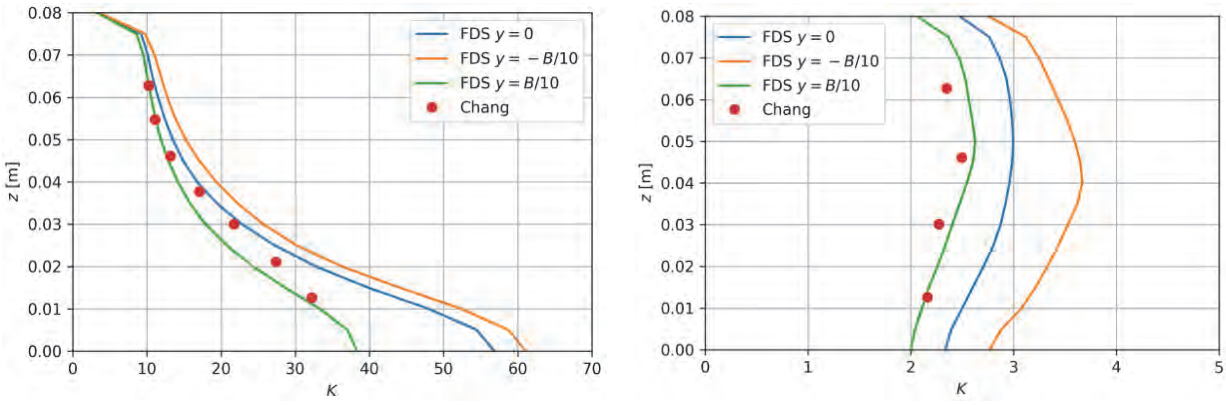

(a) (b)

Figure 5: Vertical profiles of normalized concentration along (a) Line 1 and (b) Line 2.

The unsteady FDS simulations gave more acceptable results over a range of Reynolds numbers. Vertical time-averaged distributions of normalized tracer concentration K are presented in Figures 5 (a) and (b), where $K = \rho u_{\mathrm{ref}} H^2/Q$, ρ is concentration, $Q = 8.45 \times 10^{-6}$ m^3/s is the flow rate of the tracer gas source and the averaging period is 8 seconds. The reference velocity at building height, $u_{\mathrm{ref}} = 10.6$ m/s, was inferred from related experiments in the same facility (Chang & Meroney, 2001; Ham & Bienkiewicz, 1998). Line 1 is on the face of the building upstream of the vent and Line 2 on the building downstream of the vent. A circulation of the flow in the cavity between the buildings causes the tracer gas to be convected toward the upstream building. Hence, the concentrations are noticeably higher at the base of the building and decrease with height (figure 5a). The concentrations on the face of the downstream building (figure 5b) are an order of magnitude smaller. In Figure 5 (a), the concentration at the centreline ($y = 0$) matches the data quite well. The concentrations on either side ($y = \pm b/10$) show an asymmetry which is consistent with unsteadiness in the flow. A similar conclusion is drawn from Figure 5 (b).

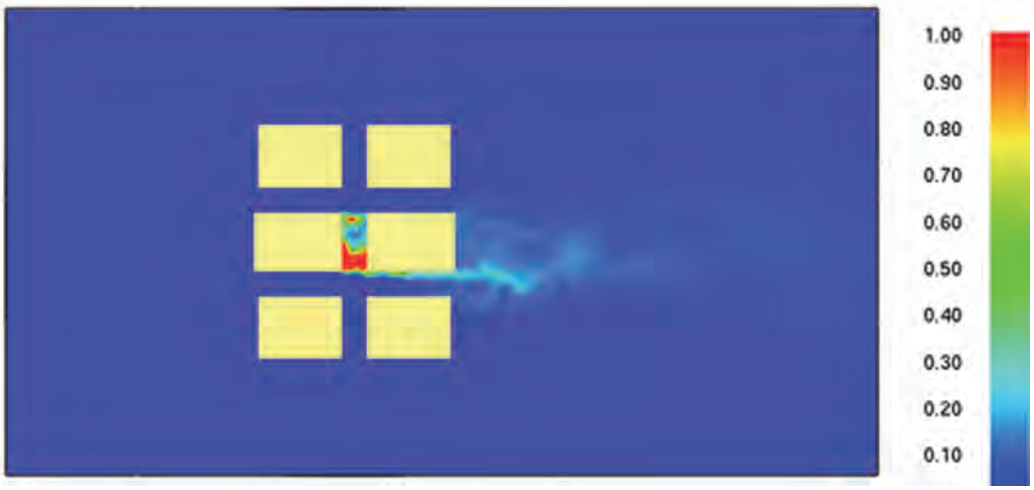

Figure 6: Instantaneous contours of tracer concentration at the horizontal mid-plane of the building array, $z = H/2$, with red contours indicating concentrations of $\rho > 10^{-3}$ kg/m^3. Note flow is from left to right and the second downstream row of buildings has not been modelled as it is expected to have little influence on near-field dispersion.

Observations of the flow field at various points in time reveal that the concentration plume tends to be biased towards one end of the street canyon, and only switches end occasionally. Figure 6 is an instantaneous contour plot of tracer concentration where the plume is biased in the negative y direction. It is interesting to note that the experiments did not indicate this

effect, and it was likely to have been averaged out by the tracer gas measuring instrumentation.

The study shows that FDS can be used to predict scalar concentrations with reasonable accuracy. Sufficient averaging time would need to be simulated to provide a complete picture since the plume clearly shows a movement from side to side and in different building arrangements this may cause excessive swings in predicted concentration. Too short an averaging time may lead to incorrect conclusions.

The RANS simulations, in a steady state mode, may not capture the intermittency of turbulence in the canyon. Further study is required using LES and unsteady RANS simulations to develop a further understanding of this effect.

4. SUMMARY

FDS shows good potential for studying the impact of smoke from metro fires, and the validation studies carried out against experiment give confidence in the full-scale predictions as well as pointers to an appropriate methodology for prescribing boundary conditions and for the critical assessment of the resulting predictions. The level of validation for the RANS simulations, although as yet incomplete, have also indicated limitations of steady state methods in this context.

The current study has focused on orthogonal flow, whereas it is generally necessary to also consider non-orthogonal winds in design simulations. In future work we intend to examine an atmospheric wind model based on Monin-Obukhov similarity theory which has recently been introduced to FDS (McGrattan et al, 2017).

5. REFERENCES

Architectural Institute of Japan (2016) AIJ benchmarks for validation of CFD simulations applied to pedestrian wind environment around buildings. ISBN978-4-8189-5001-6, AIJ, Tokyo. URL: https://www.aij.or.jp/jpn/publish/cfdguide/index_e.htm

Chang, C.H. Meroney, R.N. (2001) Numerical and physical modeling of bluff body flow and dispersion in urban street canyons. *J. Wind Eng. Ind. Aerodyn., 89*, *1325-1334*

Chang, C.H. Meroney, R.N. (2003) Concentration and Flow distributions in urban street canyons: wind tunnel and computational data. *J. Wind Eng. Ind. Aerodyn., 91*, *1141-1154*

Chang, C.H. (2006) Computational fluid dynamics simulation of concentration distributions from a point source in the urban street canyons. *J. Aerosp. Eng. 2006.19:80-86*

Gousseau, P., Blocken, B., van Heijst. G.J.F. (2013). Quality Assessment of Large-Eddy Simulation of Wind flow around a high rise building: Validation and Solution Verification. *Computers and Fluids 79 120-133*

Ham, H.J., Bienkiewicz, B. (1998) Wind tunnel simulation of TTU flow and building roof pressure. *J. Wind Eng. Ind. Aerodyn., 77&78*, *119-133*

Jarrin, N. (2008) Synthetic inflow boundary conditions for the numerical simulation of turbulence. *PhD thesis, University of Manchester*

McGrattan, K., McDermott, R., Hostikka, S., Floyd, J., Vanella, M., Weinschenk, C., Overhold, K. (2017) Fire Dynamics Simulator Technical Reference Guide, NIST Special Publication 1018-1, Sixth Edition. URL: https://pages.nist.gov/fds-smv/manuals.htm

Tominaga, Y., Mochidab, A., Yoshiec, R., Kataokad, H., Nozue, T., Yoshikawaf, M., Shirasawa, T. (2008) AIJ guidelines for practical applications of CFD to pedestrian wind environment around buildings. *J. Wind Eng. Ind. Aerodyn. 96 1749-1761*.

ON THE AERODYNAMICS OF WATER MIST FROM A VENTILATION DESIGNER'S PERSPECTIVE

I. Riess, M. Steck,
Amstein + Walthert Progress AG, Zurich, Switzerland

ABSTRACT

For a long time, the tunnel community discussed the application of water mist systems in road tunnels. In some European tunnels, water mist systems have been installed. In large-scale fire-tests, it has been demonstrated that water mist can inhibit the development of massive fires. However, there are only very few studies available on the interaction of a water mist system with other safety provisions in the tunnel, such as communication, egress and ventilation.

In a research project, we investigated the mutual influence of water mist and tunnel ventilation. Water mist has a significant impact on tunnel aero- and thermodynamics, e.g. on airflow resistance, flow rates, temperature distribution and smoke stratification as well as smoke propagation. From our research, we obtain a better understanding of the coordination required between water mist application and ventilation operation.

The following effects of the water mist on the ventilation are described in this article:

- Water droplets are accelerated by the airflow. An additional pressure resistance counteracts the longitudinal flow.
- The volume increase due to water evaporation is evaluated and compared to the volume reduction achieved by rapid cooling of hot fumes.
- Downstream of the fire, the tunnel air is saturated with water vapor. Further cooling leads to condensation.
- The pressure resistance of the fire is affected by water mist application.

The investigation is based on analytical modelling of the flow phenomena and on numerical modelling in FDS (Fire Dynamics Simulator). The numerical results are compared with the analytical models.

Keywords: tunnel ventilation design, emergency ventilation, water mist, flow resistance

1. INTRODUCTION

Fixed firefighting systems (FFFS) based on water mist injection are a hotly debated topic for a long time. Compared to sprinkler systems in buildings, the application of water mist in tunnels is less common. Currently, the technology is implemented in some European road tunnels to prevent large fires at an early stage. Previous studies on FFFS mainly focus on the efficacy in terms of fire extinction [7], [8], [9]. Some studies include cost-benefit analysis [6]. In national design codes such as the German RABT 2015 [3] or the Austrian RVS 09.02.51 [5], FFFS are mentioned without giving specific requirements on coordination with other safety equipment. Currently, the safety engineer cannot draw from established design practice. Especially, the interaction of the water mist system with other safety provisions in the tunnel such as communication, egress and ventilation is not yet adequately researched.

The present study focuses on the interaction of water mist application and longitudinal ventilation in road tunnels. Physical processes are analytically described based on aero- and thermodynamics. A quantification of the influencing factors for the ventilation design and operation is derived from the results. Numerical simulation CFD has been used in order to verify the analytical models.

2. ANALYTICAL STUDY

In the first part of the study, various physical phenomena of droplet dispersion, break-up and evaporation are analyzed separately. Figure 1 shows a selection of the physical phenomena. There is no fire considered in Figure 1. There is no fire depicted in Figure 1, as the focus of the study lies in the interaction of FFFS and tunnel ventilation

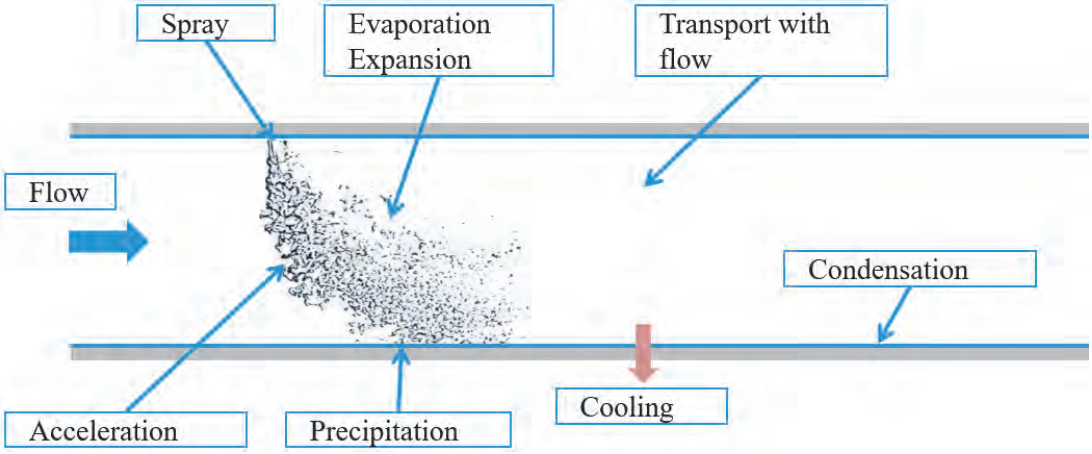

Figure 1: Physical phenomena observed in water mist application.

2.1. Pressure resistance due to water injection

Based on force equilibrium, the kinetics of a single water droplet are described. A typical droplet diameter of 0.5 mm is assumed, based on previous studies [7] and [10]. The droplet is assumed as solid sphere, vertically injected into the longitudinal airflow. The aerodynamic resistance of the droplet can be modelled similar to the steady state flow around the sphere with the resistance depending on the local Reynolds number. The lift of the droplet is neglected, as the density of water and air differ greatly. Consequently, the force equilibrium consists of three mathematical terms: inertia, flow resistance and gravity.

The movement of the droplet is then calculated by integrating the differential equation over time. Regardless the initial injection velocity, the droplet is quickly accelerated by the tunnel airflow. Its steady-state sink rate is achieved very early. The horizontal velocity reaches 99% of the airflow velocity before the droplet even reaches the lower half of the tunnel profile. Derived from this findings, it is a safe assumption, that the whole amount of injected water is accelerated to the longitudinal airflow velocity before the droplets reach the road surface.

The momentum of the accelerated water is lost, when the droplets fall out to the road surface. This causes a pressure drop, which can be calculated from the conservation of momentum. The pressure acting against the airflow direction Δp_w can be expressed as

$$\Delta p_w = -\frac{\dot{m}_w u_a}{A_T} \tag{1}$$

with the mass flow of injected water $\dot{m}_w$, airflow velocity u_a and tunnel cross section area A_T. The additional thrust of the jet fans required is computed by multiplication of (1) with A_T. For

an injection area of 750 m^2 with a water flow rate of 6 mm min^{-1} and a desired airflow velocity of 3 m s^{-1}, the thrust required to balance the pressure loss amounts to 225 N.

2.2. Impacts on volume

The evaporation of water droplets leads to a density decrease and a volume increase of the airflow. On the other hand, cooling of hot fumes increases the density and reduces the volume. In this section, these two counteracting effects are addressed.

The conversion of water to water vapor mainly takes place in the hot region close to the fire. Under the assumption of constant pressure and temperature for air and water vapor, both volume flows can be added up as a mixture of two ideal gases

$$\dot{V}(T) = \underbrace{\dot{V}_a(T_0) \cdot \frac{T}{T_0}}_{air} + \underbrace{\dot{V}_a(T_0) \cdot x \cdot \frac{m_{mol,a}}{m_{mol,v}} \cdot \frac{T}{T_0}}_{vapor} \quad (2)$$

with initial airflow temperature T_0, initial airflow volume $\dot{V}_a$, local temperature after fire T, absolute humidity x and molar masses m_{mol} of air and vapor.

A comparison of the airflow rates with and without FFFS is given in Table 1. The flow rates are calculated for a point 30 m downstream of the fire. For this location, the Austrian code RVS 09.02.51 [5] defines a maximum temperature to be achieved by FFFS operation. Apparently, the volumetric effect of cooling the hot fumes with FFFS outweighs the volume increase by evaporation.

Table 1: Comparison of downstream airflow rates with and without FFFS

	With FFFS	Without FFFS
Flowrate upstream of fire	150 m^3 s^{-1}	150 m^3 s^{-1}
Heat release rate	≤ 30 MW	30 MW
Temperature 30 m* downstream of fire	50 °C*	131 °C**
Rel. humidity 30 m downstream of fire	100%	n.a.***
Flowrate 30 m downstream of fire	195 m^3 s^{-1}	214 m^3 s^{-1}

* requirement RVS [5]
** calculated according to RVS [4]
*** not applicable for temperature >100 °C

If the initial airflow rate is reduced, without FFFS the temperature will increase, and with FFFS the absolute humidity will be reduced. Therefore, the volume flow just downstream of the fire is always smaller with FFFS than without.

Further downstream of the fire, the saturated air is continuously cooled down until the temperature equals the initial temperature. At this point, the total volume flow with FFFS differs only marginally from the flow without FFFS.

2.3. Evaporation and Condensation

The absorption of heat by water evaporation is limited due to saturation of humid air. For this reason, a large part of injected water remains in the area around the fire. The other part is in solution as vapor in humid air (saturated) and transported downstream.

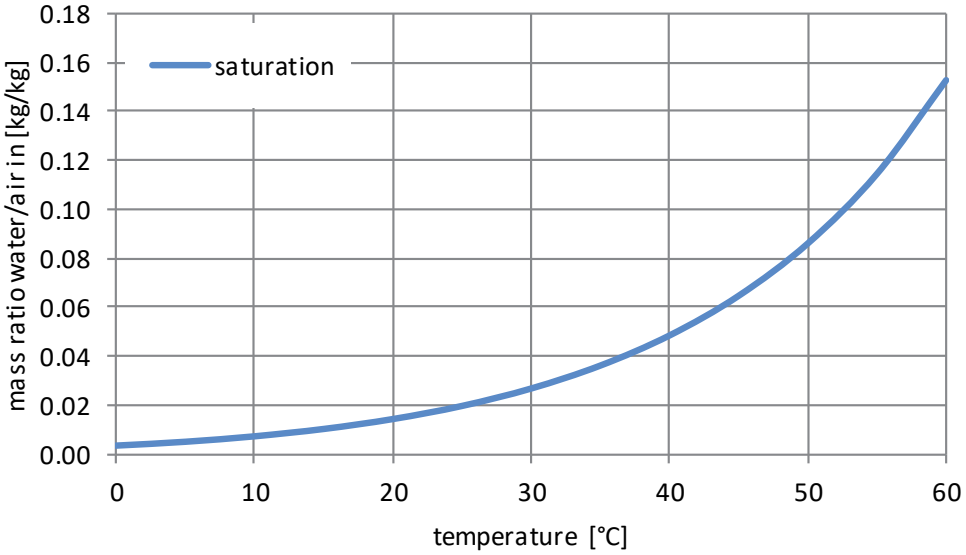

Figure 2: Maximum water content in saturated humid air.

In order to cool down the heat from the fire to 50 °C downstream 30 m from the fire, saturated humid air can carry 86.3 g water per kg dry air. Assuming an initial airflow rate of 150 m^3 s^{-1} or 180 kg s^{-1}, a maximum amount of water of 15.5 kg s^{-1} can be utilized for evaporation cooling. While this seems little compared to a typical water mist flow rate of 75 kg s^{-1} (6 mm min^{-1} on an area of 750 m^2), the heat absorbed through evaporation corresponds to a heat rate equivalent of 35 MW.

By reducing the longitudinal flow, the absorption capacity and thus the cooling effect by evaporation is reduced accordingly. Still, the water droplets support the cooling of the tunnel air, as the droplets absorb heat and transport the heat to the tunnel wall or to the road surface, where it is transferred to the concrete.

With increasing distance from the fire, the saturated air cools down and leads to condensation on the road surface and the tunnel wall. During this process, the evaporation enthalpy is released as heat into the concrete. The condensed water is absorbed by the tunnel drainage.

2.4. Throttling effect

The pressure drop due to a fire in tunnel or duct flow is known as *throttling effect,* because a fire acts like a local reduction of the tunnel cross section [11]. Although this effect is significant to the aerodynamics of tunnel fires, analytical or empirical models are scarce and provide little reliability. For the analytic calculation of the pressure drop (in [Pa]) due to the fire plume in a tunnel, an empirical relation was published by Dutrieue et al. [1]

$$\Delta p_{fire} = \frac{Q^{0.8} {u_a}^{1.5}}{{D_h}^{1.5}} C \qquad (3)$$

where the variables denote: Heat release rate Q in [MW], airflow velocity u_a in [m s^{-1}], hydraulic diameter D_h in [m] and the empirical constant $C \approx 41.5 \cdot 10^{-6}$. This approach is used for the analytical part of the present study. Obviously, there are not many tunnel or fire specific parameters contained in the relation, such as tunnel geometry, fire geometry, plume height, etc.

Numerical simulations by the authors indicate, that the pressure resistance of a fire depends on various parameters which are not included in equation (3). It should only be used as an approximation. Currently, a research project is prepared to investigate the throttling effect in more detail.

3. NUMERICAL MODELLING

Numerical calculations have been carried out applying the Fire Dynamics Simulator (FDS, V6.5.2). The FDS model for fire plume behavior, droplet dispersion and evaporation in turbulent flow is well validated against experimental results [2].

For this study, a 10 m wide and 5 m high tunnel section is modelled with a length of 350 m, whereof 200 m are decisive for the evaluation. The domain is subdivided into five isometric zones with different mesh sizes. In order to resolve the flow phenomena in the vicinity of the fire, a fine mesh of 0.125 m is chosen in this area to determine the wall friction and the local pressure drop from obstacles adequately. The airflow velocity at the tunnel entrance is set to 3 m/s. This is defined as a constant boundary condition. Tunnel walls and carriageway are modelled as solid concrete walls with a roughness of 3 mm.

A rectangular wood crib with an energy content of approx. 67'000 MJ represents the burning material. Instead of modelling single wood beams, the crib is assumed as continuum with reduced density. Its initial dimensions are 6.0 m x 3.0 m x 2.5 m (length x width x height). A complex pyrolysis model is applied with specified material and fuel data as well as natural combustion. Consequentially, the material of the fire source is consumed by the fire.

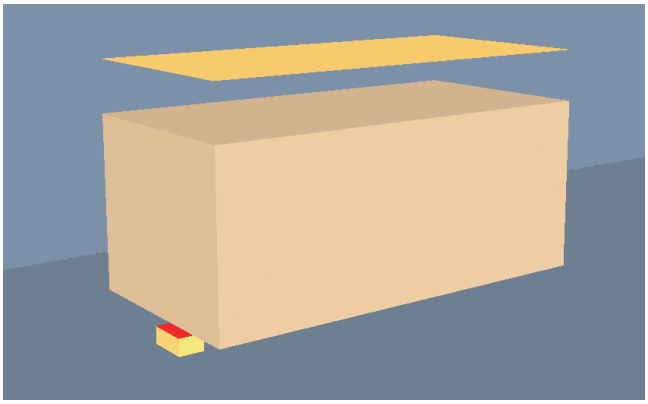

Figure 3: Covered wood crib model with burner for ignition.

The spray model consist of 24 nozzles whereof each nozzle releases 62.5 l min^{-1} water at an injection velocity of 10 m s^{-1} and an injection angle between 0° (vertical downward) and 70°.

In order to analyze the influence of different contributions to the total pressure loss, the following scenarios are simulated separately:

- Empty tunnel
- Tunnel with wood crib
- Tunnel with wood crib fire
- Tunnel with FFFS (no crib)
- Tunnel with wood crib fire + FFFS

In case of the empty tunnel, the arising pressure loss is only due to wall friction. This scenario represents the basis for all simulations. The data for each scenario is taken in the same time interval and averaged over tunnel cross section and time. Thereof, the total pressure loss for each scenario is determined which indicates a valuable parameter in the ventilation design.

The numerical results for the total pressure losses are summarized in Figure 4. Obviously, the wood crib only has a marginal influence on the pressure loss. The pressure loss due to the injection of water mist is much higher than the wall friction of the empty tunnel. Without FFFS, the averaged heat release rate (HRR) of the ignited wood crib is 25.2 MW. A significant

pressure loss is caused by the fire. The fire plume and also the water mist impact the surrounding flow of the wood crib. Consequently, its pressure resistance changes. It also changes while the wood crib is consumed by the fire.

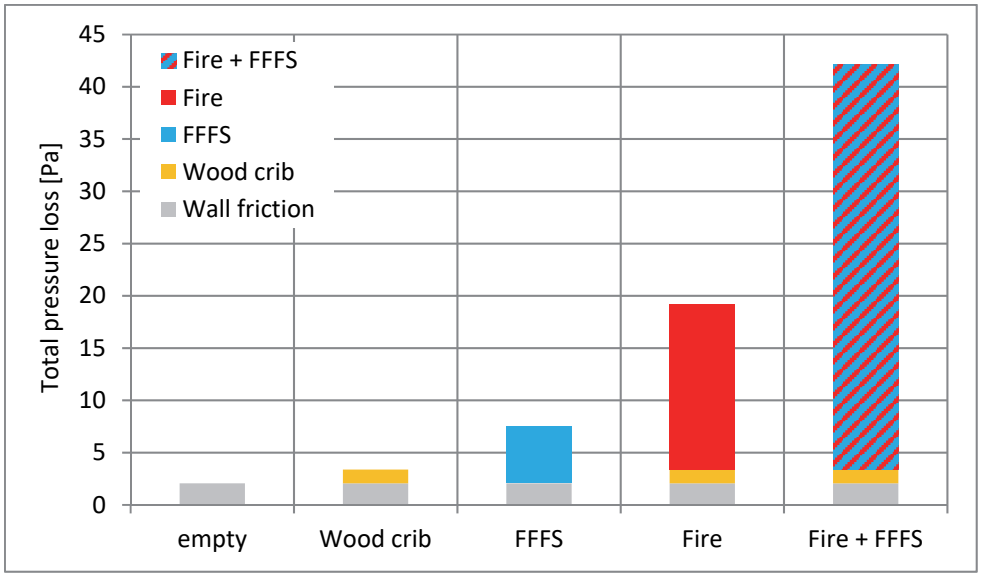

Figure 4: Composition of total pressure loss calculated with FDS.

It appears as an unjust simplification to break down each scenario into individually calculated contributions. The scenario including fire and FFFS shows a noticeably higher overall pressure loss than the sum of the individual contributions. The pressure resistance of the fire seems to be affected by the injection of water mist.

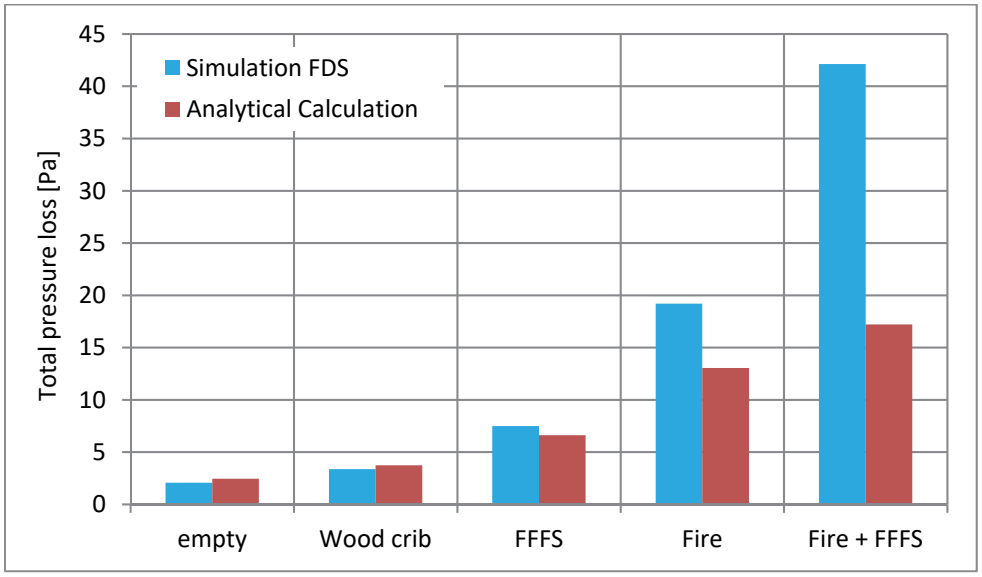

Figure 5: Comparison of analytical study and FDS simulations.

A comparison between analytical and numerical results is provided in Figure 5. The results for the empty tunnel, tunnel with wood crib and tunnel with FFFS are matching well. Theory and simulation show a high correlation as long as no fire is simulated.

If the fire simulation is included, a significant discrepancy is visible. It can be attributed to the fire's pressure resistance. For the geometry applied in this study, the relation of Dutrieue et al.

[1] appears to underestimate the pressure drop significantly. This is even more apparent if the water mist is added to the simulation.

A first indication of the causes is visualized in a picture of the secondary flow just upstream of the fire source, see Figure 6. Increased secondary flow causes increased flow velocity gradients at the tunnel wall adding to friction losses. More research is required in order to quantify the impact of the throttling effect and of the secondary flow driven by the water mist application.

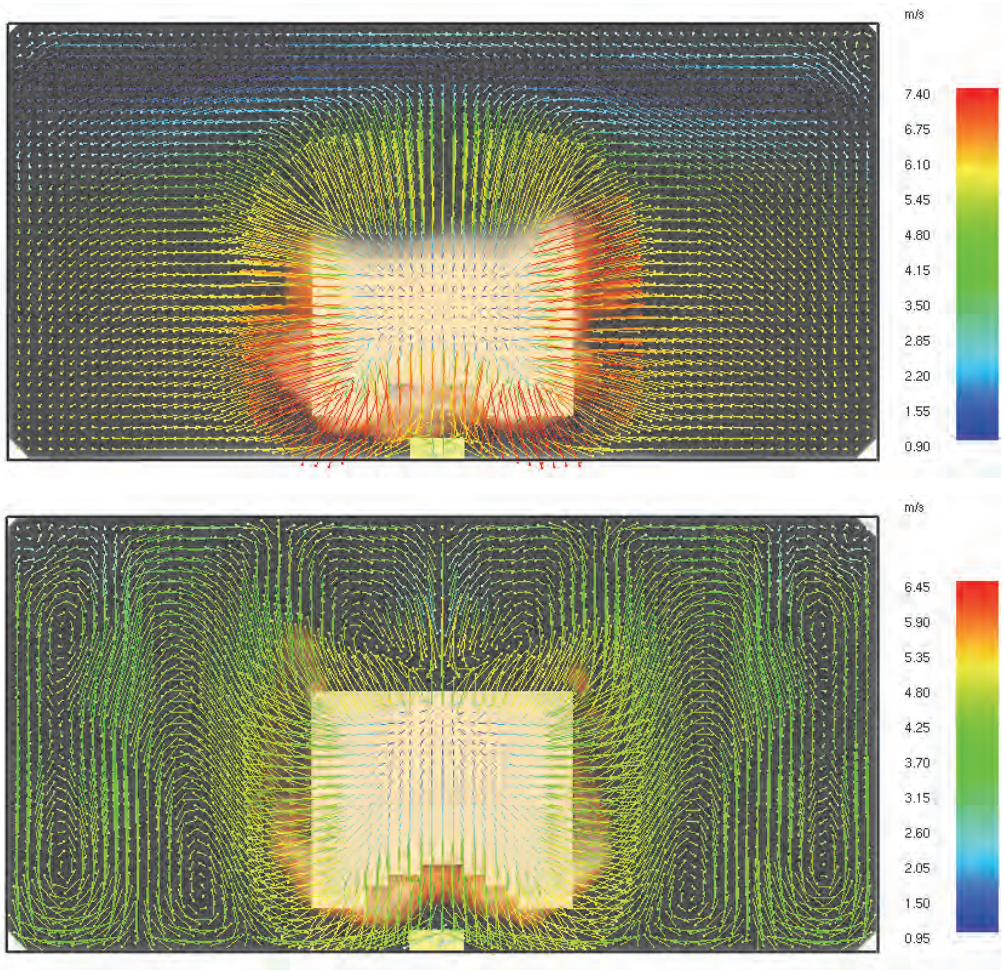

Figure 6: Tunnel cross-section just upstream of the fire source without FFFS (above) and with FFFS (below).

4. IMPACT ON DESIGN AND OPERATION

From our analysis and simulation that extended well beyond the results presented in this article, we derive some recommendations regarding design and operation of emergency tunnel ventilation for water mist operation.

Longitudinal ventilation:

- The system shall be designed to the same airflow as required without water mist system.
- The pressure drop caused by water mist has to be taken into account (equation 1).
- The stack effect can be calculated from the design fire size reduced by 50%.
- The longitudinal ventilation shall be operated at a reduced airflow velocity of
  - 1.5 to 2.0 m s^{-1} in tunnels with free-flowing unidirectional traffic.
  - 1.0 m s^{-1} in tunnels with bidirectional or congested traffic.

Local smoke extraction:

- The extraction system shall be designed without taking the water mist system into account.
- The stack effect can be calculated from the design fire size reduced by 50%.
- The water mist application does not require changes to the operation of the ventilation system.

We do not recommend to change a ventilation concept from smoke extraction to longitudinal ventilation based on the assumption of a risk reduction by the water mist system. Instead, we follow the recommendation given by PIARC [9]. The decision whether or not to install a water mist system may be supported by an assessment of the costs and benefits. The selection of the ventilation concept shall thereby be based on a project specific risk assessment.

5. CONCLUSIONS

The findings of the study can be summarized as follows:

- The water mist causes an additional pressure drop that has to be overcome by the longitudinal tunnel ventilation.
- The pressure drop of the fire (throttling effect) has to be included in the design of the tunnel ventilation, although further research is needed to support or refine the published models.
- The water evaporation does not add to the total volume flow rate in the tunnel.
- The operation of longitudinal ventilation systems shall be adapted to support the water mist operation in order to reach an optimum of smoke propagation and fire suppression.

6. REFERENCES

[1] Dutrieue R., Jacques E., Pressure Loss Caused by Fire in a Tunnel, 12th Int. Symp. Aerodynamics and Ventilation of Vehicle Tunnels, Barcelona, 2006

[2] Fire Dynamics Simulator, Technical Reference Guide, Volume 3: Validation, V6.5.2, NIST Special Publication 1018-3, August 2016

[3] FGSV, Richtlinien für die Ausstattung und den Betrieb von Straßentunneln, RABT 2015, Draft June 2015

[4] FSV, Richtlinie Tunnelausrüstung, Belüftung, Grundlagen RVS 09.02.31, June 2014

[5] FSV, Richtlinie Tunnelausrüstung, Ortsfeste Brandbekämpfungsanlagen RVS 09.02.51, August 2014

[6] ILF, A+W Progress: Wirtschaftlichkeit automatischer Brandbekämpfungsanlagen in Straßentunneln, FE 15.0564/2012/ERB, February 2014 (unpublished)

[7] ILF, STUVA, UR: Wirksamkeit automatischer Brandbekämpfungsanlagen in Straßentunneln, Berichte der Bundesanstalt für Strassenwesen Heft B 135, Februar 2017

[8] Li Y. Z., Ingason H., Influence of ventilation on road tunnel fire with and without water-based suppression systems, Fire Research, SP report 2016:36

[9] PIARC, Fixed Fire Fighting Systems in Road Tunnels: Current Practices and Recommendations, Report 2016R03EN, February 2016

[10] Saebo A.O., Wighus R., Droplet Sizes from Deluge Nozzles, SP Fire Research, A15 1074531, April 2015

[11] Vaitkevicius A., Carvel R., Colella F., Investigating the Throttling Effect in Tunnel Fires, Fire Technology, July 2015

USE OF WATER MIST SYSTEMS IN SMOKE EXTRACTION SYSTEMS FOR IMPROVING PERFORMANCES OF EXHAUST FANS

Frédéric Waymel, Laurent Plagnol,
Egis Tunnels, France

ABSTRACT

The aim of this paper is to present a concept in order to reduce the temperature through fans used in case of fire for smoke extraction and to increase their performance. High smoke temperature generally appears in case of heavy goods vehicle fire in tunnels. This leads to a significant reduction of the mass flow rate extracted in the tunnel and may affect the confinement of smokes within the tunnel extraction zone where the semi-transverse ventilation is applied. The use of water mist inside smoke extraction ducts allows reducing the smoke temperature upstream exhaust fans and to recover mass flow rate and also total pressure on smoke exhaust fans. Conceptual principles and sizing rules are described in the following paper. Theoretical examples are also presented giving advantages and drawbacks.

Keywords: Exhaust fan, Smoke temperature, Water mist, Improvement of mass flow rate

1. BACKROUND

1.1. Remind of semi transverse ventilation principles

The semi-transverse ventilation remains one of the main relevant systems to achieve fire safety objectives in bi-directional road tunnels where passengers can be blocked at both sides of a fire. One of the principles of this strategy is the confinement of the smoke in the dedicated fire zone (smoke extraction zone) in order to reduce the smoke propagation along the tunnel. To achieve this confinement objective, minimum fresh air velocities, also called confinement velocities, must be reached at both side of the fire zone as shown on the following figure. The principle of confinement velocity was introduced by Casalé and Biollay (2001) and Telle and al. (2002). Those velocities lead to mass flow rates of fresh air Qm_{conf1} + Qm_{conf2} entering into the fire zone that must be extracted by the fan in addition to the mass flow rate Qm_{conb} released by the combustion of material.

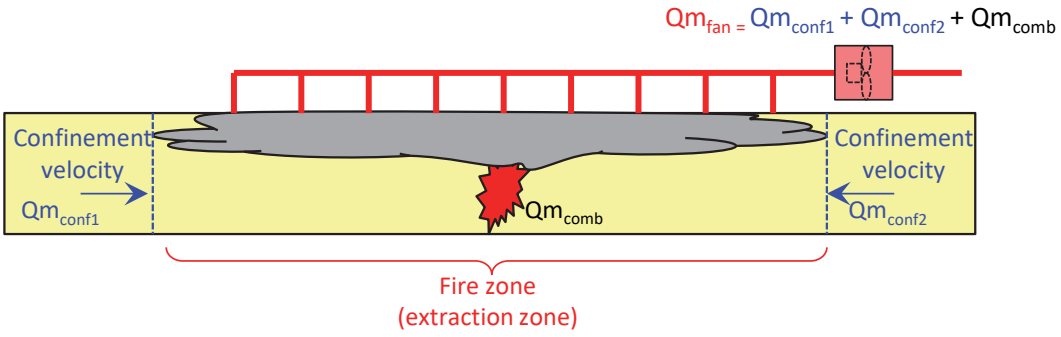

Figure 1: Principle of semi-transverse smoke extraction system

1.2. Behaviour of smoke extraction fans due to thermal effects

One of major issues is the behavior of the fan when exposed to fire conditions especially for road tunnels in which dangerous heavy goods vehicles are allowed and where the design fire can consequently exceed 50 MW. The flow extracted by the fan can reach temperatures close to 400°C for which smoke exhaust fans have been fire rated.

For a tunnel with a cross section of 60m² and a 75 MW design fire, the recommended confinement velocity is at least 1 m/s and the corresponding mass flow rate to be extracted is around 150 kg/s. As shown in Figure 1, this mass flow rate can easily be achieved under nominal fresh air conditions with a fan having a nominal volume flow rate of 125 m^3/s for the pressure duty point of 600 Pa. However, if the design of the fan is done by considering only the fan curve under those fresh air conditions, the mass flow rate significantly decreases with hot smoke and the confinement velocity cannot be satisfied. Moreover, it can also be observed that the total pressure delivered by the fan is drastically reduced. Those results are the consequences of the smoke density which is lower than the normal fresh air density (see also Gebrig and Buchmann (2012)).

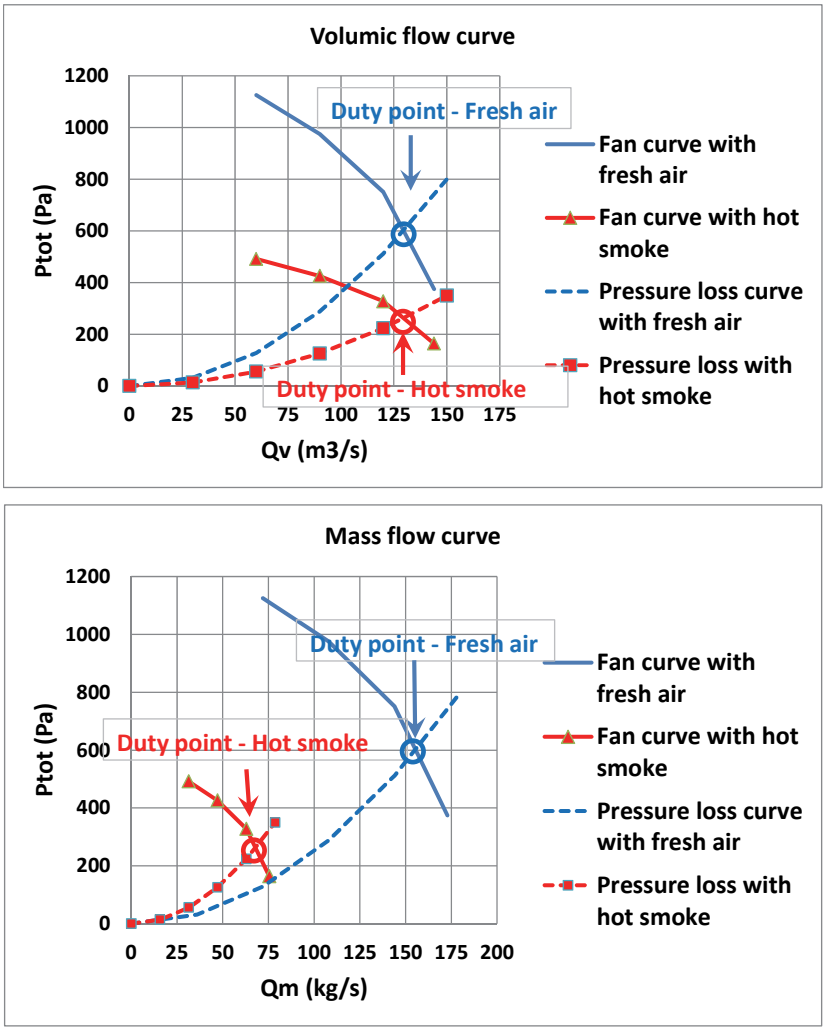

Figure 2: Fan flow curves and pressure loss system curves under fresh air and hot smoke conditions (400°C)

1.3. Consequences on the design

To achieve the requested mass flow rate under hot smoke conditions, the volume flow rate of the fan generally needs to be over-sized in order to compensate the behavior under hot smoke conditions. The rule to be applied for the volume flow rate capacity of the fan must consider the expanded mass flow rate to be extracted and can be evaluated as follow:

$$Qv_{fan} = \frac{Qm_r}{\rho_s} = \frac{\rho_0}{\rho_s} Qv_0$$

- Qv_{fan} : Volume flow rate of the fan (m^3/s)
- Qm_r : Requested mass flow rate to be extracted (kg/s)
- Qv_0: Fresh air volume flow rate entering into the fire zone based on the confinement velocity (m^3/s)
- ρ_0 : Nominal density of fresh air entering into the fire zone (kg/m^3)
- ρ_s: Smoke density through the fan (kg/m^3)

Depending on the smoke density through the fan, the volume flow rate to be extracted can be significantly higher than the flow rate entering into the fire zone. For instance with a temperature of 400°C, the flow rate through the fan can exceed more than twice the flow rate entering into the fire zone.

Moreover in order to compensate the decrease of the total pressure developed by the fan under hot smoke conditions, the pressure duty point must be calculated for the expanded volume flow rate Qv_{fan} but with the initial fresh air density ρ_0.

The following curves show duty points achieved with an oversized fan for the same tunnel example as the one presented in the previous section. In that case, the requested mass flow rate of 150 kg/s can be achieved under hot conditions with a fan flow volume flow rate oversized at 300 m^3/s and a total pressure of 3 100 Pa under fresh air normal conditions.

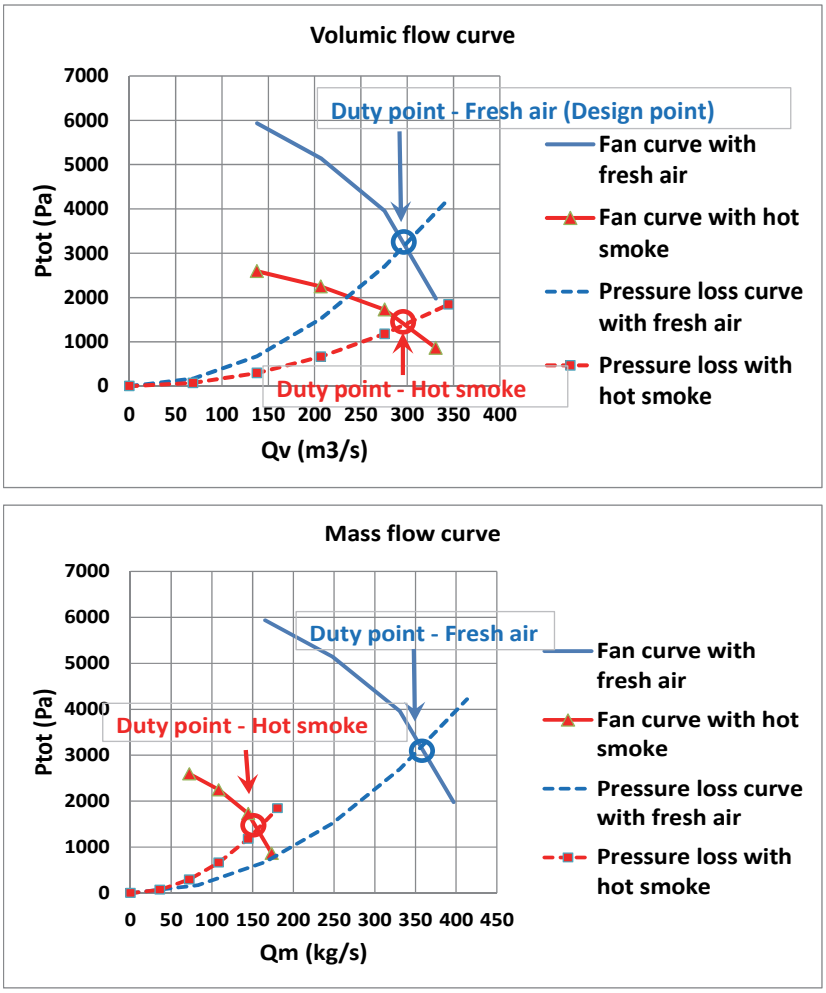

Figure 3: Fan flow curves and pressure loss system curves under fresh air and hot smoke conditions with oversized fan (400°C)

2. WATER MIST IN SMOKE EXHAUST DUCTS

2.1. Presentation of the concept and sizing rules

As presented in the previous chapter, the high temperature of smoke through exhaust fans can lead to a significant increase of the required fans volume flow rate. This may lead to a rise of fan size or number of fans. Additional civil requirements and power demand are also expected.

In order to reduce those impacts, a water mist system can be installed in the smoke exhaust duct upstream the ventilation plant. The principle is to cool the smoke flow rate before entering into exhaust fans in order to recover density and to improve the behavior of fans in case of fire. This principle is described in Figure 4.

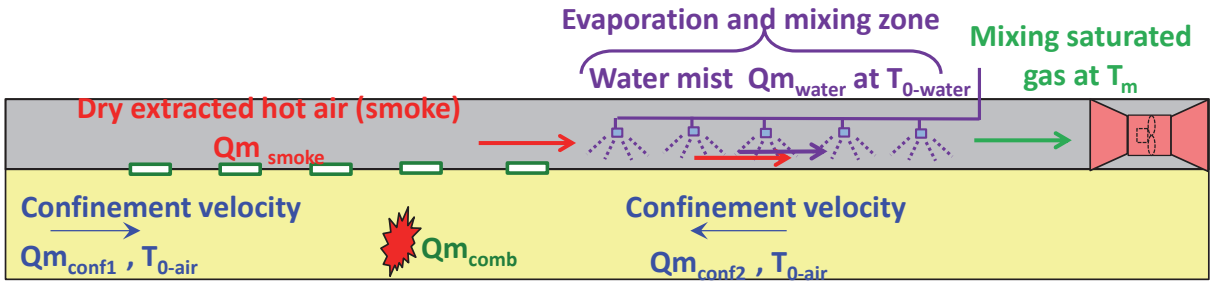

Figure 4: Concept using water mist in smoke exhaust ducts

Cooling effects are provided by the evaporation of water droplets up to the saturation point. Figure 5 gives as a remind that the latent heat for water evaporation is based on Regnault formula and also the saturated vapor pressure depending on gas temperature is based on Clapeyron. This shows that the latent heat remains very high even when the gas temperature increases. The saturated vapor pressure rises exponentially with the gas temperature which means that a large quantity of evaporated water can be introduced in dry air (or hot smoke) for higher temperatures in order to provide significant cooling effects. However, in the meanwhile as shown in Figure **6**, dry air ratio at saturation point drops which can finally reduce the mass flow rate of fresh air extracted in the tunnel necessary for the confinement of smokes into the fire zone. A compromize needs consequently to be found for the mixing gas temperature achieved at the inlet of smoke exhaust fans in order to have significant cooling capacity provided by the water evaporation up to the saturation point and by keeping at the same time a good ratio of dry air density in the mixing gas.

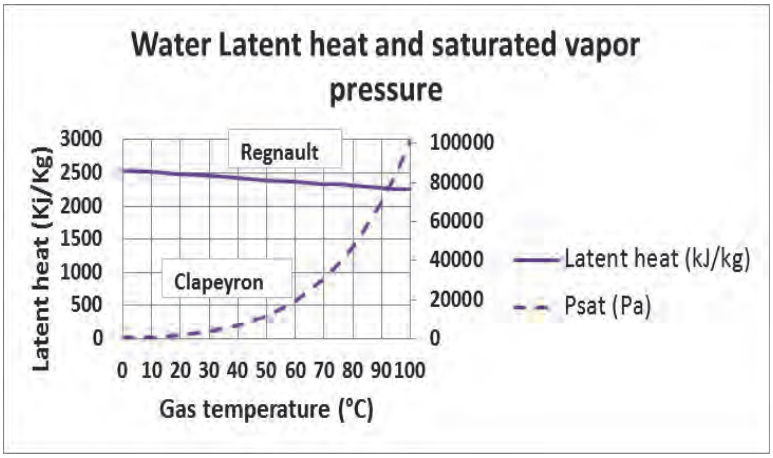

Figure 5: Psychometric properties of water

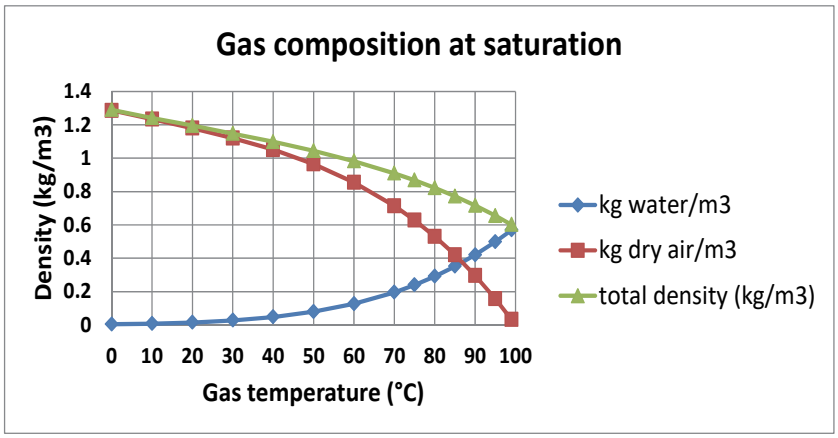

Figure 6: Gas composition at saturation point

The mixing gas temperature T_m can be calculated considering that the cooling load *(CL)* provided by the water evaporation at saturation point at T_m is equal to the cooling requirement *(CR)* for decreasing the smoke temperature at T_m. This rule can be expressed by the following equations:

$$CL = CR$$

$$CL = Qm_{water}(T_m).[Lv(T_m) + Cp_{water}.(T_m - T_{0-water})]$$

$$CR = 0.7.HRR - Qm_{smoke}(T_m).Cp_{air}.(T_m - T_{0-air})$$

With :

- $Qm_{water}(T_m)$: Mass evaporated water flow rate at saturation point at T_m (kg/s)
- $Lv(T_m)$: Latent heat of evaporation at Tm (J/kg)
- Cp_{water} : Heat capacity of water (J/kg/K)
- $T_{0-water}$: Initial water temperature in water mist pipes (°C)
- HRR : Fire total heat release rate (W)
- Qm_{smoke} : Mass flow rate of smoke to be extracted (considering also fresh air due to confinement velocity) (kg/s)
- Cp_{air} : Heat capacity of air (J/kg/K)
- T_{0-air} : Initial temperature of fresh air entering in the fire zone (°C)

The following figure shows the mixing duty point achieved for the example presented in the first chapter. The temperature of the mixing gas is in that case close to 60°C.

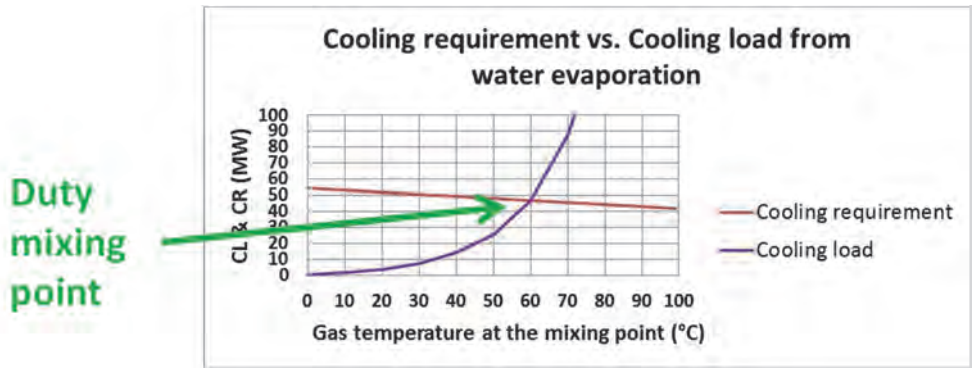

Figure 7: Duty point

2.2. Theoretical application

The implementation of water mist systems in ventilation ducts has already been done in Austria in Gleinalmtunnel but the purpose was only for reducing smoke temperature through existing fans due to the fact that they were not fire rated (See Kaiser, Kern (2010)). At the current time as far as it is known from the state of the art, it does not exist any tunnel where water mist systems have been installed in ducts for the topic presented in this paper. This section is consequently dedicated to the presentation of a theoretical application. Theoretical analyses have been performed for a typical bidirectional road tunnel with one lane per traffic direction where a semi-transverse ventilation is requested in such a situation when a fire occurs. The tunnel cross-section is 50 m². Characteristics of the study case are presented in Figure 8.

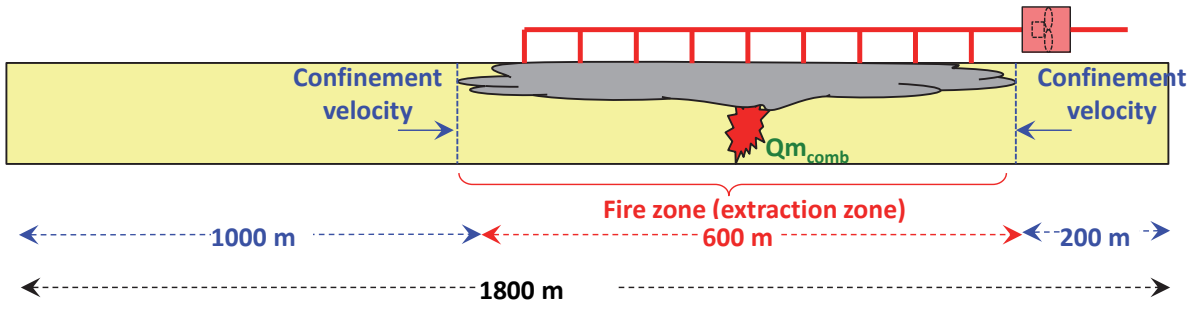

Figure 8: Case study

Analyses have been done for a design fire of 100 MW located at 500 m from the exit portal. The confinement velocity considered in that case at both side of the extraction zone is 1.25 m/s which leads to a mass flow rate to be extracted of 150 kg/s.

The following table provides the results of the preliminary sizing for fans and the water mist system. As shown, fan capacities can be significantly reduced with the water mist system. Moreover, by keeping the same total pressure on fans, the duct size is about half the size of the duct without water mist. On the other hand, the requested water flow rate of 24.6 L/s for the water mist leads to an installation including 100 nozzles pressurized at 80 bars. A water tank of around 100 m³ capacity is also recommended in order to secure the water supply.

Table 1: Pre-sizing parameters without and with water mist in the smoke exhaust duct

Configuration	Expected smoke temperature through fans (°C)	Expanded Qv to extract (m3/s)	Number of fans	Nominal flow rate per fan (m3/s)	Nominal Total pressure (Pa)	Max. Water flow rate (L/s)	Duct size (m²)
Without water mist	490	320	2	160	~ 2100	N/A	15.5
With water mist	61.7 (mixing point temperature)	180	1	180	~ 2100	24.6	8.7

More detailed analyses have been with 1D simulations performed on Zephyr software developed by Egis Tunnels. The model is presented in Figure 9.

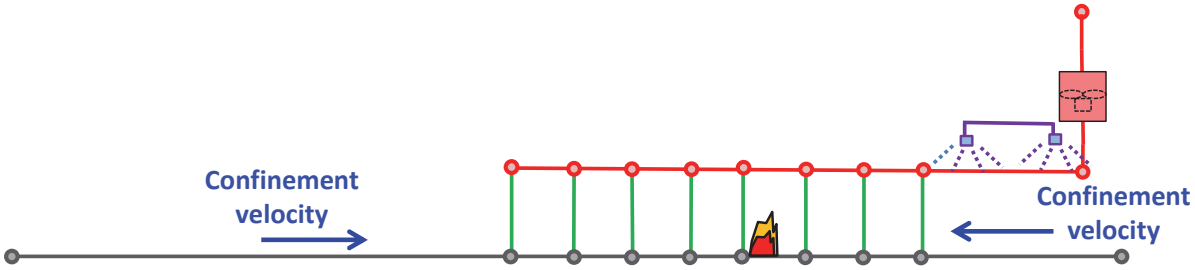

Figure 9: Zephyr 1D model

The following figure shows the smoke temperature through fans over the time. Without water mist, this temperature exceeds 480°C and can be reduced at around 65°C with the water mist at steady state when the water flow rate reached 24.6 L/s.

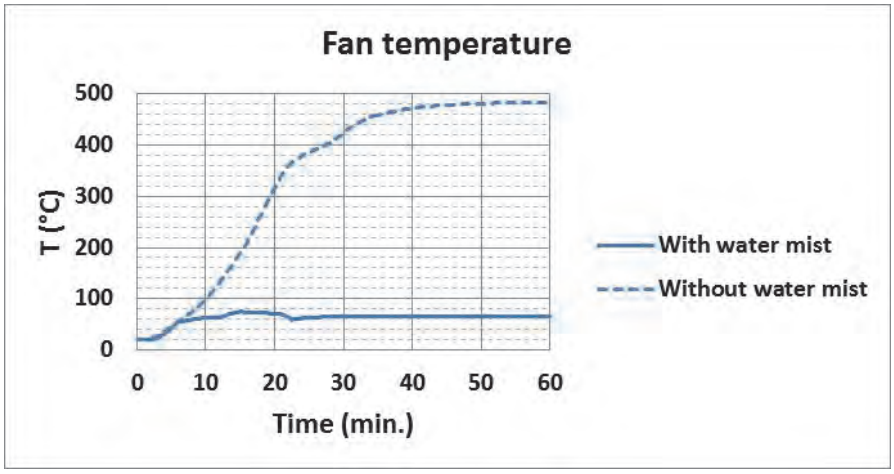

Figure 10: Duty point

As shown in Figure 11, mass flow rates of smoke extracted in both cases without and with water mist converge to the requested value of 150 kg/s for achieving the confinement velocity of 1.25 m/s at both side of the extraction zone in the tunnel. Without water mist, the value is significantly higher at the beginning of the fire (385 kg/s) due to the fact that the fan system is oversized and smokes are still cold. Then, it decreases with higher smoke temperatures. With water mist, the total mass flow rate through the fan includes the smoke and the evaporated water mass flow rates. This total mass flow rate is more stable as a consequence of the smoke temperature which never exceeds 80°C all along the simulation.

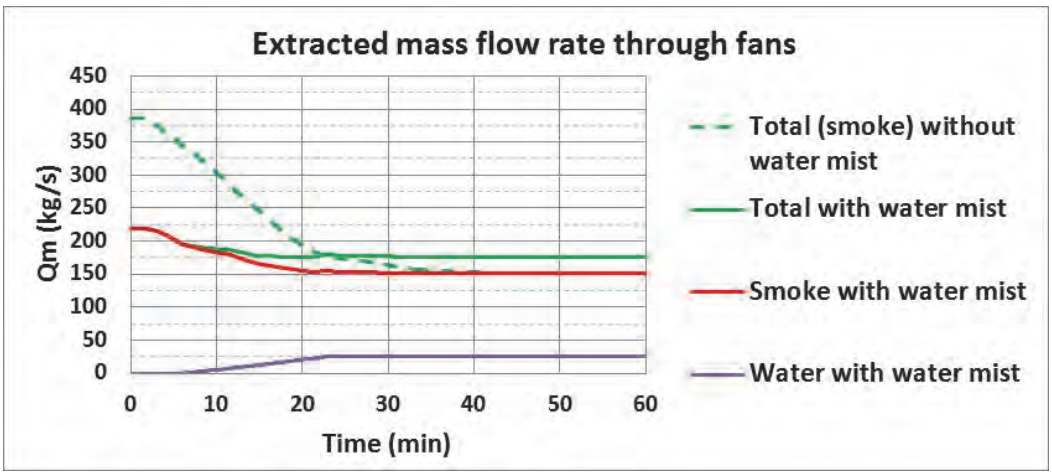

Figure 11: Mass flow rates through fans

3. BRIEF CONCLUSION AND FURTHER INVESTIGATIONS

High smoke temperatures through exhaust fans especially in case of heavy goods vehicle fire in road tunnels lead to significant reduction of fan capacities to extract mass flow rate in the tunnel and to provide total pressure in order to compensate the pressure losses. Those effects are generally compensated by oversizing the ventilation system including not only the increase of fan size or number of fans, but also the duct size. Using a water mist system in smoke extraction ducts is an alternative solution. For the theoretical application presented in this paper, the total fan capacity including flow rates and power demands is approximately divided by two with a water mist system. However, the space, the power demands and investment costs saved for the ventilation plant is on the other hand compensated by the water mist system. The main advantages of the proposed solution is the possibility to optimize the smoke exhaust duct size whose cost saving can be estimated between 3 and 5 million € depending on the construction method. Other benefits could also be introduced such as installing fans without fire rated certificate or even less heavy fans with brushless motors which operates below 60°C.

Further investigations could be performed such as:

- The evaluation of water droplet evaporation efficiency taking into account the influence of high velocity (up to 20 m/s) in extraction ducts.
- The minimum distance requested between the water mist zone and fans.

4. ACKNOWLEDGMENT

Authors would like to thank Peter Sturm from the University of Graz who provided interesting information on the water mist system which was installed in Gleinalmtunnel in Austria to compensate the absence of fire resistance on existing exhaust fans before the complete refurbishment of the ventilation system.

5. REFERENCES

Casalé E, Biollay H. (2001). *A fully controlled ventilation response in the case of tunnel fire "confinement velocity"*. Safety in Road and Rail Tunnels, Fourth International Conference, Madrid, Spain

Telle D, Vauquelin O. (2002). *An experimental evaluation of the "confinement velocity"*. Tunnel Fires, Fourth International Conference, Basel, Switzerland

Gebrig S., Buchmann R. (2012). *Impact of density variations in the exhaust duct on smoke extraction and fan operation point*. Tunnel Safety and Ventilation, Sixth International Symposium, Graz, Austria

Kaiser C., (2010). *From the classical Fire Fighting Water Supply to Structure and Smoke-Gas Cooling, taking the Gleinalm Tunnel as an example, part I*. Tunnel Safety and Ventilation, Fifth International Symposium, Graz, Austria

Kern H., (2010). *From the classical Fire Fighting Water Supply to Structure and Smoke-Gas Cooling, taking the Gleinalm Tunnel as an example, part II*. Tunnel Safety and Ventilation, Fifth International Symposium, Graz, Austria

MASS FLOW OF AIR IN TUBES AND EXHAUST DUCTS OF ROAD TUNNELS UNDER TRAFFIC CONDITIONS

[1]B. Frei, [2]H. Huber, [2]D. Jurt, [2]M. Imholz, [2]R. Stockhaus

[1]Aicher, De Martin, Zweng AG, Lucerne, Switzerland
[2]Lucerne University of Applied Sciences and Arts, Switzerland

ABSTRACT

This paper reports advances in measuring the mass flow of air in five Swiss road tunnels under traffic conditions. The measurement techniques applied are the constant-emission and the pulsed-emission tracer methods in single- and multi-point sampling mode.

Here we report strategies to overcome difficulties caused by unsteady flow conditions in tunnel tubes under traffic by using the pulsed-emission tracer method. In addition to a method already published in a previous contribution for the application in exhaust ducts, we have now completed a thorough investigation on measurement uncertainties for traffic tubes.

Our recent review of measured mass flow of air in exhaust ducts of a Swiss tunnel showed good agreement for both tracer-dosing and sampling methods. It confirms results and observations reported in our earlier contributions to this conference. The ability of the pulsed-emission tracer method to determine leakages and mass flows of air during night closures of tunnels has been demonstrated.

We conclude with the state of the art of knowledge and an outlook to further developments.

Keywords: Tracer gas measurement, mass flow of air, exhaust leakage, measurement uncertainty, road tunnel, traffic conditions

1. INTRODUCTION

Since 2002 the constant-emission tracer method has been used by scientists and engineers of the Lucerne University of Applied Sciences and Arts (HSLU) to determine mass flow and leakages in exhaust ducts and tubes of twenty-two road tunnels in Switzerland and Europe. Determining mass flow of air and leakages in exhaust ducts under difficult conditions is still a challenge (difficult flow profiles, limited time slots for measurement campaigns, and rough conditions etc.). Several papers have reported measurement campaigns and comparisons of measurement methods. The pulsed-emission tracer gas method (PEM) was described in earlier contributions (Frei /2010/, Frei /2012/) to this conference and has the potential to overcome many of the described difficulties. The pulsed-emission tracer gas method was recently downscaled and adapted to determine mass flow of air in evacuation stairwells of Swiss high-rise buildings (Frei /2016/).

2. CONSTANT- AND PULSED-EMISSION TRACER GAS METHOD

Fast measurement and control devices and the development of data acquisition tools led to the application of the pulsed-emission tracer gas method (PEM) to determine mass flow of air with lowest measurement uncertainty. Frei /2010/ and Frei /2012/ reported first applications in exhaust ducts and computed measurement uncertainties for these tracer methods. The methods are illustrated in Figure 1.

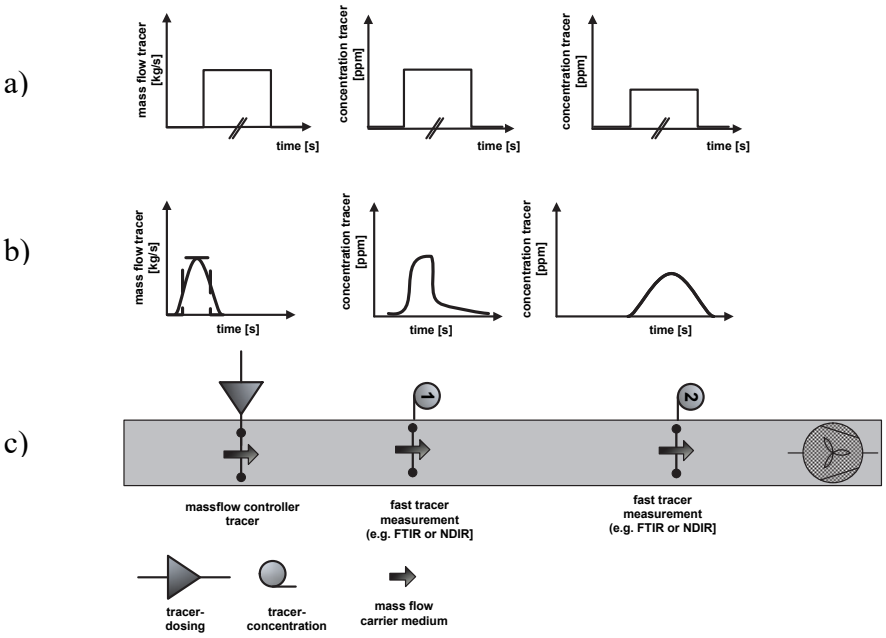

Figure 1: Experimental set-up of the constant- and pulsed-emission tracer method in exhaust ducts or tunnel tubes. (a) Dosing, (b) response, (c) duct layout.

The highly turbulent flow in exhaust ducts and tubes of road tunnels mixes tracer gases such as sulfur hexafluoride SF_6, nitrous oxide N_2O, or carbon dioxide CO_2 over short distances. The single-point or multi-point sampling of the tracer gas is done downstream. The mass flow of the carrier medium can be determined precisely from the dosing mass flow and the resulting downstream concentration of the tracer gas (or its integral) and is completely independent of the flow profile. Equipment used to measure concentrations: Infrared Photo-acoustic Spectroscopy (IR-PAS), Non-Dispersive Infrared Spectroscopy (NDIR), and Fourier Transformation Infrared Spectroscopy (FTIR).

3. APPLICATIONS OF TRACER METHODS IN SWISS TUNNELS

3.1. Determination of mass flow rates in tubes under traffic conditions

The authors have experimentally determined mass flows in tunnel tubes under traffic conditions since 2005 with the Constant-Emission Method (CEM), and since 2012 with the Pulsed-emission Method (PEM). The road tunnels Gotschna near Klosters, Schöneich in Zurich, Spier in Lucerne, Flüelen UR, and Bözberg AG were investigated. (Table 1).

Table 1: Measurement campaigns in tubes of Swiss road tunnels to determine mass flow of air by tracer methods. Ranges of the distance from dosing to sampling, $x_{D\text{-}S}$, and of measured mass flows during campaign.

Tunnel	Traffic	$x_{D\text{-}S}$ [m]	Method	Equipment	Convection	Mass flow air [kg/s]
Gotschna GR	No	847 1110	CEM	IR-PAS	natural, forced	177 - 264
A1 Schöneich ZH	Yes	62 213	CEM	IR-PAS	natural	189 - 365
A2 Spier LU	Yes	800	CEM	IR-PAS	natural	206 - 587
A4 Flüelen UR	Yes	 224	CEM PEM	NDIR FTIR NDIR	natural forced	 239 - 409
A3 Bözberg AG	Yes	365	CEM	FTIR NDIR	natural	180 - 420

Figure 2: Multi-point tracer sampling on road level of the tunnel Schöneich in Zurich (left) and on exhaust chimney of the tunnel Spier near Lucerne.

In the Swiss road tunnel Spier near Lucerne, it was possible to determine the exact mass flows in the tunnel tube and in the exhaust chimney. The tracer methods can also detect unwanted recirculation from exhausts to tunnel portals. The two tracer methods are ideal for measuring mass or volume flows under real traffic conditions without obstructing traffic in the main tunnel cross-section.

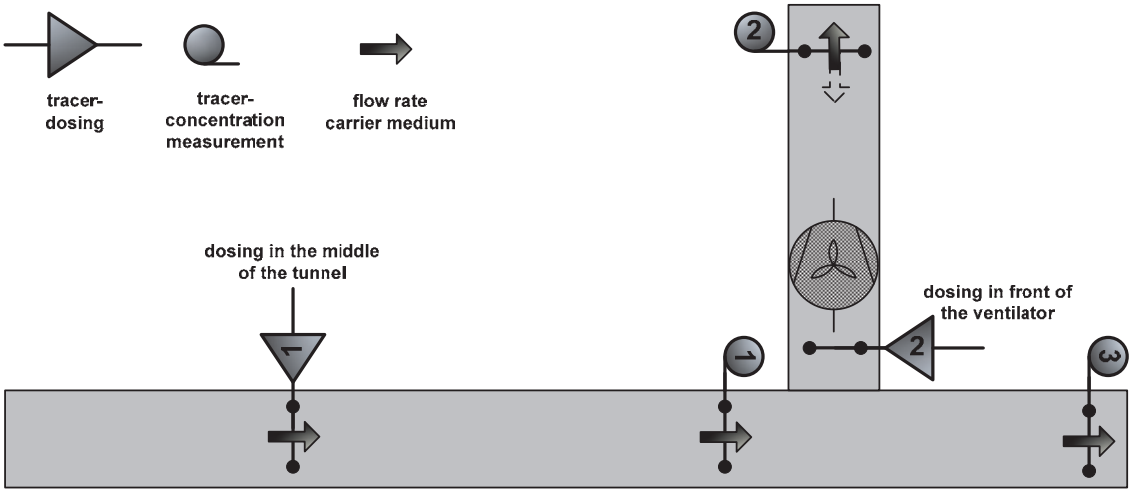

Figure 3: Experimental set-up to quantify ventilation efficiency in tunnel Spier LU.

3.2. Determination of mass flow rates in exhaust tubes of the Swiss tunnel Mappo-Morettina TI

The two tracer methods to determine leakage were compared for the first time during night-time closure in the Swiss road tunnel Mappo-Morettina near Locarno TI. Of particular interest was the validation of the mass flow measurement with both tracer methods in single- and multi-point mode at the first measuring station 96 m downstream of dosing. The agreement between the two tracer gas dosing and sampling methods is good and lies within the measurement uncertainties (Table 2). This demonstrates for the first time that tracer gas measurements with dosing distances below 100 m (i.e. 39 d_h) produce reliable results.

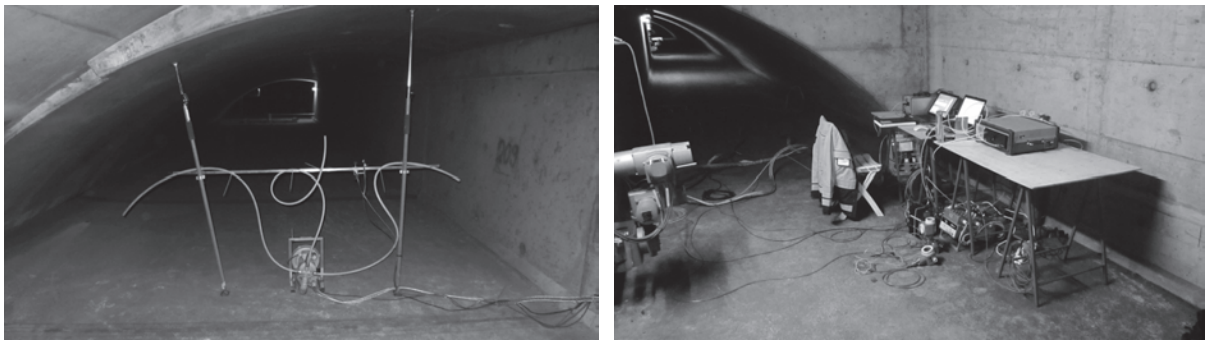

Figure 4: Multi-point sampling in exhaust duct (left) and measurement devices in supply duct at measurement site MS 2 (right) in the Swiss tunnel Mappo-Morettina near Locarno TI.

Table 2: Experimental results obtained by pulsed-emission method with single- and multi-point sampling at measurement site MS 1 (xD-S = 96 m) in Mappo Section.

PEM	**MS 1**	**FTIR**	**single-point**		**MS 1**	**NDIR**	**multi-point**	
pulse	uneven integral	trapezoidal integral	m [kg/h]	m [kg/s]	uneven integral	trapezoidal integral	m [kg/h]	m [kg/s]
1	198.646	199.466	421,896	117.2	198.318	198.097	422,297	117.3
2	129.286	128.249	425,178	118.0	129.344	129.540	424,985	118.1
3	128.132	128.690	429,070	119.2	127.654	127.396	430,678	119.6
PEM		**mean:**	**425,381**	**118.2±5.0**		**mean:**	**425,986**	**118.3±5.0**
CEM	**MS 1**						**422,280**	**117.3±5.9**
dev. (Δ/m_{PEM})								**0.8%**

In the Mappo-Morettina tunnel, experiments with pulses in series were carried out (Figure 5). With knowledge of the distance between the sampling points, it is possible to roughly calculate on-site leakage and flow velocity (or volume flow) from the peaks of the pulses.

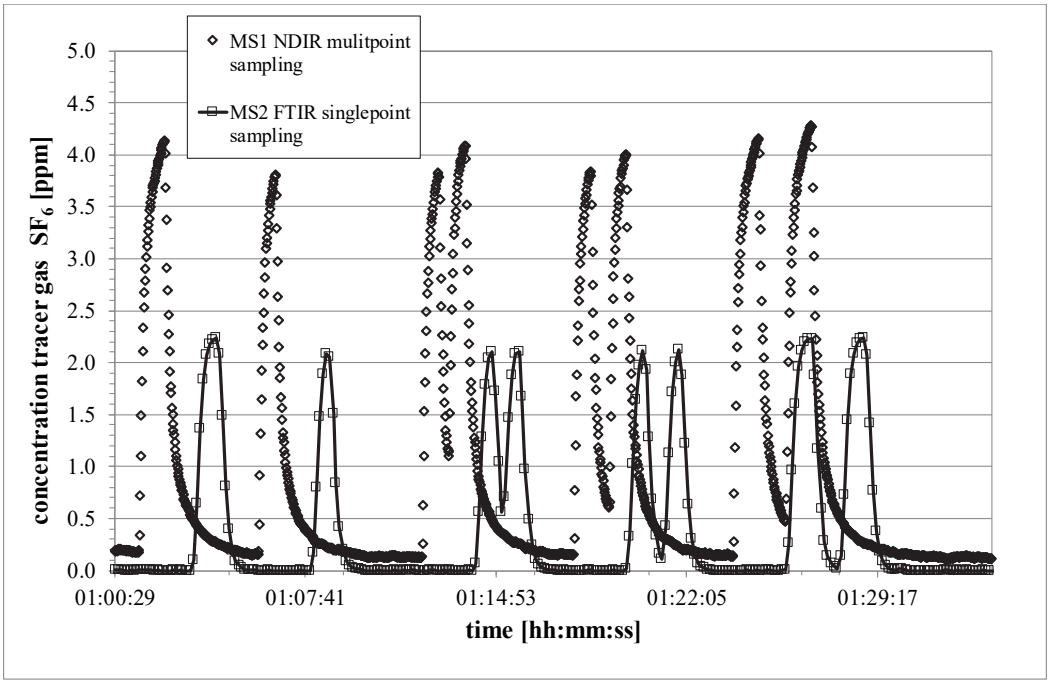

Figure 5: Series of pulses downstream at measurement site MS 1 (xD-S = 94 m) and site MS 2 (xD-S = 2303 m) in Morettina section.

In this measurement campaign rectangular pulses were generated because of the short available times slots during night closures of the tunnel and the crowded measurement program. The authors of Frei /2010/ describe measurement campaigns with normally-distributed dosage pulses.

Table 3: Experimental results obtained by pulsed-emission method (PEM) with single- and multi-point sampling at measurement site MS 1 (xD-S = 94 m) and MS 2 (xD-S = 2303 m) in Morettina section.

PEM	**MS 1**	**NDIR**	**multi-point**		**MS 2**	**FTIR**	**single-point**	
pulse	uneven integral	trapezoidal integral	m [kg/h]	m [kg/s]	uneven integral	trapezoidal integral	m [kg/h]	m [kg/s]
1	258.152	258.192	323,774	89.9	140.703	140.611	594,036	165.0
2	171.582	170.974	319,573	88.8	91.777	92.044	597,452	166.0
3	346.449	345.953	315,884	87.7	183.320	183.971	596,977	165.8
4	348.686	348.700	314,435	87.3	183.897	183.290	596,199	165.6
5	533.646	534.159	312,845	86.9	281.197	280.095	593,707	164.9
PEM		**mean:**	**317,302**	**88.1±3.7**		**mean:**	**595,674**	**165.5±6.9**
CEM	**MS 1**			**88.3±4.4**	**MS 2**			**181.1±9.1**

Table 3 shows that the two measured mass flows (PEM vs. CEM) at measuring point 2 (MS 2) differ by 15.6 kg/s (9.7%). This is within the spread of the extended measurement uncertainty of the two tracer gas methods. The agreement at the measuring station 1 (MS 1) in the Morettina section at 94 m (46 d_h) after the dosing point is very good. The results from the individual pulses differ only marginally.

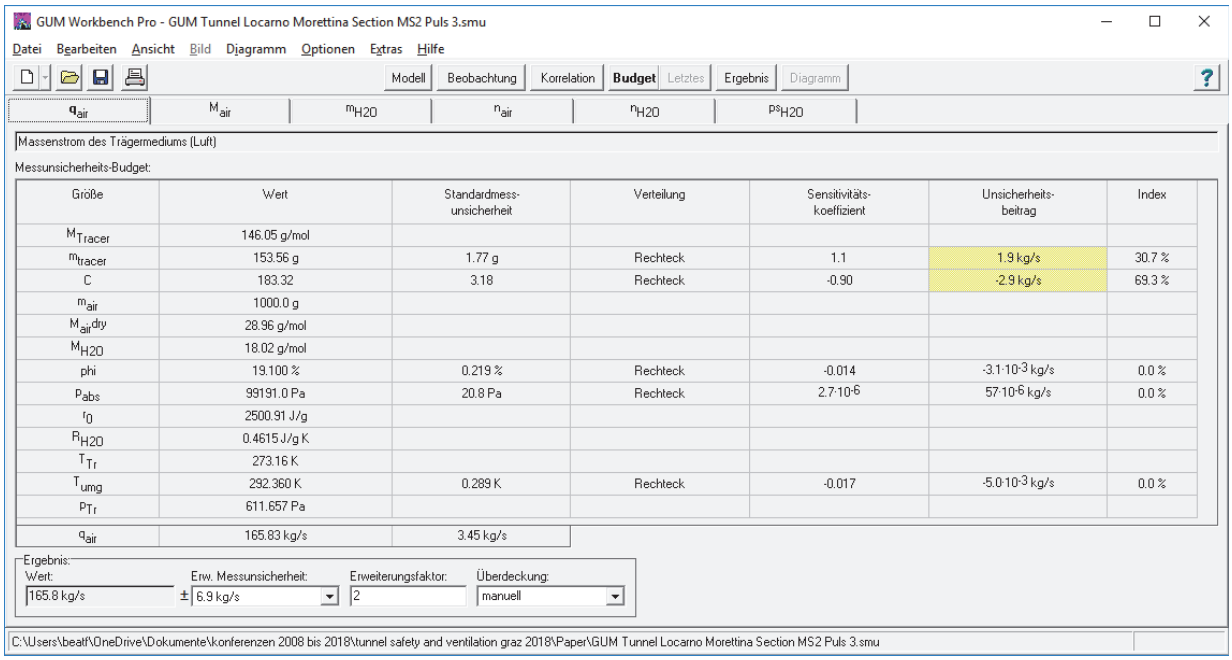

Figure 6: Budget for measurement uncertainty of pulse 3 at MS 2 (multi-point sampling).

The development of the complete assessment of measurement uncertainty according to the ISO-Guide Guide *Expression of measurement uncertainty* (GUM /1995/) was described in Frei /2012/ (Figure 6). Recently, the Monte Carlo method has also been used in an explorative way to evaluate measurement uncertainty for the pulsed-emission method (for Monte Carlo method see Lafarge and Possolo /2017/).

3.3. Determination of reference velocities in the Swiss tunnel Flüelen UR

Another research project revealed limits of the measurement of reference velocities by the constant-emission method under transient conditions. For this reason, the relationship of representative mean flow velocities and flow velocities measured near the tunnel wall is subject to uncertainties (see Grässlin et al. /2014/). In this research project, the authors were aware of the transient nature of flow and took this into account with the PEM. We have shown that (i) the differences in the sampling method have a negligible effect on the accuracy of the mass flow measurement in the tunnel tube and (ii), the mean flow velocities derived from the mass flow agree well with the locally measured velocities. The shape of the velocity profile in the tunnel cross-section must also be considered. The experiments in the tunnel Flüelen demonstrated the potential of the PEM in tunnel tubes.

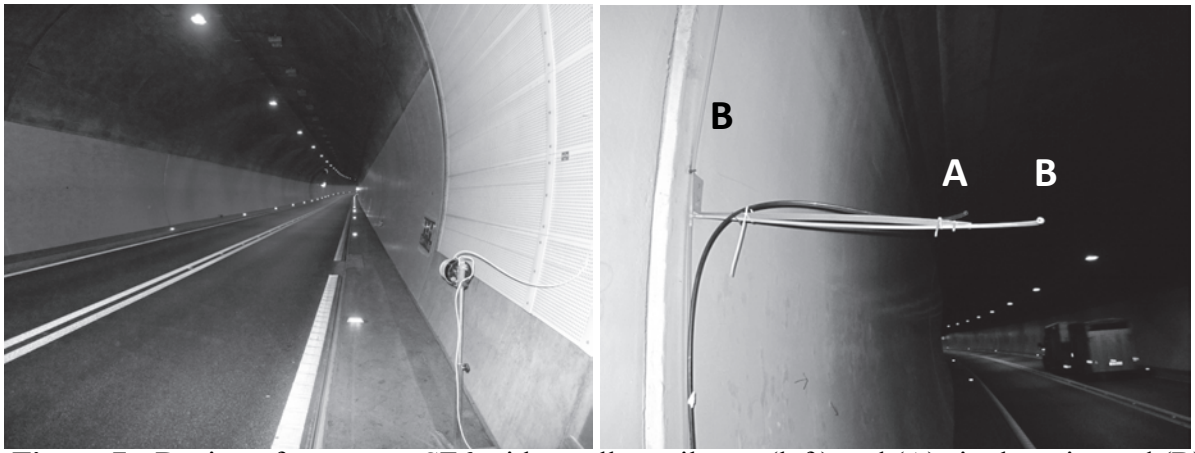

Figure 7: Dosing of tracer gas SF6 with small ventilators (left) and (A) single-point and (B) multi-point sampling in the tunnel Flüelen UR (right).

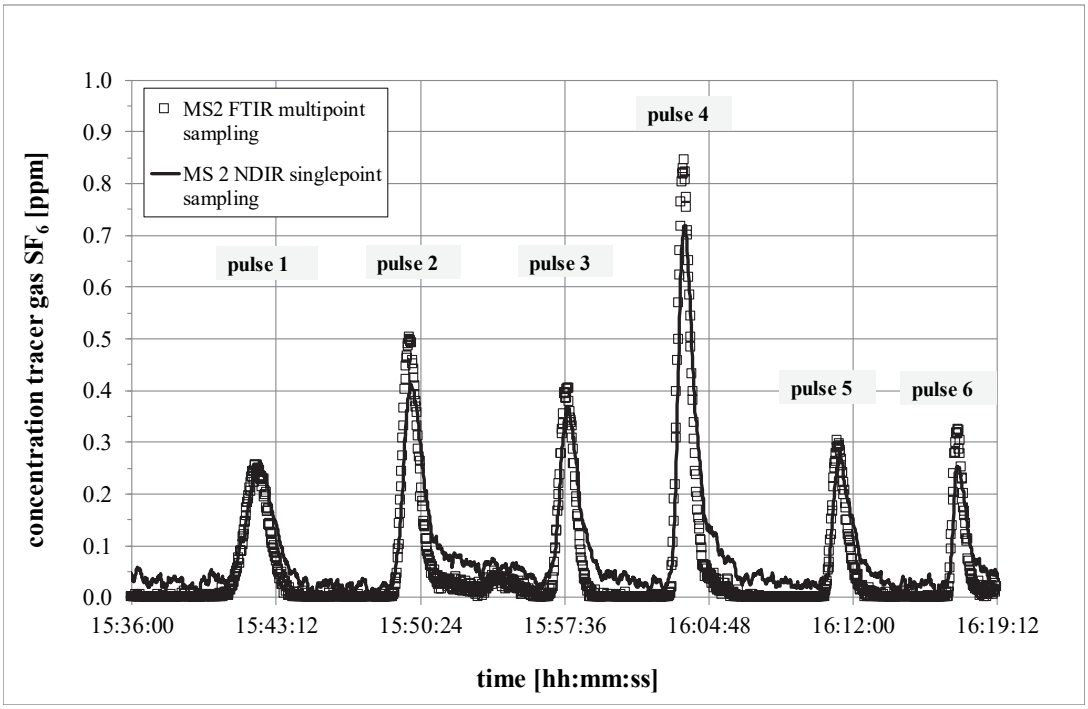

Figure 8: Comparison of single- and multi-point sampling of tracer gas SF6 at measurement site MS 2 (xD-S = 679 m) in the tunnel Flüelen UR.

Six concentration pulses were analyzed and compared in LAB-View® by two different integration methods "uneven" and "trapezoidal". The integration result is independent of the integration method (Table 4).

Table 4: Experimental results obtained by pulsed-emission method with single- and multi-point sampling at measurement site MS 2 (xD-S = 679 m) in tunnel Flüelen UR.

pulse	MS 2	FTIR	multi-point		MS 2	NDIR	single-point		
	uneven integral	trapezoidal integral	m [kg/h]	m [kg/s]	uneven integral	trapezoidal integral	m [kg/h]	m [kg/s]	**dev.$_{sp-mp}$ [%]**
1	21.280	21.221	825,840	229.4	20.997	20.988	833,760	231.6	**1.0**
2	29.924	29.895	903,240	250.9	29.114	29.040	928,440	257.9	**2.8**
3	21.161	21.174	1,285,560	357.1	20.943	20.956	1,298,880	360.8	**1.0**
4	41.444	41.340	1,044,720	290.2	41.372	41.514	1,046,520	290.7	**0.2**
5	14.467	14.446	1,231,560	342.1	13.589	13.5556	1,311,120	364.2	**6.5**
6	12.132	12.127	1,474,200	409.5	11.078	11.121	1,614,240	448.4	**9.5**

According to Table 4, the differences between the sampling methods at measuring site 2 (MS 2), 679 m after dosing, are small. The results suggest that single-point sampling is sufficient if dosing is correctly done. This greatly simplifies measurement campaigns in tunnel tubes under traffic conditions. With substantially shorter dosing distances, multi-point dosing would be required.

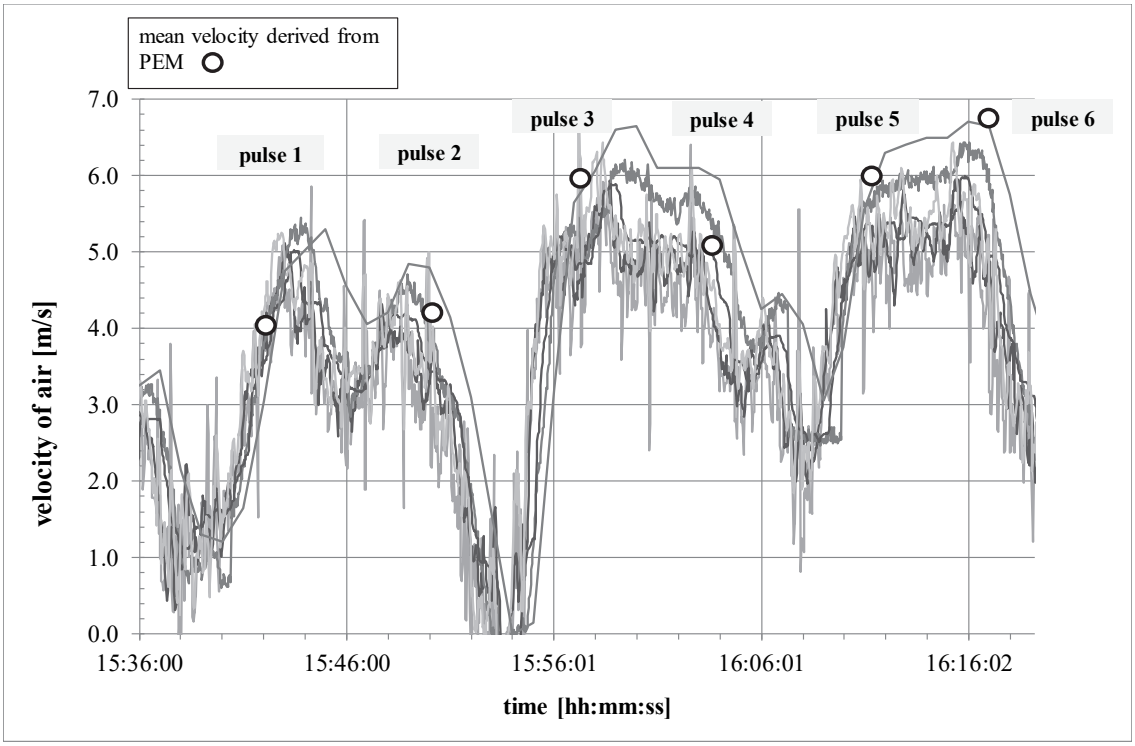

Figure 9: Comparison of velocities derived from mass flow by PEM and velocity measurement devices in tunnel Flüelen UR.

Figure 9 shows that the pulses 1 to 4 give well comparable flow velocities in the tunnel cross-section. The deviations of pulses 5 and 6 are larger. This is also evident from Table 4, where the differences between single- and multi-point sampling are more pronounced for pulses 5 and 6.

4. CONCLUSIONS AND OUTLOOK

Measurements during night-time closure have shown that PEM and single-point sampling are well suited for measuring mass flows and derived quantities. The measurement uncertainties determined with the GUM method (Guide to the Expression of Uncertainty in Measurement, GUM /1995/) are small. The PEM is superior to the CEM in all comparisons. The tracer gas consumption is reduced significantly, and the robustness of the PEM under unsteady flow conditions is remarkable. The disadvantages of CEM reported by other authors can be overcome by PEM, fast FTIR analysis, and single-point sampling, and are no longer considered as problems of PEM (see Melchior T. et al. /2014/ and Viertel M. et al. /2016/).

The pulse method opens up a broad field for the exploration of turbulent flows in tunnel cross sections at high Reynolds numbers. The first author plans studies on the Taylor diffusion of tracer pulses over long distances in exhaust ducts of road tunnels for later publication.

5. ACKNOWLEDGEMENTS

We would like to thank Marco Bettelini (Amberg Engineering), Urs Grässlin, Uwe Drost (both Lombardi Engineering), Petr Pospisil and Ludwig Ilg (both IP Engineering) for helpful technical discussions. For giving continuous scientific inspiration we are thankful to Peter William Egolf (HEIG-VD) and Alfred Moser (Science Services).

6. REFERENCES

Frei B. et al. /2016/; Measurement of Air Flow Rates in Evacuation Stairways of high-rise Buildings by Tracer Gas Methods; in Proceedings of the 12th REHVA World Congress Clima 2016, Aalborg May22-25, ISBN: 87-91606-36-5.

Frei B., Kägi A. /2010/; Recent Developments and Applications of Tracer Gas Methods in Road Tunnels; in Proceedings of the 5th International Conference Tunnel Safety and Ventilation, Graz 3. - 4. May 2010, ISBN: 978-3-85125-106-7.

Frei B., et al. /2012/; Determination of Ventilation Efficiency in Road Tunnels by using Tracer Methods; in Proceedings of the 6th International Conference Tunnel Safety and Ventilation, Graz 23. - 25. April 2012, ISBN: 978-3-85125-210-1.

GUM /1995/; Guide to the expression of measurement uncertainty, International Standardization Organisation, Geneva.

Lafarge Th., Possolo A. /2017/; NIST Uncertainty Machine, User Manual Version 1.3, National Institute of Standards and Technology, Gaithersburg MD, USA.

Grässlin U. et al. /2014/; Airflow Measurement in Road Tunnels; in Proceedings of the 7th International Conference Tunnel Safety and Ventilation, Graz 23. - 25. April 2012, ISBN: 978-3-85125-320-7.

Melchior T. et al./2014/; in Proceedings of the 6th International Symposium on Tunnel Safety and Security, Marseille 12. - 14. March 2014, ISBN: 978-91-87461-52-1.

Viertel M. et al. /2016/; Complex Commissioning and Quantitative Testing of the Gotthard Base Tunnel Ventilation System; in Proceedings of the 8th International Conference Tunnel Safety and Ventilation, Graz 25. - 26. April 2016, ISBN: 978-3-85125-464-8.

NEW METHODOLOGIES FOR VOLUME FLOW MEASUREMENTS IN DUCTS

Martin Viertel, Erwin Eichelberger
PÖYRY Switzerland Ltd.

ABSTRACT

Standards for measurements of fluid flow rate in closed conduits such as the ISO 3966 date back to the 1970's. This does not mean that the therein described methods loose validity nowadays, but it can be said that technology and therefore the possibilities have evolved since. Especially time and material costs when implementing for example the 25-sensor Log-Tchebycheff methodology limit its application potential.

This paper addresses a new methodology for volume flow rate measurements. It discusses the pros and cons of the method, which makes use of the combination of Computational Fluid Dynamics (CFD) with on-site measurements.

CFD computations are used to compute velocity profiles of a flow in the cross-sectional area of interest of the conduit. The simulation results are then used to define the suitable positions of measurement in the cross-section of the duct. The volume flow rate is calculated by multiplying the measured velocity with a factor dependent on the measurement location, derived by the preliminary CFD simulation. The required amount of velocity sensors is reduced to a minimum of 2, compared to the 25 sensors usually needed for a Log-Tchebychef measurement.

Iterative control mechanisms are described which minimize the error of the CFD results and therefore the resulting, calculated volume flow rate. The methodology is successfully put into practice and the results are compared to a Log-Tchebycheff grid measuring same volume flow rate in parallel. The comparison of the resulting volume flows shows a deviation of less than 4.62 % between the two methods.

Keywords: Fluid flow measurement, Log-Tchebycheff, Mercenier, CFD, Single Point measurements, exhaust duct commissioning

1. INTRODUCTION

Flow rate measurements in ducts are needed whenever a new tunnel is commissioned or when parts of the ventilation system have been replaced. The measurements have contractual binding. This means that the results have to be reliable, accurate and as best done by following prescribed established norms and standards (ISO 3966 [3], VDI/VDE 2640 [2]).

Traditional standardized more elaborate methods include the tracer gas method, the equal area method and, last but not least, the Log-Tchebycheff method (LTM).

All of the above methods are described in detail in [2]. These mostly time-consuming and expensive setups have been compared by Melchior et al. [4] in regards to accuracy, ease of setup as well as detailed pros and cons. As an example of complexity, the standardized Log-Tchebycheff method requires a minimum of 5x5=25 measurement points or sensors to yield plausible results.

In comparison to the more complex measurements above, single point measurements were also compared in [4]. As expected, higher deviations from results of the more elaborate methods were recorded.

This paper aims to demonstrate how the above methods can be simplified to a 2-point measurement (2SP) with accuracy comparable to LTM, with the help of CFD simulations.

2. WHY IS IT SO DIFFICULT TO ACCURATELY MEASURE VOLUME FLOW?

The flow velocity profile in ducts varies with the geometry of the duct, friction coefficient and last but not least by the flow rate itself. Also, similarity of the profiles between the different flow rates is *not always* given. See Figure **1** as an example for such measured velocity profiles within a duct.

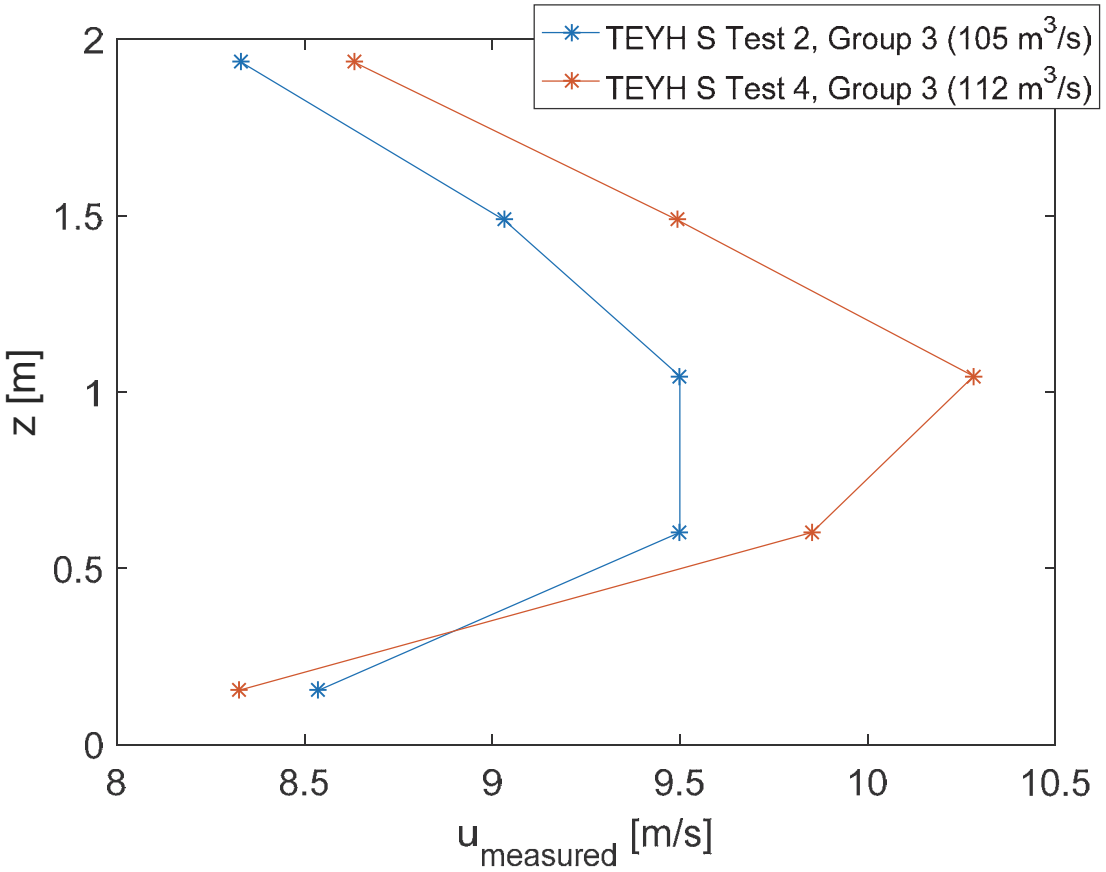

Figure 1: Example of measured velocity profiles in the same duct, in the same cross section for different flow rates

To determine the flow rate within a duct the real velocity profile has to be accounted for to determine the average velocity. This average velocity multiplied by the area of the measurement cross section results in the volume flow.

There are several options to find the average velocity and therefore the flow rate. One could increase the amount of flow sensors in the duct so as to cover all the "specialities" of the profile, or, make an assumption of the profile, which is then used or confirmed to determine the correct flow. The quality of the assumptions always has a direct impact on the end result.

3. NEW AND TRADITIONAL CONCEPT

According to Melchior et al. [4] the Log-Tchebycheff method (individual 25 point measurements) has excellent consistency, accuracy and repeatability. In conclusion of this paper it was though advised to correct the Log-Tchebycheff coefficients with a method developed by Mercenier et al. [1] to better account for the flow in the corners of the duct. The necessity of this correction stems from the standardized coefficients having been computed for rectangular cross sections and not for random shapes such as an exhaust duct of a tunnel.

Log-Tchebycheff with Mercenier correction (LTM) is an established standardized traditional measurement method for volume flows. It assumes a fully developed velocity profile in the duct

and determines, according to the geometry of the duct, the position of the measurement points as such, so that the average of the flows measured in these locations correspond to the average flow in this section of the duct.

The new concept presented in this paper is actually not new at all. The velocity profiles, which were previously assumed, are now computed with CFD simulations. The advantage of CFD is that one can account for the real 3D flow situation in the duct and is therefore not bound to trusting the assumption of a fully developed velocity profile as in the LTM method. Furthermore, all the specialties of the flow within the duct can be accounted for, such as upstream disturbances, obstacles, curves, friction coefficients, etc.

Once the velocity profile is "known" by CFD simulations, one could dare to only use 1 single measurement point to "fix" the correct profile, and therefore immediately know the flow rate.

This new method not only promises to have more accurate velocity profile assumptions, but also massively reduces the required amount of sensors or measurement points and therefore the time needed on site as well as the costs incurred.

4. INCREASING CERTAINTY OF CFD ASSUMPTIONS AND PROFILES

If the friction coefficient of the duct is not previously known, which is normally the case, it has to be assumed for the CFD simulations. In this case the CFD profiles will likely not be accurate and the flow rate measurements with 1 single measurement point will not yield satisfactory results. The influence of the friction coefficient on the resulting volume flow is estimated to be about 3%.

In Figure 2 we propose an iterative mechanism to check for the quality of the computed CFD velocity profiles and adjust the parameters accordingly.

The criterion of quality chosen requires a minimum of 2 single point measurements (2SP) to be installed. The volume flow $\dot{Q} = f(z, u_{measured}, \lambda_{friction})$ is a function of the position of where the measurements are installed z, the measured velocity $u_{measured}$ and the friction coefficient $\lambda_{friction}$. If the correct CFD profile was found, i.e. the correct $\lambda_{friction}$ was assumed, then $\dot{Q}_1 = f(z_1, u_{measured,1}, \lambda_{friction})$ should ideally be equal to $\dot{Q}_2 = f(z_2, u_{measured,2}, \lambda_{friction})$. So the criterion of quality of the CFD profiles is $\Delta\dot{Q}_{1,2} = \left|\dot{Q}_1 - \dot{Q}_2\right| \overset{!}{\Rightarrow} MIN$. Of course, this cross check can be expanded to act on more than 2 single point measurements as to give a "second or third opinion" about how good the CFD profile really reflects the actual profile.

To further eliminate faux pas, we suggest to choose the position of these two measurement points wisely. A good starting point is to place 1 point to where the maximum velocity in the cross section is suspected by the preliminary CFD simulation. This rule of thumb has the advantage of minimizing a positioning error, as the velocity change rate in this location with respect to location is usually minimal. Also, the fluctuations of the computed flow rate, and therefore the uncertainty in the measurement, are generally smaller in this position (smaller $u_{measured}$ results in higher multiplication factors B_{CFD} to find flow rate, see Chapter 5). On the contrary to the flow near u_{max}, the flow closer to the walls has a much steeper gradient, which in turn requires high precision in positioning the sensors, as every centimeter deviation from the planned placement results in strong deviations of the measured from the expected flow.

It should be mentioned that the here described new concept, as well as the standardized Log-Tchebycheff and equal area methods, requires a stationary, fully developed velocity profile. Therefore the measurement section should be at a reasonable distance from disturbances such as corners, restrictions, obstacles, etc. upstream of the flow.

5. WORKFLOW OF THE NEW CONCEPT

The following schematics shows the workflow concept of the 2 point volume flow measurement, based on CFD results. Herein summarized are all of the above mentioned tips and tricks.

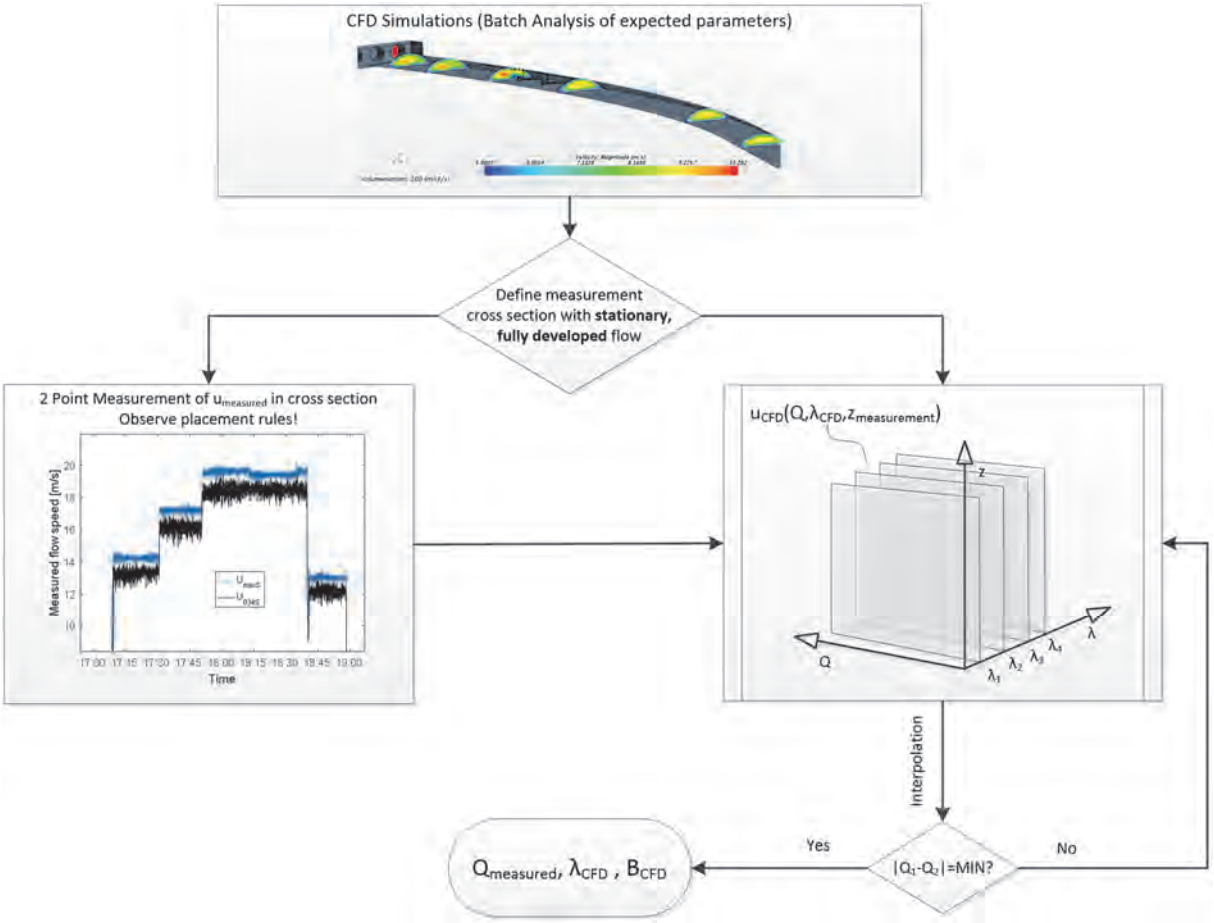

Figure 2: Workflow of the new concept of duct flow rate measurements

The proposed workflow results in the wanted flow rate of the duct $\dot{Q}_{measured} \cong Q_1 \cong Q_2$, whereas $Q_1 = u_{measured,1} * B_{CFD,1}$ and $Q_2 = u_{measured,2} * B_{CFD,2}$, the friction coefficient λ_{CFD} which *should* correspond to the actual λ_{duct} and $B_{CFD}(z)$ which is defined as the factor which multiplies $u_{measured,z}$ to get the flow rate $\dot{Q}_{measured}$. The latter factor is useful for repeated measurements in the future or quick online cross checks while measuring on site.

6. COMPARISON WITH LOG-TCHEBYCHEFF MEASUREMENTS

The new concept was applied in a couple of tunnels and compared to Log-Tchebycheff grid (LTM) measurements installed in parallel in the same cross section. The results are plotted in Figure 3.

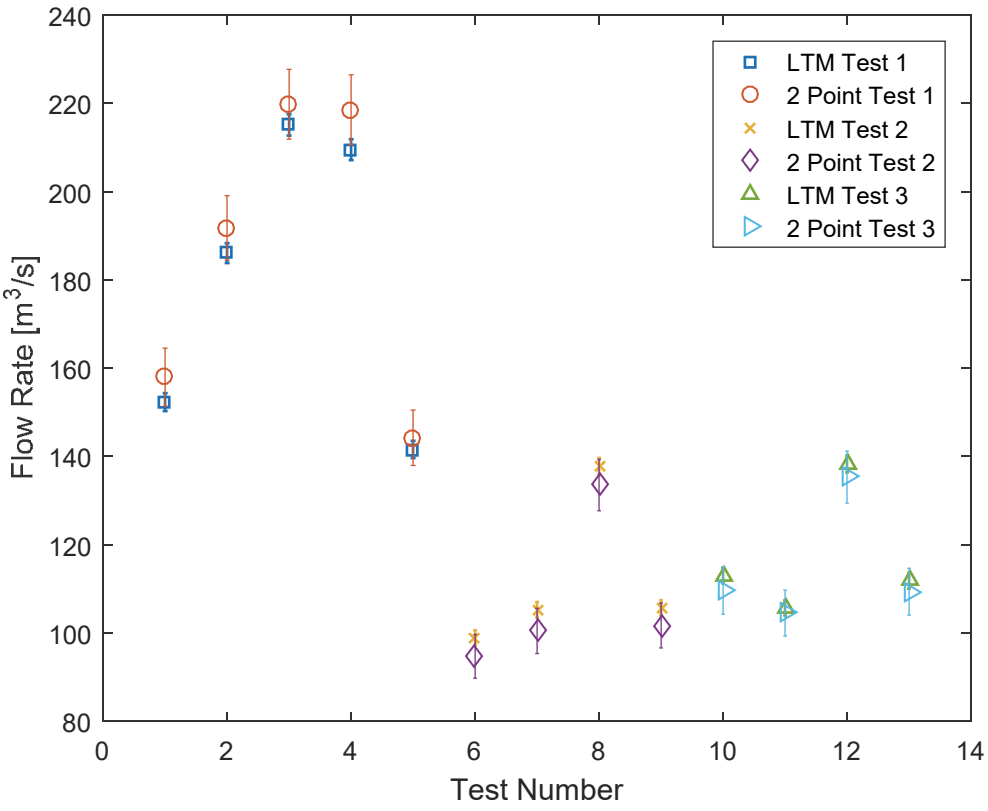

Figure 3: Flow rate result comparison between Log-Tchebycheff method corrected with Mercenier (LTM) and 2SP measurements with CFD profile assumptions. The error bars shown for the 2SP measurements indicate the 95%-confidence interval. This interval only includes errors propagating from measurement errors of the sensors.

The deviation of the 2 single point measurements from the LTM varied between +0.79% and -4.62%. The average deviation was found to be -2.01%. The partly non-stationary operating points of the exhaust fans lead to relatively high discrepancies in the measurements of tunnel 2 und 3 (Test 2, Test 3) which were not corrected for in the post processing of the LTM grid measurements shown here. Also, differences between cross section plans, essential basis for the CFD calculations, and the actual built tunnel sections could not be considered for the test cases 2 and 3. Minor corrections of the 2SP model could be done by scaling the CFD velocity profiles to fit the actual geometry.

All in all, good results were obtained as described above. The maximum 95% confidence interval (uncertainty, 1.96*standard deviation of the result) for the applied 2SP-Method evaluated over all measurements is ±2.88% of the measured volume flow rate.

Generally speaking, measurement errors when applying the LTM method are made by:

- Measurement uncertainty of the sensors
- LTM factors defined for rectangular cross sections and applied to random duct shapes (assumption of velocity profiles)
- Assumption of fully developed flow
- Error when positioning the sensors in the predefined locations by the LTM factors
- Calculation of the effective cross section area

Measurement errors made by the 2SP measurements are made by:

- Measurement uncertainty of the sensors
- Error when positioning the sensors

- Accuracy of the CFD velocity profile
- Accuracy of the geometrical model of the duct

The error of both methods can be compared by assuming both methods were executed with the same type of sensors. Disregarding the effect of wrong geometry, which influences both methods, the error of the 2SP measurements vary between ±1.91% and ±2.67%. As expected, the LTM measurements show a lower error between ±0.58% and ±0.88%. This difference is mainly due to the fact, that in the LTM method the resulting flow rate is an average of more single point measurements and therefore 1 outlier has less influence on the final result. 2SP measurements can be improved in this regard, by adding more sensors and averaging the resulting flow rate (see previous chapters) between them, effectively becoming "3SP" or "4SP" measurements.

7. PROS AND CONS OF THE NEW METHOD

The aim of the development of the here presented new concept of measurement is to minimize costs and time needed. Table 1 shows an estimate of the time and material costs per cross section to be measured. It is to be noted that the time needed for the 2SP measurements for preparation (CFD) and post processing do not scale with number of cross sections. It is estimated that for every further cross section to be evaluated the time for these tasks increases by a maximum of 10-20%. This results in significantly lower time costs when executing more than 1 cross section measurement. In addition the required time for the preliminary CFD simulations and the subsequent post processing can be further reduced due to the use of parametrized batch runs.

A resulting big advantage of this method over LTM, equal area and/or tracer gas methods is the "plug and play" kind of installation and post processing, especially when more than 1 or repeated measurements are needed.

Table 1: Time and material cost estimates for LTM grid measurements and 2 single point measurements. The estimate is valid for 1 cross section to be measured and for purchasing new sensors. Please note that this table is valid for 1 specific case. Measurements in further cross sections, if not done in parallel (for leakage measurements for example), do not require a new set of sensors.

	Cost [hours]		
Concept	**2 single point measurements**	**LTM grid measurements**	**Comment**
Preparation incl. CFD	17	12.75	Assumption: all plans needed are readily available.
Installation / per cross section	0.5	7	
Measurement / per operating point	0.17	0.5	
Deinstallation / per cross section	0.2	2.5	
Post processing	4.5	0.1	Conservative estimate
TOT	**22.4**	**22.85**	

	Cost [CHF]				Comment
Installation material	Fr.	150.00	Fr.	1,000.00	per cross section to be measured
Sensors	Fr.	1,100.00	Fr.	10,000.00	per cross section to be measured
TOT	Fr.	1,250.00	Fr.	11,000.00	

As well as costs, the accuracy and consistency of the method, as described above, is generally comparable to the LTM method.

A negative point of this method is that it heavily relies on the CFD results. We have shown quality control mechanisms to keep this from being an issue. Nevertheless, validated CFD codes and accurate geometry models must be used. Errors in the CFD calculations stem from incorrect ambient conditions, incorrect material properties, incorrect boundary conditions or more general errors like the size of the considered simulation domain.

It has to be remembered that the flow velocity in this method is only measured at 2 locations, therefore the CFD solution elsewhere has to be trustworthy. The 2SP method can be further expanded into a 3 or 4 point measurement without significant increase in time or material costs. This would increase the certainty of the results as described above.

8. SUMMARY AND OUTLOOK

In this paper we showed how the new concept of 2SP measurement using CFD profile assumptions is derived. In addition the presented method is compared to LTM grid measurements in the same cross section in 3 tunnel exhaust ducts.

The comparison showed that the new concept deviates from the results of the LTM by $Q_{LTM}{}^{+0.79\%}_{-4.62\%}$. In terms of consistency, accuracy and repeatability the method is comparable to LTM grids. The overall 95% confidence interval of the 2SP measurements is ±2.88% (uncertainty).

The error varies between ±1.91% and ±2.67% in the here presented test cases. As expected, the LTM measurements show a lower error between ±0.58% and ±0.88%.

The major advantage over LTM grid measurements is its time on site and cost efficiency as well as the ability to deviate from the assumption of a fully developed velocity profile which underlie the LTM method. Actual geometries, disturbances and further anomalies of the duct can be considered in the CFD simulations and therefore show a more accurate representation of the flow within the duct.

In the future this new concept, i.e. the processing, could be implemented in the anemometers, so as to be able to do the necessary iterations online and on site. The resulting flow rates would therefore be immediately available after or during the measurements, as it is the case when employing LTM measurements.

9. REFERENCES

[1] Mercenier, Patigny, Pirson, *Integration de la carte des vitesses dans une section driote d'une conduite - Extension de la methode Log-Tchebycheff pour les sections rectangulaires aux sections d'autre forme,* Societe Belge des Mecaniciens Vol. 28 – 1982, Dez. 1982

[2] VDI/VDE Richtlinien, *Netzmessungen in Strömungsquerschnitten – Allgemeine Richtlinien und mathematische Grundlagen (Blatt 1, Blatt 3),* Juni 1993

[3] ISO 3966:2008, *Measurement of fluid flow in closed conduits – Velocity area method using Pitot static tubes*, Second Edition, 2008-07-15

[4] Melchior, Ruckstuhl, Buchmann, *Comparative study of flow measurement methods in road tunnel exhaust ducts*, ISTSS 2014 conference proceedings, 2014

[5] JCGM 100:2008, GUM 1995, Evaluation of measurement data – Guide to the *expression of uncertainty in measurement*, First Edition, September 2008, www.bipm.org

REALIZATION OF SACCARDO NOZZLES AS MEANS OF LONGITUDINAL VENTILATION IN SACHSELN TUNNEL IN SWITZERLAND: AN APPLICATION EXAMPLE

Rehan Yousaf[1], Erwin Eichelberger[1], Samuel Gehrig[1],
Joachim Grossmann[2], Jürgen Steltmann[2]
[1]Pöyry Switzerland Ltd
[2]TLT-Turbo GmbH, Germany

ABSTRACT

In the framework of improving the safety of Sachseln tunnel in Switzerland, a 5 km long road tunnel, serving a two-way traffic receives an updated ventilation system comprising of a central exhaust fan and a set of Saccardo nozzles, located at each of the portals.

Although the concept of generating longitudinal flow by means of Saccardo nozzles in tunnels is not new, its use is not frequently seen in Swiss tunnels. As part of the commissioning process demanded by the "Swiss Federal Roads Office (German Acronym: ASTRA)", a numerical proof of concept for the Saccardo design was necessary.

The paper presented here is an application example that draws attention towards the implementation of Saccardo nozzles installed at the portals of the existing Sachseln tunnel. The aim of the conducted work is to recognize and exploit the optimization potential of Saccardo nozzles using 3-D **C**omputational **F**luid **D**ynamics (CFD) in an existing tunnel.

This study formed the basis of a cost-efficient and optimized implementation of the Saccardo nozzle ventilation in Sachseln tunnel.

Keywords: Longitudinal Ventilation, Saccardo nozzle, CFD simulation, proof of concept

1. INTRODUCTION

Within the maintenance project Tunnel Sachseln, the Sachseln tunnel shall be refurbished to comply with current guidelines, standards and specifications. The main refurbishments are a) provision of a safety gallery running parallel to the main tunnel and b) optimizing and supplementing the tunnel ventilation with new Saccardo nozzles at each portal. Saccardo nozzles are advantageous in cases with reduced tunnel height, increased tunnel availability requirements or in tunnels with an extremely corrosive atmosphere. However planning a comparable redundancy level as with jet fans, the number of the installed nozzles have to be doubled. Moreover, they need to be planned for both portals in order to counter both blowing directions. These installation demands can lead to corresponding increase in the investment costs. The purpose of this paper is to present an application example of a longitudinal ventilation in a Swiss road tunnel by means of Saccardo nozzles.

2. OVERVIEW

2.1. Tunnel Sachseln

The Sachseln tunnel has a total length of 5192 m. The longitudinal ventilation within the tunnel is realized by Saccardo nozzles. The Saccardo fans and relevant installations are installed in the newly built ventilation rooms located on the top of each portal. The accessibility of the new Saccardo buildings is independent of the tunnel traffic. It is important to note that the layout of the existing portals differ from one another. The north portal is equipped with a logistic niche whereas the south portal comprises of an open gallery on one side as shown in Figure **1**.

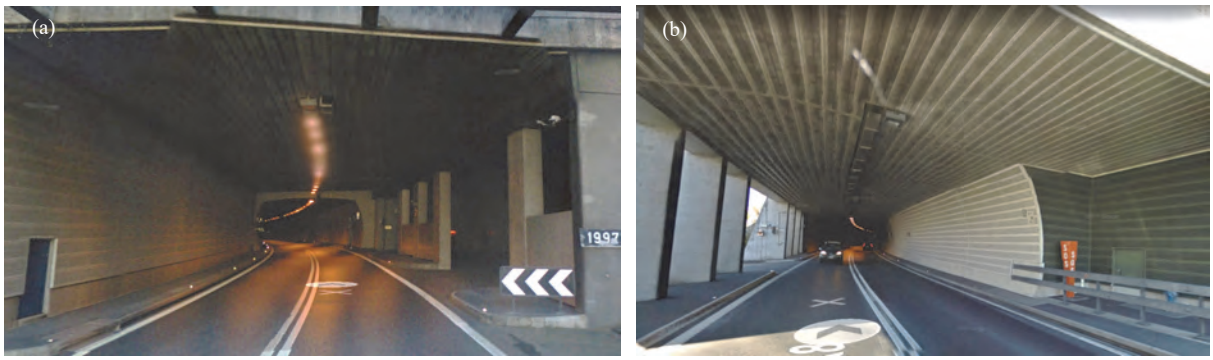

Figure 1: (a) Tunnel portal north, including logistic niche and (b) portal south, including open gallery (Source: Google Maps)

2.2. Saccardo nozzles

Saccardo nozzles, used for impulse ventilation are based on induction of one or more high-velocity jets into the tunnel. The kinetic energy of the high-velocity jet is transferred into the kinetic energy of slower-moving tunnel air. The efficiency of an impulse ventilation is limited due to the generated turbulence, friction losses of the high-velocity air near the walls and geometrical obstacles related to the tunnel geometry and traffic. Saccardo nozzles supply ambient air into the tunnel by fans situated in a fan chamber outside of the tunnel. A schematic layout of a Saccardo nozzle is shown in Figure 2.

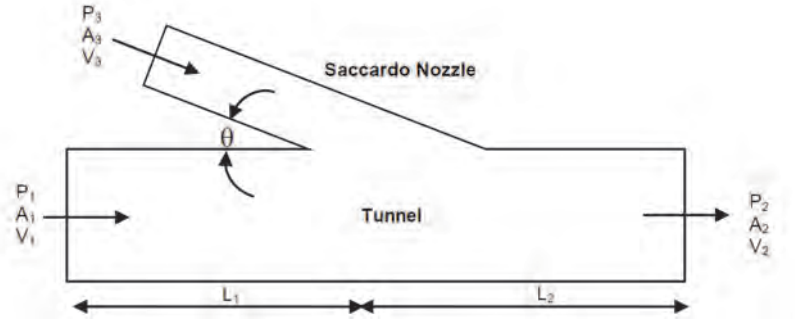

Figure 2: Schematic representation of a Saccardo nozzle

The following main parameters are relevant for the design of the impulse ventilation employing Saccardo nozzles:

- Nozzle cross section (A_3)
- Effective injection velocity (v_3)
- Injection angle (θ)

Due to the limited installation height above the tunnel clearance gauge, a rectangular nozzle geometry is often used. Ideally the injection angle should be such that the jet is fully aligned with the tunnel axis thereby maximising the potential thrust. The air jet should be prevented from getting attached to the tunnel surfaces (Coandă effect) resulting in unwanted additional frictional losses. An injection angle (θ) of approx. 10 to 30 degree is often recommended. The in-flow rate is limited by the appropriate and economic fan speed (the total power required increases as third power of the flow rate). In addition, the injection velocity is limited by the maximum flow velocity which acts on vehicles and people within the tunnel.

For the evaluation of the installation efficiency of Saccardo nozzles in the current project, the effective rise in the static pressure along the tunnel axis is evaluated. The following momentum exchange equation is used for calculating the installation efficiency (η):

$$\frac{p_2 - p_1}{\frac{1}{2}\rho v_2^2} = 2\frac{v_3}{v_2}\frac{A_3}{A_2}\left[\eta_j \frac{v_3}{v_2}\cos(\theta) + \frac{A_3}{A_2}\frac{v_3}{v_2} - 2\right] + \frac{p_3 \frac{A_3}{A_2}\cos(\theta)}{\frac{1}{2}\rho v_2^2} \qquad \text{Eq. 1}$$

It is important to note that while deriving the installation efficiency, a number of simplification and assumptions were considered (e.g. see references [1], [2], [4] and [5]) and therefore need to be appropriately considered while using the definition of installation efficiency as a criteria.

3. AIM & OBJECTIVES

Prior to the commissioning tests ASTRA demanded the contractor to provide a preliminary proof of the appropriate installation of Saccardo nozzles using 3-D CFD simulations. The original criteria of design performance was chosen to be the installation efficiency of 0.9. It is important to note that this value was an aimed value based on the simplified formula mentioned by F.Tarada [1] and Tabarra [2]. As the project evolved, this value was considered as secondary, the primary being the achievement of the required minimum thrust of 2400 N and the resulting minimum airflow of 2.8 and 3 m/s in the northern and southern tunnel cross sections respectively (as defined in revised project phase). The major focus of the work turned at investigating the current situation and taking appropriate measures to optimize the Saccardo ventilation (reduce pressure losses due to jet impingement and Coandă effect, improve operational design etc.). The aim was achieved by following objectives:

1. 3-D CFD numerical simulations to pre-assess and optimize the design of Saccardo nozzles for thrust and installation efficiency, thereby keeping the air velocity in the driving zone (2 m above ground) below 10 m/s.
2. On site commissioning tests to show the appropriate working of the Saccardo nozzles as predicted by the simulations with the optimized Saccardo design.

4. 3-D CFD NUMERICAL SIMULATIONS

In order to evaluate the geometrical effect of the Saccardo nozzles in Sachseln tunnel, the simulation domain considered the exit of the fan, the nozzles and a part of the tunnel including the portal region. The numerical domain geometrically modelled using AutoCAD Inventor 2014, meshed and simulated using the CFD software StarCCM+ [3].

4.1. Geometry & Mesh

The geometry of the complete Saccardo nozzle construction and tunnel section from the portal up to 300 m inside the tunnel was modelled as shown in Figure **3**.

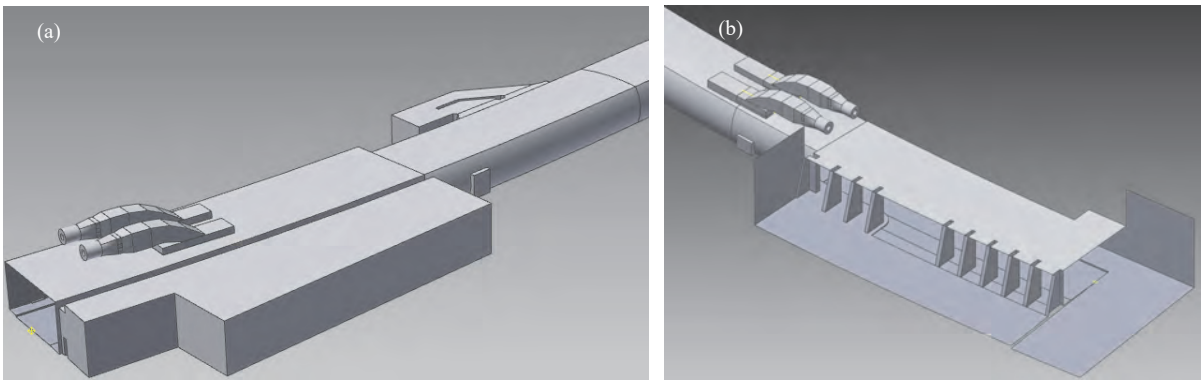

Figure 3: (a) CAD Model of north portal including niche and (b) south portal including open side gallery

For a sufficient representation of the jet flow conditions at the end of the Saccardo nozzle and within the adjacent niche and open gallery, the complete computational domain of each portal was meshed with approx. 10 million cells as seen in Figure 4.

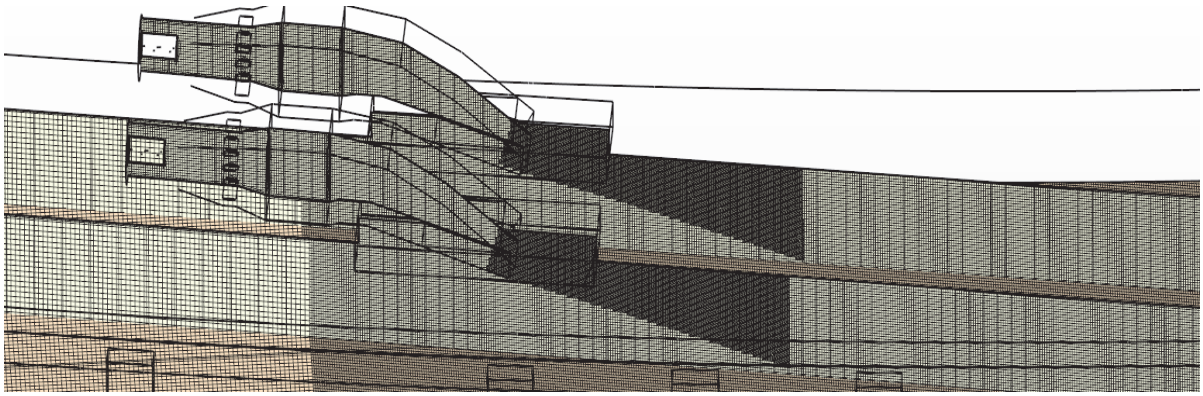

Figure 4: Example of the used mesh for the numerical calculation with local refinements

The computational grid is locally refined in regions with steep flow gradients e.g. near the nozzle. In addition to the local refinement, the wall boundaries have been resolved by "prism layers" to ensure accurate flow conditions near the walls. The validation of grid insensitivity was carried out using preliminary steady state simulations.

4.2. Boundary conditions

The CFD simulations for the numerical proof of Saccardo design are without consideration of thermal effects, portal pressure difference, wind pressure, traffic, etc. As an additional simplification, the swirl flow after the fan and the suction-side pressure losses are not taken into account. In the simulation model, only the volumetric flow of the two fans and the tunnel geometry are specified.

The following relevant boundary conditions were taken into account for the simulations:

Ambient conditions:	20°C, atmospheric pressure
Volume flow:	45.75 m^3/s per Saccardo nozzle
Fluid modelling:	Isotherm ideal gas, transient und steady state, (k-ε) turbulence model, two-layer wall model
Wall friction coefficient:	λ=0.015

The remaining variables are calculated as a result of the simulation. The influence of the pressure loss in the non-modeled tunnel section is taken into account with a corresponding pressure loss coefficient at the associated CFD system boundary.

4.3. Simulation Variations

In addition to the base case (planned situation), further variations were investigated in order to assess the influence of different parameters on the installation efficiency and the associated pressure/thrust increase. For the project, a total of 6 simulation variations were investigated. This paper presents only 3 of the 6 investigated simulation variations.

5. RESULTS

5.1. Variation 1: North portal, base case

The base case for the north portal includes the presence of the aerodynamically open side niche near the portal. The evaluation of the air flow shows a strong influence of the niche near to the Saccardo nozzles. In addition, the alignment of the nozzles seem not to follow the curved tunnel geometry (see Figure 5).

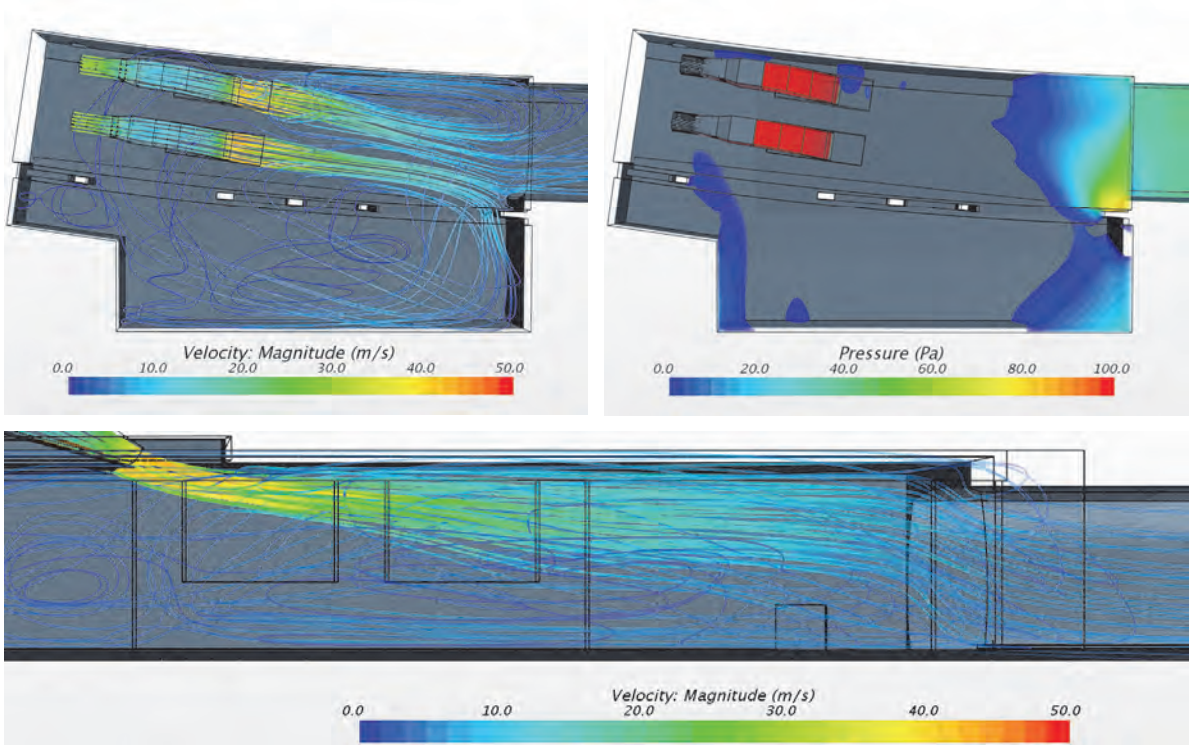

Figure 5: Streamlines of the injection jet and the resulting pressure rise (base case)

It can been seen in Figure 5 that the influence of the jet separation at the ceiling is not dominant onto the resulting airflow (i.e. less influence of the Coandă-Effect at ceiling) but due to the inappropriate horizontal jet alignment, the jet impinges the tunnel walls at the cross-section change. The evaluation of the pressure shows a non-homogeneous pressure development in the tunnel with local high pressure peaks at point of jet impingement. Based on the results, it can be stated that the alignment of the Saccardo nozzles and the non-uniform pressure development cause the jet to "get pushed" into the niche area, causing a vortex flow with a slight overpressure in the niche area.

The major base-case dependent parameter and results are given below:

Injection angle, θ:	23.5	[°]
Injection velocity, v_3:	38.2	[m/s]
Pressure rise within tunnel:	45.4	[Pa]
Generated thrust:	2156	[N]
Installation efficiency, η:	0.61	[-]

The rather low installation efficiency is caused by the unfavorable flow alignment of the nozzles, the open side niche and the pressure losses at the cross-section change after the open side niche.

5.2. Variation 2: North portal, design optimization

As a result of variation 1, improvements to the geometrical and operational design of the nozzle such as slightly rotating the nozzle along the vertical axis, increase the jet velocity and closing the side niche were investigated in further variations. The presented variation (variation 2) is a combination of an operational improvement i.e. higher jet velocity and constructional improvement i.e. closing the niche. The results are shown in Figure 6.

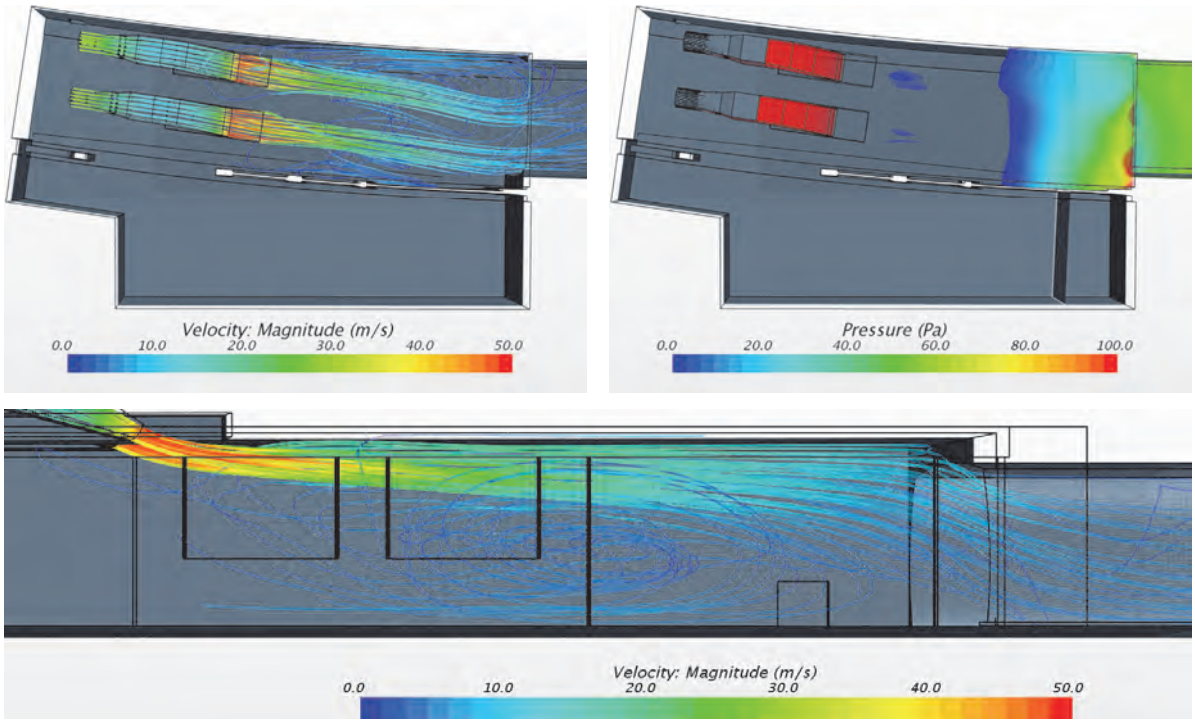

Figure 6: Streamlines of the injection jet and the resulting pressure rise (improved case)

In contrast to the base case, it can be seen that the pressure is built up at an earlier location and follows an even distribution but the unfavorable impingement at the tunnel wall at the cross-section change is still not completely rectified, instead the Coandă-Effect slightly increased due to higher jet velocity. The resulting air speed in the driving zone at 2 m above ground, remains below 10 m/s.

The major "optimized case" parameter and results are given below:

Injection angle, θ:	23.5	[°]
Injection velocity, v_3:	44.2	[m/s]
Pressure rise within tunnel:	59.0	[Pa]
Generated thrust:	2836	[N]
Installation efficiency, η:	0.69	[-]

The results show an increase of 30% in the generated thrust value and an increase in the installation efficiency of about 13% compared to the base case. The relatively low increase in efficiency is due to additional losses associated with the higher injection velocity.

5.3. Variation 3: South portal, base-case

The nozzle layout and operational parameter used in the optimized case for the north portal were employed to investigate the flow behavior at the south portal. The results are shown in Figure 7.

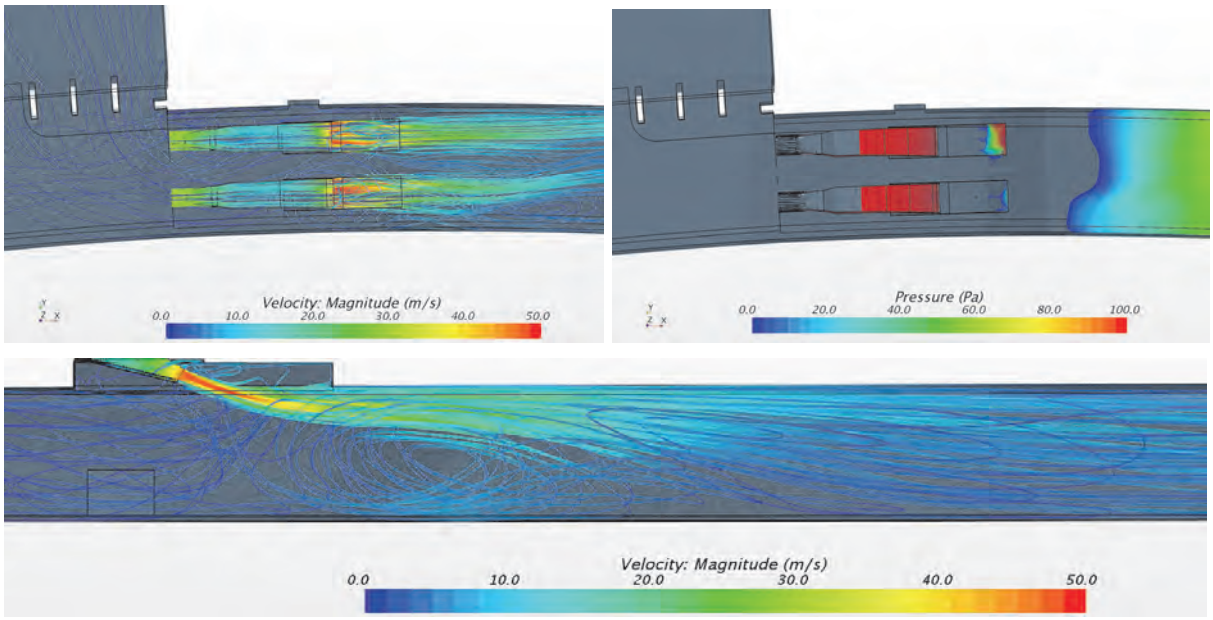

Figure 7: Streamlines of the injection jet and the resulting pressure rise (base case)

The results show that the open side gallery located prior to the Saccardo nozzles has a minor influence on the flow. The streamlines show that the supply air from the portal flows mainly through the first 3 open gallery sections and is then redirected into the tunnel. This fact leads to a non-uniform flow within the tunnel cross-section prior to the nozzle location. The evaluation of the pressure shows slight asymmetry and distraction of the jet leading to a local vortex generation. The flow is seen to be uniformly developed at about 150 m downstream of the nozzle outlets. The resulting air speed in the driving zone, 2 m above ground, remains below 10 m/s.

The major base-case dependent parameter and results for the south portal are given below:

Injection angle, θ:	23.5	[°]
Injection velocity, v_3:	44.2	[m/s]
Pressure rise within tunnel:	72.3	[Pa]
Generated thrust:	3506	[N]
Installation efficiency, η:	0.85	[-]

The lower installation efficiency in comparison to the expected value is caused by the unfavorable portal flow through the gallery. The efficiency is still higher compared to the north portal Saccardo nozzles due to no jet deflections and due to the absence of area change losses.

6. COMMISSIONING TESTS AND VERIFICATION MEASUREMENTS

In addition to the numerical proof of the installation efficiency, detailed flow measurements have to be carried out in the tunnel to demonstrate the achievement of the required flow and thrust conditions in the tunnel. At commissioning of the Saccardo fans, the contractor is obliged to measure the air flow speed in the tunnel. A measurement campaign with flow measurements at 25 grid points 300 m downstream of the Saccardo nozzles is planned. These grid measurements (log-Tchebycheff method) of the resulting air flow have to be according to the VDI 2640 and ISO 5802 standards. The planned date of these measurements is at the end of march 2018 and therefore cannot be presented in the paper. The comparison of the CFD results and the on-site measurements will however be shown at the 9th international conference ‘Tunnel Safety and Ventilation’ in June 2018 in Graz.

7. CONCLUSIONS

The results for the north portal show that by taking appropriate operational and construction measures i.e. increasing the jet velocity and closing the open side niche, the effective thrust could be increased by almost 30 % (2836 N) and the installation efficiency by about 13% (0.69) compared to the initial design. In order to reach an installation efficiency of 0.9 (following the efficiency definition in Eq.1), further constructional/operational measures need to be taken because of the unfavourable existing tunnel layout. The major of which being the adjustment in the alignment along the vertical axis to avoid the impingement of jet on the side wall and along the horizontal axis to reduce further the Coandă-effect.

At this point certain project constraints need to be considered. One of the major constraints being the already built ventilation building and the included openings in the floor of the ventilation building towards the tunnel (in tunnel ceiling). An appropriate alignment at this stage would have consequences such as additional internal pressure drops due to further installations (bends etc.), eventual non-uniformity in flow at the suction side of the fans (due to re-placement of fans), increase in Coandă-effect and possible increase in the air speed in the driving zone (> 10 m/s at 2 m above tunnel floor). All practicable, time and cost-efficient measures for the north portal, as accepted by the contractor and tunnel operators, were considered in the present investigation (adjusting the flow, closing of the niche etc.). It was seen that further optimization involve cost and time intensive measures.

The results for the south portal show that by employing the nozzle layout devised for the north portal, it is possible to achieve a thrust of 3506 N and an installation efficiency of 0.85.

Although some improvements and optimizations potential has been recognized as a result of the detailed 3-D numerical simulations, the proposed geometrical optimization and resulting improvement in the simulated thrust values were accepted by the concerned authorities.

The effectiveness of the numerical study is highly acknowledged by all the involved parties, especially the client as it helped them to check and “pre-optimize” their ventilation layout prior to the final commissioning tests (planned to be performed end of March 2018). In the absence of such numerical investigations as a “pre-study”, the optimization and rectification work after the commissioning phase might have led to cost intensive measures.

The work presented here shows the importance of involving numerical investigations already during the early project phases. The results show a strong influence of the considered tunnel layout and ventilation system onto the installation efficiency and therefore no generalities should be drawn for other tunnel layouts.

8. ACKNOWLEDGMENT

The authors would like to acknowledge the active support of all the involved parties, especially the ASTRA.

9. REFERENCES

[1] F. Tarada, R. Brandt, Impulse Ventilation for Tunnels – A State of the Art Review, AVVT13, New Brunswick, 2009
[2] M. Tabarra, R.D. Matthews and B.J. Kenrick, The revival of Saccardo ejectors – history, fundamentals, and applications, AVVT10, Boston, 2000
[3] STAR-CCM+ v12.04, Siemens PLM Software, https://mdx.plm.automation.siemens.com/star-ccm-plus
[4] P. Altenburger, I. Riess und R. Brandt, Control of longitudinal airflow in road tunnels in case of fire, ASTRA, Bundesamtes für Strassen, 2010
[5] David C. Wilcox, Basic Fluid Mechanics, 1st Edition, DCW Industries, Inc. 1997

STATISTICAL DISTRIBUTION OF AIR FLOWS IN RAIL TUNNELS AND RESULTING RISK OF FLOW REVERSAL DURING FIRE INCIDENTS

[1]Peter Reinke, [2]Matthias Wehner
[1]HBI Haerter AG, Switzerland
[2]HBI Haerter GmbH, Germany

ABSTRACT

In tunnels without mechanical ventilation, the movement of air is governed by pressure forces induced by the traffic, the underground aero-thermal conditions and the meteorological conditions outside the tunnel. Together, these forces may lead to different flow directions of air in the tunnel during normal operation. In case of a subsequent "hot incident" in an inclined tunnel, the heat of the fire causes a thermal draught, which superposes with the aforementioned pressure forces of normal operation. Depending on the strength and direction of the different forces, the heat of fire may turn a down-flow to an up-flow of air and smoke.

The flow direction of air and smoke affects the self-rescue, the evacuation and the fire-fighting activities in the tunnel. A change of the flow direction during an incident might become highly critical for the following reasons:

- Previously tenable egress and access paths become unexpectedly filled with smoke.
- Occupants and emergency services are suddenly exposed to non-tenable conditions, become disoriented and cannot identify the proper egress and access direction.
- The change in flow direction is accompanied by high flow velocities which disturb the smoke stratification and, thus, reduce the visibility in the incident tube.

In this paper, the possibility of changing flow directions in the event of a fire in a typical rail tunnel with monotonic inclination and without mechanical ventilation shall be presented. The results are based on one-dimensional simulations of the tunnel environment prior to fire. The daily and annual changes of the aero-thermal conditions of tunnels are considered. Statistical distributions of flow conditions for high-speed rail tunnels in Germany and France are given illustrating the impact of, for example, tunnel slope, ground overburden, weather conditions and train operation. The paper gives a better insight into the flow conditions prior to fire and the resulting possibility of changing flow directions during an incident.

Keywords: tunnel environmental conditions, natural thermal draught, flow reversal upon fire, rail tunnel incidents

1. INTRODUCTION

Most of the existing high-speed rail tunnels in Europe have the following features:

- Single-tube, twin-track layout
- Uniform, monotonic inclination
- Not equipped with mechanical ventilation

In such inclined rail tunnel tubes, the flow direction of air is influenced by the pressure differences induced by moving trains, outside wind acting on the portals, meteorological pressure differences across mountain rims and / or thermal draught due to the different average temperatures inside and outside the tunnel. Together, these pressures may lead to an up- or downflow of air in the tunnel during normal operation.

At the onset of a fire and the accumulation of hot smoke in the tunnel, the average tunnel air temperature increases. In the initial phase of a fire, the smoke propagation follows the prevailing air flow direction. After a while, the upwards directed, fire-induced pressure force might become dominant and the flow direction of the smoke/air may turn. Smoke may rapidly spread to other parts of the tunnel, which were smoke-free before. This change of flow direction occurs only if the flow of air and smoke is initially directed downwards. The change of smoke direction, the high flow velocities and the turbulence lead to the rapid mixing and entire filling of major tunnel sections by smoke. This typically unexpected smoke behaviour poses an additional threat for the egress and rescue activities in the event of an emergency.

In order to better assess this risk, a statistical analysis of the environmental conditions inside of rail tunnels is necessary. Quantifying the possibility of flow reversal requires the modelling of a tunnel's aero-thermal conditions for an entire year taking the train operation and the daily as well as seasonal changes of outside conditions into account.

2. OBJECTIVES

The range of pressure fluctuations and resulting air flows in a high-speed rail tunnel shall be determined. For this purpose, common features of tunnels and their operation conditions shall be identified. The aerodynamic and thermal conditions of these tunnels shall be modelled by varying key influential parameters considering their daily and yearly cycles. The parameters to be changed shall include length, inclination, rock/ground overburden, free cross-sectional area, train headway and train directions.

3. LIMITATIONS

Amongst others, the following aspects are NOT in the focus of this paper:

- Individual tunnels but generic cases only[1]
- All possible conditions and tunnels types but selected conditions and types only
- Pressures and air flows during immediate train passages but conditions shortly after trains have left the tunnel or have stopped
- Analysis of smoke propagation during fire incidents but of flow prior to incident only

4. MODELLING OF TUNNEL ENVIRONMENT

The environmental conditions inside a tunnel, i.e. the tunnel climate, are described, amongst others, by the temperature, the humidity, the pressure variations, the air velocity and the concentrations of dust, pollutants or natural gas. Heat from the ground, the technical installations and trains (traction power waste heat, air conditioning, etc.) influence the aero-thermal conditions. Additionally, the rate of air-exchange with the ambient via portals and shafts as well as the outside weather conditions determine the conditions inside tunnels (see Figure 1). The outside climate and the thermal behaviour of the ground are influenced by several parameters which vary from tunnel to tunnel. On the one hand, all these parameters would need to be evaluated for each individual tunnel. On the other hand, a categorisation of the tunnels allows insight into the dominant physical processes and a simpler extrapolation of results to tunnels which are not investigated in detail. Therefore, a generic analysis shall be undertaken by defining a reference case and variation of selected parameters.

[1] The work at hand forms part of the Franco-German research project REHSTRAIN (see Chap. 9). Therefore, the study is based on typical parameters of high-speed tunnels of France and Germany; [Krokos, Wehner, 2017a/b]

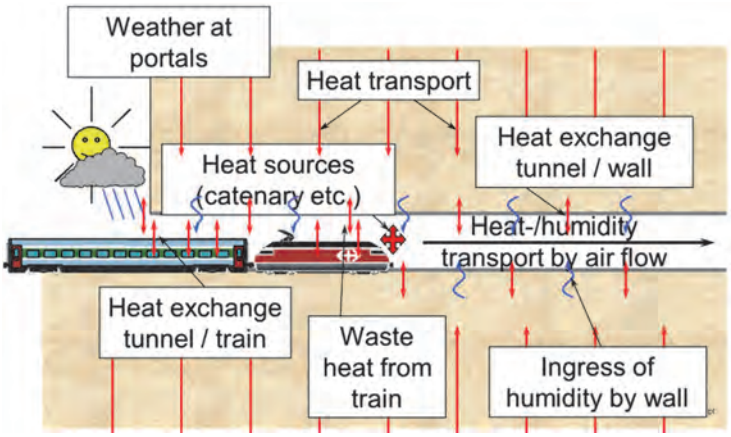

Figure 1: Factors affecting tunnel climate (tunnel environment)

Modelling the tunnel climate requires taking into account the following key phenomena:

- Pressure forces induced by moving trains and resulting motion of air
- Pressure forces induced by temperature/density difference between outside and inside
- Pressure force by meteorology (wind, pressure difference across mountain rims
- Heat and humidity transport by bulk motion of air including exchange of air at portals
- Heat sources in the tunnel (rolling stock, trackside equipment)
- Heat transfer between tunnel air, tunnel walls and surrounding ground/rock
- Heat transfer by condensation and evaporation of water at tunnel and train walls
- Heat transfer from and to trains

For the purpose of this study, the numerical codes THERMOTUN and THERMO are used:

- THERMOTUN (7) is a program for the simulation of aerodynamic and ventilation phenomena in rail and metro tunnels and based on the method of characteristics. Tunnel properties are modelled in a one-dimensional manner. The program allows modelling complex tunnel systems computing air velocities, pressure variations, traction power, temperatures, propagation of smoke and pollution in a tunnel. THERMOTUN is a development of Dundee Tunnel Research (www.thermotun.com).
- THERMO (2.1) is simulates the thermal conditions in rail tunnels. THERMO considers the thermodynamic interaction between trains, the tunnel air as well as the tunnel wall enabling the program to include heat transfer from the ground and the trains. Tunnel properties are modelled in a one-dimensional manner. The heat transfer in the surrounding rock is approached with a cylinder symmetric shell structure. When coupled with THERMOTUN the program includes the air-induced velocities and the heat load from trains (traction power, loss from catenary systems, auxiliary systems etc.). The computation of the humidity of tunnel air considers water ingress from the portals, the trains and the tunnel walls. The amplitudes of the yearly and daily temperature fluctuations at the portals are considered as well in order to provide a long-term analysis of the tunnel climate. THERMO is a development of HBI (www.hbi.eu).

In THERMOTUN and THERMO, the simulation domain is split into discrete elements. In THERMO, the tunnels are divided into segments and tranches, the latter being a subdivision of the former. The surrounding rock is divided into (generally) axisymmetric shells. The length of a shell is identical to the length of the tranche it belongs to.

THERMO is based on a forward Euler discretization using an explicit procedure. While this procedure imposes constraints on the ratio of the time step to the spatial step to ensure convergence, this constraint does not pose any problems for typical tunnel applications.

5. COMBINATION OF THERMOTUN AND THERMO BY MATLAB

In order to simulate the varying aero-thermal conditions in rail tunnels for a complete year, different time scales need to be considered:

- Simulation of the train aerodynamics requires high temporal resolution ("in range of less than seconds") resulting in long computation time.
- Simulation of the tunnel environment requires low temporal resolution ("in range of hours") resulting in short computation time.
- Simulation of an entire year of tunnel operation for calculation of the distribution of up- and downwards directed thermal draught flows requires low temporal resolution ("in range of hours"), however, resulting in long computation time to cover a whole year incl. several years for prior convergence of the ground temperature distribution

The different simulation tools are integrated by MATLAB to the scheme shown in Figure 2.

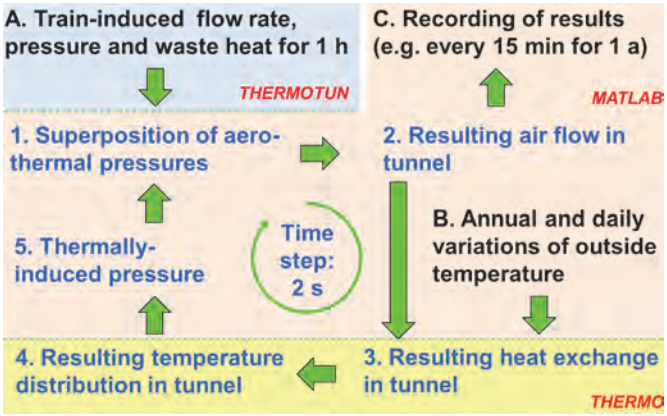

Figure 2: Loop of simulation using THERMOTUN, THERMO and MATLAB

The scheme allows an efficient computation of the tunnel environment considering the different relevant time scales and the purpose of the computations.

6. ASSUMPTIONS AND COMMON DATA

Assumptions and key parameters used for all simulations are given in Table 1 and Table 2.

Table 1: Assumptions for all calculation cases

Parameter	Assumption
Tunnel height profile / vertical alignment	Constant slope
Tunnel rock/ground overburden	Constant and uniform
Rock/ground properties (e.g. heat conductivity)	Constant in radial and longitudinal direction
Wind or barometric pressure difference on portals	None
Rock initial temperature profile	Constant along length
Outside temperature profile	Annual + daily sinusoidal curve
Train operation	Passenger trains with constant headway and velocity

Table 2: Constant parameters for all calculation cases

	Parameter	Data	
Ambient	Normal pressure at sea level	101.3	kPa
	Elevation above sea level	300	M
	Medium yearly outside temperature (Kassel/Lyon climate)	11.25	°C
	Annual amplitude	+/- 8.0	K
	Daily amplitude	+/- 3.5	K

	Parameter	Data	
Tunnel	Wall friction factor (Darcy-Weisbach)	0.021	---
	Wall density (concrete)	2000	kg/m³
	Wall heat capacity (concrete)	880	J/kg/K
	Wall heat conductivity (concrete)	1.0	W/m/K
	Water seepage	0	g/km/s
	Equipment heat release	70	W/m
	Sum of pressure loss factors for both portals	1.6	---
Ground	Density	2700	kg/m³
	Heat capacity	800	J/kg/K
	Heat conductivity	3.0	W/m/K
	Water seepage	None	
Train	Reference train type	Hypothetical multi-unit as 2-unit ICE3	
	Overall length	400	M
	Cross-sectional area	11	m²
	Perimeter	11.5	M
	Surface area	4600	m²
	Travel speed	250	km/h
	Skin friction factor (Darcy-Weisbach)	0.012	---
	Nose and tail loss coefficients	0.05 / 0.07	---
	Rolling resistance factor	0.00075	---
	Mass	900'000	kg
	Thermally active mass	60	% of mass
	Body heat capacity	450	J/kg/K
	Temperature at entry	Equal to outside temperature	
	Maximum traction power	16	MW
Kassel (D) and Lyon (F) taken as representative locations of the French-German high-speed rail networks.			

The objective of the numerical analysis is to study the sensitivity of the results regarding the main influential factors. A reference tunnel with standard train operation is defined. For the purpose of studying the sensitivity of results, variations from the reference case are introduced (see Table 3). All chosen parameters are based on the analysis of the typical range of tunnel parameters and typical parameters of trains and train operation.

Table 3: Variable parameters of the calculation cases

Parameter	Reference case	Variations
Tunnel length	3.0 km	1.5 km, 5 km, 7 km
Free cross-sectional area	80 m²	40 m², 60 m², 100 m²
Hydraulic diameter (coupled with cross-sectional area)	9.18 m	6.45 m, 7.95 m, 10.26 m
Inclination	1.25 %	0.5 %, 3 %, 4 %
Average uniform height of ground overburden	75 m	25 m, 150 m, 300 m
Initial ground temperature related to overburden height	13.5 °C	12 °C, 15.75 °C, 20.25 °C
Traffic type	Twin-direction	Single-direction
Number of trains	3 per h and direction	2 per h and direction
Traffic headway (coupled to number of trains)	20 min	30 min
Traffic staggering for opposite directions	10 min	15 min
Operating time per day	24 h	20 h

7. RESULTS

7.1. Aero-thermal conditions during a year of operation

Selected results are shown in this section in order to illustrate the steps during the analysis. Figure 3 shows the train induced-pressure fluctuations and resulting longitudinal air flow in the middle of the tunnel for the reference case during 1 h of train operation, i.e. with 6 train crossings with alternating direction. The results do not include any other impact, e.g. no impact of thermal draught, wind at portals, shafts, crossovers, etc. At individual tunnels, these other effects might become influential as well.

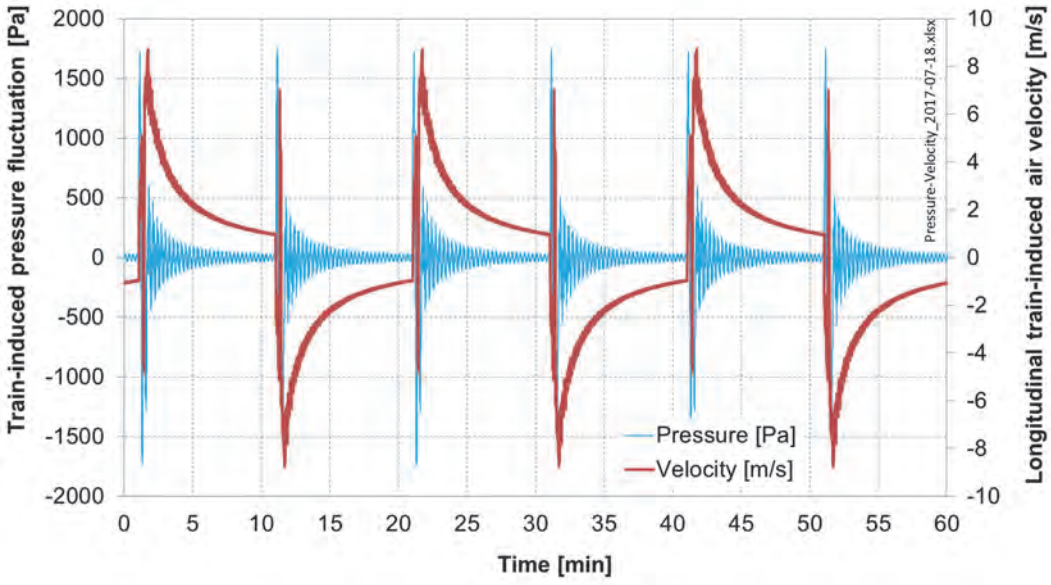

Figure 3: Pressure and longitudinal velocity of air in middle of tunnel (bi-directional traffic with 20 min headway for each direction)

The pressure patterns obtained with THERMOTUN as shown in Figure 3 are used as input for the computation scheme according to Figure 2. Here, the train-induced pressures are superposed with the thermal draught pressures and other meteorological pressures, if any. Two exemplifying results showing the averaged tunnel temperatures resulting from THERMO are shown in Figure 4 and Figure 5:

- Figure 4 shows the impact of tunnel length on the tunnel air temperature. As a general rule, the longer the tunnel is, the higher the temperature. In shorter tunnels, the daily and yearly oscillations of the temperature cover a larger range than in the longer tunnels.
- Figure 5 shows the impact of tunnel slope on the tunnel air temperature. Steeper tunnels lead to higher temperatures and the daily and yearly oscillation of the temperatures cover a larger range.

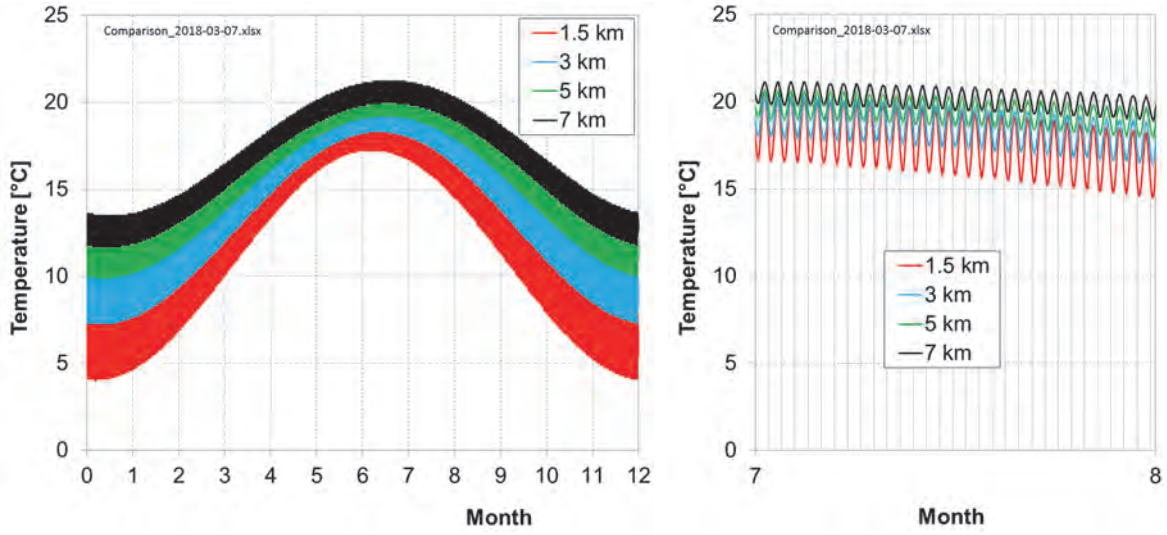

Figure 4: Average tunnel temperature for different lengths (left: 1 year; right: August only)

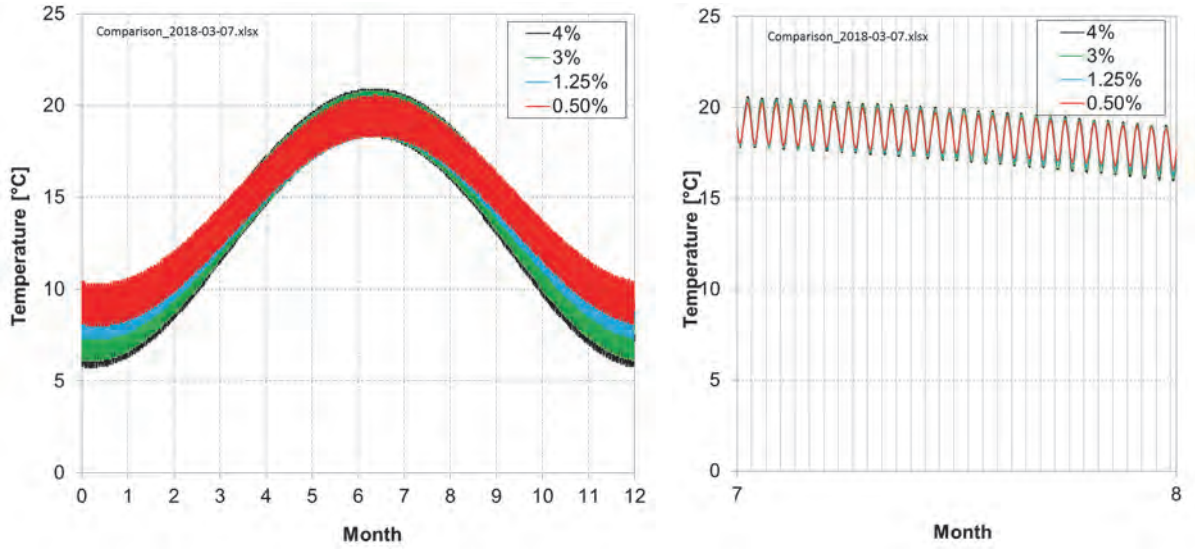

Figure 5: Average tunnel temperature for different slopes (left: 1 year; right: August only)

7.2. Resulting natural flow of air

For the statistical analysis, the flow velocities are taken at fixed time steps. In order to reduce the impact of velocity fluctuations during the immediate passage of a train, the flow velocity prevailing immediately before train entry is monitored for the statistical evaluation.

According to Figure 6, the shortest tunnel of the analysis (1.5 km) exhibits a downflow of air for approximately 40% of the operation time. With an increasing length of tunnels, the proportion of operation time with natural downflow of air decreases. The tunnel gradient supports extreme up- or downwards directed air velocities, however, the slope has no considerable impact on the frequency of up- or downflow.

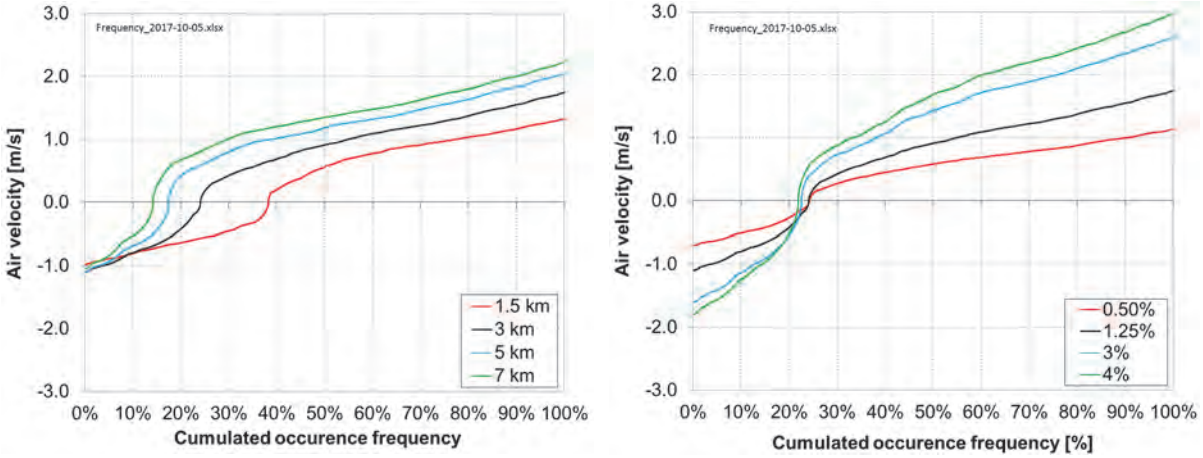

Figure 6: Occurrence frequency of natural air flow for different tunnel lengths and slopes (left: variable tunnel length; right: variable tunnel inclination)

In addition to the results for different lengths and slopes of the tunnel as shown in Figure 6, further parameters were analysed. Together, the consequences of these variations from the reference case on the natural flow in the tunnels are summarized in Table 4.

Table 4: Impact of varying tunnel parameters on natural flow (Parameter range of Table 2)

Variation of parameter	Impact on downflow (thermal draught to lower portal)
Increasing length of tunnel	Decreasing proportion of downflow; more extreme velocities
Increasing slope of tunnel	Almost no influence on proportion of downflow; more extreme velocities due to increase of "driving height" for draught
Increasing free cross-sectional area of tunnel	Slight increase of proportion of downflow; slightly more extreme velocities due to smaller flow resistance
Increasing ground / rock overburden	Decreasing proportion of downflow; almost no impact on velocities; Higher temperature due to higher overburden
Traffic "2 tracks up- and downhill" to "downhill only" to "uphill only"	Increasing proportion of downflow; almost no impact on velocities; "2 tracks up- and downhill" leads to lowest air-exchange and highest tunnel temperatures on average
Longer headway	Slight increase of proportion of downflow; no impact on velocity; "Longer headway" means less heat release from trains
"Traffic" to "No traffic"	Increasing proportion of downflow; no impact on velocity; "No traffic" means no heat release from trains
"20 h" or "24 h" operation	No significant impact
Modelling of ground / wall properties	Adiabatic walls: almost 50 % of operation natural downflow; "Isothermal wall" (wall at average annual outside temperature) about 30 % of operation with downflow; "Axisymmetric shells": about 25 % of operation time with natural downflow.

8. CONCLUSIONS AND SUMMARY

For the statistical distribution of natural air flows in rail tunnels prior to an incident and for the range of parameters investigated in this study, the following is noted:

- Short tunnels with small rock/ground overburden are likely to experience downflow.
- Longer and steeper tunnels experience higher natural flow velocities.
- The ground modelling (adiabatic, isothermal, etc.) has an impact on the flow statics.
- Fires in tunnels with natural ventilation include for substantial parts of operation time the risk of flow reversal (up to about 40 % of yearly operation time).
- Flow reversal as additional risk of fire incidents in inclined tunnels without mechanical ventilation should be considered as part of the fire safety assessment.

9. ACKNOWLEDGEMENT

The support by the French National Research Agency (ANR) and German Federal Ministry for Education and Research (BMBF) as part of the research project "REsilience of the Franco-German High Speed TRAIn Network" (REHSTRAIN) is gratefully acknowledged.

10. REFERENCES

E. Krokos, M. Wehner (2017a), Joint research project REHSTRAIN, "Analytical and Numerical Evaluation of the Initial Aero-Thermal Conditions in Tunnels – Milestone Report", 19.07.2017

E. Krokos, M. Wehner (2017b), Joint research project REHSTRAIN, "Analytical and Numerical Evaluation of Fire Events in Tunnels – Milestone Report", 29.09.2017

DYNAMIC TUNNEL MODEL – CURRENT PRACTICE

Axel Bassler, Roman Felix,
Nabla Engineering, Switzerland/Germany

ABSTRACT

A tunnel model programmed in the mathematical platform Matlab/Simulink enables a smooth development of a uniform and comprehensive work tool for all planning and operational phases. The tool can be universally applied during the entire lifecycle of the tunnel structure:

- Dimensioning of the ventilation system
- Control design
- Approval of ventilation controls in coupling with SPC
- Generation of risk analyses
- Optimization of the ventilation system in operation

The added value of a digital tunnel ventilation model is demonstrated in a tunnel put into operation in Germany in 2016 (1.8 km two-way traffic) in comparison to the conventional methods. The impediments to the application of these tools no longer exist in the technical and practical realization but rather predominantly in the traditional project planning procedures.

The public procurement frequently builds on traditional service concepts. Innovative approaches which particularly alter the timing of services and the concepts of the services themselves can thus only succeed if the boundary conditions for the application of these approaches are created by the client.

Keywords: tunnel model, design of ventilation, design of ventilation control, initial operations, risk analysis

1. INTRODUCTION

The aerodynamical and ventilation technical features of a tunnel can be described mathematically well in the well-known, defining flow-mechanical equation for the conservation of mass, momentum and energy. A static approach to states of equilibrium continues to present an adequate method for simple longitudinal ventilation systems without regulation. More complex ventilation systems that include control engineering elements, however, require a dynamic approach to the conditions. While a static approach to states of equilibrium with simple mathematical tools (e.g. table calculations) is still realizable, the dynamic and thereby transient approach to the flow conditions requires a solution of coupled differential equations in time and space. The application practice exhibits that a description of the ventilation technical phenomena in one-dimensional formulation is sufficient for the usual questions.

In the concrete case, the resulting differential equations are programmed in Matlab/Simulink and combined in a corresponding tunnel model. The tunnel model then represents the flow-mechanical properties of the actual tunnel. In this way, relevant mathematically-supported analyses and tests of the tunnel are possible in the planning phase as well as during the initial operation and in subsequent operation.

The mathematical platform Matlab/Simulink selected for the realization enables the easy use of the tunnel model for the most diverse cases of application. The tunnel model can be directly applied in the design and dimensioning of the tunnel ventilation system (NablaVent). Furthermore, the use of the tunnel model is very simple possibility for the design of the closed loop system with Simulink (NablaControl) (see Figure 1).

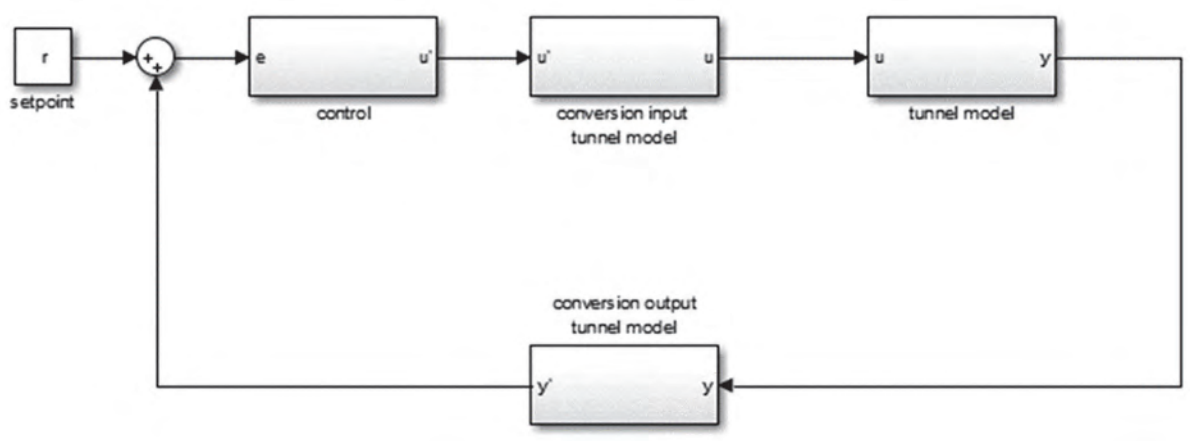

Figure 1: Block diagram image of the closed loop with the tunnel model (controlled system)

In another application, the tunnel model can be connected directly with the SPC responsible for the control via a corresponding interface in the program platform. The strength of the interfaces available in the mathematical platform is evident here in the industry standard. This application is very helpful in the course of the initial operation of tunnel ventilation systems.

Last but not least, the complete closed loop of the ventilation system can be integrated in a risk analysis tool (NablaRisk) also programmed in the mathematical platform Matlab. With this, it is guaranteed that the flow calculations used in the risk analyses will conform to the actual conditions installed in reality.

2. DESCRIPTION OF THE TUNNEL

The practical application of the tunnel model has proved worthwhile until now. For example, it was implemented in the applications described above in a tunnel set in operation in 2016. This tunnel, located in southern Germany, is a 1.8 km long tunnel for two-way traffic. The middle incline of the tunnel is 2.1 % eastwards. Both tunnel zones near the portals were built using a cut-and-cover method with a length of 80 m on the western side and a length of 126 m on the eastern side. The mined section between these exceeds a length of 1590 m and is fitted with a suspended ceiling. The tunnel cross-section in the suspended ceiling section is approximately 49 m^2 and in the section with jet fans (without a suspended ceiling) is approximately 62 m^2.

The tunnel has a smoke extraction system with controllable smoke extraction flaps. Jet fans are positioned in two groups at the east portal to influence the longitudinal air flow. While the jet fans in the groups near the portal (SVG2) are continuously adjustable by means of a frequency converter, the jet fans of the other group (SVG1) are simply switched on or off.

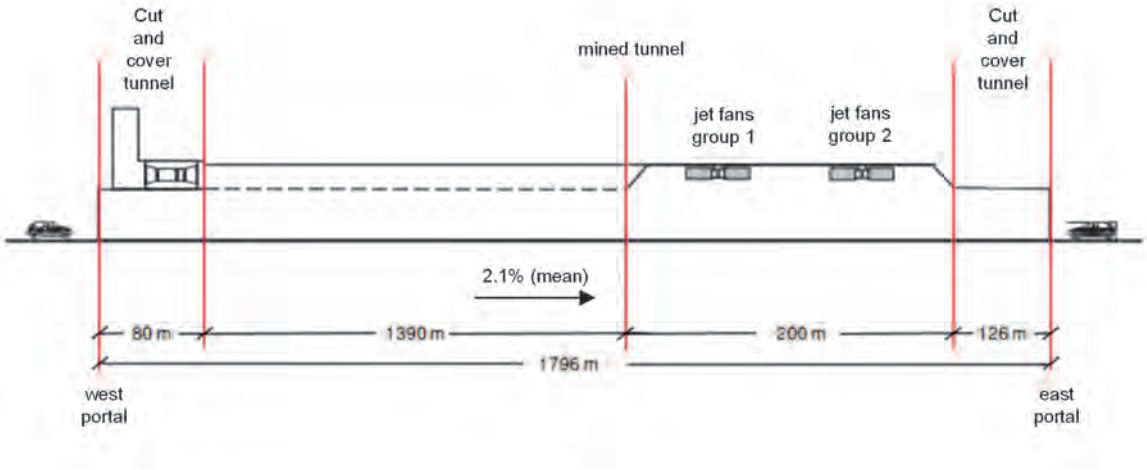

Figure 2: Configuration of the tunnel studied

The tunnel has a total of 5 emergency exits with a distance of 300 m between each. The emergency exits NA1 to NA4 lead to a single rescue tunnel running westwards parallel to the tunnel tube. The emergency exit NA5 leads directly into the open through a separate escape tunnel. The rescue tunnels are equipped with a positive pressure ventilation system which is used during both normal operation and in the event of fire.

3. DIMENSIONING OF THE VENTILATION SYSTEM AND CONTROL DESIGN IN THE EVENT OF FIRE

A mathematical description of the flow-mechanical properties of the tunnel is required the calculations for both the dimensioning of the ventilation system and for the control design. The transient Bernoulli equations are essentially applied for this. The non-linear differential equations resulting from this compare the sum of all impulse entries arising from the various influences with the flow velocity.

The pressure effects of the jet fans, the friction (wall, vehicles), the pressure loss at entries and exits, the extraction points and the thermal fire stimulants are taken into account. The thermal fire stimulants are additionally released through the 1-D energy equation for the balancing of the heat flows relevant to the temperatures in the tunnel. The fire itself is modelled as a heat source with thermal power that varies in time.

The realization of the simulation model occurs in Matlab/Simulink. This program includes a commercial software, The MathWorks Inc., for numerical calculations. The numerous toolboxes are a great advantage of the software. Thus, it is, for example, possible with the OPC Toolbox to directly link the simulation model with an SPC.

The dimensioning of the ventilation led to the installation of two axial ventilators with an extracted quantity of 110 m^3/s each with a total pressure of approximately 3200 Pa. The axial ventilators are equipped with electric motors with a motor nominal capacity of 500 kW. The axial ventilators with fixed blades are constantly controlled by frequency convertors. The necessary partial load points can be started up without difficulty in normal operation. Three frequency convertors are principally available as a result of redundancy observations. In the event of fire, the frequency convertors serve only as a starting aid. The axial ventilators are directly connected to the network through an electrical bypass once the nominal speed has been reached.

A total of 7 type 1120 jet fans with a static thrust of 1150 N and a motor nominal capacity of 30 KW are installed in two jet fan groups.

In the event of fire, the fumes are extracted out of the driving area by the smoke extraction flaps if the fires are located in the suspended ceiling area. To compensate for the asymmetries (location of fire, wind pressure, resistance in the tunnel), jet fans are activated to influence the longitudinal air flow if necessary. The objective is to attain a bilaterally symmetrical as possible inflow to the location of the fire. In the sections near the portals, a clean longitudinal air flow comes from the jet fans whereby the maximum velocity of the air flow is adjusted to a target value of 1.5 m/s towards the portal.

A PID controller with an anti-windup and a low-pass filter for the differentiator is used for the ventilation control (see block diagram image below).

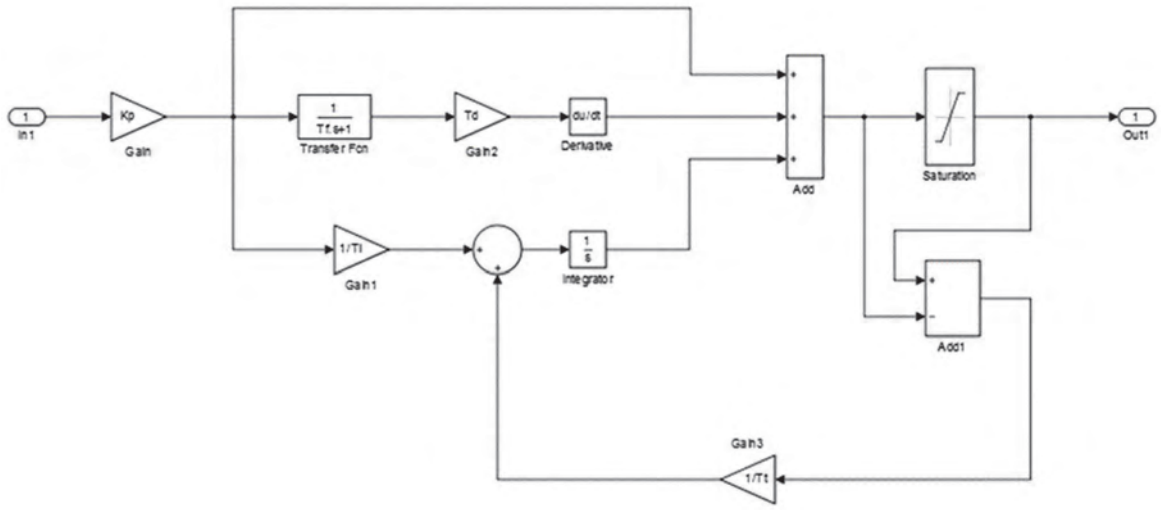

Figure 3: Block diagram of PID controller with anti-windup and low-pass filter

Although the non-linear model of the tunnel describes the dynamics of the tunnel air flow well, it is not suitable for the traditional design of controllers on account of its non-linearity. Therefore, a linearity of the model is necessary. It is clear that the linear model of a low-pass of the first order with dead times illustrates a sufficiently good approximation of the actual conditions for the tunnel.

- $P(s) = \frac{K}{1+\tau*s} * e^{-\theta*s}$

with:

- K: Strengthening of the system [-]
- τ: Time constant of the system [s]
- θ: Dead time for the system [s]

The parameters of the linear model can be simply, quickly and reliably defined for both extraction and longitudinal air flow conditions by means of a regression procedure and a simulated jump method in the dynamic tunnel model.

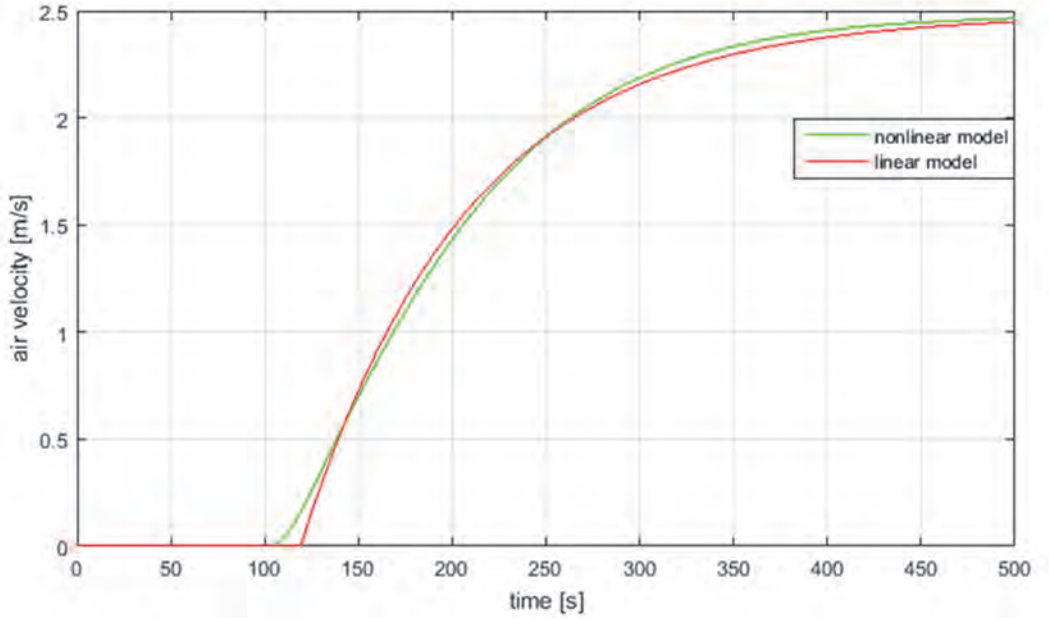

Figure 4: Behavior of the linearized model vs. the exact model for the extraction.

Line segments with dead times lead to an additional phase shifting and thereby to a reduction of the phase reserve. This can result in strong overshooting or instable behavior. The IMC (internal model control) structure explicitly recognizes the dead time. The error signal of the controller is released from the predicted dead time which leads to very good design results. Furthermore, the IMC structure can be mathematically traced back to a standard PID controller. The return of the IMC structure to a PID controller provides the advantage that the controller still only exhibits a design parameter of λ_{IMC}. The design parameter is also accessible to the intuition. With rising λ_{IMC}, the robustness of the system increases and agility simultaneously decreases.

The analysis of the closed loop with respect to stability and robustness as well as the command action and disturbance behavior occurs mathematically with the variation of the design parameter λ_{IMC} on the model of the closed loop.

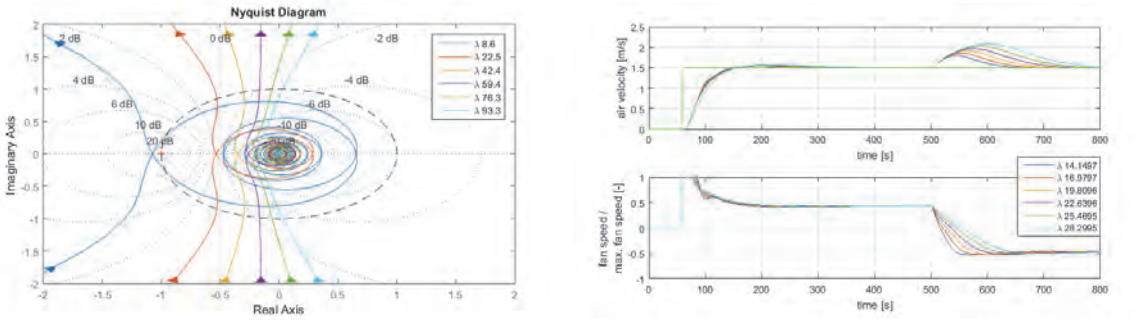

Figure 5: Stability analysis (Nyquist Diagram) and management and disturbance behavior

The controller settings could thus already be determined and verified for the tunnel in a numerical method long before the initial operation. It becomes clear in the course of the initial operation that the numerically ascertained control parameters were better suitable than the parameters derived from the jump functions in the actual tunnel. The disturbance-free design in the model appears to be significantly preferred here.

Table 1: Recommended Control Parameters for the PID Controller

	λ_{IMC}	*Kp*	*Ti*	*Tt*	*Tf/Ts*	*Tt*
Longitudinal Ventilation	43.7	3.1	115	12	8.4	37.2
Extraction	22.5	4.1	61.8	4.9	3.0	17.4

4. APPROVAL OF THE VENTILTION CONTROL IN COUPLING WITH THE SPC

In the course of the preparation of the realization specifications, the executing company approached the building contractor with the request to allow the adaption of the controller structure already stipulated in the building contract to the SPC to be operated in the realization. This request was approved subject to the proof of the equivalence of the solution. The proof was produced in a coupling of the SPC intended for the tunnel with the already available tunnel model. The ventilation control programmed in the SPC could then already be tested in the factory and months before the installation in the tunnel.

The coupling of the tunnel model with the SPC occurred via the OPC interface in Matlab. Because this interface represents the industry standard, the communication between the SPC located in the manufacturer's factory and the tunnel model located on a PC could be established.

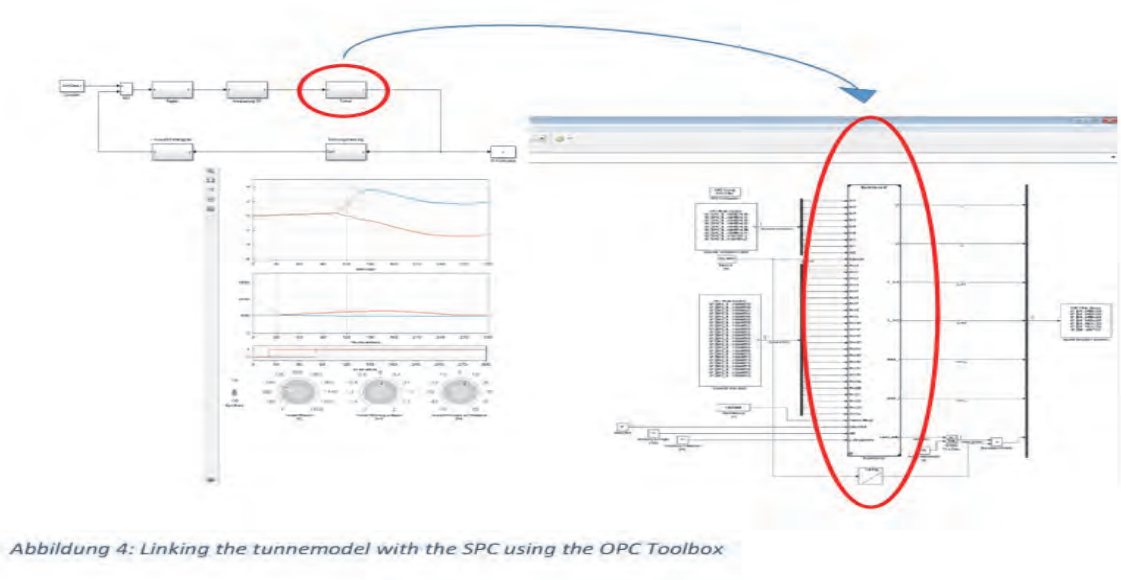

Figure 6: Coupling of the tunnel model with an SPC

5. RISK ANALYSIS

In relation to the optimization of the construction processes with respect to the adherence to the initial operation deadline agreed upon in the building contract, the question arises as to if and under what conditions it is permissible to operate the tunnel with only one axial ventilator. The aerodynamic attempts during the initial operation of the ventilation systems had exhibited that the ventilation system fulfills all ventilation technical requirements and still commands aerodynamic reserves as well. The proof of equal safety required for the operation is produced by means of a safety evaluation. In this, the safety evaluation fulfills the requirements set by the Federal Highway Research Institute and essentially incorporates a quantitative risk analysis.

The risk analysis tool applied and likewise programmed in Matlab is oriented on an event tree and commands various models for the calculation of the relative extent of damages. For the corresponding fire scenarios with the tunnel ventilation, the tunnel ventilation model already developed from the planning is coupled with the risk analysis tool. That is, the ventilation calculations based on the risk analysis are carried out with the model of the actually installed ventilation system. The coupling of the tunnel model of the ventilation with the risk analysis tool is enabled by the common program platform Matlab. This way the agreement between the relations simulated in the model and the actual realized conditions can be significantly improved. The credibility and the capacity of the safety evaluation increase considerably.

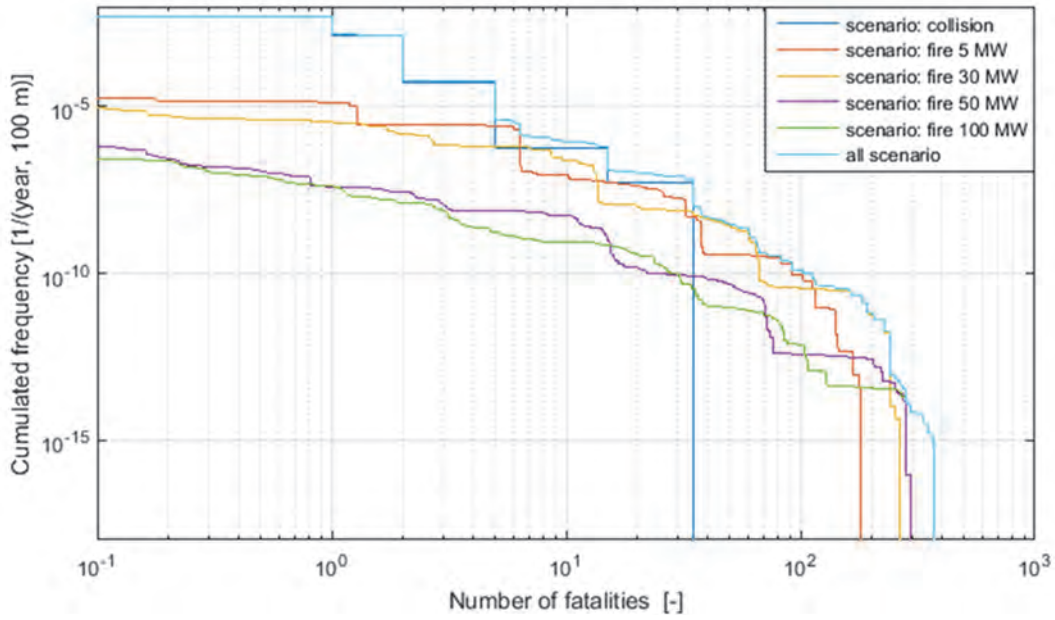

Figure 7: Results of the risk analysis

It is exhibited in the concrete scenario that the tunnel operation with an axial ventilator is only possible under some conditions. Under the effect of compensatory safety measures:

- Velocity reduction from 80 km/h to 50 km/h
- Fast fire detection (Supervision in the tunnel center and/or automatic confirmation of the fire pre-alarm)

An adequate safety level is reached in comparison to the RABT reference tunnel. Through this, a reliable guideline for the handling of exceptional scenarios could be developed for both the initial operation and the subsequent operation.

6. SUMMARY AND OUTLOOK

The implementation of a digital tunnel model in design, construction and operation of tunnel ventilation systems generates a substantial added value in comparison to the conventional methods. By modifying the tunnel to an efficient mathematical program, the physical properties linked to the ventilation for diverse analysis and decisions are accessible at any desired point in time of the life cycle of a tunnel. The quality and the availability of flow-mechanical predictions increase.

For example, the question could already be answered at an early phase in the construction planning as to whether the installation of a suspended ceiling can be omitted in the course of a tunnel retrofitting. With the aid of risk analysis, it can be realistically demonstrated using the tunnel model if a proof of equal safety is possible and what specific requirements are to be fulfilled for the frequently delayed safety and ventilation planning in detail.

With the aid of the optimization algorithms available in the mathematical programs, the ventilation control, e.g. with respect to the optimization of the energy consumption, could also be analyzed and improved in operation.

The impediments to the application of these tools no longer exist in the technical and practical realization but predominantly in the traditional project planning procedures. The public procurement frequently builds on traditional service concepts. Innovative approaches which particularly alter the timing of services and the concepts of the services themselves can thus only succeed if the boundary conditions for the application of these approaches are created by the client.

7. REFERENCES

[1] Directive 2004/54/EG of the European Parliaments and the Council from 29 April 2004 for the Minimum Safety Requirements for Tunnels Belonging to the Trans-European Road Network; 07.06.2004

[2] Guidelines for the Equipment and Operation of Road Tunnels RABT 2006; Research Committee for Roads and Transport (D); Edition 2006

[3] B66, Evaluation of the Safety of Road Tunnels, FE 03.0378/2004/FRB, Federal Highway Research Institute (BAST), November 2007

[4] Hagenmeyer, V. und M. Zeitz: Flachheitsbasierter Entwurf von linearen und nichtlinearen Vorsteuerungen, Automatisierungstechnik, 52:3-12, 2004.

[5] Astrom, K.J.: Control System Design, Department of Mechanical and Environmetal Engineering, University of California, Santa Barbara, 2002.

[6] Mituhiko Araki, Hidefumi Taguchi, Two-Degree-of-Freedom PID Controllers, International Journal of Control, Automation, and Systems Vol. 1, No. 4, December 2003

[7] Daniel E. Rivera, Internal Model Control: A Comprehensive View, Department of Chemical, Bio and Materials Engineering, College of Engineering and Applied Scienes, Arizona State University, October 27, 1999

[8] Seborg, Edgar, Mellichamp, Doyle, Process Dynamics and Control, Third Edition, John Wiley & Sons, Inc.2011

EFFECTIVENESS OF THE SAFEGUARDING SUPPORTIVE SYSTEM (SSS) AS A RESIDUAL RISK REDUCTION MEASURE IN TUNNEL ENVIRONMENT - QUANTITIVE EVALUATION OF VALIDITY OF THE SSS AND BEHAVIOR OF TUNNEL WORKERS

[1]R. Hojo, [1]K. Hamajima, [2]M. Tsuchiya, [1]S. Umezaki, [1]S. Shimizu
[1] Mechanical System Safety Research Group, Japan Organization of Occupational Health and Safety, National Institute of Occupational Safety and Health, Japan
[2]ADVANTAGE Risk Management Co., Ltd., Japan

ABSTRACT

The "Safeguarding Supportive System (SSS)" was newly established to prevent human error and intentional unsafe behavior of workers at workplace of tunnel. The SSS is a system to control and prevent human error and intentional unsafe behavior from the mechanical side (hardware side) using an appropriate Information and Communication Technology (ITC) combination. In the present study, the effectiveness of the SSS was evaluated with behavioral analysis procedure (feedback and no-feedback conditions). In addition, stress symptoms and work loads of subjects (workers) during the experiment were measured with self-report questionnaires. We conducted the experiment at a tunnel workplace of a company A. Baseline behavior of workers without the SSS condition and behavior under the SSS condition were measured. Then the parameters total work time, mechanical outage time and work time were calculated and compared between the baseline and the SSS conditions. The average total work time of workers under the SSS condition was significantly longer than that of the baseline condition. We assumed that irregular work occurred once per 30 min out of 8-hour-work time. Then the mechanical outage time was calculated using an average total time of each condition (16 times x the number of outage machines x total time). The machine outage time of the SSS condition was significantly shorter than that in the baseline condition. There was no difference in the work times between the SSS and the baseline conditions, but repeated factors were effective in both conditions. Decrease rates of total work time from the first work of the feedback group was greater than that of the no-feedback condition. In the self-reported questionnaires, 7 subjects reported stress decrease or no-change during the experiment. Even if the total time took longer in the SSS condition than in the baseline condition, the machine outage time was shorter in the SSS condition than in the baseline condition. In addition, it was suggested that some feedback of the work possibly promote further work

of the workers. The usage of feedback might be applied as a good promoter for self-encouragement for working. These results suggest that the introduction of the SSS guarantees both, safety and operation efficacy. It is possible that some feedback to the performed work promote further work. Also, it was suggested that repeated factor of the work in the present study played the role as promoter for further work too. Results of self-reports indicated that the present experiment was not stress for more than half of the subjects. It would be possible that more precise analysis of reinforcement procedures including feedback helps to establish more effective learning processes of the work.

Keywords: Safeguarding Supportive System (SSS), Tunnel construction, Behavior analysis

1. INTRODUCTION

Recently, the percentage of non-regular and short-term employees has increased, while the percentage of expert workers, who have supported safety at the workplace with long-term experience, has decreased in Japan. Therefore, the method of ensuring safety through individual awareness is no longer suitable in Japan, which is also the case for tunnel work sites in Japan. The aging of workers at tunnel constructions is developing. Some of the

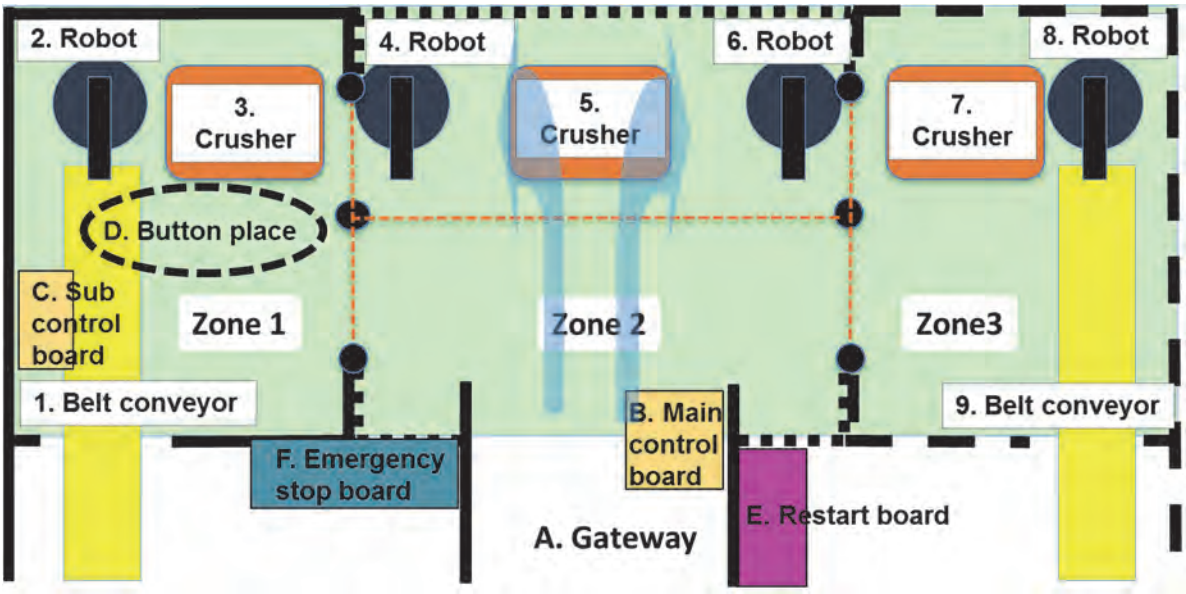

Figure 1: Work place for experiments
1-9 means machines in the work place. Zone 1 (Left, Solid line) has a belt conveyor, a rock crusher and a robot. Zone 2 (Middle, Dotted line) has 2 robots and a rock crusher, assuming rock crush work. Zone 3 (Right, Broken line) has same machines as zone 1. Under the SSS condition, machines 1-3 are stopped, and all machines are stopped in the usual stop condition. A. Gateway, B. Main control board, C. Sub control board, D. Button place, E. Restart board, F. Emergency stop board.

manual works in tunnels should be automated as much as possible and the safety of workers should be managed by electronic devices such as ICT, which is not depending on human attentiveness. At the same time, it would be necessary to promote some standardized systematic operational manuals for workers with little experience. Especially in manufacturing industry, accidents by workers who lack experience in non-routine works, such as cleaning robots, inspection, maintenance and setup, still occur at workplaces that have introduced an integrated manufacturing system (IMS). The 3-step method of inherently safe design measures, safeguard and providing complimentary protective measures and information for use, is a risk-reduction measure for safety ensured by ISO 12100/JIS B 9700, which is the safety standards for machines (Safety of machinery-Basic concepts, general principles for design). However, dangerous point-approach work occurs at actual workplaces, such as driving, adjustment, processing, troubleshooting, maintenance, repairing and cleaning machines during operating of these machines. Therefore, risk cannot be reduced sufficiently through safety standards for machines alone. New risks occur in IMS from combining mechanical equipment. ISO11161—"Safety in an Integrated Manufacturing System" — does not offer an effective method of ensuring safety in dangerous point-approach works. Some users at actual work sites sometimes still apply risk-reduction methods, depending on the workers' attentiveness. Therefore, many uncertainties exist in this risk-reduction method. A severe accident might occur if human error happens and the expected effect cannot be obtained as a result.

In the present study, we tried to apply the SSS to a tunnel construction site. Once human error occurs, it would be connected to a severe accident in the tunnel. Based on the worldwide situation, it is necessary for the Japanese tunnel construction to consider risk-reduction strategies that match real work sites. We have established a new risk-reduction method named Safeguarding Supportive System (SSS), which targets the tunnel construction site.

The SSS focuses on the residual risk after implementing the 3-step method of ISO 12100/JIS B 9700. The aim of the SSS is to provide effective residual risk-reduction using a combination of appropriate information and communication technology (ICT) equipment without depending on workers' attentiveness. Workers' qualifications (licenses) and rights (provided by ability and skill), the target machine, the work content, the place of the work and the operation time would become clear by introducing SSS. Under the SSS, work will only be allowed when ID information and the target machine of the tag held by a worker are matched with information from the control machine

located in the work area. Therefore, it is possible to prevent dangerous side errors caused by human error. Nevertheless, the SSS should be used in parallel with the "protection plan" — the education and training management were already introduced in Japan. The SSS is not a substitute for the protection plan.

Aim of the present study: The "**Supporting Protective System** (SSS)" was originally established to prevent human error and intentional unsafe behavior of workers at workplaces of integrated manufacturing systems (IMS). The SSS is the system to control and prevent human error and intentional unsafe behavior from the mechanical side (hardware side) using an appropriate Information and Communication Technology (ITC) combination. We examined the applicability of the SSS to a tunnel construction site. In the present study, the effectiveness and usefulness of the SSS were evaluated with behavioral analysis procedures. In addition, stress symptoms and work loads of subjects (workers) during the experiment were measured with self-report questionnaires.

MATERIALS AND METHODS

Subjects: Ten graduate school students (M = 9, F = 1).

Work place for the experiment: The workplace for the experiment (Figure 1) was built in the National Institute of Occupational Safety and Health, Japan (JNIOSH). We assumed the work place as a manufacturing industry, including irregular work such as cleaning, teaching or maintenance of robots. All subjects participated under the following 2 experimental conditions for 4 times each.

The SSS condition: Three machines in zone 1 were stopped and the rest kept working. A subject entered the work place from the gateway (Figure 1 - A), hung a tag (3 x 3 cm,

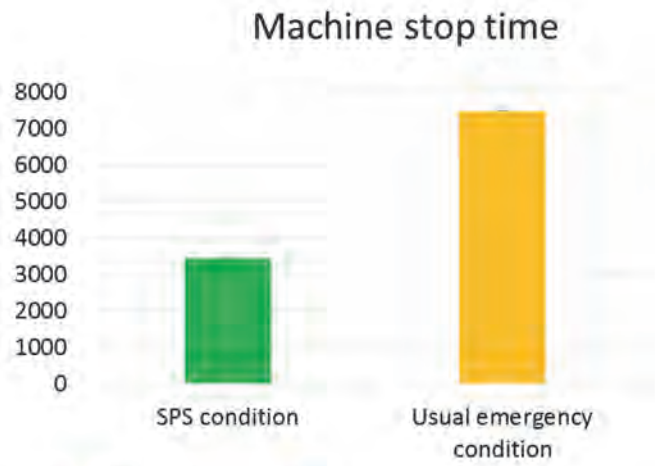

Figure 2: Total time (sec) of the SSS condition and usual emergency condition group

Omron, Japan) over the main (Figure 1 - B) and the sub control boards (Figure 1 - C), for stopping 3 machines, for the confirmation of the own authority and for selecting work in zone 1. After that the subject moved to a button place (Fig.1D). The subject was required to the press button 4 times each at the upper and the bottom locations of the belt conveyor. The subject hung a tag to the sub and the main control boards again and pushed the restart button of the restart board (Figure 1 - E).

Usual emergency stop condition: After stopping all machines by pushing an emergency button of the emergency stop board (Figure 1 - F), the subject moved from the gateway to zone 1, and was required to push the button 4 times each at the upper and the bottom locations of the belt conveyor at the button place. After leaving zone 1, the subject released the emergency, moved to the restart board. Half subjects were assigned to the feedback condition and the rest of them to the no-feedback condition, respectively.

Feedback condition: Five subjects in the feedback group were able to see the button-press time (work time) on the screen of the tablet and described the total time (time from the start to the end) by the experimenter immediately after the session.

No-feedback condition: The other five subjects were assigned to the no-feedback condition. The work time on the tablet screen was hidden by a sheet of paper. Also, the total time was not told the subjects in the no-feedback group.

The average total times of the SSS condition and the usual emergency stop condition were compared and analyzed by the Student's t-test. Statistical analysis of the effects of repeated sessions were performed with a repeated one-way analysis of variance (one-way ANOVA). All numerical values are expressed as the mean and se. Values of $p < 0.05$ were considered statistically significant. All statistical analysis were performed using the EZR software version 1.27 (Saitama Medical Center, Jichi Medical University, Saitama, Japan).

RESULTS

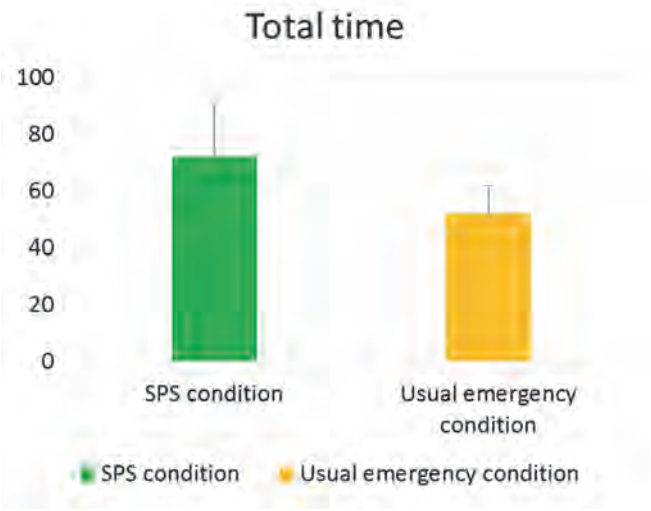

Figure 3: Machine stop time (sec) of the SSSS condition and usual emergency condition group

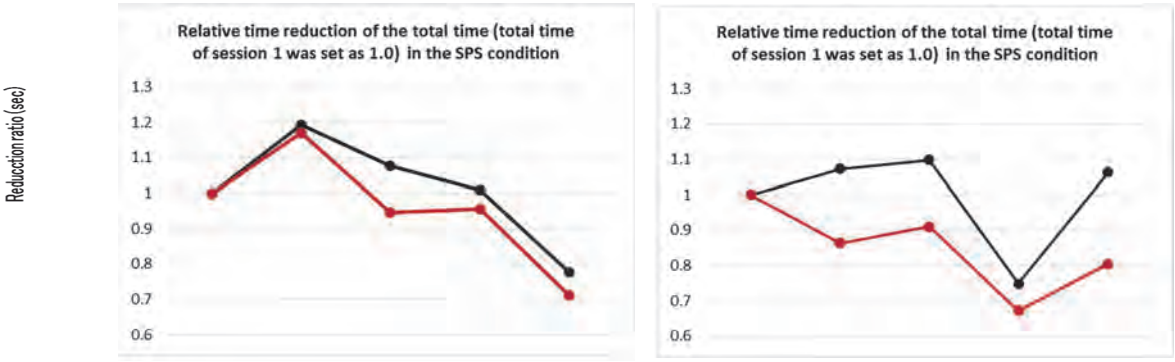

Figure 4: Relative time reduction with session repeat. Total time of session 1 was set as 1.0

The average total time of the SSS were 78 ± 8.7 and of the usual stop condition groups 54 ± 4.4 seconds (Figure 2).

We assumed that irregular work occurred once per 30 min out of 8-hour-work time. Then the mechanical outage time was calculated using an average total time of each condition (16 times x the number of outage machines x total time). The machine outage times of SSS and the usual stop conditions were 3,744sec (62.4 min) and 7,776 sec (129.6 min), respectively. There was no difference in the work time of the upper and the bottom locations of the belt conveyor between the SSS and the usual stop conditions, but repeated factors were effective in both conditions. If the total time was compared with those of the

first work, the feedback group had a greater decrease than the group with the no-feedback condition. In self-reported questionnaires, 7 subjects reported stress decrease or no-change during the experiment.

DISCUSSION

Even if the total time took longer in the SSS condition than in the usual stop condition, the machine outage time was shorter in the SSS condition than in the usual stop condition. In addition, it was suggested that some feedback to the performed work possibly promote further work. The usage of feedbacks might be applied as a good promoter for self-encouragement for working. These results suggest that the introduction of the SSS guarantees both, safety and operation efficacy. It is possible that some feedback to the work promote further work. Also, it was suggested that repeated factor of work in the present study played the role as promoter for the work. Results of self-reports indicated that the present experiment was not stressful for more than half of the subjects.

PERSPECTIVES

It would be possible that more precise analysis of reinforcement procedures including feedback helps to establish more effective learning processes of the work. Then, the SSS would be suitable for tunnel sites.

REFERENCES

1. EN ISO12100: 2010, Safety of machinery –Basic concepts of general principles for design (2003), (in Japanese).
2. International Organization for Standardization, ISO11161, Safety of machinery – Safety of integrated manufacturing systems – Basic requirements (2007).
3. Japanese Industrial Standard, Safety of machinery-General principles for design-Risk assessment and risk reduction −Part 2, JIS B 9700-2 (2004), pp.4-15, (in Japanese).
4. Massimi P and Van Gheluwe JP, Community legislation on machinery comments on directive 89/392/EEC and directive 91/368/EEC, Nikkei Mechanical, Nikkei Business Publication Inc. (1994).
5. Ministry of Health, Labor and Welfare, Ordinance of Industrial Safety and Health (Revision), Article24-3 (2014). <http://www.mhlw.go.jp/bunya/roudoukijun/anzeneisei14/dl/120521_01.pdf>, (accessed on 20 September, 2017).

6. Ministry of Health, Labor and Welfare, Sekkei Gijutsusha, Seisan Gijutsukanrisha ni taisuru Kikaianzen ni kakawaru kyouiku ni kannshi chuisubeki jikou ni tsuite (2014), <https://www.jaish.gr.jp/anzen/hor/hombun/hor1-55/hor1-55-32-1-0.htm>. (accessed on 20 September, 2017), (in Japanese).
7. Ministry of Health, Labor and Welfare, Section 9 Industrial Robot (Articles 150-3 to 151) (2015), <http://www.japaneselawtranslation.go.jp/law/detail/?id=1984&vm=04&re=01>, (accessed on 20 September 2017).
8. Ministry of Health, Labor and Welfare, Guidelines for comprehensive safety standards of machinery (Overview), revision (2007), <https://www.jaish.gr.jp/anzen/hor/hombun/hor1-48/hor1-48-36-1-0.htm>, (accessed on 20 September, 2017).
9. NihonKantokushiKyokai, Human Error Taisaku Book (2011).
10. Rodo Shinbun Sha (2017), <https://www.rodo.co.jp/column/10133/>, (accessed on 21 September, 2017), (in Japanese).
11. The Japan Machinery Federation, Subcommittee report 2014, Supporting Protective System under Integrated Manufacturing System (2014), (in Japanese).
12. The Japan Machinery Federation, Subcommittee report 2015, Supporting Protective System under Integrated Manufacturing System (2015), (in Japanese).
13. The Japan Machinery Federation, Subcommittee report 2016, Supporting Protective System under Integrated Manufacturing System (2016), (in Japanese)

TECHNOLOGIES FOR THE IMPROVEMENT OF JETFAN INSTALLATION FACTORS

Fathi Tarada, Karl Else
Mosen Ltd., United Kingdom

ABSTRACT

Three different technologies for the improvement of jetfan installation factors, namely deflection vanes, slanted silencers and MoJets, were calculated using 3D CFD and their performance was compared to that of a conventional jetfan. For a fixed installation height of 1.7 m, the MoJet exhibited an in-tunnel thrust enhancement of 61% above that of a conventional jetfan, with slightly reduced power consumption. Slanted silencers increased the installation factor compared to a conventional jetfan, but the in-tunnel thrust was reduced due to restrictions on the fan diameter. The deflection vanes tested in this study were not effective in increasing the in-tunnel thrust, due to the attachment of the jet to the tunnel floor.

Keywords: tunnel, ventilation, jetfan, installation factor, efficiency, thrust

1. INTRODUCTION

Alternative technologies have been proposed for the improvement of jetfan installation factors, including deflection vanes (with or without a clearance between the jetfan outlet and the vanes, Lotsberg (1997)), the Banana Jet (slanted silencers, Witt and Schütze (2008)) and the MoJet (a development on the original concept using silencers with an inclined outlet, Tarada (2018)). Each of these technologies implies different space requirements, power consumption, installation factors and induced tunnel velocities.

Bench thrust tests were simulated for a conventional jetfan and a MoJet to establish baseline values for the fan mass flow, power absorbed and axial thrust. The technologies were then tested in a tunnel environment and the values for the shaft power, axial thrust, tunnel airflow velocity and installation factor were calculated. The limitations of using the concept of installation factor in a strongly swirling, 3D flow-field in a tunnel are discussed.

2. CFD MODELLING

The calculations reported in this paper were undertaken using ANSYS CFX, a commercially available general-purpose CFD code.

A typical CFD model investigated in this study can be seen in Figure 1 below. The model represents a 211.6 m long section of tunnel, within which a single jetfan is located along the tunnel centreline at the tunnel soffit, 52.8 m from the upstream end. The height of the tunnel is 6.75 m, and is 16 m wide.

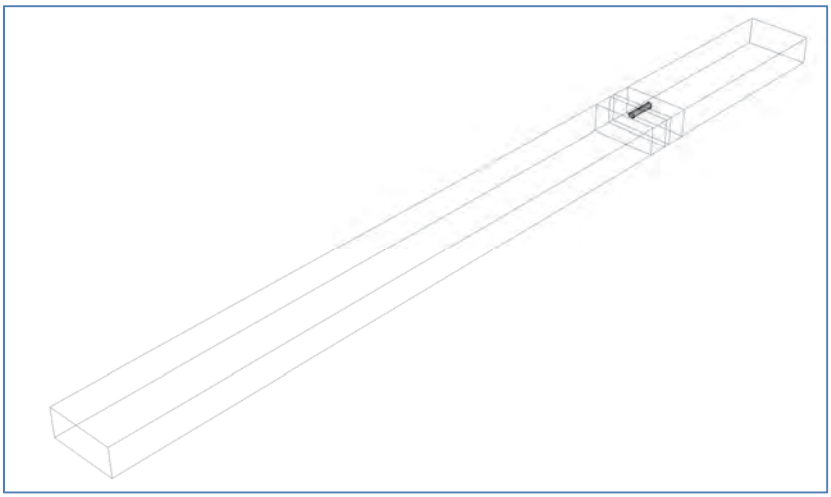

Figure 1: CFD Model of Tunnel including Jetfan

The detailed geometry of the jetfan hub, blades and motor was included in the same CFD model as the tunnel geometry. Blade rotation was simulated using the multiple frame of rotation option in ANSYS CFX, with circumferential averaging. The mass flow through the jetfans was not prescribed but was calculated through the CFD code based on a blade rotational speed of 1500 rpm, corresponding to the speed of a four-pole motor. Reductions in blade rotational speed due to induction motor slippage were not accounted for. The k-ω SST model of turbulence (Menter, 1993) was employed, which assisted in identifying any areas of flow separation. The tunnel walls, floor and soffit were assumed to have a uniform sand roughness height of 0.03 m, giving an equivalent friction factor (λ=4f) of 0.024.

Boundary layer meshes were attached to all solid surfaces to resolve sharp velocity gradients. Within the fans and silencers, these boundary layer meshes were calculated via 30-layer prisms with an initial layer approximately 0.1 mm thick within a jetfan, and with an expansion factor of 1.2 (Figure 2). Along the tunnel, the boundary layer mesh was 10-layer with an initial layer 0.3 m thick and an expansion factor of 1.1. A typical y^+ value for the last cell (downstream) along the (rough) tunnel surfaces was 315, while a typical y^+ value on the fan blades and silencers was 15. Table 1 lists the number of CFD cells used for each type of technology tested.

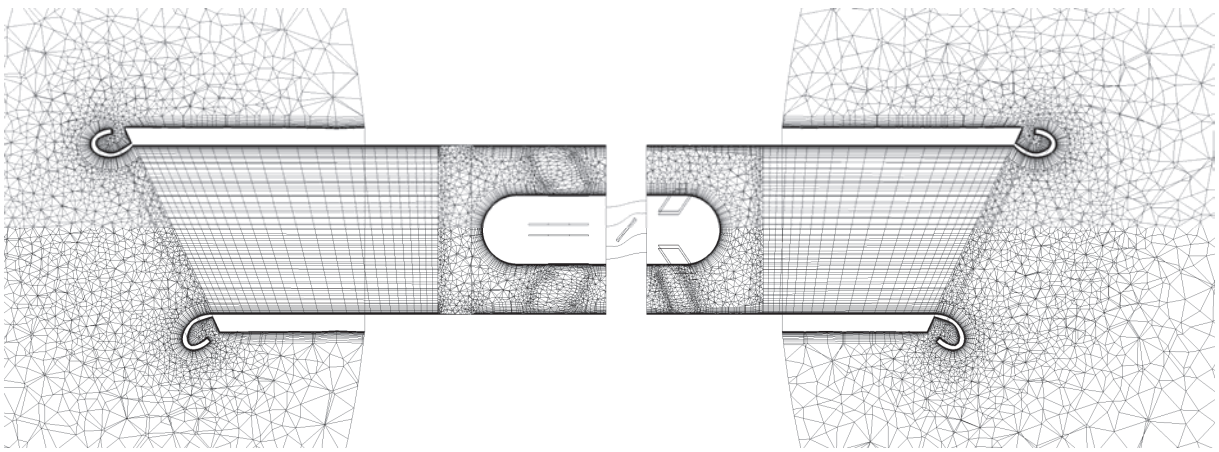

Figure 2: Mesh for MoJet Bench Thrust Test

Table 1: Number of CFD cells employed in the simulations

Technology	**Conventional jetfan**	**Deflection vanes**	**Slanted silencers**	**MoJet**
Number of CFD cells	25.1 million	72.3 million	25.6 million	27.1 million

3. TECHNOLOGIES INVESTIGATED IN THE STUDY

The four technologies selected for this study are well established in engineering practice (conventional jetfan, deflector vanes and slanted silencers) or represent a recent innovation (MoJet). The fan, casing, silencer and centrebody geometries for all four technologies were provided by a major manufacturer of tunnel ventilation equipment.

The same available installation height of 1.7 m was assumed for all four jetfan technologies. The silencers attached to the fans were selected with 100 mm thickness, and were arranged to be 150 mm below the tunnel soffit.

The jetfan internal diameter for the conventional jetfan, deflection vanes and MoJet was set at 1.25 m. A smaller jetfan diameter (1 m) had to be selected for the slanted silencers (with a 7° angle to the horizontal) to keep the jetfan to just within the 1.7 m installation height limit. All four technologies had "2D" lengths of silencers installed on either side of the fan, where "D" is the internal diameter of the fan.

A mid-range blade pitch angle of 33.4° was selected for the initial calculations with the 1.25 m diameter jetfans. A blade pitch angle of 39° was also tested for the MoJet, to approximately match the shaft power absorbed by the conventional jetfan.

The deflector vanes included a flat section followed by vanes set at 25° from the horizontal. Following the fan manufacturer's guidance, the deflector vanes were installed at a distance of 0.504 m from the silencers at both ends of the jetfan (Figure 3).

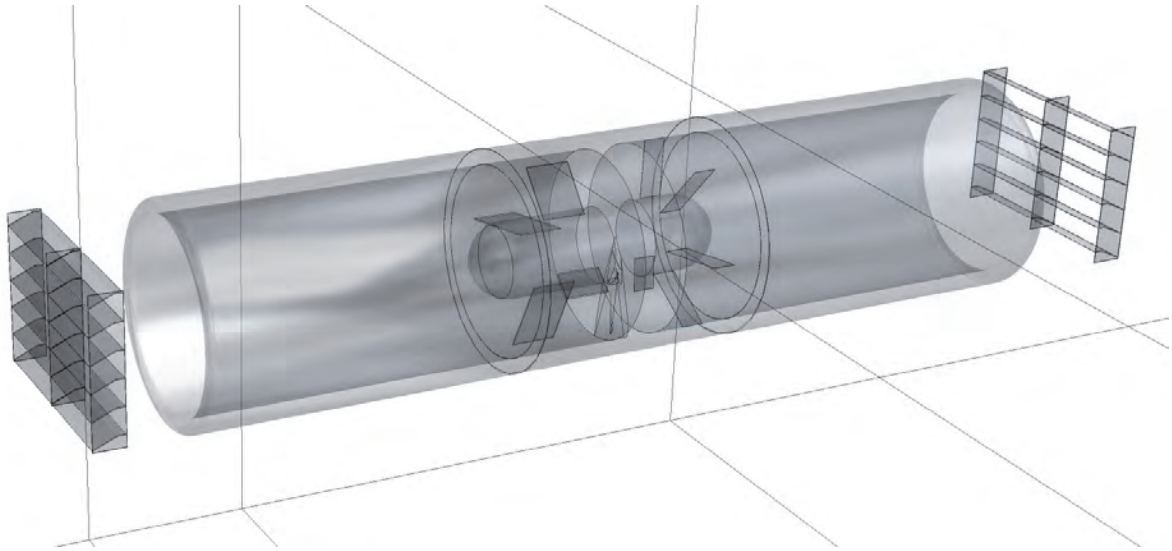

Figure 3: Jetfan with Deflector Vanes

4. CFD RESULTS

4.1. Bench Thrust Results

Bench thrust calculations were undertaken for the conventional jetfan and MoJet options, to provide a baseline for comparison with experimental data. The results are summarised in Table 2. The density of air in still conditions can be taken as 1.185 kg m^{-3}. The fan shaft power was estimated as the product of the blade torque and the rotational speed in radians per second.

Table 2: Bench thrust results (1.25 m diameter fans)

	Conventional jetfan	**MoJet**
Blade pitch angle	33.4	33.4
Blade torque (Nm)	285.6	275.3
Fan shaft power (kW)	44.9	43.2
Fan mass flow (kg/s)	50.57	51.38
Thrust (N)	1759	1815

Compared to measurements, the calculated conventional jetfan thrust is overstated by around 5% due to the neglect of the induction motor slippage. The deviation of the MoJet thrust is expected to be less than 5%, because the reduced motor torque causes less slippage.

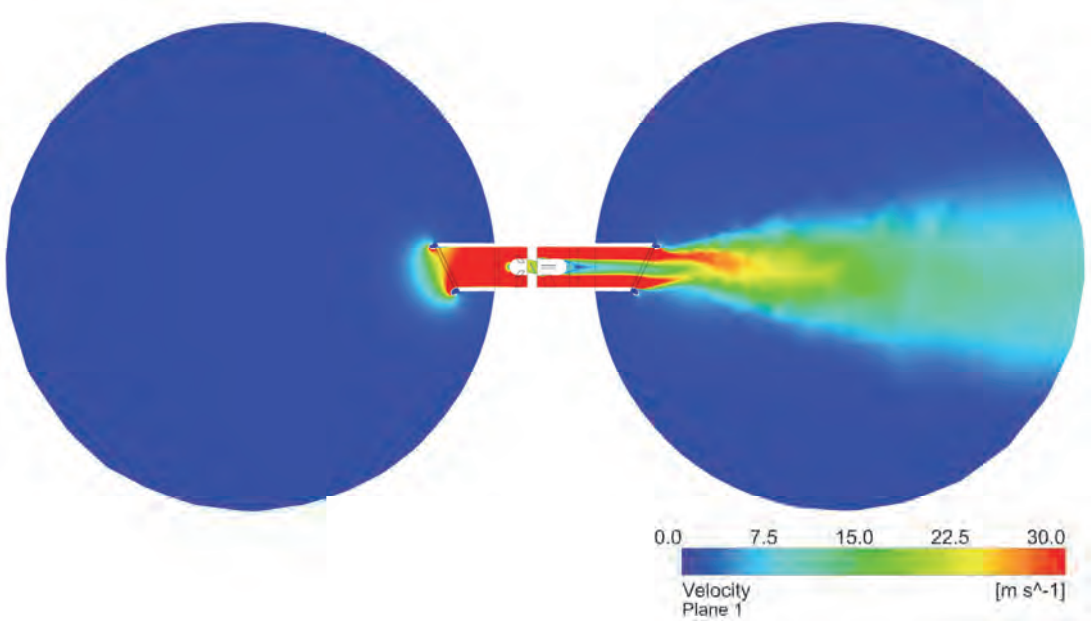

Figure 4: Bench Thrust Test for MoJet (Velocity Contours)

4.2. Tunnel Installation Results

The effective thrust of a jetfan in a tunnel, T, is lower than the bench thrust, due to confining effect of the tunnel soffit (which reduces the mass flow through the fan) and because of the friction on the tunnel walls, which is represented by the installation efficiency η_i. The value of T is calculated as:

$$T = \eta_i \rho A_A v_A (v_A - v_T) \quad \text{(Equation 1)}$$

where A_A is the cross section of the jetfan outlet, v_A the jet average velocity and v_T the velocity in the tunnel beyond the direct influence of the jetfan intake and discharge. The installation factors were interpreted from the CFD results on the basis of the methodology described by Tarada (2016), as follows:

$$\eta_i = 1 - \Delta T / T_{max} \quad \text{(Equation 2)}$$

where

ΔT = increase in skin friction drag above standard case

= skin friction drag predicted by CFD – standard skin friction drag

and

Skin friction drag in 3D CFD = Sum of predicted wall, soffit and roadway drag forces

Standard skin friction drag = $\frac{1}{2}\rho v_T^2 \lambda \frac{LA_T}{D_h}$

where

L = tunnel length (m)

A_T = cross-sectional area of tunnel (m^2)

D_h = hydraulic tunnel diameter (m)

Since the installation factor relies upon one-dimensional consideration of the tunnel airflow, it may be of limited value in a tunnel with strongly swirling flow, such as jetfans with internal struts removed, as discussed below.

Table 3 summarises the jetfan performance values obtained in the study.

Table 3: Summary of Jetfan Performance

	Conventional jetfan	**Conventional jetfan (struts removed)**	**MoJet**	**MoJet**	**MoJet (struts removed)**	**Slanted silencers**	**Jetfan with deflectors**
Blade pitch angle	33.4	33.4	33.4	39	39	43	33.4
Tunnel airflow velocity (ms^{-1})	2.66	2.60	3.04	3.62	3.89	2.56	2.26
Installation factor	0.84	0.74	0.92	1.00	0.97	0.98	0.60
Fan shaft power (kW)	56.7	53.1	48.2	56.3	53.7	22.7	56.4
Fan mass flow (kg/s)	49.0	50.0	52.2	57.4	57.6	33.6	49.4
% of conventional jetfan in-tunnel thrust	100%	91%	124%	161%	156%	86%	74%

4.3. Conventional Jetfan

The jet discharged from a conventional jetfan adheres to the tunnel soffit due to the Coanda effect, causing a loss of in-tunnel thrust due to friction between the jet and the soffit.

When installed with 150 mm clearance to the tunnel soffit, the mass flow through the conventional jetfan is reduced by 6.1% from its bench test value, due to the confining effect of the soffit on the inlet silencer. Taking the reduced mass flow into account, the installation factor calculated from the CFD results is very close to the value provided by the Kempf correlation (1965):

$$\eta_i = \left[0.0192 \left(\frac{z}{D_A} \right)^2 - 0.144 \frac{z}{D_A} + 1.27 \right]^{-1} \qquad \text{(Equation 3)}$$

where D_A is the outlet diameter of the jetfan and z denotes the distance between the centre axis of the jet at the outlet and the tunnel wall. This result is somewhat surprising, since Kempf did not include any swirl in his measurements. The CFD calculations indicated a significant swirl velocity of up to 10 m/s at the discharge from the silencer following the fan (Figure **6**). Removing the struts holding the fan centrebody (which is aerodynamically equivalent to replacing the struts with drop-rods) increases the outlet swirl, but neither improves the installation factor nor the tunnel airflow velocity.

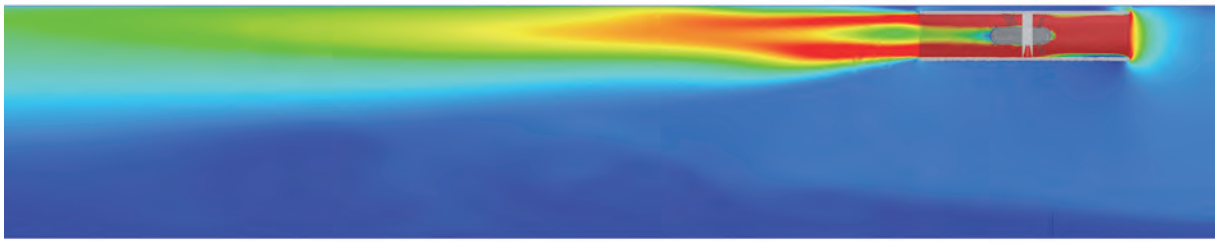

Figure 5: Velocity Contours for Conventional Jetfan (Colour Legend as per Figure 4)

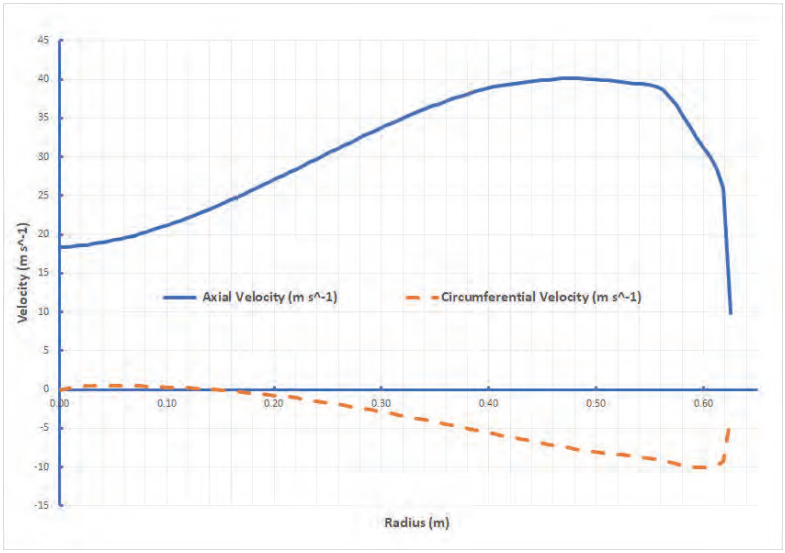

Figure 6: Axial and Circumferential Velocities at Discharge from Conventional Jetfan Silencer with Struts (33.4° Blade Pitch Angle)

4.4. MoJet

The MoJet design tested in these calculations comprises silencers with trailing edges that are inclined at 25° from the vertical. The trailing edge is circular in shape, with a diameter (1.379 m) greater than that of the fan (1.25 m). A convergent/divergent bellmouth is attached to the trailing edge, with a minimum diameter of 1.332 m. The bellmouth is designed to avoid separation of the flow at the lower edge of the MoJet inlet silencer, and the same bellmouth is designed to turn the flow at the upper edge of the MoJet discharge silencer.

Since the inlet and outlet areas of the MoJet silencer are significantly greater than the fan area, there is less resistance to the fan airflow, and the MoJet results therefore exhibit higher mass flow and less power consumption than conventional jetfans with the same blade pitch angle.

The increase in the cross-sectional area of the MoJet silencer leads to a significant pressure recovery downstream of the fan, and to a reduction in the discharge velocity. Approximately 22% of the kinetic energy of the flow is recovered as static pressure in the MoJet outlet silencer. This pressure recovery leads to an increase in the force exerted by the MoJet onto the tunnel air, while the reduction in discharge velocity reduces the aerodynamic friction between the jet and the soffit. The Coanda effect is also reduced by the effect of the bellmouth in turning the flow away from the tunnel soffit. These factors explain the high (near-unity) installation factors reported for the MoJet in Table 3.

The MoJet results for a 33.4° blade pitch angle show a 24% increase in the in-tunnel thrust compared to a conventional jetfan, with 15% less absorbed power. In order to compare the MoJet with a conventional jetfan of equivalent power consumption, the MoJet blade pitch angle was increased from 33.4° to 39°. This enhances the MoJet in-tunnel thrust to 161% of the conventional jetfan in-tunnel thrust, with slightly less power consumption than the conventional jetfan. Removing the struts (i.e. replacing them with drop-rods) reduces the installation factor slightly, but installation factor is an unreliable parameter for prediction of this complex swirling flow-field. Using drop-rods in a MoJet delivers a significant increase in the tunnel air velocity with less power consumption – arguably the main issues of interest to tunnel designers.

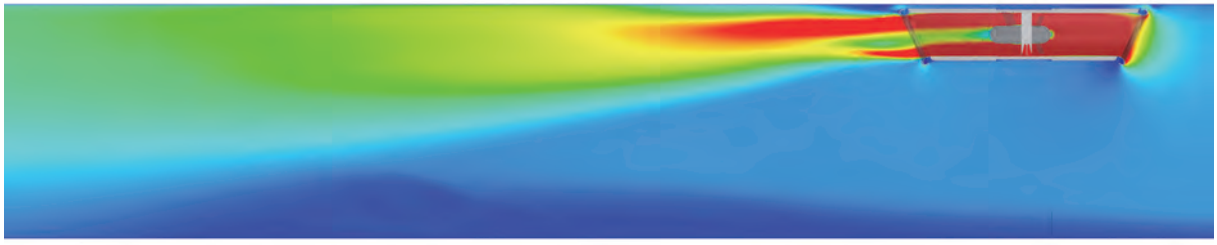

Figure 7: Velocity Contours for MoJet with 39° Blade Pitch Angle, with Struts (Colour Legend as per Figure 4)

4.5. Slanted Silencers

The installation factor is improved by the use of slanted silencers compared to a conventional jetfan, but this improvement does not adequately compensate for the loss of thrust due to the reduction of the jetfan diameter from 1.25 m to 1 m. This loss in thrust occurred even though the blade pitch angle was increased to the maximum allowable value without stalling, namely 43°. The in-tunnel thrust with slanted silencers is reduced to 86% of the conventional jetfan thrust, with a corresponding reduction in tunnel air velocity. The loss of thrust due to a reduction in fan diameter with slanted silencers would occur in any height-restricted space, and is not a result of the 1.7 m clearance assumed in this study. However, due to the reduction in fan diameter to 1 m, the thrust/power ratio with this option is better than any of the 1.25 m diameter fans tested here.

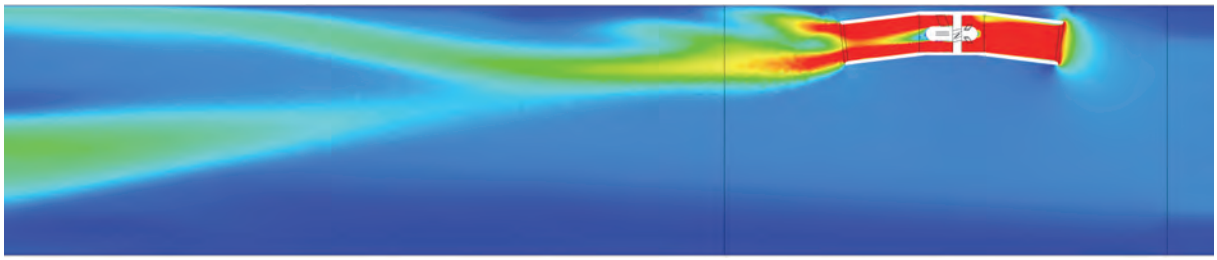

Figure 8: Velocity Contours with Slanted Silencers (Colour Legend as per Figure 4)

4.6. Jetfan with Deflectors

The result with deflectors shows that the swirl in the discharge flow is eliminated, and the flow is efficiently directed downwards (Figure 9). However, the jet then attaches to the tunnel floor, and significant friction is generated there. The installation factor is therefore rather poor at only 0.60, and the tunnel air velocity is less than that with a conventional jetfan. It is recognised that a better result could have been obtained by deflectors that are better designed. The authors contacted three fan manufacturers with a request for improved deflector geometry, but no response was received.

The authors originally planned to test the same deflectors coupled directly to the ends of a jetfan. However, given the poor performance observed with the detached deflectors, the CFD calculations with the coupled deflectors were abandoned.

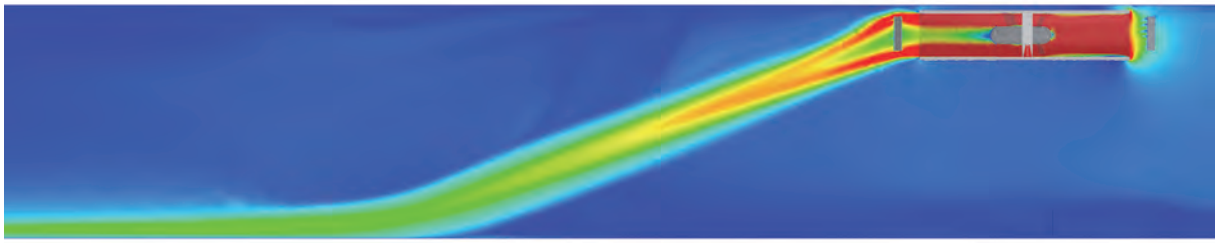

Figure 9: Velocity Contours with Deflectors (Colour Legend as per Figure 4)

5. CONCLUSIONS

Each technology that purports to improve the tunnel installation factor can have an effect on the jetfan itself (e.g. in terms of reduced or enhanced mass flow), as well as having an effect on the tunnel air (e.g. by deflecting the jet away from the tunnel soffit, or enhancing the pressure force exerted on the tunnel air). The most promising technology identified by this study has been the MoJet, which can increase the in-tunnel thrust by 61% above the conventional jetfan value, with a slightly reduced power consumption. A research project is underway at the Institute of Aerodynamics at RWTH Aachen University to manufacture 1:18 scale models of jetfans with different silencer geometries including slanted silencers and MoJets using 3D printing, and to measure their tunnel installation factors. Full-scale tests of MoJets in a tunnel are also planned.

6. REFERENCES

Kempf, J. (1965), *Einfluss der Wandeffekte auf die Treibstrahlwirkung eines Strahlgebläses*, Schweizerische Bauzeitung, 83. Jahrgang, Heft 4, Seiten 47-52.

Lotsberg, G. (1997), *Investigation of the Wall-friction, Pressure Distribution and the Effectiveness of Big Jetfans with Deflection Blades in the Fodnes Tunnel in Norway*, 9th International Symposium on Aerodynamics and Ventilation of Vehicle Tunnels, Aosta Valley, Italy.

Menter, F. R. (1993), *Zonal Two Equation k-ω Turbulence Models for Aerodynamic Flows*, AIAA Paper 93-2906.

Tarada, F. (2016), *Innovation in Jetfan Design*, 7th International Symposium on Tunnel Safety and Security, Montreal.

Tarada, F. (2018), *Optimised Tunnel Ventilation Device,* International PCT Patent Application Number PCT/GB2018/000029.

Witt, K.C. and Schütze, J. (2008), *Effective Thrust Transformation inside Tunnels with Jet Fans (Banana Jet),* 4th International Conference 'Tunnel Safety and Ventilation', Graz.

BEST PRACTISE IN THE USE OF BANANA JET® IN TUNNELS AND METROS

[1]Karsten C. Witt
[1]Witt & Sohn AG, Germany

ABSTRACT

In practice longitudinal jet fan ventilation system designers do not take full advantage of the 30 - 50% performance improvement that Banana Jet® systems make possible. The fans can be better positioned in the tunnel, the fan size can be optimized and the flow direction is better adjusted compared to traditional straight jet fans. With less interference between downstream fans a significantly reduced number of larger fans can be placed close together resulting in dramatically reduced cable length and installation cost.

Unfortunately often CFD simulations do not model Banana Jet® systems correctly sometimes resulting in CFD results which are contrary to the basic laws of physics. This paper attempts to provide some guidance of how to improve that situation.

1. INTRODUCTION

In a very large proportion of road tunnels jet fans are being used as the main source of ventilation or to support other ventilation effects. Also in railway tunnels and metros jet fans are a major component in the ventilation systems. For more than 10 years a special form of jet fans, popularly called "Banana Jet® "with slanted silencers have been installed. By guiding the jet away from restrictive surfaces the aim is to improve the efficiency of the overall ventilation system. Based on hundreds of installations around the world some lessons have been learned.

A traditional jet fan is installed with the inlet and outlet, typically with fans and silencers, parallel to the ceiling or walls. Their function is to blow into the tunnel thereby accelerating the air column inside the tunnel. However, only a portion of the energy (called thrust) coming out of the fan is effectively translated into air movement. The air flow coming out of the fan is expanding with an angle of around 6 - 8°, some of this thrust is hitting the ceiling without transferring any energy to the air column of the tunnel. Also the friction losses of the air stream following the ceiling due to the Coanda effect and losses due to the background velocity in the tunnel further reduce the overall efficiency of the traditional jet fan. Typically only 65 - 70% of the energy in the air stream of the traditional jet fan is translated into useful thrust.

By slanting the fan outlet away from the ceiling the losses from the expanding jet stream hitting the ceiling can virtually be eliminated. Also there will be little or no Coanda effect further improving the efficiency. Measurements have also proven that the background velocity is lower in such ventilation systems. In essence the efficiency of such a "Banana Jet®" system is around 90 - 95%.

In practice, the actual Banana Jet® Systems have not taken full advantage of the possibilities that this type of fan can offer. The fans could be better positioned in the tunnel, the fan size could be optimized and the flow direction adjusted.

When all possibilities would be used the overall cost of installing such a Banana Jet® System is typically less than half the cost of a traditional jet ventilation system. Especially large savings can be achieved in reducing the number of fans needed, the total power to be installed and the length of the cables required.

Unfortunately many CFD analyses trying to simulate Banana Jet® fan ventilation systems are using assumptions that are too crude. In some CFD simulations, contrary to the laws of physics, traditional jet fan systems are "shown" to create higher air flow speeds compared to Banana Jet® fan systems using the same fan sizes despite generating less than 65 - 70% of the usable effective thrust.

2. PREDICTING THE BANANA JET® ADVANTAGE

2002 - 2006 in 3 tunnels the difference in air speed and thrust between Banana Jet® fans and traditional jet fans were measured. To reduce the measurement uncertainty the only modification between the measurement series was to straighten the silencers from Banana Jet® to traditional jet fans by using transition pieces. The fans themselves were left in position so that the mounting location and the fan, motor, impeller plus silencer were exactly the same. The increase in thrust was in all cases found to be between ~25 - 35%.

Using these three tunnels as the base case 12 CFD simulations were done, calibrating the results with the measurements (Figure 1). All simulations assumed empty tunnels so that the results could be compared to the measurements and can be reproduced in a commissioning situation.

T/B: Square tunnel profile, 2 fans @ corner, size 710:

Traditional jet fan (TJ)

Banana Jet® fan (BJ)

Figure 1: Example CFD simulation of Collombey tunnel (Bibliography Nr. 5)

After the model had been calibrated, 8 different tunnel profiles were investigated. There were 2 round tunnel profiles (with 1 and 2 fans in parallel), 3 square profile (with 1 fan in the middle, with 1 fan in the corner and with 2 fans in each corner), 2 cases with niches (with one and 2 fans) and finally one configuration with a fan in a corner niche (Figure 2).

Configuration	Thrust improvement [%] [1] compared to TJ at different tunnel air speeds [m/s]						
	2 m/s	3 m/s	4 m/s	5 m/s	6 m/s	7 m/s	8 m/s
	45 %	**47 %**	50 %	52 %	55 %	57 %	60 %
	41 %	**43 %**	45 %	**47 %**	50 %	52 %	55 %
	38 %	41 %	44 %	47 %	50 %	53 %	**56 %**
	35 %	(38 %)	40 %	43 %	45 %	**48 %**	50 %
	33 %	**35 %**	37 %	**39 %**	42 %	45 %	48 %
	27 %	**29 %**	32 %	34 %	37 %	39 %	42 %
	19 %	**21 %**	(23 %)	**25 %**	28 %	31 %	34 %
	15 %	18 %	21 %	24 %	27 %	**30 %**	(33 %)

[1] tolerances: +/- 10%

○ → Actual measurements of tested tunnel

Bold → Results of CFD analysis

Rest → Predicted values

Figure 2: Predicting the Banana Jet® Advantage (Bibliography Nr. 5)

Key to the simulations was to get the correct outlet flow pattern from the Banana Jet® fan, i.e. the correct spreading of the jet and the speed differential over the cross section of the jet as it expands the further away from the fan it goes. To be able to estimate the influence of the air speed, 4 additional simulation were done with different air speed compared to the base model for each tunnel configuration.

As can be seen from the results, depending on the average air velocity that is to be achieved, the Banana Jet® improves the thrust by 15 - 60%. Given that, most tunnels need air speeds in an empty tunnel of around 3 - 5 m/s it is safe to assume as a first approximation an improvement of 20 - 40%.

Based on these calibrated tunnel CFD models, the scenarios were run again with tunnels filled with cars. There the reduction of thrust was between 2 - 12% depending on the tunnel configuration. This is much less than some CFD models have found. We suspect, as stated in the 3rd chapter of this paper that the mistakes are in the CFD models which e.g. they almost certainly do not take into account the minimum 15% losses from the Coanda effect.

Subsequent commissioning measurements in at least 100 tunnels have found the theoretical improvement in thrust to be conservative. In no case were the measured values below the expected contractual values agreed with the customers.

3. OPTIMAL INSTALLATION

There seem to be some uncertainty of how to get the best out of this technology. In most cases the fans are placed the same way as traditional jet fans. In the following some suggestions of how to optimize Banana Jet® systems.

3.1. Reducing installation height

To minimize the losses resulting from the expanding jet behind traditional fan, they are typically mounted 1/2 of the diameter of the fan from the ceiling. Banana Jet® can be mounted directly at the ceiling. With more space available the diameter of the fans can be increased. Since the thrust goes to the power of 4, i.e. $T_2 = T_1 \times (D_2/D_1)^4$ this allows larger fans to be installed. Fans are typically built according to the DIN R20 series, i.e. each size about 12 - 14% larger than the previous size.

So taking advantage of the 0.5 D gap used by traditional jet fans, Banana Jet® can be build at least 2 sizes larger (i.e. ~ 1.25% D), even taking into account the around ~15% D extra space needed for the bending silencers (Figure 3). A size increase of 25% allows for an increase in thrust by ~ 250%! The number of fans to be installed will be reduced by 60%. So in a tunnel instead of installing 20 fans, 8 fans will suffice. The electrical installations, cables, physical installation cost and maintenance will be significantly reduced.

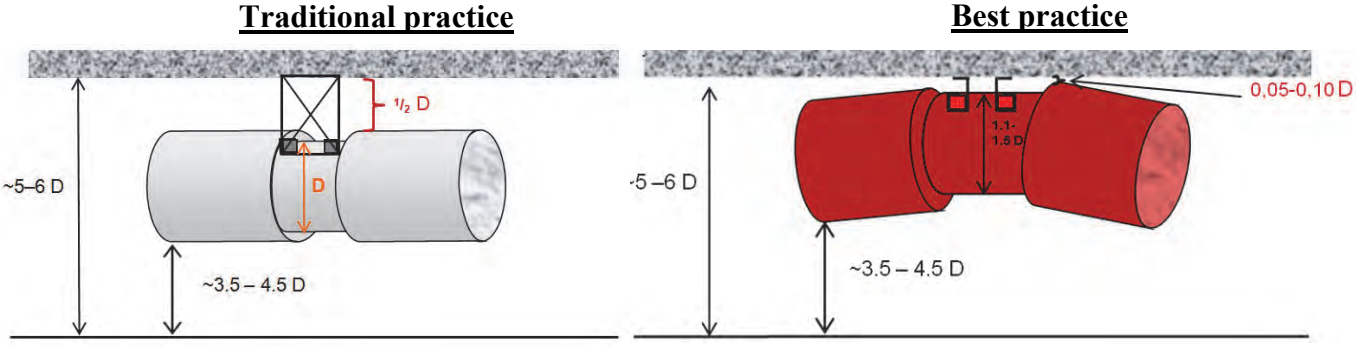

Figure 3: Installing maximum size Banana Jet® close to the ceiling

Even if for noise reasons the silencers have to be very long this can be achieved because only around 1/3 D silencer lengths need to be angled. The rest of the silencer can be straight. If even lager fans are to be installed e.g. 3 times the diameter of a traditional jet fan this method can be used to reduce the extra space need from the angling of the silencers from 15 % to 5%. The increase in thrust per fan is ~400% (Figure 4)!

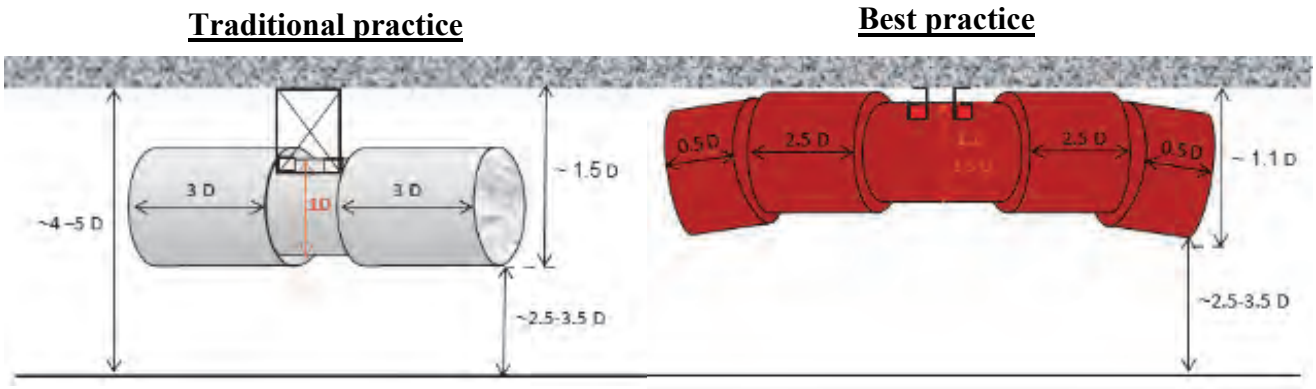

Figure 4: Reducing the maximum deflection

3.2. Angling silencers

Straight, traditional jet fan with silencers can only blow the air in one direction which is straight parallel to the ceiling. Silencers are typically mounted with 8 - 24 bolts in the flanges of the jet fan. The same is the case for Banana Jet® fans. This makes it possible to direct the flow of the air in more than one direction. This is useful in a number of situations:

- Jet fans in corners/niches or semi enclosures. When space is at a premium or typically in square tunnels where the fans are placed in corners or niches, the jet stream can be angled away from those restrictive surfaces further improving the efficiency compared to traditional jet fans. A special case are tunnels where there are some kind of air duct in the middle of the tunnel e.g. for removing smoke using a damper/duct system from fires in the tunnel. In those cases the fans are hung enclosed by 3 sides. Angling the silencers away from the wall into the tunnel will result in an improvement compared to traditional jet fans of 60-70% (Figure 5).

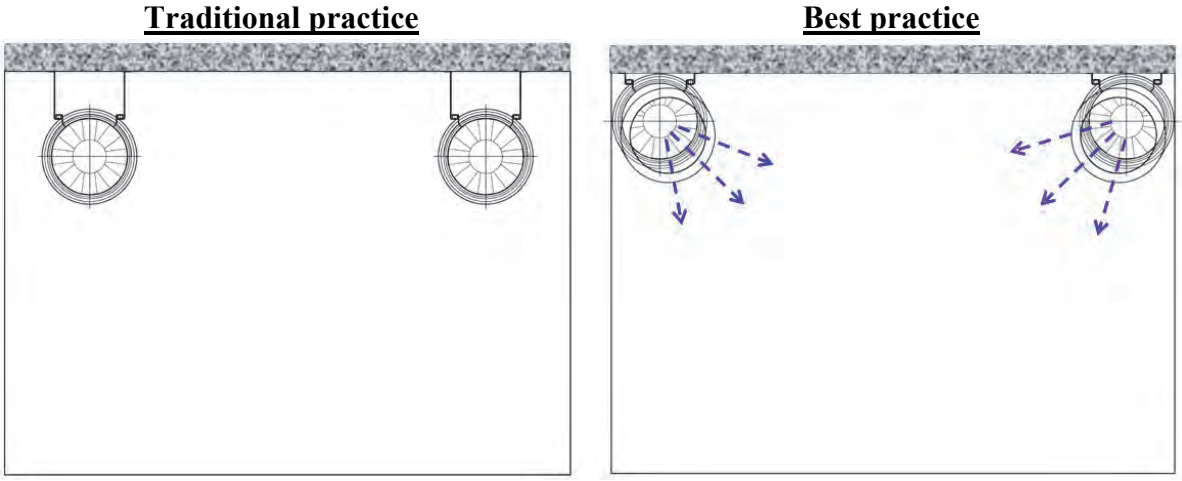

Figure 5: Positioning Banana Jets® optimally in the corners of square tunnels

- Jet fans side by side. Since the traffic envelope where jet fans can be hung is restricted in most cases jet fans are hung in pairs or even 3 or 4 fans side by side. The result is that the expanding air column of the air leaving from traditional jet fans will cross each other and create turbulence and losses. By angling the air flow away from each other using Banana Jets® these losses can be further reduced (Figure 6).

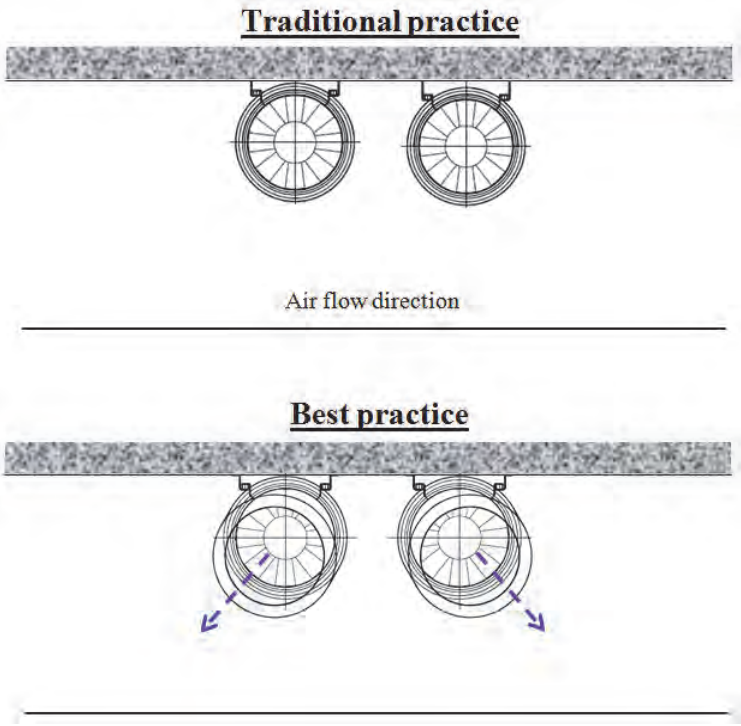

Figure 6: Optimizing the air flow distribution in a tunnel

This has a further advantage: The majority of the air speed in a tunnel filled with cars during a traffic stoppage will be at 2/3 of the height. Simulations done on the Shiraz tunnel in Iran showed that there is very little air velocity amongst the cars and especially in the corners of the tunnel leading to very high CO/CO_2/NOx concentrations around the cars. By using Banana Jet® s the air speed around the cars can be increased. When they pointing more to the corners CFD simulations and 2 dimensional analyses show a reduction in CO/CO_2/NOx concentrations of 25 - 35% (Figure 7). In addition, the simulations showed a reduced temperature level below the ceiling, a just very slight increase in the middle of the tunnel and virtually the same temperature distribution at road level.

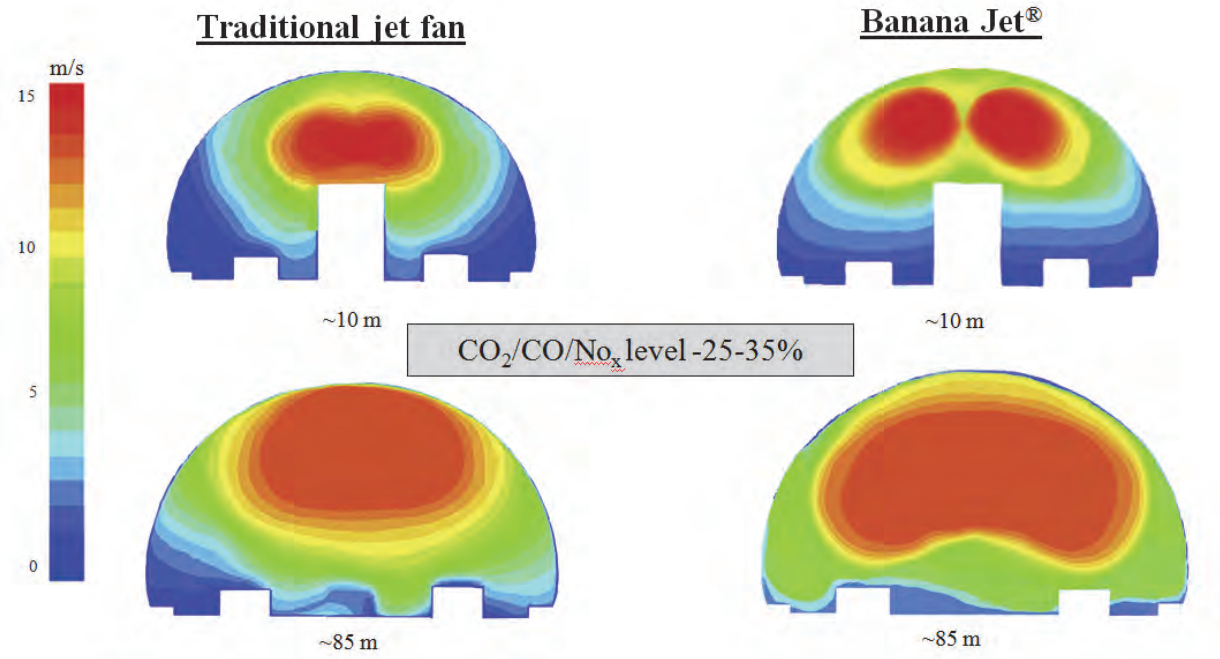

Figure 7: Performance of jet fans in ventilation of an urban tunnel under traffic jam condition (Bibliography Nr. 5 and Witt & Sohn AG simulation)

- Jet fans angled to follow tunnel contours. Few tunnels are completely straight. In many cases, there are bends in the road. Traditional jet fans will blow into these bends with resulting efficiency losses. Again Banana Jet® can be angled removing some of these losses.

- Jet fans angled to avoid ancillary equipment. Few pressure losses calculations or CFD analysis of the ventilation systems of tunnel take into account that fans are not the only equipment mounted outside the traffic envelope under the tunnel ceiling. In this area are also mounted the lamps, road signs, surveillance cameras, emergency signage, loud speakers and lots and lots of other ancillary equipment. With an air stream from traditional jet fans mainly below the ceiling, there are substantial losses that should be taken into account (but never are). Again, the intelligent angling of silencers can direct the high-speed air stream away from such obstructions improving overall system efficiency.

3.3. Reducing cable length

Traditional jet fans are typically place at a distance of 100 m along the length of the tunnel. If special design requirements do not make it necessary to install fans along the full length of the tunnel, the fans are typically installed close to the portals to reduce the length of the installed cables, because the cost of jet fan cables are anything but trivial. It is not uncommon that the average cable cost per fan exceeds the cost of the fan. Banana Jet® allows for a significant improvement in the cable installations (Figure 8).

- The air profile behind Banana Jet® is very different compared to traditional jet fans generating much lower air speed under the ceiling, they interfere much less with downstream jet fans. This allows the fans to be spaced closer together, typically 60 m.

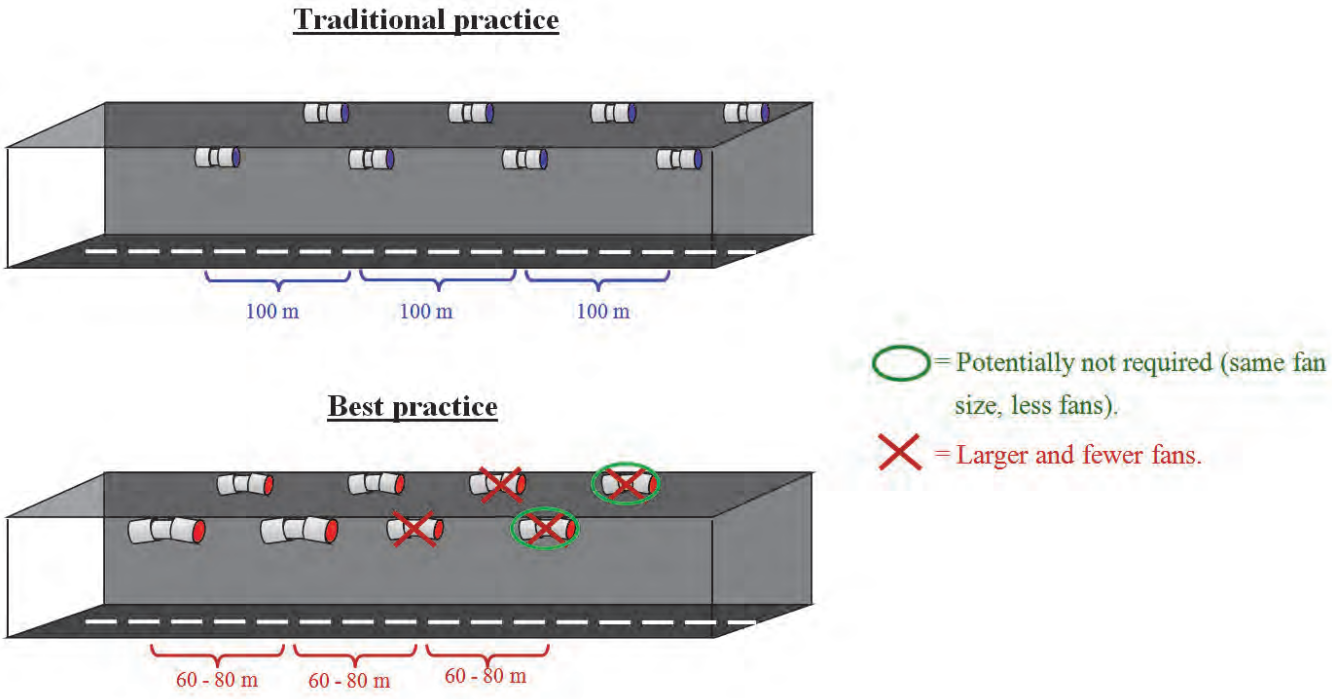

Figure 8: Reducing cable length by installing Banana Jet® systems

- If the diameter is increased, the number of fans, as described above, can be further reduced. Not only are the average cable length reduced, the average size of the cable is smaller since the limitation of voltage drops legally permitted result in ever increasing cable diameter the longer the cables are.

4. MISTAKES IN MODELING JET FANS

It has become very popular to model the ventilation systems using CFD. Unfortunately the quality of this modeling is sometimes not very good and we have seen many mistakes made. At times the result is directly misleading. This paper will not make recommendation about how best to do that modeling, just point out some of the more serious errors when modeling jet fans and in particular when the aim is to compare them to Banana Jet®.

4.1. Using a too simple model of a jet fan

In some models the analyst simply assumes that the air comes out uniformly behind a jet fan or even a "U-form" at the fan outlet. That is not the case. The rotational element of the air flow can be almost eliminated by using turning vanes behind the impeller (which also significantly improves the fan efficiency.) The true air distribution just a couple of D behind the fan looks more like the flame of a candle with an high speed inner core and lower airspeed at the periphery (see also Figure 1).

4.2. Ignoring Coanda effect

In no CFD model have we ever seen the Coanda effect modelled. There may be some, but these have never been presented to us. Since the Coanda effect reduces the efficiency of a traditional jet fan by around 15% this is a major mistake making nonsense of most CFD comparisons with Banana Jet®. When having carried out detailed comparisons of Banana Jet® and traditional jets in actual tunnels we found that most simple models using simple pressure drop calculations use a friction factor that is too high. (Compared to what one would expect be if one calculates a simple duct in an air conditioning system.) This is probably to adjust for the losses from the Coanda effect. The overall results of these simple calculations are therefore by and large correct, but they result in much lower air speed for Banana Jet® compared to what is measured.

4.3. Not adjusting for different background velocity

The air speed profiles in tunnels are assumed to be quite uniform. So when adjusting the effective thrust for background velocity in a tunnel with a series of jet fans typically the average air velocity is being used. That is incorrect. Measurements have found that the inlet velocity for traditional jet fans 100 m downstream is about 30 - 50% higher than the average air velocity. For Banana Jet® the contrary is true. There the air velocity is 50 - 70% of the average velocity. Any model that does not achieve this difference for downstream fans is obviously flawed and not useful for a meaningful comparison.

4.4. Placing Banana Jet® incorrectly

Some simulations locate the Banana Jet® incorrectly such as too far away from ceiling and not bending silencers away from obstructions. As we saw earlier, Banana Jet® can be placed differently in the tunnel and angled so as to further reduce losses and optimize for example the $CO/CO_2/NOx$ concentrations. When for simplicity the same location and flow direction is used the result obviously is suboptimal. Just placing the fan 0.5 m closer to the ceiling will mean that the air speed is 30% lower when it hits the first truck/cars compared to being hung at the same height as traditional jet fans.

4.5. Turning on jet fans too close to the fire (turbulent flow)

Fire scenarios attempt to create a certain stratification of the smoke in the event of a fire. (Although in real life fire experiments burning cars and buses in tunnel show that this is probably a very optimistic assumption.) If at all possible the fans just upstream from the fire, just as in the fire management in enclosed car parks, should not be turned on or at least be the last fans to be turned on. This reduces the chance of blowing high speed air into the fire and

maximizes the chance of creating a laminar flow. This goes for both traditional and for Banana Jet®. Obviously the same scenario should be adopted when doing the CFD simulation. In some simulations we have seen that the fire is assumed in the most unfavourable location for Banana Jet® resulting in a claim that visibility is more reduced with Banana Jet®.

4.6. Ignoring signage, lamps and other equipment outside the traffic envelope

Especially in city tunnels there is a lot of equipment and particularly lamps which are very close to the outlet of the jet fans. CFD models making comparisons between these 2 types of fans should take that into account as the traditional jet fan will in all cases lose a lot of thrust against those obstructions, so that in practice they have to be moved or dismounted because the otherwise would be blown down.

4.7. Assuming too high traffic load in case of fire

As a fan maker we should maybe be happy when the CFD simulator assumes the tunnel to be completely filled with cars when there is a fire resulting in much higher required thrust. That a tunnel jammed full of cars will develop a catastrophic fire is unlikely. Stopped cars do not have catastrophic accidents. A high-speed crash can realistically only occur at the portals of the tunnel in case a motorist has not notice the slow down in front. Reversing the airflow would allow the smoke to be exhausted by the portal leading the stopped cars free to safely exit the tunnel.
The more interesting case, which is rarely modelled, is the visibility and concentration of noxious gases when there is a slow down or stoppage inside a tunnel, which is a much more likely event. As stated above, the directed faster airflow among the cars may be of significant advantage

4.8. Over-pessimistic location of trucks/busses (in Europe by law making right lane only)

Not that we believe some CFD analyst have malicious intent, but too frequently have we seen scenarios where all high vehicles are placed right in front of the outlet of the Banana Jet® fans. (Even then and even without the Coanda effect the "improved" performance of traditional Jet fans is not very large.)
Especially in Western Europe these scenarios are unlikely as by law in most tunnels trucks and buses have to stay in the right-hand lane.

5. SUMMARY

Banana Jet® has proven their superior performance in all jet fan ventilation systems we are aware of. They inherently have a 25 – 30% higher efficiency because the do not suffer from the direct losses at the fan. In some types of tunnels and installations the direct advantage can be as high as 60% as proven by measurements and CFD calculations. Selecting and installing them intelligently can further increase their performance.
Not only do Banana Jet® reduce the energy consumption for the end user, but the overall cost in terms of number of fans required, cable length and sizes, switch gear, installation cost etc. holds significant benefits for the contractor.

One hindrance in the more wide spread use of such systems seem to be the incomplete CFD modelling of these systems and many wrong assumptions. Not only do these models underestimate the losses from traditional jet fans, especially by not taking into account the Coanda effect, they also do not use the degrees of freedom that Banana Jets® offer in their selection and installation. One often overlooked benefit of Banana Jet® is that they can create higher air velocities around the cars, especially in the corners compared to traditional jet fans in the case of the very common slow moving or even stooped traffic and thus reducing inhalation of polluted air by the user of the tunnels.

6. BIBLIOGRAPHY

[1] *Optimierung von im Tunnel installierten Strahllüftern*, Modell, Dr. Witt; Witt & Sohn AG 2002

[2] *Tunnel de Collombey*, *Strömungsmessungen,* Matthias Marti; HBI Haerter AG 2004

[3] *Hauptstrasse T8/A8 Tunnels Balmenrain und Uznaberg, Messungen der Lüftungsanlage,* Petr Pospisil/ Martin Ilg/ Matthias Marti; HBI Haerter AG 2003

[4] *Performance of Banana Jet® fans verified by CFD simulations*, Bernado Vazquez/ Karsten C. Witt, Buro Happold Ltd./ Witt & Sohn AG 2010

[5] *A numerical investigation into the performance of two types of jet fans in ventilation of an urban tunnel under traffic jam condition.* Esmaeel Eftekharian/ Alireza Dastan/ Omid Abouali/ Goodarz Ahmad; Tunneling and underground space technology 44 (2014) 56 - 67

REFURBISHMENT OF AXIAL FANS FOR TUNNEL VENTILATION SYSTEMS

Frits van Vemden, Fred van Jaarsveld,
Zitron Nederland

SUMMARY:

During recent years Zitron Nederland has refurbished numerous axial and jet fans for tunnel ventilation systems. Examples are the Arlbergtunnel, the Perjentunnel and the Bosrucktunnel in Austria and the Kerenzertunnel, the Fäsenstaubtunnel, the Belchentunnel and the Leissigentunnel in Switzerland. In this paper Zitron Nederland will share the experiences gained during these refurbishment projects and present some of the lessons learned.

Following topics will be discussed in the paper:
- Scope of refurbishment
- Overhaul of impeller and blades, renewal of blades and bearings
- Overhaul of major components (drive motors, fan isolation dampers, ducting etc.) and surface treatments
- Renewal and improvement of fan sensors and controls, communication with control system
- Re-commissioning of fans and ventilation systems
- Logistical aspects of refurbishment projects “under traffic”

1. GENERAL

Electrical and mechanical equipment for road and rail tunnels are commonly designed for life cycles of 20 to 40 years.

Fans for ventilation systems, jet fans for longitudinal ventilation and axial fans for fresh air supply and extraction of polluted air and smoke are typically designed for a life time of 25 (jet fans) to 40 years (axial fans).

This design life time is considerably shorter than the design life time of the tunnel itself which will be at least 100 years. Therefor refurbishment of electro-mechanical components such as jet and axial fans will be a necessity. Also upgrading of tunnel ventilations systems with the goal to comply with EU-regulations creates an opportunity for refurbishment of existing equipment.

2. JET FANS

Jet fans are designed for a life time of approx. 25 years. In practice jet fans often need to be refurbished after approx. 15 years of operation. The main cause of failure is the drive motor, more specifically the motor bearings.

Specifications quite often call for motor bearings which are “greased for life”. In practice drive motor suppliers guarantee bearings for a L10 lifetime of max. 40.000 hours. This number means that 90% of the bearings should reach min. 40.000 hours of operation, 10% of the bearings may fail.

Jet fans and its drive motors need to be certified for 250 or 400 ºC for 90 or 120 minutes. To comply with this requirement, motor suppliers select a high temperature (high viscosity) grease which has acceptable lubrication properties at high temperatures at the cost of the lubrication properties at ambient temperature.

Suppliers of lubricants have recommendations for shelf and service life of their greases. The values vary but are far from the 25 years which is theoretically required for “life time greased bearings”.

It is recommended to apply grease nipples on motor bearings to enable re-lubrication.

Smaller jet fans should have a greasing tube with a nipple on the fan casing for accessibility.

Drive motor housings are made from cast iron or aluminium with a surface protection. The experience learns that, also when a surface treatment to suit the highest corrosion category (C5) is applied, after 10 to 15 years severe corrosion to the motor housings may occur.

For a “mid-life refurbishment” of jet fans customers may decide to renew the drive motor in its whole or to dismount the motor, replace the motor bearings, check winding insulation and renew the surface treatment of the motor housing. Jet fans should be dismounted from the tunnel and transported to a work shop for this.

For an overhaul or renewal of the drive motor the jet fan impellers must also be removed. This enables cleaning and dye penetrant inspection of the blades. The impeller hubs will have to be cleaned and possibly be re-coated. Removal of jet fan impellers from the motor shaft after a number of years of operation often proves to be a challenge where hydraulic tools are required. Blades often show damages due to objects passing through the fan. After re-assembly the impeller must be re-balanced.

Renewal of motors can cause problems as current regulations dictate high efficiency class motors which can affect frame size and shaft dimensions. A replacement with an dimensionally identical motor may then not be possible.

Nowadays jet fan casings and jet fan silencers for road tunnel ventilation are largely fabricated from stainless steel.

When jet fan silencers are fabricated using rivets and/or spot welding, damage may occur caused by shear stresses on the joints induced by vibrations. Silencer parts should be joined by continuously welding. Spot welding and riveting should be avoided.

Due to the need for tunnel closures, the use of dedicated vehicles/hoisting equipment and the man-hours involved refurbishment of jet fans is, compared to the initial investment, relatively expensive. An additional initial investment to extend operating life will quickly be worthwhile.

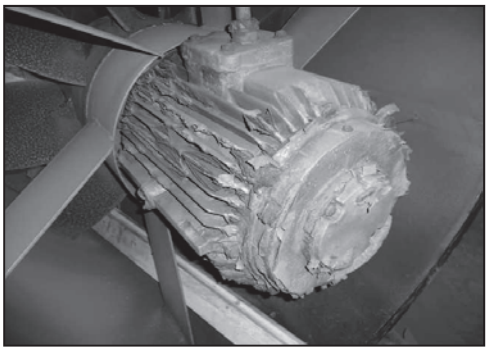

Figure 1: Corroded jet fan motor

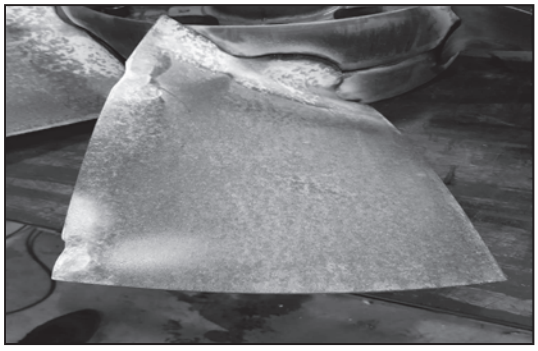

Figure 2: Damaged jet fan rotor

3. AXIAL FANS

Depending on actual operating conditions axial fans for fresh air supply and extraction of polluted air will need a major overhaul after approx. 20 years. Fan system components to consider are:

- Drive motor
- Impeller
- Instrumentation and sensors
- Static parts such as fan casings, diffusors, inlet bells/grids, ducting and guide vanes
- Flexible connections
- Fan isolation damper

To enable overhaul of impeller and drive motor these components should be dismounted and be transported to a dedicated work shop. Ideally hoisting equipment and installation hatches are foreseen to enable taking out the complete fan unit or at least the motor/impeller combination. In case no hoisting equipment is foreseen temporary hoisting equipment will have to be installed.

3.1. Drive motor

An overhaul of a drive motor consists typically of following activities:

- Replacement of the bearings
- Replacement of bearing temperature sensors (winding temperature sensors remain)
- Replacement of encoder
- Check of stator winding insulation (when not adequate re-winding is required)
- Check of drive shaft and seats
- Re-balancing of rotor
- Cleaning, repair or renewal of surface treatment

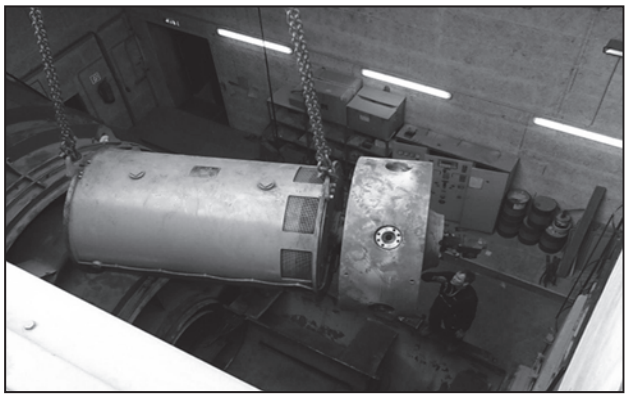

Figure 3: Disassembly of motor/impeller

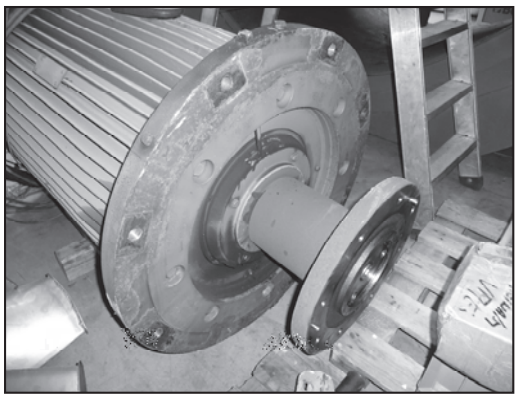

Figure 4: Disassembled motor

3.2. Variable speed drives

When fans are driven by variable speed drives, the capacitors of variable speed drives deteriorate with time and need to be renewed after 10 to 12 years.

3.3. Impeller

The impeller must be removed from the drive shaft. Often this will required special hydraulic removal tools.

Overhaul of an impeller mainly comprises of:

- Dismounting blade adjustment mechanism, blades, blade suspension and blade bearings
- Cleaning and dye penetrant or X-ray checking of blades, blade spindles and hub
- Renewal of bearings, seals, (blade) bolts and fasteners
- Re-apply surface treatment of the hub
- Balancing of the assembled impeller

Special attention and often special tooling is required to remove the impeller from the drive shaft. Fan manufacturers often use modified or custom made bearings. A simple 1:1 replacement of blade bearings can result in considerable damage.

Blades may show small damages due to foreign objects passing through the fan. Depending on the severity of the damages and the results of the non-destructive tests renewal of the blades may be required.

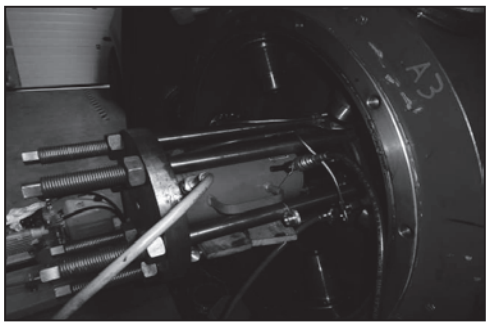

Figure 5: Disassembly impeller

Figure 6: Disassembly blade

Special attention needs to be given to the blade suspension bolts, often made of high tensile strength material. After dismounting these have to be renewed.

Blades of impellers with blades adjustable at standstill can be stuck due to deposits or corrosion and prove impossible to remove. In that case machining will be required and blades will have to be renewed.

Figure 7: Mechanical removal blade

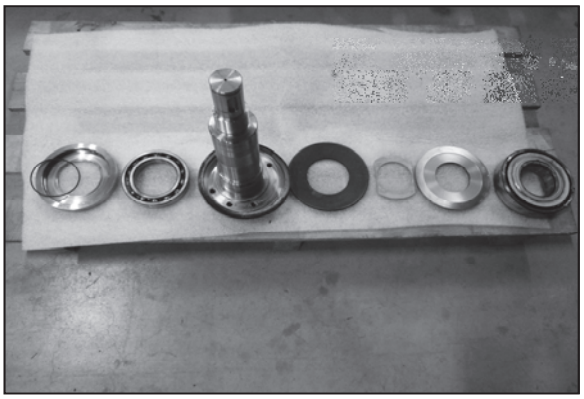

Figure 8: Parts blade suspension

Nowadays with material analysis and 3D scanning techniques it is possible to make a good quality copy of existing blades. Nevertheless it is recommended to check blade loads in relation to the high temperature requirement in case of emergency exhaust fans.

3.4. Static parts

Static parts such as fan casings, diffusors, inlet bells/grids, ducting and guide vanes, usually made from carbon steel with a multilayer surface treatment will show signs of corrosion in various degrees after 10 to 15 years of operation. For a durable refurbishment, the corroded parts should be cleaned thoroughly by pellet blasting.

Ideally the static parts should be dismounted and transported to a work shop where blasting and application of new layers of surface treatment can be done in a controlled environment. Pellet blasting in the fan room causes a lot of dust. Used pellets contaminated with paint and oxidized particles are often considered as chemical waste with special disposal regulations.

Application of layers of paint in fan rooms under non-optimal conditions require special attention as the layers of paint may show delamination.

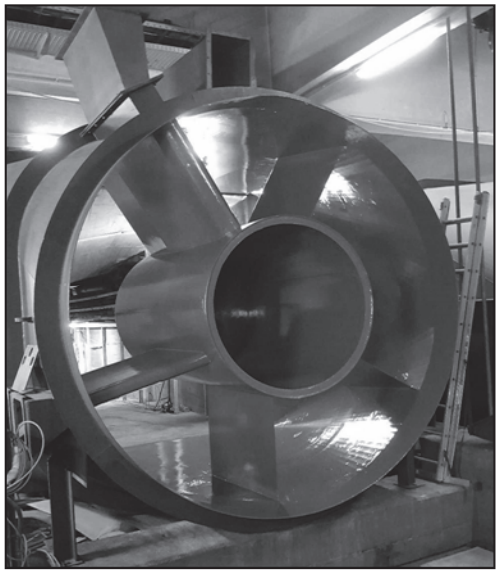

Figure 9: Fan casing after treatment

Figure 10: Delamination after treatment

Dry ice cleaning with CO_2 pellets is a good alternative for cleaning and removal of deposits. Only the deposits remain after cleaning and need to be disposed. Dry ice cleaning is inadequate to remove the corrosion and subsequent application of new layers of paint.

3.5. Fan isolation damper

During a fan refurbishment also the fan isolation damper should be cleaned, the bearings of the damper blades need to be renewed. The actuator will have to be dismounted and sent to the original supplier for renewal of seals and checking the switches.

3.6. Hydraulic unit

Refurbishment of the hydraulic unit powering the blade adjustment mechanism consists of following activities:

- Check and measurement of the oil pumps
- Remove oil and clean the system
- Check of temperature, pressure and level sensors, replacement if required.
- Renew seals
- Renew tubes
- Fill with new oil
- Renew surface treatment

3.7. Fan instrumentation

For a safe and accurate operation large tunnel ventilation fans should be equipped with following instrumentation:

- Speed and sense of rotation
- Measurement of temperature of motor windings and motor bearings
- Volume measurement
- Fan pressure measurement
- Stall monitoring system
- Vibration measurement in X- and Y-axis
- Blade angle measurement system (in case of a fan with blade adjustable during operation)

Knowing the speed and the sense of rotation of the fan is essential for a safe start of the fan. Volume and pressure measurement is required for an accurate control of the ventilation system. Temperature and vibration measurement enables condition monitoring of fan and drive motor.

Older fans with hydraulically adjustable blades often are equipped with a limited number of blade angle indications by means of a cam shaft. An analogue blade angle position signal enables an active stall monitoring system which contributes to safe fan operation at maximum loads.

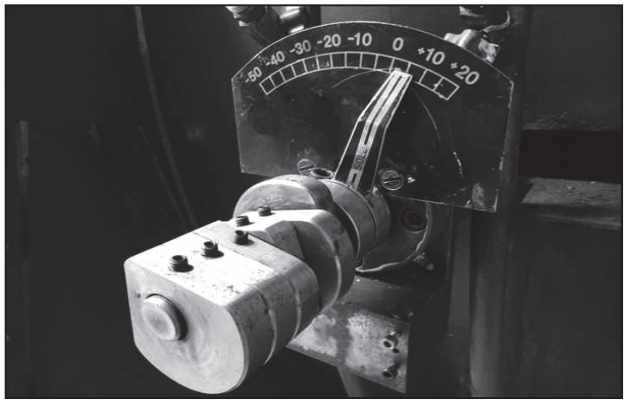

Figure 11: "Digital" blade position

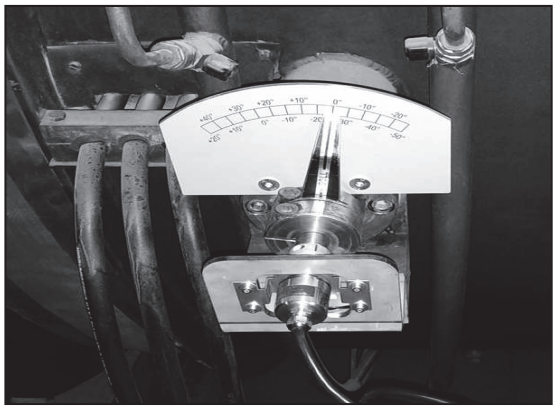

Figure 12: Analogue blade position

When the fan is already equipped with the above instrumentation, the equipment should be thoroughly checked if not renewed completely. Signals must be validated during re-commissioning.

In case some of the instrumentation is not present, we recommend to install this additionally.

When the ventilation system control system is also renewed during a refurbishment of the tunnel equipment, careful consideration must be given to the moment of switching from the existing to the new control system. Refurbished fans with new instrumentation often have to be re-commissioned before the next fan to be refurbished can be taken out of operation. New instrumentation may not be compatible with the existing control system.

4. Logistical aspects

A full closure of an existing tunnel for a longer period of time is usually not acceptable to the public. In winter periods alternative routes may not be available. This means that as a rule, fan refurbishment has to be carried out during temporary or even partly tunnel closures during the night.

In these cases the actual available working time including the time frame for bringing equipment in and out of the tunnel is very limited. Working in parallel at multiple fans is usually not possible because of minimal ventilation requirements. This will extend lead times for refurbishment. Working in tunnels “under traffic” is inherently more dangerous than working in new built tunnels. Accurate registration of staff working in tunnels, enforcement of health and safety regulations and the use of well-instructed and experienced personnel is of the utmost importance for an accident free execution of the work.

SMOKE DETECTION IN ROAD TUNNELS LEADING TO AUTOMATIC INCIDENT RESPONSE

[1]Matthias Lempp, [1]Natalie Riklin, [1]Vincent Butty, [2]Franz Zumsteg,
[3]Markus Eisenlohr, [3]Peter Wartmann;
[1]HBI Haerter AG, CH, [2]US+FZ Beratende Ingenieure, Switzerland
[3]FEDRO Federal Roads Office, Switzerland

ABSTRACT

The numerous tunnels with two-way traffic in the Canton of Grisons, Switzerland, are all monitored from one common control centre. In an emergency, automatic responses control the safety systems. The operator is not expected to intervene manually during the initial phase. Therefore, fire and smoke need to be detected automatically and the ventilation system has to respond with a high degree of reliability. In long and steep two-way tunnels with a smoke extraction system, rapid and precise detection is especially crucial. Under these conditions, the automatic differentiation between a moving and a stationary smoke source is particularly challenging.

The Swiss directive [2] released in 2007 aims at a rapid detection. According to this directive new and refurbished road tunnels in Switzerland are required to be equipped with a smoke detection system in addition to the thermal linear sensor. The first of the two systems to trigger the alarm, initiates all necessary reactions of the safety system.

This paper focusses on smoke detection and the triggering of the appropriate ventilation response. The evaluation routine was optimized using a simulation model and numerous data sets obtained from smoke tests. However, in the case of an initially moving smoke source, a trade-off between a quick reaction and a precise detection has to be accepted.

The article covers the following subjects:

- Presentation of the refurbishment of the Crapteig Tunnel
- Requirements and functional description of the automatic smoke detection in case of a fire incident
- Results of smoke tests with stationary and moving smoke sources
- Limitations of smoke detection for automatic ventilation control
- Proposals regarding further measures for the improvement of the reliability of smoke detection and standardised test procedures

Keywords: Tunnel safety, smoke detection, ventilation control, test procedures

1. INTRODUCTION

The Crapteig Tunnel is part of the A13 route, an alternative to the Gotthard route. The tunnel opened to traffic in 1996. It is 2.2 km long, has a slope of 6.5% with 2 lanes uphill and 1 lane downhill. From 2015 to 2017 the electromechanical equipment of the tunnel was refurbished and upgraded in night shifts.

The emphasis of the original transversal ventilation system design was on maintaining sufficient air quality during normal operation.

The tunnel was equipped with a distributed air exhaust and supply system, which was divided into two sections (Figure 1). This system design managed normal operation satisfactorily.

However, fire tests conducted in 1998 already showed that due to the lack of controllable dampers and without jet fans, the ventilation system could not satisfactorily control the smoke propagation. The distributed air exhaust system with extraction slots every 10 m needed to be triggered by temperatures exceeding 100°C in order to enable a more concentrated air extraction over the fire location. These temperatures were not achieved in the fire tests despite a test fire of 5 MW. Furthermore, the control of the bulk air velocity in the tunnel using the fresh air inlets was not sufficient.

To eliminate the safety deficit, two projects were launched. The aim of the first project was to upgrade the electromechanical equipment and refurbish the ventilation system to the current standards of the Swiss Federal Road Office FEDRO [1], [2]. These measures were carried out during the years 2015 to 2017. The second project consists of building a new parallel safety gallery, according to the requirements of [4] and [3]. The emergency exits are expected to be operational by 2022.

2. REFURBISHMENT OF THE CRAPTEIG TUNNEL

Major changes to the original ventilation system were necessary in order to fulfil the requirements of the current FEDRO standards, whilst not lowering the previous safety level during the execution phase.

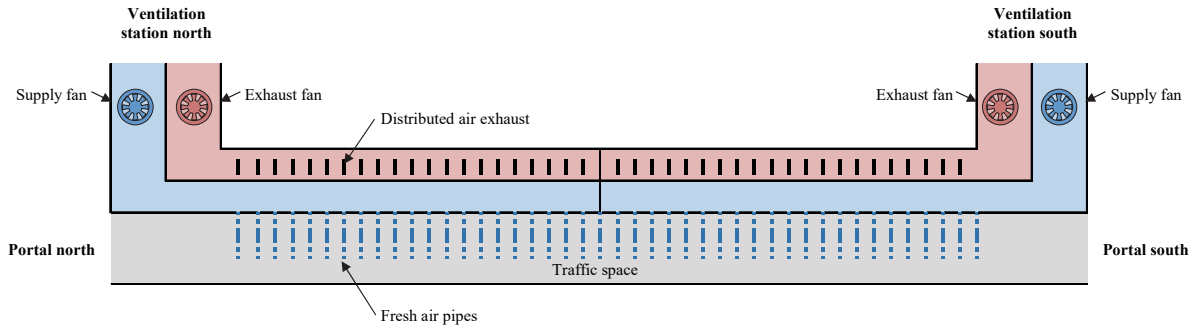

Figure 1: Ventilation system before the refurbishment

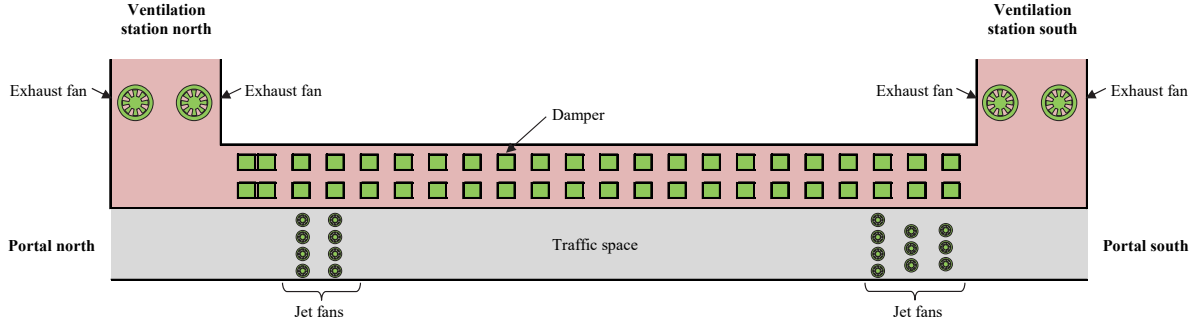

Figure 2: Ventilation system after the refurbishment

The following modifications were undertaken:

Ventilation stations:

- Replacement of the axial fans (2 supply and 2 exhaust fans) by 4 axial exhaust fans. The fans are equipped with variable pitch in motion to be able to cover varying pressure differentials. Additionally the limitations of the available power supply required the use of variable speed drives in order to limit the starting current.
- Since distributed fresh air is no longer required for the fresh air demand, all axial fans are redirected to the existing exhaust stacks.

Ventilation ducts:

- All fresh air orifices were sealed. Following this step, smoke exhaust dampers were installed every 90 m along the former fresh air duct.
- The former supply and extraction ducts were aerodynamically connected.
- After completion of the new exhaust system, 5 over-head niches for jet fans were built. This step required temporary partitioning of the new exhaust duct. The jet fans were installed and commissioned according to the progress of work.

Traffic space:

- In addition to the existing thermal linear sensor 2 groups of 3 velocity sensors, 25 smoke detectors and 4 opacity sensors were newly installed. The passively ventilated smoke detectors are mounted under the intermediate ceiling along the centreline of the tunnel.

3. INCIDENT PROCEDURE

According to the FEDRO standards [6] the first main alarm of the thermal detection or the designated smoke sensors triggers all safety systems. The systems then switch to the operation mode predetermined by the control system. Subsequent alarms do not overrule the active alarm.

The opacity monitors only control the ventilation during normal operation.

Due to the limitation of available manpower at the operations centre, a manual intervention by the operator into the automated procedure is considered unpractical. The main focus of the operator is to support the rescue forces.

The fire detection systems in the traffic space consist of smoke detectors every 90 m and the thermal linear sensor along the whole tunnel length. While the smoke detector and the thermal linear sensor affect the ventilation system and the other equipment directly, the video system provides a possibility for the operator to get additional visual information.

Figure 3 shows an extract of the reflex matrix giving information on the correlation between detection and reaction.

detection \ reaction		Incident lighting	Traffic lights		Ventilation		Video signals
			warning	at the portals	preparation	incident	
Manually by tunnel user							
Thermal detection	Pre alarm						
	Alarm						
Smoke detection	Stationary smoke sources						
	Moving smoke sources						

Figure 3: Extract of the reflex matrix for the Crapteig Tunnel

The detection of a localised fire or smoke source automatically starts the smoke extraction system: opening 2 pairs of dampers, starting up the 4 extraction fans and initiating the control process for the longitudinal air flow. In general the latter consists of a symmetrical air flow in the tunnel cross section, from both portals to the extraction point. If the incident is close to a portal the system reaction depends on the direction of the airflow at the moment when the main alarm is set off. With air flowing into the tunnel the smoke is extracted through the dampers whereas with airflow out of the tunnel the smoke is pushed out of the portals using jet fans.

4. REQUIREMENTS FOR THE SMOKE DETECTION

[2] requires a smoke sensor at every tunnel cross section where dampers are located. The technical manual [5] states the following key requirements for smoke detection:

- Use of two smoke concentration threshold values (GW1 = 10 1/km, GW2 = 30 1/km). Exceeding the threshold value GW1 starts the smoke evaluation routine and computes the smoke propagation velocity. GW2 triggers the alarm stationary smoke source.
- Distinguish between mobile and stationary smoke sources, starting with the assumption of a mobile source.
- Take into account the smoke propagation velocity and the bulk air velocity in the tunnel.

Whereas requirements exist for thermal linear detectors and their testing [2], [8], no specifications are given for the testing of the smoke evaluation routine.

In the design process, the ventilation engineer has to define a detailed functional description based on the above-mentioned requirements. Further assumptions are necessary, e.g. sample rates, averaging or the storage of the status of each smoke detector. It is inevitable that all persons involved in the process need to meet high technical and communicative demands.

5. FUNCTION OF THE SMOKE DETECTION

The smoke evaluation routine analyses the sequence of the data of the smoke detectors. The smoke source is either a vehicle that has already stopped or a moving vehicle. For the safety of the tunnel users it is essential to determine the correct position of the stationary incident. As long as the smoke source is still moving or the location of the stationary source is not identified, the air extraction must not be activated since an air extraction at the wrong location would endanger the tunnel users by moving smoke from the incident location through the tunnel to the distant extraction point.

In the Crapteig tunnel and 10 other tunnels in the Canton of Grisons, the same smoke evaluation routine is implemented. The main features of the routine are:

- Estimate of the smoke propagation velocity using the sequence of the smoke detector signals
- Use of a limited spatial evaluation zone for the smoke detectors considered in the smoke evaluation routine

The correct implementation of the smoke evaluation routine is verified before conducting a smoke test. The state of the art is to simulate values for single smoke detectors in a specific sequence and to check the reaction of the smoke evaluation routine. The values are mimicked using the manual-simulation mode on the user interface. The ventilation engineer specifies the test sequence for each project individually.

6. RESULTS OF SMOKE TESTS WITH STATIONARY AND MOVING SMOKE SOURCES

During real fires as well as in tests it is very unlikely that smoke detectors are triggered in a linear sequence. Thermal effects and the turbulent bulk air velocity influence the movement of smoke. The distribution of smoke in the traffic space is irregular and the smoke concentration varies, as shown in Table 1.

In the Crapteig Tunnel tests, the smoke consisted of a dense white aerosol as seen in Figure 4. This procedure does not require protection measures of the tunnel lining since the heat development is small but still buoyant enough to make it rise to the ceiling. The tests included stationary as well as moving smoke sources.

Figure 4: Moving smoke source in the Crapteig tunnel

Table 1: Smoke distribution with moving smoke source. In test A, the vehicle is moving against the direction of the bulk air flow; in test B, both directions are the same. The smoke source and the absolute value of the vehicle speed and the bulk air velocity are comparable in tests A and B.

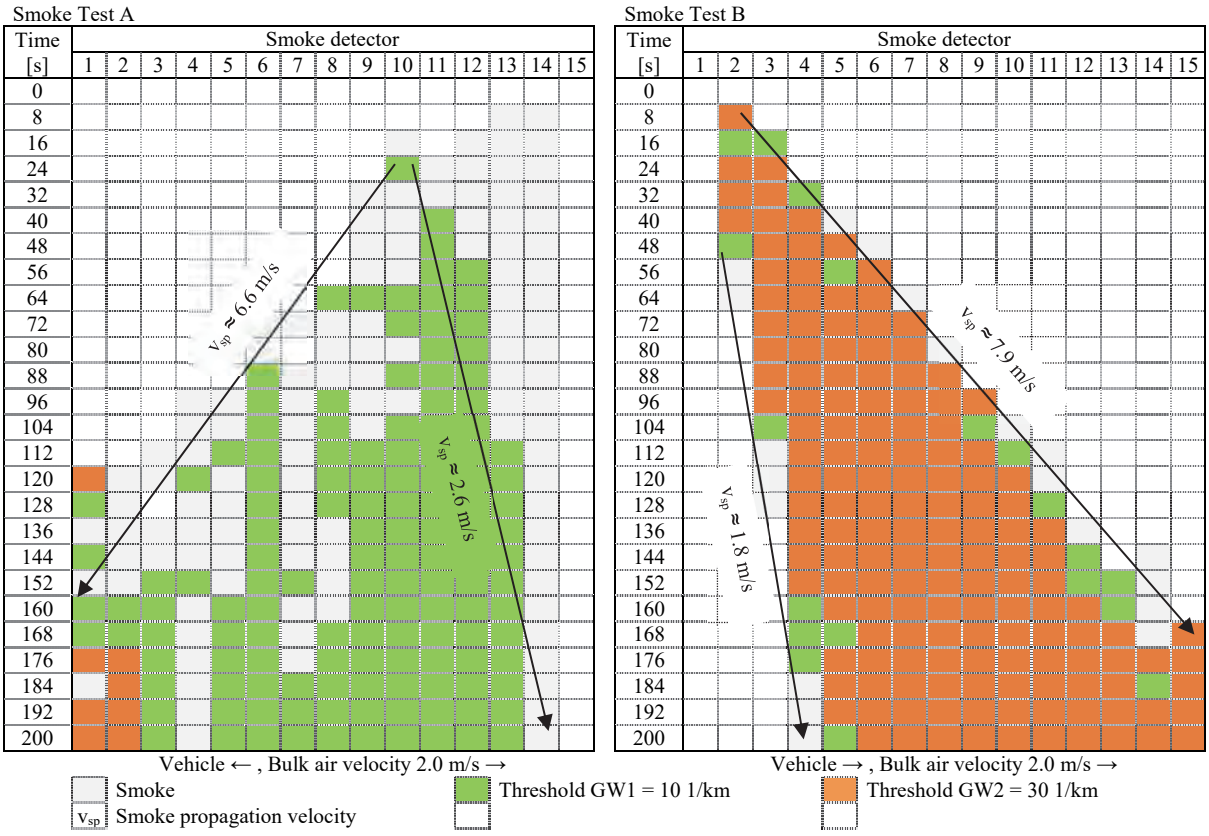

Observations from the Crapteig smoke tests are:

- Stationary smoke sources are detected with great reliability.

- The evaluation of the stopping point of moving smoke sources (approx. 20 m^3/s smoke generation, driving speed 40 km/h) has shown to be reliable as long as the direction of the bulk air velocity and the moving smoke source are equal.
- If the direction of the bulk air velocity is opposite to the direction of travel of the moving smoke source, it is likely that the calculated location will have an offset with respect to the true location of the vehicle. In the Crapteig Tunnel, the longest offset with the current *Grisons routine* under unfavourable circumstances was up to 800 m.
- As shown in Table 1, the detected opacity is strongly reduced if the direction of the bulk air velocity is opposite to that of the moving smoke source. Reasons for this are the higher dilution by the approaching fresh air and the more intensive turbulence. In combination with the implemented spatial evaluation zone in the Grisons routine these effects can lead to a disregard of smoke detectors outside the zone.

The tests with moving smoke sources in the Crapteig Tunnel confirmed results from tests in other tunnels where, under certain circumstances, the correct position of a moving vehicle could not be evaluated.

7. OPTIMISING THE SMOKE EVALUATION ROUTINE

Taking into account experiences from several tunnel projects a new evaluation routine was developed and optimised by using the existing 35 data sets from smoke tests. In January 2018 an additional test series with moving smoke sources expanded the data set. Smoke generation with low smoke concentrations, simulating a starting fire was of special interest. An entire data set of 55 tests was pre-processed and then used in the optimised smoke evaluation routine HBISD^{plus}. This routine allowed performing a parameter study. The following parameters were examined:

- Increase of the spatial evaluation zone. This zone specifies the spatial expansion of smoke detectors used in the smoke detection routine.
- Influence of the threshold values for GW1 and GW2.

Table **2** shows the comparison of the currently implemented *Grisons routine* to the routine HBISD^{plus} with 16 different parameter sets.

Table 2: Results of the parameter study for moving smoke sources for the current state Grisons routine and the optimised HBISD^{plus} routine

	Grisons routine	HBISD^{plus} GW1 = 10 1/km, GW2 = 30 1/km				HBISD^{plus} GW1 = 30 1/km, GW2 = 30 1/km			
		evaluation zone ±3 SD	evaluation zone ±5 SD	evaluation zone ±8 SD	no evaluation zone	evaluation zone ±3 SD	evaluation zone ±5 SD	evaluation zone ±8 SD	no evaluation zone
Not detected	5.5%	3.6%	1.8%	1.8%	1.8%	1.8%	0.0%	0.0%	0.0%
Out of range	18.2%	5.5%	7.3%	7.3%	5.5%	14.5%	16.4%	14.5%	12.7%
+/- 3 to 4 SD	9.1%	9.1%	7.3%	7.3%	7.3%	3.6%	3.6%	3.6%	3.6%
+/- 1 to 2 SD	32.7%	36.4%	38.2%	38.2%	38.2%	34.5%	38.2%	38.2%	36.4%
Exact	34.5%	45.5%	45.5%	45.5%	47.3%	45.5%	41.8%	43.6%	47.3%
Not acceptable	32.7%	18.2%	16.4%	16.4%	14.5%	20.0%	20.0%	18.2%	16.4%
Acceptable	67.3%	81.8%	83.6%	83.6%	85.5%	80.0%	80.0%	81.8%	83.6%

	HBISD^{plus} GW1 = 30 1/km, GW2 = 75 1/km				HBISD^{plus} GW1 = 75 1/km, GW2 = 75 1/km			
	evaluation zone ±3 SD	evaluation zone ±5 SD	evaluation zone ±8 SD	no evaluation zone	evaluation zone ±3 SD	evaluation zone ±5 SD	evaluation zone ±8 SD	no evaluation zone
Not detected	20.0%	20.0%	21.8%	21.8%	9.1%	3.6%	7.3%	9.1%
Out of range	9.1%	9.1%	7.3%	7.3%	12.7%	10.9%	10.9%	10.9%
+/- 3 to 4 SD	3.6%	3.6%	3.6%	3.6%	9.1%	7.3%	7.3%	7.3%
+/- 1 to 2 SD	27.3%	25.5%	23.6%	25.5%	30.9%	36.4%	32.7%	32.7%
Exact	40.0%	41.8%	43.6%	41.8%	38.2%	41.8%	41.8%	40.0%
Not acceptable	32.7%	32.7%	32.7%	32.7%	30.9%	21.8%	25.5%	27.3%
Acceptable	67.3%	67.3%	67.3%	67.3%	69.1%	78.2%	74.5%	72.7%

The results of the parameter study are:

- For tests with a stationary smoke source, the location was determined with a high degree of temporal and spatial accuracy. The verification of a stationary source takes approximately 50 secs.
- The currently implemented *Grison routine* leads to acceptable results in 67% of the cases. Acceptable is defined here as an aberration of max. 2 smoke sensors or 180 m.
- The routine with the best performing parameter set leads to an acceptable smoke detection in 86% of the tests.
- The best parameter set contains unchanged threshold values GW1=10 1/km and GW2=30 1/km but with abatement of any spatial evaluation zone.

Videos of real incidents prove that it remains impossible for an automatized routine to detect moving smoke sources with absolute reliability. Smoke might not impinge the detectors and the smoke detectors are not necessarily triggered in a regular sequence. With respect to these facts, a detection rate of 86% is high.

8. EXPERIENCE WITH SMOKE DETECTION FOR AUTOMATIC VENTILATION CONTROL

Since 2007 smoke detectors are part of the standard equipment in Swiss road tunnels. The experience gathered from the use of smoke detectors in road tunnels is presented below:

- The threshold values GW1=10 1/km and GW2=30 1/km are adequate for smoke detection.
- Incidents with little heat development are detected significantly faster with smoke detection than with thermal detection.
- Using a transgression of the threshold GW1 to trigger reactions such as stop lights at the tunnel portals is considered inappropriate due to the high number of false alarms when referring only to GW1.
- Bulk air direction and velocity have an important effect on the dilution of smoke from a slowly moving source and therefore on smoke detection.

9. IMPROVEMENTS FOR SMOKE DETECTION AND TEST PROCEDURES

The proposed improvements are:

- Standardisation of the smoke evaluation routine.
- Standardisation of the virtual smoke detection tests with defined sample data (FAT of control system). A set of virtual data shall be predefined to set the minimal standard of what the executed smoke routine must handle successfully.
- Standardisation of on-site tests especially for moving smoke sources.
    - Factors to be standardised are smoke quality and quantity, heat development of the source, speed of the moving source and bulk air conditions.
    - These tests shall be carried out in form of a general test for detection and ventilation.
- Standard tests with moving smoke sources combined with additional heat sources are desirable, however technically challenging and at the time, not state of the art.

10. SUMMARY AND CONCLUSIONS

The refurbishment of the Crapteig Tunnel including a state of the art ventilation system and up to date detection methods was fulfilled successfully within the given time and cost frames. Whereas the ventilation system functions very reliably there is still room for improvement of the detection of incidents. The major challenge here, is detecting any type of moving smoke source and assigning its stopping location to the correct fire zone within the tunnel.

The current smoke evaluation routine functions reliably, but it is known to occasionally determine the wrong position of a stopped vehicle if the smoke detectors are not triggered in a constant sequence. Hence efforts were made to improve the situation. The key step was to develop an optimised smoke evaluation routine. For the optimization of the smoke evaluation routine, 55 data sets of smoke tests were used. This process led to the optimised smoke evaluation routine HBISD^{plus} with an increase in the detection reliability of incidents from 67% to 86%. In spring 2018 this optimised routine has not been implemented in any tunnel yet. Approval is expected for Tunnel Crapteig until summer 2018.

Potential for further improvement of reliable smoke detection remains. This is due to the circumstance that the FEDRO guidelines are not specific enough in this area and allow room for interpretation, starting with the design of the system and ending with the testing of the software. This will allow for a more efficient use of the already installed hardware and achieving a higher safety standard at moderate costs.

This will allow for a more efficient use of the already installed hardware and achieving a higher safety standard at moderate costs.

The current FEDRO standard uses thermal and smoke monitoring to detect incidents. In the first phase of an incident, the concept relies on automatic processes, without requiring the operator to intervene or adjust the ventilation system control. The smoke detection concept is confirmed by the high success rates, when correctly implementing a well-engineered smoke detection routine. Further, the standardization of the smoke detection routine design and its testing must be a future goal.

11. REFERENCES

[1] Swiss Federal Roads Office: Directive 13 001, Lüftung der Strassentunnel, V2.03, 2008

[2] Swiss Federal Roads Office: Directive 13 004, Branddetektion in Strassentunneln, V2.10, 2007

[3] Swiss Federal Roads Office: Directive 19 004, Risikoanalyse für Tunnel der Nationalstrassen, V1.01, 2014

[4] Standard SIA 197/2, Design of tunnels – road tunnels, 2004

[5] Swiss Federal Roads Office: Fachhandbuch 23 001-11510, Brandmeldeanlage Tunnel, V2.10, 01.01.2018

[6] Swiss Federal Roads Office: Fachhandbuch 23 001-11315, Funktionen der Lüftungssteuerung, V2.00, 01.01.2015

[7] Council of the European Union, EU: Directive on Minimum Safety Requirements for Tunnels in the Trans-European Road Network, 2004/54/EG, 2004

[8] Council of the European Union, EU: Directive on Fire detection and fire alarm systems - Part 22: Resettable line-type heat detectors, 54-22, 2015

[9] Zumsteg, Steinemann, Eisenlohr: On the road to safer tunnels, Conference "Tunnel Safety and Ventilation", 2016, Graz

RAPID INCIDENT DETECTION IN TUNNELS THROUGH ACOUSTIC MONITORING – OPERATING EXPERIENCES IN AUSTRIAN ROAD TUNNELS

[1]Franz Graf, [2]Martin Gruber
[1]JOANNEUM RESEARCH Forschungsgesellschaft mbH, Austria
[2]ASFINAG Bau Management GmbH, Austria

ABSTRACT

AKUT is an innovative tunnel safety system based on the automatic detection of abnormal noises. Analyses on all live AKUT systems show that all relevant incidents in these tunnels were first detected by AKUT. The head start provided by AKUT in these incidents ranged from several seconds to over 11 minutes. Furthermore, false alarms were also explained. The analyses resulted in very low numbers of false alarms, which when paired with the high detection performance, led to extremely positive feedback from the operator. Aspects of microphone maintenance and cleaning will also be discussed using experience gained in a tunnel that has been operating for 8 years.

Keywords: Acoustic tunnel monitoring, AKUT, microphone, operating experience, maintenance, detection rates

1. INTRODUCTION

The rapid detection of critical incidents in tunnels is essential for the triggering of emergency responses and the evacuation of people involved in accidents in the tunnel. Immediate reaction by the operators in the traffic management centre is not only important for the persons in the tunnel – rapid response is also important for the protection of the infrastructure.

In order to enable such rapid incident detection, JOANNEUM RESEARCH combined forces with ASFINAG (Austrian Motorway and Expressway Network Operator) to jointly develop a system for the acoustic monitoring of tunnels – AKUT. Comprehensive research and field tests were carried out between 2002 and 2009 leading to implementation of the first AKUT pilot system for ASFINAG in the Kirchdorf tunnel in 2010. Over the next 4 years, between 2010 and 2013, ASFINAG tested and evaluated the system in live operation. Parameters such as the detection rate, the head start over other safety systems and false alarm rates were of primary interest. However, other aspects underlying the decision to rollout the AKUT system in the ASFINAG network were the effort for maintenance, service and repair.

Due to the extremely positive evaluation results, in 2014 ASFINAG decided to rollout the system throughout Austria in all tunnels in hazard classes 3 and 4. The general agreement between ASFINAG and JOANNEUM RESEARCH provides for a total of 56 tunnel systems to be equipped with AKUT by 2029. When completed, approximately 3,500 microphones will have been installed in ASFINAG tunnels and the safety in Austrian tunnels will have been increased in 24/7 operation.

2. ACOUSTIC TUNNEL MONITORING – HOW IT WORKS

The soundscape of noise occurring in tunnels is dominated by the sounds emanating from passing vehicles such as engine, rolling and air flow noise. Noise anomalies such as accidents, tyre squealing and even people shouting are detected by the microphones located in the tunnel. The distance between microphones is approximately 125 m, whereby a video camera and a microphone are installed at the same location.

Specially trained acoustic detectors recognise the abnormal sounds in real-time and allocate them to predefined noise classes. Accidents and other critical incidents in the tunnel are always accompanied by distinguishable sounds. These sounds occur at the instant in time of the incident - not after a delay - and can be detected immediately.

The huge advantage of acoustic detection is that AKUT can react **directly** to the critical incident (e.g. accident noise after a collision). This means that AKUT can trigger an alarm in the traffic management centre just 0.7 seconds after the incident. Other safety systems usually recognise the consequences of an accident **indirectly** (e.g. slow drivers, queues, etc.) and hence require a longer amount of time to trigger an alarm.

After rapid detection by AKUT, the operator can immediately capture the situation by activating the corresponding camera and trigger the appropriate actions. This saves valuable time and provides the parties involved in the accident and the following vehicles with the maximum of emergency response and accident prevention measures.

Currently, the following sound classes are detected:

- Accident/tyre burst
- Tyre squeal
- Door slam
- Honking
- Voices/shouting (VoiceScan)

3. HARDWARE STRUCTURE

The first elements in the signal chain are the microphones mounted in boxes located in the tunnel. The microphones are encased in a special membrane that protects them from water and fine dust ingression. The membrane does not require any additional cleaning. The microphones are cleaned as part of the normal, periodic tunnel washing activity. If the protective membrane needs replacing, this can be done within a few seconds.

There are three variations for the hardware structure layout. Depending on the available infrastructure in the tunnel, one of the following variants can be selected:

<u>Variant 1: Microphone and Smartcam</u>

In this variation, the microphone is directly connected to the Smartcam. The Smartcam digitalises the audio signal and generates an IP-data stream that is transmitted over a network (optical or electrical).

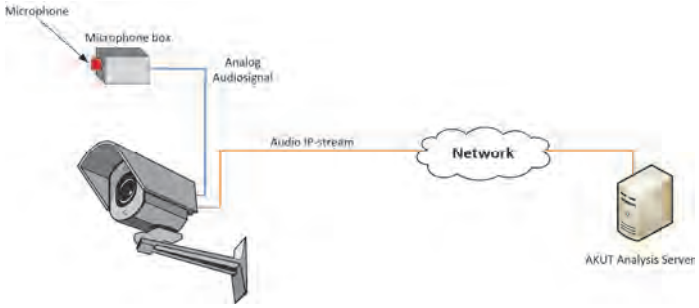

Figure 1: System structure when using Smartcams

Variant 2: Separate Audio Network

The audio signals in this variation are transmitted to the analysis server via a separate audio network. This variation is used if an existing video system is to be refurbished with AKUT.

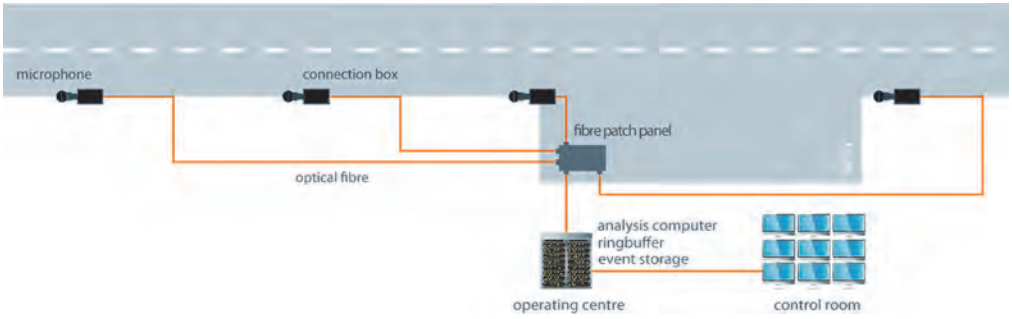

Figure 2: System structure when using an audio network

Variant 3: Combined Audio and Video Network

If the audio and video networks are combined in a similar fashion to variant 1, then the costs for the data transmission devices can be saved. The audio and video signals from a location are transmitted together on a single cable (optical or electrical).

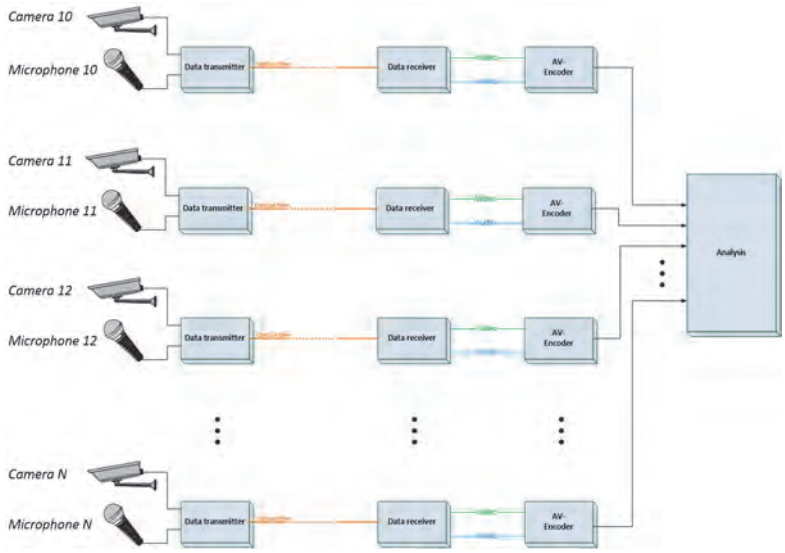

Figure 3: System structure when using a combined audio and video network

4. AKUT INSTALLATIONS

As of March 2018, AKUT systems have been installed in 22 tunnels run by ASFINAG in Austria and in the Southwick tunnel in Great Britain. Currently, 1150 microphones run in 24/7 operation and trigger alarms for abnormal noises.

In Austria, as of March 2018, 3 AKUT systems are under construction, 4 systems are in the planning stage, and 27 tunnel systems are in ASFINAG's construction programme up to 2029. When completed, ASFINAG tunnels will contain approximately 3,500 microphones.

In parallel to the activities in Austria and Great Britain, work is in progress on the rollout of AKUT systems in other countries.

5. OPERATIONAL EXPERIENCE

5.1. Evaluation of current systems using the ASFINAG incident database

The first AKUT systems for ASFINAG went online in the middle of 2016. Over 1.5 years of operational data with these first AKUT systems are now available. Specifically, the following systems were analysed:

Table 1: Overview of tunnels used for the incident analysis

Tunnel	Length in m	Number of bores	Number of microphones	Average Daily Traffic Volume
Bosruck, A9	5,505	2	122	17,470
Ehrentalerberg, A2	3,345	2	75	30,623
Falkenberg, A2	1,090	2	26	30,623
Lendorf, A2	800	2	20	30,623
Trettnig, A2	450	2	12	30,623
Götschka, S10	4,435	2	86	37,298
Neumarkt, S10	1,970	2	38	37,298
Pernau, S10	245	2	4	37,298
Lest, S10	545	2	12	37,298
∑ 9 Tunnel	**∑ 36.77 km Bore length**		**∑ 395**	

The ASFINAG incident database, where all events are documented in detail, was used as the basis for the following analyses. As a first step, all incidents were evaluated that have been documented in the incident database since July 2016. Each incident was analysed in detail using the alarm messages and alarm lists from the traffic control system. The evaluation primarily followed the order in which the alarm messages occurred after an incident.

In the period from July 2016 to February 2018, a total of 28 incidents were documented in the incident database for the specified systems. Of these 28 incidents, nine were not included in the analysis. From the nine that were not evaluated, six occurred outside the tunnel and the entrance portal or gallery area (where no microphones are installed), the data set for one incident was not complete. One incident was a vehicle underbody fire, and in one event, the vehicle merely rolled onto the traffic lane without causing any further damage. This means that 19 incidents were relevant for further evaluation. Table 2 shows the classification of these 19 incidents.

Table 2: Classification of the relevant incidents

Incident type	
Rear-end collision	5
Collision of 2 vehicles	4
Collision of a vehicle with the infrastructure	10
Total	**19**

The results of the analysis show that all 19 incidents were detected quickest by AKUT, without exception. This means that the operators first received an alarm message from AKUT for every incident, whereby the cameras were then activated and the operator could observe what was happening in the tunnel after approximately 0.7 seconds.

Figure 4 shows the head start AKUT provides via its alarms. It can be seen that for 58% of the incidents, the time advantage provided by AKUT was up to one minute, and for 42% of the incidents, the time advantage was greater than one minute. The largest head start compared with other safety systems was 11 minutes and 46 seconds. Two incidents were exclusively alerted by AKUT.

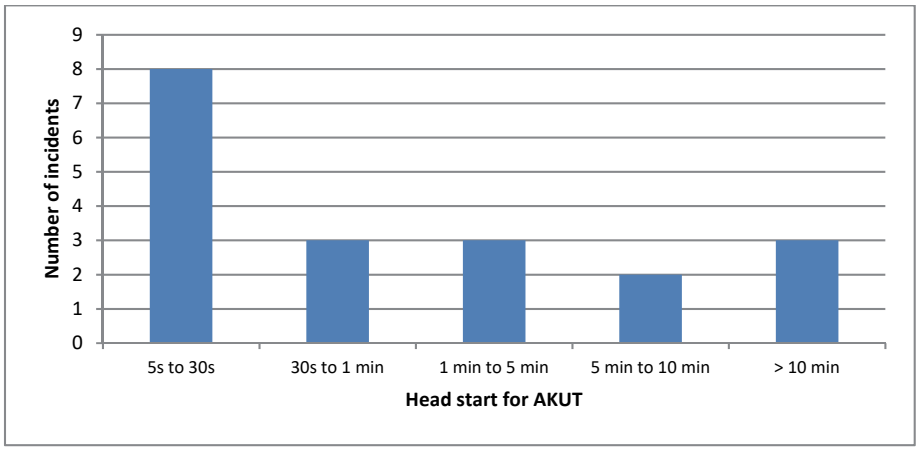

Figure 4: Head start provided by AKUT compared to other tunnel safety systems

In this context, it is also interesting to note which safety systems reported incidents to the traffic control system in second place after AKUT. Table 2 shows the distribution of the alarms provided by other safety systems.

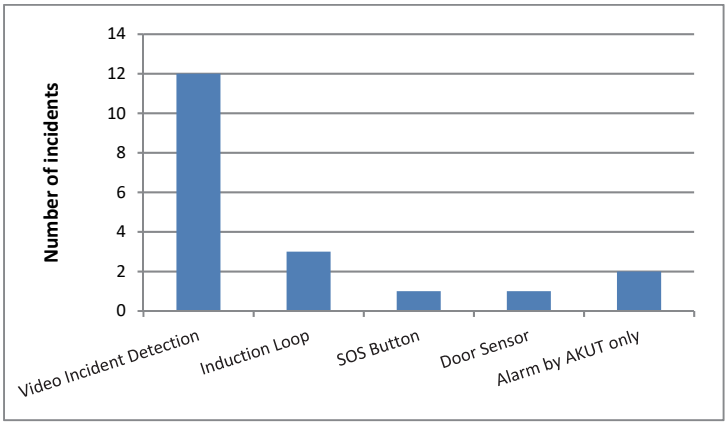

Figure 5: Distribution of alarm reports by other safety systems that reported alarms in second place after AKUT

5.2. Detection of loose manhole covers

Water is removed from the tunnel via tunnel drains and corresponding shafts that are closed with manhole covers. The manhole covers are bolted down with several bolts to prevent them from jumping out, for example by the suction effect caused by a passing truck.

During the operation of AKUT systems, operators in the traffic control centres noticed that the detectors also reacted to loose manhole covers. Since traversing loose manhole covers causes a noise impulse which sounds similar to the slamming of a door, the noise of a loose manhole cover was largely detected as a “door slam”.

Several events were documented, where AKUT detected loose manhole covers very early on and triggered an alarm. After the alarm had been verified by the operator, the offending tunnel bore was immediately closed and repairs effected.

AKUT was thus able to successfully prevent serious traffic accidents caused by “open manholes”. The detection of loose manhole covers was not considered in the product development phase. In the meantime however, the long-term operation of AKUT has shown that the detection of loose manhole covers is an essential contribution to the prevention of critical incidents in tunnels.

5.3. False alarms

The main task of a detection system in the safety domain is of course the detection of real incidents. On the other hand, the number of false alarms is an enormously important criterion for the practical operation of a system. If too many false alarms occur, the system will not be taken seriously by the operators and at some in the near future, it will be switched off. This section therefore focusses on the typical number of false alarms triggered by the AKUT system in live operation.

To do this, evaluations were carried out for incidents from 2016 through 2018 for different tunnels. Tunnels in eastern and western Austria were analyzed, along with short and long tunnels.

Evaluation of the Bosruck Tunnel September 2016

The evaluation in Table 3 shows that the Bosruck Tunnel had 29 false alarms in the month of September 2016. This corresponds to 0.96 false alarms per 24 hrs for the complete tunnel system with a length of 11,010 m. If false alarms were to be nominalized to kilometer bore length, this would correspond to 0.0877 false alarms per 24 hrs per kilometer.

Table 3: Evaluation of false alarms in the Bosruck Tunnel, September 2016

	Sound class	Number of false alarms per month	False alarms per km bore length and per 24 hrs
Tunnel analyzed: Bosruck	Accident / tyre burst	1	0.003
Bore length: 11,010 m	Tyre squeal	12	0.0363
Number of microphones: 122	Door slam	16	0.0484
	Honking	0	0
	TOTAL	**29**	**0.0877**

Three further evaluations follow. They can be explained analog to the evaluations shown above.

Evaluation tunnel sequence S10 September 2016

Table 4: Evaluation false alarms tunnel sequence S10, September 2016

	Sound class	Number of false alarms per month	False alarms per km bore length and per 24 hrs
Tunnel analyzed: Götschka, Neumarkt, Pernau, Lest	Accident / tyre burst	8	0.018
Bore length: 14,390 m	Tyre squeal	21	0.048
Number of microphones: 140	Door slam	65	0.15
	Honking	0	0
	TOTAL	94	**0.216**

Evaluation Ehrentalerberg tunnel, March 2017

Table 5: Evaluation false alarms Ehrentalerberg tunnel, March 2017

	Sound class	Number of false alarms per month	False alarms per km bore length and per 24 hrs
Tunnel analyzed: Ehrentalerberg	Accident / tyre burst	6	0.0298
Bore length: 6,690 m	Tyre squeal	6	0.0298
Number of microphones: 75	Door slam	20	0.0996
	Honking	1	0.0049
	TOTAL	33	**0.164**

Evaluation Flirsch tunnel January 2018

Table 6: Evaluation false alarms Flirsch tunnel, January 2018

	Sound class	Number of false alarms per month	False alarms per km bore length and per 24 hrs
Tunnel analyzed: Flirsch	Accident / tyre burst	0	0
Bore length: 2,252 m	Tyre squeal	0	0
Number of microphones: 19	Door slam	17	0.243
	Honking	0	0
	TOTAL	17	**0.243**

The analysis of the false alarm rate shows that, in general, the number of false alarms on AKUT systems is very low. Coupled with an excellent detection performance (see section 5.1), this is also the main reason why AKUT is well accepted by operators in traffic control centres and is regarded as valuable support for daily operation.

5.4. Cleaning and maintenance

The maintenance of safety equipment in tunnels is an essential topic for tunnel operators. The frequency of required maintenance actions, fault susceptibility and the associated availability of a system are of primary concern for the operator after commissioning of a system is complete.

The AKUT system in the Kirchdorf tunnel went live in 2010. The AKUT system in Kirchdorf tunnel consists of 49 microphones and the total bore length is 5,614 m. The Average Daily Traffic Volume is 19,330.

Experience over the past 8 years of operating the tunnel can be summarized as follows:

- No form of maintenance of repair work has been required for the microphones or the signal transmission devices since commissioning in 2010
- No form of cleaning work has been carried out on the microphones or the protective membrane since 2010
- Not one microphone has failed since 2010
- In 8 years of operation, the server hard disks only had to be replaced twice as they were defective

However, the Kirchdorf tunnel analysis server will be completely replaced by a new server, since several hard drives are defective and the exchange of disk drives after 9 years is no longer economically viable.

In summary, it can be said that the maintenance costs for AKUT systems facing a tunnel operator are very low and do not represent significant extra effort.

6. SUMMARY AND CONCLUSIONS

The acoustic tunnel monitoring system – AKUT is an innovative safety system for tunnels that is based on the automatic detection of abnormal sounds (accident, tyre squealing, etc.). Thanks to the large installed base in Austrian tunnels, it has been possible to gather comprehensive operational data since 2016 and use it for analysis and explanations. The detected incidents were analyzed. The foundation was provided by the ASFINAG incident database. The evaluations show that 19 relevant incidents have occurred since mid-2016. All 19 incidents were detected by AKUT first, without exception. The head start provided by AKUT ranged from 5 s to 11 minutes 46 s. Two incidents were only detected by AKUT. The false alarms on different systems were also evaluated. The results show approximately 0.08 to 0.24 false alarms per 24 hrs and per km tunnel bore length. Due to the very low false alarm rate and the excellent incident detection performance, AKUT is well accepted by operators. Experience regarding maintenance and cleaning is available from the pilot system, which has been in operation since 2010. From 2010 to 2018, no periodic maintenance or repair work was carried out on the system components (e.g. microphone and data transmission devices). Neither was cleaning required and no microphone was replaced, since no microphone has failed since 2010. All in all, AKUT has provided excellent operational service in Austrian tunnels and during this period, AKUT has made an important contribution to the increase in safety in ASFINAG's tunnels.

ON THE DETECTION OF TRAFFIC CONGESTION AND VENTILATION CONTROL

Marco Bettelini, Samuel Rigert
Amberg Engineering Ltd., Switzerland

ABSTRACT

Traffic congestion has a fundamental impact on ventilation operation in case of unidirectional traffic, particularly if a longitudinal ventilation system is used. Existing technologies for congestion detection are generally based on CCTV, inductive loops in the pavement or other kinds of counting devices. New radar-based technologies recently became available on the market. In the framework of ventilation design for Zürich's Northern Bypass, a specific experimental campaign for comparing and assessing three potentially viable technologies (traffic counting sensors, CCTV and newest-generation radar sensors) was carried out in the 3.3 km long Gubrist tunnel. Based on the results, the relative advantages and drawbacks of the different technologies could be assessed under real-life conditions. Both CCTV and radar sensors proved to be viable technologies for this specific application. Based on the results, it was decided to implement a radar-based solution in the short Katzensee tunnel (0.58 m) and a CCTV-based solution in the three tubes of the Gubrist tunnel (3.3 km).

Keywords: Traffic congestion, ventilation control

1. INTRODUCTION

Traffic congestion plays a fundamental role for ventilation control in case of fire incidents in road tunnels with unidirectional traffic. Strategies devised for fluid unidirectional traffic are generally straightforward and very effective. Conversely, compromises are called for in case of congestion, with vehicles at rest downstream of the fire location. Under these conditions, strategies developed for fluid traffic directly endanger part of the persons in the tunnel and are not allowable. These drawbacks are particularly significant whenever ventilation systems without smoke extraction are used. Proper congestion detection is needed for implementing the most appropriate and effective ventilation strategy at any time.

Existing technologies for congestion detection are generally based on CCTV, inductive loops for vehicle-detection and counting devices. Recently, new radar-based technologies became available on the market, but have so far hardly been implemented for detecting traffic congestion in road tunnels.

In the framework of ventilation design for the 3.3 km long Gubrist Tunnel (Zürich, Switzerland, with two existing tubes to be renovated and a third one under construction), existing technologies were initially assessed in a qualitative manner. The open literature was investigated and several carriers of expert knowledge were consulted. The findings pointed out many open issues with a high level of relevance for ventilation design and operation. For this reason, an experimental campaign for comparing and assessing three potentially viable technologies was carried out between June 2015 and February 2016 in the first tube of the Gubrist tunnel (direction Bern-St. Gall) over a length of 1.4 km. The following systems were tested: traffic counting (Tri-Tech sensors), CCTV and newest-generation radar sensors.

2. TRAFFIC CONGESTION AND VENTILATION CONTROL

The most appropriate ventilation concept for tunnels up to 2-3 km length with one-way traffic is generally longitudinal ventilation. Only tunnels with bi-directional traffic or longer tunnels (prescriptions vary between different countries) are equipped with a smoke-extraction system.

Emergency-ventilation control in longitudinally ventilated tunnels is quite simple in case of fluid traffic. Vehicles between the fire location and exit portal can leave the tunnel unhindered and do not need to be considered. Vehicles and persons between the entrance portal and the fire location are trapped and need to be protected by the ventilation system through full smoke control. The ventilation control system shall achieve the critical velocity in driving direction.

In case of traffic congestion, the situation is much more complicated. Vehicles and persons are blocked on both sides of the fire location. The common ventilation strategy in such a case is to establish a moderate ventilation velocity, typically 1 to 1.5 m/s, for preventing loss of smoke stratification. This ventilation-control strategy should maintain as long as possible adequate self-rescue conditions for most persons.

Having these two widely different ventilation scenarios in mind, one fundamental prerequisite for optimum ventilation control is rapid detection of traffic congestion. At fire detection, information about the traffic situation is required. The allowable time delay for congestion detection should be smaller than the one for fire detection. This is usually in the range of one minute.

It should be noted that specific ventilation strategies for traffic congestion are generally required also for semi-transverse ventilation systems with smoke extraction. The consequences of using less appropriate ventilation strategies are however in most cases significantly less severe.

In the case of Zürich's Northern Bypass, with high congestion frequency, the situation is as follows:

- Tunnel Gubrist (3.3 km, ventilation system with smoke extraction): Information on traffic congestion is relevant but not vital.
- Tunnel Katzensee (0.58 km, longitudinal ventilation): Information on traffic congestion is essential since mechanical ventilation is used only in case of fluid traffic (Bettelini and Rigert, 2014).

From the point of view of ventilation control, there are two types of congested traffic:

- Type 1: Traffic or vehicles at speed below about 10 km/h (in case of fire, faster vehicles can generally leave the tunnel without being overtaken by the smoke).
- Type 2: One or several vehicles stopped in the tunnel.

From the point of view of ventilation control, congestion is only relevant if it is located between fire location and exit portal.

3. DETECTION METHODS

Today's standard device for the detection of congestion, or traffic monitoring in general, are inductive loops. They are installed in the pavement and allow detecting vehicles, which pass or stop over the loop. Inductive loops allow for local ("point") measurements and are very reliable.

Traffic-counting devices, installed above a traffic lane, offer a similar functionality. They also allow for local ("point") measurements of vehicles passing or stopping directly under the devices. The big advantage against inductive loops is that they are not installed in the pavement and thus can be replaced without construction works and in short time.

CCTV allows full monitoring of traffic conditions in a tunnel. CCTV usually offers a comprehensive incident detection, including in general the detection of stopped vehicles, congestion, wrong-way driver and more. CCTV allows for area observation. Incidents are detected up to distances of roughly 80 m or even 150 m if the visibility conditions are favorable.

Its reliability is a steady concern. Optical effects (reflections, unfavorable light conditions) or bad visibility can cause false detections or prevent detections. Incident detection is thus not consequently used in tunnels for automatic incident detection.

New long-range radars also allow for area observations of traffic patterns, such as stopped vehicles or congestion. According to manufacturers, vehicles can be detected up to a distance of about 500 m. A major advantage compared to CCTV is certainly that optical conditions (light, fog, smoke) have no influence on detection capabilities. Since it is a new measurement method, there is not much experience about the reliability of long-range radars in tunnels.

The three detection methods considered herein have partially large differences in their capabilities to detect congestion or stopped vehicles. Traffic-counting systems can only survey the tunnel cross-section at the location where they are installed. Radar and CCTV cover a more or less extended area. The entire tunnel (or test section of the experimental campaign respectively) can be monitored. Thus, there are no fundamental limitations for detection of congestion because of the length or location of the congestion.

Table 1: Preliminary assessment of capability to detect different types of congestion

Detection method	Stopped vehicles	Short congestion	Congestion over entire tube
Radars	**Yes**	**Yes**	**Yes**
CCTV	**Yes**	**Yes**	**Yes**
Traffic counting	**No**	**No**	**Yes**

Due to the fundamentally different measurement principle, data from the traffic-counting system are not entirely comparable to the two measurement methods with area coverage. Careful comparison of data is possible with the observation sections of CCTV and radar in which the measurement cross section of the traffic counting system is located.

4. TEST CAMPAIGN

4.1. Sensor description

The goal of the experimental campaign was to compare and assess three potentially viable technologies. The experimental campaign was carried out between June 2015 and February 2016 in tube 1 (driving direction towards St. Gall) of the Gubrist tunnel (highway A1, Switzerland). The tunnel is well known for its high traffic volumes and daily congestion.

The following systems were accounted for: Traffic counting (Tri-Tech sensors, using a combination of doppler radar, ultrasound and passive infrared technologies in a single unit), CCTV and newest-generation radar sensors type ClearWay developed by Navtech. Two radar sensors were rented and installed in the tunnel just for the experimental campaign. For congestion detection with CCTV, the already installed cameras (type analogue) were used to get images from the tunnel. A new system for incident detection (using the existing cameras) and storage of images was installed for the duration of the experimental campaign. The traffic counting system is currently used by the ventilation control system for congestion detection. The raw data were used and analyzed by a slightly adapted evaluation routine to match the congestion criteria used for CCTV and radar.

4.2. Setup

The test setup in the tunnel is presented in Figure 1.

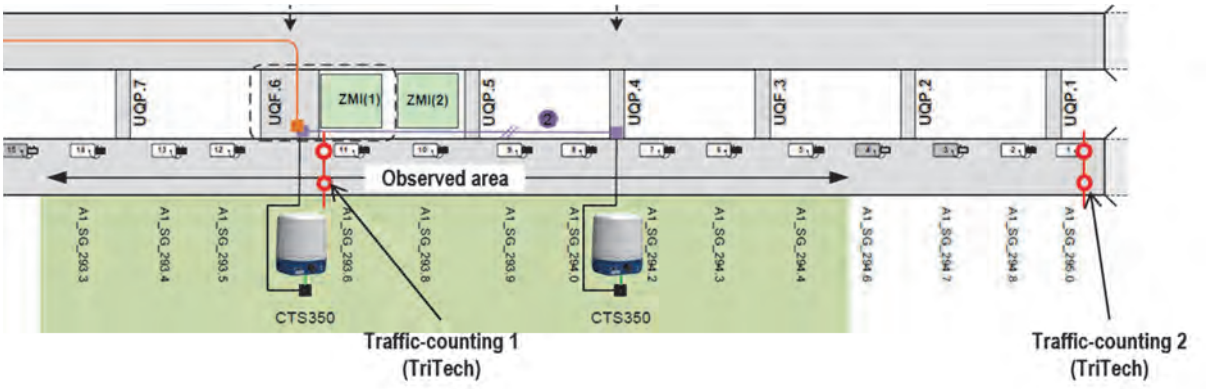

Figure 1: Test setup

The three detection systems cover different areas:

- The traffic counting system is a point measurement. Congestion is only detected if it occurs at the location of the sensors
- CCTV monitors an area of the tunnel. Each camera can detect congestion within a range of up to roughly 80 to 150 m. The cameras are installed in an interval of 150 m. Consequently, observation sections of 150 m length are defined, where each section is evaluated individually.
- Radar monitors an area of the tunnel. According to the manufacturer, each radar covers a range with a radius of 500 m. The evaluation software allows splitting this range into observation sections of any desired length. Observation sections with 100 m length were chosen, corresponding to for fire detection sections used in Swiss road tunnels.

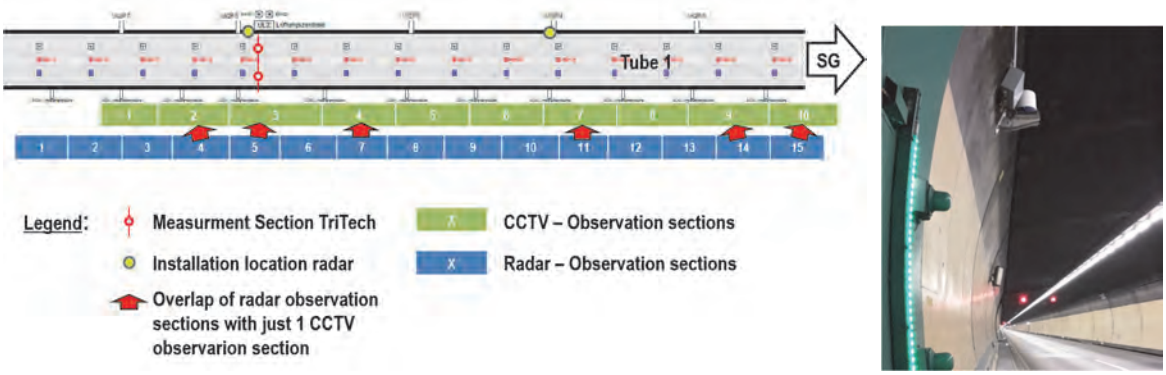

Figure 2: Coverage of radar and CCTV and measurement points of traffic counting system

As illustrated in Figure 2, there are in total 15 observation sections for radar, 10 observation sections for CCTV and 1 measurement cross-section for the traffic counting system. The observed tunnel section covered by the detection systems has no curves and accounts for approximately half of the tunnel, from the center to the exit portal (length of about 1.4 km).

4.3. Measurement campaign

The measurement campaign started with the installation of the additional equipment in June 2015 and the duration was limited to one year. Calibration of the different systems was initially a major issue. CCTV and radar are originally trimmed to detect dense traffic situations for traffic management. Their usual parameters for incident detection filter unimportant events, which are not relevant for tunnel operators (e.g. stop-and-go situations). This allows reducing the number of alarms issued to the traffic control center, but leads to a considerable delay of alarms of the order of 1 minute (depending on system calibration). Conversely, using automatic congestion detection for fire ventilation, the number of alarms is not important since the system will treat them automatically, but the detection of a congestion event should happen as rapidly

as possible. A large effort was carried out initially for calibrating CCTV and radar as consistently as possible. Since these two systems use entirely different parameters, this task was complex.

5. RESULT EVALUATION

5.1. Methodology

Each congestion event detected by one or more of the three systems was recorded in a file with time stamp. The CCTV system additionally recorded images over the entire measurement period allowing for a visual verification of the correctness of congestion detection.

In a first step, the recorded congestion events were assessed on correctness. Wrong detections (congestion events recorded although not present in the tunnel, congestion events not recorded although present in the tunnel) were separated from correct detections applying the following rules:

- A congestion event detected from two different systems at the same time and at the same location was qualified as correct detection, congestion was present in the tunnel.
- A congestion event detected only by one system represented possibly a wrong detection.

In case of doubts about the validity of a recorded congestion event, the camera images were used for validation. However, due to the high number of detected events, this time-consuming approach could not be followed in a systematic manner.

5.2. Number and duration of congestion events

A high number of short events extending over just one observation section were found. For both systems, radar and CCTV, a minimum duration for congestion events was defined to reduce the number of events whenever the traffic (velocity, density) was fluctuating around the congestion criteria. Congestion events with just the minimum duration correspond to stop-and-go events, with low relevance for comparison of the two systems. The probability is high, that these events are detected by just one of the detection systems (radar or CCTV). The traffic counting system will have anyway almost no chance to detect such events. Of importance for comparison are the congestion events, which have a longer duration and an extension over several observation sectors. A minimum duration of 8 minutes was defined for relevant congestion events.

The ClearWay radar detected more events than CCTV (see Table 2). The only exception was radar's observation sector 15, where the corresponding CCTV's observation section 10 detected around 15% events which were not detected by radar. This is due to the limited range of the radar discussed in section 5.3.

The higher number of events detected by radar is due to its independency from adverse meteorological situations or visibility conditions in the tunnel. In case of heavy rain outside the tunnel, a lot of humidity is transported into the tunnel and disturbs the functionality of CCTV routines. CCTV does often not correctly detect congestion in such situations.

Table 2: Comparison of number of detected congestion events for observation sections

CCTV observation section	2	3	4	7	9	10
Radar observation section	4	5	7	11	14	15
Events detected only by radar	18%	32%	9%	7%	10%	5%
Events detected only by CCTV	0%	0%	2%	0%	3%	15%
Events detected simultaneous	83%	68%	88%	93%	86%	80%

5.3. Detection range of radar

Comparing the number of congestion events recorded by CCTV and radar, Figure 3, the radar shows well-defined peaks along the tunnel axis. The events detected by CCTV are more evenly distributed over the different observation sections. The peaks are located around the location of the two radar positions (observation sections 5 and 10/11, see Figure 2). Most of these additionally detected events are stop-and-go events, with a very short duration. These events could be declared as wrong detections. However, they occur only in case of very dense traffic situations, when the probability for a real congestion is high.

If the two peaks are not considered, the number of events detected by radar and CCTV is similar. There are only two important exceptions:

- The radar observation section 15 (located around tunnel km 294.4) detects only around 60% of the events detected by CCTV.
- The radar observation sections 1 to 3 (located between tunnel km 292.8 and 293.2) detect only between 20% and 60% of the events detected by CCTV in the same area.

It can be concluded that the observation range of the radar is more limited than originally believed and dependent on the driving direction of vehicles. This leads to a very important conclusion concerning the range of the radar sensors for congestion detection in tunnels:

- Range in driving direction: 400 m
- Range against driving direction: 100 m.

The reason for this large difference is probably related to the aerodynamic shape of the vehicles. The front side of cars creates less or weaker reflections of radar waves than the backside.

The above-mentioned limitations of the measurement range were observed under intense traffic conditions. Better results could probably be achieved in case of lower traffic intensity.

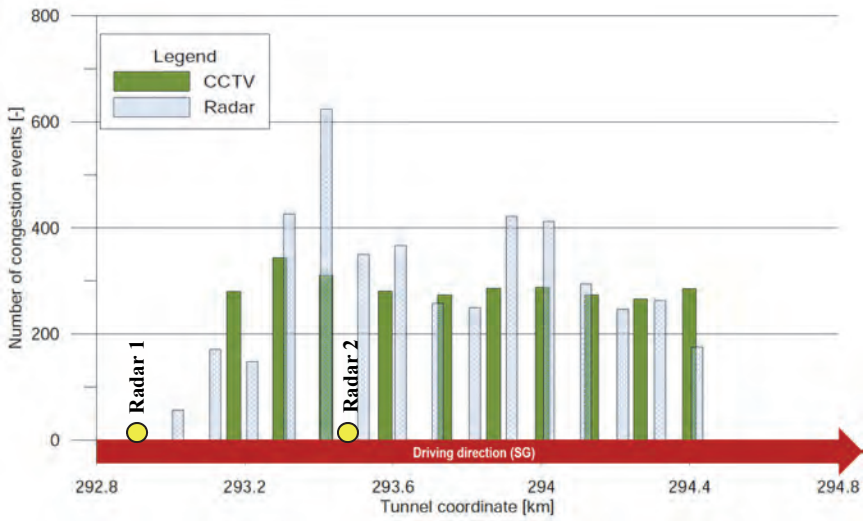

Figure 3: Number of congestion events

5.4. Detection time and temporal delay

Detection time or starting time of congestion events should be identical. Just the traffic counting system has clear drawbacks, as it is based on measurements in discrete cross-sections and congestion has first to develop to that measurement cross section to be detected. Thus, the focus of the evaluation of detection time is laid on radar and CCTV. In this section, only congestion events are considered, which were detected by both radar and CCTV.

The evaluation results lead to the following conclusions:

- Median delay of detection time between radar and CCTV was around 30 seconds, if all events are considered. Possible causes for the delay are the different perspective situations of radar and CCTV, as well as different algorithms for congestion detection. Especially in dense traffic situations, CCTV detects congestions only when it occurs close to the camera position (up to about 80 m).
- Delay is slightly reduced for larger congestion events developing over several observation sections. Congestion events extending over several observation sections are easier to detect than stop-and-go events which occur only for short time and in just one observation section.
- There were no explicit indications that one of the detection systems is faster than the other. The location of the first occurrence of the congestion seems to influence the delay. If it occurs close to the one of the radars, the faster detection comes from radar.
- The maximum delay is the consequence of special conditions with bad visibility or unusual traffic conditions affecting CCTV detection capabilities.

5.5. Influence of meteorological conditions

It was observed that in case of heavy rain the humidity level in the tunnel rises strongly. The high humidity reduces the image quality and affects the proper functionality of the CCTV system. Under these conditions the high humidity level reduces the quality of the images. It becomes blurred and the red breaking lights of the vehicles enlighten the whole image. This leads to very difficult conditions for analyzing the images through the CCTV system. The CCTV system often recorded "debris" (small objects on the road) instead of congestion in the log file during such conditions. Further investigations would be necessary for verifying, if this kind of detection could be interpreted as congestion by the ventilation control system.

No influence on the radar's detection quality through different meteorological conditions could be observed during the whole test campaign.

6. SUMMARY AND CONCLUSIONS

The presence of congestion has a significant impact on the selection of the most appropriate road-tunnel ventilation strategy. Three methods for detecting congestion in road tunnels have been extensively and systematically evaluated by means of an experimental campaign carried out in Swiss highway tunnel Gubrist. The following systems were investigated:

- Tri-tech vehicle-counting devices
- CCTV with image analysis
- New-generation radar sensors.

The traffic-counting system showed clear and distinct drawbacks against the other two systems. The two measurement cross-sections located at a distance of roughly 1.5 km were not adequate for detecting a similar number of congestion events as radar and CCTV, which both monitor the whole range. In case of fire, this technology could miss a significant number of congestion episodes or detect them too late (after fire detection), which would let the ventilation control start the ventilation scenario for fluid traffic. The situation could be improved by reducing the distance between measurement cross-sections.

New-generation radar systems proved to be well suited for congestion detection in road tunnels. The detection quality of radar and CCTV is basically comparable. Both systems detect the relevant congestion events with an acceptable time delay and accurate location. Deviations have been identified only for rather irrelevant congestion events. These are stop-and-go situations, where the criteria for congestion (primarily velocity limit) are fulfilled for a few seconds only. The detection of such events is dependent on the location of the congestion event in relation to the location of the detection device (radar or camera). The closer the location of the congestion

event to the detection device, the higher the chance for detection. Not relevant congestion events have been recorded mainly by the radar system, in great number.

The observation range of the radar for detection of congestion in tunnels was shown to be smaller than declared. Reliable detection can be expected:

- up to distances of about 100 m from the installation location of the radar against the driving direction
- up to distances of about 350 m from the installation location of the radar in driving direction.

The difference is explained with the aerodynamic shape of cars. The aerodynamically shaped front side creates weaker radar reflections than the rather flat backside.

Congestion detection is of special importance in tunnels characterized by high traffic volumes and longitudinal ventilation. An activation of the ventilation system in the fluid-traffic-mode could lead to undesired consequences. The experimental campaign revealed, that common solutions for detection of congestion (traffic counting) are not always appropriate.

There are no normative or legislative prescriptions concerning the detection of traffic congestion. Systems with the capability to monitor the whole tunnel and not just a few cross-sections are recommended for tunnels with high congestion probability. Simple traffic-counting systems could detect congestions with an undesired high delay.

Radar systems have additional advantages in case of difficult visibility conditions (portals with illumination from outside of the tunnel, wet conditions in the tunnel). The high measurement range of radar is only an advantage in straight tunnels.

Radar and CCTV systems are commonly designed for application in traffic monitoring. The corresponding congestion criteria cannot be compared to those requested by the ventilation-control system. A system working for traffic monitoring is designed for preventing unnecessary alarms. An excessive number of alarms could not be handled by the operators working with the system. In the case of ventilation control, all congestion alarms received form radar or CCTV are treated automatically and the number of alarms is not an important factor. These different requirements have influence on the detection criteria and device calibration. Some parameters can be easily adapted, other ones cannot be adapted. For applications of radar or CCTV in tunnels for detection of congestion for ventilation control, the systems should be specifically designed and calibrated for exactly this application. Otherwise, the effort for parametrization of the system is huge.

Based on the results of this test campaign, it was decided to implement a radar-based solution in the Katzensee tunnel (0.58 m) and a CCTV-based solution in the three tubes of the Gubrist tunnel (3.3 km). The main reason is that adverse environmental conditions have a much larger impact on the short Katzensee tunnel, where congestion detection has a much more significant impact on ventilation control. The more conventional solution was deemed adequate for the Gubrist tunnel, which is significantly less demanding from this point of view.

7. AKNOWLEDGEMENTS

The authors thank the Swiss road authority FEDRO, particularly Mr. Marco Knecht, and the GEVII who supported the experimental campaign and allowed publishing these results. Thanks are also due to Siemens for the invaluable support during the test campaign.

8. REFERENCES

Bettelini M., Rigert S. (2014). Ventilation and escape facilities for short cut-and-cover urban tunnels. *Paper presented at the 7th Symposium 'Tunnel Safety and Ventilation'*, 12-13 May 2014, Graz.

FAST FIRE DETECTION BY LINEAR TEMPERATURE SENSOR CABLE AND ITS APPLICATION

Ichiro Nakahori, Tatsuya Oshiro, Kengo Fukuda,
Takuya Matsumoto and Shigeru Abe
Sohatsu Systems Laboratory Inc., Kobe, Japan

ABSTRACT

The authors have developed a fast fire detection algorithm using the temperature data from the linear temperature sensor cable which can detect a fire of 12 L N-Heptane on 1.0 m^2 plate (equivalent to 370 MJ fire) within 30 seconds. The developed fast fire detection algorithm is effective as a pre-alarm of fire and can be used to trigger emergent switching of video cameras as well as fire emergency ventilation strategy such as the zero-flow ventilation control for drivers' safe self-evacuation. As the developed algorithm has a challenge of false alarm, the paper will present a counter-method to suppress false alarm by monitoring and processing the temperature evolution continuously after the pre-alarm has been issued. Verification of the fast fire detection algorithm will be provided using the data collected from an actual tunnel fire test and none-fire tunnel normal operation.

Keywords: linear temperature sensor cable, tunnel fire, fast fire detection, heat sensor, fire alarm

1. INTRODUCTION

There is a valuable report paper [Maevski et. al, 2015] which is concerned with a comparative study on fire detection system performance using different types of sensors at actual vehicle fire test and false alarm record during a long-term operation at an actual tunnel.

The report describes the following sensors which are currently applicable to and used in tunnel fire detection system:

- Infrared camera
- Linear temperature sensor cable
- Flame and smoke sensor
- Spot heat detection sensor

A plate fire of 1 or 2 MW with diesel oil was ignited inside a vehicle for fire detection that thermocouples were mounted at key places and flammable components were removed. Infrared camera and linear temperature sensor cable met the requirement of detecting the fire within 2 minutes. Other sensors could not detect the fire or could detect it but at more than 2.5 minutes. In case of airflow existing prior to the fire, flame and smoke detector was better than other sensors, and linear temperature sensor cable came after it.

It is reported in the paper [Maevski et al, 2015] that infrared camera never issued a false alarm, and linear temperature sensor cable ("sensor cable") issued only one false alarm. The false alarm case with the sensor cable was due to a parking maintenance vehicle which radiated heat. Infrared sensor could not stop false alarm which was caused by light bloom at the tunnel portal in spring and fall. It was also reported that infrared sensor would reduce fire detection accuracy unless cleaning up the dust on sensor.

Based on the report [Maevski et. al, 2015], the authors of the present paper have concluded that sensor cable which is suitable to detect fire location is the best among those sensors in fire

detection performance, robustness, and practical use. Figure 1 illustrates a cut model and fire detection system with sensor cable. A typical sensor cable embeds semiconductor temperature sensors at standard intervals of 5 or 8 m along its length and can determine a fire location in a tunnel by means of measuring temperature.

The paper deals with a fast fire detection algorithm using sensor cable. First a present status of fire detection with the sensor cable will be described. Then a fire experiment to which the fast fire detection algorithm is applied will be explained, followed by introducing two mathematical formulas of the algorithm which will detect a 370MJ plate fire within 30 and 60 seconds respectively.

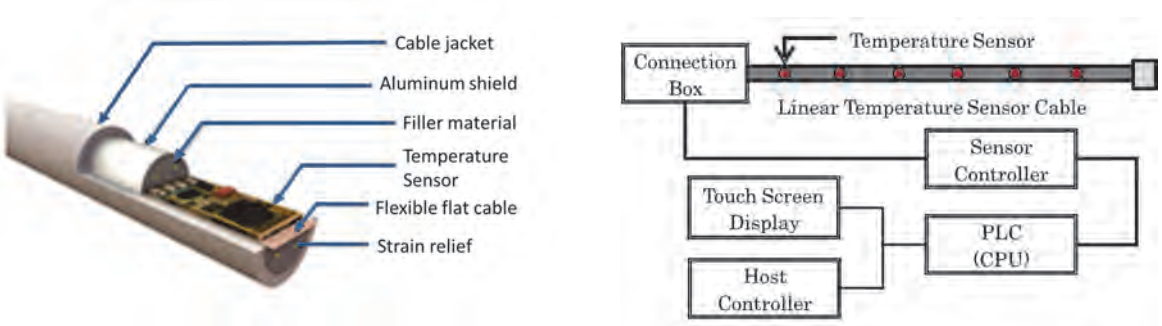

Figure 1: Cut model of linear temperature sensor cable and the detecting system using it

2. FIRE DETECTION BY LINEAR TEMPERATURE SENSOR CABLE

The fire detection algorithm with sensor cable has already been proven to work and widely applied in the tunnels worldwide. Temperature measurements at each sensor in the cable are scanned to a controller at pre-determined and constant time interval. The signal processing software provided by the sensor cable supplier runs on the controller and calculates temperature difference in each sensor with the original calculation method. The controller selects a sensor which indicates the largest temperature rise and generates an alarm if the difference is larger than a pre-set threshold. The controller usually sets two thresholds, low and high. If the difference exceeds the low threshold, the controller generates a pre-alarm. If the difference exceeds the high threshold, the controller generates an alarm.

It has been verified that the sensor cable can detect fire at high accuracy. However, the temperature sensors are covered by a few layers of capsule as shown in Figure 1 and it takes time for the heat to reach the sensors exceeding the threshold. If the threshold is set to too low value, it becomes hard to distinguish temperature rise caused by natural temperature change and tunnel fire. It was considered for long that small scale fire detection with the sensor cable was never possible in short time.

Japan regulation calls out 2 L gasoline fire on 0.5 m^2 plate has to be detected within 30 seconds. The regulation seems to be the one that assumed fire flame detection with an optical method. There is no condition mentioned on airflow velocity in the regulation. The architecture of the sensor cable is considered impossible to meet the regulation. The initial response triggered by the fast fire detection, however, is critical to fire risk reduction [Sakaguchi et. al, 2016] and fire scale estimation [Nakahori et. al, 2014], and will be effective in fire emergency operations.

Having looked into the unique characteristics of the sensor cable which capture temperature rise of individual sensors and monitor temperature rise profile in the neighboring sensors, the authors developed a fast fire detection algorithm with considering not only each temperature rise but also the rise profile, which can detect 12 L N-Heptane fire on 1 m^2 plate (equivalent to 370MJ fire) within 30 and 60 seconds. The developed algorithm is applied to two temperature data measured with a sensor cable at actual tunnel fire tests.

3. FIRE TEST

Table 1 summarizes a fire test where sensor cable was mounted at upper part of the wall in two lane traffic and long-distance tunnel. Temperature data collected at the test are illustrated in time and space domain as in Figure 2. Please note that both are same scale fire but under different airflow velocity.

Table 1: Fire test conditions and fire locations detected by sensor cable

	Fire scale	Total energy	Airflow velocity	Detected fire location
Case A	**1.0 m², 12 L**	**370 MJ**	**0 m/s**	**No. 13, No.14 sensors,**
Case B			**2.0 m/s**	**No. 15 ssensor**

Remark: fire plate is directly under No. 13 sensor.

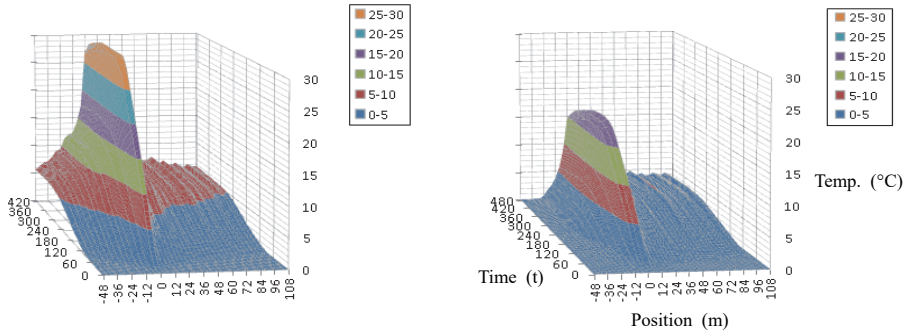

Case A Case B

Figure 2: Temperature increases in space and time

4. TEMPLATE FOR FAST FIRE DETECTION ALGORITHM

4.1. Selection of a temporary fire location

Let N be a total number of semiconductor temperature sensors embedded in equal distance in the sensor cable, i be a semconductor sensor number ($i = 1, 2, \cdots, N$) and $T(i,t)$ °C be temperature ouput of the semoconductor sensor i at time t. Suppose a sensor temperature $T(i,t)$ is updated at time t. A temperature change of the sensor i between time t and $t - \Delta t$ is represented by Eqn. (1).

$$H_{\Delta t}(i,t) = T(i,t) - T(i,t-\Delta t)\ ,\ i = 1, 2, \cdots, N \qquad (1)$$

A set of sensors which satisfy the Eqn. (2) are selected as $\{H_{\Delta t}(i,t)\}$

$$H_{\Delta t}(i,t) \geq ThP_F \qquad (2)$$

where ThP_F is the threshold. Let sensor i be P_F which shows the largest value in $\{H_{\Delta t}(i,t)\}$. The largest temperature change is $H_{\Delta t}(P_F,t)$. If there are multiple sensors indicating the same largest change, then smallest P_F is chosen.

4.2. Setting a hypothesis for fire breakout

To capture the characteristics of this temperature distribution, a spatial sum of the temperature rise is introduced. A sum of temperature rise between time t and $t - \Delta t$ in $2M + 1$ sensors including the sensor i is defined as Eqn. (3).

$$\sum_{2M+1} H_{\Delta t}(i,t) = H_{\Delta t}(i-M,t) + \cdots + H_{\Delta t}(i,t) + \cdots + H_{\Delta t}(i+M,t) \qquad (3)$$

Spatial sums of the temperature change in $2M+1$ sensors including P_F with the largest temperature rise during $\Delta t = 10$ and $\Delta t = \Delta t_A$ are calculated.

$$H_{10}(i,t) = T(i,t) - T(i,t-10) \quad (4)$$

$$H_{\Delta t_A}(i,t) = T(i,t) - T(i,t-\Delta t_A) \quad (5)$$

$$\sum_{2M+1} H_{10}(P_F,t) = H_{10}(P_F - M,t) + \cdots + H_{10}(P_F,t) + \cdots + H_{10}(P_F + M,t) \quad (6)$$

$$\sum_{2M+1} H_{\Delta t_A}(P_F,t) = H_{\Delta t_A}(P_F - M,t) + \cdots + H_{\Delta t_A}(P_F,t) + \cdots + H_{\Delta t_A}(P_F + M,t) \quad (7)$$

If spatial sums of Eqn. (6) and (7) are satisfied for two thresholds ThH_{10} and $ThH_{\Delta t_A}$ °C,

$$\sum_{2M+1} H_{10}(P_F,t) \geq ThH_{10} \quad (8)$$

$$\sum_{2M+1} H_{\Delta t_A}(P_F,t) \geq ThH_{\Delta t_A} \quad (9)$$

a hypothesis of a fire breakout at the temporary fire location at the sensor P_F is set and the fire detection algorithm moves on to testing step whether the hypothesis is correct or not.

4.3. Testing a hypothesis for fire breakout

Four testing procedures are applied to see if the fire breakout hypothesis is correct. Each testing procedure calls out a pair of evaluation value $E_V(i)$ and associated threshold $E_T(i)$ ($i = 1, 2, 3, 4$), and if-them rule is applied to judge TRUE or FALSE as follows:

$$If\ E_V(i) \geq E_T(i)\ then\ \text{Testing}\ i\ is\ \text{TRUE}\ else\ \text{FALSE} \quad (10)$$

If all the testing ends TRUE, then the hypothesis is accepted and an alarm will be generated. If the testing ends FALSE, then the hypothesis is rejected and no fire breakout is concluded.

4.3.1. Testing 1

The evaluation value is defined as Eqn. (11).

$$E_V(1) = \frac{H_{\Delta t_A}(P_F,t)}{\Sigma_{2M+1} H_{\Delta t_A}(P_F,t)} \quad (11)$$

$E_V(1)$ is checked against $E_T(1)$, threshold value. $E_V(1)$ is normalized with the spatial sum of the temperature rise at $2M+1$ sensors including a hypothetical fire location sensor. $E_V(2)$, $E_V(3)$ and $E_V(4)$ are normalized in the same way $E_V(1)$.

4.3.2. Testing 2

The evaluation value is defined as Eqn. (12).

$$E_V(2) = \frac{\Sigma_3 H_{\Delta t_A}(P_F,t)}{\Sigma_{2M+1} H_{\Delta t_A}(P_F,t)} \quad (12)$$

$E_V(2)$ is checked against $E_T(2)$, threshold value.

4.3.3. Testing 3

The evaluation value is defined as Eqn. (13)

$$E_V(3) = \frac{\Sigma_{2M+1} H_{10}(P_F,t-10)}{\Sigma_{2M+1} H_{\Delta t_A}(P_F,t)} \quad (13)$$

$E_V(3)$ is checked against $E_T(3)$, threshold value. No temperature rise was observed in the fire test until 20 seconds after fire ignition. Spatial sum of temperature rise at 20 seconds after fire breakout is checked.

4.3.4. Testing 4

The evaluation value is defined as Eqn. (14).

$$E_V(4) = \frac{\Sigma_{2M+1} H_{10}(P_F,t)}{\Sigma_{2M+1} H_{\Delta t_A}(P_F,t)} \quad (14)$$

Rapid temperature rise during 10 seconds between 20 and 30 seconds after the fire ignition was observed in the fire test. It should be noted that this kind of rapid temperature rise was not observed after the fire growth was completed. Spatial sum of temperature rise during 10 seconds $E_V(4)$ is checked against $E_T(4)$, threshold value.

5. FAST FIRE DETECTION ALGORITHM WITHIN 30 SECONDS

Fast fire detection algorithm with parameter Δt_A set at 30 seconds and parameter M at 5 is studied. Temperature rise of 12 L N-Heptane fire on 1 m^2 plate at 30 seconds after ignition is provided in Figure 3. The fire plate is placed under the sensor No. 13. In case A, $H_{30}(13,30)$ $(i = 13, \Delta t = 30, t = 30)$ of the sensor No. 13 and $H_{30}(14,30)$ of the sensor No. 14 indicate the highest temperature rise under breeze airflow. In case B, $H_{30}(15,30)$ of the sensor No. 15 indicates the highest temperature rise under 2.0 m/s airflow velocity. P_F of Case A and that of Case B are 13 and 15, respectively.

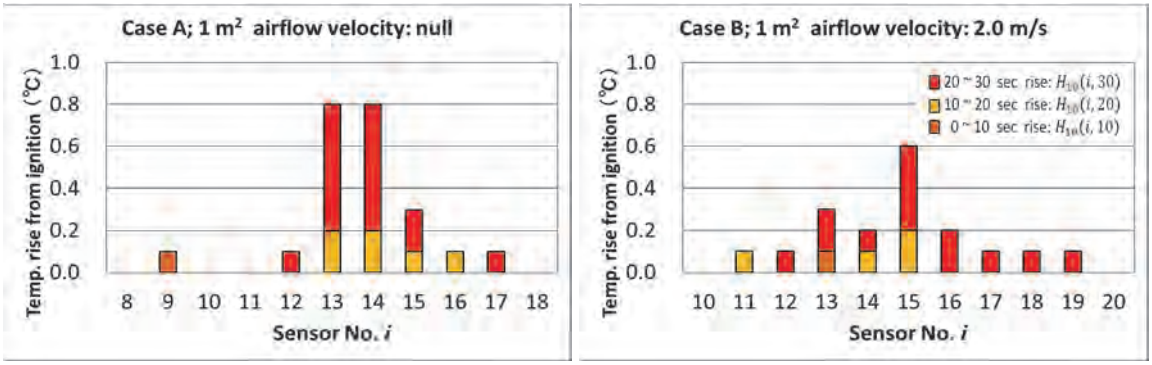

Figure 3: Distribution of temperature rise for 30 seconds after ignition

5.1. Selection of a temporary fire location

Since we focus on the temperature change at each semiconductor sensor during 30 seconds, set Δt equal to 30 in Eqn. (1).

$$H_{30}(i,t) = T(i,t) - T(i,t-30), \;\; i = 1,2,\cdots,N \quad (15)$$

The temporary fire location, which is the sensor number P_F showing the largest value in $\{H_{30}(i,t)\}$, is selected in the manner as mentioned in 4.1.

5.2. Setting a hypothesis

Since each safety zone where sprinklers are activated is defined every 50 m in Japan, we set $2M + 1 = 11$ $(M = 5)$. In fact the temperature rises outside these 11 sensors are zero in Figure **3**. Spatial sums of the temperature change in 11 sensors including P_F of the largest temperature rise during 10 and 30 seconds are calculated as follows.

$$\sum_{11} H_{10}(P_F,t) = H_{10}(P_F-5,t) + \cdots + H_{10}(P_F,t) + \cdots + H_{10}(P_F+5,t) \quad (16)$$

$$\sum_{11} H_{30}(P_F,t) = H_{30}(P_F-5,t) + \cdots + H_{30}(P_F,t) + \cdots + H_{30}(P_F+5,t) \quad (17)$$

Eqn. (16) is obtained by setting $M = 5$ in Eqn. (6) and Eqn. (17) is obtained by setting $M = 5$ and $\Delta t_A = 30$ in Eqn. (7). If Eqn. (16) and (17) are satisfied for two thresholds ThH_{10} and ThH_{30} °C,

$$\sum_{11} H_{10}(P_F, t) \geq ThH_{10} \quad (18)$$

$$\sum_{11} H_{30}(P_F, t) \geq ThH_{30} \quad (19)$$

then the hypothesis of fire breakout is set at the sensor number P_F.

5.3. Testing a hypothesis

Evaluation values for Testing are as follows:

$$\text{Testing 1: } E_V(1) = \frac{H_{30}(P_F,t)}{\Sigma_{11} H_{30}(P_F,t)} \quad (20)$$

$$\text{Testing 2: } E_V(2) = \frac{\Sigma_3 H_{30}(P_F,t)}{\Sigma_{11} H_{30}(P_F,t)} \quad (21)$$

$$\text{Testing 3: } E_V(3) = \frac{\Sigma_{11} H_{10}(P_F,t-10)}{\Sigma_{11} H_{30}(P_F,t)} \quad (22)$$

$$\text{Testing 4: } E_V(4) = \frac{\Sigma_{11} H_{10}(P_F,t)}{\Sigma_{11} H_{30}(P_F,t)} \quad (23)$$

Testing the hypothesis is executed in the manner as mentioned in 4.3

5.4. Thresholds

The evaluation values and actual thresholds used in this paper are shown in Table 2. The threshold values are determined to detect the test fire of Case A and Case B. Relatively small value is chosen for the threshold values in the temporary fire location selection and the fire hypothesis formation so as to not miss the fire breakout. As Testing 1 and Testing 2 use spatial sum of temperature rise during 30 seconds after fire ignition in order to check the spatial shape of temperature rises, the evaluation formula is called spatial filter, while Testing 3 and Testing 4 use change of spatial sum during 10 seconds in order to check the rate of temperature rises, the evaluation formula is called temporal filter.

Table 2: Summary of evaluation values and threshholds in fast fire detection algorithm

	Evaluation value	Threshold	Notes / Check point
Fire location selection	$H_{30}(i,t)$	$ThP_F = 0.3$	Pick up max value more than ThP_F .
Hypothesis forming	$\Sigma_{11}H_{10}(P_F, t)$	$ThH_{10} = 0.5$	Spatial sum of 11 sensors temperature rise during 10 s or 30 s. Hypothesis is checked by Test 1 ~ 4.
	$\Sigma_{11}H_{30}(P_F, t)$	$ThH_{30} = 1.1$	
Testing 1 (Space filter)	$E_V(1)$ Eq. (20)	$E_T(1) = 0.28$	Temperature rise for 30 s of the fire location.
Testing 2 (Space filter)	$E_V(2)$ Eq. (21)	$E_T(2) = 0.50$	Sum of 3 sensors temperature rise during 30 s.
Testing 3 (Temporal filter)	$E_V(3)$ Eq. (22)	$E_T(3) = 0.10$	Sum of 11 sensors temperature rise during 10 s from $(t-20)$ s to $(t-10)$ s.
Testing 4 (Temporal filter)	$E_V(4)$ Eq. (23)	$E_T(4) = 0.80$	Sum of 11 sensors temperature rise during 10 s from $(t-10)$ s to t s.

5.5. Verification in Normal Operations

The developed fast fire detection algorithm is applied to the sensor data recorded at an actual tunnel. As there was no fire in the tunnel, the data is considered in normal operations. The testing procedures used the threshold values provided in Table 2. With those threshold values, there is no false alarm generated in processing one full day sensor data as shown in Table 3.

For the data taken in winter at the Yoka Tunnel, 67 false alarms are observed if only Testing 1 is applied. All four testings, however, never end TRUE for the 67 cases, and no false alarm is generated. There is no false alarm for the Yoka Tunnel summer data in case only Testing 1 and Testing 2 are applied. Study results using the Mitani Tunnel data indicate possible false alarm caused by high temperature vehicle. Testing 4 rejects the fire hypothesis due to the high temperature vehicle, concluding no fire breakout.

Table 3: Numbers of nuisance alarms by fast fire detection algorithm

Tunnel	Date	Number of Hypotheses	Number of false alarms				
			Testing 1 alone	Testing 2 alone	Testing 3 alone	Testing 4 alone	All Testings
Yoka	**8/2/2014**	6500	67	118	5989	30	0
	20/8/2013	268	0	0	254	1	0
Mitani	**19/8/2017**	20	1	12	20	0	0

6. SIMPLIFIED FIRE DETECTION ALGORITHM WITHIN 60 SECONDS

6.1. Temparature rise at 60 seconds after ignition in fire tests

Figure 4 illustrates temperature rise evolution during 60 seconds after fire ignition at fire location and its neighbourhood.

6.2. Evaluation values for detection

The evaluation value is defined in the similar way to the fire detection within 30 seconds. Namely the evaluation value with spatial sum of temperature change during 10 seconds $\sum_{11} H_{10}(i,t)$ $(i = 1,2, \dots N)$ and spatial sum of temperature change during 60 seconds $\sum_{11} H_{60}(i,t)$ are compared to thresholds for fire detection.

The thresholds used in fast fire detection within 30 seconds for the evaluation of $\sum_{11} H_{10}(P_F,t)$ and $\sum_{11} H_{30}(P_F,t)$ were set at relatively small value to avoid missing fire breakout. It generated many fire hypotheses and rejected them all in testing procedures.

Temperature will rise enough and become stable when time elapses 60 seconds after fire ignition. It is expected that the threshold can be selected so as to always accept fire hypotheses. Thus there is no need for the hypotheses testing.

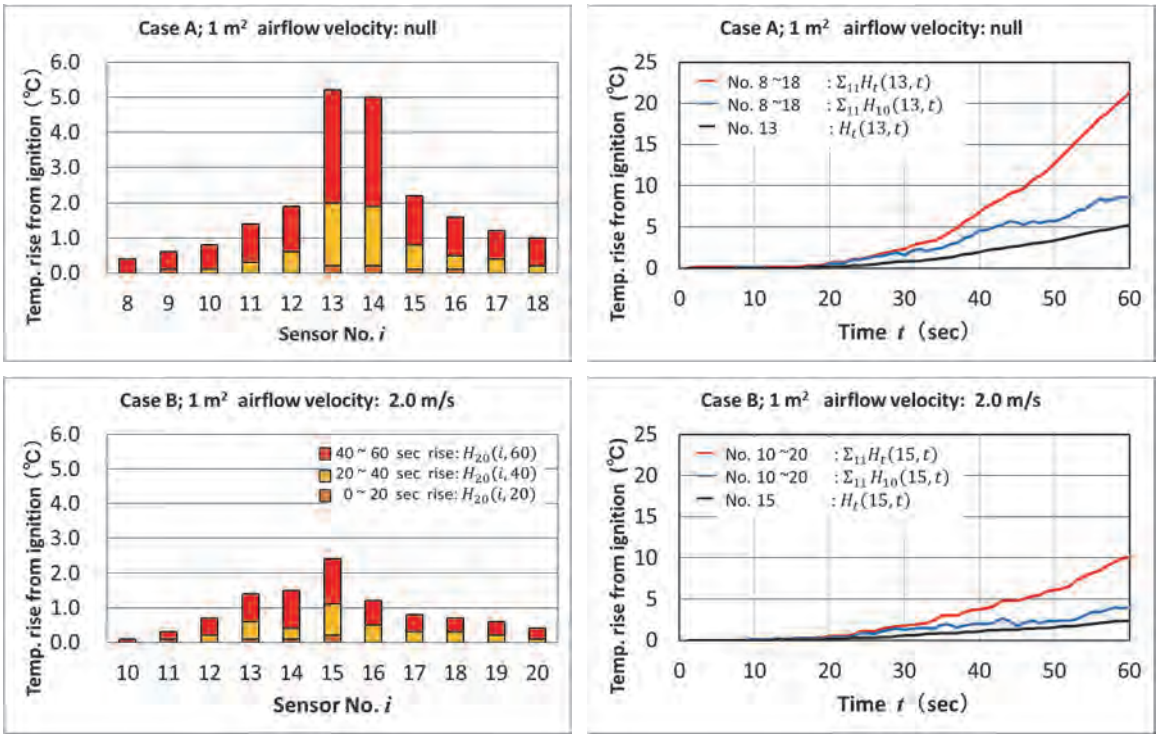

Figure 4: Distribution of temperature and fire location sensor and sum of its neighbour temperature rises for 60 seconds after ignition

6.3. Thresholds

The evaluation values at 60 seconds in Figure 4 are summarized in Table 4.

Table 4: Evalution values at the elapsed time of 60 seconds at the fire test

		Evaluation values at one minute after ignition		
Fire Test		$H_{60}(F_P, 60)$	$\Sigma_{11}H_{10}(F_P, 60)$	$\Sigma_{11}H_{60}(F_P, 60)$
Case A	F_P**=13**	5.2	8.7	21.3
Case B	F_P**=15**	2.4	4.0	10.1

Table 4 indicates that a set of $\{H_{60}(i,t)\}$ is selected which satisfy Eqn. (24) to detect fire within 60 seconds.

$$H_{60}(i,t) \geq 2.0\ °C \tag{24}$$

The temporary fire location, which is the number P_F of sensor which shows the largest value in $\{H_{60}(i,t)\}$, are selected in the manner as mentioned in 4.1. The simplified detection algorithm is to check if the following two tests are accepted.

$$\sum_{11} H_{10}(P_F,t) \geq 3.8\ °C \tag{25}$$

$$\sum_{11} H_{60}(P_F,t) \geq 9.5\ °C \tag{26}$$

If they are accepted at the same time, fire alarm is generated.

6.4. Verification in Normal Operations

The simplified algorithm was studied using the recorded data of the sensor cable during the normal operations at actual tunnel. The maximum value of the temperature rise of individual sensor during 60 seconds $H_{60}(i,t)$, and two evaluation values of hypothesis $\sum_{11} H_{10}(j,t)$ and $\sum_{11} H_{60}(k,t)$ are shown in Table 5. Note that P_F has not been decided yet. The sensor number which takes the maximum does not mean $P_F = j = k$. They may not take the maximum at the same time t. It is confirmed that no false alarm will be generated even if the same sensor indicates the maximum at the same time.

Table 5: Maxima of evaluation values for 60 seconds detection in non fire tunnels

Non fire		Maxima of Evaluation values		
Tunnel	**Date**	$H_{60}(i,t)$	$\Sigma_{11}H_{10}(j,t)$	$\Sigma_{11}H_{60}(k,t)$
Yoka	**8/2/2014**	1.9	3.6	17.3
	20/8/2013	0.9	1.4	6.5
Mitani	**19/8/2017**	0.7	1.1	2.7

7. APPLICATION OF FAST FIRE DETECTION ALGORITHM

False alarm is not avoidable in fast fire detection within 30 seconds for a model fire on the 1 m^2 fire plate. Taking a wrong action in responding to a false alarm may lead to a fatal incident. Thus, the alarm issued within 30 seconds should be limited to actions, such as the zero-flow ventilation control [Nakahori et. al, 2013], which avoids a fatal risk. We should regard it as equal to “pre-alarm” of a conventional detection system. In contrast, since temperature will rise high enough, the simplified algorithm within 60 seconds becomes reliable enough to generate no false alarm. The alarm issued by this algorithm would be equal to "alarm" in the conventional sense. Table 6 summarizes examples of actions initiated by the two different fire detection algorithms.

Table 6: Operations for fire suppression and evacuation in 370 MJ fire progress

Elapsed time	Actions
30 seconds (pre-alarm)	**・Alerting operators in control room.** **・Switching camera to fire zone.** **・Starting low speed airflow control automatically.** **・Starting to fully record temperature for estimating fire scale.**
60 seconds (alarm)	**・Notifying fire station.** **・Blocking traffic to tunnel automatically.** **・Starting sprinkler systems for fire protection.**

8. CONCLUSIONS

The developed algorithm implements calculation of evaluation value, and if-then type comparison with threshold. It searches sensors indicating high temperature rise, sets up a hypothesis on fire location with the high temperature rise sensor, calculates evaluation values as spatial sum of the temperature rise of the sensor at the fire location and sensors in its neighbourhood, and checks four different testing by comparing evaluation value with threshold. If all four are accepted TRUE, then the system generates fire alarm.

The threshold is chosen in a way that can detect 370 MJ model fire on 1 m^2 plate within 30 seconds. The algorithm has been applied to sensor cable data recorded during normal operations at an actual tunnel and verified to generate no fire alarm.

The simplified algorithm has been proposed to detect the same model fire within 60 seconds. This algorithm derived from the detection algorithm within 30 seconds by means of replacing the parameter value 30 with 60 seconds. There is no need for this algorithm to test whether or not hypothesized fire alarm is TRUE, because sensor temperature rise becomes high enough. It is considered that false alarm is barely generated in the 60 seconds detection algorithm.

The sensor cable and the developed fire detection algorithm will allow selection of appropriate risk reduction and avoidance measures from early stage of fire growth.

The thresholds of the developed algorithm are preferably selected in tunnel fire tests. However single fire test can't cover entire situations of actual tunnel fires. 3D fire simulation such as Fire Dynamics Simulator ("FDS") is a viable and effective way to complement actual fire data as it allows to investigate details of tunnel fire. Experience, knowledge and insight shall be accumulated in fire test and 3D simulation study to optimize the evaluation formula and threshold.

9. REFERENCES

Maevski, I., Josephson, B., Klein, R., Haight, D., & Griffith, Z. (2015). *Final testing of fire detection and fire suppression systems at Mount Baker Ridge and First Hill Tunnels in Seattle.* 16th International Symposium on Aerodynamics, Ventilation & Fire in Tunnels (ISAVFT), Seattle. pp. 745-754. BHR Group.

Nakahori I., Jiang S., & Vardy A.E. (2013). Zero-flow response to fire in longitudinal-ventilated tunnels. 15th International Symposium on Aerodynamics, Ventilation & Fire in Tunnels (ISAVFT). Barcelona. pp. 323-336. BHR Group.

Nakahori, I., Sakaguchi, T., Nakano, A., Atsushi Mitani, & Vardy, A.E. (2014). *Real-time Estimation of Heat Release Rates in Tunnel Fires.* 7th International Symposium on Tunnel and Ventilation, Graz. pp.12-13. Graz University of Technology.

Sakaguchi, T., Nakahori, I., Kohl, B., Senekowitsch, O., & Vardy, A.E. (2016). *Consequence Anlysis of False Fire Detection in Road Tunnels.* 8th International Conference on Tunnel Safety and Ventilation, Graz. pp. 25-26. Graz University of Technology

DEVELOPMENT OF A FULL PROBABILISTIC RISK MODEL TO ASSESS THE PERFORMANCE OF LONGITUDINAL VENTILATION SYSTEM FOR FIRES IN TUNNEL

[1]Matteo Pachera, [1,2] Bart Van Weyenberge, [1,2]Xavier Deckers,
[1] Fire Engineered Solution Ghent, Ghent, Belgium
[2]Ghent University-UGent, Dept. Flow, Heat and Combustion Mechanics, Belgium

ABSTRACT

The current paper investigates the coupling of quantitative risk assessment (QRA) methods with one-dimensional (1D) tunnel ventilation models. The coupled approach allows to perform multiple simulations with different fire scenarios with a limited computational cost. This provides a holistic view of the response of the ventilation system in case of fire. The analysis is applied to a case study where four variables are considered in the model: the Heat Release Rate (HRR), the location of the fire, the wind pressure and the effectiveness of the ventilation system to operate on demand (described by the number and reliability of jet fans). The ventilation conditions in the tunnel are analysed considering different number of jet fans installed. The QRA allows to compare the failure probability associated with the ventilation strategy and the number of installed jet fans.

Keywords: Tunnel ventilation, risk analysis, HRR, fire location, wind

1. INTRODUCTION

Tunnels have always been considered strategic structures for the transportation of people and goods. Severe fires occurred in the late 90's with large damages for the structure and fatalities, (Carvel & Beard, 2005) (Ingason, Li, & Lönnermark, 2015). These disasters led to a renewed interest in fire safety in tunnels with several research projects (Haukur, Kumm, Nilsson, Lönnermark, & Claesson, 2012), (Ingason, Li, & Lönnermark, 2015). These research projects highlighted how fires in tunnels can be more severe than similar fires in an open environment, with HRR peaks higher than 200 MW.

In the design phase the choice of the fire scenario plays an important role in the creation of a fire safety design which meets the objectives and boundary conditions set by the different stakeholders. By means of a deterministic approach, the designer defines one or more fire scenarios that are used to design the ventilation strategy. The choice of the design scenario is either imposed by national regulations or in the case these are not available, the designer relies on his experience and ethics. The quantitative risk based methods provide a possibility to analyse fire safety systems and to take the variety of possible scenarios into account. The latter approach, although more complicated, provides a holistic view of the safety level of the structure (Fernandez, Fraile, Del Rey, & Alarcon, 2013) (Deckers, Lappano, Van Weyenberge, & Merci, 2016) (Van Weyenberge & Deckers, 2014) (Van Weyenberge, Deckers, Caspeele, & Merci, 2018).

With quantitative risk based methods, the ventilation strategy is associated with a failure probability which takes into account the possible fire scenarios with their occurrence probability. Acceptable safety levels and performance criteria can be different, depending on the scope of the project. Where the objective is to assess life safety, results in terms of smoke spread, evacuation times and eventually the number of fatalities are required. The FN curves relate the number of fatalities to the occurrence probability.

In this paper, the scope of the analysis is different, as the evacuation process is not taken into account and the performance criteria are based on the smoke propagation in the tunnel. A longitudinal ventilation strategy works properly if the velocity induced by the ventilation system is greater than the velocity required to confine the smoke (Li, Lei, & Haukur, 2010). Alternative performance criteria could allow a limited smoke backlayering, which can be estimated with (Li, Lei, & Haukur, 2010). In order to estimate the velocity along the tunnel for several scenarios an efficient computational tool is required to simulate the ventilation (Carvel & Beard, 2005). Therefore, a simplified 1D model has been developed to estimate the longitudinal velocity and to consider the effect of the different variables on the flow field in the tunnel. The 1D models have a limited accuracy compared to three-dimensional models. However, in a preliminary design phase it is useful to study several scenarios, rather than giving accurate results for few selected cases.

A case study is designed considering a specific tunnel configuration. The paper presents the failure probability of the ventilation system, linking the results in a straightforward way to the involved variables. The proposed approach provides an overview over the aerolic response of the flow in the tunnel. The sensitivity of the assumptions in the ventilation design are clearly represented. The operational reliability of the ventilation system in the tunnel can be determined, which is useful in the design of new tunnels or to evaluate the safety level in existing tunnels.

2. DESCRIPTION OF THE NUMERICAL MODEL

The 1D models are often used to design the ventilation system in tunnels. However, the results are strongly dependent on the operating conditions and the configuration of the tunnel. The fire load, the atmospheric conditions and the location of the fire cannot be controlled by the designer, who should choose a conservative scenario for the design of the ventilation strategy. If the choice is too conservative the cost of the project will rise due to the high redundancy of the ventilation system. The designer should accept a low level of risk in order to limit the possibility of smoke spread and the installation costs under an acceptable level.

Some input variables are chosen in order to consider the possible operating conditions of the tunnel:

- The wind at the portal can induce an over- or underpressure depending on the wind direction and on its magnitude. The wind conditions are recorded near the site of the tunnel and these data can later be used as boundary conditions at the portals.
- The power of the fire can change depending on the vehicle type. Different values for the HRR are considered for cars, busses or HGV. The HRR of the single vehicle is also combined with the traffic density of the vehicle type.
- The position of the fire affects the temperature distribution along the tunnel and the pressure losses in the tunnel.
- The reliability of the ventilation system, here taken as the number of jet fans operating on demand, has a direct effect on the effectiveness of the system which can be described as the capability of the ventilation system to confine the smoke.

The variables presented before are integrated in a risk model where they are sampled and used as boundary conditions for the 1D ventilation model. The first three variables are considered continuous, so they are sampled using a random model. There are several methods able to sample continuous variables: Monte Carlo Sampling, Latin Hypercube Sampling, Orthogonal Sampling and Sobol Sequences. The first three methods generate random sequences, while the last one generates quasi-random low-discrepancy sequences. The Latin Hypercube Sampling (LHS) is chosen because of its simplicity and its capability to evenly spread the samples over the domain of research. The possibility of failure of one or multiple jet fans is taken into account

in the study with an event tree method. The failure probability of a ventilation system can be calculated by multiplying the probability of failure of the single event by the probability of the event to occur.

$$P_f(u < u_{cr}) = \sum_{i=1}^{n} P(u < u_{cr} | \, scen_i) \, P(scen_i) \qquad \text{Eq. 1}$$

The failure occurs when the longitudinal velocity at the fire section is lower than the corresponding critical velocity and the smoke can spread upstream the fire. The critical velocity is chosen in this paper as the failure criterium, but a reduced backlayering length could be used instead. The critical velocity can be estimated with several methods (Wu & Bakar, 2000) (Li, Lei, & Haukur, 2010) (Oka & Atkinson, 1995) (Thomas, 1958) (Kennedy, 1996), but in the current study the proposed correlation in (Li, Lei, & Haukur, 2010) is used.

$$u_{cr}^* = \begin{cases} 0.81 Q^{*1/3} & if \; Q^* < 0.15 \\ 0.43 & if \; Q^* > 0.15 \end{cases} \qquad \text{Eq. 2}$$

Where u_{cr}^* and Q^* are the non-dimensional velocity and the non-dimensional HRR, the critical velocity is later corrected for sloped tunnels (Atkinson & Wu, 1996) (Carvel & Beard, 2005).

$$u_{cr}^*(\vartheta) = u_{cr}^*(0°)(1 + 0.033 \, \vartheta) \qquad \text{Eq. 3}$$

This allows to consider the variation of the critical velocity in the different parts of the tunnels.

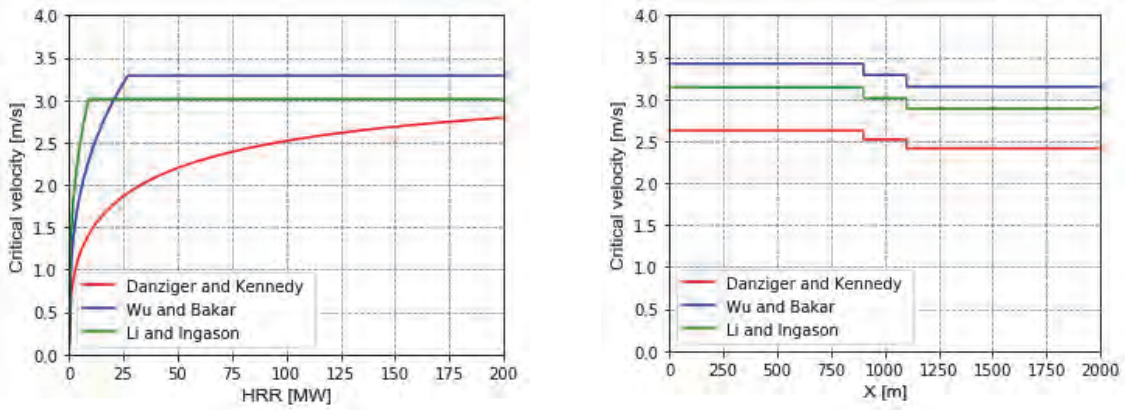

Figure 1: Critical velocity as function of the HRR and of the fire location.

In case a limited smoke backlayering is allowed, this is estimated with the equation proposed in (Li, Lei, & Haukur, 2010):

$$\frac{L}{H} = \begin{cases} 18.5 \ln(0.81 \, Q^{*\frac{1}{3}}/u^*) & if \; Q^* < 0.15 \\ 18.5 \ln(0.43/u^*) & if \; Q^* > 0.15 \end{cases} \qquad \text{Eq. 4}$$

The risk model is coupled with a fluid dynamic model which is capable to simulate the tunnel with a 1D approach. The 1D model is chosen due to its suitability for tunnels and thanks to its limited computational cost. The model used in this research was developed at FESG to simulate a single branch tunnel. In a single branch model, the equation of mass conservation is automatically fulfilled. The momentum equation, Bernoulli equation, is solved for steady state conditions along the whole tunnel:

$$\frac{1}{2}\left(f\frac{L}{D_h} + \sum \beta\right)\rho u^2 + \Delta P_{fan} + \Delta P_{fire} + \Delta P_{wind} + \Delta P_g = 0 \qquad \text{Eq. 5}$$

The buoyancy force in the tunnel is modelled with the approach proposed by Merci (Merci, 2008), considering the density of the gas ρ variable as function of the temperature.

$$\Delta P_g = \int_0^L \rho g \sin(\alpha)\, dx \qquad \text{Eq. 6}$$

The pressure rise induced by the jet fans is calculated with a momentum source change (Tarada & Brand, 2009):

$$\Delta P_{fan} = \frac{A_f}{A_t}\rho(u_f - u_t)u_f \qquad \text{Eq. 7}$$

The wind pressure is calculated based on the weather conditions at the portals. The wind velocity and the angle are calculated based on the one site measurements. The wind pressure at the portals is calculated as:

$$P_{wind} = \frac{1}{2}\rho\, u_{wind}^2\, c_p \qquad \text{Eq. 8}$$

The coefficient c_p is calculated based on (Blendermann, 1975), Figure 2, for a given wind condition the pressure difference at the portals is calculated, Figure 3. A negative pressure induces a velocity that is opposite to the ventilation flow, while a positive pressure induces a velocity in the same direction to the ventilation flow.

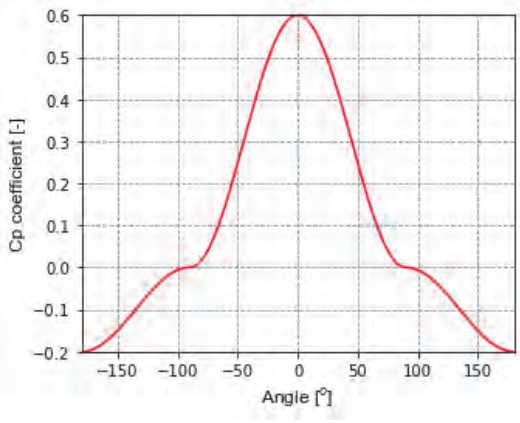

Figure 2: Wind pressure coefficient.

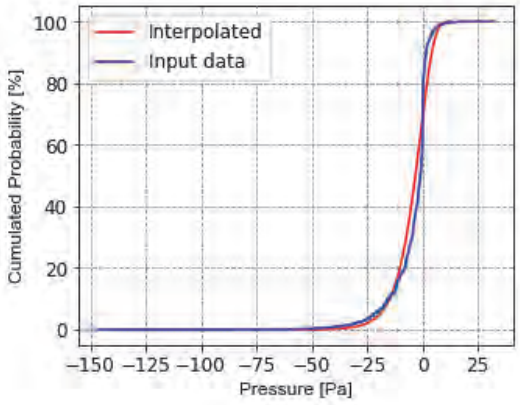

Figure 3: Cumulative wind pressure distribution.

The heat losses through the walls of the tunnel are not calculated by solving the energy equation, but are modelled with a simplified approach proposed by Ingason (Carvel & Beard, 2005). The temperature rise induced by the fire is equal to:

$$\Delta T_{fire} = \frac{2\dot{Q}}{3\,\dot{m}\,c_p} \qquad \text{Eq. 9}$$

While the temperature decay downstream the fire is described by the following equation:

$$T(x) = T_{Amb} + \Delta T_{fire}\exp\left(-\frac{hPx}{\dot{m}\,c_p}\right) \qquad \text{Eq. 10}$$

The current approach solves the equation controlling the fluid motion in a simplified way. But in this study several simulations are required, therefore these simplifications are acceptable. The results of the 1D model have been compared with those provided in (Carvel & Beard, 2005)(Merci, 2008) in order to evaluate the capabilities of the proposed model. However, the results are not reported here for sake of brevity.

The fire load in the tunnel changes depending on the vehicles that are allowed in the tunnel: cars, busses and trucks. The possible fire loads in the tunnel are related to the traffic conditions

and to the HRR of the single vehicle. The traffic conditions considered for this specific case-study are summarized in Table 1.

Table 1: Traffic conditions in the tunnel

Vehicle	Car	Bus	HGV	Tanker
HRR average	7 MW	30 MW	100 MW	200 MW
Traffic %	70 %	20 %	8 %	2 %

The values of the HRR for the different vehicles are calculated based on (Ingason, Li, & Lonnermark, 2015) (NFPA 502, 2010) (Yuguang & Spearpoint, 2007). The distribution of the HRR for the given traffic conditions is presented in Figure 4 and Figure 5.

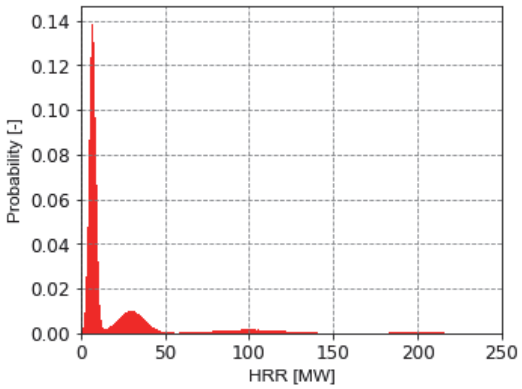

Figure 4: HRR of vehicles.

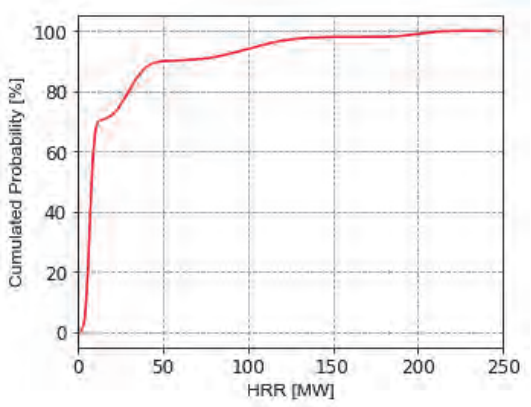

Figure 5: Cumulated distribution of HRR.

3. DESCRIPTION OF THE TUNNEL UNDER INVESTIGATION

The case study proposed in the paper is a road tunnel dug under a river or a canal. The tunnel is 2.0 km long and it has a V shape, the lowest point of the tunnel is at -20 m with respect to the portals, Figure 6. The orientation of the north portal is -135° and the orientation of the South portal is 45°, Figure 7.

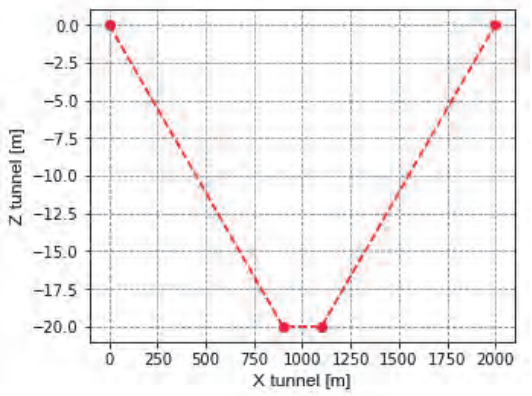

Figure 6: Tunnel's z-profile.

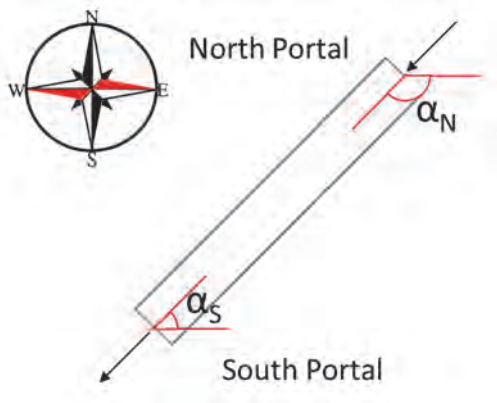

Figure 7: Orientation of the tunnel.

The cross section of the tunnel is rectangular and constant along the length of the tunnel, Figure **8**. The width of the tunnel is 11.0 m and the height is 5.0 m, in the tunnel there are 3 lanes plus a pedestrian way for evacuation. The hydraulic diameter of the tunnel is 6.875 m and the area of the cross section is 55 m^2. Figure 8 shows that there is no space to allocate the jet fans above the traffic lanes. There is only 1.3 m available on the side due to the space required for the

installation, 0.2 m. The installed jet fans have an external diameter of 1.3 m and an internal diameter of 1.1 m, the discharge velocity is 30 m/s and the installation efficiency 0.80 (Beyer, Sturm, Saurwein, & Bacher, 2016) (Rijkswaterstaat, 2005).

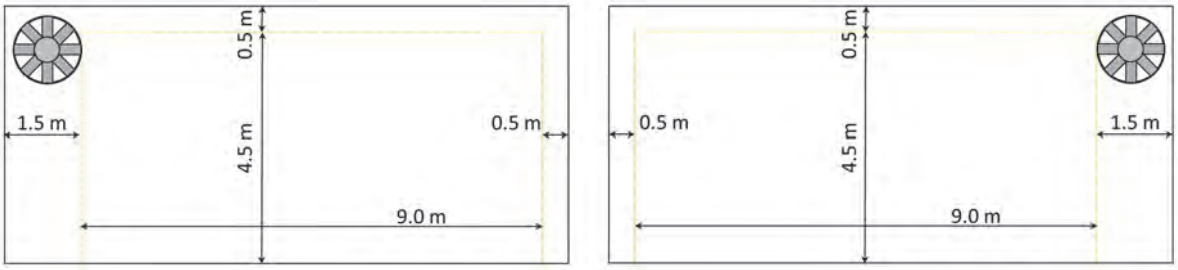

Figure 8: Cross sections of the tunnel.

4. RESULTS

In the case study different configurations are investigated. First, the number of jet fans operating on demand is modified in order to show how the probability of failure (being described as not reaching the critical velocity) changes. Before executing the simulations, it is necessary to perform a sensitivity analysis to evaluate the reliability of the calculation. The accuracy of the calculation varies with the number of evaluated samples. Therefore, it is necessary to determine the minimum number of samples required to perform an analysis which is independent from the number of chosen samples, Table 2.

Table 2: Sensitivity analysis for the Latin Hypercube Sampling method.

N sample	10	100	1'000	10'000	100'000	1'000'000
Failure	1	3	67	708	6928	69496
Failure %	10 %	3 %	6.7 %	7.08 %	6.928 %	6.9496 %
Error %	3 %	4 %	0.3%	0.13 %	0.022 %	-
Time	3 s	5 s	37 s	246 s	2196 s	21056 s

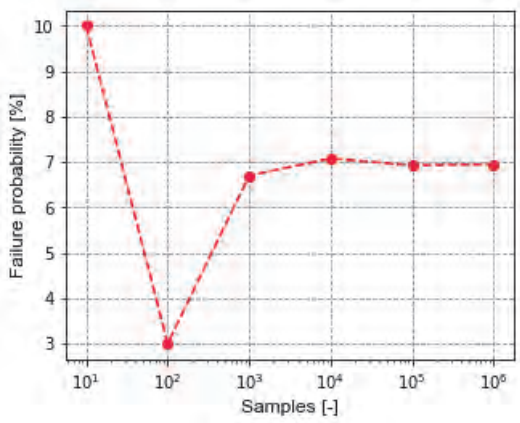

Figure 9: Sensitivity analysis: failure probability.

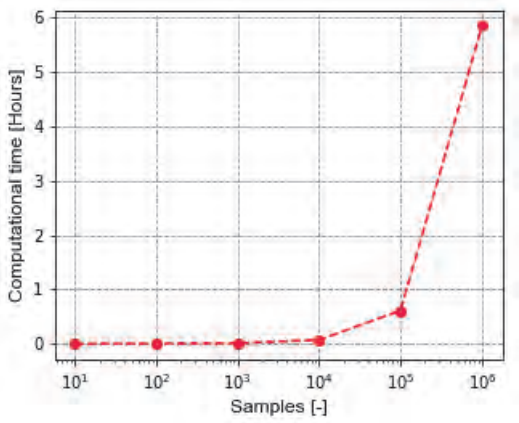

Figure 10: Sensitivity analysis: computational time.

The failure probability is presented as function of the number of samples in Figure 9. The computational time grows together with the size of the samples; therefore, it is necessary to make a trade-off between the accuracy of the method and the computational time. Due to low discrepancy between the results obtained with 10^5 and 10^6 samples, about 0.02%, the first sample size is chosen for the next analysis.

The tunnel is simulated with different number of jet fans operating on demand. The results are later combined together in order to consider the effect of the failure of some devices. This is done by combining the failure probability in the tunnel with less jet fans installed and the reliability in terms of operating on demand. The probability of one jet fan to fail on demand (maintenance) is assumed to be 5%. The probability of two jet fans to fail on demand is 0.25% and the probability of all jet fans operating on demand is 94.75%. The total probability of failure of one configuration with n jet fans is:

$$P_f(u < u_{cr}) = P_f(u < u_{cr})\big|_{n_b} 0.9475 + P_f(u < u_{cr})\big|_{n_b-1} 0.05 + P_f(u < u_{cr})\big|_{n_b-2} 0.0025 \qquad \text{Eq. 11}$$

In order to reduce the complexity of the model once there is a failure of one of the jet fans, the remaining ones are evenly distributed along the tunnel. This simplification avoids the addition of another variable which controls the jet fans that is not operating on demand.

Table 3: Failure probability.

N jet fans	Simple P_f	Combined P_f
0	98.9 %	98.9 %
1	96.0 %	96.2 %
2	78.8 %	79.7 %
3	46.2 %	48.0 %
4	23.3 %	24.6 %
5	12.1 %	12.7 %
6	7.8 %	8.1 %
7	4.9 %	5.1 %
8	3.4 %	3.5 %
9	2.7 %	2.7 %
10	2.2 %	2.2 %

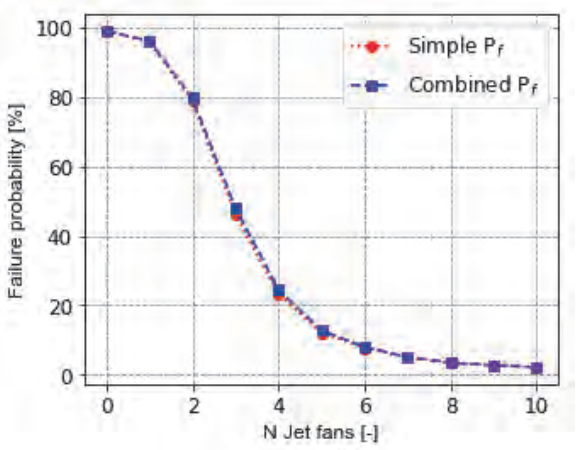

Figure 11: Failure probability as function of the number of installed jet fans.

In Figure 11 and Table 3 the failure probability for different jet fans configurations is presented. The failure probability is presented before and after taking into account the failure probability of some jet fans. The results show that the increase of failure probability is limited when the jet fans' reliability is taken into account, less than 2%.

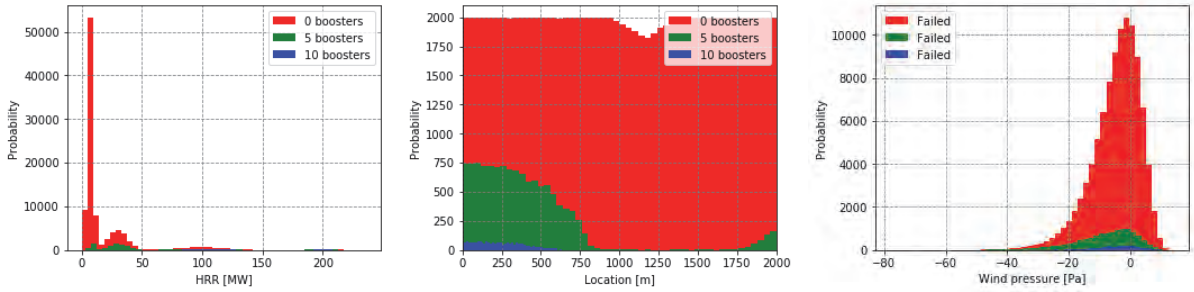

Figure 12: Probability distributions for HRR, fire location and wind pressure with 0, 5 and 10 jet fans.

The results are presented also in a graphical way showing the operative conditions that lead to a failure of the ventilation system for few selected configurations, Figure 12.

5. DISCUSSION

The results from the case study indicate that by increasing the number of jet fans, the risk of smoke spread and associated backlayering decreases Figure 11. However, this information doesn't give a complete understanding of the response of the ventilation to a fire event. The possibility to combine several parameters for a specific tunnel allows to define design criteria specific for each project, new or existing. On top of that the developed model allows to answer questions relevant to many parties. For instance, what is the maximum design fire that a specific ventilation system is able to handle? And how does this change if not all the jet fans are available? The largest fire where the ventilation system will still avoid back-layering can then be determined based on the available number of jet fans. Figure 13 describes, how for a ventilation system with 10 available jet fans, the maximum HRR is around 28 MW when the most conservative location in the tunnel and the most conservative wind conditions are taken into account. If 1% of the scenarios (combinations of wind load and fire location in the tunnel) are allowed to have smoke spread larger than the objective (no back-layering), than it is possible to increase the HRR limit to 60 MW. Similarly, if 5% of the cases are allowed to be exceeded, then the largest fire is 75 MW.

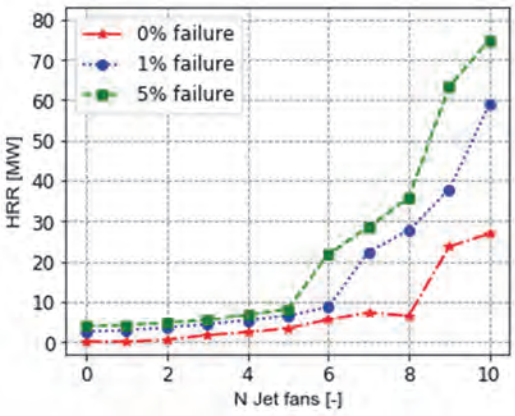

Figure 13: Critical HRR for different failure probabilities.

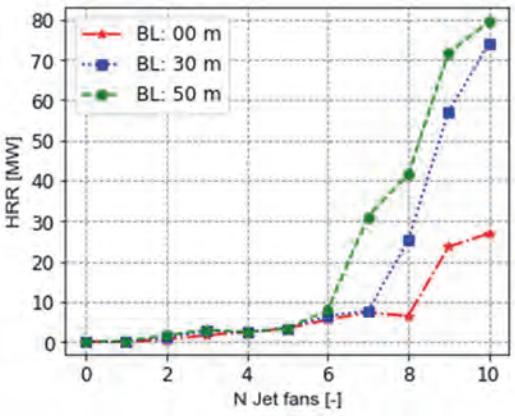

Figure 14: Critical HRR for different performance criteria.

Until now the ventilation was considered to fail if the critical velocity was not reached, but a limited backlayering length can be also used as a design criteria. When is it acceptable to have some back-layering and to what extend? In order to tackle this problem, also the performance criteria was taken as a variable. This can typically range from no back-layering to 30 m or 50 m. It is the authors' point of view the proposed criteria might be acceptable depending on the case, as long as the stratification is maintained (has to be proven by CFD). Allowing a backlayering length of 30 m or 50 m it is possible to extend the acceptability range for the ventilation system. The maximum HRR considered to be safe for a given ventilation configuration is presented in Figure 14 for different accepted backlayering lengths. Adjusting the performance criteria for smoke spread and allowing a limited back-layering the ventilation system can still operate successfully for larger design fires. Therefore, the critical HRR that is confined by the ventilation increases allowing a larger backlayering length.

The wind pressure plays an important role in the tunnel and affects the longitudinal velocity in the tunnel. Strong wind at the portals have a low probability to occur, Figure 3, because these values lay on the tails for the probability curve. In deterministic design, typically the 90 or 95 percentile of the wind is taken into account. If the wind pressure exclude those extreme values that have low probability to occur the largest fire where the ventilation system will still avoid back-layering increases, Figure 15. The combination of different performance criteria and boundary conditions allows to create different limit conditions for the HRR, Figure 16.

Accepting a limited backlayering and excluding the extreme wind conditions it is possible to extend the critical HRR for all the different ventilation configurations. Considering the configuration with 10 jet fans the maximum HRR increases from 27 MW to 74 MW when allowing 30 m backlayering and limiting the wind conditions between 5 and 95 % of the cases. The maximum HRR can be further extended to 79 MW allowing 50 m backlayering and limiting the wind conditions between 10 and 90 % of the cases.

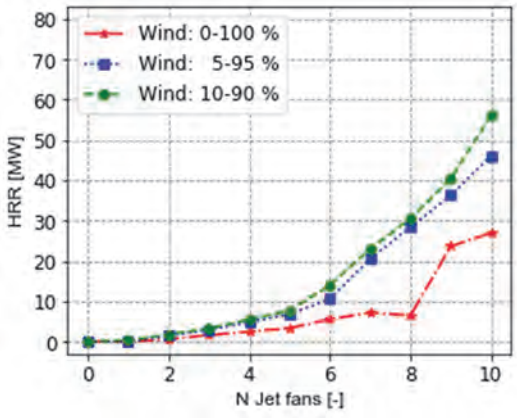

Figure 15: Critical HRR for different wind pressures.

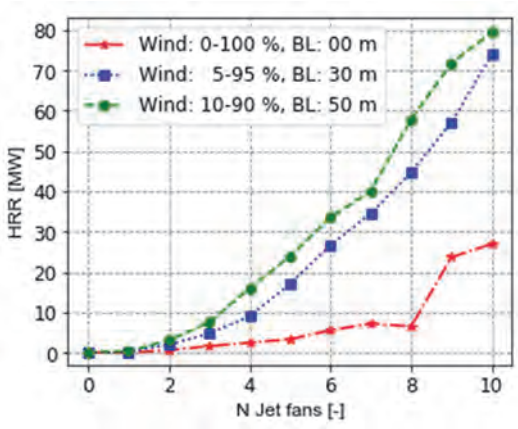

Figure 16: Critical HRR for different back-layering lengths and wind pressures.

6. CONCLUSIONS

The current paper presents the capabilities of a combined tool for the analysis of the ventilation in tunnels. A risk assessment method is combined with a one-dimensional model for the analysis of the longitudinal ventilation in case of fire. With the risk analysis the operative conditions of the tunnel were varied based on the possible fire scenarios (position and HRR), weather conditions (wind pressure), and effectiveness of the ventilation system to operate on demand (described by the number and reliability of jet fans). The approach shows in a quantitative way how the probability of the ventilation failure is influenced by the number and reliability of the jet fans. The results allow to evaluate the maximum fire size that a specific ventilation system is able to handle. It is possible to represent the largest fire size where the back-layering will be limited (e.g. 30 m) and the wind pressure is not exceeded in 90% of the time. The current approach can be used to verify the operative conditions of tunnels which are already built providing a holistic view of the response of the ventilation system to the fire event. The current method could also be used also to design a new tunnel or to determine the cost-benefit of limiting the residual risk (extreme wind) in discussions on the acceptable risk level. This allows the designer to support the decision maker and client in setting up the functional requirements on design and minimal operating conditions.

7. REFERENCES

Association, N. F. (2015). *NFPA 502, Standard for road tunnels, bridges, and other limited access highways.*

Atkinson, G. T., & Wu, Y. (1996). Smoke control in sloping tunnels. *Fire Safety Journal*, 335–341.

Beyer, M., Sturm, P., Saurwein, M., & Bacher, M. (2016). Evaluation of jet fan performance in tunnels. *8th International Conference on Tunnel Safety and Ventilation.*

Blendermann, W. (1975). *On a probabilistic approach to the influence of wind on the longitudinal ventilation of road tunnels.*

Carvel, R., & Beard, A. (2005). *The handbook of tunnel fire safety.* Thomas Telford.

Deckers, X., Lappano, M., Van Weyenberge, B., & Merci, B. (2016). Quantifying the Effect of Input Parameter Uncertainty on the Resulting Risk Level for Fire in Rail Tunnels. *7th International Symp. on Tunnel Safety and Security*, (S. 671-682).

Fernandez, S., Fraile, A. I., Del Rey, I., & Alarcon, E. (2013). Probabilitic approach for longitudinal ventialation system design in fire situations. *15th International Symposium on Aerodynamics, Ventilation and Fire in Tunnels*, (S. 67-80).

Haukur, I., Kumm, M., Nilsson, D., Lönnermark, A., & Claesson, A. (2012). *The METRO project.* SP.

Ingason, H., Li, Y. Z., & Lönnermark, A. (2015). Runehamar tunnel fire tests . *Fire Safety Journal*, 134-149.

Ingason, H., Li, Y. Z., & Lönnermark, A. (2015). *Tunnel fire dynamics.* Springer.

Kennedy, W. D. (1996). Critical velocity: past, present and future. *One Day Seminar Smoke and Critical Velocity in Tunnels.*

Li, Y. Z., Lei, B., & Haukur, I. (2010). Study of critical velocity and backlayering length in longitudinally ventilated tunnel fires. *Fire Safety Journal*, 361-370.

Merci, B. (2008). One-dimensional analysis of the global chimney effect in the case of fire in an inclined tunnel. *Fire safety journal*, 376-389.

NFPA 502. (2010). *Standard for Road Tunnels, Bridges, and Other Limited Access Highways.* National Fire Protection Association.

Oka, Y., & Atkinson, G. T. (1995). Control of smoke flow in tunnel fires. *Fire Safety Journal*, 305-322.

Rijkswaterstaat. (2005). *Aanbevelingen ventilatie van verkeerstunnels.* In Dutch.

Tarada, F., & Brand, R. (2009). *Proceedings of 13th International Symposium on Aerodynamics and Ventilation of Vehicle Tunnels. BHRG. New Brunswick, New Jersey, USA*, (S. 95-107).

Thomas, P. J. (1958). The movement of buoyant fluid against a stream and the venting of underground fires. *Fire Safety Science*.

Van Weyenberge, B., & Deckers, X. (2014). Development of a risk assessment method for fire in rail tunnels. *6th International Symp. on Tunnel Safety and Security.*

Van Weyenberge, B., Deckers, X., Caspeele, R., & Merci, B. (2018). Development of an integrated risk assessment method to quantify the life safety risk in buildings in case of fire. *Fire technology*.

Wu, Y., & Bakar, M. A. (2000). Control of smoke flow in tunnel fires using longitudinal ventilation systems--a study of the critical velocity. *Fire Safety Journal*, 363-390.

Yuguang , L., & Spearpoint, M. (2007). Analysis of vehicle fire statistics in New Zealand parking buildings. *Fire technology*, 93-106.

REPRODUCTION OF HUMAN BEHAVIOR IN RISK MODELS – VALIDATION OF THE RELEVANT RISK PARAMETERS BASED ON PROBAND TESTS

[1]Anne Lehan, [2]Oliver Senekowitsch
[1]Bundesanstalt für Straßenwesen, Germany
[2]ILF Consulting Engineers, Austria

ABSTRACT

Under certain conditions, risk analyses must be carried out as part of the quantitative safety assessment of road tunnels. In addition to object-, traffic- or event-specific parameters, there are also a number of input parameters that are fixed in the risk model and whose variation is usually not planned - this also applies to parameters of human behavior. In the course of various test series on the escape and reaction behavior of road users in road tunnels in the event of an incident, various behavioral parameters were determined and analyzed. The obtained values are compared with the conventional model parameters, used in the Austrian tunnel risk model. In addition to the reduction of the overall risk, based on the currently acquired behavioral parameters, it can be shown that the assessment of self-rescue related safety measures is more or less invariant under the change of behavioral parameters investigated, if a comparative assessment approach is used.

Keywords: tunnel, risk analysis, risk assessment, real life field test, human behavior

1. INTRODUCTION

One main objective of the safety measures in tunnels is to ensure self-rescue in case of an incident. In the course of equipping a tunnel with operational and safety equipment, a quantitative safety assessment using a risk analysis approach must be carried out under certain conditions. Efficient risk models also have modules that depict human behavior. In addition to object-, traffic- or event-specific parameters that are systematically varied, there are also a number of input parameters that are fixed in the model and whose variation is usually not provided. Among other things, this applies to many parameters for describing human behavior. The basic parameters used in the Austrian tunnel risk model have not been validated or updated since the introduction of the model about 10 years ago.

In the course of a series of tests conducted by the Federal Highway Research Institute (Bundesanstalt für Straßenwesen) on the influence of fixed fire-fighting systems (FFFS) on self-rescue behavior, tests were carried out for the first time in which the reaction and escape behavior of tunnel users was investigated qualitatively and quantitatively [1]. The results provide a basis for checking the data stored in the risk models.

For the first time, the paper will present new insights into evacuation and reaction behavior in connection with the possible updating of risk models.

2. EVACUATION BEHAVIOR IN TUNNELS

In general, the evacuation behavior of persons can be divided into several phases. At the beginning is the pre-evacuation phase, which includes all events before the start of the evacuation and ends with the decision to escape. Of particular interest here is the duration of this phase and which characteristics of the event lead to whether and when the tunnel user decides to escape. In the following evacuation phase it can be distinguished between a pre-movement phase and a movement phase. During the pre-movement phase, the tunnel user searches for information and selects an escape route. The movement phase includes all behavior that the tunnel user displays during the evacuation until he reaches an escape target.

This approach is reflected in the Kuligowski's 4-phase model [2], where the first two phases of Kuligowski correspond to the pre-evacuation phase, the third phase corresponds to the pre-movement phase and the fourth phase corresponds to the movement phase. In phase 1, situational clues are perceived which are interpreted in phase 2 and evaluated with regard to their risk. In phase 3 an action decision is made, which is carried out in phase 4. Based on this pattern, the behavior of tunnel users before and during evacuation is reproduced in the Austrian tunnel risk model. Phases 1 to 3 are represented by a reaction time. Reaction time is understood to mean the realization of the situation as well as the processing and includes the period of time from the vehicle's standstill at the event situation until leaving the vehicle. The movement phase is mainly modelled and determined by different escape velocities. The escape velocity expresses the average speed at which the subject moves out of his vehicle to reach a safe area (here: emergency exit). A more detailed connection to the relevant parameters in the Austrian tunnel risk model is given in section 4.

3. TEST PERSON EXPERIMENTS IN REAL TUNNELS WITH AUTOMATIC FFFS

To gain further insights into the escape and reaction behavior of road tunnels with the system types high pressure foam (foam) and high pressure water mist (water-mist), two real life field tests were conducted with the aim of determining the influence of the FFFS on the behavior and experience of road users [1].

Table 1: Number of test persons (pairs) for each experimental setting

Parameter	Including activation of FFFS	Without activation of FFFS
foam	16	14
water-mist	28	26
Pairs	3(6)	3(6)

Table 1 shows the number of participants, separated by persons who experienced an activation of the FFFS and the number of those who served as so-called control subjects. In a random, yet controlled set-up, the escape behavior of the participants inside and outside the vehicle was observed. Participants drove a car into the tunnel and were confronted with a simulated accident with smoke propagation. After stopping the vehicle on approaching the accident, an announcement requested them to evacuate. In case of the subjects of the event group "with FFFS" the FFFS was activated for 2 minutes during the announcement (see Figure 1).

Figure 1: Experimental situation after activation of FFFS – Foam (left) – Water mist (right)

The participants had 3 minutes from the start of the announcement to react. The trial ended when one of the following criteria occurred: Attempt to make an emergency call via mobile phone; turning the vehicle; reaching certain targets: Emergency exit, emergency call station; the test person remains in the vehicle for 3 minutes; getting out and remaining in the scenario for 3 minutes. Figure 2 shows the experiment set-up in the tunnel.

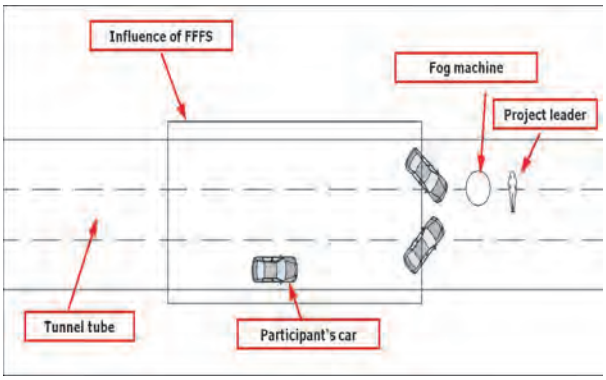

Figure 2: Schematic representation of experiment set-up

4. PARAMETER COMPARISON AND DISCUSSION

The Austrian tunnel risk model TuRisMo 2.0 according to [3] forms the basis for the investigation of the influence of representative behavioral parameters on risk models. TuRisMo is based on an integrative approach which allows a detailed analysis of road tunnels as an overall system, including the evaluation of a variety of risk mitigation measures. A detailed description of the Austrian tunnel risk model can be found, for example, in [3], [4] and [5], the implementation of a FFFS (water mist) and the illustration of its effectiveness in the tunnel risk model can be found in [6].

The modelling of evacuation procedure and in particular of human behavior during such, is based on four basic assumptions:

- Persons in the tunnel begin self-rescue when a) they are prompted to do so by suitable installations by the operating personnel or b) visibility falls below a critical value due to the concentration of fire smoke.
- Persons who are requested to escape by the operating personnel need a certain reaction time to actually leave the vehicle.
- Persons escape with a statistically distributed walking speed to the nearest emergency exit but never over the fire site.
- A certain percentage of people do not leave the vehicle's location despite limited visibility or request for self-rescue.

These assumptions are represented by three model parameters, namely – reaction time (time to perceive, process and decide) – escape velocities (demographically inspired velocity distribution) and share of non-evacuating persons (because of reduced mobility, injuries or impropriate behavior).

4.1. Derivation of the model parameters from the test subjects' experiments

The data on self-rescue and evacuation behavior recorded in the course of the trial were analyzed with regard to the behavioral parameters used in the Austrian tunnel risk model. Due to the consistent homogeneity of the data sets without activating the FFFS, the statistical analysis for this case was carried out on the basis of the combined data set of both tunnels. When the FFFS was activated, response times, escape velocities and proportions of non-evacuating persons were investigated separately for the two tunnels with the different FFFS types in order to identify tunnel-specific and system-specific influences. The results of the analysis are presented in Table 2 together with the values normally used in the Austrian tunnel risk model.

Table 2: Analysis of real person test data with and without activation of FFFS

Parameter	without activation of FFFS		including activation of FFFS	
	TurRisMo standard value	Experimental results	Experimental results (foam)	Experimental results (water-mist)
Reaction time	53 seconds	30 seconds	54 seconds	40 seconds
Escape velocities	1.15 m s^{-1}	1.9 m s^{-1}	1.7 m s^{-1}	2.6 m s^{-1}
Share of non-evacuating persons	3 %	%	13 %	32 %

The Austrian tunnel risk model takes account of reaction time and the proportion of non-running persons in the Austrian tunnel risk model in terms of an average value. For this reason, the values shown in Table 2 already correspond to the values used in the parameter study, cf. Section 6; in contrast, the escape velocities are taken into account in the risk model via a discrete probability distribution. The distribution applied as standard is based on assumed escape velocities which are differentiated according to age and gender and taken from the evacuation model BuildingExodus, cf.[7] as well as on the demographic distribution of the Austrian population[8]. In the course of the parameter study, this distribution is replaced by the discrete actual distribution of the escape velocities from the test persons. Both distributions are shown in Figure 3.

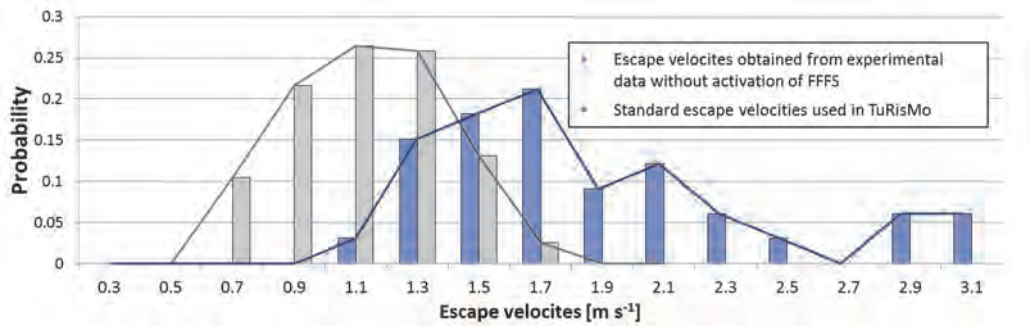

Figure 3: Probability distribution of escape velocites

4.2. Discussion of model input parameters and general validity

4.2.1 Response times

The normally assumed response time of approximately 60 seconds in the Austrian risk model, which includes the time from stopping the vehicle and following the self-rescue request to leave the vehicle, can be regarded as conservative, even without comparison with the significantly shorter response times from the test subjects. Nevertheless, it must be noted that the test persons were confronted with an experimental set-up and were aware of the experimental character of the situation. A certain expectation and thus a - in comparison to a real situation - faster reaction can therefore be assumed. The resulting response times of 30-54 seconds are therefore to be regarded as optimistic.

4.2.2 Escape velocities

The actual escape velocities determined from the two studies are comparatively high and deviate significantly from the standard values usually used in risk analyses. Particularly striking is the fact that, contrary to other assumptions (see[9],[10],[11]), particularly high speeds were

recorded in the case of very limited visibility. Some of the respondents literally ran out of the danger zone. With regard to this behavior, it should be noted that the presence in the area of the activated water mist (high walking speeds were mainly encountered with this type of plant) is unpleasant and therefore the drive to leave this area quickly is high. It should also be borne in mind that the limitation of visibility (and its effect on escape velocities) in the experimental set-up cannot be directly transferred to the conditions of a real fire (effect of the FFFS combined with dense fire smoke was not investigated).

4.2.3 Share of non evacuating persons

In view of the comparatively low data set from the real tests, the shares of non-evacuating persons of 3% in the risk model and 2% in the test persons without activation of the FFFS can be interpreted as equivalent. In the Austrian risk model non-evacuating persons remain at the vehicle's location for the entire simulation period of 900 seconds and are thus exposed to the dangers of heat and flue gases over a long period of time. The interpretation that all test persons who did not initiate an escape reaction within the duration of the experiment (180 s) would not initiate an escape over a period of 900 seconds even in an actual fire is therefore presumably conservative. In addition, it can be assumed that the decision to flee and leave the vehicle is facilitated by the perceivable real threat and the observation of other evacuees (group effect).

5. PARAMETER STUDY – EFFECT OF HUMAN BEHAVOIR ON THE QUANTITATIVE ASSESSMENT OF SAFETY MEASURES

The effect of a change in evacuation behavior parameters on the absolute risk values of a model tunnel, calculated with the Austrian tunnel risk model, has already been investigated in prior studies [13]. As a result of the parameter improvement, with respect to experimental obtained data, a reduction of approx. 25% of the overall risk value for a more or less generic bidirectional model tunnel without FFFS has been found. More diverse results were obtained for the same model tunnel if the effects of FFFS are taken into account. A detailed discussion of the change in absolute risk and about the possible effect of FFFS activation on human behavior can be found in [13]. Although the absolute risk value may change with a change in evacuation behavior parameters, the comparative assessment method used in the Austrian tunnel risk model is considered to be very robust against variation of background parameters.

5.1. Model tunnel

In order to investigate the influence of changed behavioral parameters on the outcome of risk assessments and to examine the invariance with respect to the variation of background parameters, the Austrian tunnel risk model is applied to a 1000-meter long bi-directional model tunnel, which characteristics are summarized in Table 3.

Table 3: Model tunnel – relevant parameters

Parameter	Value
length	1000 m
inclination	3 %
traffic type	Bi-directional traffic
emergency exit distance	500 m
traffic volume	20.000 veh/day
traffic composition	14.5 % hgv, 0.5% bus

5.2. Results

Starting from the characteristics of the model tunnel, specific parameters were varied to reflect the action of four risk mitigation measures. The changed parameters are shown in Table 4 for the reference model tunnel as well as for the tunnel including different risk mitigation measures.

Table 4: Model implementation of risk mitigation measures

Risk mitigation measure	Parameter	Value in reference case	Value after application of measure
Additional emergency Exit	Emergency Exit Distance	500 m	333 m
Improved incident detection	Detection time	37 s	7 s
Portal barriers	Time until tunnel closure	90 s	60 s
Smoke extraction system	Ventilation system	Longitudinal	LL + Smoke Extraction

Two risk assessments were carried out based on the same set of reference tunnel and risk mitigation measures. In the first study standard evacuation parameters which are normally used in the Austrian tunnel risk model were applied. These parameters were changed in the second study, according to the findings of the person experiments described in chapter 4, c.f. Table 2 and Figure 3. Within each risk assessment the four risk mitigation measures were evaluated and the resulting risk values were compared to the reference risk profile arising from the reference model tunnel. The results are depicted in Figure 4 and Figure 5. Due to more optimistic behavioral parameters, the risk values arising from adapted evacuation parameters lead to consistently lower risk expectation values. Standard behavioral parameters lead to risk values between 0.221 (reference case) and 0.132 (smoke extraction) expected fatalities per year. In contrast, risk expectation values between 0.171 (reference case) and 0.128 (smoke extraction) were found for adapted behavioral parameters. The overall risk reduction arising from variation of behavioral parameters is in good agreement with the findings of prior studies [13]. On average 18% risk reduction in the present, compared to 25% in the prior one.

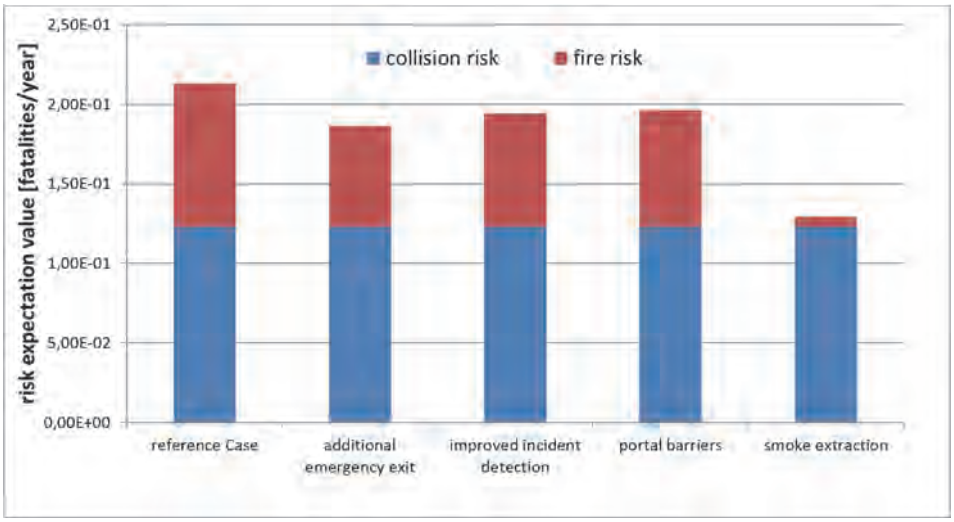

Figure 4: Risk values with respect to standard behavioral parameters

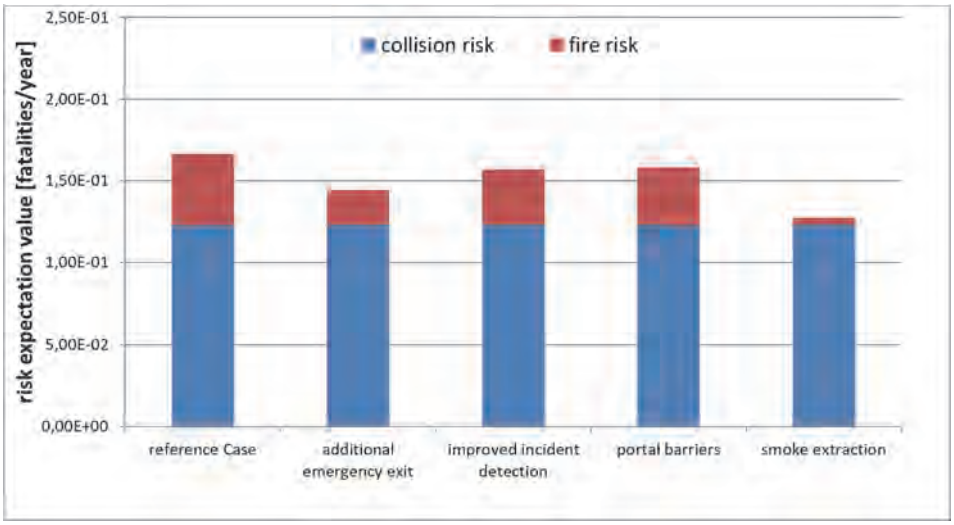

Figure 5: Risk values with respect to behavioral parameters based on person experiments

In the application of the Austrian risk model, decisions are made based on the relative comparison of reference risk profile, which is given from the application of the risk model on a reference tunnel, and the risk value of the actual tunnel. The actual tunnel may include notable deviations from regulatory guidelines as well as additional measures. Since parameter variations, which do not favor specific measures or tunnel designs, will cancel out in this kind of relative assessment approach, the Austrian tunnel risk model is believed to be very robust against parameter uncertainties. In order to investigate this behavior, the risk reductions due to risk mitigation measures, as they result from the risk model, is compared in Figure 6, for the two choices of behavioral parameters (standard parameters and experimentally obtained parameters). It is found that three of the investigated measures – improved incident detection, portal barriers and smoke extraction system – lead to almost exactly the same percentage of (fire) risk reduction for both choices of behavioral parameters. Only risk reduction following from an additional emergency exit increases from approximately 30% to 50%, if the optimistic behavioral parameters are used. However, also for this case risk reductions are comparable (same order of magnitude). Thus, the robustness of the comparative risk assessment approach is confirmed.

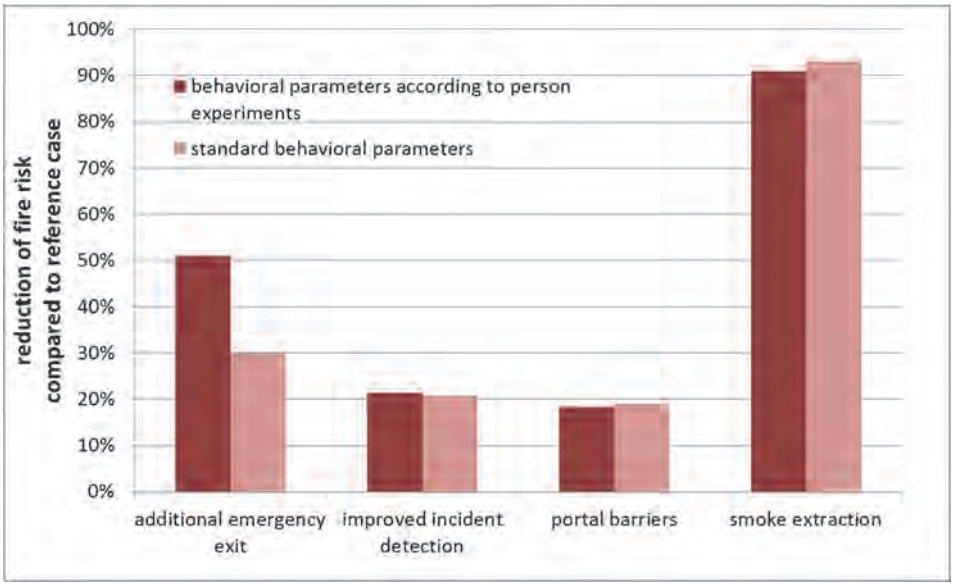

Figure 6: Reduction of fire risk compared to reference case

6. DISCUSSION AND CONCLUSION

The test data show both significantly higher escape velocities and much shorter reaction times compared to conventional model input parameters. Nevertheless, it should be noted that these good results may also be due to the fact that the test situation was a test situation and the test persons were aware of it. Due to the expectations regarding the confrontation with an incident, the situation alone in the tunnel and the claim to accomplish this task well, influences on the result cannot be ruled out. Nevertheless, it is still necessary to make an estimate between the fundamentally conservative, conventional assumptions and the nevertheless very optimistic results with regard to escape speeds and reaction times. This conclusion can be drawn independently of the installation or activation of a FFFS.

Contrary to this, the proportion of non-evacuees must be discussed differently. Without activation of the fire-fighting system, the value of 3% stored in the risk model corresponds well with the evaluations of the test persons, whereas activation of the FFFS shows a significant increase in the proportion of non-evacuating persons. Even if the proportion of persons who are not reacting is presumably overestimated due to certain restrictions with regard to the short duration of the experiment and, in some cases, the lack of a group effect, it is advisable to discuss the consideration of this effect in the risk assessment and to consider suitable countermeasures to compensate for the escapism.

In summary, the comparison of the parameter values stored in the model and the parameter values derived from the test persons shows a fluctuation range within which the real expected value is likely to be found (nota bene: in reality, however, a large fluctuation range can be expected in individual cases as well [12]). It can be stated that, on the one hand, the courses of action as depicted in risk models are close to the actual challenges that evacuees have to overcome. On the other hand, the few behavioral parameters introduced for specific modelling and derived on the basis of plausibility considerations and empirical reports are well in line with the evaluations of the real tests. The parameters currently used in practice for mapping human behavior tend to be conservative, resulting in an overestimation of the absolute value of the fire risk.

However, parameter variations which do not favor specific measures or tunnel designs, cancel out, if the assessment is based on a comparative approach and both, reference profile and risk value of the tunnel, are calculated with the same background parameters. The study shows that this is the case for the presented change in behavioral parameters. The risk reduction due to specific counter measures, which are themselves connected with the self-rescue process, is more or less invariant with respect to the adaption of the told parameters. It can therefore be concluded that risk models which are using comparative assessment criteria, as in the case of the Austrian tunnel risk model, are robust against parameter uncertainties. These findings can contribute in improving confidence in such models.

It is nevertheless necessary to continuously check existing models whether they are up-to-date with regard to all input parameters and to make adjustments to new findings if necessary. This process can help to ensure the quality and validity of such models. In addition to the evaluation of behavioral patterns in real-life accidents and fires, realistic experiments in real tunnel facilities provide a valuable contribution along this path.

7. REFERENCES

[1] Mühlberger, A, Plab, A. & Probst, T. (2016). Analyse des Reaktions- und Fluchtverhaltens von Tunnelnutzern bei einer aktivierten Brandbekämpfungsanlage anhand von Realversuchen (FE 15.0607/2014/ERB). Unveröffentlichter Projektbericht der Universität Regensburg im Auftrag der Bundesanstalt für Strassenwesen, Deutschland.

[2] Kuligowski E.: The process of human behavior in fires: US Department of Commerce, National Institute of Standards and Technology, 2009.

[3] Österreichische Forschungsgesellschaft Straße-Schiene-Verkehr: RVS 09.03.11 Tunnel-risikoanalysemodell, Wien, 2015.

[4] Forster C., Kohl B., Wiesholzer S.: Methodologies for accurate risk modeling in the context of integrted quantitative risk analysis, 16th ISAVFT, BHR Group, Seattle, 2015.

[5] Nakahori I., Sakaguchi T., Kohl B., Forster C., Vardy AE.: Risk assessment of zero-flow ventilation strategy for fires in bidirectional tunnel with longitudinal venitlation, 16th ISAVFT, BHR Group, Seattle, 2015.

[6] Bundesanstalt für Straßenwesen: Wirksamkeit automatischer Brandbekämpfungsanlagen in Straßentunneln (FE 15.0563/2012/ERB).

[7] Ando K., Ota H., Oki T.: Forecasting the flow of people, Railway Research Review, Vol. 45, No. 8, 1988.

[8] Statistik Austria: Statistisches Jahrbuch 2003, Verlag Österreich, Wien, 2004

[9] Mayer, G.: Brände in Straßentunneln: Abschätzung der Selbstrettungsmöglichkeiten der Tunnelnutzer mittels numerischer Rauchausbreitungssimulation. Dissertation, Aachener Mitteilung Straßenwesen, Erd- und Tunnelbau, Heft 47, 2006.

[10] Jin, T.: Irritating effects on fire smoke on visibility, Fire Science and Technology, Vol. 5 No 1, S. 79-90, 1985.

[11] Galea E.R., Lawrence P.J., Gwynne S., Filippidis L., Blackshieds D., Cooney D.: Building Exodus – The evacuation model for the building industry. Theory Manual, Fire Safety Engineering Group, University of Greenwich, London, 2017

[12] Martens, M.H.: Modelling Human Behaviour in Tunnels – Expectations and Reality. In: 4th International Conference "Tunnel Safety and Ventilation", Graz, 2008.

[13] Kohl, B., Lehan, A., Senekowitsch, O.: Abbildung des menschlichen Verhaltens in Risikomodellen für Tunnelbrände: Validierung relevanter Eingangsparameter auf Basis von Probandenversuchen, Proceedings of STUVA-Conference 2017, Stuttgart, pp 405-411.

EXPERIMENTAL INVESTIGATION OF WALKING SPEED IN A FULL-SCALE DARKENED TUNNEL

[1,2]Miho Seike, [2]Nobuyoshi Kawabata, [2]Masato Hasegawa,
[2]Noritada Yamashita, [2, 3]Yung-Chi Lu
[1]Toyama Prefectural University, Japan, [2]Kanazawa University, Japan
[3]Chia-yi county fire bureau, Taiwan

ABSTRACT

When a large fire occurs in a tunnel, the ceiling lights are often covered with dense smoke so that pedestrians must evacuate in total darkness. The walking speed in such situations has not been studied, although the average walking speed in dark architectural spaces is reported to be 0.3 m/s. The walking speed in a dark tunnel is the slowest walking speed that can be expected in an evacuation situation. This speed must be clarified to allow designers to accurately assess a tunnel's fire safety. We measured the walking speed of participants wearing eye masks to simulate darkness in a full-scale tunnel. The experiments were performed in an obsolete full-scale tunnel named the ex-Tonokuchi tunnel in Fukui in November 2016. This horseshoe-shaped tunnel is 488 m long (total length), 6.6 m wide and 5.4 m high. The participants walked along 150-m-long lanes that were divided into several sections with or without obstacles. The walking speed was inferred from the longitudinal and transverse locations of each participant, recorded every 5 s. The results showed that the participants' walking speed was approximately normally distributed in the range from 0.2 to 0.8 m/s with an average value of 0.48 m/s when obstacles were present. The walking speed in a lane without obstacles ranged from 0.6 to 1.0 m/s with an average value of 0.74 m/s.

1. INTRODUCTION

Tunnels are large and long spaces, and fires in tunnels can scale from just a few to over a hundred megawatts. Any pedestrians in the tunnel will need to evacuate from this large space that will also fill with thick smoke. As many tunnels in Japan have no ventilation system, smoke behaviour is influenced by the tunnel's longitudinal inclination, natural ventilation and traffic ventilation, so that modelling the pedestrian environment is difficult. Additionally, several tunnels in Japan have no emergency announcement system; hence, pedestrians must judge for themselves whether they need to evacuate or not. We have measured the evacuation speed and walking speed in experiments in a full-scale tunnel filled with smoke and with and without lighting [1–4]. When walking normally, as they would in the workplace, pedestrians' average walking speed is 1.3–1.5 m/s and the maximum walking speed is 2 m/s [1, 3]. We also found that the walking speed distribution remains nearly constant up to the extinction coefficient 0.4 m^{-1}, which means that the distribution approximates the normal distribution curve [4]. Moreover, in an evacuation situation where an emergency announcement has played, the evacuation speed ranges between 1.5 and 3.5 m/s up to the extinction coefficient of 0.4 m^{-1}, and the maximum evacuation speed decreases with dense smoke [1–3]. The walking speed in this situation is also approximately normally distributed [4]. We reported that the maximum evacuation speed could be limited by the speed at which pedestrians share information in the case without an emergency announcement [5], which has an important impact on the reliability of agent-based evacuation simulations [5].

When a large fire occurs in a tunnel, ceiling lights are covered with dense smoke, so the environment may be in near-total darkness. The walking speed in darkened architectural spaces is reported to be around 0.3 m/s [6], but the walking speed in a darkened tunnel has not been studied. In the Sekisho tunnel fire, some evacuees used their mobile phones as a light, but the

evacuation environment was filled with dense smoke, making even these light sources ineffective [7]. Without considering the influence of smoke and toxic gases on the human body, evacuees' walking speed in a darkened space would be the lowest walking speed in that space. To measure this limit, we used a full-scale tunnel to investigate the fundamental characteristics of walking speed in dark tunnels. We simulated darkness by having participants wear eye masks, and we did not use smoke to irritate their respiratory systems. Our data are then relevant to modelling the middle to late stages of an evacuation, after smoke has cleared somewhat.

2. EXPERIMENTS

2.1. Experimental tunnel

Experiments were performed in the obsolete ex-Tonokuchi tunnel in Fukui in November 2016 (see Fig. 1). The horseshoe-shaped tunnel is 488 m long (total length), 6.6 m wide and 5.4 m high. The region allocated for the experiment (a longitudinal interval and transverse sections) is diagrammed in Fig. 2. The longitudinal direction is indicated by x, and the origin is set at checkpoint 1 (CP1).

Figure 1: Evacuation experiments in a full-scale tunnel with ceiling lights

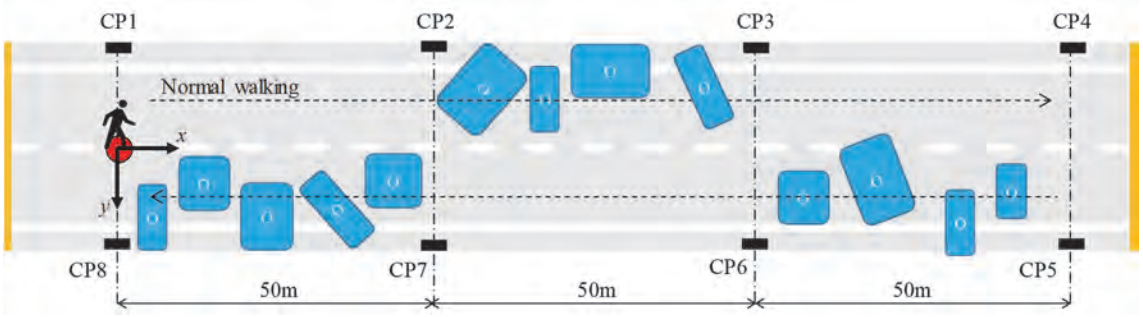

Figure 2: Schematic of evacuation experiments in a full-scale tunnel

2.2. Methodology

We measured the walking speed under conditions of zero visibility to investigate the fundamental characteristics of traffic flow in tunnel fires. Participant instructions included the following:

For normal walking: 'Please walk in the tunnel as you normally walk.'

The participants walked in 150-m-long lanes marked in several sections with or without obstacles. Three obstacles were installed in the measuring route as diagrammed in Fig. 2. The obstacles were tents in four shapes and were set at random locations to prevent participants from remembering the locations. Before the experiments, participants were told to walk carefully because obstacles would be present.

The walking speed was inferred from the longitudinal and transverse locations of each participant, recorded every 5 s by three research assistants.

2.3. Participants

Forty subjects participated in the experiments (male: 36; female: 4; the average age was 23.5 years). The participants wore a safety vest, dust mask and helmet.

3. RESULTS

Our experiments focused on zero-visibility conditions, and we chose reference data from the literature that was collected under similar conditions. Jin and Yamada [8] took data with irritant smoke in a space, and Frantzich and Nillson [9, 10] measured pedestrians in an environment with an extinction coefficient of 1.5 m^{-1}.

Figures 3 and 4 show the walking speed probability distribution and averaged walking speed, respectively, comparing present data vs. those from Jin and Yamada [8]. The vertical axis in Fig. 3 shows the percentage of the number of participants who walked in the indicated velocity range divided by the total number of participants. Both data sets in these plots were collected without obstacles in the walking path.

Jin and Yamada [8] investigated the effects of visibility by measuring the walking speed of 10 participants in a 20-m-long corridor filled with smoke. The participants were directed to walk along the side of the corridor until they saw an emergency board placed in front of the wall. The smoke was produced by burning wood. These tests were intended for disaster prevention in road tunnel fires in Japan, and the results are widely referenced in the building safety literature. Therefore, this section briefly outlines the experimental conditions in [8] to facilitate comparison with the results of the present study. The ceiling lights were normal lights, and the experiment was repeated during a power failure, with no lights. However, the influence of lighting was negligible in [8] because of the thick smoke; hence, the results are not much different if the lights are on or off, as can be seen in Figs. 3 and 4. In [8], the walking speed through irritant smoke was 1.1 m/s at maximum, 0.4 m/s at minimum and 0.7 m/s on average. If the environment has an extinction coefficient in the range 0.32–0.48 m^{-1}, the minimum walking speed is close to 0.3 m/s in a darkened room [6]. The walking speed in [8] is slow because the participants had to stop when they saw an emergency notice board. In the present study, participants walked at a maximum speed of 1.2 m/s, a minimum of 0.3 m/s and a mean of 0.7 m/s, which is close to Jin and Yamada's results in [8]. In the situation without obstacles in our experiments, we consider that the pedestrians walked along the tunnel wall slowly because the tunnel space was rather simple. The minimum walking speed we measured, 0.3 m/s, matches Togawa's report [3], but the mean walking speed we measured was 0.7 m/s, which is larger than Togawa's measurement [3].

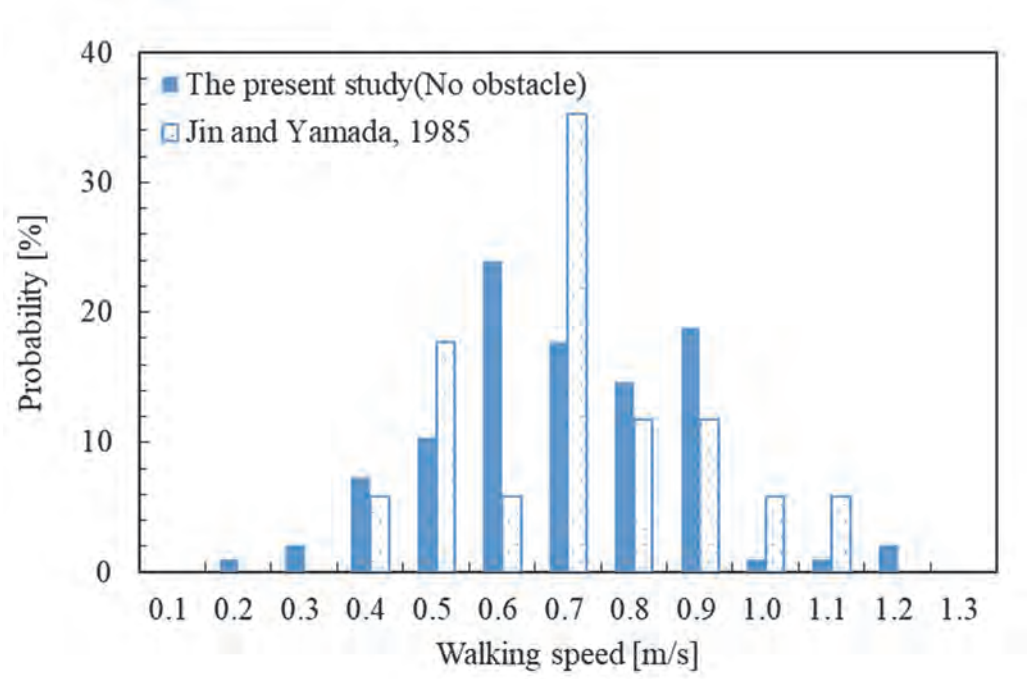

Figure 3: Walking speed probability distribution (present study vs. that of Jin and Yamada [8])

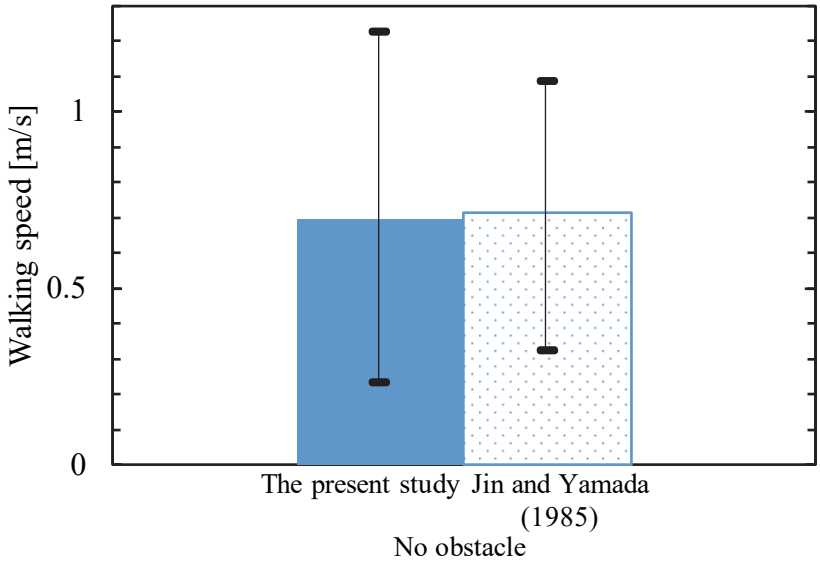

Figure 4: Average walking speed (present study vs. that of Jin and Yamada [8])

Next, we compared our data with the results of Frantzich and Nillson [9, 10]. They conducted the experiments in dense smoke (extinction coefficient: over 1.9 m^{-1}). In [9, 10], the walking speed was measured in a 37-m-long tunnel filled with artificial smoke of glycerol (irritant) and acetic acid (non-irritant), with obstacles of real vehicles placed in the tunnel.

Figures 5 and 6 show the walking speed probability distribution and average walking speed, respectively, for our data and the data from [9, 10]. The vertical axis in Fig. 5 shows the percentage of participants who walked in the indicated range, as in Fig. 3. Both data sets were measured from an obstructed pathway.

Frantzich and Nillson [9, 10] reported that the walking speeds through irritant smoke with lights on are 0.8 m/s at maximum, 0.2 m/s at minimum and 0.5 m/s on average for smoke with extinction coefficients ranging from 1.9 to 7.4 m^{-1}. This minimum walking speed is slower than that measured in [6], even with lights on. With the lights off, Frantzich and Nillson [9, 10] found that the walking speed through irritant smoke was 0.7 m/s at maximum, 0.3 m/s at minimum and 0.5 m/s on average for smoke with extinction coefficients ranging from 2.6 to 4.9 m^{-1}. The present results (maximum 0.9 m/s, minimum 0.1 m/s and mean 0.5 m/s) are close to Frantzich and Nillson's results. We consider that the walking speeds were slower in our experiment when obstacles were present because pedestrians followed the wall and stayed close to the edges of obstacles, thus increasing the total length of their evacuation. The average speed was less than 1.0 m/s, which is slower than the standard value used for disaster planning. The minimum value was also lower than that which Togawa [6] reported, at 0.1 m/s.

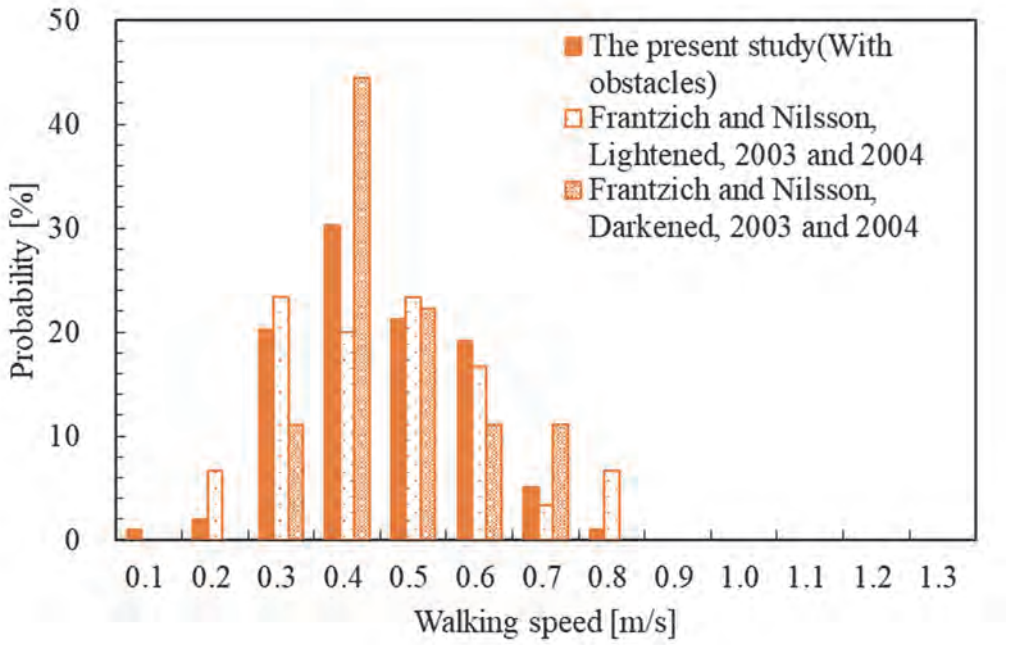

Figure 5: Walking speed probability distribution
(present study vs. that of Frantzich and Nillson [9, 10])

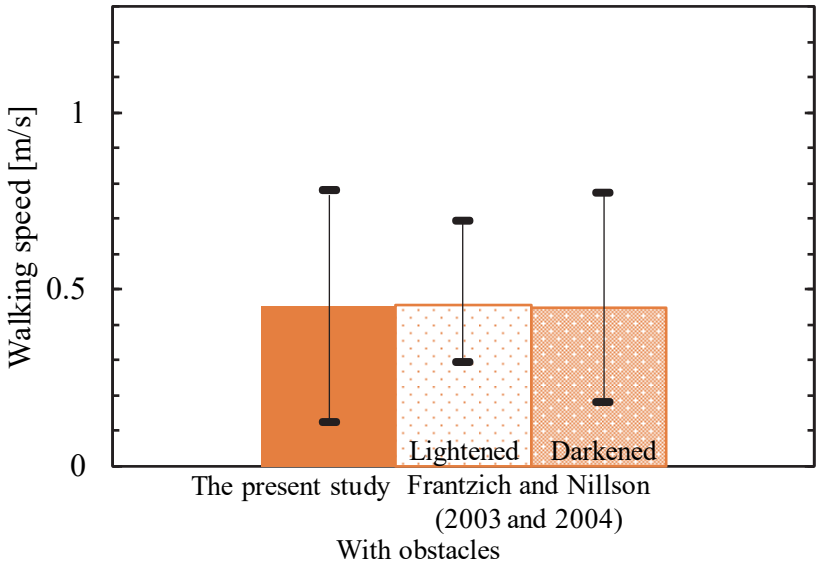

Figure 6: Average walking speed (present study vs. that of Frantzich and Nillson [9, 10])

4. CONCLUSIONS

We measured the walking speed in a darkened full-scale tunnel to investigate the fundamental diagram for evacuating pedestrian traffic in tunnel fires.

We found that the participants' walking speed was approximately normally distributed in the range from 0.2 to 0.8 m/s with an average value of 0.5 m/s when walking in a lane with obstacles. The walking speed in a lane without obstacles ranged between 0.6 and 1.2 m/s with an average value of 0.7 m/s.

5. ACKNOWLEDGEMENT

This work was supported by JSPS KAKENHI Grant Number JP16H03122. We would like to thank the Fukui Prefectural Civil Engineering Office for their help in using the ex-Tonokuchi tunnel.

REFERENCES

[1] Seike, M., Kawabata, N., and Hasegawa, M., Experiments of Evacuation Speed in Tunnel Filled Smoke, Tunnelling and Underground Space Technology Vol. 53, 2016, pp. 61-67. http://doi.org/10.1016/j.tust.2016.01.003

[2] Seike, M., Kawabata, N., Hasegawa, M., and Lu, Y. C., Evacuation speed distribution in smoke filled full-scale tunnel experiments, 8th International Conference Tunnel Safety and Ventilation - New Developments in Tunnel Safety -, Graz, 2016, pp. 189-195.

[3] Seike, M., Kawabata, N., and Hasegawa, M., Evacuation speed in full-scale darkened tu nnel filled with smoke, Fire Safety Journal, Vol. 91, 2017, pp. 901-907. http://10.1016/j. firesaf.2017.04.034

[4] Yamashita, N., Kobayashi, T., Nakano, H., Seike, M., Kawabata, N., and Hasegawa, M. Experimental investigation for evacuation speed curve in smoke filled tunnel, 8th Japan/Korea/Taiwan Joint Seminar for Tunnel Fire Safety and Management, 2017, pp. 405-407, Kanazawa, Japan.

[5] Seike, M., Kawabata, N., and Hasegawa, M., Quantitative Assessment Method for Road Tunnel Fire Safety -Development of an evacuation simulation method using CFD-deriv ed smoke behavior-, Safety Science, Vol. 94, 2017, pp. 116-127. http://doi.org/10.1016/j .ssci.2017.01.005

[6] Togawa, K., and Watanabe, H., Safety Plan I, Viewpoint of safety plan, Committee of planning and design, architectural institute of Japan, 1981, p. 26 (in Japanese).

[7] Tokachi Mainichi Newspaper, Inc., May 29th 2011 (in Japanese).

[8] Jin, T., and Yamada, T., Irritating Effects of Fire Smoke on Visibility, Fire Science & Technology, 5:1, 1985, pp. 79-89.

[9] Frantzich, H. and Nilsson, D., Utrymninggenomtätrök: beteendeochförflyttning [Evacuation in Dense Smoke: Behaviour and Movement], Department of Fire Safety Engineering and Systems Safety, Lund University, Report 3126, 2003, p. 75.

[10] Frantzich, H. and Nilsson, D., Evacuation Experiments in a Smoke Filled Tunnel, Proceedings of the 3rd International Symposium on Human Behaviour in Fire, Interscience Communications Ltd., London, 2004, pp. 229-238.

DISCUSSING THE INFLUENCE OF CONGESTION ON TUNNEL SAFETY – USING THE EXAMPLE OF THE WATERVIEW TUNNEL IN AUCKLAND, NZL

[1]Bernhard Kohl, [2]Sumi Eratne,
[1]ILF Consulting Engineers Austria GmbH, Austria
[2]New Zealand Transport Agency, New Zealand

ABSTRACT

Persistent traffic congestion is expected with high probability in unidirectional road tunnels in urban expressways around the world. The new Waterview Tunnel in Auckland (NZL) is a typical representative of this type of tunnel. Located in a crucial section of the Auckland motorway system, this new tunnel is expected to be used to capacity from the very beginning of its operation, including congestion in the tunnel in peak hours. Minimising congestion inside the tunnel by traffic management measures on the adjacent network may not provide the optimal network solution. Therefore acceptability of various levels of congestion was investigated in a risk assessment study, applying the Austrian tunnel risk model TuRisMo 2. The paper presents a general discussion of the effects of congestion on fire risk and collision risk in unidirectional tunnels with longitudinal ventilation. Taking the example of the Waterview Tunnel, these effects are quantified and the specific results are discussed, intending to deduce relevant findings for similar tunnels.

Keywords: Risk assessment, congestion, fire risk, collision risk, unidirectional tunnels, longitudinal ventilation

1. INTRODUCTION

There is a common understanding that congestion in a unidirectional tunnel with longitudinal ventilation is a relevant risk factor, which requires special attention and specific risk mitigation measures. The common approach to avoid or minimize congestion inside the tunnel, is to restrict the access to the tunnel by adequate traffic management measures. For tunnels located in rural parts of the road network this approach is normally applicable without major implications. But in urban areas, on trunk roads with very high traffic loads, which are closely connected to the urban road network, this approach may not be applicable, because it could compromise the traffic flow in the adjacent network.

The new Waterview Tunnel in Auckland (NZL) is a typical representative of this type of tunnel. Located in a crucial section of the Auckland motorway system this new tunnel is expected to be used to capacity from the very beginning of its operation, including some congestion in the tunnel in peak hours. Minimising congestion inside the tunnel by traffic management measures on the adjacent network may not provide the optimal network solution due to negative effects on the rest of the network. Hence alternative options were investigated including balancing a higher level of congestion in the tunnel with optimized traffic operations over the whole network. As the Waterview Tunnel is representative of urban tunnels with high traffic loads, this topic is relevant to a large number of existing tunnels as well as to future tunnels.

2. THE EFFECTS OF CONGESTION ON TUNNEL USER RISK

Typically the type of tunnels addressed in this paper is characterized by two separate tubes with two or more driving lanes each and longitudinal ventilation. Most studies investigating the effects of congestion on tunnel user risk focus on the perspective of fire safety. Whereas under normal traffic conditions, vehicles in front of a vehicle on fire are able to leave the tunnel without being affected by smoke, in a congestion, when cars are also queuing downstream of the fire, there is no option for smoke management that will completely avoid endangering some people [1].

However, a broader view reveals that collision risk may be influenced by congestion as well. Congestion typically is characterized by a sudden drop of driving speed at the beginning, followed by a phase of low driving speed (slowly moving or stop and go traffic). This effect can be well illustrated by the predicted speed profiles for various traffic scenarios of the Waterview Tunnel (Figure 1).

Whereas the first effect increases the likelihood of front-end-collisions, the second phase of a congestion is less critical: there might be collisions, but as a consequence of the low driving speed most probably without casualties.

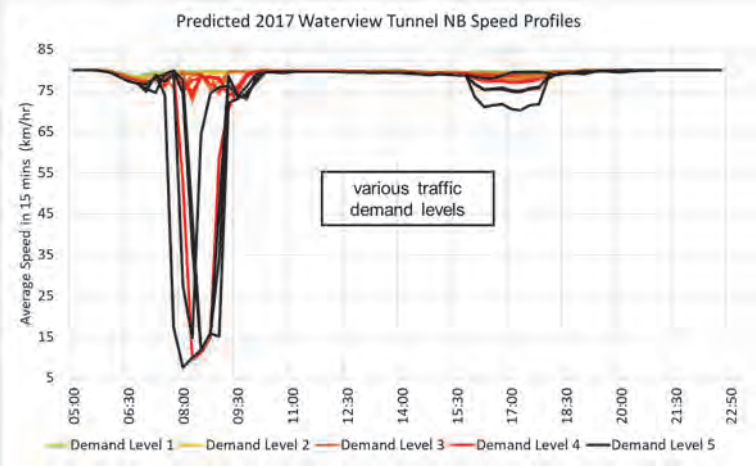

Figure 1: Waterview Tunnel – northbound tube – predicted speed profiles for various traffic scenarios

Consequently in the low speed phases, the collision risk will be lower than in normal operation. Hence it can be concluded that congestion may have negative as well as positive aspects on collision risk and the critical phase is the beginning of congestion (the back of the developing queue of traffic).

3. THE WATERVIEW TUNNEL

3.1. The Waterview Tunnel project

The Waterview Connection Project is a 4.5 km in length and includes 2.5 km of twin three lane motorway tunnels constructed using a TBM. The tunnels pass under a built up residential area and a major local arterial carrying over 50,000vpd before surfacing and connecting into a full motorway to motorway interchange linking SH20 to SH16. The location plan is shown in Figure 2.

The tunnels consist of three 3.5 m lanes and a 200 mm offset to barriers to give a 10.9 m roadway width. The posted vertical clearance is 4.6 m, with 4.9 m clearance provided. The internal tunnel diameter is 13.1 m and the excavation diameter is 14.46 m. The driven tunnel lengths for southbound tunnel northbound tunnel are 2398 m and 2410 m respectively. The maximum longitudinal tunnel gradient is 5 per cent and the minimum horizontal tunnel radius is 1500 m. Minimum cover at the portals is about 10 m and maximum cover is about 50 m above tunnel crown.

A service culvert is located underneath the roadway, formed by 3.7 m wide, 2.2 m high and 2 m long precast culvert units. This culvert is backfilled to a height of about 3.6 m above invert to generate the width required for the three traffic lanes.

16 mined cross passages are located within the driven tunnel alignment and two cross passages are located within the ventilation buildings at either the portals. Total length of driven cross passages is about 186 m with the average length for each cross passage about 11.6 m. The

longitudinal spacing between each cross passage is about 150 m. The cross passage located at the lowest tunnel point also contains the low point dewatering sump.

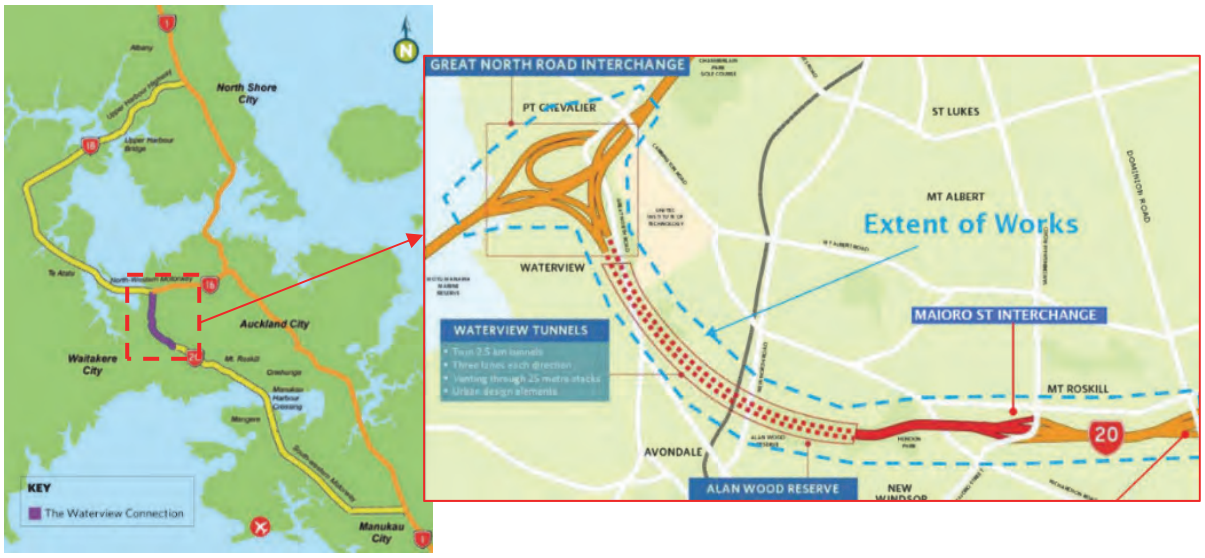

Figure 2: Waterview Tunnel – Location Plan

3.2. Waterview Tunnel characteristics

3.2.1. Structural elements and tunnel safety equipment

The most important tunnel characteristics with respect to safety are compiled in the subsequent tables and figures. In summary, it can be concluded that the tunnel has a very high safety standard.

Table 1: structural elements

Parameter	Waterview Tunnel
Tunnel system	2 tubes, unidirectional traffic
Tunnel length	northbound 2,500 m / southbound 2,590 m
Longitudinal slope	see Figure 3
Number of traffic lanes	3 traffic lanes; lane width 3,5 m; 0,2 m offset to crash barrier profile fixed at tunnel wall; no emergency lane or walkway
Cross section characteristics	bored tunnel profile – details see 3.1
Emergency exits (cross passages to second tube)	maximum distance 150 m
Traffic discontinuities inside or next to the tunnel (ramps, merging zones)	ramps close to northern portal

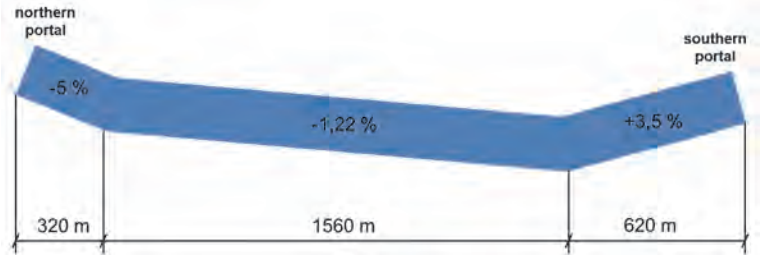

Figure 3: Schematic representation of longitudinal slopes in the tunnel

Table 2: Tunnel safety equipment

Type of element	Waterview Tunnel
Tunnel surveillance	Full-time tunnel supervision via tunnel control centre
Detection systems	Automatic incident detection system (CCTV), linear heat detection cable
Tunnel closure	Lane closure system using variable message signs (VMS), traffic signal at tunnel portal
Evacuation	Egress signage, emergency lighting, public address system, radio broadcast and visual information panels for occupant information, optical and acoustical marking of egress doors
Traffic signage	Variable message signs (VMS) at the entrance portal and inside tunnel,
FFFS	Deluge system with a water discharge rate of 10 mm/min
Tunnel ventilation	Longitudinal ventilation system with jet fans; exhaust through ventilation building on both exit portals (for normal operations – to avoid emissions at tunnel portals)

3.2.2. Operational strategies and procedures

To provide a safe operation of the tunnel, numerous operational strategies and emergency procedures are in place. The subsequent information refers to the information which was taken as basis for the risk assessment study.

Detection of an incident: Tunnel incidents are detected by the automatic video detection system installed in the tunnel. Typically a fire is also linked to irregularities in traffic flow (stopped or slowly moving vehicle, collision); the operator detects the fire when watching the image of such an incident depicted on the video screen and triggers a fire alarm. Alternatively/additionally a fire can be detected by the automatic fire detection device (linear heat detector) as soon as it has developed to a size which is able to trigger an alarm.

Congestion: If the average speed goes below 20 km/h, an automatic alarm is triggered to inform the operator.

Breakdown of vehicle/collision: Closure of affected lane throughout the whole tunnel; if the middle lane is affected – closure of 2 lanes; signaling of a speed limit of 50 km/h in access to the tunnel; immediate intervention by incident response crew, based outside both tunnel portals.

Fire: As soon as a fire is confirmed, an automatic fire response mode will be initiated with respect to the location of the incident detected. The affected tunnel tube is closed and in the neighboring tube the traffic lane adjacent to the cross passage doors is closed as well. If a tunnel evacuation is required, tunnel occupants will be instructed to evacuate the tunnel. In case of a fire, the deluge system installed will be activated without delay, as soon as a fire is declared and the fire location is confirmed.

Fire ventilation: Once a fire is declared, the tunnel ventilation is shut down. As soon as the operator confirms that there are no occupants downstream of the fire location the emergency mode of ventilation is activated and the ventilation is operated with critical velocity (approximately 3 m/s) in driving direction. In congested scenarios, the ventilation system remains off during the evacuation phase.

3.2.3. Traffic characteristics

During peak hours in the morning and in the evening the motorways in and around Auckland as well as the main roads in the city are overloaded and extended congestion occurs frequently. As a consequence, congested traffic is to be expected also for Waterview Tunnel. As for the tunnel, congestion most likely will be caused by the fact that the traffic coming in and going through the tunnel exceeds the capacity of adjacent open sections. In the northbound direction

the SH20 splits up into 2 ramps entering the SH16. Hence, congestion on the SH16 causes vehicles backing back on the ramps and into the tunnel. The southbound direction is less critical. As input to the risk assessment study, traffic data (AADT and traffic distribution over time) was provided for different traffic scenarios. The focus was on high traffic scenarios (highest share of congestion) with an AADT of 43,722 vehicles/day northbound and 36,943 vehicles/day southbound.
The maximum traffic speed in the tunnel of both cars and HGV is 80 km/h in free flow traffic.

4. RISK ASSESSMENT STUDY

4.1. Objectives of risk assessment study

During the design phase of Waterview Tunnel, a first risk study was elaborated, justifying and specifying in detail the safety-relevant tunnel configuration and equipment (including operational aspects). This study indicated that the risk level was ALARP (hence acceptable) – i.e. the residual risk was assessed as being "as low as reasonably practicable" taking cost-benefit considerations into account. This outcome was based on the assumption, that congestion in the tunnel can be minimized and that it would be possible to avoid frequency of congestion higher than 1% by traffic management measures.

This was taken as a reference situation for the new risk assessment study, which was pursuing the subsequent objectives:

- analyse the influence of a level of congestion higher than 1% of the time on the personal risk of tunnel users, applying a system-based quantitative risk model [2] [3] [4];
- as reference case, the risk level of the tunnel according to the initial design and assuming a congestion level of 1% shall be taken – representing the situation which initially was assessed as "ALARP";
- evaluate the differences in risk comparing the situation with increasing level of congestion (up to 8%) to the reference case;
- identify and assess additional risk mitigation measures – as far as required.

4.2. Approach

For the quantitative risk assessment study the Austrian Tunnel Risk Model TuRisMo is applied. The Austrian Tunnel Risk Model (TuRisMo) is defined in the Austrian tunnelling guideline RVS 09.03.11 [4] and fulfils the requirements of EC Directive 2004/54/EC on minimum safety requirements for tunnels on the trans-European road network.

This methodology uses a fully integrated approach that allows for the detailed analysis of many kinds of safety measures and for interactions between different safety measures. Factors such as the installed equipment and boundary conditions such as traffic conditions are taken into account rigorously. The method combines a quantitative frequency analysis based on statistical evaluations and a quantitative consequence analysis that includes (i) a (mechanical) collision-only part, and (ii) a distinct fire consequence model. Figure 4 shows a schematic representation of the overall structure of the method. Details of the various sub-models of the overall method have been given elsewhere [4], [5] and [6] and are not reproduced herein.

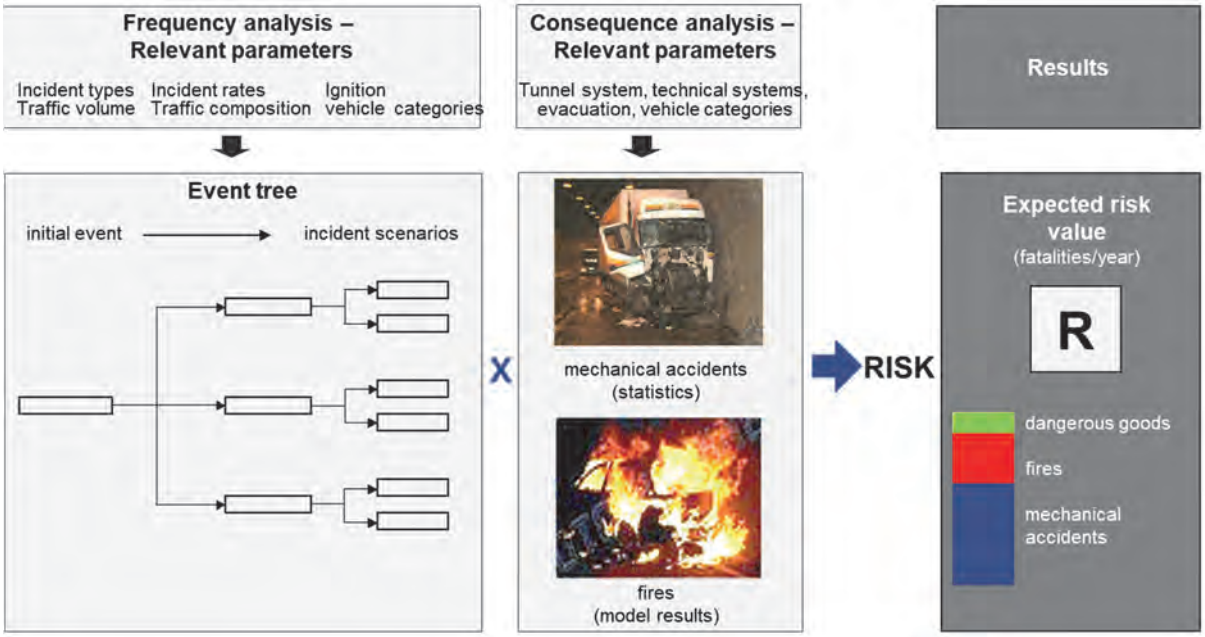

Figure 4: Schematic representation of the TuRisMo methodology

The risk model includes two different scenarios of congestion:

- **Congestion as a consequence of a preceding incident** (vehicle breakdown or collision): this scenario represents the initial phase of a congestion period (when the queue is building up), a situation which may induce "secondary" incidents (secondary collisions and fires)
- **Congestion due to traffic overload:** this scenario represents a standing / slow moving queue which is caused by traffic bottlenecks inside or outside the tunnel. In this scenario, the speed is so slow that collisions will most probably only cause material damage, but no casualties.

Similar to a congestion following an incident, a congestion which is caused by traffic bottlenecks is also characterized by a sudden drop of driving speed at its beginning (as can be seen in the chart in Figure 1). Hence, the initial phase of such congestion may induce secondary collisions quite similar to the congestion scenario caused by preceding incidents.

With respect to traffic flow conditions, the risk model includes 3 different fire events:

- **Primary fire scenario:** During normal traffic flow, a vehicle has a collision or a break-down and catches fire.
- **Secondary fire scenario:** An incident causes a traffic jam. A vehicle hits the rear end of the queue and catches fire.
- **Tertiary fire scenario:** A vehicle in a standing / slow moving queue catches fire

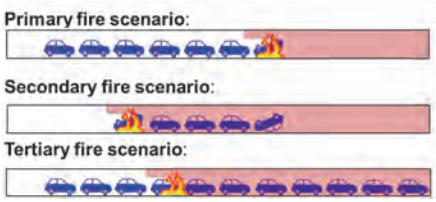

Figure 5: Types of fire events

The risk assessment study investigated:

- how these 3 fire events influence fire risk, and
- the influence of the level of congestion on the risk shares related to these 3 different fire events.

4.3. Discussion of Results

4.3.1. Collision risk

Figure 6 illustrates the results of the quantitative risk analysis of the Waterview Tunnel showing the expected risk values and the respective risk shares (collision, fire) for the northbound tunnel tube. Additionally, the risk for different congestion levels is shown:

- no congestion: no traffic congestion in the tunnel (0%) and no additional secondary collisions at the tail of a traffic jam (theoretical case to show the influence of congestion)
- 1-8% of congestion: different amount of hours with congested traffic (88-701h per year), including the influence of secondary collisions at the tail of a traffic jam in the tunnel

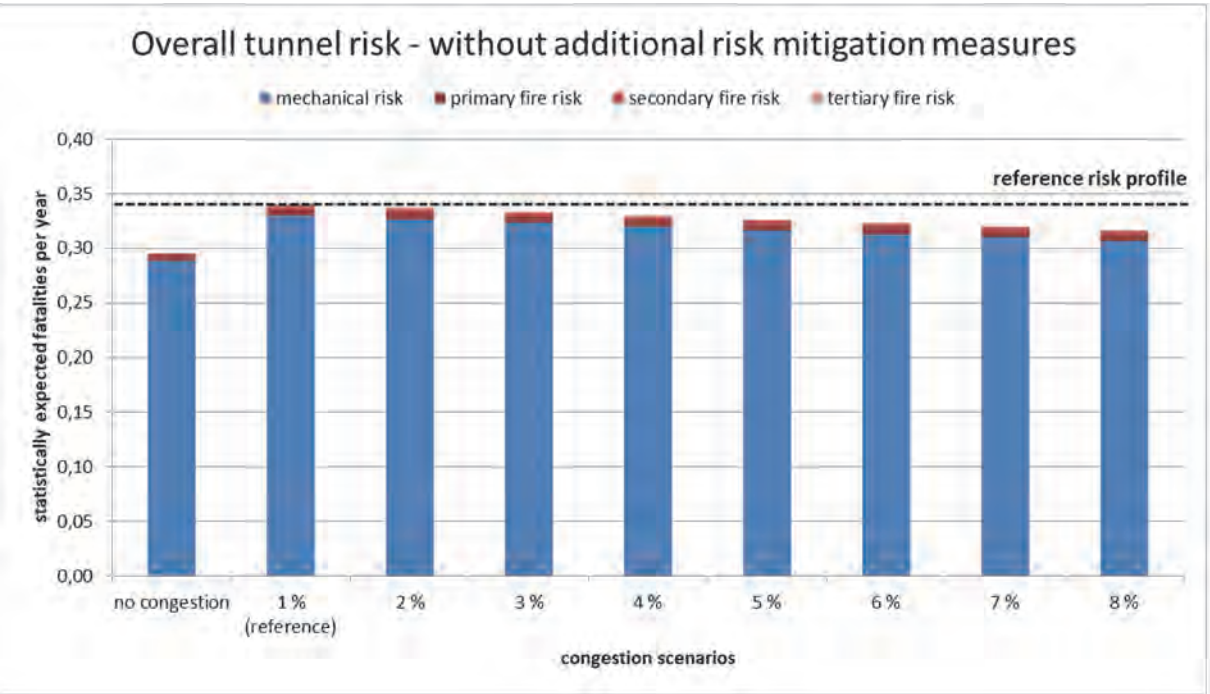

Figure 6: Collision and fire risk in northbound tunnel tube for different frequencies of congestion – expected risk value, without additional measures

These results can be explained as follows:

- The collision risk dominates the overall risk and thus as well the differences in overall risk due to the influence of congestion.
- There is a significant increase in collision risk from "no congestion" to "regular congestion" 1% of the time. This increase in risk is due to secondary incidents which may be caused in the initial phase of a congestion, caused by the sudden drop in velocity as shown in Figure 1.
- As can be seen in the speed profiles as well, this drop in velocity happens just once at the beginning of congestion, independent of how long it persists. For this reason a further increasing level of congestion reduces collision risk, because collisions in a slowly moving queue are extremely unlikely to cause casualties.
- The fire risk is very low – which can be explained by the low likelihood of fire incidents in general, the limited consequences of fires due to the good egress conditions and the effects of FFFS; hence the differences in fire risk due to the influence of congestion are low as well.
- The fire risk increases slightly with longer-lasting congested scenarios, but the influence is negligible in comparison to collision risk.

4.3.2. Fire risk

In Figure 7 the effect of different congestion levels on the overall fire risk is shown for the northbound tube (the fire risk shown in these figures corresponds to the respective values in Figure 6).

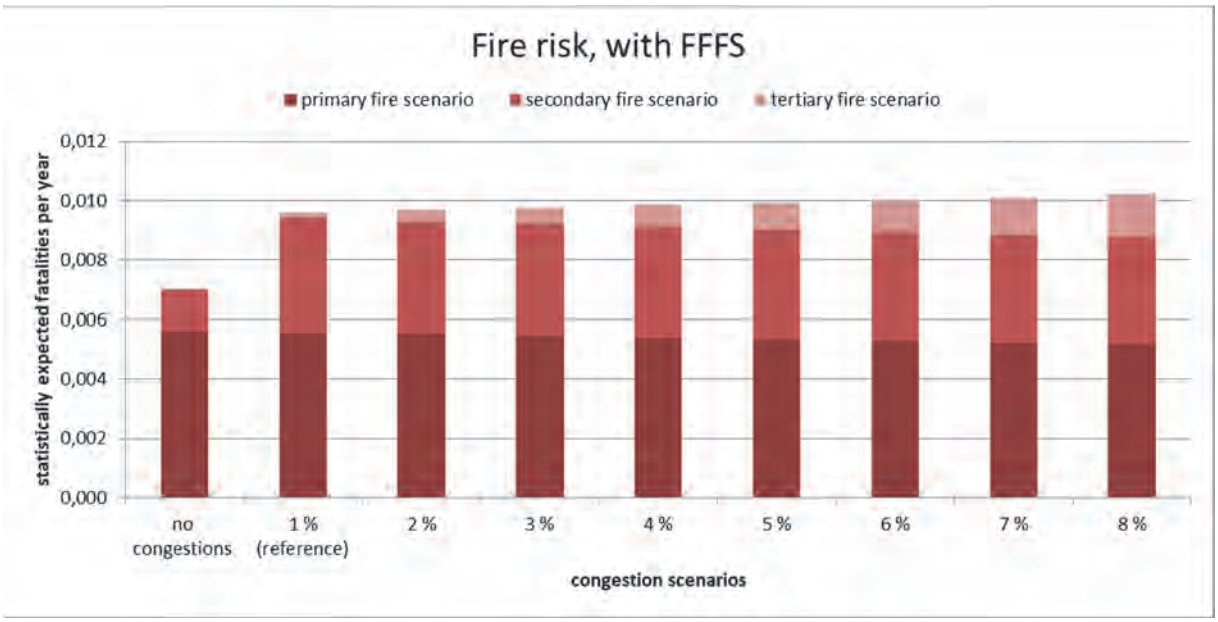

Figure 7: Share of different fire scenarios in fire risk, without additional measures – northbound tunnel tube

These results can be explained as follows:

- The results for the primary fire scenario represent the fire risk related to a normal traffic situation (without congestion). It corresponds to appr. 50% of the overall fire risk in the cases with congested traffic. The primary fire risk is mainly due to persons who do not behave as advised (they stay where they are instead of evacuating).
- This risk share of the primary fire scenarios is slightly reduced with an increasing level of congestion – for the same reasons as explained for the collision risk.
- The secondary fire risk shows a sharp increase between a situation without congestion in comparison to 1% regular congestion; this is due to the increase in secondary collisions caused by the beginning of congestions, as explained for the collision risk.
- The tertiary fire risk is the part of fire risk which is increased steadily by an increasing level of congestion; but even in the case with 8% congestion the share in total fire risk is lower than the share of the other fire scenarios.
- Compared to the other types of fires the primary fire event has a much higher frequency but much lower consequences – whereas the secondary and tertiary fire risk are typically caused by incidents with very low frequency and high potential consequences.

4.3.3. Risk mitigation measures

Based on the results, no further risk mitigation measures would be required to reach a safety level equal to or below the reference risk profile. Nevertheless it was decided to implement the subsequent traffic management measure as additional risk mitigation measure for congestions:

- Pre-warning on congestion inside the tunnel by variable message signs on the tunnel approach routes

The congestion warning will be shown on the motorway sections upstream of the tunnel and it will be combined with a speed reduction to 50 km/h. It is assumed that the pre-warning system will increase the awareness of motorists with respect to the slow moving queue and the reduced

velocity will reduce the consequences of a potential collision. It was demonstrated in the risk study that by implementing this measure a reduction in collision risk by 7% can be achieved.

5. CONCLUSIONS

When discussing general conclusions on the basis of the results of one specific risk study for an individual tunnel, due care needs to be taken. The results of the risk assessment study for Waterview Tunnel seem to support the idea, that in unidirectional tunnels with longitudinal ventilation and a high traffic load, overall risk may be reduced by increasing congestion; this seems to be in contradiction to the common assumption that congestion increases risk. Discussed more specifically, the results may give rise to the subsequent considerations:

- The idea that fire is risk is increased by congestion in an unidirectional, longitudinally ventilated tunnel is not questioned by the results of the study
- However, it could be demonstrated that a high standard of fire safety (FFFS and good egress conditions) is able to minimize this effect
- A longer duration of a phase with congested traffic reduces collision risk
- However, the initial phase of congestion requires specific attention; adequate traffic management measures like congestion warning (combined with speed limits) seem to be suitable measures to mitigate negative effects inside the tunnel

Taking these results into account it seems to be possible to accept a higher level of congestion in such a tunnel, if adequate measures are in place. However, in any case, such a decision should be based on a detailed, risk based investigation, taking all relevant risk factors into account.

6. REFERENCES - EXAMPLE

[1] B. Kohl, O. Senekowitsch, I. Nakahori, T. Sakaguchi, A.E. Vardy (2017). *Risk assessment of fire emergency ventilation strategies during traffic congestion in unidirectional tunnels with longitudinal ventilation* (proceedings of ISAVFT 2017). BHR, Lyon, France.

[2] PIARC, *"Risk Analysis for Road Tunnels"*, 2008 R02, 2008.

[3] PIARC, Technical Committee C.4 – Road tunnel Operation, *"Current Practice for Risk Evaluation for Road Tunnels"* Rep. No. 2012R23.

[4] FSV (Austria Society for Research on Road, Rail and Transport), *„Guideline RVS 09.03.11 Methodology of Tunnel Risk Analysis"*, Vienna, 2015.

[5] Nakahori I, Sakaguchi T, Kohl B, Forster C and Vardy AE, *„Risk assessment of zero-flow ventilation strategy for fires in bidirectional tunnel with longitudinal venitlation"*, 16th ISAVFT, BHR Group, Seattle, 2015.

[6] Forster C, Kohl B and Wiesholzer S, *„Methodologies for accurate risk modeling in the context of integrated quantitative risk analysis"*, 16th ISAVFT, BHR Group, Seattle, 2015.

UPGRADING OF ROAD TUNNELS DURING NORMAL OPERATION

Anne Reinisch BSc MSc, Dipl.-Ing. (FH) Andreas Jörg,
Dipl.-HTL-Ing. Mag. (FH) Alexander Wierer;
ASFINAG BMG, Austria

ABSTRACT

The aim of this work is to show the complexity of requirements, which can influence an upgrading project of road tunnels. To fulfill the actual standards and laws for road tunnels, processes for the release are given. So the influences of any work on the systems integrated into a tunnel or any construction work can implicate other conditions, which need to be evaluated from a completely different point of view.

It will be shown, that this complexity can be worked through when the project influencing conditions are considered preliminary to the project setup. With the analysis, the different foci for each project can be prioritized.

Keywords: road tunnels, upgrading projects, ASFiNAG, STSG

1. INTRODUCTION

Tourism, transit, and business are only a few reasons for the increased traffic volume of the last 20 years. For adaption and upgrading works in road tunnels, this implies a rethinking of the strategies managing the traffic stream during the construction works. The aim is always, that tunnel users (customers) reach their destination safely, comfortably and without interferences.

In Austria, the ASFiNAG is responsible to operate the highways and motorways. In the network of about 2.223km, 166 tunnel with an overall length of about 401km (Data: March 2018) convey special challenges to the traffic management system during upgrading projects of these tunnels. One vision of the ASFiNAG is the highest possible availability of the network for the customers. Especially the alpine topology, the seasonal weather and high traffic volumes are challenging this aim during construction works.

In the preliminary considerations of an upgrading project of road tunnels boundary conditions and requirements influencing the following set up for the project. The complexity of these conditions and their dependencies of each other will be discussed in section 2. As every tunnel is unique and so the upgrading project, the used measures will be discussed further on certain examples in section 3. In section 4, a summary of the conclusions for future projects will be further examined.

2. PRELIMINARY CONSIDERATIONS ON TUNNEL UPGRADING PROJECTS

During the planning period and before starting any construction works in the tunnel, some preliminary considerations about the influencing conditions need to be made. This should be done from the customer and traffic manager point of view (stakeholder specific) as well as from the project process point of view. In the following, these requirements and boundary conditions are discussed in detail.

2.1. Traffic and customer specific boundary conditions and requirements

Before starting an upgrading project of a tunnel, the tunnel will be analyzed in detail. This means its location, the existing facilities, the traffic volume and the resulting risks have to be contemplated.

When thinking about the general set-up during the upgrading period of a tunnel, traffic flow statistics will help to set the arrangements and timetables. It is crucial to know the traffic volume and its distribution in time. Including this knowledge into the considerations for the traffic arrangements, like the lane management, leads to more satisfied customers, safe construction zones and optimized schedules for traffic guidance.

The existing facilities influence security and possibilities for traffic guidance. Ventilation, lighting, tunnel control and the equipment in terms of traffic are just some points which are inducing the project setup. So it might be possible, that bidirectional traffic is not possible due to non-conform set up of the ventilation system.

As Austria is a country with a lot of tourism in summer and winter, the aim is always to keep the traffic on the highways and motorways, because closing sections of the route will always lead to complications, especially in urban areas. With the alpine topology, as already mentioned in the introduction, alternative routes can bring special challenges like seasonal weather and the course of the road. Especially for tourists without knowledge of local conditions this leads to a higher risk of accidents and to get lost on the way. In winter the tourism in some regions needs special considerations for the traffic guidance. These points should be taken into account in the traffic management as well. Having construction zones during holidays in the country or neighbor countries can implicate traffic jams due to the high traffic volume on the streets.

Considerations about traffic guidance mainly arise from the circumstances of the traffic volume and the location. When having a tunnel next to a city, rush hours become more important for the schedule of the construction and so the traffic guidance. In regions with less traffic, but next to a village or small town, night operations of the construction work can result in discontented residents due to the construction traffic.

Risk analyses are a very important tool to evaluate the project set-up planned. Sometime it could be necessary to set risk-reducing actions, like reducing the velocity, setting additional security equipment, like section controls or a fire brigade at the portals and so on. So they support the assessment of the possibilities of the traffic guidance and ensure the highest possible security for the operation of the tunnel, for the tunnel users and the workers. Depending on the project it may be possible, that alternative routes need to be evaluated as well. Later an example will be discussed where these special things had been considered.

So it can be seen, that the boundary conditions and requirements for a project are very complex and so different situations for the traffic guidance, shift models and so on evolve. The conditions looked at are similar for every project, the difference is the weighting. This means it is unfeasible to make a general statement and the evolving solutions on the boundary conditions.

2.2. Project-Process specific boundary conditions and requirements

Besides the already named requirements, process-specific conditions need to be considered as well. Time is the first thing which comes to mind when thinking about a construction. The user needs the improvements as soon as possible, but multifarious projects need more time. The process itself can depend on the necessities of the upgrading scope. If only a few things need to be done, the construction time becomes shorter and the other way around.

Implementing the new equipment, different tests need to be done, controllers have to be implemented, flow measuring devices need to be calibrated, the lighting control needs to be set up and door opening forces need to be measured, to just name some examples. Overall, everything needs to be tested on functionality and conformity to given regulations like the STSG (National Road-Tunnel-Security-Law of Austria), directives for the traffic system (RVS) and Austrian and European Standards.

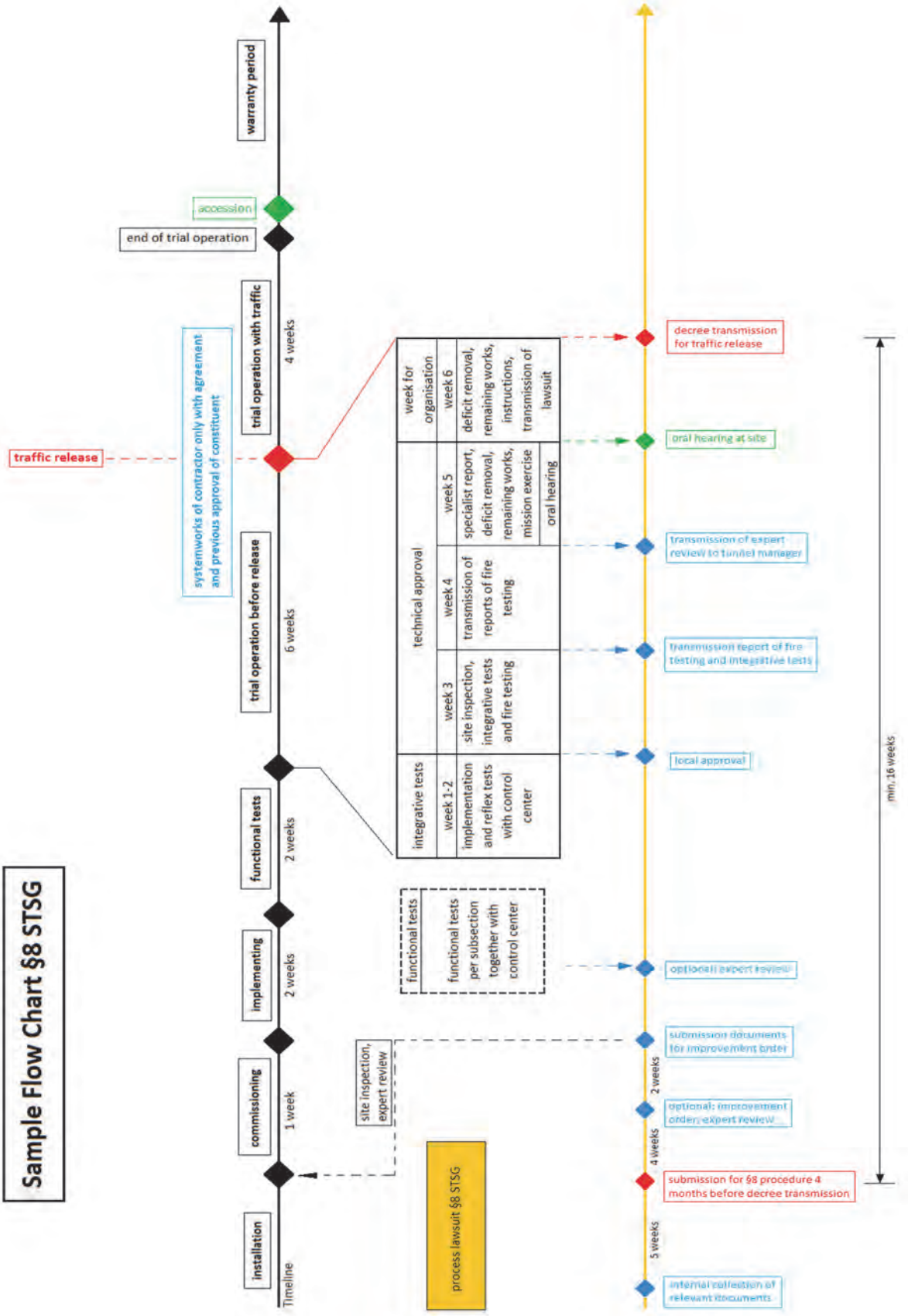

Figure 1: Sample flow chart §8 STSG procedure (translated from BMVIT 2015)

The main tests which need to be done are:

- Data point tests
- Function and reflex tests
- Leakage measurement
- Air flow measurements (ventilation system), adjustment of the control system
- Fire tests.

Before, during and especially in the end of a project the "BMVIT", the federal ministry for transport, innovation, and technology in Austria is involved in the projects and releases the tunnel in the end. This phase is the so-called "commissioning phase". It means, that the administrative procedure has to be considered in the preliminary phase of the project.

In **Figure 1** the §8 STSG commissioning procedure can be seen schematically. The tests which are done after the implementation of the technical and security equipment need to follow certain steps and will be observed by experts to guarantee an impartial inspection and release. The process itself needs at least 16 weeks, to check the documents and the reports out of the tests. In existing tunnels, this additional schedule brings new challenges to the implementation process, because the traffic needs to flow even if the release of the new equipment is not finished already. This means the existing systems need to be kept alive until the release of the new systems is given.

For the phase of implementing and testing, a daily schedule should be made from the contractor already at the beginning of the project, to be able to evaluate it with the different parties (supervisors, testing engineer, and maintainer) involved.

3. CHALLENGES ON CERTAIN EXAMPLES

In **section 2** certain requirements, boundary conditions, and preliminary considerations for upgrading projects with influence on the traffic had been discussed. In this section, certain examples should give an overview of different approaches to implement the considerations in the project setup.

High influence on the chosen model for the traffic guidance evolves from the availability and utilization of the local street network and the tunnel itself. For example, approaches can be whole stops during the night in one tube, blocked single lanes and/or reduced velocity of the traffic.

If the tunnel only has one tube, it gets more complex and alternative routes have to be evaluated for the time during the stops. This can be done during some months (like in Arlberg-Tunnel), only during the night or just for a few hours with changing the direction of the traffic.

If it is not possible to close one tube and work in the other one, due to nonconformity of one tube for contraflow traffic, this tube has to be upgraded first with an additional operation and security equipment.

The following subsections will explain used strategies in 2 selected tunnels.

3.1. Plabutsch-Tunnel

As bypass to the city of Graz, the Plabutsch-Tunnel was built in the 1980's and the first tube opened in 1987. Due to yearly rising traffic volume, a second tube was built and opened in 2004. Now the Plabutsch-Tunnel is a tunnel with two tubes and two lanes each. It has a length of about 9.8km in the direction of Spielfeld and 9.75km in the direction of Linz.

Today the yearly daily traffic volume of this tunnel is about 40 000 cars, with rising tendencies. Currently, the tunnel is adapted to the actual standards for the conformity by law (STSG).

After evaluating the statistics and risk analyses, a strategy for the traffic management during the construction time had been developed. This allows, to handle the project with respect to the requirement of availability. So one tube of the tunnel is closed during the night for construction works, while the other tube is operated with bidirectional traffic. During the day both tubes will be kept open under normal operating conditions.

Figure 2: Location Plabutsch-Tunnel

The most special thing at the construction site is the very strict obedience of the closing times of the tunnel. In the morning at 5 o'clock the tunnel has to be opened with normal operation (unidirectional traffic), otherwise the rush hour traffic would go through the city and traffic jams will result. This means the construction zones have to be build up every day at 8 pm and closed at 5 am. With an overall construction time until February 2020, this has to be done around 600 times. To ease this procedure, one tube had been closed before starting the construction itself during the nights for about 2 weeks, to be able to install removable traffic guidance systems. Additionally to the traffic guidance systems for bidirectional traffic in one tube of a tunnel, bollards (able to drive over), an entranceway lighting and additional traffic signals had been installed. With this measures, the safety of the drivers during the night had been increased a lot.

In **Figure 3** the traffic guidance of the Plabutsch-Tunnel during the upgrading works can be seen. Due to the location of the exit "Graz Webling", the traffic needs to be guided back to the normal lane directly after the gallery.

Essentially the upgrading of the Plabutsch-Tunnel includes restoration and renewal of the power supply, data network, and control and communication system installations. The video monitoring system is updated and an acoustic detection system will be integrated together with the installation of the security equipment in the 20 new cross ways (17 accessible, 3 traversable).

Upgrading projects in urban regions, like the Plabutsch-Tunnel, implicates special challenges due to the high traffic during rush hours. In this example, new cross ways need to be made. Due to blasting operations during the night, every piece of debris has to be cleaned in the morning to ensure unaffected and secure traffic flows during the day. To finish the work in this kind of projects on point means, sometimes, to use more manpower and machines.

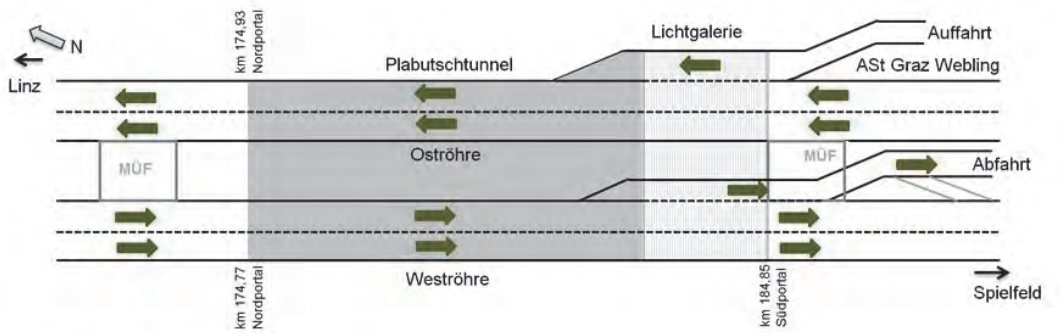

a) traffic guidance during the day

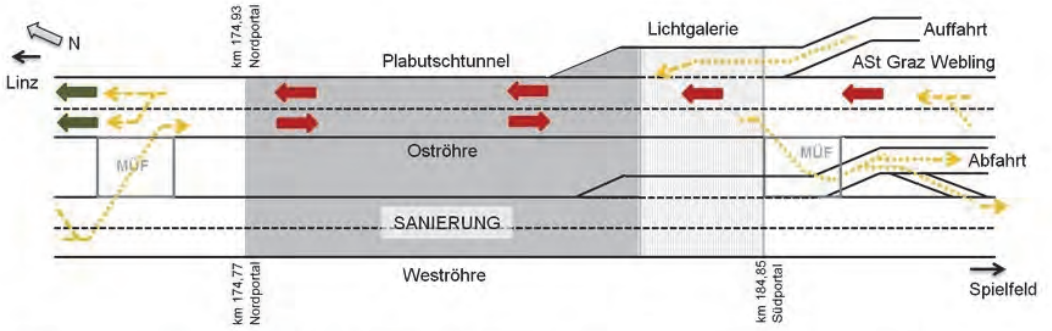

b) traffic guidance during the night (construction phase 1 - stop in the eastern tube, bidirectional traffic in western tube, construction phase 2 - stop in western tube, bidirectional traffic in eastern tube)

Figure 3: Traffic guidance Plabutsch-Tunnel (Reinwald M. 2018)

3.2. Tunnel Dalaas

The 1.8 km long tunnel Dalaas on the S16 Arlberg highway is situated between the interchanges „Wald am Arlberg“ in the east and „Dalaas“ in the west and bypasses the municipal area of Dalaas in the middle of the “Klostertal”-valley. The single-tube tunnel was opened in 1979 and is operated in bidirectional traffic with one lane per driving direction. The average traffic volume is about 13 400 cars per day with a 9.6% share of heavy traffic, with rising tendencies.

In 2017 the tunnel has been refurbished and adapted according to the state of the art and to fulfill the conformity by national law (STSG).

With regard to the operating and safety equipment, the following main measures have been implemented:

- Realization of a new power supply concept
- New tunnel data network and tunnel control system
- Installation of a video and audio monitoring
- Renewal of tunnel ventilation including the emergency exits
- New equipment of the emergency call system

The main measures from a civil engineering point of view had been the construction of two new emergency exits and the constructional fire protection inside the tunnel. In addition, two new buildings for technical equipment had to be built.

The topography of the tunnel in the Valley, with only one alternative route, crossing the village of Dalaas, and the parallel installation of new security and operation equipment, while maintaining the existing systems until the final approval, formed the challenging requirements of this project.

To deal with the boundary of only one low capacity alternative route the construction works were divided into two phases. In the first phase new escape ways and new buildings where constructed. Most of the construction took place during the day without influencing the traffic flow. Although, in order to allow a safe supply of the construction site, the velocity in the tunnel had been reduced to 60 km/h.

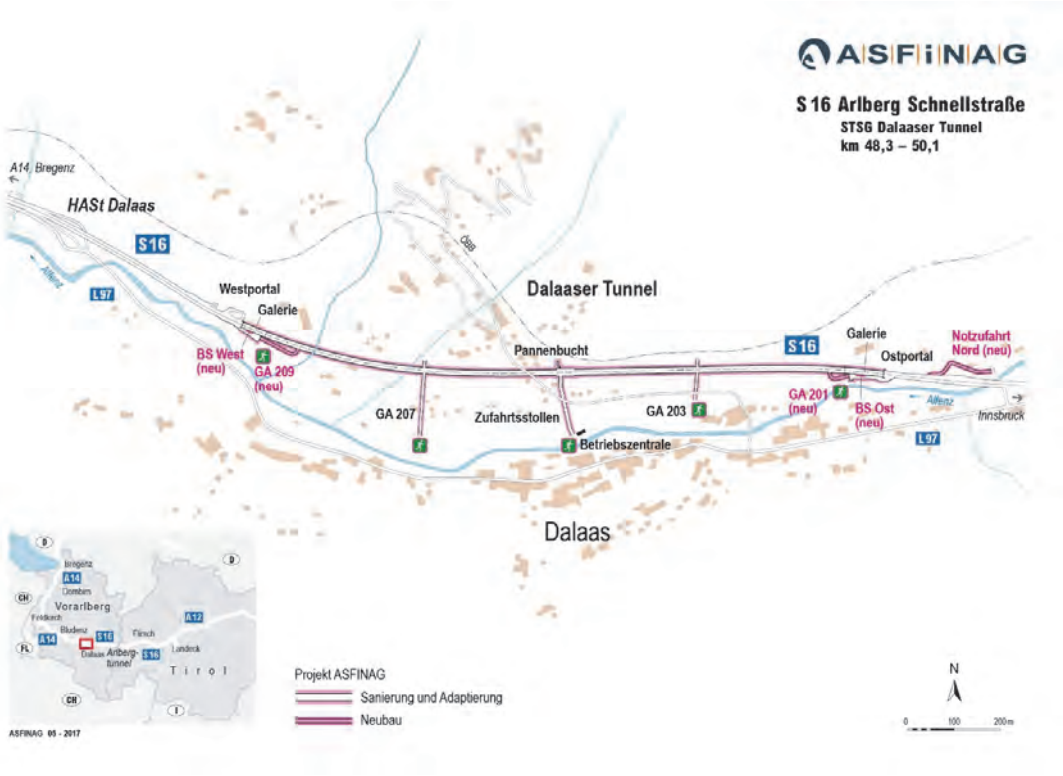

Figure 4: Location tunnel Dalaas with actual (after upgrading) situation of escape ways

In the second construction phase, the tunnel was closed during the night, to do the installation works inside the tube. During the day, the tunnel had been operated with reduced speed. Closing the tunnel had been crucial for executing tasks where the existing safety systems have to be deactivated. In this phase, the power supply system was renewed and the new ventilation system had been installed.

When the tunnel was closed, the traffic stream had to take the only alternative route through the village of Dalaas. Because of the geographical conditions, there are no additional routes possible without extensive detours. Due to these restrictions and based on the known distribution of the traffic volumes, the barriers were set up between 8:00 pm and 6:00 am. The aim was to minimize the additional traffic load on the alternative route and so to reduce the impact on the residents. Unfortunately, the relocation of the work into the night has led to an additional burden on local residents because of the noise from the construction site. Hence, supplementary measures had to be taken in this respect, e.g. temporary noise protection.

The second main requirement when setting up the project was the demand for parallel operation of the existing and the new electromechanical and safety equipment. Only after positive commissioning of the new systems by the tunnel authority the dismounting and removal of the old equipment could start.

This requirement implies parallel installation of cables and constructions, stepwise renewal and replacement of electromechanical equipment and temporary measures. Equipment cannot be placed at the future installation site, as existing electrical distributors were still in operation and occupied the space.

A particular challenge are subsystems, which are not completely renewed. In this project, the existing sensor cable system for fire detection is further used. Throughout the testing phase, the system was adapted to the new requirements (with additional fire zones) each night. During the day, under normal operation, it had to run with the old setup.

The upgrading projects of the Plabutsch-Tunnel and the tunnel Dalaas had similar aims in the first sight, but after analyzing the traffic situation, the location, and the possibilities, different set-ups need to be made.

4. SUMMARY / CONCLUSIONS / LESSONS LEARNED

Until spring 2019 the road tunnel of the highway and motorway traffic system need to be upgraded to conform to the actual STSG and the European Directive 2004/54/EG. To reach this goal, a lot of tunnels needed to be upgraded in parallel. This requires an efficient project management even before the upgrading project is set-up. During the last years, different strategies to evaluate possible risk of a project during the planning period had been improved. So risk analyses had been discussed more and more intensively and the influences not only on the project itself, but the stakeholders around the project had been evaluated too.

As it can be seen from the short summaries of the mentioned projects in ***section 3***, the requirements and boundary conditions are very complex and influence each other. Depending on the location, the scope of the upgrading project and the traffic volume, requirements and boundary conditions need to be weighed.

During the last years, the massive amount of upgrading project necessitated a considerable and comprehensive preliminary consideration. Thus in the future, the perceptions of the past are involved in the set-up of an upgrading project.

5. REFERENCES

ASFiNAG. (2017). internal documents of the projects. Austria.

BMVIT. (2015). Sektion IV Verkehr - Gruppe Straße, Abteilung ST2 Technik und Verkehrssicherheit. *Dienstanweisung zum Verfahrensablauf Tunnelsicherheit*.

Company Homepage ASFiNAG. (2018, 03 20). Retrieved from https://www.asfinag.at/

Reinwald, M. (20. 03 2018). Sanierung und Anpassung an STSG A9-Phyrn Autobahn - Plabutschtunnel. Winidschgarsten: ASFiNAG BMG.

TUNNEL REFURBISHMENT FROM THE PERSPECTIVE OF THE OPERATING CONTROL CENTER

Paul Sattinger
evon, Austria

ABSTRACT

The refurbishment of traffic tunnels presents great challenges on the availability of the affected road section, on the technical equipment providers, and also on those responsible for the operation and monitoring of the tunnel who have to guarantee safe and freely flowing traffic.

As a supplier of traffic control systems for several monitoring stations run by ASFiNAG, regional organizations and international operators, including in Belgium and the United Arab Emirates, we know well which methods and processes have proved themselves allowing us to provide the successive and seamless integration of new system components into the sovereign domain of a traffic management centre.

The goal at the beginning of any refurbishment program is to map the construction phases, which are formulated in civil engineering terms, from a software perspective in order to be able to identify the exact traffic and management phases for the monitoring centre. All required software measures must follow a clear rollout concept when implementing these phases so that all participants from construction, monitoring and operation are involved. However, the rollback concept is even more important than the rollout concept to ensure that a state of safe operation can be switched into should unexpected failures and malfunctions occur. The entire concept for such measures covers an agreed upon procedural model for commissioning, tests, acceptance test, qualification of operating personnel as well as system modifications.

In addition to the provision of new technical functions, modern integration concepts increasingly focus on aspects of cyber security, whose implementation is accompanied by additional time costs and further technical challenges.

Keywords: Control system, traffic control centre, rollout and rollback concepts, parallel operation, cyber security

1. INTRODUCTION

Practically all tunnels in Austria are monitored by a supervisory control centre. Hence any civil works in the tunnel and on its control will have a direct effect on the tunnel control centre and vice versa, a technical change in the tunnel management system can have an effect in the tunnel.

1.1. Reasons For Technical Changes In Tunnel Control Systems

In order to satisfy the demand for high levels of safety, modern tunnel systems have become complex systems and subsequently have an enormous density of electromagnetic actuators and sensors. In ASFiNAG jargon, all these components are grouped into the term Tunnel Operation and Safety Equipment (in German, BuS). The signal from each BuS component is connected to the tunnel control system.

Due to the high density of BuS in modern tunnels, there is in practice no refurbishment measure or other adaptation of the tunnel system that does not also require modifications to be made to the BuS and hence the tunnel control system.

Experience shows that the following situations lead to the necessity of refurbishment measures and changes to the tunnel systems.

- Component ageing
  The lifetime of a tunnel system, from a civil engineering perspective, is very long, yet that of the energy supply is considerably shorter and even more so for actuators and

sensors, which need to be replaced frequently. It is assumed that the server computer on the tunnel control level requires replacement every five years for reasons of IT security, availability of spare parts and manufacturer guarantee.

- Changes to the legal framework
  In Europe and Austria, the current minimum tunnel safety requirements in the trans-European road network must be fulfilled [Directive 2004/54/EC of the European Parliament and of the Council of 29 April 2004]. The road tunnel safety law (in German STSG) in Austria is derived from this and is applicable to all tunnels from 500m in length for motorways and trunk roads.
- New capacity requirements
  Civil engineering measures to increase the vehicle capacity of tunnel systems are very often required in European conurbations, but in Austria, only exist in the form of new systems and not as changes to existing systems.

1.2. Reference Systems

Evon has been installing traffic control centres at home and abroad since 2011. There are special circumstances requiring consideration for every systems, and suitable methods and procedures need to be worked out in partnership with the client in order to tackle the successive and seamless integration of new system components into the sovereign domain of the traffic control centre.

Figure 1: rVMZ Hohenems [2011]

Figure 3: SHEIKH ZAYED TUNNEL Abu Dhabi including control room, United Arab Emirates [2013]

Figure 2: rVMZ Klagenfurt - central control room Carinthia - ZWK [2015]

Figure 4: Tunnel management system Vlaamse tunnels, Belgien [2016]

2. CHALLENGES

When carrying out refurbishment activities, the traffic flow needs to be altered so that civil work, commissioning activities, or tests and acceptance tests, can be carried out in the subsequently traffic-free sections. These various traffic flows, which correspond very closely to the civil works phases, are called traffic phases.

A quality-assured process must be adhered to when integrating new external systems into a traffic control centre (henceforth TCC) that guarantees correct operation of the tunnel from the TCC. Before any integration work can commence, the new tunnel system components must be modelled in the TCC software control system and the configuration of the tunnel interfaces (IEC60870-5-104 or OPC UA) need to be prepared. Subsequently, this software model must be subjected to an individual signal test together with the central tunnel software. The successfully tested software is then migrated to a TCC integration system to enable functional testing of the combination tunnel – traffic control centre. The new software can only be switched into testing and live operation in the TCC once the functional tests have been successfully completed, thus establishing operative running of the new or modified external system. These working phases are called integration phases.

The particular challenge for tunnel refurbishment lies in the planning, harmonization and execution of the tunnel-related traffic phases and in the TCC-related integration phases.

2.1. Typical Traffic Phase Models for Tunnel Refurbishment

For the following analysis, we have selected three typical procedures of refurbishment concepts. The phases of a procedure represent the construction stages, means e.g. during two-way traffic in bore 1, construction work will be carried out in bore 2. In procedure 2.1.1 Twin-Bore Tunnel, Refurbishment In Four Phases, Without Client (RV4oC) and 2.1.2 Twin-Bore Tunnel, Refurbishment In Four Phases, With Client (RV4mC), an intermediate phase is planned between the bore wise refurbishment, in which both tubes are operated in one-directional traffic. Procedure 2.1.3 Two-Way Tunnel Traffic, Refurbishment in Day/Night Operation (GVTN) is completely different from 2.1.1 Twin-Bore Tunnel, Refurbishment In Four Phases, Without Client (RV4oC) and 2.1.2 Twin-Bore Tunnel, Refurbishment In Four Phases, With Client (RV4mC), here a single-bore tunnel in day-night operation is refurbished.

In Procedure 2.1.1 Twin-Bore Tunnel, Refurbishment In Four Phases, Without Client (RV4oC) and 2.1.2 Twin-Bore Tunnel, Refurbishment In Four Phases, With Client (RV4mC) a client is mentioned, this client is an operator station operated directly by the tunnel server.

2.1.1. Twin-Bore Tunnel, Refurbishment In Four Phases, Without Client (RV4oC)

Table 1: Traffic phases for the refurbishment of a twin-bore tunnel in four phases, without client

Phase		Description	Control
0	*TW DR1*	*Enablement of an existing bore for two-way traffic.* - *Additional traffic signs* - *Additional entry lighting, etc.* *To enable the refurbishment of DR2*	*Original tunnel control Integration in TCC*
1	*OW DR2*	*Two-way traffic flow of an existing bore (DR1) and a refurbished bore (DR2)* *Use: to cover traffic peaks during civil works with two instead of one tunnel bore (summer holiday traffic, …)*	*Original tunnel control and new tunnel control TCC operation with two remote stations*
2	*TW DR2*	*Refurbished bore (DR2) with two-way traffic flow* *To enable the refurbishment of DR1*	*new tunnel control integrated in TCC*
3	*OW DR1*	*Refurbishment of both bores complete*	*new tunnel control integrated in TCC*
TW .. two-way traffic / OW.. one-way traffic / DR .. direction / TCC .. traffic control centre			

2.1.2. Twin-Bore Tunnel, Refurbishment In Four Phases, With Client (RV4mC)

Table 2: Traffic phases for the refurbishment of a twin-bore tunnel in four phases, with client

Phase		Description	Control
0	*TW DR1*	*Enablement of an existing bore for two-way traffic.* - *Additional traffic signs* - *Additional entry lighting, etc.* *To enable the refurbishment of DR2*	*Original tunnel control Integration in TCC*
1	*TW DR2, Client*	*Refurbished bores (DR2) for two-way traffic.* *To enable the refurbishment of DR1*	*new tunnel control no integration in TCC, Tunnel operation with tunnel system in TCC*
2	*OW DR2*	*One way traffic of the existing bore (DR1) and a refurbished bore (DR2)* *Use: to cover traffic peaks during civil works with two instead of one tunnel bore (summer holiday traffic, …)*	*Original tunnel control and new tunnel control TCC operation DR1, tunnel system for DR2*
3	*OW DR1*	*Refurbishment of both bores complete*	*New tunnel control integrated in TCC*
TW .. two-way traffic / OW.. one-way traffic / DR .. direction / TCC .. traffic control centre			

2.1.3. Two-Way Tunnel Traffic, Refurbishment in Day/Night Operation (GVTN)

Table 3: Traffic phases for the refurbishment of a single bore tunnel in day/night operation

Phase		Description	Control
0	*TW day*	*Tunnel is operated with the existing equipment during the day*	*Original tunnel control* *Integration of existing equipment in the TCC*
1	*TW night new*	*Tunnel is enabled with the new equipment and operated at night* *(Traffic is blocked)*	*New tunnel control* *Separate integration in TCC* *Daily change of configuration*
TW .. two-way traffic / DR .. direction / TCC .. traffic control centre			

2.2. Risk Assessment From The Traffic Control Centre Perspective

Table 4: Risk assessment matrix

Risk description	Traffic phase model	Probability	Effect
Monitoring gaps, BuS components are temporarily not monitored	*RV4oC*	*2*	*4*
	RV4mC	*1*	*4*
	GVTN	*3*	*4*
Operating errors due to lack of clarity caused by having more than one visualization system in the control centre	*RV4oC*	*0*	*5*
	RV4mC	*4*	*5*
	GVTN	*0*	*5*
Malfunctions in shared operational resources by TCC and tunnel control (videowall)	*RV4oC*	*0*	*4*
	RV4mC	*3*	*4*
	GVTN	*0*	*4*
Traffic guidance malfunction due to insufficient integration time	*RV4oC*	*2*	*5*
	RV4mC	*1*	*5*
	GVTN	*4*	*5*
Technical malfunction due to insufficient integration time	*RV4oC*	*2*	*3*
	RV4mC	*1*	*3*
	GVTN	*4*	*3*
Malfunctions in higher level processes due to lack of connection between the new and old tunnel systems	*RV4oC*	*3*	*4*
	RV4mC	*3*	*4*
	GVTN	*0*	*4*
Insufficient training of operating personnel due to frequently changing phases	*RV4oC*	*2*	*3*
	RV4mC	*2*	*3*
	GVTN	*3*	*3*
Malfunctions in shared operational resources by the old and new tunnel control	*RV4oC*	*1*	*4*
	RV4mC	*1*	*4*
	GVTN	*4*	*4*
1..very low / 2 .. low / 3 .. medium / 4 .. high / 5 ..very high			
BuS .. German acronym for Tunnel Operation and Safety Equipment			

3. IMPLEMENTATION OF REFURBISHMENT INCLUDING THE CONTROL CENTRE

The goals of attaining the highest possible quality and safety during refurbishment work are reached by the implementation and adherence to the following rules.

- Definition of required traffic phases
- Standardized approach to software integration
- Consideration of a rollback concept to enable the change back to a safe operating state in the case of faults.

3.1. Selection Of The Traffic phase Models

Not only is it necessary to include the civil engineering expert in the basic planning of a tunnel refurbishment scheme, other representatives must be included from the electromechanical equipment, tunnel-related software and in particular the traffic control centre domains.

An agreed upon traffic phase model considers the following major boundary conditions:

- All civil engineering measures can be carried out as far as possible without the presence of traffic
- All electrical and mechanical activities can be carried out as far as possible without the presence of traffic
- Before any change to traffic flow is made, all technical changes to the tunnel and control centre software have been implemented and sufficient time for tests is available
- The total number of different traffic phases is to be kept as low as possible
- Parallel systems for operation in the traffic control centre are to be avoided
- The parallel operation of new and old controllers in tunnel systems are to be avoided
- The required traffic phases are logically consistent and fulfil legal requirements.
- A risk assessment has been carried out

3.2. Standardized Approach for Software-Related Integration

The quality of integration can be considerably increases by using a standardized approach. A common approach is:

1. Integration of external systems
    a. Base tests
    b. Test of individual signals
    c. Function test
2. Simulation of operation (if possible)
3. Test operation (client tests accompanied by the supplier)
4. Live operation

Particular emphasis should be placed on the function test, which not only tests the correct functioning of individual components, but ensures the interplay of traffic control centre, tunnel control and tunnel peripherals.

An integration test is mandatory for the start of switching each traffic phase live.

3.3. Consideration Of A Rollback Concept

Many software integration concepts are forwards-facing and plan using a step-by-step approach to complete full deployment. An equally important component however is having a rollback scenario that enable a change to the last known safe operating state should tests not be successful. The following technical rollback mechanisms have proved themselves in tunnel and control centre systems:

- Copies of the control system for the current and previous traffic phase are available in parallel and can be “switched live”.
- A change can be revoked by restoring incremental backups
- A change can be revoked by restoring a total backup (not possible with large systems!)
- New phases are installed in parallel systems and “switching” is achieved by changing the system

4. SECURITY ASPECTS

Tunnel systems and traffic control centres are more susceptible to cyber-attacks during construction or refurbishment phases than during stable operation.

4.1. Threat Scenarios

The following threat scenarios are evident, particularly during system refurbishment activities.

- The attacker achieves access to control hardware at the construction site
- The attacker achieves access via networks that are not completely protected during the construction phase
- The attacker achieves access with temporary access codes meant for installation
- Operating systems have security flaws since the planned updates are only planned before the final handover of the installation to live operation
- Virus protection is only established at the end of the construction phase
- Temporary internet access is established by the supplier companies
- Firewalls are only established at the end of the construction phase
- Authentication via secure transmission protocols is waived during the construction phase
- Regular system backups are not performed during the construction phase
- System fault messages are ignored due to the sheer volume of information created during the construction phase

4.2. Cyber Protection Measures For The Systems

The protection of systems during the construction and refurbishment phases can be increased via technical, organisational and personnel measures. All activities are focussed on prevention, mitigation or restoring.

The following measure are to be particularly recommended during the construction phase [K. Jacobsen, 2018]:

Table 5: Measures for the cyber protection of the systems

Type of measure	Measure	Effect
Technical	*Access control using secure user passwords*	*Prevention*
Technical	*Use of virus protection*	*Prevention, mitigation*
Technical	*Use of firewalls*	*Prevention*
Technical	*Biometric access data to computer systems*	*Prevention*
Technical	*Regular execution of security updates*	*Prevention*
Technical	*Regular execution of system backups*	*Recovery*
Technical	*Use of VPN for remote access*	*Prevention*
Technical	*Use of access control systems at construction sites*	*Prevention*
Technical	*Check of existing access control systems*	*Prevention*
Technical	*Data encoding on transport paths*	*Prevention, mitigation*
Technical	*Use of data protocols with reliable authentication*	*Prevention, mitigation*

Organisational	*Interventions by an IT security specialist*	*Prevention, mitigation*
Organisational	*Creation and implementation of a security concept*	*Prevention, mitigation, recovery*
Organisational	*Implementation of binding regulations for the remote access by external service provider*	*Prevention*
Organisational	*Definition of access rights at construction sites*	*Prevention*
Organisational	*Evaluation of status reports*	*Prevention, mitigation*
Personnel	*Regular training and qualification of personnel with software tasks at the construction site*	*Prevention*
Personnel	*Sensitization of the entire workforce at the construction site*	*Prevention*

5. SUMMARY/OUTLOOK

Achieving the highest possible quality and security during refurbishment not only requires meticulous planning and good coordination between all involved parties, but also sufficient time during the construction phase. Proven models are available for the different technical and traffic-related requirements during the refurbishment of tunnel and traffic control centres that emulate all phases of the work in terms of construction and control. It must be noted that the models have different risks associated with them.

5.1. Outlook: Cyber-security law in Austria

The goal of the European IT-security directive is to improve the protection of critical infrastructure throughout the EU against disturbances and attacks. The EU directione for network and information security (NIS directive) came into force on August 8th, 2016. The member states now have two years to implement the directive in national law. In Austria, a cyber-security law is currently in work, whereby the title has not yet been decided upon. [NIS EU directive is in force – what does this mean for the SME?, WKO, October 10th, 2016]

5.2. Consideration of increased cyber-security measures for tunnel refurbishment

The measures introduced in this document to increase cyber-protection during construction and refurbishment phases will, together with the new cyber-security law, definitely increase the level of security.

The particular challenge for system operators and constructors, however, will be that the consideration of the new security measures will require additional time effort. Additional time that will have a negative effect on the construction period and the flexibility of construction processes.

6. REFERENCES

RICHTLINIE 2004/54/EG DES EUROPÄISCHEN PARLAMENTS UND DES RATES, 29. April 2004

Wirtschaftskammer Österreich (10. Oktober 2016). NIS-Richtlinie der EU in Kraft getreten – was bedeutet sie für KMU?

K. Jacobsen (2018). Erkenntnisse aus dem Projekt Cyber Security. Dürr Group

CONTROL SYSTEMS IN CITY TUNNELS

Lars Elertson
Swedish Transport Administration, Sweden

ABSTRACT

The aim of the article will describe, in general, the basic design for Control Systems (CS) in Road Tunnels according to high Traffic flow mainly in City Tunnels in Sweden. The Control Systems (CS) handle Software logic in many Infrastructure projects, but there is not much recommendation or guidelines in this subject. This technical article gives some hints about how to construct CS in Road Tunnels.

1. INTRODUCTION

"Tvärförbindelse Södertörn" a planned 20 km new road connection south of Stockholm, from road 73 at Haninge to European Highway E4 in the Stockholm area. This road connects E4 with road 77 and will be used for transports from the South-East and specially from the new harbour terminal in Nynäsham. A large amount of heavy traffic are to be expected. This project is part of the national plan for road projects for Swedish Transport Administration, STA.

Tvärförbindelse Södertörn in brief

- Masmo Tunneln, length approx.1 km
- Glömsta Tunneln, length approx. 1 km
- Flemingsberg Tunneln, length approx. 3 km

Figure 1: Tvärförbindelse Södertörn.

The tunnels are designed with the aim of creating a safe journey, with parallel tunnel tubes without oncoming traffic, which is part of the Safety Concept for Swedish Transport Administration. Ramp tunnels connect the main tunnel to the surface road network. The tunnel system will be monitored and controlled by the regional Traffic Control Centre "Trafik Stockholm".

Each Tunnel is autonomous and they are equipped with a Local Control and Monitoring System. The Control systems monitors approx. twenty technical Sub-Systems. For example CCTV, detection systems such as automatic fire detection for smoke and heat, Traffic Systems, Electrical Systems, PA-Systems, Radio Systems, Communication Systems, a Fixed Fire Fighting system and Waste Water Systems. The ventilation concept is based on longitudinal ventilation. Specific Action plans for fires and accidents are developed for handling Fires and automatic closing of the tunnel.

2. DESIGN CRITERIA

- Large City Tunnels has three different tasks and they are integrated in one Control System.
  - Safety Systems, Fire and smoke detection. Fixed Fire Fighting System, Local Evacuation Sequences and Fire Ventilation and Tunnel sensors.
  - Traffic Systems, Traffic Signs, Barriers and traffic sensors.
  - Systems for Electric Power Supply, Tunnel Environment Ventilation, Wastewater and Climate Control.
- One brand for Control Systems for controls and monitoring for the road tunnels technical system.
- Total system integration. The Control system is a common tool for operation and maintenance.
- Distributed and autonomous logic. Maintains functionality in case of serious malfunction in centralized systems.
- System Redundancy. The Control system is a safety system and is constructed to handle one fault for safety related functions.
- User Friendly. Similarities with Windows. "Clickable" symbols. Texts in Swedish for operators.
- User friendly in case of incidents, maintenance and Fault finding. Easy access to panels for operating, indication, alarms and access to Document Database.
- Constructed using STA's Guideline for Graphic User Interface.

3. CONTROL SYSTEM DEFINITIONS.

3.1. Control Components

Programmable Logic Controller (PLC) The PLC is a small industrial computer originally designed to perform the logic functions executed by electrical hardware (relays, switches and mechanical timers). PLCs have evolved into controllers with the capability of controlling complex process, and they are used substantially with SCADA and in DCS-systems.

Human machine Interface (HMI) The HMI is a software and hardware that allows operators to monitor the state of a process. The operator can operate connected objects or modify control settings to change the control objective, and manually override automatic control operations in the event of an emergency. The HMI also allows a control engineer or operator to configure set points or controller algorithms and parameters in the controller. The HMI displays process status information and historical information. The location, platform and interface may vary a great deal. For example, an HMI could be a dedicated platform in the Control Centre or a laptop on a wireless LAN or a browser on any system connected to Internet.

ASÖ = *Swedish* Anläggningens Styr Övervaknings System. *Eng.* Plant Control System *Ger.* Anlagen Leith System

ASÖ AÖ = PLC with Tunnel Overall Functionality (Control of tunnel ventilation, Sequence Control and Lighting.

ASÖ Server = Human Machine interface with graphics and control panels.

ASÖ Client = Operator's console (Stationary or portable).
ASÖ DO = PLC with Distributed Functionality (Control of Objects within a DO. i.e. Jet Fans, High and Low Volt Switch Gears, Barriers, Traffic Signs, Telematics equipment and Lighting.
DO = Tunnel Section for Electrical and Communication equipment to minimize consequence of serious errors or malfunction.
ASÖ AS = PLC with Autonomous Control Systems for i.e. Fan Stations or Waste Water.
ASÖ RIO = Distributed In / Output Cards connected to PLCs.

4. CONTROL SYSTEM HIERARCHY FOR ROAD TUNNELS.

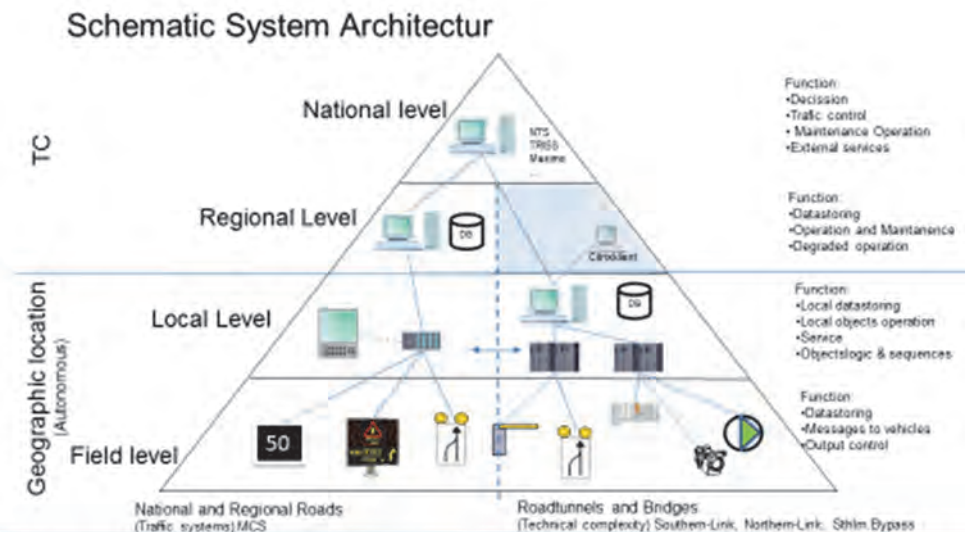

Figure 2: System Hierarchy for Infrastructure in Region Stockholm

5. REGIONAL CONTROL SYSTEM, TRAFIK STOCKHOLM

The tunnel system will be monitored and controlled by a traffic control center with the National Traffic Control System (NTS).

The tunnel system is monitored and checked by the STA's regional Traffic Center, Traffic Stockholm. From there, all traffic is monitored within the region (24/7). In the traffic center there are traffic controllers and operating technicians for continuous monitoring of highways, tunnel installations and drawbridges in the region. The personnel use the technical system NTS. It is a decision-support system with pre-programmed Action Plans (AP) that manage tunnel fires and traffic accidents, as well as traffic regulations in connection with operations and road work during tunnel maintenance.

NTS uses Action Plans (AP) for handling traffic accidents and fires. The AP is a sequence that sends commands to ASÖ. In ASÖ these commands are handled by different objects related to geographical and logical groups for i.e. Ventilation, Lightning, Traffic and Radio and voice messages. One example of a logic group is for Tunnel Ventilation and consists of a number of Jet Fans, Air flow sensor, Environmental detectors and best available Camera.

6. FUNCTIONALITY IN AN ACTION PLAN FOR A FIRE SCENARIO

This is a short description of what happens with all technical systems in a Fire Scenario when a fire occur and the operator confirms and leads trough the selected Sequence.

- The Fire is indicated by Tunnel sensors with a Fire/Smoke Alarm to ASÖ in the Tunnel to the NTS.
- The best possible camera is conected to the alarm. Then the operator will then confirm the fire or reject it in case of a false alarm.
- The operator gets a proposal to start a Pre Programmed Action Plan (AP) which handles a Tunnel Fire. It is a sequence of commands. See figure 3.
- The Pre Programmed Action Plan sends commands using the Local Communication Platform (LCP) to the Plant Control System (ASÖ). Now the Fire ventilation program starts from logic in the Controller for Superordinate systems (ASÖ-AÖ). Then more commands will follow from the sequence and more systems/objects will start working from logic in locally controllers (ASÖ-DO) by using different fieldbuses for Tunnel Road Signs with Symbols and Messages, Lightning, Barriers, Radio Messages, Jet Fans and more….
- When it is time for the sequence step for the Fixed Fire Fighting system to start, one command from the AP to the ASÖ-AÖ with its logic selects the geographical ASÖ-DO. The Controller use fieldbuses to communicate with ASÖ-RIO with is then connected by cable to open one section with its FFFS-valve. From the CCTV actions are also observed. See figure 4.
- To ensure the right pressure in the FFF-System pressure transmitters are connected to the Locally Control System (ASÖ-AS) and the logic will ensure that more pumps starts automatically when the pressure is decreasing.
- Now passengers from vehicles can save themselves through the Emergency Exits and the fire will be suppressed by the FFF-System.

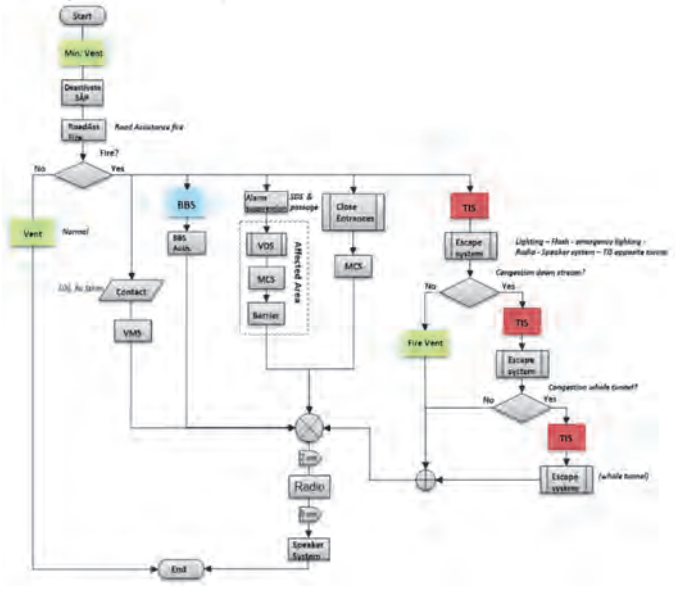

Figure 3: Action Plan in NTS

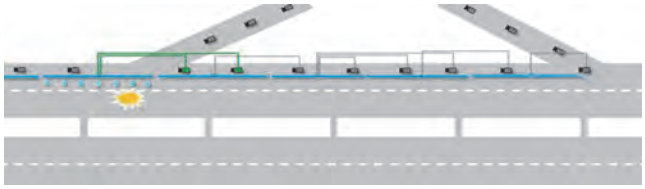

Figure 4: Layout FFFS and Cameras

7. RISK MINIMISING MEASURES

- ✓ All Safety-systems are constructed to handle one fault.
- ✓ All Safety-systems have 100% redundancy which means switching to another system without delay or malfunction.
- ✓ Systems which include safety are: NTS, Communication, Water Pressure Station, Control System and Output card with cable connection to FFFS-valves.
- ✓ Unbreakable Power Supply for safety Systems for 60 minutes to ensure people to save themselves through the Emergency Exits.
- ✓ Unbreakable Power Supply for Emergency services for 8 hours.
- ✓ Pre-Programmed Action Plans. Operators can handle the situation by following a step by step sequence in a difficult and dramatic situation.
- ✓ If there is a communication failure with the Tunnel there will be an automatic opening of the BBS-valves from the Control System if the Temperature rise to >90°C.

Risk minimizing is also dependent of people and how they are trained in critical situations and also about "Murphy's Law".

"Murphy's Law is an adage or epigram that is typically stated as: Anything that can go wrong, will go wrong"

8. CONTROL SYSTEMS DIFFERENT TASKS

- ASÖ integrates technical systems for Tunnel control, monitoring and operation.
- ASÖ acts as a Safety Systems: Fire and smoke detection. Fixed Fire Fighting System, Local Evacuation Sequences.
- ASÖ acts as a Traffic Systems: Traffic Signs and Barriers,
- ASÖ acts for Normal operation of Tunnel Ventilation, Waste Water Systems, Electric Power Supply and Climate Control
- ASÖ acts as a Maintenance tool: Regularly monitoring of time for running object and objects alarms. Fault finding tool for High priority alarms.
- ASÖ acts for Data collection and storage to Data Bases locally for Alarm and Event-handling and measurements.
- ASÖ integrates technical systems for Tunnel control, monitoring and operation.

9. PROGRAMMING AIDS IN FORM OF FUNCTIONAL DESCRIPTION TEXTS, MATRIX OR FUNCTIONAL SCHEDULES

How can we explain all technical details for the automation engineer? The automation engineer has to make all logic to achieve a safe and reliable Tunnel System. Without this information there will not be any functionality at all, just 20 technical systems who are switch off, without any interaction between them.

In the construction scope, proper construction documentation must be included. This is of great importance for the system integrators to fulfil his work, especially for programing of Tunnel Ventilation and Waste Water. In the he scope for system integrators, this has to be done:

- ➢ Detailed Input/output Lists with data and description of objects and sensors.
- ➢ Construct all Input and output cabling and fieldbuses to objects and sensors.
- ➢ Construct all Cubicles with hardware; Controller, Electric supply, I/O and Communication cards.
- ➢ Construction of the software application programs.

There are different approaches of documentation to accomplish the Software application.

- Text description
- Excel documents
- Graphical function drawings
- Graphical layout of the Tunnel Ventilation

Text description

This is the most common way to describe different technical systems and objects in process applications i.e. Waste Water and Climate Control. The document normally requires a descriptt-tion of object, alarms, interlocking, parameters and normal and unnormal operation for one type object or a complete system.

Matrix layout with Excel

This kind of documents is mainly for Tunnel Ventilation Control and contains all Fans and sensors in their geographical locations and how the equipment should operate in different operating modes. A text document is still required for a more detailed description how to understand the requested function. It have one benefit that Excel-files could be imported directly to a modern Control System with some software tool.

Graphical Function plans

(Power-plant documentation according to VGB-standard. VGB is the European technical association for Power and Heat Generation)

This is a very detailed documentation and it describes how the Graphic Function blocks in the software for the control system are connected for the right function. See figure 5.

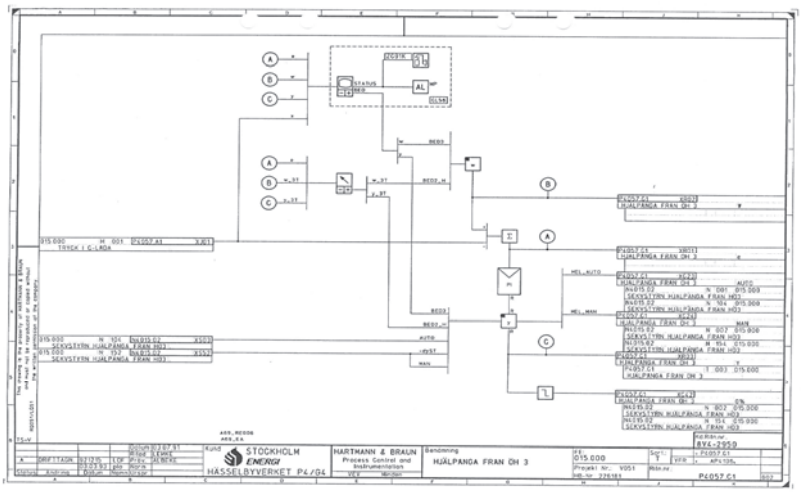

Figure 5: Example of a Function plan

Graphical Layout of the Tunnel Ventilation System

STA used this approach in “Norra Länken” in Stockholm and it shows a graphical layout of the Tunnel Ventilation System with all information included for all fire cases and for environment ventilation. See figure 6. The reason for this was to make it so useful so it could be used as basic data for software applications and it can be used in the testing phase for an easy verification of the control strategy. The layout shows in this overview format all Fans and Air-Ventilation Stations. It gives information on how the tunnel are sectioned into different

ventilation areas and the names of the different tunnels. Each drawing shows a fire scenario in a specific location and how the control system shall control each fan. All values are made from simulations runs. There are also text describing general rules and principles. For the reader, the colour marking helps understanding what happens under different scenarios. The Graphical Layout of the tunnel system consists of two parts, Fire-ventilation and Environment Ventilation.

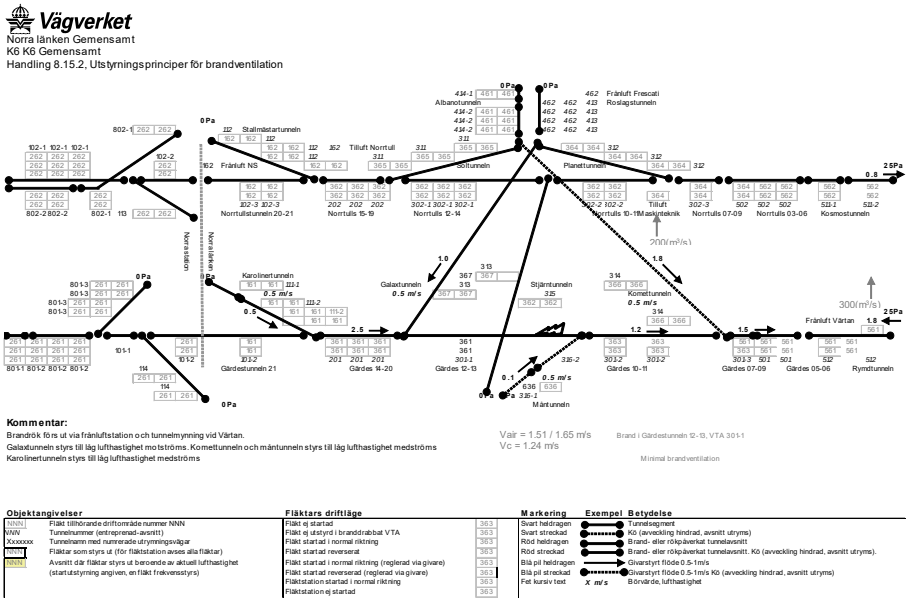

Figure 6: Graphical Layout of the Tunnel Ventilation System

10. MALWARE PREVENTION

This new treat is important and has to take seriously. Most important is to ensure that central equipment for Communication are in secured places. All Windows software not necessary for Control Systems has to be removed and of course using of safe Passwords. Today much time has to be used on upgrading Software on technical systems for latest versions for Malware protection. STA has now a guideline for Information Security which is written for contractors with demands incorporated in the main contract for installations. One useful standard is IEC 62443 and especially group 3 which is written for System Integrators.

11. CLOUD FREE CONTROL

STA has demands to handle Hardware in Infrastructure project regarding Road Tunnels in Installations contracts. Autonomous Control Systems means that logic for Control is placed as near as possible to the controlled objects in secure (locked) and ventilated spaces.

12. HANDLING OF HIGH PRIORITY SYSTEM ALARMS FOR OPERATORS IN TRAFFIC STOCKHOLM

The different technical systems in the safety concept are in some cases a form of redundancy to each other. This means that the tunnel is still considered to have sufficient safety to be open to traffic even in the event of failure of certain individual technical systems for a limited period of time. However, if there are system failures of parts or whole technical system, then it has consequences that are difficult to assess by an operator in the traffic management center. If safety is not considered sufficient, then there is a need to close all or part of the tunnel for various types of system failures. As a basis for decision, there is an operator instruction as a help tool for system failure. For some types of system failure, a few compensatory measures

may be taken to mitigate the effect and "buy time" before corrective maintenance/action can take place. Lower technical safety standards should be compensated as such:

- Traffic control, speed reduction and Traffic sign messages
- Enhanced guarding of Road Assistance
- Maintenance measures

The basic prerequisite is that there are temporary system failures and the consequences of these. Where closing of certain tunnel sections is required, it is the question of closing after some elapsed time. See Table 1 as an example for alarm priorities for Control System failure.

Priority 1 - Immediate action.
Priority 2 - Compensatory action and call back up personal according to Maintenance routines.
Priority 3 - Next scheduled Maintenance job.

In case of failure or interference in a technical system the tables below indicate in certain cases that the impact on traffic is severe. There are compiled alarms which indicate that there is reduced functionality from an important technical system. It is assumed that Traffic operators monitor these compiled alarms and receive support in action plans and instructions for guidance. This instructions could also be made as a software function in a Control System for all technical systems.

Table 1: Example of instruction for Control System ASÖ

ASÖ	**Traffic impact**	**Compensatory measure**	**Maintenance action**
ASÖ out of order	Close Tunnel in 20 min		Prio 1
1 ASÖ-AÖ out of function (one of two)	No impact (Redundancy in action)		Prio 3
1 ASÖ-DO out of function	Closure of affected Traffic section in 20 min		Prio 1
1 ASÖ-DO in Ramp Tunnel	Close the ramp within 20 min		Prio 1
1 Communication, Electrical and Control cubicle out of order	Speed reduction (50) upstream of the affected traffic section	Increased preparedness Road Assistance	Prio 2
1 Communication, Electrical and Control cubicle out of order in Ramp Tunnel	Speed reduction (50) upstream of the ramp	Increased preparedness Road Assistance	Prio 2

13. REFERENCES

[1] Contracts for the Installation of Mechanical and Electrical Systems, E4 The Stockholm Bypass, Trafikverket, Swedish Transport Administration, September 2017, www.trafikverket.se

[2] Contracts for the Installation of Mechanical and Electrical Systems, Norra Länken, Stockholm, Trafikverket, Swedish Transport Administration, June 2010, www.trafikverket.se

KEEPING CROSS PASSAGES SMOKE-FREE – RESULTS FROM FULL SCALE TESTS IN RAIL TUNNELS

[1]Thomas Thaller, [2]Peter Sturm, [3]Johannes Rodler

[1]ÖBB Infrastruktur AG, Austria
[2]IVT / Graz University of Technology, Austria
[3]FVT mbH, Austria

ABSTRACT

Investigations concerning smoke dispersion in a rail tunnel were content of a research project, which was performed in the already finished section KAT1 of the Koralmtunnel in Austria. Full scale tests were performed, covering fires with a max. heat release rate of up to 21 MW. Smoke dispersion was monitored using video cameras and related temperature distributions at various sections of the tunnel were recorded. Focus of the investigation was the smoke dispersion in the region of the cross passages where passenger evacuation will happen.

The tests shall provide supporting information for the selection of the proper escape doors (swinging doors or sliding doors) which will be installed for passenger evacuation via the cross passages. In order to provide sufficiently safe conditions during the self-evacuation phase, smoke shall not restrict the escape possibilities. The tests aimed at investigating the interaction between fire load, smoke production rate and escape possibilities as a function of the installed ventilation system and the aforementioned parameters.

Keywords: safety in railway tunnels, fire tests, smoke dispersion, egress doors for cross passages

1. INTRODUCTION

Modern railway tunnels consist of two single-track tubes, which are connected via cross passages at a maximum spacing of 500 m. As soon as their length exceeds the maximum distance to be covered by the failsafe running function, an emergency stop station in the tunnel has to be provided. The both tunnel projects Semmering Base Tunnel (SBT) with a length 27 km, as well as the Koralm Tunnel (KAT) with a total length of 33 km, are currently under construction and contain one emergency stop station roughly in the middle of the tunnel. Both projects are the key elements of the new ‘Südbahn’ between Vienna and Klagenfurt and are part of the Baltic-Adriatic TEN corridor.

The most serious problem of a rail tunnel under operation is the possibility of an incident with fire. Hence the decisive scenario for the risk assessment is the case ‘passenger train under fire’. From this perspective, the protection of passengers is seen as the major goal in case of an incident. In case of a fire a passenger, train should either stop at the emergency station if it has not passed it yet or exit the tunnel. The most unfavorable scenario is given when a train is forced to stop between portal and emergency station, thus passengers have to be evacuated via the closest cross-passages.

This requirement calls for smoke-free egress ways. Mechanical ventilation has to provide a positive pressure difference between the non-affected and the incident tube in order to avoid smoke penetration into the safe area, hence maintaining this pressure difference is of utmost importance.

As part of an ÖBB funded research project full scale fire tests were carried out from October 2016 until January 2017 in the already built section KAT1 of the Koralmtunnel. The tests contained fires with a maximum heat release rate of up to 21 MW. Main objective was to gain

knowledge about the conditions while an incident particularly with regard to the smoke propagation at the different development phases of the fire.

2. PROBLEM DESCRIPTION

2.1. Smoke-free egress ways

On the one hand cross passages are used for housing the technical equipment needed for tunnel operation and safety issues, on the other hand they are used as escape routes into the safe area in case of an incident.

The mechanical ventilation system of the SBT is designed to serve this purpose [1]. In case of a stop in the emergency station, smoke will be extracted and fresh air supplied to the rescue rooms. In case of a stop between the rescue station and the portal, fresh air will be supplied to the non-affected tube and smoke extracted from the incident tube. Figure 1 depicts an incident situation between east portal and emergency stop station. Due to the resulting pressure difference, smoke cannot penetrate into the safe area.

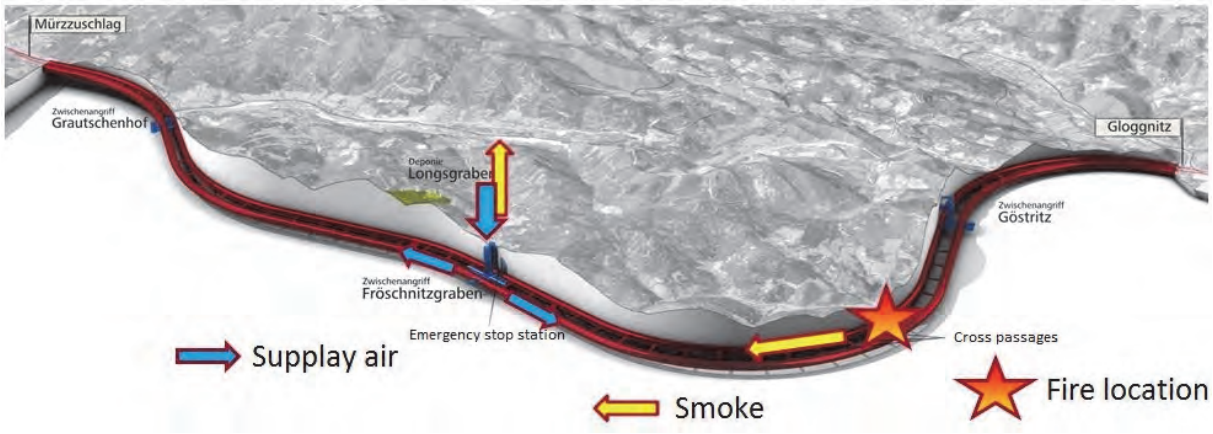

Figure 1: Sketch of the ventilation of the Semmering-Basistunnel in case of fire between east portal and emergency stop station

2.2. Escape doors

There are manifold and partly even contradictory requirements when it comes to railway equipment of railway tunnels. This applies in particular to the escape doors of the cross passages. On the one hand, the doors have to stay tight regarding smoke despite the constant change of pressure and suction caused by the passing trains. On the other hand, they have to keep their functionality as escape doors in case of an incident, meaning the force, necessary to open it, must not exceed 100 N.

In the design phase for the approval of the railway authorities for both projects SBT and KAT, swing doors were planned. These double wing swing doors – the wings open in both directions – meet the requirements regarding escape routes best because they can be used as escape doors in both directions depending on which tube is affected. Alternatively, the use of sliding doors should also be possible (see Figure 2).

Figure 2: Potential door systems – swing door left, sliding door right

3. FULL SCALE FIRE TESTS

3.1. Objectives

Full scale fire tests with maximum heat release rates of up to 21 MW and a smoke / exhaust air volume flow of up to 150 m³/s were performed to investigate the interaction between fire size, smoke production as well as smoke penetration into cross passages with open doors.

The activation of the incident ventilation in the SBT causes partially high pressure differences (>200 Pa) between both tubes, thus preventing smoke penetration from the affected tube into the escape routes (QS). As a consequence of such high pressure differences, mechanical equipment (doors, dampers …) might be restricted in its functionality, respectively require extra force to be handled.

The performance of cross passages doors (swing resp. sliding doors) at this high pressure differences, was another issue to be observed within the tests. Furthermore, the technical equipment needed in order to keep the cross passages free of smoke should be determined. Simultaneously, it was examined whether the max. tolerable door opening force of 100 N was not exceeded.

3.2. Test setup and ventilation

The tests were performed in the section of the Koralm Tunnel KAT 1 where the carcass works are already completed.

Figure 3 shows a schematic sketch of the Koralmtunnel with tunnel section KAT 1 between the eastern portal and the shaft Leibenfeld.

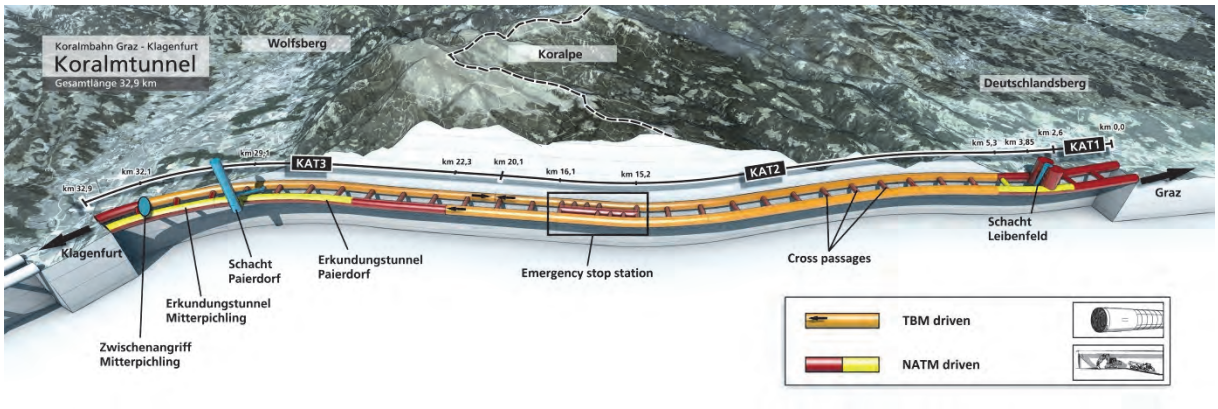

Figure 3: Sketch of the Koralm Tunnel

Cross passage QS02 was used for the tests. A swing door was mounted into the existing shear wall at one side and a sliding door at the other as a boundary to the test tunnel. The fire source was situated approx. 60 m away from the cross passage in western direction. Figure 4 shows the test setup.

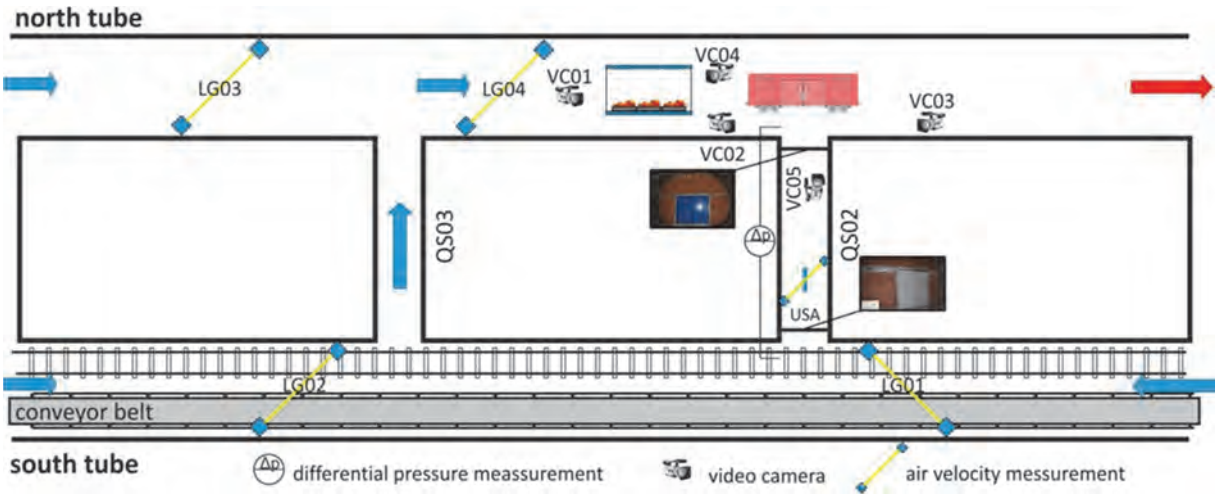

Figure 4: Sketch of the test section

Because of the high tested heat release rates with fire loads of up to approx. 21 MW a structural fire protection was necessary in order to avoid damage to the inner lining of the tunnel. A maximum allowable wall temperature of 120°C was defined by the tunnel owner. A fire protection box, double lined with fire resistant boards, served for this purpose (see Figure 5). It was 20 m in length and had a cross-section of 5 m by 5 m. In order to simulate the reduction of the tunnel section resulting from a train, an obstacle having the size of a train wagon was erected on a scale of 1:1 and situated directly in front of the access point to the cross passage.

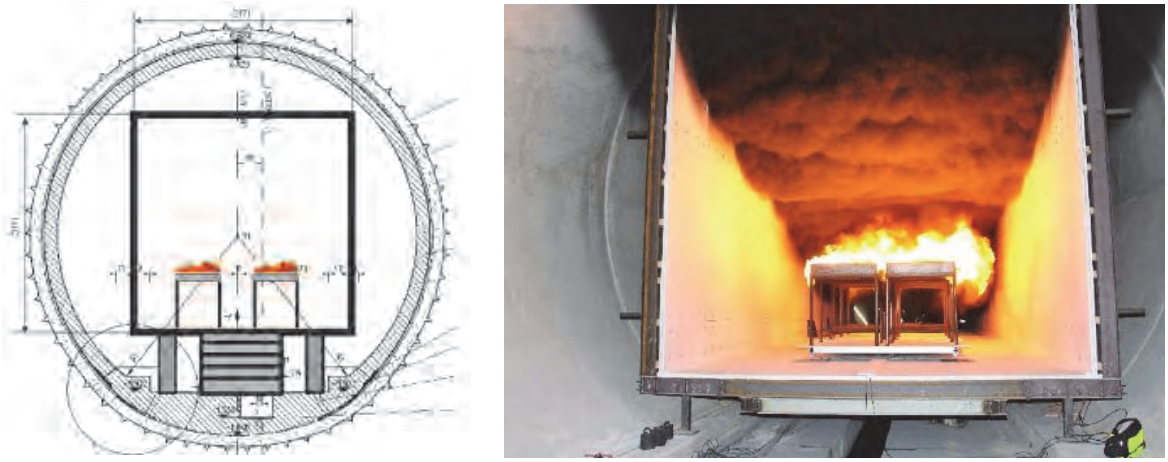

Figure 5: Fire box for thermal insulation

As an additional safety measure – and as a further test object – a high-pressure water mist system (HPWMS) was installed at the ceiling of the fire protection box, which should ensure a reduction of the temperature of the hot combustion gases if necessary.

The ventilation of the tunnel was mainly performed via the eastern portal of the southern tube and the cross passage QS03, which was opened to the northern tube. The suction of the smoke was ensured by axial fans in the brattice at the east portal of the northern tube. At the boundary, the two sections KAT1 und KAT2 were aerodynamically separated by brattices. A detailed description of the test setup can be found in [2] and [3].

3.3. Measurement and monitoring system

To get the major important testing parameter such as pressure difference, temperature profile, longitudinal flow velocity, oxygen content in the air, etc. a sophisticated measurements and monitoring equipment was implemented at the tested areas in both running tunnels. The following parameters were monitored:

- pressure difference between cross passage and both tubes employing measuring transducer (pressure measurement Δp in Figure 4)
- air velocity at various regions within the tunnel employing ultrasonic anemometers (sensors LGxy in Figure 4)
- temperature profiles at various locations downstream of the fire, employing PT100 sensors (see temperature sensors Sx,y in Figure 6)
- temperature distribution in and at the concrete surface and in the fire resistant boards within the fire box using PT100 sensors (see temperature sensors Sx,y in Figure 6)
- smoke dispersion via video cameras (see video camera VCxy in Figure 6)
- CO and CO_2 concentrations downstream of the fire (only within special tests)

Figure 6 shows the location of the temperature sensors and the video cameras.

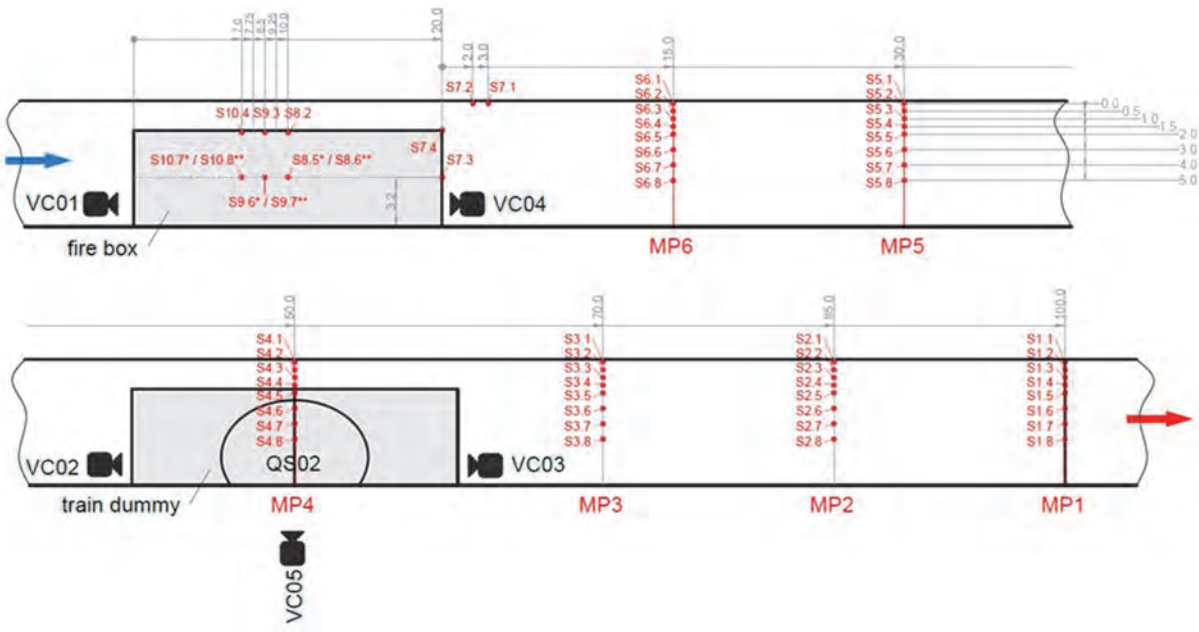

Figure 6: Location of the temperature sensors (Sxy) and the video cameras (VCxy)

3.4. Heat release rate

The heat release rate was measured on basis of a high precision measurement of the loss of mass (high precision scales) and then multiplying the mass burnt by the calorific value of the fuel. In order to get a sophisticated visualization of the smoke distribution, a mixture of gasoline (5 liter per pool) and diesel (20 liter per pool) was used as fuel. This mixture was burnt in pools with a size of 1 m² at the surface. An increase in the number of pools resulted in an increase of the fire size.

Table 1 shows the major important parameters of the respective tests. The highest fire load was reached at test #13 with a peak heat release rate of 21 MW. It was tried to keep the air velocity upstream of the fire source on a constant level. Nevertheless, the values changed permanently because of the local conditions.

Table 1: Parameters of the respective tests

Test No.	No. of pools	HHR average	HHR maximum	Duration	Air velocity at start	Air velocity average
[#]	[#]	[MW]	[MW]	[min]	[m/s]	[m/s]
BV 1	2	2.3	4.0	00:15	1.54	1.30
BV 2	4	5.5	7.9	00:13	1.12	1.75
BV 3	2	2.3	4.0	00:16	0.60	1.22
BV 4	4	6.0	7.7	00:10	1.00	1.49
BV 5	6	7.2	11.5	00:12	1.20	1.74
BV 6	8	9.5	14.3	00:12	2.00	2.16
BV 7	8	14.5	19.5	00:08	1.43	1.77
BV 8	4	4.1	6.7	00:14	0.64	1.32
BV 9	4	6.0	8.0	00:10	1.23	1.54
BV 10	8	11.0	18.1	00:10	1.40	1.54
BV 11	6	5.0	9.3	00:17	2.30	2.21
BV 12	6	8.8	11.0	00:11	2.40	2.13
BV 13	10	9.0	**21.0**	00:16	2.00	1.91
BV 14	10	7.9	18.5	00:21	1.20	1.38

4. RESULTS

The air speeds achieved during the tests upstream of the fire location, were in the range of 1.5 to 2.2 m/s. These quite moderate air velocities resulted in clear smoke and temperature layering downstream. Even the dummy wagon structure at QS02 did not induce any relevant increase of turbulence.

The maximum gas temperature in the fire box amounted to 615°C, the maximum gas temperature outside the box, measured 15 m downstream of the box (MP6), did not exceed 300°C (test #14). At the same time, the maximum concrete wall temperature did not exceed the critical value of 120°C (sensor S7.1, see Figure 7) although it has to be mentioned that during test #14, the HPWMS had to be activated in order not to exceed this value. Temperatures in the tunnel downstream the fire did not exceed 40°C at the height of approx. 2 m above ground (head level).

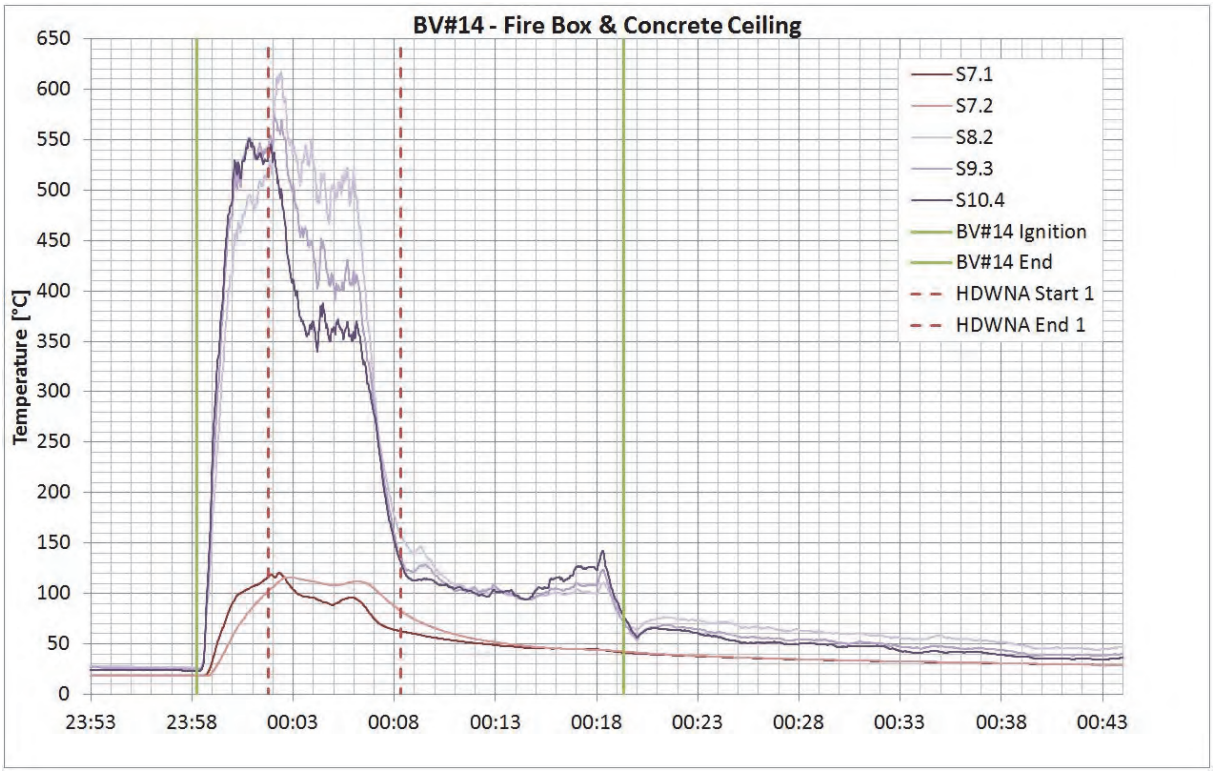

Figure 7: Fire test #14, temperatures in fire box (S8.2, S9.3, S10.4) and at concrete ceiling (S7.1, S7.2)

Ventilation was activated in such a way that at the cross passage QS02 a pressure difference of some 60 Pa between the two tubes was maintained in most cases. In this cross passage, the sliding door towards the clean tube was always kept closed while the swing door towards the smoke-filled incident tube was always kept open. This pressure difference resulted, due to the leakage through the closed door, in a small air flow of approx. 1 m/s towards the incident tube. This velocity was sufficient, despite the open door to the incident tube, to prevent any smoke from entering the cross passage.

Especially at tests with very high fire load, the relatively low air velocities in the upstream area of the fire (< 2.5 m/s) resulted in the formation of a backlayer with lengths > 100 m.

Before the fire tests #13 and #14, the door opening forces were examined at different pressure conditions in both tubes. These tests showed that even without any pressure difference between the two tubes the door opening force for the swing door already adds up to approx. 100 N. As expected, the door opening force increased with the increase of the pressure difference between the tubes.

The door open force for the sliding door, also without a pressure difference between the running tunnels, is approx. 120 N. Although it can be expected that this value can be signifycantly reduced by an elaborate adjustment of the door. In contrast to the swing door, the door-opening force did not change with the increase of the pressure difference.

Table 2 shows the measured door-opening forces for swing doors and for sliding doors at various differences of air pressure.

Table 2: Door opening forces for swing door and sliding door at various differences of air pressure

SWING DOOR				SLIDING DOOR			
Date	Time	Differential pressure	Force	Date	Time	Differential pressure	Force
[TT:MM:JJ]	[hh:mm]	[Pa]	[N]	[TT:MM:JJ]	[hh:mm]	[Pa]	[N]
20.01.2017	17:10	0	**100**	20.01.2017	17:08	0	**120**
	17:13	20	**120**		17:12	20	**120**
	17:20	60	**155**		17:18	60	**115**
	17:23	80	**180**		17:22	80	**120**
	17:26	100	**210**		17:25	100	**120**
	17:07	200	**280**		17:05	200	**115**

5. CONCLUSION

It can be concluded that an air speed of >1 m/s in the open cross passage (egress) door is sufficient in order to avoid smoke penetration into the safe area. This was demonstrated during the tests. However, in realistic cases running trains in the tunnel could negatively influence the pressure situation during the first phase of the incident. However, as running trains in the non-affected tube have to reduce their velocity remarkably in case of an incident situation, this effect shouldn`t be too strong.

The design fire size for a passenger train incident is 28 MW. The tests performed with a maximum heat release rate up to 21 MW resulted in regions where passengers would be in acceptable temperatures due to convective heat downstream the fire (max. 40 C at head level) and visibility conditions were maintained acceptable.

The activation of the HPWMS resulted in a massive decrease of the temperature downstream the fire location. However, it has to be mentioned that the momentum of the injected water spray resulted in increased turbulence and hence in a strong downwash of the smoke which reduced visibility remarkably.

The necessary air velocities ≥ 1 m/s require pressure differences between both tubes in the range of 60 Pa and more. Due to this fact, sliding doors seems to be preferable as the requirement of keeping the door-opening force <100 N can be achieved more easy.

6. REFERENCES

[1] Gobiet G., Langner V., Hagenah B.: New Semmering Base Tunnel, Project description and ventilation concept; Proceedings of the 6th Symposium 'Tunnel Safety and Ventilation', 23-25 April 2012, Graz Austria, ISBN 978-3-85125-210-1, pp 1-8, 2012

[2] Sturm P. et. al: Full scale fire experiments for smoke propagation investigations in long rail tunnels; Proceedings of the 17th Int. Symposion on Aerodynamics, Ventilation & Fire in Tunnels, 13-15 September 2017, Lyon, France

[3] Sturm P., Thaller T., Rodler J.: Smoke propagation in the region of cross-passages in long railway tunnels – Results from full scale tests; Geomechanics and tunnelling = Geomechanik und Tunnelbau. Volume 10, Issue 6, S. 694-699

HYDRAULIC ISOLATION FROM AIR ENTRAINMENT AS A NOVEL SMOKE CONTROL MEASURE FOR ADHERED SPILL PLUMES

M. Houchin, M. Gilbey
WSP Ltd, Guildford, United Kingdom

ABSTRACT

Over-site development (OSD) above railway stations presents opportunities to better integrate transportation into an urban environment. The OSD can be a combination of above or within any station development and in either case can affect the smoke and heat control within the station, as well as reduce the amount of space available for plant and other railway systems.

This paper describes a situation where proposed OSD would penetrate into a station volume giving rise to challenges in controlling smoke. In overcoming this challenge a novel semi-passive smoke control measure for adhered spill plumes was investigated and is presented within this paper. Fire Dynamics Simulator models are presented which demonstrate the potential effectiveness of hydraulic isolation of the rising spill plume in reducing the total volume of smoke to be extracted from a high level smoke reservoir in a larger atrium.

Rail specific applications are discussed, including the pairing of jet fans to impose a preferential flow towards the edge spill chimney. A design formula is presented to determine the appropriate width spill chimney for the natural ventilation of smoke.

Keywords: Smoke Control, Spill Plumes, Railway Station Ventilation

1. INTRODUCTION

This paper aims to investigate the potential for a novel passive smoke control measure using spill plume chimneys to hydraulically separate the rising plume from the ambient air that is usually entrained within it. The application is similar to that of a channelling screen.

Passive smoke control measures such as channelling screens have been previously been used to reduce air entrainment into thermal spill plumes (Law, 1986), and by proxy, to reduce the extract mass flow rate required to maintain a constant smoke layer depth. Empirical design formulae for the performance of such screens were not considered as applicable to the application to the geometry and smoke control concept that was being considered for this application. The performance of the proposed smoke control system was therefore analysed using Computational Fluid Dynamics (CFD).

Despite the use of CFD in this application, the use of empirical formulae remains a fast and robust alternative to the use of CFD (Morgan et al., 1999). In recognition of this design formulas for determining the appropriate chimney width for natural ventilation of the smoke were developed and are presented, along with possible applicability to mechanically assisted exhaust.

2. SMOKE SPILL PLUMES

Transverse-type smoke management systems have the principal aim of extracting a sufficient volume of smoke from a reservoir to maintain a defined boundary between the smoke and the evacuation environment below it. This results in a tenable region below the smoke layer where evacuees can have sufficient visibility to discern their evacuation route and be in an environment where they are unlikely to be overcome by the presence of asphyxiating gasses and untenably high smoke temperatures.

The achievement of a smoke interface above the evacuation route can be achieved via two methods. Firstly, the volume of smoke entering the ceiling reservoir can be decreased, and secondly, the mass flow rate of the high level smoke extractor or natural vent can be increased. Decreasing the volume of smoke entering the ceiling reservoir in a free plume is often not possible because the mass flow rate of smoke entering the ceiling reservoir is a function of parameters that cannot be easily controlled in a fire scenario (namely the convective component of the fire heat release rate and the room dimensions). Increasing the mass flow rate of the extract or vent system is relatively simple, therefore, this is typically the primary method for controlling the depth of the smoke ceiling reservoir.

The mechanics of air entrainment into an adhered spill plume have been understood to a good degree of engineering usability for many decades. Numerous analytical models exist for predicting the mass flow rate of smoke entering a ceiling reservoir and they are used extensively in the design of smoke extract systems. Thermal spill plumes can be divided into two categories; adhered spill plumes and free spill plumes (Harrison & Spearpoint 2009). Adhered plumes are characterised by a continuous wall extending above the vertical opening into the atrium which acts to adhere the smoke to it. Free plumes in comparison are created where there is no vertical wall to bound the flow above the vertical opening.

The typical spill plume comprises of three components. Firstly a ceiling reservoir is generated from the upward motion of the smoke which starts to fill the room with smoke. This reservoir propagates along the ceiling until it reaches the opening of the room into a larger space, commonly known as the Atrium. As the flow exits the room, it rotates out of the opening and towards the ceiling of the atrium, which is commonly referred to as the rotating spill region. There is a minor amount of air entrainment within this region and as the smoke rises, further entrainment occurs within the spill plume, until the flow reaches the full height of the Atrium, whereby a secondary ceiling reservoir is formed.

3. PROPOSED SPILL PLUME MITIGATION MEASURES

For this application there was a situation where a portion of the platform was covered by OSD leaving a clear height of about 6 m from the platform to the OSD. The concourse around the OSD was a good deal higher at about 17 m. The smoke extract system was located at the second and higher roof level. It might have been possible to extend smoke ducts down to the lower height platform level, but this would have reduced the space available for OSD. The smoke was therefore allowed to travel along the lower height area and then rise to the upper ceiling.

Allowing the smoke to travel along the ceiling and then rise to the upper ceiling created a significant amount of smoke. As the smoke rolls around the edge of the lower reservoir it tends to entrain more outside air. The resulting volume of smoke threatened to make the smoke control system very large. Methods to reduce the amount of air entrainment were therefore reviewed.

Reducing the volume of smoke to be extracted in the atrium ceiling reservoir was achieved by hydraulically separating the rising spill plume from the ambient air by way of an isolation chimney. Smoke that flows through the vertical opening and into the atrium is captured by the chimney, therefore only the volume of smoke that passes through the opening needs to be extracted or vented to the atmosphere (plus some small volume of air entrained in the rotating spill plume).

The mass flow rate of smoke that needs to be extracted from the atrium smoke reservoir to maintain a constant smoke layer depth (given a constant fire heat release rate), with the use of a spill plume chimney, is a function of the mass flow rate of smoke leaving the vertical opening, the width of the spill plume chimney and the height of the spill plume chimney above the vertical opening.

Figure 1 shows the typical presentation of an adhered spill plume. Note the four stages of the adhered spill plume; stage A is the axisymmetric plume originating at the heat source, stage B is the flowing smoke layer in the fire origin room, stage C is the adhered spill plume and stage D is the horizontal ceiling flow in the atrium. The proposed smoke control measure is chiefly concerned with the elimination of stage C. There is then the possibility to allow the smoke to enter the atrium at high level, bypassing stage C, with the atrium extract grille requiring to extract approximately the same volume of smoke as is flowing out of the fire origin room (plus some small volume of air entrained in the rotating region). This represents a reduction in the mass flow rate required by the following as per Harrison & Spearpoint (2010):

$$m_{p,3D} = 0.3Q_c^{1/3}W_s^{1/6}d_s^{1/2}z_s + 1.34\dot{m}_s \quad (1)$$

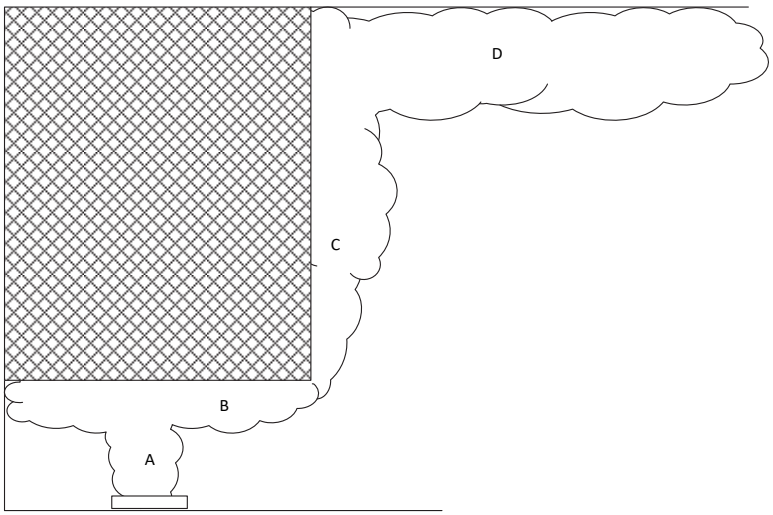

Figure 1: Typical adhered spill plume configuration

Figure 2 shows the proposed mitigation measure to eliminate the air entrainment into the adhered spill plume. The adhered spill plume is hydraulically separated from the ambient air by way of a chimney extending to the roof of the atrium. Whilst the chimney also takes up space, it was calculated to take up less space than dropper ducts passing down through the OSD, but could also be made of transparent toughened glass, thus still allowing natural lighting and views through the OSD. In effect, the chimney became a false or double façade the type of which is used in some buildings to reduce heat losses or gains to the occupied spaces.

Ideally, the chimney would incorporate mechanical ventilation to extract the smoke directly from the rotating spill edge region. In the event that smoke does spill over the edge of the spill edge chimney, mechanical ventilation at the roof (installed for the case of a free plume within the atrium) can be activated in order to extract smoke from the upper ceiling reservoir. Balancing of the ventilation is unneeded due to the large delta between the spill edge chimney and atrium flow rate.

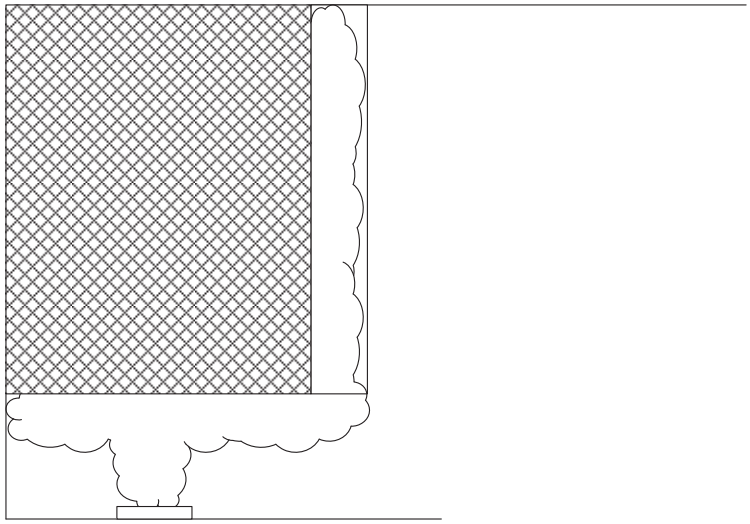

Figure 2: Proposed mitigation measure for adhered spill plumes

BRE report 368 (Morgan et. al, 1999, p. 23) gives some indication that boundary edge exhaust slots can be used to prevent the transition of smoke from the fire compartment to the atrium, however no calculation method is given to determine the width of the slot exhaust.

4. FDS MODELLING METHOD

Fire Dynamics Simulator was used to simulate the adhered spill plume problem. A simplified case of a spill plume from an enclosed room into a larger atrium was set up with an adhered plume chimney to extract smoke rising from the spill edge. This represents a case comparable to the experimental set up from Poreh et al. (2008) and the FDS model from Tilley & Merci (2009). An 'open' boundary condition was applied to the lower section of the atrium walls to allow a make-up air path for the extract vent, similar to previous experimental configurations.

The computational domain of the FDS model measured 30 m wide, 20 m high and 25 m deep, with the fire origin room having width and depth of 10 m and a ceiling height of 5 m (**Figure 3**).

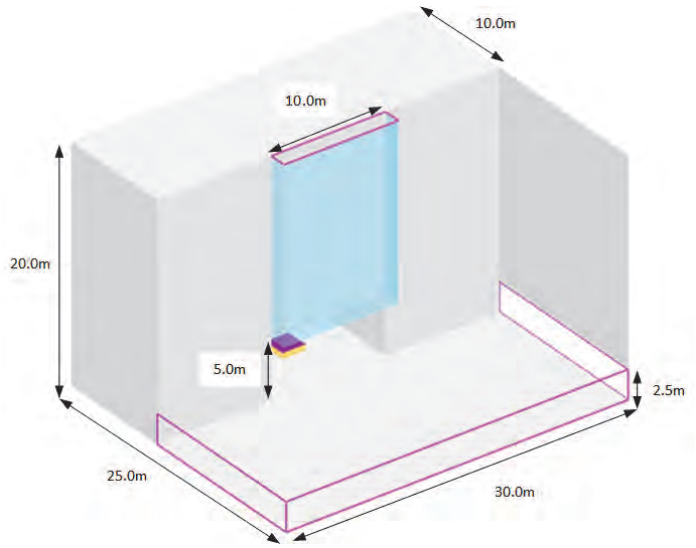

Figure 3: FDS representation of the atrium set up. A 1.5 m deep edge spill chimney has been included

The depth of the chimney was increased by one grid cell per simulation, up to a depth of $W_s/W_c = 5$ m, where W_s is the width of the room opening and W_c is the depth of the chimney. This represents a range of chimney widths to determine a relationship between chimney width and smoke entrained into the spill plume. Simulations were run until the smoke layer interface was constant. Initially the spill plume entrainment was calculated using equation 2, serving as the initial extract rate for the roof exhaust patch. The depth of the smoke layer in the FDS model was then compared to the design formulae to ensure that the correct flow rate was imposed on the roof exhaust grille.

The steady state fire heat release rate was set to 1 MW, with a soot yield of 0.1 kg/kg and a mass extinction coefficient of 8700 m^2/kg.

Subsequent simulations were completed with edge spill chimneys. The mass flow rate of the roof extract grille was iterated until the smoke layer depth matched the original adhered plume simulation. This allowed for a direct relationship between the adhered plume entrainment and chimney width to be derived.

The smoke layer interface was characterised by the iso-surface of 1°C temperature rise above ambient. This is the definition used by Kumar, Thomas & Cox (2008). This was also visually verified with the smoke visibility.

The chimney opening was set to an open boundary within FDS, with a damper placed above the upper ceiling smoke reservoir within the atrium to measure the spill plume entrainment rate for various chimney widths. In practical applications, the edge spill chimney would have a damper placed at the opening and be connected to a mechanical ventilation system to extract smoke within the rotating spill region.

5. 3D ADHERED SPILL PLUME RESULTS

Initially a simulation was completed to verify the modelling methodology. A mass flow rate was calculated that maintained a constant clear height above the vertical opening of 5 m, with the post-processed iso-surface of 1°C temperature rise indicating the smoke layer interface.

Figure 4 shows the smoke layer interface defined by the iso-surface of 1°C temperature rise, averaged over the last 50 seconds of simulation time. The smoke layer interface is maintained at 5 m above the vertical opening, suggesting that the FDS model is well matched to the design formula given in equation 2.

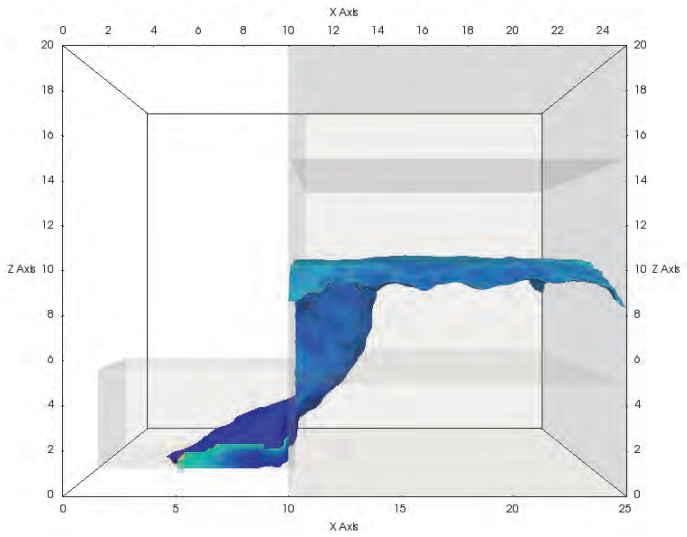

Figure 4: Average iso-surface of a 1°C temperature rise characterizing the smoke layer interface. Averaging is taken over the last 50 seconds of the simulation

The width of the chimney was increased by 0.2 m per simulation, with iterations of the mass flow rate at the atrium being performed until the clear height above the vertical opening was equal to 5 m. Increasing the width of the chimney reduces the mass flow rate required at the atrium roof to maintain a constant smoke layer depth.

Figure 5 shows the mass flow rate ratio m_c / m_{p3D} as a function of the chimney width, with the width of the room opening W_s at 10 m. A proposed analytical function has been fit to the data:

$$a = e^{-0.28W_cW_s} \tag{2}$$

Such that:

α = ratio of extract rate with (m_c) and without chimney (m_{p3D}) for specific opening width.

w_c = width of edge spill chimney.

w_s = width of room opening.

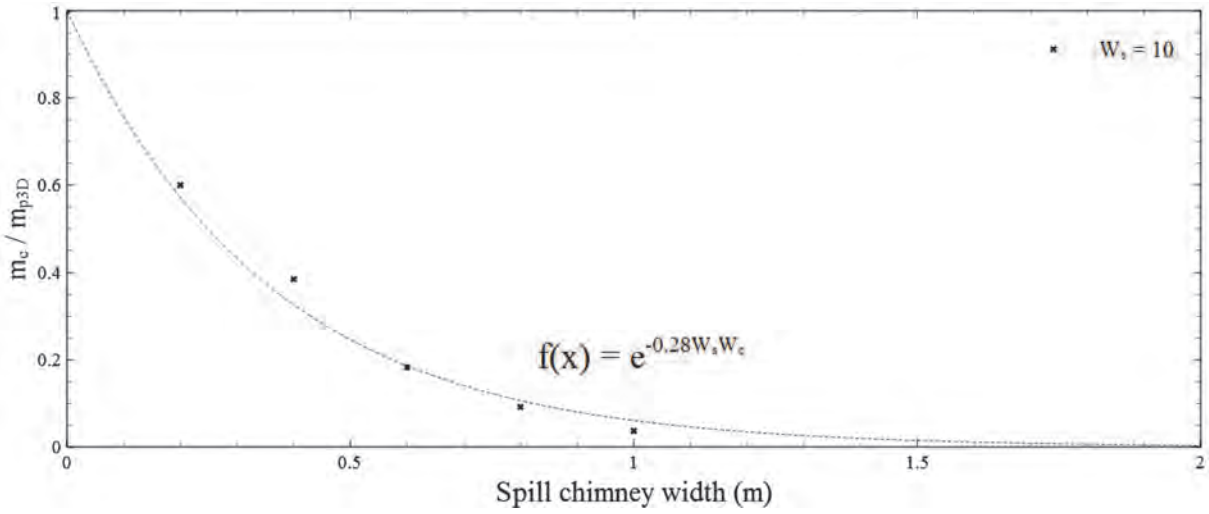

Figure 5: Extract rate ratio as a function of spill chimney width

It can be seen from Figure 5 that the chimney was capable of making a significant reduction in the required mass flow rate of smoke exhaust from the system. Chimney widths of up to 1 m appeared to be optimal.

Equation 2 has only been validated for the specific room dimensions described in Figure 3 with a fire size of 1 MW. Therefore further work is required to determine the applicability of the above function to generic fire and room sizes.

6. RAIL SPECIFIC APPLICATIONS

This method of air entrainment isolation was applied to a railway station where was a possibility of a train fire underneath an Oversite Development (OSD) which protruded into the station volume. Either smaller chimneys could be placed on either side or in this application, due to site constraints, the chimney was placed on one side and jet fans used to direct the smoke within the trackway (bounded by downstands) towards the edge spill chimney. Powered ventilation was then be added to extract the smoke within the chimney, expelling it to the outside air. Figure 6 shows the typical configuration of the jet fan and chimney system in operation.

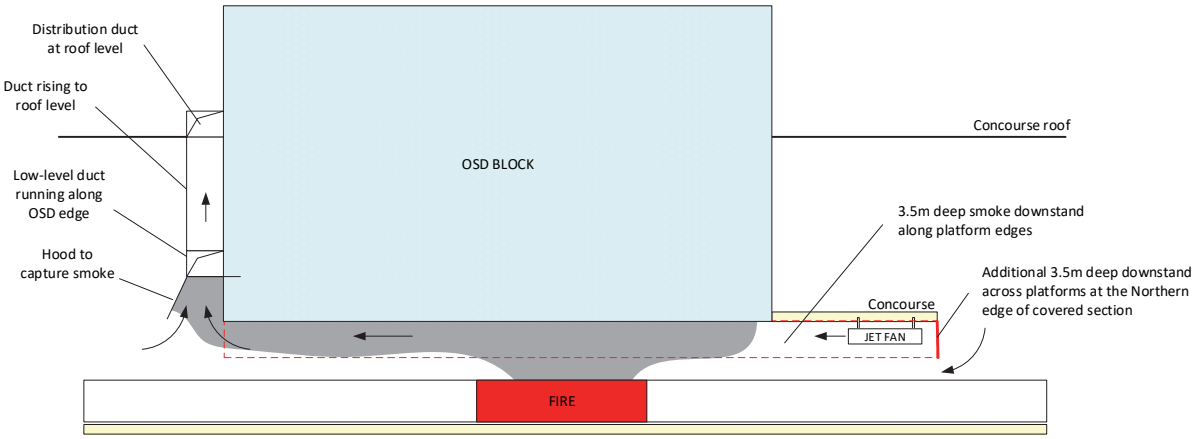

Figure 6: Edge spill chimney with jet fans to direct flow towards specific edge

The above configuration was tested within FDS to verify the applicability of the theory to a fire scenario underneath an OSD within a railway station. **Figure 7** shows the effectiveness of the proposal, with the entirety of the smoke being extracted.by the edge spill chimney and the jet fans.

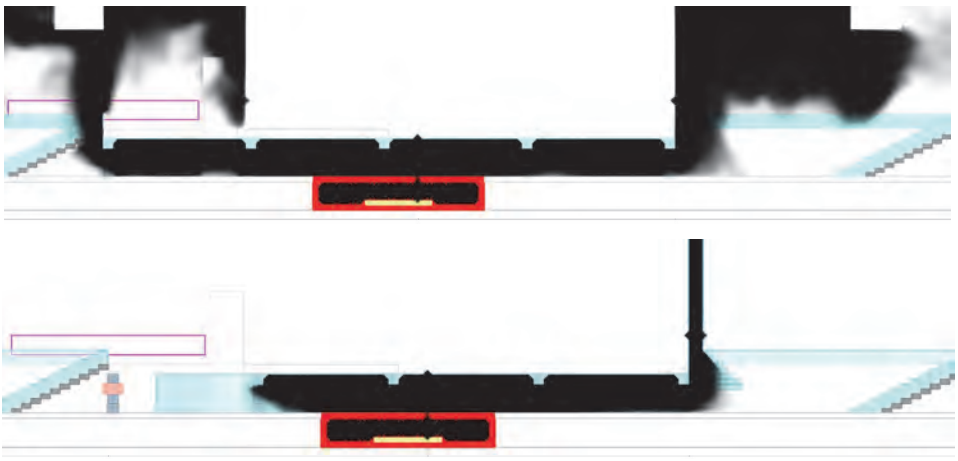

Figure 7: Comparison of smoke concentration within a station volume with a spill plume (top) and edge spill chimney installed with jet fans (bottom)

The visibility contours shown in Figure 8 demonstrate the predicted effectiveness of the jet fan and edge spill chimney combination. The top image shows the visibility contours after 1200 seconds for the case with the smoke spilling off the edges of the concourse and into the concourse roof area. Regions of smoke approaching 7.5 m of visibility was predicted on the concourse connecting bridge. The concourse to the right of the image was also predicted to start to be exposed to smoke. In comparison, the bottom image shows the effect of adding the edge spill chimney and jet fans. The concourse was predicted to have a smoke visibility of above 30 m throughout the whole station, with all of the smoke being extracted from the edge spill chimney.

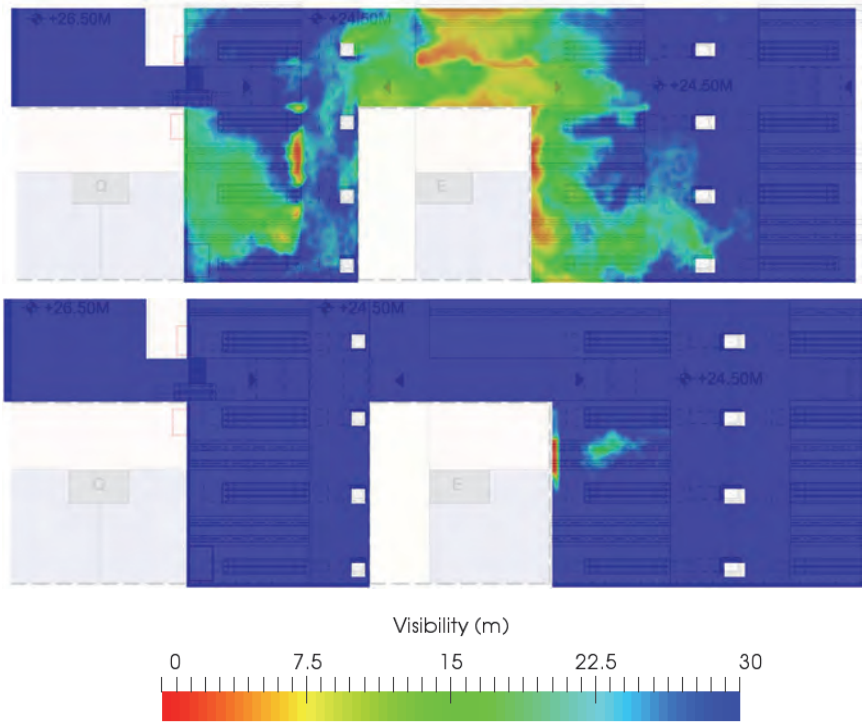

Figure 8: Comparison of visibility for fire scenario under an OSD using roof extract after spill edge (top) and extract from a spill edge chimney (bottom)

7. CONCLUSION

Fire Dynamics Simulator models have been presented to demonstrate the effectiveness of hydraulic isolation of the rising spill plume in reducing the total volume of smoke to be extracted from a high level smoke reservoir in a larger atrium.
Rail specific applications have been discussed, including the pairing of jet fans to impose a preferential flow towards the edge spill chimney.
A design formula has been presented to determine the appropriate width spill chimney for the natural ventilation of smoke.

8. BIBLIOGRAPHY

Harrison, R., & Spearpoint, M. (2009). Characterisation of balcony spill plume entrainment using physical scale modelling.

Harrison, R., & Spearpoint, M. (2010). Physical scale modelling of adhered spill plume entrainment. Fire Safety Journal, 45(3), 149-158.

Harrison, R., & Spearpoint, M. J. (2009). A review of simple entrainment calculation methods for the thermal spill plume. International Journal on Engineering Performanced-Based Fire Codes. Accepted for publication.

Kumar, S., Thomas, P. H., & Cox, G. (2008). Novel analytical approach for characterising air entrainment into a balcony spill plume. Fire Safety Science, 9, 739-750.

Law, M. (1986). A note on smoke plumes from fires in multi-level shopping malls. Fire Safety Journal, 10(3), 197-202.

Morgan, H. P., & Gardner, J. P. (1990). Design principles for smoke ventilation in enclosed shopping centres. Garston, UK: Building Research Establishment.

Morgan, H. P., Ghosh, B. K., Garrad, G., Pamlitschka, R., De Smedt, J. C., & Schoonbaert, L. R. (1999). Design methodologies for smoke and heat exhaust ventilation. BRE 368, Construction Research Communication Ltd, Londres, R.

Poreh, M., Marshall, N. R., & Regev, A. (2008). Entrainment by adhered two-dimensional plumes. Fire Safety Journal, 43(5), 344-350.

Tilley, N., & Merci, B. (2009). Application of FDS to adhered spill plumes in atria. Fire technology, 45(2), 179-188.

9. NOMENCLATURE

α ratio of mass flow rate extraction with and without spill chimney

d_s Flowing layer depth of smoke ceiling reservoir (m)

$\dot{m}_c$ Mass flow rate requires to maintain an atrium smoke layer depth Z_s with chimney width (m^3/s)

$\dot{m}_{p3D}$ Mass flow rate required to maintain an atrium smoke layer depth Z_s with a 3D spill plume (m^3/s)

Q_c Convective component of heat release rate of fire (kW)

W_c Width of spill plume chimney (m)

W_s Width of opening of fire origin room (m)

Z_s Reattachment height of spill plume above opening (m)

FINDINGS ABOUT THE COMPLEXITY AND CRITICAL FACTORS REGARDING INACCURACY OF DETERMINING THE INSTALLATION EFFICIENCY OF JET FANS

Thomas Pleninger
Lechner & Partner ZT GmbH, Austria

ABSTRACT

This paper deals with the challenges of determining the installation efficiency of jet fans in tunnels and analyses different methods in terms of effectiveness and accuracy.
In most cases, the number of jet fans in a tunnel is a tradeoff between technical and economical aspects. The definition of an appropriate installation factor in ventilation design is sometimes difficult, since not all governing factors are known by the time the ventilation design is carried out. Also, there is little research available on how to choose an appropriate installation factor for a given tunnel geometry. Thus, the ventilation designer's only chance is to consider a very conservative factor, often leading to excessive reserves. This approach has obviously a negative economic impact.
For the current paper, the installation factors have been determined experimentally in the new-built tunnels of "Tunnelkette Klaus" (A9, Austria). In order to create a methodology for other tunnels, a CFD model was developed using ANSYS CFX.
The measurements showed a significant sensitivity of the results to a variety of unexpected factors. Particularly the way of determining the static pressure was critical. Furthermore, accumulated measurement error can be high, as other measured values (e.g. air velocity, values for determining air density, cross section area of the tunnel) also have to be considered.
For CFD simulations, mesh quality, turbulence models, boundary conditions (especially those for the jet fan) and the method of determining the jet fan's thrust can have a severe influence on the resulting installation efficiency. Eventually, the experimental data showed good agreement with the model-based findings. Hence some best practices and guidelines are worked out.

Keywords: installation efficiency, jet fan, longitudinal ventilation, tunnel ventilation

1. NOTATION

Latin:

A	m^2	cross section area
c	$m\ s^{-1}$	absolute velocity
F	N	thrust
k	-	installation efficiency
n	s^{-1}	rotation speed
no	-	number
p	Pa	pressure
P	kW	power transferred to fluid (jet fan)
Q	$m^3\ s^{-1}$	volume flow (jet fan)
T	°C	air temperature
u	$m\ s^{-1}$	blade linear velocity
v	$m\ s^{-1}$	airflow velocity

Greek:

β	°	relative flow angle (jet fan)
Δp	Pa	pressure difference
ζ	-	hydraulic resistance
λ	-	Darcy friction factor
ρ	$kg\ m^{-3}$	air density
ψ	-	load coefficient (jet fan)

Indices:

0	reference state
2	outflow
JF	jet fan
MS	at/over measured section
t	total
th	theoretical
T	tunnel
TS	test stand
u	circumferential

2. INSTALLATION EFFICIENCY OF JET FANS

This section gives a brief overview of research on the installation efficiency of jet fans.

Kempf (1965) investigates the installation efficiency of jet fans in tunnels with a rectangular cross section using a model-geometry. The resulting installation efficiencies depend on the distance of the jet fan to the wall and are all higher than 0.83 for a geometry without niches. Also working with model geometry, Rohne (1988) mechanically measures the friction on a wall (flat surface) caused by one to four parallel jet flows with a margin of error of ± 10%. A comparison of his work can be found in his third paper on the topic (Rohne, 1988), showing lower friction forces per jet with increasing number of jets. He also investigates the losses of a single jet at a vaulted ceiling using a similar method (Rohne, 1991). Martegani et al. (1994) investigate the installation efficiency of jet fans in ANAS 505 (Italian tunnel profile) tunnels using a wind-tunnel model. The resulting efficiencies are in good agreement with Kempf (1965), while further results show no dependency on tunnel Reynolds number and decreasing efficiency with increasing swirl. A jet fan manufacturer suggests using a diagram to determine the installation efficiency depending on the distance of the jet fan to the wall (Bopp, 2003). Similar to the findings from Kempf (1965), it ranges from 0.83 (jet fan touches the wall) to 0.99. Beyer et al. (2016) have conducted measurements in two tunnels and developed a CFD-model based on their collected experimental data. Here the installation efficiencies are up to 20% lower than those mentioned by Kempf (1965).

3. MEASUREMENTS

Measurements were carried out in July 2017 in the new-built tunnels of "Tunnelkette Klaus" (Falkensteintunnel, Speringtunnel, Klauser Tunnel; A9, Austria), while four different measurements in Klauser Tunnel are presented here.

3.1. Determination of installation efficiency

The definition of momentum transferred from the jet fans to the tunnel, the thrust in tunnel,

$$F_T = \frac{\Delta p_{MS} + \zeta_{MS} * \rho * 0{,}5 * v_T^2}{no_{JF}} * A_T \tag{1}$$

is determined from the pressure difference, tunnel airflow velocity and air density (by measuring air pressure and temperature) using a similar method as in Beyer, et al. (2016) based on the theoretical background in Meidinger (1964). The installation efficiency

$$k = \frac{F_T}{F_{JF,TS} * \frac{\rho}{\rho_0} * \left(1 - \frac{v_T}{v_{JF}}\right)} \tag{2}$$

is the fraction of the thrust in tunnel F_T and the jet fan's thrust at the test stand $F_{JF,TS}$ – with corrections for air density and the velocity quotient.

3.2. Fan data

A summary of jet fan specification (Kolkman & Van Vemden, 2016) can be found in the table below, while some cells contain two values: in/against preferred flow direction.

Table 1: Jet fan specifications

fan diameter	1200	mm
nominal thrust	835	N
nominal rotation speed	1465	r min^{-1}

nominal shaft power	18.5	kW
shaft power at test stand	18.2/18.4	kW
thrust at test stand $F_{JF,TS}$	888/855	N

3.3. Measurement set-up and taking

For determining the installation efficiency experimentally, the following measured quantities were recorded: pressure difference Δp, tunnel airflow velocity v, air temperature T and air pressure p. The set-up can be seen in the figure below, while measurements were carried out over either one or two pairs of jet fans. In the case of lay-bys in the measured section, the section is extendend, to ensure a distance of 100 m from the lay-by to the end of the measured section.

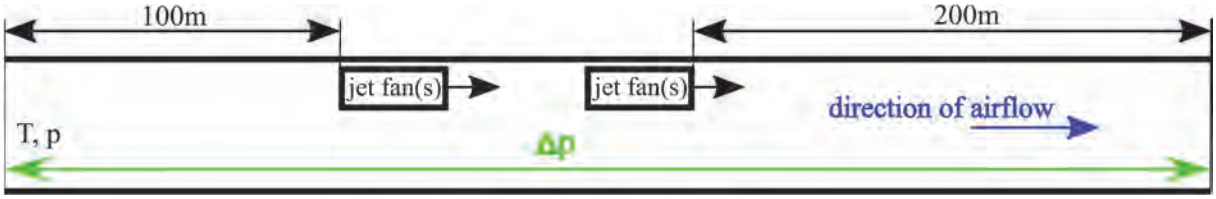

Figure 1: Measurement set-up

Eight sets of measurements in four different measured sections have been carried out in Klauser Tunnel: four for determining hydraulic resistance of the measured section, and four with jet fans in the corresponding section running at nominal speed for determining the thrust in tunnel, while tunnel airflow direction has always been in driving direction. Air pressure and temperature have been taken at the beginning of each measurement cycle, while pressure difference and tunnel airflow velocity were recorded every second and then averaged over a period of 10 minutes for thrust-measurements and 15 minutes for hydraulic resistance-measurements. Tunnel airflow velocity has been measured using either calibrated tunnel sensors (A) or using a grid of 20 vane anemometers (B). All anemometers have been calibrated, with the calibration data being considered in measurement data analysis. To ensure that only static pressure is taken into account, the end of each hose connected to the differential pressure meter has been placed inside an otherwise airtight junction box with several 0.5 mm-holes on its bottom.

Table 2: Measurement equipment

measured quantity	measurement device	range	calibration error	unit
pressure difference	Halstrup Walcher P26	-50 – 100	±0.3	Pa
air pressure	Greisinger GTD 1100	300 – 1100	±1.5	hPa
air temperature	Greisinger GTD 1100	-10 – 50	±0.6	°C
tunnel airflow velocity (A)	tunnel sensors (Durag)	-40 – 40	±0.2	$m\ s^{-1}$
tunnel airflow velocity (B)	Schiltknecht MiniAir64 Makro	0 – 20	±0.2 ±1.5% mv.[1]	$m\ s^{-1}$
tunnel cross section area	according to documentation	53.7	+0.5 / -1.4	m^2

3.4. Results

Measurement results show installation efficiencies of 0.83 and larger. In general, efficiencies tend to be higher, when only one pair of jet fans was investigated. The influence of tunnel airflow velocity on the installation efficiency was found to be insignificant. The Darcy friction factor is higher in measurements 2 and 3, as they include a lay-by in the measured section. Differences between the measurements where the calibrated tunnel sensors were used (A) for tunnel airflow velocity measurement and those were a grid of 20 anemometers was used (B) are minimal.

Results in Table 4 (B1) have been obtained by averaging the anemometers' values, while in Table 5 (B2) a CFD simulation has been used to calculate the average airflow velocity in tunnel. So, the geometry of the grid of 20 anemometers has been chosen well, as differences in results are very small. Table 4 and Table 5 show slightly higher measurement errors, which is caused by slightly higher calibration errors of the anemometers.

[1] of measured value

Table 3: Measurement results (A)

No.	Jet fan no.	v_T in m s^{-1}	F_T in N	λ	k	Accumulated measurement error		Accumulated measurement error and confidence intervals	
1	1. 2	2.27	640	0.0134	0.833	-6.0%	+5.1%	-8.3 %	+7.7%
2	3 – 6	3.36	612	0.0199	0.852	-7.0%	+6.4%	-9.3%	+9.2%
3	7. 8	1.97	677	0.0203	0.887	-7.1%	+6.6%	-11.2%	+11.6%
4	9 – 12	4.47	573	0.0159	0.845	-7.3%	+6.6%	-8.0%	+7.5%

Table 4: Measurement results (B1)

No.	Jet fan no.	v_T in m s^{-1}	F_T in N	λ	k	Accumulated measurement error		Accumulated measurement error and confidence intervals	
1	1. 2	2.29	637	0.0122	0.842	-6.3%	+5.5%	-8.5 %	+8.1%
2	3 – 6	3.30	603	0.0188	0.838	-7.6%	+7.4%	-9.8%	+10.2%
3	7. 8	2.00	675	0.0189	0.886	-7.5%	+7.3%	-11.5%	+12.4%
4	9 – 12	4.52	578	0.0163	0.842	-8.7%	+8.7%	-9.5%	+9.8%

Table 5: Measurement results (B2)

No.	Jet fan no.	v_T in m s^{-1}	F_T in N	λ	k	Accumulated measurement error		Accumulated measurement error and confidence intervals	
1	1. 2	2.31	637	0.0120	0.842	-6.3%	+5.5%	-8.5 %	+8.1%
2	3 – 6	3.32	603	0.0185	0.839	-7.6%	+7.4%	-9.7%	+10.1%
3	7. 8	2.02	675	0.0186	0.886	-7.4%	+7.3%	-11.5%	+12.3%
4	9 – 12	4.55	578	0.0160	0.843	-8.7%	+8.7%	-9.5%	+9.8%

3.5. Measurement error and measurement uncertainties

In general, two kinds of measurement uncertainties were evaluated for installation efficiency: accumulated measurement (calibration) error and 95%-confidence intervals. The former was evaluated using the measurement error of all the instruments used, while the latter has been determined for averaged values – pressure difference and tunnel airflow velocity. As the time used for averaging is large enough, the influence of the confidence intervals to the total measurement uncertainties is negligible in most cases.

3.6. Pressure measurement inaccuracies

The variation of confidence intervals in different measurements is mainly caused by pressure signal quality (see Figure 2) showing a part of the pressure signal of two measurements.

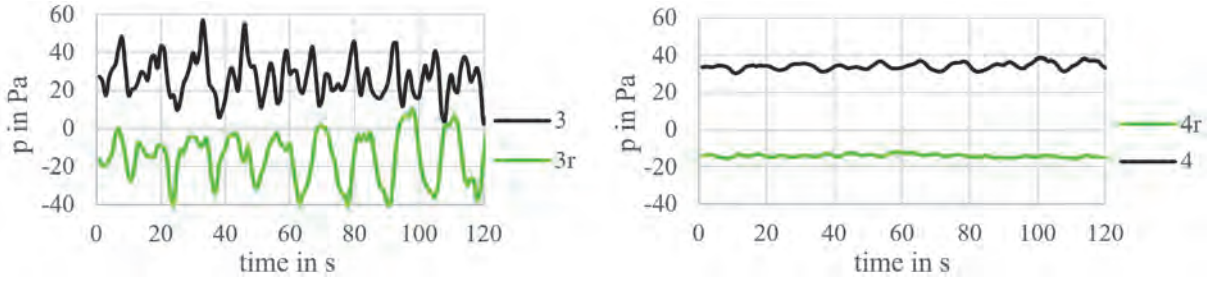

Figure 2: Pressure signal measurement 3 (left), pressure signal measurement 4 (right)

Green curves are measurements for determining hydraulic resistance, black curves for thrust in tunnel. Weather outside the tunnel might have an influence on the pressure measurement: All the measurements were carried out in the afternoon/evening in summer, while a thunderstorm was taking place during measurement 3. Confidence intervals increase from measurement 1 to 3, having its lowest value in measurement 4 (after the thunderstorm), see Table 3 to Table 5.

4. NUMERICAL MODEL

4.1. Geometry and meshing

A section of 480 m of the Klauser Tunnel east-tube – starting from the entrance portal – has been used for the model, including one pair of jet fans. The tunnel cross section profile has been extruded along a 3D-path provided by the tunnel construction company. The fluid volume includes the jet fans' silencers. The mesh, which can be seen in Figure 4, has been generated by ANSYS Meshing only using the "sweep" method resulting in 99.47% hexa-elements, the rest being wedges (3 sided prisms).

Figure 3: Silencer/fan housing inside (left) and outside (middle), jet fans in Klauser Tunnel (right)

Table 6: Mesh quality

	average	maximum	minimum
Skewness	0.13	0.69	-
Aspect ratio	25	752	-
Orthogonal quality	0.96	-	0.35

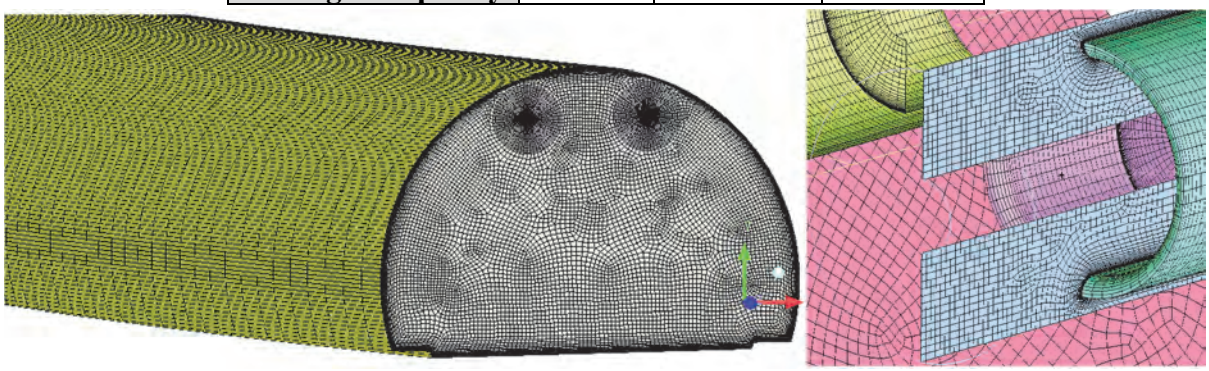

Figure 4: Mesh (left), mesh detail (right)

4.2. Boundary conditions and models

For the tunnel flow, a velocity inlet and a pressure outlet are used. Jet fans are modeled using velocity inlets/outlets (with a constant volume flow) and smooth no-slip walls, while data to calculate the boundary conditions (velocity components) is obtained from the jet fan's test stand report (Kolkman & Van Vemden, 2016). In addition, the fact that the fans were installed with different preferred flow direction is taken into account. The circumferential velocity component of the jet fans is calculated based on a relative outlet flow angle of β_2=27° (Fernández Oro, et al., 2009). The tunnel wall is modelled with a roughness of 2 mm. For the incompressible fluid, the kω-SST model with automatic wall functions is used.

4.3. Postprocessing

Thrust in tunnel is determined by obtaining mass-flow averaged static pressure at the same distances to the jet fans as in the measurement (see Figure 1). Since the simulation includes the

silencers, the jet fans' thrust has to be determined: It is calculated by evaluating the mass flow averaged dynamic pressure at the exit-plane of the silencers. Further calculations are carried out according to section 3.1.

4.4. Results

The simulations show an installation efficiency of 0.840 for a tunnel speed of 2.27 m s^{-1}, while the thrust in tunnel is 628N. More detailed results and data on critical factors can be found in the following sections. RMS-residuals were in the order of magnitude 10^{-5}, while simulations usually converged within less than 100 iterations.

4.5. Influence of mesh quality

For a mesh independence study four different grids were generated (see Figure 5). When looking at the results, the difference between the finer meshes (~10^7 and ~$2*10^7$ nodes) is only 0.07% for installation efficiency and 0.15% for thrust in tunnel. Consequently, the mesh with ~10^7 nodes has been used for all further calculations to save computation time. However, it was also noticed that results for installation efficiency and thrust in tunnel both decrease significantly when using coarser meshes.

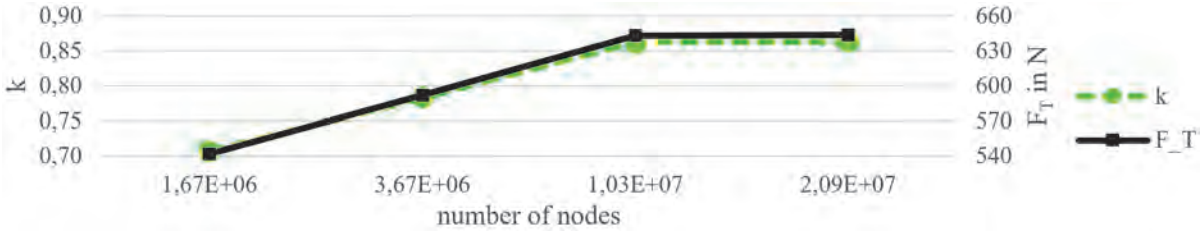

Figure 5: Results of mesh independence study

4.6. Influence of fan model

As no detailed data (e.g. fan curves) on jet fans was available, a very simple fan model – constant volume flow – has been chosen, while volume flow and thus longitudinal and circumferential velocity components differ in the two fans, to take the fact into account that they were installed with counterrotating axes. This section focuses on the importance of the fan model.

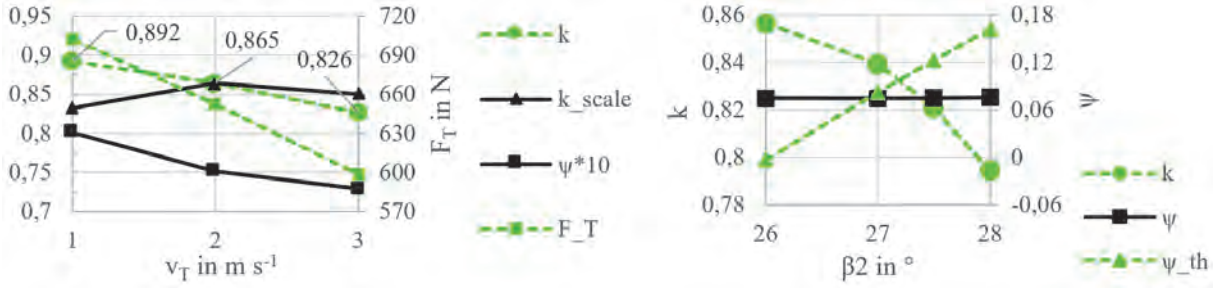

Figure 6: Influence of tunnel airflow velocity (left), influence of swirl (right)

In the left plot, a dependency of the installation efficiency on tunnel airflow velocity can be seen, while when – just for visualization – scaling the installation efficiency with the load coefficient (Carolus, 2013)

$$\psi = \frac{\Delta p_t}{\frac{\pi^2}{2}\rho\, D^2\, n^2} \tag{3}$$

to v_T = 2 m/s (here), there is no such dependency (k_{scale} in Figure 6). The right plot indicates that installation efficiency decreases with increasing swirl. This finding is also confirmed by measurements by Martegani, et al. (1994). In addition to equation 3, the load coefficient from fan velocity calculation (Carolus, 2013)

$$\psi_{th} = \frac{c_{u2}}{0{,}5 * u} \tag{4}$$

has been evaluated at several relative outflow angles to further validate the relative outflow angle of β_2=27° as the relation between those values is plausible.

The effect on different volume flows has been investigated by varying the volume flow through the fan while retaining the flow angles to simulate operation at different rotation speeds. Installation efficiency, thrust in tunnel and power transferred to the fluid (calculated from the jet fan's total pressure rise) have been evaluated: All 3 values increase with increasing volume flow, although at a different rate. In order to adapt the fan model to the different operating point in the tunnel, volume flow has been increased by 4.4% from test-stand values, as this produces thrust conditions similar to the measurements.

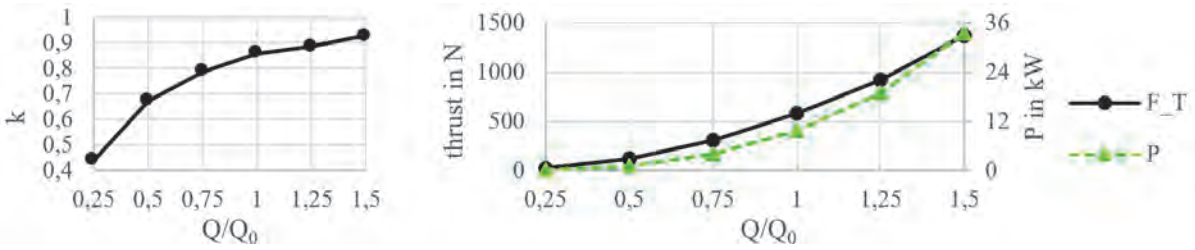

Figure 7: Influence of volume flow

4.7. Contour Plots

Figure 8 shows contour plots. The left image shows airflow velocity in the plane of the jet fans' axes and the right one shows wall shear on the tunnel wall above the fans.

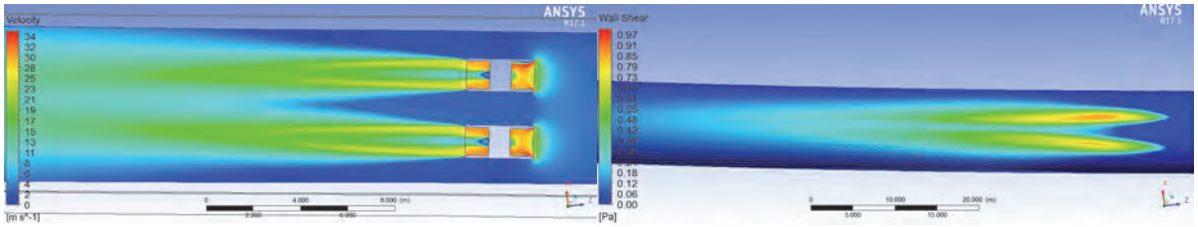

Figure 8: Velocity contour plot (left), wall shear contour plot (right)

The wall shear is asymmetrical, which is caused by the asymmetric boundary conditions of the fans, especially the different circumferential velocity component (see section 4.2 and 4.6). Another influence of the swirl can be seen in the fact that the jets slightly point to each other although jet fans are mounted parallel to the tunnel axis.

5. CONCLUSION, BEST PRACTICES AND FUTUTRE WORK

A comparison of installation efficiencies from measurements and from simulation shows that the measured installation efficiencies are a bit higher, while showing almost no dependency on tunnel airflow velocity. The latter has been published before (Martegani, et al., 1994). Nevertheless, other researchers published other findings: results of measurements and CFD simulations in Beyer, et al. (2016) show a dependency on tunnel airflow velocity. Simulation results in this paper also show a dependency on tunnel airflow velocity which – in this case – can be caused by the fan model, see section 4.6. So, a next step would be including the jet fan's rotor in the simulation.

In general, the number and size of tunnel fittings at the tunnel top near the jet fans can have an influence on the installation efficiency, see the image in Figure 3 for an overview on those fittings in Klauser Tunnel.

For measuring static pressure differences in tunnels, ensuring there are no influences from dynamic pressure is important, while velocity measurements using calibrated tunnel sensors are sufficient. In general, highly precise instruments should be used to keep accumulated measurement error at a minimum. Furthermore, measured values should be averaged over a time of at least 10 minutes, depending on signal quality.

When developing a numerical model for determining the installation efficiency, great effort has to be put into the mesh: no tetra meshes shall be used and a mesh-independency-study is inevitable. In general, all data for boundary conditions should be thoroughly validated, as they can have a great impact on the results, as swirl for instance.

The findings in this paper not only confirm proven methods for determining the installation efficiency, but the numerical model also introduces a methodology for determining it more precisely. Considering the - sometimes contradictory - results of other research that has been conducted in that area, it seems obvious that more research has to be carried out in this relatively small field. However, the economic impact definitely suggests a need for a profound database. Using the methods from this paper for determining the installation efficiency in tunnels with a rectangular profile – including geometries with niches and deflectors – would be a next step.

6. ACKNOWLEDGEMENTS

I want to thank the folks at Lechner&Partner ZT GmbH, especially DI Dr. Guntram Lechner, without whose support this paper would not have been possible.

7. REFERENCES

Beyer, M., Sturm, P., Saurwein, M. & Bacher, M., 2016. Evaluation of Jet Fan Performance in Tunnels. *8th International Conference 'Tunnel Safety and Ventilation'*, pp. 298-315.

Bopp, M., 2003. *Ventilatoren Lieferprogramm Strahlventilatoren.* Zweibrücken: TLT-Turbo GmbH.

Carolus, T., 2013. *Ventilatoren.* 3. Hrsg. Wiesbaden: Vieweg+Teubner Verlag, Springer Fachmedien.

Fernández Oro, J., Argüelles Díaz, K., Santolaria Morros, C. & Ballestores-Tajadura, R., 2009. Impact of the tip vortex on the passage flow structures of a jet fan with symmetric blades. *Proceedings of the Institution of Mechanical Engineers, Part A: Journal of Power and Energy, Vol 223, Issue 2*, pp. 141-155.

Kempf, J., 1965. Einfluss der Wandeffekte auf die Triebstrahlwirkung eines Strahlgebläses: ein Beitrag zur Aerodynamik der Tunnellüftung. *Schweizerische Bauzeitung*, pp. 47-52.

Kolkman, B. & Van Vemden, F., 2016. *Abnahmemessung Strahlventilator JZR 12-18.5/4 A09 Tunnelkette Klaus,* Hengelo, The Netherlands: ZITRON Nederland BV.

Martegani, A., Pavesi, G. & Barbetta, C., 1994. An experimental Study on the longitudinal Ventilation System. *Proceedings of the 8th International Symposium on Aerodynamics & Ventilation of Vehicle Tunnels.*

Meidinger, U., 1964. Längslüftung von Autotunneln mit Strahlgebläsen. *Schweizerische Bauzeitung*, pp. 498-501.

Rohne, E., 1988. The friciton losses on walls caused by a row of four parallel jet flows. *6th International Symposium on the Aerodynamics and Ventilation of Vehicle Tunnels*, pp. 151-164.

Rohne, E., 1991. Friction Losses of a Single Jet due to its Contact with a Vaulted Ceiling. *Aerodynamics and Ventilation of Vehicle Tunnels*, pp. 679-687.

ELECTRIC MOBILITY AND ROAD TUNNEL SAFETY
HAZARDS OF ELECTRIC VEHICLE FIRES

[1]L. D. Mellert, [1]U. Welte, [2]M. Hermann, [2]M. Kompatscher, [3]X. Ponticq,
[1]Amstein + Walthert Progress AG, Switzerland
[2]VersuchsStollen Hagerbach AG, Switzerland
[3]Centre d'études des tunnels, France

ABSTRACT

This experimental study illustrates that severe damage of electric vehicle batteries can immediately lead to uncontrollable fires with high-energy release, strong smoke generation and so far untypical smoke emissions. The experiment was conducted in a real tunnel environment and investigated the effects of a lithium-ion battery used in a full electric vehicle approved for traffic – there were no crash tests with vehicles nor were there any analyses on the probability of such damage. Since potential causes for electric vehicle fires in road tunnels are mechanical (e.g. crash) and thermal (e.g. fire) damage to their batteries, four different scenarios were tested, each following a worst-case approach. The study concludes that the thermal fire hazards of electric vehicles are comparable to those of conventional vehicles. In the immediate vicinity and in unfavourable ventilation situations, however, electric vehicle fires may lead to new and potentially more severe chemical hazards. Analyses point to critical concentrations of heavy metals such as cobalt, lithium and manganese in form of aerosols. These pollutants do not occur in such high concentrations in conventional vehicle fires and are toxic for both humans and the environment. It is assumed that the existing operational and safety equipment in road tunnels is sufficient to cope with these new threats – therefore, no technical adjustments are recommended. Overall, increasing electric mobility will not lead to a reduction of tunnel safety, but in certain aspects, it will change the hazard situation in road tunnels and ultimately will have an impact on incident management in particular.

Keywords: electric vehicles, lithium-ion batteries, experimental measurements, tunnel safety

1. INTRODUCTION

Technical development and the intentional promotion of low-emission vehicles have led to an increasing electric mobility in many European countries. New registrations of electrically powered vehicles are rising steadily in Switzerland, even though their share of the entire motor vehicle fleet remains small (ca. 2%). Virtually all forecasts imply a significant increase of all sorts of electric vehicles; for Switzerland, it is expected that the number of electric vehicles will grow continuously in the years to come, ultimately leading to a penetration rate of over 40% in the year 2050 ([1]). Even though the effective numbers might vary between countries, a high proportion of electric vehicles on European roads and in tunnels must be considered very likely in the future.

1.1. Research questions and project goals

Electric vehicles are defined as vehicles that are powered by electrical energy, encompassing pure battery as well as hybrid electric vehicles. Typically they obtain their energy from high-capacity batteries which, due to their high energy content and highly reactive chemical components, are associated with fire hazards and other chemical or electrical risks ([6];[8]). With increasing urbanisation ([9]) and the observable tendency to shift traffic underground ([2]), the safety question for these new technologies is now being voiced. For special traffic infrastructure

with limited ventilation, escape or rescue possibilities, as is typical in road tunnels, two questions arise regarding the specific hazard situation:

- Do electric vehicle fires in road tunnels cause different hazards compared to conventional vehicle fires?
- Is there a need to adapt technical safety equipment or future operations of road tunnels?

To answer these questions, the characteristics of electric vehicle fires need to be investigated in the real environment of a road tunnel. From literature, only limited information can be derived. Although the safety of electric vehicle batteries is subject to controversial debate in research as well as the media in general, the hazards emanating from such fires in road tunnels have not been examined comprehensively so far ([3];[4]). With respect to road tunnels, possible fire hazards of electric vehicle batteries (e.g. gas emission, smoke development, etc.) are discussed primarily theoretically or with the aid of models and have only been investigated in isolated experiments – and then not in the real environment (see [3];[6];[7]).

In order to close this knowledge gap, the present research project was launched with the support of the Swiss Federal Roads Office (FEDRO) and the French Centre d' Études des Tunnels (CETU). The study was to examine experimentally whether the increasing share of electric vehicles will lead to changing hazards in road tunnels due to their different energy storage systems. Since the majority of electrified vehicles will be passenger cars, the experiment concentrated on these; electrified heavy vehicles and motorcycles were intentionally excluded from the considerations. The project had the following objectives:

1. Experimental analysis of the effects of a typical electric vehicle fire in a road tunnel
2. Description of the different fire consequences of an electric and a conventional vehicle in a road tunnel, due to their energy storage systems
3. Identification of possible impacts on road tunnel operations, and adequate mitigation measures

1.2. Approach and hypothesis

The main difference between a conventional vehicle with an internal combustion engine (ICE vehicle) and an electric vehicle (EV) is, apart from the electrified motor, their energy storage. While the energy of the former is mostly stored in the form of liquid fossil fuels (e.g. gasoline, diesel), the latter uses rechargeable batteries made of highly reactive chemical components. Since the superstructure of both vehicles may be assumed as mainly comparable, the experiment concentrated on the root cause of the hazard differences: the battery.

With this approach, crash and fire tests with complete vehicles were deliberately excluded from the study. Such experiments have already been described in literature, although without special regard to road tunnels ([7];[10]). The main goal, now, was to analyse the greatest possible effects of damaged EV batteries from a passenger car in a road tunnel, hence a worst-case approach. To get significant conclusions, various test scenarios had to be conducted, each maximally damaging a high-capacity battery of a typical EV in a different way. The whole project was grounded on the hypothesis that "*compared to conventional vehicles, electric vehicles lead to increased fire hazards in road tunnels due to their energy storage*".

2. METHOD

The experimental situation had to be established in such a way that the relevant parameters could be recorded correctly. Because influencing factors, such as product-specific protective measures on the battery systems had to be eliminated, individual modules of an EV battery were investigated in the experiment. There was no battery management system to ensure chemical and electrical safety of the modules, and no protective battery housing to guarantee its mechanical safety. The results were then scaled up to the battery level.

2.1. Test material

As rechargeable energy storage systems for EV, the most promising technologies currently are lithium-ion batteries. This term generally refers to batteries, in which the element lithium is used as active material in pure or bound form and where lithium ions move from the anode to the cathode during discharge and back when charging. Because of their high reactivity, lithium-ion batteries tend to develop a thermal runaway when damaged mechanically, thermally or electrically ([11]). The battery then heats up automatically and very quickly (>10 °C/min) through chemical processes, and leaves its stable operating range. Battery fires with large energy release, leakage and gas venting are the consequences. The main goal of the experiment was to investigate these effects of a lithium-ion battery in a road tunnel environment. The battery modules used in the experiment were fully usable and new components of a fully EV that is approved for traffic (see Table 1); they were completely charged (>95%) for the experiment.

Table 1: Characteristics of the investigated lithium-ion battery system

Characteristic	**Description**	
Number of cells	96 cells in 8 modules	
Electrode active material	Anode: Graphite	Cathode: $LiNiMnCoO_2$
Electrolyte	Lithium hexafluorophosphate ($LiPF_6$)	
Energy (gross/net)	33.182 / 27.2 kWh	
Specific energy (gross/net)	0.14 / 0.12 kWh/kg	
Thermal runaway	From 210 °C typical. High charge promotes thermal runaway.	

2.2. Measurement concept

In the event of a fire involving EV, apart from the conventional combustion gases (e.g. CO, CO_2 etc.), the formation of new, highly toxic pollutants is of special interest. Because of this theoretically expected difference to conventional vehicle fires, the experiment focused specifically on gas analysis. Pollutants and aerosols were measured in the test tunnel 160 m downstream of the test site at approx. 1.5 m above road level. In addition, thermal parameters were measured and visual characteristics of the provoked battery fires were recorded on video. The experiment was conducted in the test facilities of VersuchsStollen Hagerbach AG (VSH), which offer a real and safe environment for large fire tests with a reference to road tunnels. The site had a varying cross-section, being 56 m^2 at the test site and 43 m^2 at the measuring site.

The test area had to be constantly ventilated throughout the entire experiment for safety and measurement reasons. In order to control air flow and to prevent dilution by added fresh air after the test site, the bypass (pink) to the main ventilation duct (blue) shown in Figure 1 was closed with a gate during all tests. The measurements of the pollutant concentrations and the flow velocities in the main ventilation section could thus be determined conclusively and reliably.

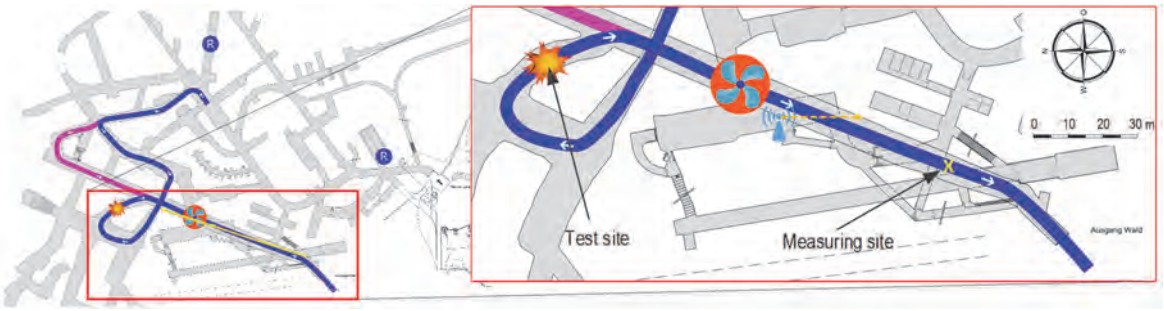

Figure 1: Layout of the test area: test site (fire), main ventilation section (blue) with closed bypass (pink), fan and measuring site (yellow)

The driving fan was located in the fire tunnel downstream of the test site (see Figure 1 and Figure 2). It was placed in the centre of the fire tunnel and provided a constant, homogenised air flow with an average speed of 1.0 - 1.5 m/s. All kinetic, thermal and chemical risks for the test personnel arising from the experiment were mitigated with appropriate safety precautions.

Figure 2: Test site (left) and subsequent fire tunnel where samples were taken (right)

2.3. Test scenarios

Possible fire scenarios in road tunnels involving an EV are mechanical damage (e.g. crash, object impact) and thermal stress (e.g. fire in a road tunnel, fire of EV itself) of its battery. These main scenarios were used as a basis for the experiment; in total, four identical modules were damaged in different ways, ultimately leading to a thermal runaway (see Table 2). The exact cause of the battery damage and its probability of occurrence in reality were not defined: The aim of all test scenarios was to achieve the maximum damage to the battery modules and ensure the resulting thermal runaway.

The forces required for the mechanical damage of the battery modules were generated by explosive methods – but the batteries themselves were not blown up. Depending on the test, the force was applied via a steel plate on which a sufficient explosive charge was mounted for acceleration in the direction of the battery module or through a penetrating projectile. Ideal quantities of explosives for the scenarios were determined in specific preliminary tests.

Table 2: Test scenarios of the experiment

#	Scenario	Illustration
1	**Wedge-shaped penetration**: Detonation of explosive charges accelerated a steel plate in the direction of the battery module. As a result, the wedges on the underside penetrated evenly into the two cell rows of the battery module, where they remained and caused electrical short-circuits.	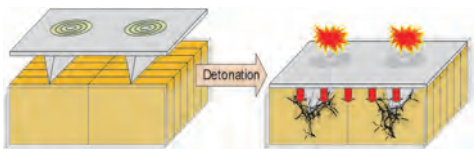
2	**Blunt impact**: Detonation of explosive charges accelerated a steel plate in the direction of the battery module. The module thus suffered a blunt impact over its entire surface so that all cells were structuraly damaged without penetration.	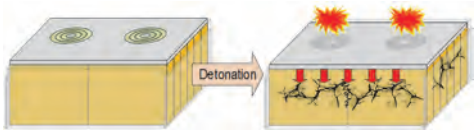
3	**Central puncturing**: Battery module was shot at centrally with an explosively formed projectile (EFP) from a distance of 10 cm. As a result, both cell rows were to be damaged with a continuous penetration of all 12 cells.	
4	**Thermal stress**: Battery module was evenly underfired with a propane gas fire until the module caught fire. The fire source was then removed and the thermal runaway of the battery observed.	

3. RESULTS AND DISCUSSION

The tests were carried out on 27 and 28 November 2017 in the Hagerbach test tunnel according to a test concept drawn up beforehand. All measurements started at the time of damage and ended after the battery modules had completely reacted. The results shown in Table 3 are mean values over the listed test durations.

Table 3: Freight / release quantities (measurement uncertainty of ±10%)

Parameter	**Test 1 («wedge»)**	**Test 2 («plate»)**	**Test 3[1] («puncture»)**	**Test 4 («fire»)**
PH_3 [g]	< 0.4	---	< 0.4	---
F^- as HF [g]	1.1	3.1	< 1	< 0.5
PO_4-P as H_3PO_4 [g]	< 1.5	< 1.5	11.3	< 1
Co [g]	457	567	190	364
Li [g]	107	124	42	92
Mn [g]	445	536	184	349
F^- Aerosol [g]	152	160	68	126
NO [g]	< 1	1.1	< 1	1.5
NO_2 [g]	< 1	< 1	< 1	< 1
CO [g]	76	181	97	141
CO_2 [g]	8’500	6’000	2’000	7’800
TVOC [g]	20	196	93	32
∑ Aromate [g]	1.6	8.6	3.2	3.1
Benzene [g]	1.1	3	1.6	1.7
Toluene [g]	0.2	1.1	0.5	0.4
Xylene [g]	0.1	0.6	0.3	0.2
Styrene [g]	0.1	3.0	0.5	0.6
Duration	*16 min*	*21 min*	*16 min*	*26 min*

At the beginning of all scenarios, the damaged battery modules emitted large amounts of black and very dense smoke. It rose directly to the tunnel ceiling and drifted in stable layers from the test site to the ventilation fan in the subsequent fire tunnel, where turbulence destratified the smoke layers. Growing combustion processes gradually reduced the smoke emissions in all scenarios. In addition to typical combustion gases, other pollutants were detected, which are relevant because they do not occur in conventional ICE vehicle fires. The measurements indicate increased amounts of the toxic heavy metals Cobalt, Manganese and Lithium (dust-bound aerosols). It is noteworthy that the cause of damage has no significant influence on the released quantities of pollutants: in a worst-case, the whole chemical potential of a battery is set free. Contrary to expectations, no large quantities of HF were found[2].

Whereas the different mechanical damaging scenarios led to almost simultaneous thermal runaways of all cells, thermal stress did not result in a uniform reaction of the whole module: in this scenario, a distinct chain reaction from one cell to another could be observed, ultimately leading to the longest test duration (see Table 3). After the tests, the modules had no voltages left. It was shown that severe mechanical and thermal damages to EV batteries instantly lead to uncontrollable fires with high-energy releases. However, the general hypothesis that the fire

[1] In test 3, the measurement encompasses only the time during which 50% of the module was destroyed.

[2] It is assumed that considerable quantities of HF were formed in the experiments, but due to its highly hygroscopic properties it very quickly reacted with moisture from the environment and presumably deposited somewhere in the tunnel on the way from the test site to the measuring site (approx. 160 m).

hazard in road tunnels will generally increase as a result of high-capacity traction batteries in EV cannot be confirmed. The experimentally derived findings illustrate that EV batteries do not lead to an aggravation, but to changing hazards in road tunnels.

Will thermal hazards change in road tunnels?
No. The battery fires were characterized by their rapid development, their high-energy release in a short period and, in some cases, by spectacular thermal processes (deflagration, flash flames) with strong smoke formation and high temperatures. Despite these effects, however, no explosions or other thermal effects could be observed that would differ significantly from conventional ICE vehicle fires. The measurements indeed show very high temperatures of up to 750 °C within the batteries, but at a distance of 2 m practically no temperature rises were registered. It is not possible to make a reliable statement on the heat release rate (HRR) of the battery fires based on the present measurements. However, within this context, the HRR of the battery fires is not decisive. The observed temperatures (>700 °C) during the experiments suggest that lithium-ion batteries are indeed extremely energy-rich fire sources and that a battery fire will spread through the surrounding body parts and ultimately lead to a complete vehicle fire. As soon as a full EV fire has occurred, its thermal characteristics will not differ from those of a conventional ICE vehicle fire: Experimental studies with complete vehicles prove that comparable EV and conventional ICE vehicles have similar HRR (approx. 5 MW) and heats of combustion (approx. 7'000 MJ) ([3];[5];[7]).

Will chemical hazards change with regard to potential effects on humans in road tunnels?
On the small-scale: Yes. Like conventional vehicles, completely burning EV emit pollutants that result from the exothermic decomposition of the vehicle. However, due to the chemical components of lithium-ion batteries, the flue gases of an EV fire contain additional substances that are very reactive and pose a considerable health risk to humans. In the immediate vicinity and in unfavourable ventilation situations, therefore, EV fires pose new and potentially greater chemical hazards to people than fires of conventional ICE vehicles. On the large-scale however, it can be assumed that the chemical hazard situation for tunnel users will not change with increasing distance from the fire: the natural air flows in road tunnels and the ventilation systems lead to fresh air supply and dilutions and thus to increasingly lower pollutant concentrations.

Is there a need for technical adaptation in road tunnels?
No. Due to the experimental results, no adaptation of the existing operating and safety equipment seems necessary. Ventilation systems in road tunnels are central facilities to enable appropriate self-rescue for road tunnel users in the event of an incident. In Switzerland they are generally designed for major fires (30 MW) with considerable pollutant emissions (e.g. heavy vehicles). It is therefore assumed that EV fires can be adequately managed with the existing technical equipment in state of the art road tunnels.

Is there a need to adjust the management of incidents with regard to firefighting?
Concerning the choice of the extinguishing agent – No. Water is considered the best coolant for lithium-ion battery fires, although the chemical properties of the batteries practically prevent a complete fire extinguishment. Firefighting with water has the advantage that undamaged cells of a battery may be cooled and hence protected against a thermal runaway. However, for effective cooling of EV fires, very large quantities of water are required, potentially more than with conventional ICE vehicle fires. Hence, sufficient water supply is a critical factor at the site during an incident.

What about chemical hazards in other underground infrastructure?
The findings of this study point to potential relevant consequences for other, smaller underground infrastructure (e.g. car parks). To estimate the chemical fire hazards of a complete lithium-ion battery in a passively ventilated room, the experimental pollutant data can be expressed in terms of the maximum concentration values at which an exposed person suffers serious or

permanent damage after 30 minutes (immediately dangerous to life or health, IDLH[3]). For this, the following scenario is assumed: The complete battery (8 modules) as described in Table 1 is completely burnt off within 30 minutes in a volume of 1,000 m^3 (e.g. car park with 20 x 20 x 2.5 m). The room is ventilated passively with an air exchange rate of 3/h. The calculated concentrations are then compared with the IDLH values of the respective substances. Table 4 only lists the substances where critical concentrations could be detected (all other substances show concentrations that lie below the IDLH-values).

Table 4: Chemical hazards in a room with 1000 m^3 (≠ road tunnel)

Substance	Concentration (mg/m^3)	IDLH-Value (mg/m^3)	Q
Co	1'100	20	55
Li	300	0.5	600
Mn	1'100	500	2.2
F^- Aerosol	400	250	1.6
CO_2	121'000	72'000	1.68

These thoughts illustrate that heavy metal emissions are of particular importance, as they do not occur in such concentrations in conventional ICE vehicle fires. In this example, the calculated concentrations of cobalt are 55 times higher than the maximum IDLH-value; lithium is 600 times higher and manganese 2 times higher than the maximum value at which serious or lasting damage is to be expected after 30 minutes. From a scientific point of view, these findings must be verified; it is therefore recommended that heavy metal emissions from EV fires in infrastructure with restricted ventilation as well as possible contamination should be investigated in greater depth. In the context of changing mobility, these findings support emergency forces in coping with future incidents. They are also able to sensitize operators of other underground traffic infrastructure (e.g. car parks) to changing hazards.

4. OUTLOOK

Even if the original hypothesis about the increased risk from EV fires in road tunnels could not be proven, new topics were uncovered, which have to be scrutinised in further research steps.

Potential contamination

Burning lithium-ion batteries form the highly toxic, gaseous hydrogen fluoride (HF) due to the fluorine contained in the electrolytes. Being highly hygroscopic, it tends to bond very rapidly with water. In contact with firefighting water, hydrofluoric acid can form, which is a powerful contact poison that is immediately absorbed by the human skin. If contaminated firefighting water with HF or with the heavy metals Co, Li and Mn drains off uncontrolled after a fire event and is released to the environment, additional hazards arise that cannot be estimated at the present time. Since no measurements were carried out on this aspect in the study at hand, further investigations are recommended to assess the potential hazard posed by contaminations of damaged EV batteries (e.g. firefighting water, building structures, vehicle parts, equipment of emergency personnel).

Disposal of damaged traction batteries

In contrast to the test material of this research project, EV batteries are in most cases not completely reacted and chemically inert after a real mechanical or thermal damage event. This means that damaged but not completely destroyed cells of a lithium-ion battery can repeatedly emit harmful substances or even flare up again. From the emergency personnel's point of view, it is therefore important to be able to assume that damaged traction batteries no longer pose any

[3] https://www.cdc.gov/niosh/idlh/intridl4.html

chemical or electrical hazards. At present, however, there are no uniform procedures for limiting risks in this respect. In the course of the present experiment, a number of explosive methods have been revealed that might be suitable for efficiently neutralising damaged traction batteries after an incident on-site. Based on this practical experience from the experiment, further studies are to be carried out to get an effective, practicable and economic method to ensure a safe disposal of damaged EV batteries after a fire.

Effectiveness of high-pressure water mist systems in underground infrastructure
Investigations for ocean ferries have shown that the use of high-pressure water mist appears particularly suitable for EV fires, as the extinguishing agent is distributed effectively in a room and has the property of penetrating concealed places as well. The risk-based effectiveness of these firefighting systems in relation to EV fires in road tunnels and other underground infrastructure (e.g. car parks) has not been investigated thoroughly yet. A risk-oriented study on the alleged effectiveness of high-pressure water mist systems for EV fires seems recommendable.

5. REFERENCES

[1] BFE (2015): Bericht in Erfüllung der Motion 12.3652. Elektromobilität. Masterplan für eine sinnvolle Entwicklung. Bundesamt für Energie BFE, Eidgenössisches Departement für Umwelt, Verkehr, Energie und Kommunikation UVEK, Bern.

[2] Broere, W. (2016): Urban underground space: Solving the problems of today's cities. *Tunnelling and Underground Space Technology*, 55, 245-248.

[3] Colella, F., Biteau, H., Ponchaut, N. F., Marr, K., Somandepalli, V., Horn, Q., Long, R. (2016): Electric vehicle fires. Tunnel Safety & Security, 7th International Symposium, Montréal, 629-639.

[4] Gehandler, J., Karlsson, Vylund, L. (2017): Risks associated with alternative fuels in road tunnels and underground garages. SP Technical Research Institute of Sweden.

[5] Lam, C., MacNeil, D., Kroeker, R., Lougheed, G., Lalime, G. (2016): Full-scale fire testing of electric and internal combustion engine vehicles. 4th International Conference on Fires in Vehicles - FIVE 2016, Baltimore, USA, 95-106.

[6] Larsson, F., Andersson, P., Mellander, B. E. (2016): Lithium-Battery aspects on fires in electrified vehicles on the basis of experimental abuse tests. *Batteries*, 2(9), 1-13.

[7] Lecocq, A., Bertana, M., Truchot, B., Marlair, G. (2012): Comparison of the fire consequences of an electric vehicle and an internal combustion engine vehicle. 2nd International Conference on Fires in Vehicles - FIVE 2012, Chicago, United States, 183-194.

[8] Nedjalkov, A., Meyer, J., Köhring, M., Doering, A., Angelmahr M., Dahle, S., Sander, A., Fischer, A., Schade, W. (2016): Toxic Gas Emissions from Damaged Lithium Ion Batteries – Analysis and Safety Enhancement Solution. *Batteries*, 2(5), 1-10.

[9] United Nations (2014): World Urbanization Prospects: The 2014 Revision, Highlights (ST/ESA/SER.A/352). Department of Economic and Social Affairs, Population Division, New York.

[10] Wisch, M., Ott, J., Thomson, R., Léost, Y., Abert, M., Yao, J. (2014): Recommendations and guidelines for battery crash safety and post-crash safe handling. Eve-ryday Safety for Electric Vehicles (EVERSAFE), ERA-Net collaborative project, work programm "Electromobility+".

[11] Züger, B. J. (2017): Studie: Technologiefolgenabschätzung und Prüfrichtlinien von Li-haltigen Batterien. armasuisse, Eidgenössisches Departement für Verteidigung, Bevölkerungsschutz und Sport VBS, Schlussbericht V1.1.

POTENTIAL OF INTEGRATING C2X COMMUNICATION INTO TUNNEL OPERATIONS CONTROL

[1]Christian Badocha, [2]Georg Mayer, [3]Axel Norkauer
[1]Ingenieurbüro Badocha, Germany, [2]PTV Transport Consult GmbH, Germany,
[3]Hochschule für Technik, Stuttgart, Germany

ABSTRACT

Safe operation of road tunnels requires comprehensive and detailed information on all processes in the traffic space, in order to be able to react quickly and appropriately to hazardous situations. Information is provided by various sensors available on the infrastructure side. Via data transmission devices, they are connected to central control technology and allow operating centres or higher-order monitoring centres to draw direct or indirect conclusions on irregularities in the traffic space. Incidents which necessitate intervention by control technology or operators are, for example, stop-and-go traffic, congestion, slow vehicles, vehicle breakdowns, occupied emergency bays, counter-flow vehicles, objects on the carriageway, persons on the carriageway, slippery road, accidents, vehicles on fire, release of hazardous substances, exceeded maximum permissible values (visibility, CO, NO_x) etc.
At present, some of the required data are already acquired continuously by in-vehicle sensors and evaluated by on-board systems.
Therefore, the exchange of in-vehicle data with control technology on the infrastructure side bears high potential for enhancing safety in road tunnels. To use that technology called Car to X or C2X in road tunnels, the necessary basic principles, and technical requirements for its integration into tunnel operations control technology are described. It will also be shown which C2X functionalities contribute to improving the detection of incidents.

Keywords: incident detection, sensors, C2X functionalities, safety enhancement, tunnel operations technology, road tunnel operation

1. INTRODUCTION

For safe operation of road tunnels, the early detection of hazards combined with the immediate initiation of measures is crucial to protecting tunnel users. Compared to conventional detection systems which react to effects of incidents, Car to X (C2X) technology allows detection of the causes of incidents directly. Hereby, C2X is the generic term for the communication between individual vehicles (Car to Car), between vehicles and enterprises (Car to Enterprise), between vehicles and homes (Car to Home) as well as between vehicles and infrastructure (Car to Infrastructure). Table 1 below gives an overview of the different C2X concepts.

Regarding the application in tunnels, particularly the C2X concepts concerning the communication between individual vehicles (C2C) and the communication between vehicle and infrastructure are of major interest. Data are transmitted between vehicles, traffic infrastructure and control centres and assumed to be processed efficiently. One challenge is the standardization of the interfaces. Current projects are using WLAN (Wireless Local Area Network) / LTE (Long Term Evolution) for information transmission between the individual C2X participants /components. To ensure data security, it is important that all connections and interfaces are highly protected against misuse and manipulation.

Table 1: C2X concepts and their way of communicating (Lübcke, 2004)

C2X concept	Communication
Car to Car (C2C)	Communication between vehicles, e.g. traffic conditions and direction of travel
Car to Enterprise (C2E)	Communication with enterprises, i.e. retrieving customer data from office computer en route
Car to Home (C2H)	Communication with home, e.g. access to home computer, burglar alarm system (SmartHome)
Car to Infrastructure (C2I)	Communication with surrounding transport infrastructure, e.g. with tunnels, traffic lights, concerning traffic condition

2. BASIC PRINICPLES OF C2X TECHNOLOGY

Wireless communication between individual vehicles (C2C) or between vehicles and infrastructure (C2I) in combination with various in-vehicle sensors allows detection of critical incidents directly, quickly, and reliably. To do this, the data gained from C2X have to be processed in real time and transmitted to a higher-order control unit. The sections below discuss in-vehicle C2X components, C2X components on the infrastructure side and C2X components needed for communicating with other C2X participants.

2.1. In-vehicle components

Besides the components required to establish communication, vehicle-specific and safety-relevant hardware components are mounted on board a vehicle. This includes all kinds of safety equipment that a modern vehicle generally has, starting from the airbag, which, if triggered, indicates that an accident has happened, to rain and light sensors, to ESP (Electronic Stability Program) and ABS (Anti-lock Brake System), which in combination with the acceleration sensors detect unusual vehicle movement like skidding between vehicle and road surface. New generations of vehicles even offer a brake assist system which sets maximum pressure to the brake pedal as soon as the driver initiates an emergency braking. This is an application which substantially reduces response time. Forward collision warning systems use radar sensors and "observe" the traffic in front and behind the vehicle to detect imminent collision, to warn the driver and to initiate measures mitigating the severity of an accident significantly.

On the vehicle side, information exchange between control units and detectors/sensors is cable-based and uses data buses like CAN (Controller Area Network) and Flexray, for example. Some information is stored also, e.g. the tyre pressure. The on-board computer, the Application Unit (AU) is the most important component for in-vehicle control of the different components.

Another on-board hardware component is the Communication Control Unit (CCU). This unit enables the vehicle to „communicate" with its surrounding environment via mobile radio or WLAN. It reads and prepares vehicle data for the communication with the outside world. It accesses the vehicle data bus to gain information on the state of the indicators, the rain sensor or the fog lights, for example.

2.2. Infrastructure components

On the infrastructure side, stand-alone stations at the roadside, so-called Road Side Units (RSU), are the central element of wireless communication with the vehicles. Their purpose is to receive information from vehicles or transmit information to other vehicles, as needed. Thus, the RSU constitutes the intermediate point between the mobile road users and the stationary C2X participants, the traffic infrastructure, the traffic control centres the tunnel control centres, etc.

The RSU consists of a CCU, which is a WLAN receiver, and an AU. Together it is a system which is similar to that on board the vehicle. Due to the required higher data bandwidth, RSUs

and other stationary units are not linked via radio technology but via LAN (Local Area Network) in combination with the Internet or on WAN (Wide Area Network). Optical fibres providing a high data bandwidth play a key role.

The RSU also provides for bi-directional information flow between vehicle and control centre. Naturally, the communication between vehicle and RSU can only be temporary and has a low data bandwidth. In contrast, the communication from RSU to control centre is highly available, featuring a comparatively high transmission rate. The RSU not only transmits data but also preprocesses data. The functionalities assigned to the RSU are limited by the confined hardware resources, e.g. storage capacity, CPU (Central Processing Unit), etc. as well as by the finite data bandwidth. However, the control centre has full access to the RSU and can start maintenance jobs (simTD-Konsortium, 2013).

2.3. Communication technology

The elementary function of C2X technology is the communication, i.e. the exchange of data and information. Technically seen, C2X technology is based on WLAN radio technology, or to be more precise, on the IEEE 802.11 standard which is applicable to communication in radio networks and which is applied also to the private domain. Being an established and widely used standard for wireless network communication, WLAN allows the automatic exchange of information between sender and receiver even at relative speeds of 400 km/h (Lübcke, 2004). Besides WLAN on IEEE 802.11 basis, additionally DSRC (Dedicated Short-Range Communications), which is an advancement of IEEE 802.11p, has been standardized particularly for the automotive industry. DSRC, in Europe also called ITS-G5, allows bi-directional near-field communication, e.g. between vehicles (C2C) and between vehicles and roadside units (C2I). Each participant can be identified exactly. DSRC is also used for electronic toll collection (U. S. Department of Transportation, 2003); it provides for safe information exchange in a self-contained, protected radio frequency range. A high safety standard here means that – in contrast to the IEEE 802.11g standard used for not safety-relevant or consumer domains, e.g. by every WLAN-capable end-user device like notebooks etc. – separate frequency ranges are reserved for ITS-G5 applications. Therefore, disturbances emanating from other utilisations do not occur. Otherwise it may be overloaded and bear a higher risk of data loss.

From the economic point of view, the advantages of WLAN are the lower data transmission costs compared to cellular radio technologies like the widespread UMTS (Universal Mobile Telecommunications System). From the technical point of view, the advantages are the latency periods, i.e. the time needed to establish the connection between sender and receiver, which are approx. 20 times shorter and the transmission rate which is 140 times faster (Elektronik-Kompendium.de, 2015).

The disadvantage of WLAN is that the network is locally limited and has a by far shorter range compared to WWAN (Wireless Wide Area Network). WLAN based on 802.11g features a range of only 100 m compared to UMTS which has a range of 20.000 m (Weidner & Kluge, 2016) (Elektronik-Kompendium.de , 2015). Therefore, sending and receiving units have to be established densely to achieve the same availability as UMTS. If the distance of the range is exceeded, other vehicles may become intermediate nodes to ensure data connection (multi-hopping). Alternatively, the distance between the RSU may be reduced to that extent that they can exchange information directly with the CCU of the vehicles (single-hopping) (Laglstorfer, 2012).

New WWAN standards like the already introduced LTE compensate for many of the disadvantages compared to WLAN. The transmission rate is much higher than that of IEEE 802.11g, whereas the latency period is comparable. LTE and the introduction of new standards or technologies like ITS-G5 in Europa and DSRC in North America, for example, open up new potentials for C2X communication. The general structure of communication channels, though,

will not change. To ensure that communication will not be impeded by technical progress, WLAN standards in the RSU will always have to be downward compatible to slower standards used by vehicles and their CCU.

3. INTEGRATION OF C2X IN TUNNEL OPERATIONS TECHNOLOGY

Prior to the integration of C2X technology in tunnel operations control technology, the related boundary conditions or preconditions have to be established at the infrastructural environment so that both the expected or required functional scopes and the technical limitations like the radio range are provided for.

The acquisition of traffic information and the supply of complementary information are of major relevance for tunnel operators and tunnel users. Infrastructure data like tunnel length or position of nearest emergency exit or emergency telephone can be provided to users. The basic functionalities developed within the framework of simTD (research project shaping tomorrow's safe and intelligent mobility through researching and testing car-to-x communication and its applications) have to be extended if used in tunnel operations control technology. Possible new functionalities of substantial benefits to tunnel operators and tunnel users will be described in the following paragraphs.

For operators, and equally for users of tunnels, it is essential that planned or unplanned traffic incidents are identified by means of a traffic acquisition system, for example, the event of fire. With regard to tunnels, C2X functionalities cover part of the function blocks (FB) of the system structure of tunnel operations control technology. Functionalities of this category may be integrated in FB2: „Traffic engineering installations" and FB5: „Escape route signing, orientation lighting and active guidance installations" according to RABT (Richtlinien für die Ausstattung und den Betrieb von Straßentunneln).

Traffic control, for example, allows tunnel operators to issue diversion recommendations in case of incidents in tunnels, and to safeguard the site concerned. These functionalities are particularly important to enhance traffic safety. C2X extends available traffic control-related installations and functionalities, or may even replace them. Integration into tunnel operations control technology could be possible and useful in function block FB2:„Traffic infrastructure", since here traffic control, e.g. the implementation of a speed funnel, plays a role, too.

Warnings of slow vehicles, vehicles which have broken down or obstacles on the carriageway provide great safety enhancements for tunnel users when subsequently collisions may be prevented. Should traffic control measures already been taken by the tunnel operator, e.g. the tunnel closed, entering the tunnel may be prevented by means of access control forcing vehicles to stop. To activate the system, remote access is conceivable.

Emergency systems like eCall independently report as soon as on-board sensors register a severe collision. When activated, they establish a connection to the nearest emergency call centre via mobile radio providing the emergency services with relevant data on the circumstances of the accident, e.g. time, exact position of the accident car using GPS (Global Positioning System), number of passengers (Communication Department of the European Commission, 2013). Important precondition here is that mobile radio connection is available in the tunnel, of course. This, however, may not be the case since they are not always equipped with the required antennas. A similar problem is the localization per GPS in tunnels. The eCall system notes the last position of the vehicle based on its GPS signal as well as the presumably present position of the vehicle and transmits it to the centre (Filjar, 2015). This technology can also be used to transmit instructions to individual vehicles and their passengers. However, those may only be heard inside the vehicle via the on-board loudspeakers. Therefore, the functionality does not replace the loudspeaker system of the tunnel.

According to RABT, C2X technology and the necessary technical installations on the infrastructure side like RSU are considered to be at field level, directly connected to the traffic computer centre and the permanently staffed tunnel control centre. This, however, carries the risk that C2X technology which is integrated into tunnel operations control technology may not be used redundantly or autonomously if data connection to the outside world is disrupted. Therefore, it should be connected to the system control level and automation level via a subcentre (subcentre, cf. RABT) since here action can be taken based on automatic schemes set beforehand, e.g. the automatic closing of the tunnel in case a collision has occurred (detected by C2X). This ensures safe operation, even if the higher-order control level fails. A precondition is the previous filtering or prioritization to select those data which are relevant for safe tunnel operation and which are directly processed by the subcentre or tunnel control centre.

The density at which RSUs have to be positioned along the tunnel interior depends on the one hand on the tunnel geometry and the tunnel roadway design and on the other hand on the sending and receiving capacities of the RSU. A good coverage is possible with WLAN. Considering the range of approx. 100 m for IEEE 802.11g, a maximum distance of 200 m could be reached. It may however, be useful to reduce the distance to 150 m and to place the RSU alternately on both tunnel sides. It is recommended to realise the communication structure necessary to implement C2X technology in tunnels, i.e. the connection between RSU and tunnel operations control technology, as LAN on TCP/IP IPv4 (Transmission Control Protocol / Internet Protocol) or later IPv6. This is equally recommended by (Zumbroich, et al., 2007) because it allows using standardized and marketable products of communication hardware and application software.

4. POTENTIAL OF C2X AND SUMMARY

Early detection of incidents in a tunnel is of major importance. If detection time is shortened, the number of persons endangered by the incident clearly decreases because safety systems can be activated earlier, e.g. closing the tunnel, activation of ventilation, etc.

C2X technology offers a very good alternative to video detection since incidents for which video detection is used can as well be detected reliably by C2X. However, C2X technology, cannot fully replace conventional video systems (CCTV Closed Circuit Television). Video pictures are still helpful and important for operators when assessing the prevailing situation in the tunnel. However, to minimize the error rate, the use of video detection systems is to be limited to few major events or incidents (e.g. vehicle breakdowns).

The potential of C2X technology to substitute conventional tunnel operations control technology very much depends on the functions which can be realized by C2X. Traffic data acquisition systems like inductive loops can be replaced by C2X because the vehicles are used as mobile sensors generating data themselves (FCD Floating Car Data).

C2X technology can provide an enormous amount of data. These have to be filtered and prioritized according to the different interests of the parties involved.

What C2X technology cannot accomplish for the time being, is the detection of fire in tunnels, as is done by heat detectors, for example. If a vehicle is burning intensely, fire ventilation has to be activated automatically. This holds as long as vehicles or mobile phones are not equipped with their own fire detectors.

Table 2 below shows a summary of functionalities of conventional sensors which C2X can take over.

Table 2: Incident and detection matrix

	Visibility sensor	CO sensor	Fire detection system - automatic	Fire detection system - manual	Contact sensor at manually operated hazard alarm, emergency station or emergency exit	Traffic data acquisition systems (inductive loops, overhead detectors)	Rod surface sensors	Video detection systems (VDS)	C2X technology
Excessive / inappropriate speed						**x**		**x**	**x**
High traffic density / stop-and-go traffic						**x**		**x**	**x**
Congestion / risk of traffic jams						**x**		**x**	**x**
Stopped vehicle / vehicle breakdown						**x**		**x**	**x**
Occupied emergency bay						**x**		**x**	**x***
Counter-flow / reversing / turning manoeuvre								**x**	**x**
Accident								**x**	**x**
Unknown objects on carriageway / emergency bay								**x**	
Persons / animals on carriageway					**x**			**x**	
Vehicles of excess height						**x**			
Slippery road surface							**x**		**x**
Emergency call				**x**	**x**				**x**
Overheated vehicle								**x**	**x**
Vehicle on fire	**x**	**x**	**x**	**x**	**x**			**x**	**x****
Release of hazardous substances					**x**				

*) Depending on location accuracy **) if fire detector on board

The error rate of C2X still has to be validated. To do so, research projects involving tunnel operators, automotive industry and possibly major IT service providers are necessary. Reputable manufacturers are working on the Internet of Things (IoT), i.e. a networked world. The IoT will be a major stepping stone for C2X technology. It will facilitate a tremendous acceleration as regards penetration and utilization. Making all involved parties into concerned parties leads to a synergy of interests which becomes the necessary driving force spreading C2X or comparable technologies.

But as for every technical development, C2X bears risks, e.g. data disruption, false reports, data security. Full safety is impossible but compared to other technologies a very high safety level can be reached.

Data protection and data security issues are equally major aspects in the development of C2X. Like every new technology, C2X will continuously meet new challenges. So, it is necessary to update the systems (software) regularly to withstand attack scenarios.

One technology benefitting from C2X is autonomous driving. Information exchange assists the independent and autonomous, driverless driving – based on a machine-to-machine communication. Previous approaches to autonomous driving are based on navigation by means of in-vehicle sensors. This requires great processing power since a map of the route has to be calculated in real time. C2X provides information which many in-vehicle sensors may use, supporting their own calculations. This helps to reduce the required on-board processing power, and thus saves costs.

The potential of C2X is great. In the future, networking technologies will be inevitable even for traffic infrastructure. However, this postulates considerable investments which have to be politically supported by the decision-makers.

5. ABBREVIATIONS

ABS	Anti-lock Brake System		**FCD**	Floating Car Data
AU	Application Unit		**GPS**	Global Positioning System
C2C	Car to Car		**IoT**	Internet of Things
C2E	Car to Enterprise		**IP**	Internet Protocol
C2H	Car to Home		**LAN**	Local Area Network
C2I	Car to Infrastructure		**LTE**	Long Term Evolution
C2X	Car to X (generic term)		**RABT**	Richtlinien für die Ausstattung und den Betrieb von Straßentunneln (German tunnel guidelines)
CAN	Controller Area Network		**RSU**	Road Side Unit
CCTV	Closed Circuit Television		**simTD**	Sichere Intelligente Mobilität Testfeld Deutschland (Safe and Intelligent Mobility Test Field Germany)
CCU	Communication Control Unit		**TCP**	Transmission Control Protocol
CPU	Central Processing Unit		**UMTS**	Universal Mobile Telecommunications System
DSRC	Dedicated Short-Range Communications		**WAN**	Wide Area Network
ESP	Electronic Stability Program		**WLAN**	Wireless Local Area Network
FB	Function Block		**WWAN**	Wireless Wide Area Network

6. REFERENCES

Badocha, C., 2014. *Eignung von bluetooth-Daten zur Korrektur von Fahrzeugbilanzfehlern in der stationären Verkehrsdetektion.* 1 Hrsg. Stuttgart: s.n.

Bundesamt für Bevölkerungsschutz und Katastrophenhilfe, 2015. *Ereignismanagement für Straßentunnel - Empfehlungen für Betriebs- und Einsatzdienste.* Bonn: s.n.

Communication department of the European Commission., 2013. *European Commission Press Release Database.* [Online] Available at: http://europa.eu/rapid/press-release_IP-13-534_de.htm [Zugriff am 24 Januar 2016].

Elektronik-Kompendium.de , 2015. *IEEE 802.11g / WLAN mit 54 MBit.* [Online] Available at: http://www.elektronik-kompendium.de/sites/net/0907051.htm

Elektronik-Kompendium.de, 2015. [Online] Available at: http://www.elektronik-kompendium.de/sites/kom/0910141.htm

Erin-Ee-Lin, L., Boon-Giin , L., Seung-Chu, L. & Wan-Young , C., 2008. *Enhanced RSSI-Based High Accuracy Real-Time User Location Tracking System for Indoor and Otudoor Environments.* [Online] Available at: http://www.s2is.org/issues/v1/n2/papers/paper14.pdf [Zugriff am 25 Januar 2016].

Filjar, R., 2015. *Harmonised eCall European Pilot.* [Online] Available at: http://www.heero-pilot.eu/ressource/static/files/filjar_vidovic_britvic.pdf [Zugriff am 24 Januar 2016].

Forschungsgesellschaft für das Straßen und Verkehrswesen (Hrsg. 2016): *RABT – Richtlinien für die Ausstattung und den Betrieb von Straßentunneln.*

Jahn, E., Starke, H. & Seliger, U., 2013. *Maßnahmen und taktische Vorgehensweise bei der Brandbekämpfung in Straßentunneln unter besonderer Berücksichtigung von Gefahrstoffen.* Forschungsbericht Nr. 163 Hrsg. Heyrothsberge: Ständige Konferenz der Innenminister und –senatoren der Länder Arbeitskreis V Ausschuss für Feuerwehrangelegenheiten, Katastrophenschutz und zivile Verteidigung.

Laglstorfer, R. J., 2012. *Die Zukunft des intelligenten Automobils: Wirtschaftliche Markteinführungsszenarien am Beispiel Audi.* Hamburg: Diplomica Verlag GmbH.

Lübcke, A., 2004. *Car-to-Car Communication – Technologische Herausforderungen.* Berlin, s.n.

Nathansen, M., 2012. *GPS-Genauigkeit & Einschränkungen.* [Online] Available at: http://gpso.de/technik/gpsgenau.html [Zugriff am 25 Januar 2016].

simTD-Konsortium, 2013. *Sichere Intelligente Mobilität Testfeld Deutschland.* [Online] Available at: http://www.simtd.de/index.dhtml/deDE/index.html [Zugriff am 22 11 2015].

U. S. Department of Transportation, 2003. *Dedicated Short Range Communications (DSRC),* s.l.: s.n.

Weidner, M. & Kluge, H.-G., 2016. *UMTS und GSM - ein Vergleich der Technik.* [Online] Available at: http://www.teltarif.de/mobilfunk/umts/technik.html

Zulauf, C. et al., 2009. *Bewertung der Sicherheit von Straßentunneln,* Bergisch Gladbach: Bundesanstalt für Straßenwesen.

Zumbroich, M. et al., 2007. *Zukünftige Kommunikationstechniken und Integration von Straßentunneln im Bereich der TLS,* Bonn: Bundesministerium für Verkehr, Bau und Stadtenwicklung.

IMPROVED INCIDENT MANAGEMENT THROUGH A RESILIENT ORGANISATION

André Stein
graduate engineer in civil engineering
tunnel safety officer
Ponts et Chaussées Luxembourg

ABSTRACT

The European tunnel safety directive achieves improved organisation through four independent organs (administrative authority, tunnel manager, safety representative, investigative body) as well as better preparation for incidents in the tunnel through preventive incident management, consisting of the phases organising, training, exercise, post-processing and adaptation of the organisational guidelines. Nonetheless, it is impossible to ensure that every incident in a tunnel is overcome optimally and without delay. Many years of experience, observations and extensive research in the disciplines of safety, organisation, management and resilience research suggest that further progress is possible through proactive incident management (PEM). PEM consists of a distinctly established safety culture, resilient organisation and resilient technical tunnel concept. Optimized incident management can be achieved through the collaboration of the preventive incident management covered by the European directive and the new concept of the PEM.

1. INTRODUCTION

While I was on a sojourn in Brussels in late 2001 at the invitation of the EU Commission to take part in the preparations for the future directive on tunnel safety, it was clear to everyone involved that it was imperative to position ourselves better as organisations, especially with respect to the preparation of emergency services.

At that time, we spoke about preventive incident management (Figure 1), consisting of organising (instructions, alarm and emergency response plan, etc.), educating and training, conducting exercises (together with the emergency services), reviewing (training exercises and real incidents) and adapting (the organisational aspects).

For years, I was convinced that this would lead to certain success sooner or later, meaning that every incident could be handled optimally, thus achieving flawless incident management as a result. Sixteen years later, following numerous large-scale exercises and real incidents in tunnels, I am no longer convinced of this.

Figure 1: Preventive incident management

It happens to be in the nature of incidents in tunnels that they never follow the "script" of an alarm and emergency response plan. Experience teaches us that an incident which is difficult to manage occurs as a result of a combination of several unforeseeable events, each one being non-critical when regarded in isolation, but having catastrophic effects when combined.

It should also be noted that we have neglected the human dimension of incident management way too much up to now. The members of the emergency services team do not usually know the tunnel well enough, are often not familiar enough with the operational concepts and all too often conduct themselves in a suboptimal manner; in other words, they lose a lot of time through hesitation, reluctance to take responsibility and/or a lack of self-efficacy or acceptance of the situation and flexibility.

In light of the observations above, I have adopted a new approach, which I will call "proactive incident management" or PIM. In the process, optimised incident management can only be achieved by the combined effects of "preventive incident management" covered by the European directive 2004/54/EC (on minimum safety requirements for tunnels in the Trans-European Road Network) and the new concept of "**proactive incident management" (PIM)**.

PIM consists of the following sub-aspects:
- a highly developed, consolidated safety culture,
- a resilient organisation,
- a resilient (technical) tunnel concept.

Remark: this article is only concerned with the subject of the "resilient organisation".

2. THE RESILIENT ORGANISATION

The unpredictability, diversity and complexity of critical situations in tunnels and the crucial impact that the time sequence has on their consequences require emergency services to be organised resiliently.

An organisation is only resilient when it demonstrates a systemic resistance to disruptions and changes in its environment. Such an organisation is characterised by a high degree of self-regulation and remains capable of acting even in adverse circumstances, i.e. it retains the ability to operate in accordance with its purpose. This is certainly also facilitated by preparatory planning as well as educating and training employees, but above all, by having recourse to the personal and social skills of its employees at all levels of the hierarchy.

A resilient system can cope with changes in its environment and adapt to the circumstances and conditions. It is highly disruption-tolerant, so to speak.

The resilience of an organisation (Figure 2) is based on the concepts of **robustness**, **agility** and **intersubjectivity**.

Figure 2: The resilience of an organisation

"**Robustness**" is the proactive form of resilience. A robust organisation possesses the necessary resources (material, human, knowledge-based and technical) and concepts (organisational structure, plans, esprit de corps, corporate culture) to be able to react promptly. Forward-looking planning and competent, adaptable employees make it possible to meet the organisational goals when disruptions and problems arise. Ultimately, in order to remain capable of acting in difficult situations and react appropriately in such situations, a generally positive assessment of the situation within an organisation is indispensable. Every single employee within an organisation must be convinced that the resources, skills, expertise and practical experience that were acquired during comparable crises in the past will be sufficient to cope with each and every situation. In a nutshell, there is an *esprit de corps* and a sense of "we can do it".

"**Agility**" is the reactive form of resilience, often also called "vitality". Disaster response demands measures that can stabilise the situation as quickly as possible. The members of the emergency services team need space for creative solutions and thinking "outside the box". For many people, innovative improvisation is certainly a surprising but necessary counterbalance to the highly structured alarm and emergency response plan.

Agile organisations work iteratively and incrementally and make constant progress through "small steps", which are taken quickly as the situation dictates and are not necessarily contained in a manual. Freedom to make decisions and act are central to the desired innovative improvisation and are based on an open corporate culture, where creative solutions are fostered with positive encouragement and error tolerance is routine.

When major problems need to be addressed, the employees must strive for quick results and make incremental improvements. To achieve this requires acceptance of the situation, rapid adaptation to a changed environment, early detection of problems that arise and prompt implementation of countermeasures, if necessary.

Another key feature of resilient organisations is harmonious interaction between employees. This is based on the concept, meaning that there is unity within the organisation, at all levels of the hierarchy and in every team, with regard to how to assess, classify, perceive and manage a situation (such as a tunnel fire).

The creation of a resilient organisation is first and foremost a task for the strategic management level, since it requires a clear top-down approach. A company's trust in its own staff and leadership is the lynchpin of successful implementation within that company, since the fundamental prerequisite for an agile organisation is the partial transfer of responsibility away from management towards the team. It is only by decentralising responsibility that agile organisations attain the required stability and ability to act.

Creating a resilient organisation of tunnel operation requires a holistic concept with the aim of minimising the effects of a wide range of disruptions on the regular process of incident management. A considerable commitment on the part of managers and a coherent approach to targeted staff development are necessary to "leverage" non-knowledge-based human resources. Transactional leadership, error tolerance and the creation of trust between the employees and management tiers are core elements of management skills here.

The objective is for employees who have a high level of self-efficacy and are therefore capable of making decisions to accept challenges and assume responsibility.

In an ideal scenario, this is how we achieve "**role flexibility**", a concept which contradicts the narrowly defined organisational structures. Karl Weick, Professor of Organisational Behaviour and Psychology at the University of Michigan, also speaks of "virtual role systems" in this context and refers to role theory (social behaviour and role expectation). He emphasises that it is necessary for every member of an incident response team to be at least mentally capable of taking on any role within that group. That is the only way to ensure that a vacuum is not created in the organisation when there is an acute need for action. This self-regulation is also decisive for the self-care of every member of an incident response team, not least in the event of a disaster.

If role flexibility can be developed successfully amongst the staff, then the goal of the resilient organisation is not so far off.

However, it must be mentioned in conclusion that emergency service employees must be empowered to assess and accept a situation devoid of emotion in order to be able to manage disasters effectively. Good and effective training and education, practical experience, esprit de corps and camaraderie within the team are milestones along the way to achieving this goal.

In summary, it can be said that **resilient organisations** are nothing other than **groups of resilient individuals inspired by *esprit de corps*.** The management, organisational and safety culture in a company determines whether organisational resilience can be achieved.

REDUCING OF PISTON EFFECT IN METRO LINE A IN PRAGUE

Miroslav Novák
METROPROJEKT Praha a.s., Czech Republic

ABSTRACT

The new extension of metro line A in Prague was opened on the 6th of April 2015. This presentation represents a solution of reduction of piston effect caused by metro trains by placing cross passages at regular intervals of approximately 200 m.

The measurement of the flow and pressure of the air in the cross passages was carried out in cooperation with the Faculty of Mechanical Engineering of the Czech Technical University in Prague and the company METROPROJEKT Praha a.s. (3). The results are published in this presentation.

Keywords: Piston effect, cross passage, Prandtl probe, static pressure, dynamic pressure, fire gate, airflow velocity, running tunnel

1. INTRODUCTION

The metro line A was extended from station Dejvická to Nemocnice Motol station (called metro V.A) and was opened on the 6th of April 2015. The Metro running tunnels were carried out by using TBM technology (Tunnel Boring Machine). The tunnels are single-track with the diameter of 5.3 m. The design speed of Metro trains in the tunnel is max. 80 km/h and causes changes in the air pressure along the tunnels and induces flowing of air in stations. High airflow speed causes discomfort of passengers and other problems with safety conditions. Metro line V.A was designed in urban area under buildings and technical infrastructures. It was very complicated to situate ventilation shafts on the surface and any other connection with the surface was practically excluded. In case of fire, there are cross passages designed between running tunnels at regular intervals of 200 m (1). We decided to use these cross passages for a reduction of piston effect caused by metro trains. The optimum cross- section of cross passages should be comparable with the cross-section of a running tunnel with the area of 20 m^2. When the cross passages between the tunnel tubes were being designed, it was impossible for structural reasons to design cross-section 20 m^2. Finally, the cross-section area was designed 15.25 m^2. The cross passages are equipped with fire doors with the EI 90 DP1 fire resistance. Two doors 0.9 m wide each are sufficient for the purpose of evacuation. Nevertheless, this door size is insufficient for the purpose of equalising the pressure of the air caused by the piston effect of metro trains. For that reason a double- leaf gate 3.6 m wide and 2.6 m high, with the total cross-sectional area of 9.36 m^2, was installed. In normal operation conditions, gate leaves are secured in the open position by an electromagnet. In case of an accident or a fire in the metro, the gate leaves are closed by a self- closing system and two 1.2 m wide fire doors installed in the gate can be used by escaping passengers. The requirement of the fire protection standards is the separation of the running tunnels into two fire protection sections. However the requirement increases the resistance to flowing air through the cross passage and the reduction of the piston effect induced by metro trains is not fully effective. The above-mentioned measurement was carried out for analysis of effectivity of cross passages in terms of the aspect of the equalisation of pressures.

2. MEASURING AIRFLOW VELOCITY, DYNAMIC AND STATIC PRESSURE

The object of a measurement is to prove the influence of the cross passages between metro tunnels to the reduction of the piston effect and the air flow on the platforms of stations. Another reason of this measurements was to find out the values of the air pressure on the open fire doors in the cross passage in order to verify the force required to hold the door leaf.

The measuring equipment and devices were selected in connection with dynamic course of the measured quantities and the size of the measuring cross-section.

The measurement in cross-passage between parallel metro tunnels was necessary to carry out during the operation. Measurement was automatized. The dimensions of the cross passage cross-section and sizes of the gate led to the decision to use a network of total pressure probes connected in parallel for determination of the average airflow velocity and subsequently to deduce the rate of flow of air in m^3/s from it. The arrangement of the probes allowed qualified guessing at the average total air pressure over time. The total pressure probes were installed in the pattern of a grid covering the entire cross-section of a gate. It was possible to determinate the average dynamic pressure within the measuring cross-section by comparing the value of the total pressure within the grid with the static pressure in the same measuring cross-section that was determined by means of Prandtl probe. Two measuring grids were installed for the opposite directions of flow. The readings of the static pressure on Prandtl probes allowed for independent obtaining information on the static pressure very rapidly varying over time, which the force effects of air on the door leaves are related to. All measured quantities were recorded in time (cca 1s intervals) by measurement data loggers.

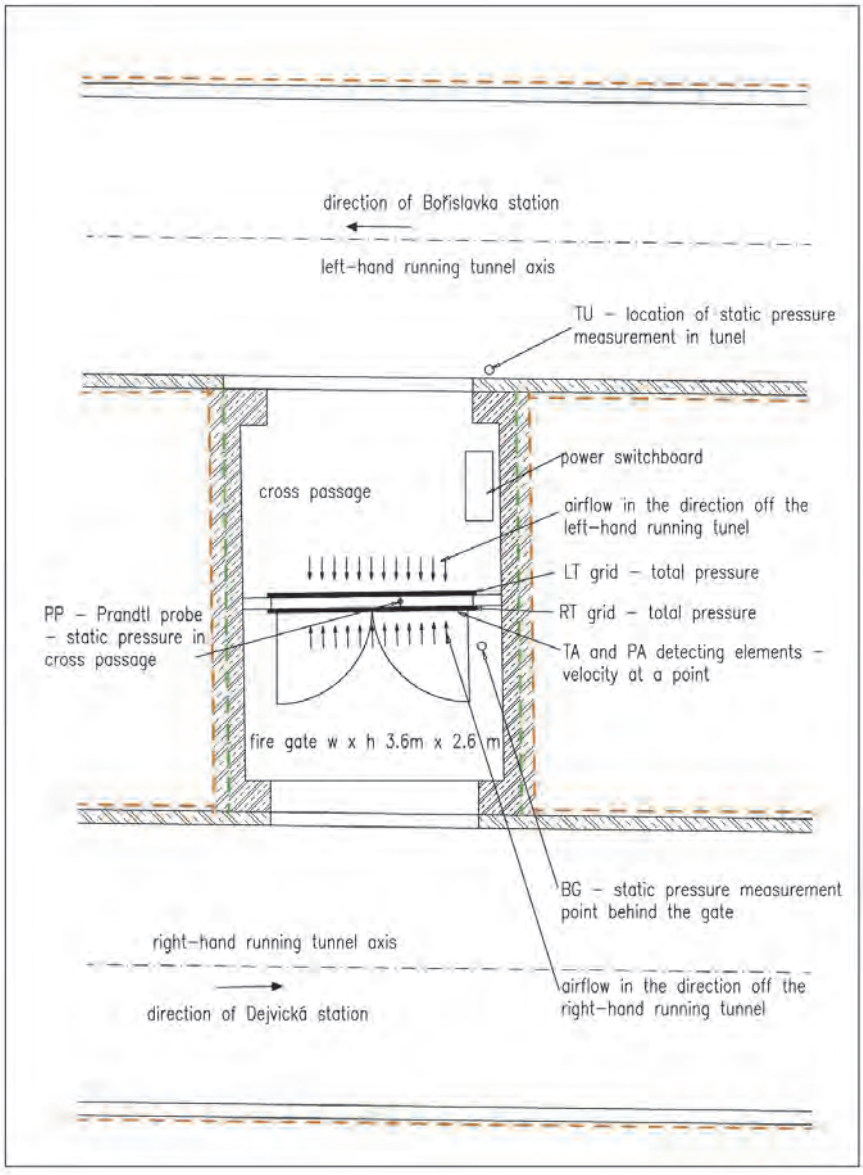

Figure 1: Metro Line V.A – The scheme of cross passage between metro tunnels

3. MEASUREMENT DESCRIPTION

The measurement equipment (fig.1) was installed in cross passage during an overnight closure (fig.2):

- Measuring grid for the measurement of the total pressure (Pa).
- Prandtl probe PS - 2 pieces located in the centre of the gate for measuring the static pressure in the cross passage (fig.3).
- Prandtl probe BG, located in the space behind the open door designed to measure the static pressure (Pa).
- Prandtl probe TU located in the LTT for measuring the static pressure (Pa).
- Thermo anemometer TA for measuring the airflow velocity.
- Propeller anemometer PA for measuring the airflow velocity (fig.3).

The values measured were evaluated; the records obtained during following periods:

- Morning rush hours 6:00 a.m. – 9:00 p.m., 120 s interval between metro trains.
- Normal intensity operation 11:00 a.m. – 2:00 p.m., 210 s interval between metro trains.
- Afternoon rush hours 4:00 a.m. – 7:00 p.m., 120s interval between metro trains.

Individual measurements – detecting elements:

- M00 (Pa) measures atmospheric pressure.
- M01 (m/s) measures total pressure and static pressure. The result is the dynamic pressure and calculation of the mean velocity of the flow within the fire gate cross-section (m/s) (fig.4).
- M03 (m/s) measures total pressure and static pressure. The result is the dynamic pressure and calculation of the mean velocity of the flow within the fire gate cross-section (m/s) (fig.4).
- M04 (Pa) measures the differences between the static pressure behind the gate (BG) and Prandtl probe PP (static pressure BG – PS; it measures the difference in the static pressure acting on the fire gate (Pa)).
- M02 (Pa) measures the differences between the static pressure behind the gate (BG) and static pressure TU. BG – TU; it measures the difference in the static pressure acting on the fire gate (Pa) (fig.5).

Extreme measured values were selected and depicted in the graph for measuring devices M01, M02, M03, M04:

TA (m/s) – thermal anemometer measurements of airflow velocity in the cross-section of the open fire gate in cross-passage (fig.7).

PA (m/s) – propeller anemometer measurement of airflow velocity in the cross-section of open fire gate (fig. 7).

Figure 2: Arrangement of the measurement grid for measuring the dynamic pressure, the installation of propeller and thermo anemometer for measuring the velocity of the air flow within the cross-section of the fire gate in cross passage

Figure 3: Arrangement of Prandtl probes for measuring static and dynamic pressure and the the propeller and thermal anemometer for measuring the velocity of the air flow within the cross-section of the fire gate in cross passage

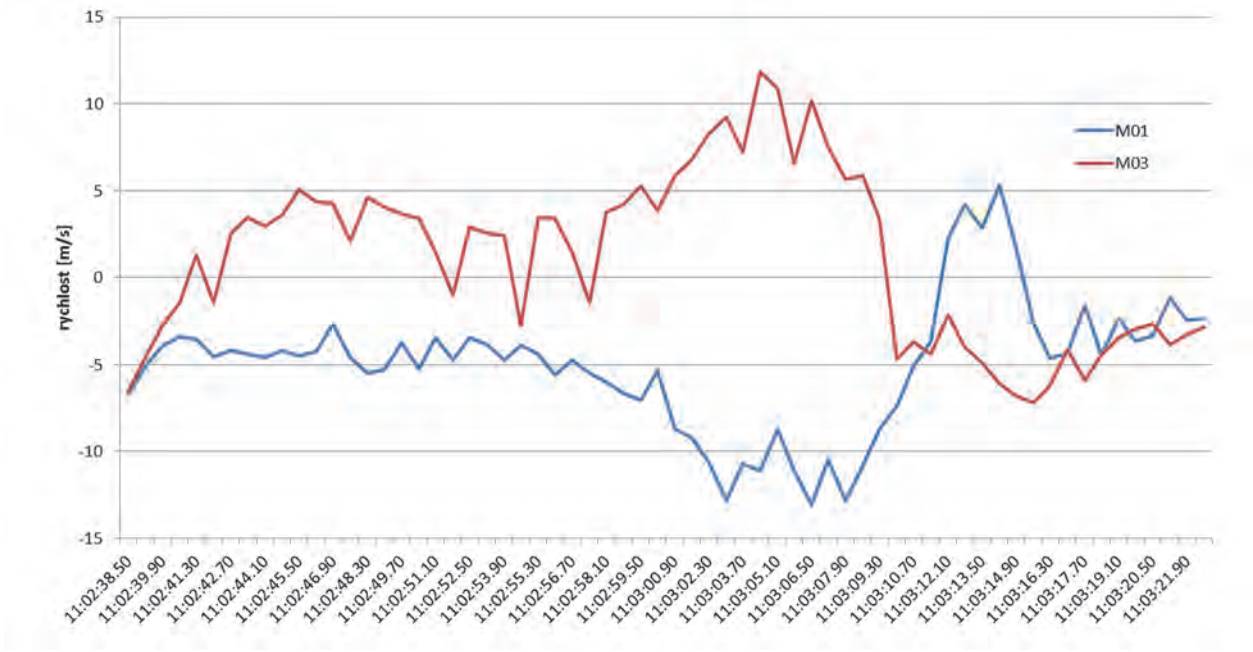

Figure 4: Extreme values of the velocity of the airflow within the cross-section of the fire gate M01 (LT-PP), M03 (RT-PP)

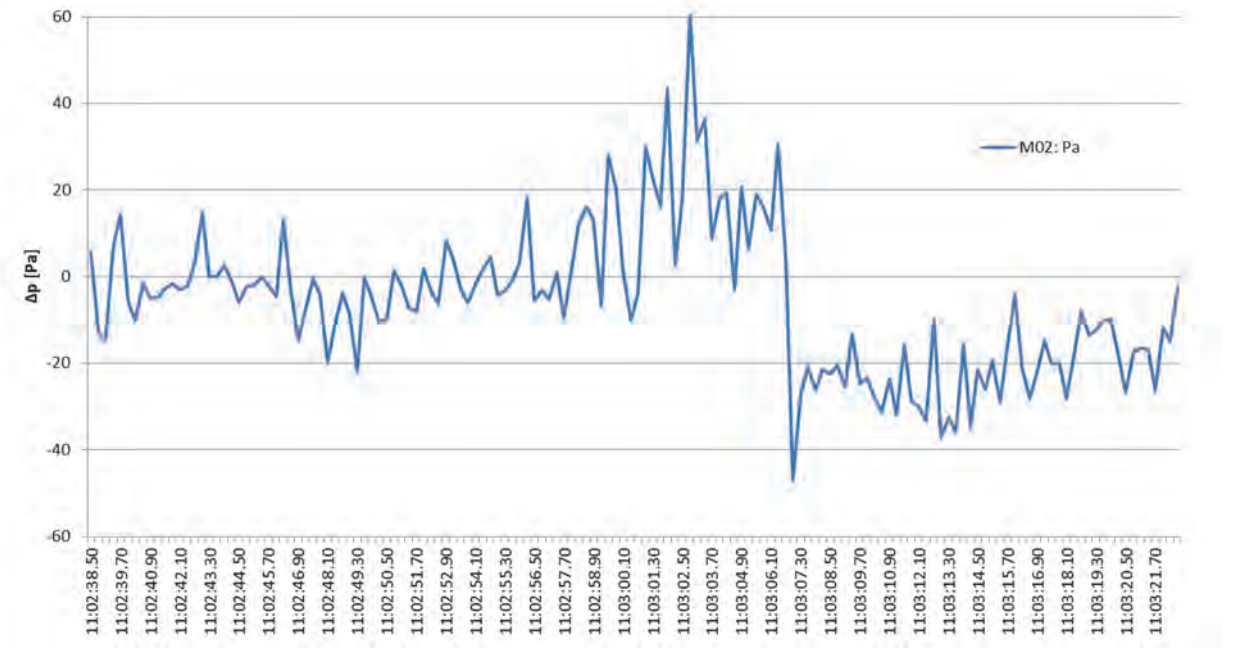

Figure 5: Extreme values of the difference between the static pressure BG (the space behind the right-hand leaf of the fire gate) and TU (static pressure in the left-hand tunnel tube) M02 (BG-TU)

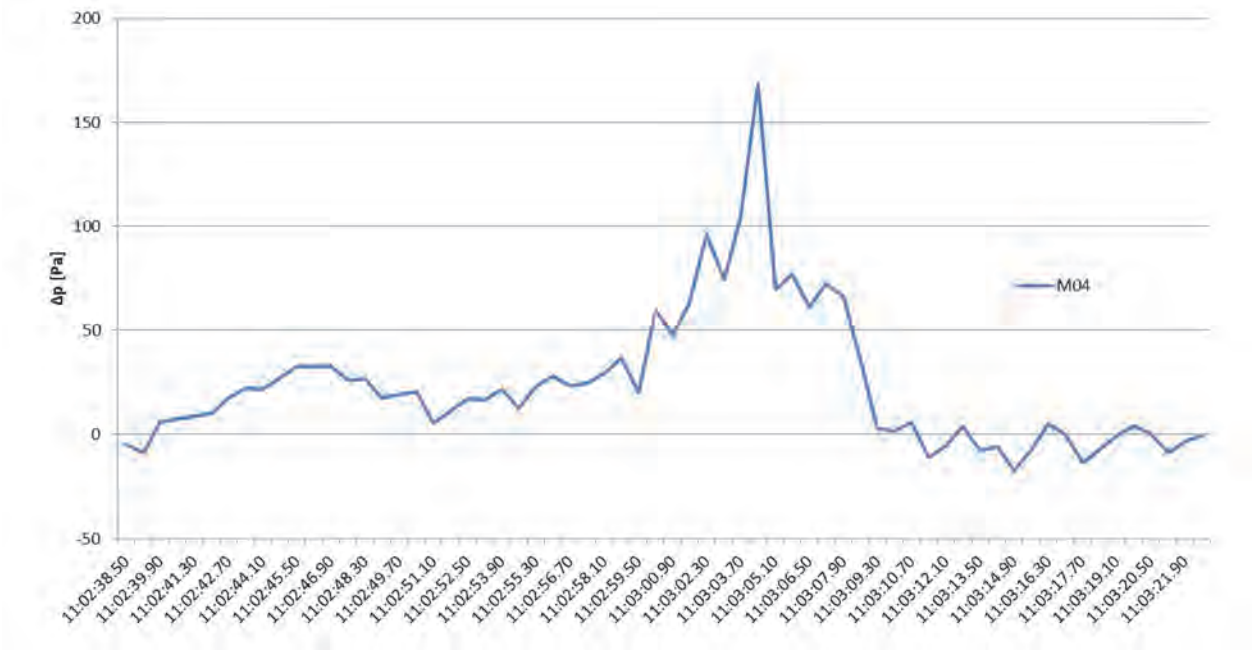

Figure 6: Extreme values of the pressure difference of the static pressure between BG (the space behind the right-hand leaf of the fire gate) and PP (Prandtl probe within the cross-section of the open fire gate) M04 (BG-PP)

4. EVALUATION OF MEASUREMENT RESULTS

The function of a cross passage from the aspect of reducing the influence of the piston effect of metro trains.

Measurements M01, M03, PA, and TA recorded average value of airflow velocity, values were determined in the 3.6 * 2.6 m profile of the open fire gate (the cross-section area of 9.36 m^2). During the passage of trains, air flew to the other running tunnel at the velocity of 14 – 18 m/s. The average value of airflow velocity during the passage of trains is 10 – 14 m/s. The amount of air flows through the cross passage:

- 90 m^3/s to 130 m^3/s during the passage of trains as an average
- 120 m^3/s to 160 m^3/s during the passage of trains as a maximum

The piston effect of a train passing through the tunnel tube at the maximum speed of 60 – 80 km/h causes the pressure of 400 to 500 Pa. The pressure induces the pulling force of 7600 to 9500 N. The pulling force of the metro trains induces the flow of air at the rate of cca 160 to 200 m^3/s. The above mentioned values were determined by a calculation according to EN 14 067-1 and EN 14 067-3 Railway applications – Aerodynamic in tunnels (2). It follows from the above-mentioned text that 60 to 70% of air circulates inside the tunnel through cross passage. The piston effect of metro trains causes a change in the pressure in cross passage, an increase in the pressure ahead of the running train of 180 Pa as the maximum and a decrease in pressure behind the running train by up to 150 Pa (M02, M04).

The above mentioned pressure changes propagate along the running tunnel at the speed of sound (cca 340 m/s) up to a station platform, where the change in pressure is subsequently equalised though the exits to the surface (escalator tunnels, staircases) and causes short-term negative excessive flowing of air (cca 6m/s). The cross passages help to equalise the pressure in metro staions. It follows from the above mentioned measurement that cross passages reduce the influence of the piston effect in metro line, but do not remove it completely. It would be

necessary to enlarge the cross passage to an area comparable with that of a running tunnel, i.e. to 20 m^2.

Passengers usually stay in the metro station for about 5 minutes on average. The maximum air flow speed in the metro station platform should not exceed 6 m/s in the short term. Higher speed could cause uncomfortable and danger conditions of the passengers.

Forces acting on open leaves of the fire gate in the cross passage

There are escape cross passages between running tunnels designed to ensure safety in case of an accident or a train fire in the tunnel. The cross passages have to be equipped with a fireproof doors/gate. The gates in cross passages are permanently open and are secured in position by electromagnets so that it is possible to close them remotely in the case of accident, a fire in the tunnel. The maximum pressure of 180 Pa acts on the open leaf (110 Pa on average):

- 180 Pa*4.7 m^2 = 846 N as the maximum
- 110 Pa*4.7 m^2 = 517 N as the average

Each gate leaf is secured by a double electromagnet with the holding force of 1500 N.

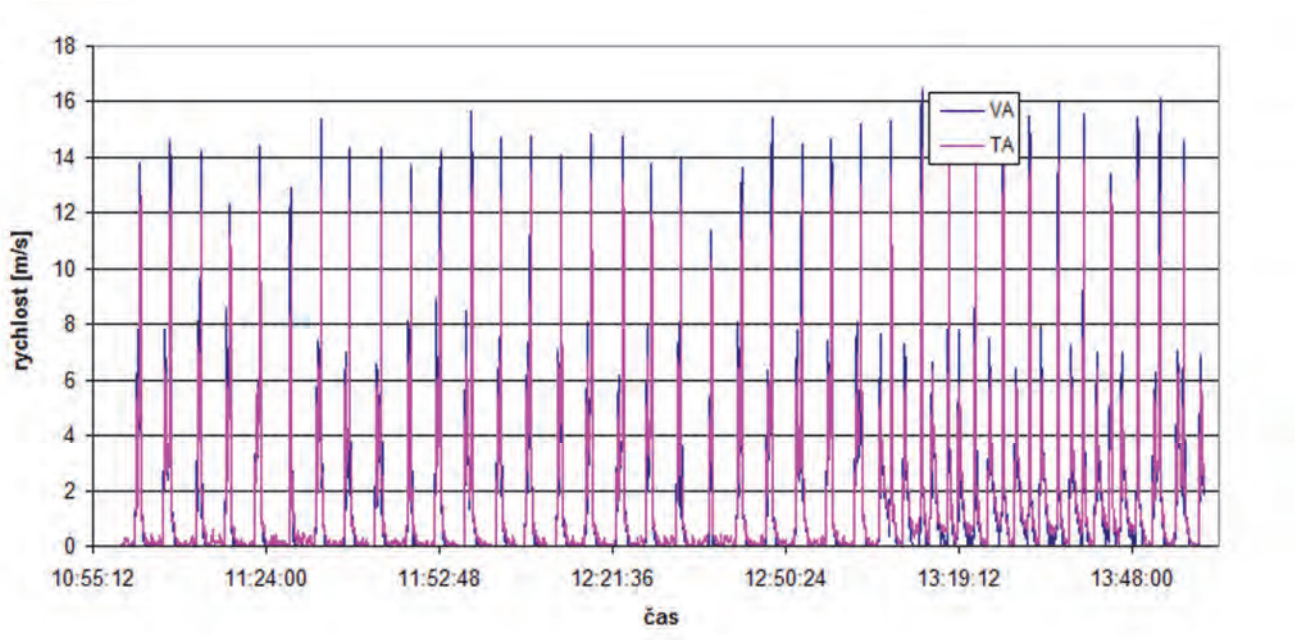

Figure 7: The measurement of the airflow velocity within the cross-section of the open fire gate – TA thermal anemometer, PA propeller anemometer

5. CONCLUSION

It follows from the above mentioned measurement that cross passages significantly reduce the influence of the piston effect during operation of metro trains, but the full reduction is not achieved. It would be necessary to enlarge the cross passage to an area comparable with that of running tunnel, i.e. to 20 m^2.

It was proved that the forces acting due to piston effect on a leaf of the open gate in the cross passage do not exceed 1000 N. The proposed fixing of a leaf of a fire gate by two electromagnets with the holding force of 1500 N is satisfactory.

6. ALTERNATIVE SOLUTIONS

A different solution of reduction of piston effect is used in the metro system with single-track running tunnels and cut-and-cover stations.

The solution is based on design of ventilation shafts to reduce the pressure of air in the tunnel induced by the piston effect of metro trains. The shafts with the cross-sectional areas of cca 16 to 20 m^2 are situated at the both ends of a station in cut-and-cover parts. The shafts connect the running tunnels with the surface. They are combined with a mechanical metro ventilation system. The undesirable changes in metro pressure originating in a metro tunnel due to the piston effect are equalised with the pressure on the surface before stations. The significant economic demands of building these shafts and necessity for obtaining free space for ending the two shafts on the surface, which is usually a serious problem in urban areas.

The platform space is separated from running tunnels by a safety wall with doors in it, which automatically open on the metro train arrival. Separate ventilation systems are necessary for tunnels and the stations. In bored one-vault stations, which were realised on Prague metro on the lines A and C and are being designed for the new line D, the safety wall would have to be too high and it is unrealistic. This system is suitable for cut-and-cover stations.

Exit double doors in metro vestibule will increase the pressure loss of air at the exit to the surface. The amount of the air flowing through the exit double doors is diminished.

7. REFERENCES

(1) Guidlane of Prague Transport Company 22-2012-01 – Principles of Fire Protection in Prague Metro Line
(2) EN 14067-1, EN 14 067-3 Railway applications – Aerodynamic in tunnels
(3) The measurement of the flow and pressure of the air in the cross passages - Faculty of Mechanical Engineering of the Czech Technical University in Prague and METROPROJEKT Praha a.s.

PRACTICAL EXPERIENCES FROM THE INSTALLATION OF THE ESCAPE WAY VENTILATION SYSTEM OF THE DALAASER TUNNEL

[1]Reinhard Kripsch,
[2]Reinhard Gertl
[1]Sirocco Luft- und Umwelttechnik GmbH, Austria
[2]ILF Consulting Engineers Austria GmbH, Austria

ABSTRACT

The Dalaaser tunnel is a 1.8 km long bidirectional road tunnel which is part of the S16 Arlberg express motorway. Two new emergency exits were added to the three existing emergency exits. The ventilation system of all escape ways was designed to fulfill the latest Austrian RVS 09.02.31 guidelines as well as the standards of the applicable Asfinag design handbook. Due to different geometrical boundaries several detailed designs had to be realized. However, the ventilation system of the escape ways is very typical for many projects which are executed these days.

The paper will show the the designer's and the subcontractor's point of view. What are the requirements during the design phase and what are the influences and required information at which stage of the execution phase? What information is generally missing or is not prepared sufficiently for the execution phase? What challenges were faced during the execution phase besides lack of time and very limited space? Specific conclusions will be drawn for both a comprehensive design process and an organized execution phase.

Keywords: escape way ventilation, emergency ventilation in road tunnels, control of ventilation system, converter driven axial fan, overpressure in escape ways

1. INTRODUCTION

The idea of this paper is to show the experiences from the designer's and the supplier's point of view in the same project but at different stages of the project lifecycle, and how they can learn from each other.

The first part of the paper will show the design process based on the applicable design basics. The results of this process are the dimensions of dampers and the operating points of the axial fans. The second part of this paper will show the supplier's process which starts at the very beginning to gather all the required information for the escape way ventilation systems. The information is generally distributed over several documents which are part of a large number of documents which were submitted to the contractor.

The renovation of the Dalaaser tunnel's escape way ventilation was strongly affected by space limitations for the equipment and the challenge of the tight timeframe which led to a partly parallel realization of construction, electrical and mechanical installations.

2. GENERAL

The Dalaaser tunnel is part of the S16 Arlberg expressway and is located in the district of Bludenz in Vorarlberg. The tunnel has a length of 1.8 km and is operated as a bidirectional tunnel. The daily average traffic is 13,400 vehicles with a share of 9.6% of heavy goods vehicles. The tunnel was constructed using the drill and blast method and has a horse shoe profile. The regular cross sectional profile is 54.5 m² and the hydraulic diameter is 7.7 m.

3. DESIGN OF ESCAPE WAY VENTILATION SYSTEM

3.1. Design Boundaries

The existing tunnel had three emergency escape tubes which led outside. During systems renovation two additional escape tubes were built in order to reduce the distance between the emergency exits and to fulfil the EU Directive 2004/54 EC [1] as well as the "Straßentunnel-Sicherheitsgesetz" (STSG) [2]. The maximum allowable distance between emergency exits is 500 m.

The design of the escape way ventilation system is based on the requirements of the Austrian guideline RVS 09.02.31 [3] and the Asfinag design handbook PLaPB [4]. The RVS [3] requires a flow velocity from the escape way towards the tunnel tube when opening the escape way door. The PLaPB [4] has more specific requirements regarding the minimum flow velocity through an open escape way door. The minimum flow velocity is 1 m/s in case of an twin bore tunnel system with cross passages between the tubes and 2 m/s in case of escape ways which lead outside. This is the case for the Dalaaser Tunnel.

3.2. Description of the Ventilation System

The ventilation system of the traffic tube consists of eight pairs of fully reversible jet fans. The jet fan pairs adjacent to the portals are controlled by frequency converters. All other jet fans are switched on and off directly. Two flow velocity measurement locations are installed at distances of approximately 400 m from each portal. Each flow velocity measurement location comprises three measurement devices.

The existing tunnel had three emergency escape tubes which led outside. During systems renovation two additional escape tubes (GA 201, GA 209) were built in order to reduce the distance between the emergency exits and to fulfil the EU Directive [1] and the STSG [2]. The former escape ways had no mechanical ventilation. In order to fulfil the requirements of RVS [3] and PLaPB [4] the new and the renovated escape ways needed mechanical ventilation. The escape way ventilation system has one axial fan with a shutting damper and a silencer at the end of the escape way and an overpressure damper installed in series combined with a shutting damper at the beginning of the escape way that connects the escape way with the main tunnel. The following figure shows the schematic layout of the escape way ventilation and the tunnel ventilation system.

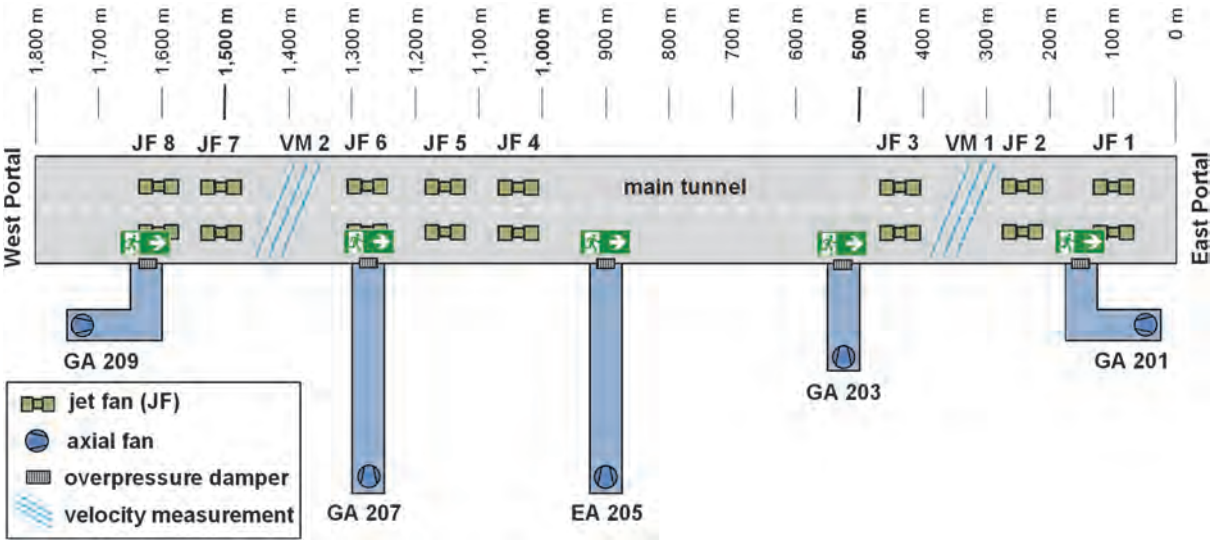

Figure 1: Schematic layout of the escape way ventilation and the tunnel ventilation system

The following table shows an overview of the length, the location and the distances between the escape ways.

Table 1: Length, location and distances between escape ways

Escape way	Length	Distance to East Portal	Distance between escape ways
GA 201	69 m	154 m	E. Portal – GA 201: 154 m
GA 203	89 m	518 m	GA 201 – GA 203: 364 m
EA 205	181 m	902 m	GA 203 – EA 205: 384 m
GA 207	185 m	1,282 m	EA 205 – GA 207: 380 m
GA 209	124 m	1,639 m	GA 207 – GA 209: 357 m

In case of a fire in the main tunnel the shutting damper between the main tunnel and the escape way opens. At the same time the shutting damper of the axial fan opens and the axial fan starts at speed n1. The axial fan draws air from outside into the escape way tube. The air then flows through the overpressure damper which keeps the overpressure between the escape way tube and the main tunnel within a range of approximately of 40 to 50 Pa.

When the escape way exit door opens the axial fan accelerates to speed n2 to achieve the required flow velocity through the open door. As soon as the door is closed the axial fan decelerates to speed n1.

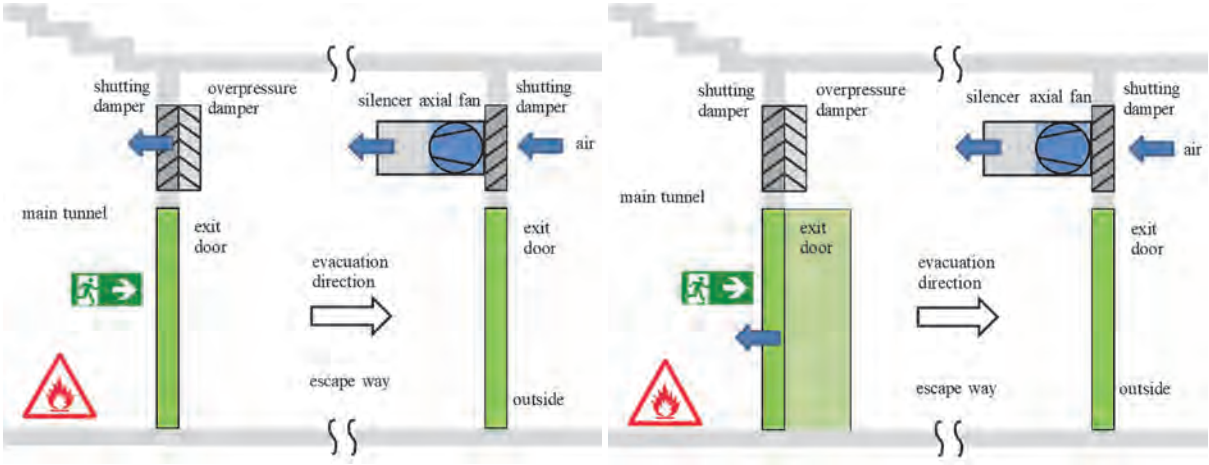

Figure 2: Concept of escape way ventilation, fan speed n1 (left) and fan speed n2 (right)

3.3. Dimensioning of Escape Way Ventilation

The dimensioning of the escape way ventilation is conducted for both fan speeds n1 and n2. The size of the fan is determined by the fan speed n2 which considers one open escape way exit door. The minimum required flow velocity through an open door is 2 m/s, see chapter 3.1. The door is 1.0 m wide and 2.2 m high. The leakage of the closed exit door is considered to be 0.05 m³/s. An additional design reserve of 25% is added. Following these boundaries and assumptions the flow rate is calculated as: (2.0 m/s * 2.2 m² + 0.05 m³/s)*(100% + 25%) = 5.6 m³/s. The external pressure loss along the flow path is calculated to be 280 Pa.

The calculation of the operating point for fan speed n1 considers the minimum possible flow rate of the fan which amounts to about 25% of n2. Therefore, the flow rate for fan speed n1 is 5.6 m³/s * 25% = 1.4 m³/s. The external pressure loss along the flow path is calculated to be about 130 Pa.

4. EXECUTION PHASE

At the execution phase the contractor (supplier) has to provide the equipment as specified in the design phase. It is basically not subject to discuss and change basic design data. In this phase the designer is not noticeable for the supplier.

4.1. Defining the Equipment Details

The first big goal is to filter the relevant information. The cross section ventilation is just one detail within a complex project. Consequently the complete contract papers cover much more than needed for these components. The Technical Report Tunnel Ventilation Design [5] compiled by the designer is just one necessary part.

The fans are selected based on the given nominal power, the required pressure increase and volume flow of the higher operating point. The diameter is defined in the specification and is one of the main figures influencing the arrangement. Of course the silencer has a bigger diameter than the fan.

It is essential to find the exact location and arrangement of each unit listed in the bill of quantities. The width and height of the dampers, as well as the exact mounting position have to be defined. It might happen that for one position of the bill of quantities different dimensions or actuator arrangements are necessary due to the given surroundings.

It is only for defined positions that the size of the damper and arrangement of the actuator can be defined. For the Dalaaser Tunnel three different arrangements at the fan side and two different arrangements at the main tunnel side for five escape ways had to be defined. Additionally mounting on different materials had to be considered. Partly the equipment had to be mounted on concrete walls, partly on steel constructions.

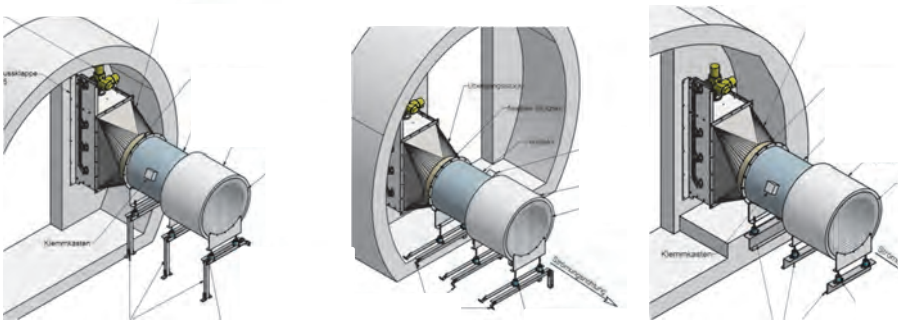

Figure 3: Three different arrangements of the damper, the drive and the fan at the end of the escape way which has access to the outside

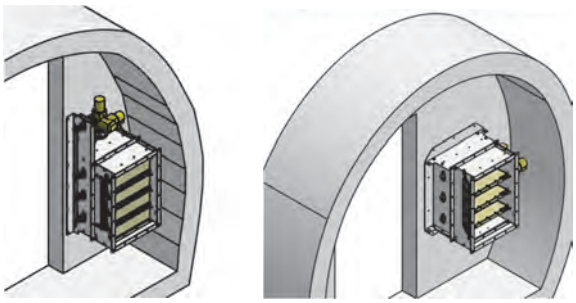

Figure 4: Two different arrangements of the overpressure damper and the shutting damper at the beginning of the escape way which is connected to the main tunnel

The following examples show some more necessary installation variations from other projects. It is very difficult to find sufficient space for the ventilation. The opening of doors has to be considered and flat channels and warping are required to place the equipment away from the escape way in order not to block the door area. The main challenges concern the installation of the now required mechanical ventilation system in existing escape ways. A lot of imagination is required of the designer to find space for the equipment and it is a challenge to build the units into this space for the supplier.

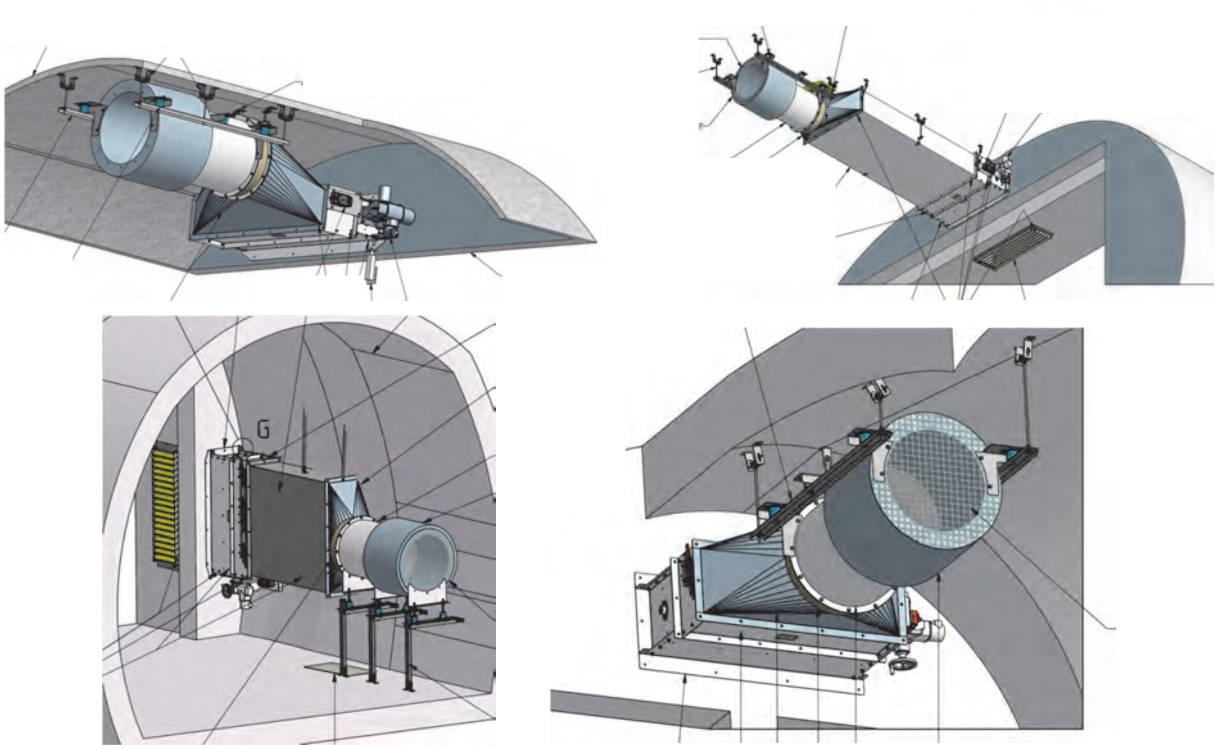

Figure 5: Examples from other projects of different system arrangements due to limited space

4.2. Design, Approval, Site Measurements and Manufacturing

The normal process is to create drawings and documents, get them approved by the client, take site measurements, implement the natural size information into the design and finally start with the production.

The necessary sequence of works of first doing the construction, then installing the steel walls and doors and at last mounting the ventilation parts on the just finished parts means that site measurements are not available for manufacturing. Therefore more attention had to be paid to the design and coordination.

4.3. Site Installation

Site works at the Dalaaser tunnel were more complicated than is usually the case because the tunnel was open for traffic during the day, and construction and installation works were executed during tunnel closures at night. The overall schedule was quite tight. This is why it was necessary to perform many works in parallel. Consequently, this led to conflicts.

Luckily, it was possible to compensate for part of the conflicts because of another project being carried out at the same time in this geographical region. Another positive factor was the supplier's optimal coordination of all works.

4.4. Commissioning and Settings

Several components involve different companies which need to work together during the commissioning of the escape way ventilation system. Electricity has to be supplied, the

control system must be in operation and other ventilation equipment such as jet fans in the main tunnel have to be operated to bring the tunnel into the required flow condition which differs in each escape way.

The settings for the escape way ventilation system are only possible if the tunnel is closed to traffic. Because moving vehicles would produce relatively high transient pressure waves which would massively affect the system.

The following table shows the settings of the fan speeds n1 and n2, as well as the differential pressure between the escape way and the tunnel and the outside. Additionally, the measured flow velocity through the emergency exit door at the beginning of the escape way is shown. It can be seen that the pressure differences above the closed doors are within the favorable range. The flow velocities through the open doors are slightly below the required value according to PLaPB [4] but fulfil the requirements according to RVS [3].

Table 2: Pre-settings and measurement results at commissioning

Escape Way	**Fan Speed**		**Pressure Difference, doors closed, at fan speed n_1**		**Air Velocity through open door to main tunnel, at fan speed n_2**				
	n1	n2	exit door tunnel	exit door to the outside	Top	Middle	Bottom	Average	
No.	Hz	Hz	Pa	Pa	m/s	m/s	m/s	m/s	
GA201	17	25	41	40	1.5	1.7	1.6	1.6	1)
GA203	23	25	50	67	1.4	1.5	1.5	1.5	
FA205	25	25	45	48	1.8	1.8	1.9	1.8	2)
GA207	20	20	47	50	1.8	1.5	1.5	1.6	
GA209	16	22	48	46	1.8	1.7	1.7	1.7	

Remarks

1) It was found that the system could be set into oscillation by closing the door at a certain fan speed. The influence of the door could be adjusted by changing the speed of the fan, changing from “oscillation every time by closing the door” to “oscillation when pushing the door hard enough” to “oscillation only when pushing the door very, very hard”. This effect was the same at both doors at the beginning and at the end of the escape way.
2) The setting was done at the required moment in accordance with the project schedule. However, at this escape way some openings for cables had not yet been closed at this time. After closing these openings of course the settings had to be adjusted as well. This was done between our time slot for commissioning and the inspection of the test engineer.

The lower operating point had to be adjusted to be very close to the minimum speed of the fan. The limiting factor for this minimum speed of the fan is the cooling of the fan’s motor. The higher operating point is set in the range of 50% of the nominal speed because the flow velocity through an open exit door was reduced compared to the design value.

The commissioning had shown the sensitivity of the ventilation system. The smallest possible change of the frequency already causes remarkable change of the pressure difference to the main tunnel when the door is closed.

Table 3: Settings and measurement results at formal commissioning inspection
Target values for n1: approx. 40Pa (max. 50Pa), for n2 range 1.0 to 1.2 m/s

Escape Way	Fan Speed				Pressure Difference, doors closed, at fan speed n_1	Air Velocity through open door to main tunnel, at fan speed n_2	
	n1		n2		exit door tunnel	Average	
No.	%	Hz	%	Hz	Pa	m/s	
GA201	25	12.5	35	17.5	31	1.3 – 1.5	1)
GA203	35	17.5	40	20	42	1.5 – 1.8	
FA205	35	17.5	40	20	40	1.4 – 1.7	
GA207	30	15	35	17.5	38	1.2 – 1.5	
GA209	30	15	40	20	38	1.5 – 1.7	

All values were slightly reduced for the pre-commissioning. No operating point is above 50% of the fan capacity.

At another project a third operating point had been defined. In this case the control of the ventilation system distinguishes between all doors closed, one door open and two doors open.

4.5. Characteristics of the Overpressure Damper

Besides the fan the overpressure damper is the second item used to make adjustments within the system. The characteristics of the overpressure damper can be influenced by using weights and lever arms.

To learn about the damper characteristic we did two steps. First a simple experiment in the workshop. We used a standard container and installed a fan and a shutting damper as well as an overpressure damper. After the first measurements we were able to define the position and size of the weights so accurately that on site only the fan speed needed to be adjusted.

In the second step the damper curves have been measured for three different weight adjustments – with low, medium and heavy weight.

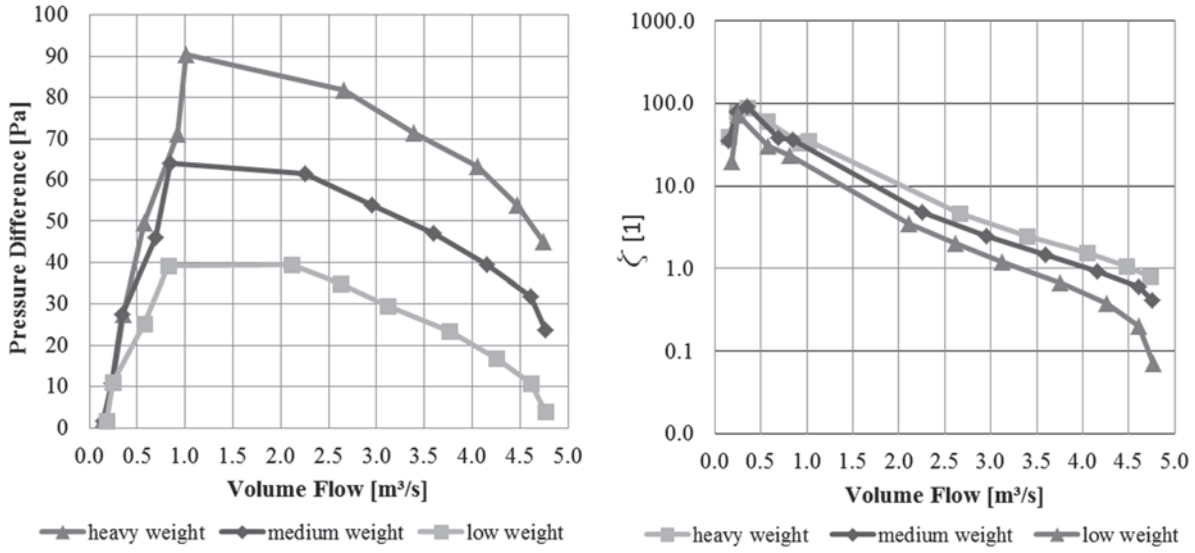

Figure 6: Characteristics of overpressure damper

5. CONCLUSION

5.1. Standardized System Designs

In a project the fans of the escape way ventilation system are usually of the same type and size. Consequently, the length, cross section and surface of the escape ways and differences in the equipment arrangement practically have no significant impact.

The study of the design data of a broad variety of projects showed that the nominal power of the fans varies from 1.5 to 7.5 kW. The fan's flow rate varies from 2.75 m³/s to 6.8 m³/s. Considering that the fan's flow rate is determined only by the type of emergency exit door which either leads outside or between tubes, it should be possible to define a standardized fan type for each of the two escape way types.

5.2. Fan Selection

When preparing this paper it was found that the fan selection is primary based on the higher operating point. But also the lower operating point needs to be valid and lie safely within the fan characteristics because in the event of a fire all axial fans are switched to fan speed n1. At the escape ways where people evacuate to the outside the axial fan speeds are switched to fan speed n2 when the exit door opens. The lower limit of the fan speed (n1) is defined by the cooling of the fan motor.

An operation at 55 or 60 Hz at the higher point should be taken into consideration, in order to be able to increase the lower fan speed.

6. REFERENCES

[1] EU Directive 2004/54/EC of the European Parliament and the Council on minimum safety requirements for tunnels in the trans-European road network, 29th of April 2004

[2] Straßentunnel-Sicherheitsgesetzt (STSG), Federal law of Austria on the safety of road tunnels, BGBl. I No. 54/2006 and changes in BGBl. I No. 111/2010 and 96/2013

[3] RVS 09.02.31, Tunnel Ventilation Design Guideline Austria, 1st of June 2014

[4] PLaBP 800.542.1000, Design Handbook Tunnel Ventilation, Technical Guideline, 1st of January 2016

[5] ILF Consulting Engineers, Technical Report Tunnel Ventilation Design, 25th of January 2017

[6] Asfinag BMG, B3 Contractual Technical Condition, 1st of October 2013

MAIN DIRECTIONS OF UPGRADING SEVEROMUYSKY RAILWAY TUNNEL VENTILATION WHEN THERE IS AN INCREASE OF THE AMOUNT OF TRAFFIC OF THE ROLLING STOCK

[1]Simon Gendler, [1]Mikhail Belov,
[2]Roman Vvedensky, [2]Michael Mogilniy,
[1]Saint-Petersburg Mining University, Russia
[2]OJSC NIPII "Lenmetrogiprotrans", Russia

ABSTRACT

The purpose of this study was developing suggestions on upgrading heating and ventilation systems of the Severomuysky tunnel with respect to rolling stock's traffic increase. To this end, field studies of heating and ventilation systems were performed in winter. Main factors determining heating and ventilation regimes were defined and technical solutions were proposed for upgrading existing systems. On the basis of theoretical and empirical data, the upgrade solutions of the heating and ventilation systems were justified in the event of double increase of rolling stock traffic.

Keywords: Railway tunnel. Ventilation, Heat regime, Unit-heater, Amount of traffic, Piston effect, Air consumption, Automatic gate. Equivalent equilibrium volumetric activity of radon.

1. INTRODUCTION

Severomuysky railway tunnel (SMT), which was finished in 2003, is the longest tunnel in Russia [1]. In order to insure safety of the tunnel, a ventilation system is used that provides an adequate air supply during an annual period and distributes the air over the traffic tunnel, service tunnel, shafts, shaft sidings and crossings and functions alongside with an outdoor air system in winter until positive temperature establishes [1,2].

The requirements towards the heating and ventilation systems demanded frost and mist prevention as well as the decrease of volumetric activity of radon in sidings' air [1,2,3].

Trains pump large amounts of cold outdoor air into the tunnel due to a piston effect; from each tunnel portal, the air travels considerable distances in the direction of train movement. Additionally, tunnel's air is cooled as a result of heat exchange with train surfaces temperature of which equals outdoor air temperature. Since it was impossible to eliminate or mitigate the piston effect of a moving train and in order to maintain positive temperature in the tunnel, an approach compensating for the cold pumped by trains was used when there were no trains traveling [1,5].

To supply air into SMT's sidings main ventilation fans are used, which are installed in a crossing that connects the ventilation shaft and traffic tunnel, alongside fans used for distributing air between the traffic and service tunnels [1]. An important element of the ventilation system is portal gates that are used to control air flows [2].

A full diagram of sidings drawn during the construction of the SMT is available in [1].

During the winter season the outdoor air entered the tunnel by means of the natural draught or/and fans as well as the piston effect from the trains through the tunnel portals and was removed through the ventilation shaft.

During the initial period of operation of the SMT, outdoor air heating was performed by unit-heaters located in ventilation buildings next to the tunnel portals and by additional unit-heaters installed in dedicated chambers 250 - 300 meters away from the west and east portals.

Despite the fact that after the unit-heaters the air temperature reached 35 - 45ºC, the closer the air approached the ventilation shaft the less compensation for the cold it could provide, what was especially true for distances beyond 3000 m from the portals.

Regular cross direction movement of the trains created in the middle of the tunnel an area of lower temperatures compared to those after unit-heaters. With the outdoor air temperature being -30ºC to -35ºC, the temperature in the area dropped below 0ºC, what resulted in frost building-up.

For this reason, it was necessary to redistribute unit-heaters along the tunnel by means of deploying additional heat-up systems 3520 m away from the east portal and 4370 m from the west portal.

Winter 2017 field studies included efficiency evaluation of the existing heating and ventilation equipment, finding its weaknesses as well as main opportunities for upgrade of heating and ventilation system in the event of a double increase in rolling stock traffic.

2. SMT's HEATING AND VENTILATION SYSTEM STUDY

2.1. The purpose and objectives of the study

The purpose of the study was to determine actual aerodynamic and heat parameters of the heating and ventilation system.

The objectives in this study dealt with:

- defining actual air consumption distribution per an SMT's siding;
- studying the piston effect created by a goods train depending on different position of the portal gates;
- evaluating unit-heater efficiency installed next to portals;
- measuring air temperature distribution along the tunnel with units installed for local air heating;
- measuring volumetric activity of radon in the traffic and service tunnel.

2.2. The results of measuring air consumption and air movement directions during SMT's operation

Air consumption and its movement directions in SMT's sidings were determined by means of air flow measurement along sidings according to methodology [2]. To measure air speed and its thermodynamic parameters MES-200 thermal anemometer [2] was used.

Air flow directions through sidings according to the measurements are shown in Figure 1.

According to the measurements, outdoor air enters the traffic tunnel (TT) through the West and East portals, then it gets heated up by unit-heaters located in ventilation buildings (VB) and by additional unit-heaters (AH). As soon as the air reaches ventilation crosscuts (7), one part of it is sent to the service tunnel where it was split into two flows. One of the flows moved towards a bypass tunnel (BT) where it mixed with air from the traffic tunnel (TT). Another air flow moved through the service tunnel towards ventilation buildings (VB) at the West and East portals, then it was heated up by unit-heaters 12 and sent into the traffic tunnel (TT) by fans 11.

Another part of the air after the ventilation crosscuts (VCrc) moved through the traffic tunnel (TT) to the crossing (Cr) and forth where was bled off through an air staple shaft into the service tunnel (ST).

After mixing, the whole air volume from the traffic tunnel (TT) and service tunnel (ST) was sent through the bypass tunnel (BT) into the ventilation shaft (VSh) to reach the surface.

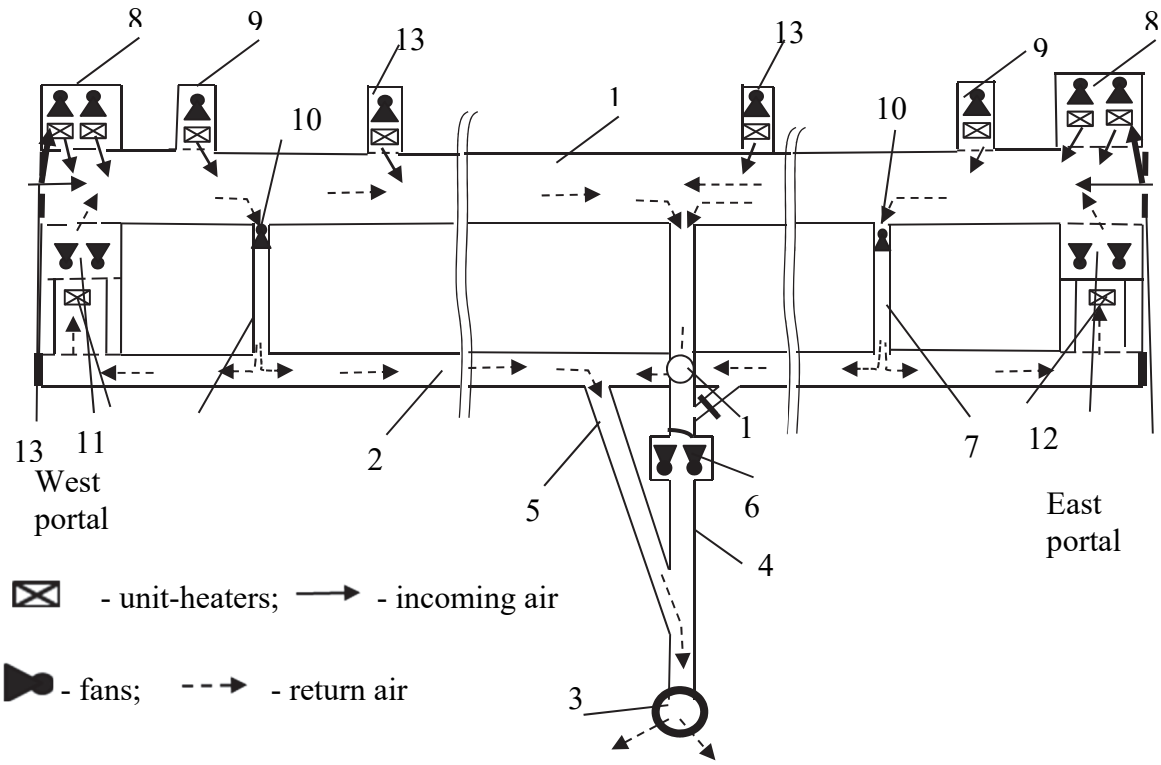

Figure 1: Ventilation scheme for Severomujsky tunnel in winter: 1 – traffic tunnel (TT); 2 –service tunnel (ST); 3 – Ventilation shaft (VSh); 4 – crossing (Cr); 5 – bypass tunnel (BT); 6 – ventilation room with main fans (VR); 7 - ventilation crosscut (VCrc); 8 – ventilation building (VB); 9 – additional unit-heaters (AH); 10 – fans for air-splitting (Fsp); 11 – fans for recirculation air (Frec); 12 - unit-heaters for recirculation air (UHrec); 13 – local unit-heaters (LH); 14 - air staple shaft (Assh); 15 – automatic gates (AG).

During the field study, main fans (VR) were off and their inputs were shut with dump doors.

During the study, airflow at the portals without trains was 35 - 50 m^3/s, service tunnel areas between the ventilation crosscuts and ventilation buildings was 6 - 19 m^3/s, the airflow that reached surface leaving the shaft amounted to 50 - 70 m^3/s. The difference between the airflow was caused by the piston effect that could not be avoided during the field study while the railway tunnel was in operation. Moreover, during observations, it was noted that not only the absolute air consumption values, but also the direction of movement changed inside both the traffic (TT) and service tunnels (ST).

2.3. Studying the piston effect created by moving rolling stock in the tunnel

In order to evaluate the piston effect of rolling stock air speed (consumption) was measured that entered the tunnel through portal sections. The measurements were performed at the East portal alongside a freight train moving westwards (the direction of a natural draught was from West to East). In order to eliminate the influence of portal's resistance on the velocity field, the measurement point was located at a distance 10 times exceeding the hydraulic diameter of the tunnel.

Air speeds were recorded every 30 seconds in the measurement point during the process. The measurement was taken before the train entered the tunnel and immediately it reached the test point. The train consisted of 85 cars. Average train's speed in the tunnel was approximately 51 kph. The results of the measurement are shown in Figure 2.

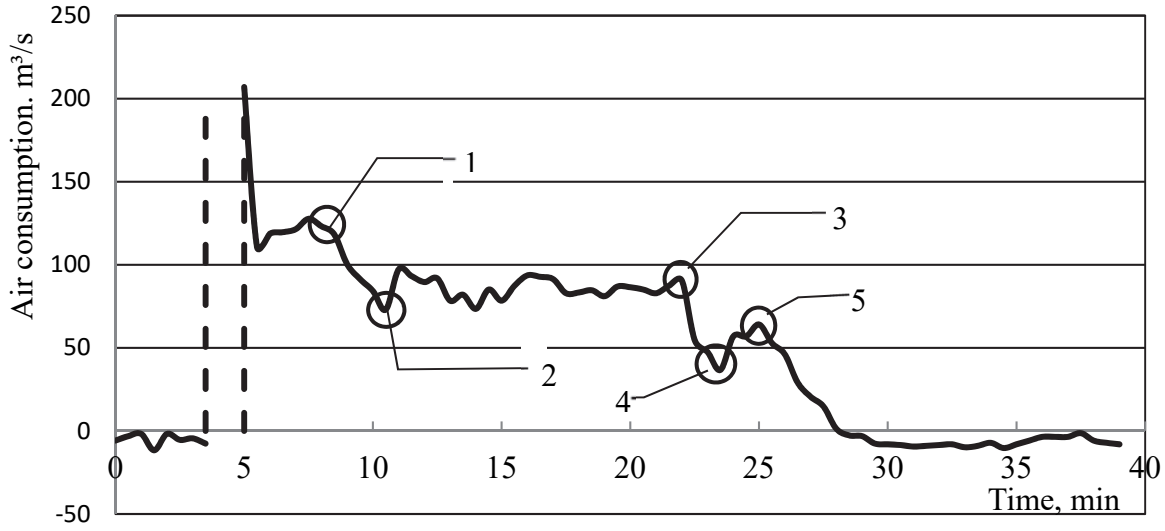

Figure 2: Behaviour of consumption on entering the tunnel with a moving rolling stock (dashed lines indicate the step time of the rolling stock at the test point).

The analysis of the measurements showed that the train by entering the portal caused the natural air flow eastwards direction to change (negative air consumption value on the diagram). A significant drop in air consumption was caused by shutting the East portal gates after the train passed by (point 1). As the train moves westwards, air consumption continuously goes down. After the West portal gates were open, the air flow at the measurement point grew by 20 m^3/s (point 2). The area of the graph between point 2 and 3 show the behavior of the amount of air entering the tunnel with a moving train, with open West portal gates. As the train leaves the tunnel, air consumption drops (point 4). As the train completely leaves the tunnel with open West portal gates, air consumption grows approx. by 25 m^3/s (point 5) due to a lower aerodynamic resistance of the tunnel. After the West portal gates are shut, air consumption drops to zero and air begins its eastward movement again. Average air consumption calculated during the existence of the piston effect was 82.2 m^3/s, and the piston effect lasts for 27 minutes.

Comparing the piston effect in winter and in summer [2] with the above mentioned settings of portal gates opening/closing shows that average air consumption nearly doubles with the gates open. Calculations performed according to paper [4] regarding the field study conditions revealed that the estimated value of the average air consumption is 74 m^3/s what deviates from the empirical data only by 10%.

2.4. Studying temperature conditions at the portal areas

Air temperatures before and after the unit-heaters installed in the ventilation building (VB) at the East portal were measured without trains and with trains leaving or entering the East portal. Alongside measuring the temperature, air volumes entering the unit-heaters were measured. The changes in temperature are shown in Figure 3. Data analysis make it possible to conclude that the direction of train's movement regarding the portal with unit-heaters exerts ultimate influence on the resulting air temperature. When a train enters the portal bringing outdoor air to the unit-heaters, return air temperature from the unit-heaters does not exceed 7 - 13°C. When a train leaves the portal, unit-heaters are supplied with tunnel air with average temperature amounting to the average temperature of an adjacent tunnel section. As a result, unit-heaters' output temperature reaches 30 - 43°C and the heated air is removed from the tunnel. The amount of air supplied to the unit-heaters does not change depending on the train's direction and is 13 - 15 m^3/s.

Thus, a unit-heater located at the exit portal virtually heats-up only the portal area and the outdoor air outside the portal, what decreases its energy efficiency.

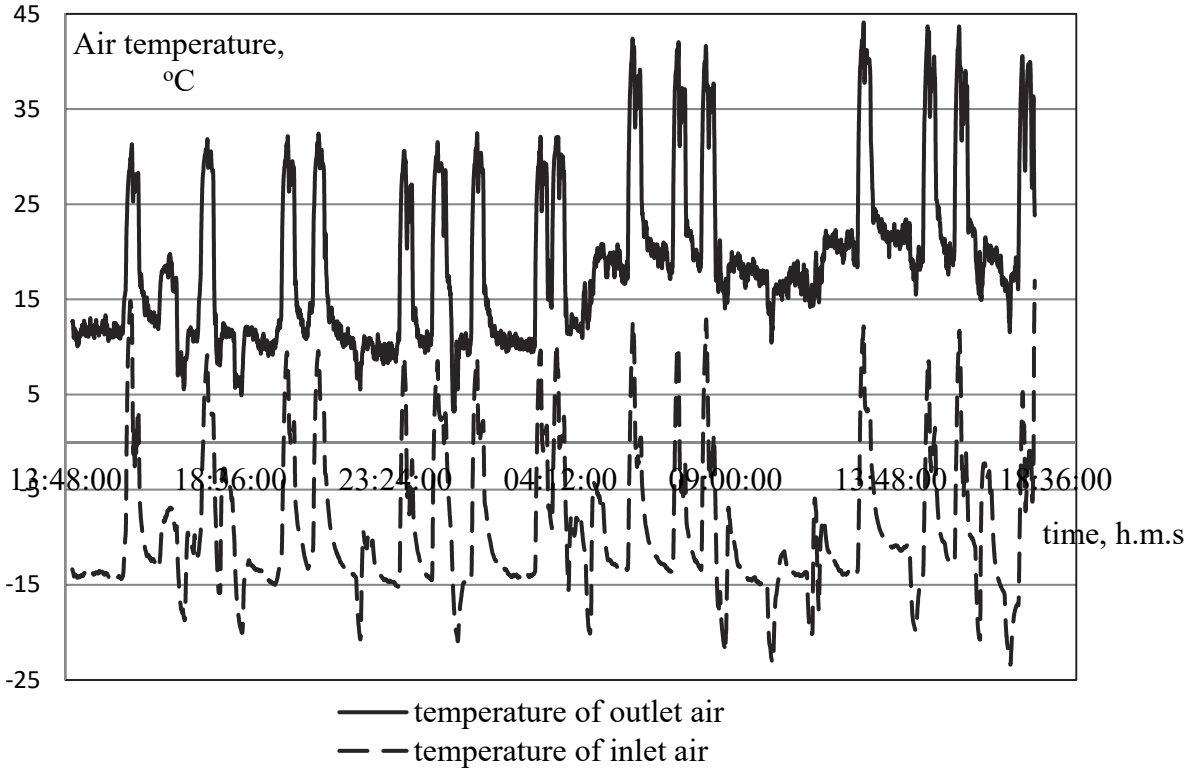

Figure 3: Inlet and outlet air temperature changes of the unit-heaters located in the ventilation building (VB).

Beside the efficiency of the portal unit-heaters average temperatures at the portal areas were measured while there was a train inside the tunnel. The cross section where the temperature was measured at coincides with the airflow measuring points. According to the data analysis shown in Figure 4, air temperature in the tunnel before a train entered was 17ºC.

After the train passes the measurement point, usually there is a significant drop of 13ºC. The temperature remains nearly constant for 18 minutes after the train leaves. It goes back to its initial values 35 - 40 minutes later.

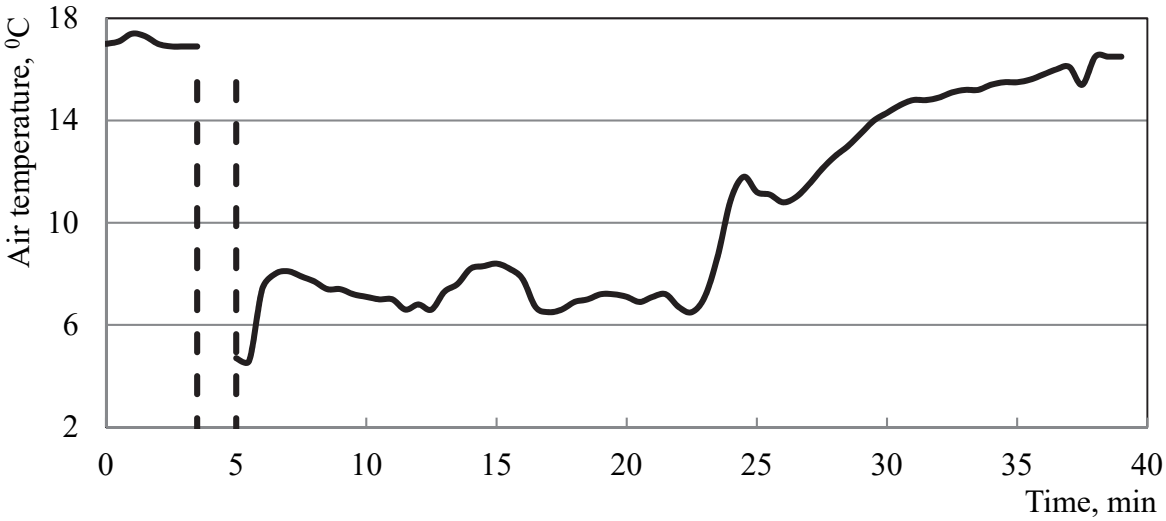

Figure 4: Air temperature changes at the entrance to the tunnel with a moving train (dashed lines indicate the step time of the rolling stock at the test point).

2.5. Temperature measurement results of the air distributed along the tunnel

The changes in air temperature along the tunnel were measured for the same heating system but after additional unit-heaters were installed at 3520 and 4370 meters away from the East and West portals correspondingly (Figure 5).

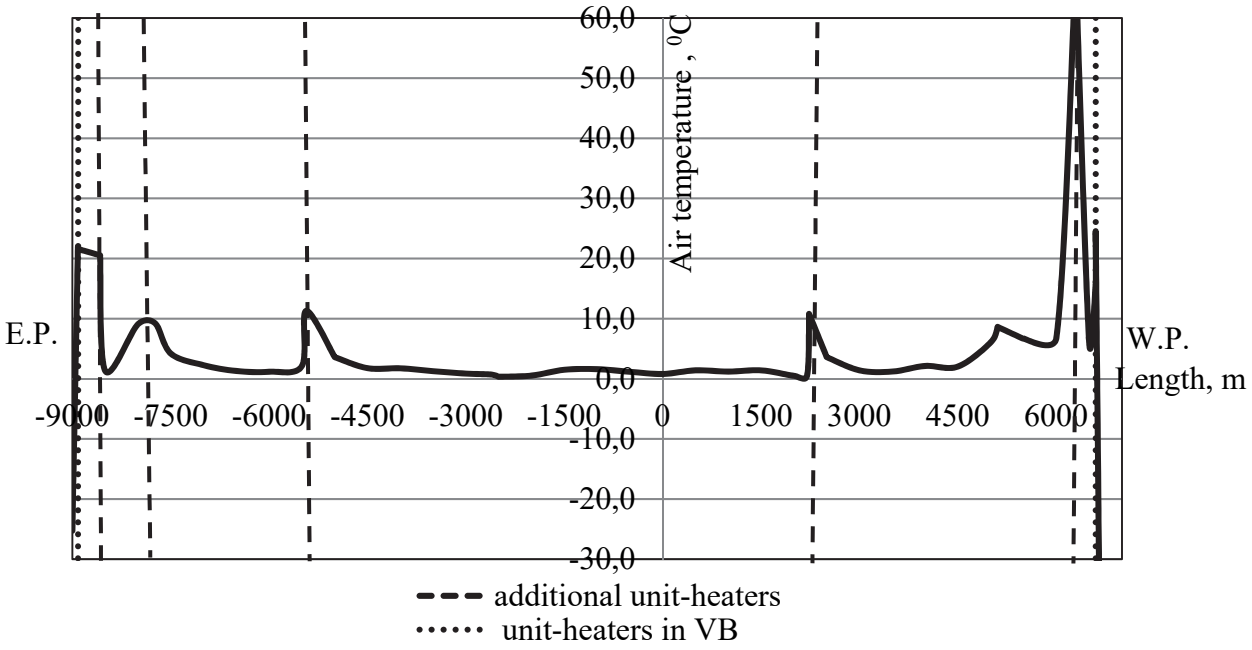

Figure 5: Air temperature distribution along the tunnel.

Data analysis showed that using the distributed heating system allowed increasing the temperature in the middle section of the tunnel up to positive values where it used to go below 0ºC.

2.6. Evaluating volumetric activity of radon in the traffic and service tunnels

The evaluation of radiation environment was performed by equivalent equilibrium volumetric activity of radon ($EEVA_{Rn}$) in the traffic and service tunnels.

The traffic tunnel shows normal values of $EEVA_{Rn}$ [7], but the service tunnel showed a 2 – 2.5 times excess of $EEVA_{Rn}$, especially in the air entering the bypass tunnel (BT). The reason for this is regular changes in air movement direction due to the piston effect and air recirculation among the portals and ventilation crosscuts that lead to the accumulation of radon in the air.

The comparison of average volumetric activity of radon in sidings and the volumes of water drained from the tunnel showed a linear correlation between those two values with a coefficient no less than 0.7.

This means it is possible to stabilize radiation environment not only through ventilation improvements, but also decreasing the amount of drain water containing radon in the tunnel.

3. APPROACHES TO UPGRADING HEAT AND VENTILATION SYSTEMS IN THE EVENT OF ROLLING STOCK'S TRAFFIC INCREASE

Field studies of existing heat and ventilation systems in the SMT helped to find out the details of their operation with current rolling stock traffic and to suggest technical solutions to upgrade the systems in the event of a double increase in the traffic.

In order to define heat and ventilation systems' parameters in the event of rolling stock's traffic increase, a simulation model was created to study the aerodynamics of the tunnel's ventilation depending on different traffic intensity and speeds in the traffic tunnel (TT) [4,6]. The considered cases included one or two trains traveling with the speed of 60 and 80 kph. Simulation results showed that the average amount of air entering the tunnel when the piston effect was online and the train speed was 60 kph was 70 m^3/s in case of one train traveling and changed to 96 m^3/s in case of two freight trains. If the speed was 80 kph, the amount of air entering the tunnel increased from 110 m^3/s to 120 m^3/s correspondingly. Those data were used to calculate air heating system capacity [5]. It turned out that in case of a double increase in rolling stock's traffic the capacity of the heat system needs to be increase two and threefold depending on train schedule and speeds.

On the basis of the field studies and simulations a number of technical solutions was proposed for operating the SMT with the increased rolling stock's traffic meeting the requirements from Section 1. The solutions include:

- deploying additional heat systems along the tunnel and simultaneous increase of unit-heaters' capacity at the portals;
- controlling the performance of unit-heaters at the exit portals to decrease energy consumption;
- ventilating the service tunnel with heated outdoor air by a separate ventilation system instead of ventilating the tunnel by means of air recirculation.

4. CONCLUSION

The following information was found on the basis of field studies and simulations:

- The main factors affecting the operation of current heat and ventilation systems of the outdoor air are traveling freight trains up 1200 meter long at a speed up to 60 kph and the temperature difference between the tunnel portals of 10 - 15ºC, extremes being from -25 to -35ºC;
- Regular changes in air movement directions due to the piston effect and air recirculation among the portals and ventilation crosscuts, what results in accumulating radon in the air, should be acknowledged as the reasons for the increase in equilibrium volumetric activity of radon in tunnel's sidings.
- To meet the requirement of preventing frost build-up in the event of a double increase in rolling stock's traffic, it is necessary to enhance the capacity of the heat system by 2 - 3 times depending on train schedule and speeds.
- The solutions proposed allow meeting the requirements that guarantee safety of the rolling stock in case of increasing its traffic.

5. REFERENCES

[1] Gendler S.G. Sokolov V.A. (2003). The choice of operation regimes for an air quality *maintenance system in the Northern Mujsky Railway Tunnel*. BHRg 11th International Symposium Aerodynamics and Ventilation of Vehicle Tunnels, Luzern, Switzerland, pp. 289-308

[2] Gendler S.G., Sokolov V.A. (2006). *The results of ventilation tests during practical use of the Severomujsky railway tunnel.* BHRg 12th International Symposium Aerodynamics and Ventilation of Vehicle Tunnels, 2006, Portoroz, Slovenia, pp. 451-462

[3] Gendler S.G., Victor N Castañeda, Ana G Belen (2011) *Control of natural air flow in road tunnels* International conference "Tunnel Safety Forum for Road and rail", Nice, France, 4-6 April, p. 155- 164

[4] Gendler S.G. (2013). *Peculiarities of control ventilation in the Kuznetsovsky railway tunnel.* BHRg 15th International Symposium on Aerodynamics, Ventilation and Fire in Tunnels, Barselona, Spain, pp. 309-323

[5] Gendler S.G., Sinjavina C.V. (2017). *Procedure of system parameters air heating definition in railway tunnels located in severe climatic condition.* The Proceedings of the Mining Institute. SP, t.224. p. 215-222.

[6] Paleev D.J., Lukashov O.J., Kosterenko V.N., Timchenko A.N. (2011). *Computer technology for task emergency control plan.* Publisher "Mining", t.6. Industrial security. Book 2. Moscow. 160 p.

[7] *Standard of a Radiation Safety* (SRS-99), 1999/2000, 115 p.

LIFE CYCLE AND TUNNEL OPERATION ASPECTS WILL DRIVE FUTURE PROJECT NEEDS

René List
ASFINAG Bau Management GmbH, Austria

ABSTRACT

For our demanding society, the usability of transportation infrastructure is of essential importance. We thus have to face the challenge of operating, maintaining and improving roadways and tunnel structures in such a way that road users can travel as smoothly as possible and without any obstructions. Whereas we are able to extend the life cycles of roadway structures, the technical tunnel equipment is exhibiting a contrast in terms of development, as the usable lifespan of information technology devices continues to become shorter. In the future we will have to find ways to successfully manage the coordination of these two diametrically opposed life cycles.

1. INTRODUCTION

As the safety equipment of tunnel structures is very large in scale, the need for refurbishment is becoming more and more frequent. On the one hand, this is due to the life cycle of the tunnel equipment, and on the other hand it is related to the increase in legal regulations aimed at guaranteeing safety in terms of tunnel operation. Examples include directive number 2004/54/EC from the European parliament dated 29 April 2004 that covers the minimum safety requirements for tunnels in the trans-European road network and the more recent EU directive 2016/1148 from the European parliament of 6 July 2016 concerning measures for a unified high level of security of network and information systems throughout the EU. Other factors that are of essential importance are the increase in traffic volume and user demand (i.e. customer demand) for a maximally usable roadway infrastructure. These factors greatly influence the planning of tunnel structures in order to meet the respective requirements.

Currently the 2,200 km long ASFINAG roadway network includes 166 tunnel structures with an overall length of app. 400 km. ASFINAG started a tunnel improvement programme in 2004, which is being implemented in the framework of the “ASFINAG 2020 safety programme”. By 2019, ASFINAG will have invested 5.7 billion euro for the structural upgrade of more than 80 tunnel structures as well as for their upgrade in terms of technical safety equipment.

The upgrading programme is not only being carried out in order to comply with the requirements included in EC Directive 2004/54 by 2019. Other specific reasons include both safe detection of incidents in a more rapid way while at the same time preventing accidents, and improving the availability of self-rescuing facilities, e.g. through the construction of second tunnel tubes. Currently 16 tunnel structures with an overall length of 59 km are either in the planning stage or the construction upgrade to add a second tunnel tube is already underway.

In order to draw the greatest possible benefit from the investments made, the focus is set on optimally utilising the lifespan of tunnel equipment components. An important challenge results from the fact that the lifecycle of the tunnel structure differs from that of the mechanical and electrical equipment. The aim is to guarantee the functionality of the overall tunnel structure (i.e. both the structural infrastructure as well as the mechanical and electrical infrastructure) by carrying out renewals in a timely manner on the basis of regular inspections and checks.

2. FUNDAMENTALS

2.1. Age distribution of ASFINAG tunnel structures

In comparison to other modes of transport, ASFINAG road tunnels are relatively new; the oldest tunnel, the Massenberg Tunnel on the Semmering expressway, was opened in 1965. Tunnel building for the Austrian motorway and expressway network reached its high point between 1986 and 2006 with the construction of the expensive mountain routes (Figure 1).

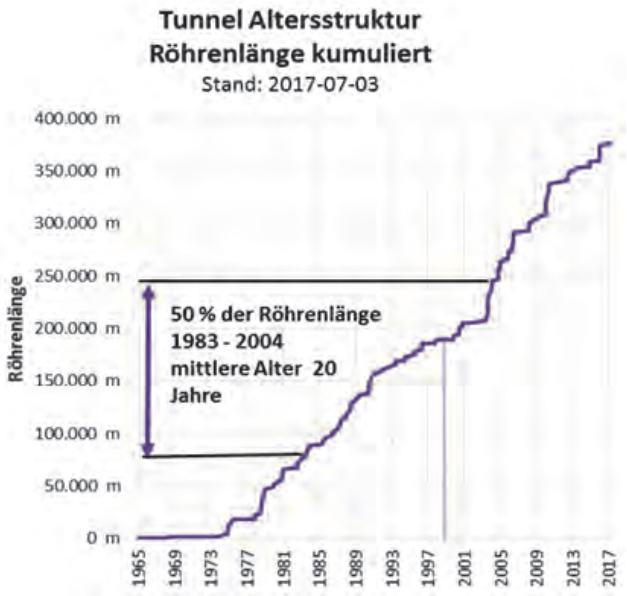

Figure 1: Tunnel condition distribution dependent on age

2.2. Maintenance and repair of the construction and the mechanical and electrical facilities

The upkeep of the construction and mechanical and electrical facilities along with their maintenance and repair are part of the infrastructure investment programme (IIP), which includes a forecast for the next six years in terms of required measures and the related costs. Out of the total investment of 500 million euro allotted to the refurbishment and the renewal of the overall network in 2017, approximately 170 million euro were spent on tunnel structures alone (Figure 2). For 2017 to 2022, investments of altogether 706 million euro are planned for tunnels.

Figure 2: ASFINAG 2017 investment plan for the roadway infrastructure

2.3. Strategic targets of ASFINAG Asset Management

Asset Management comprehensively ensures sustainable maintenance planning (i.e. the planning of required refurbishment measures) in order to guarantee the structural safety and serviceability of the overall road network while at the same time providing for the highest possible route availability of both open roadway sections and tunnels. This includes both the structural infrastructure and the mechanical and electrical infrastructure. The maintenance strategy for road tunnels has the following aims:

- Highest possible route availability through freedom from construction work
- Optimal safety for the road users
- Optimal exploitation of lifecycles; "repair the right thing at the right time"

A three-stage monitoring principle – continuous monitoring, inspection and checking – ensures the best possible standard in terms of both economic feasibility and road safety.

3. LOOKING AT LIFE CYCLES

3.1. Constructional maintenance management

Reliable recording of conditions (testing and checks) allows for the determination of the necessary repair works while at the same time optimising them on the basis of lifecycle analyses.

The following activities are regularly carried out:

- Continuous monitoring: In order to determine the functionality of the structure and the road safety in the traffic space, surveying drives through the tunnel are regularly carried out.
- Checks: Minimally every two years, the structural elements and the associated equipment and the terrain over the structure must be checked by a qualified internal engineer.
- Inspections: Every twelve years, the structural elements as well as the associated equipment and the terrain over the structure are inspected by a qualified external engineer with relevant experience in tunnel inspection. If defects and damage cannot be assessed visually, a special inspection is carried out.
- Special inspections (as required or before planned refurbishments): Special inspections include, for example, profile recording including the checking of deformation measurements in at-risk areas, surveying of pipes, measurement of carbonisation, chloride penetration or concrete cover in damaged zones.

3.2. Maintenance management for tunnel mechanical and electrical equipment

Maintenance management for tunnel mechanical and electrical equipment includes surveys of conditions based on Austrian guideline RVS 13.03.41, entitled “Operational and safety equipment for road tunnels”, which includes regulations with regard to the maintenance, checking and inspection of mechanical and electrical equipment as well as other safety equipment in order to ensure both functionality and operational reliability as well as traffic safety. On the basis of the previously mentioned RVS guideline, ASFINAG has prepared an assessment procedure, which allows for the assessment of the condition of mechanical and electrical facilities. The assessment results serve as a basis for the optimisation of refurbishment measures in terms of economic feasibility (Figure 3).

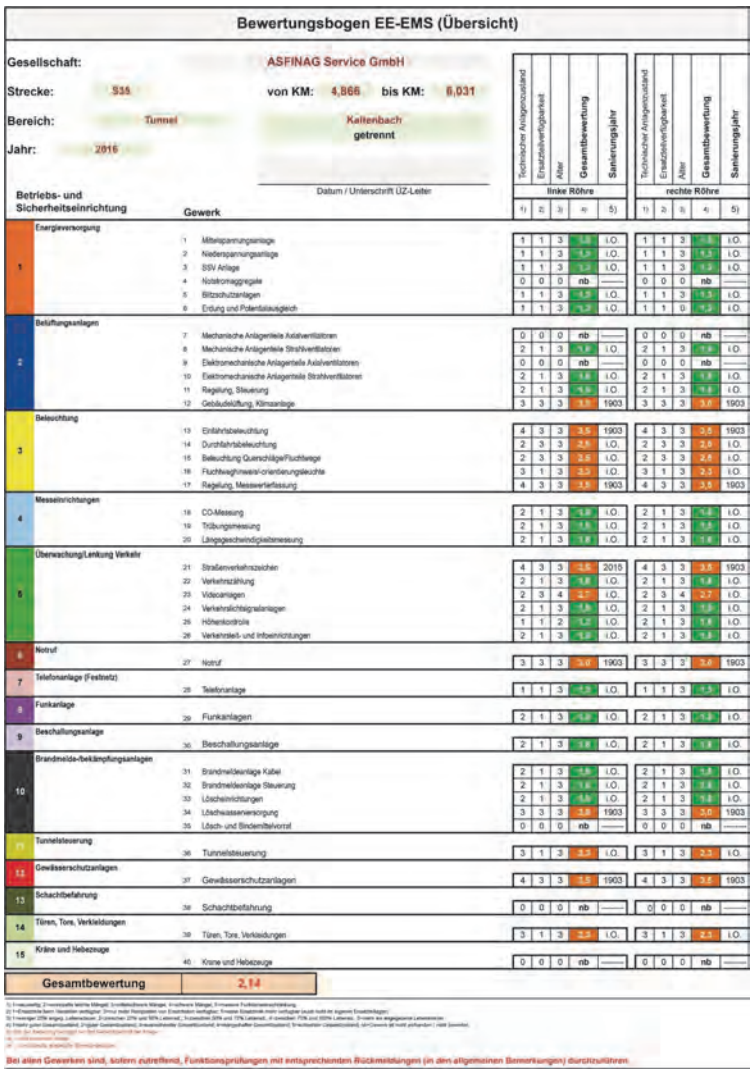

Bewertungsbogen EE-EMS (Übersicht)

Gesellschaft: ASFINAG Service GmbH

Strecke: S35 von KM: 4,866 bis KM: 8,031

Bereich: Tunnel Kaltenbach getrennt

Jahr: 2016

Datum / Unterschrift ÜZ-Leiter

Betriebs- und Sicherheitseinrichtung		Gewerk	linke Röhre: Technischer Anlagenzustand 1)	Ersatzteilverfügbarkeit 2)	Alter 3)	Gesamtbewertung 4)	Sanierungsjahr 5)	rechte Röhre: Technischer Anlagenzustand 1)	Ersatzteilverfügbarkeit 2)	Alter 3)	Gesamtbewertung 4)	Sanierungsjahr 5)
1	Energieversorgung	1 Mittelspannungsanlage	1	1	3	1,5	i.O.	1	1	3	1,5	i.O.
		2 Niederspannungsanlage	1	1	3	1,5	i.O.	1	1	3	1,5	i.O.
		3 SSV Anlage	1	1	3	1,5	i.O.	1	1	3	1,5	i.O.
		4 Notstromaggregate	0	0	0	nb	———	0	0	0	nb	———
		5 Blitzschutzanlagen	1	1	3	1,5	i.O.	1	1	3	1,5	i.O.
		6 Erdung und Potentialausgleich	1	1	3	1,5	i.O.	1	1	0	1,5	i.O.
2	Belüftungsanlagen	7 Mechanische Anlagenteile Axialventilatoren	0	0	0	nb	———	0	0	0	nb	———
		8 Mechanische Anlagenteile Strahlventilatoren	2	1	3	1,8	i.O.	2	1	3	1,8	i.O.
		9 Elektromechanische Anlagenteile Axialventilatoren	0	0	0	nb	———	0	0	0	nb	———
		10 Elektromechanische Anlagenteile Strahlventilatoren	2	1	3	1,8	i.O.	2	1	3	1,8	i.O.
		11 Regelung, Steuerung	2	1	3	1,8	i.O.	2	1	3	1,8	i.O.
		12 Gebäudelüftung, Klimaanlage	3	3	3	3,0	1903	3	3	3	3,0	1903
3	Beleuchtung	13 Einfahrtsbeleuchtung	4	3	3	3,5	1903	4	3	3	3,5	1903
		14 Durchfahrtsbeleuchtung	2	3	3	2,5	i.O.	2	3	3	2,5	i.O.
		15 Beleuchtung Querschläge/Fluchtwege	2	3	3	2,5	i.O.	2	3	3	2,5	i.O.
		16 Fluchtwegh/weis/-orientierungsleuchte	3	1	3	2,3	i.O.	3	1	3	2,3	i.O.
		17 Regelung, Messwerterfassung	4	3	3	3,5	1903	4	3	3	3,5	1903
4	Messeinrichtungen	18 CO-Messung	2	1	3	1,8	i.O.	2	1	3	1,8	i.O.
		19 Trübungsmessung	2	1	3	1,8	i.O.	2	1	3	1,8	i.O.
		20 Längsgeschwindigkeitsmessung	2	1	3	1,8	i.O.	2	1	3	1,8	i.O.
5	Überwachung/Lenkung Verkehr	21 Straßenverkehrszeichen	4	3	3	3,5	2015	4	3	3	3,5	1903
		22 Verkehrszählung	2	1	3	1,8	i.O.	2	1	3	1,8	i.O.
		23 Videoanlagen	2	3	4	2,7	i.O.	2	3	4	2,7	i.O.
		24 Verkehrslichtsignalanlagen	2	1	3	1,8	i.O.	2	1	3	1,8	i.O.
		25 Höhenkontrolle	1	1	2	1,2	i.O.	2	1	3	1,8	i.O.
		26 Verkehrslei- und Infoeinrichtungen	2	1	3	1,8	i.O.	2	1	3	1,8	i.O.
6	Notruf	27 Notruf	3	3	3	3,0	1903	3	3	3	3,0	1903
7	Telefonanlage (Festnetz)	28 Telefonanlage	1	1	3	1,5	i.O.	1	1	3	1,5	i.O.
8	Funkanlage	29 Funkanlagen	2	1	3	1,8	i.O.	2	1	3	1,8	i.O.
9	Beschallungsanlage	30 Beschallungsanlage	2	1	3	1,8	i.O.	2	1	3	1,8	i.O.
10	Brandmelde-/bekämpfungsanlagen	31 Brandmeldeanlage Kabel	2	1	3	1,8	i.O.	2	1	3	1,8	i.O.
		32 Brandmeldeanlage Steuerung	2	1	3	1,8	i.O.	2	1	3	1,8	i.O.
		33 Löscheinrichtungen	2	1	3	1,8	i.O.	2	1	3	1,8	i.O.
		34 Löschwasserversorgung	3	3	3	3,0	1903	3	3	3	3,0	1903
		35 Lösch- und Bindemittelvorrat	0	0	0	nb	———	0	0	0	nb	———
11	Tunnelsteuerung	36 Tunnelsteuerung	3	1	3	2,3	i.O.	3	1	3	2,3	i.O.
12	Gewässerschutzanlagen	37 Gewässerschutzanlagen	4	3	3	3,5	1903	4	3	3	3,5	1903
13	Schachtbefahrung	38 Schachtbefahrung	0	0	0	nb	———	0	0	0	nb	———
14	Türen, Tore, Verkleidungen	39 Türen, Tore, Verkleidungen	3	1	3	2,3	i.O.	3	1	3	2,3	i.O.
15	Krane und Hebezeuge	40 Krane und Hebezeuge	0	0	0	nb	———	0	0	0	nb	———

Gesamtbewertung 2,14

Bei allen Gewerken sind, sofern zutreffend, Funktionsprüfungen mit entsprechenden Rückmeldungen (in den allgemeinen Bemerkungen) durchzuführen.

Figure 3: Example of an assessment report including assessment results of each individual tunnel equipment component, yielding an overall assessment result

Condition recording and assessment is carried out for each individual work package or element of mechanical and electrical equipment according to weighted grading of the following aspects:

- Technical facility condition (weighting 3)
- Spare parts availability (weighting 2)
- Facility age (weighting 1)

The condition forecast together with the risk evaluation for the work package gives the time horizon for the planned maintenance and repair works (Figure 4).

Figure 4: Weighting of partial assessment results in determining the overall assessment result

3.3. Harmonisation of different life cycles

The aim is to keep restrictions for the users as low as possible (route availability and routes free of work sites) through the optimised simultaneous refurbishment of mechanical and electrical components and structural elements, and to exploit the resulting economic synergies. With regard to efficient planning of future refurbishment projects, the contrast between the lifecycles of constructional elements and mechanical and electrical facilities is becoming more and more significant. While the structure of a tunnel is designed to last 100 years or more, the lifecycles of mechanical and electrical equipment are very short in comparison. A report entitled "Life Cycle Aspects of Electrical Road Tunnel Equipment" (2012R14EN), which was already prepared by PIARC (World Road Association) in 2012, includes a diagram showing that the different mechanical and electrical systems and components differ markedly from each other in terms of life cycles (Figure 5).

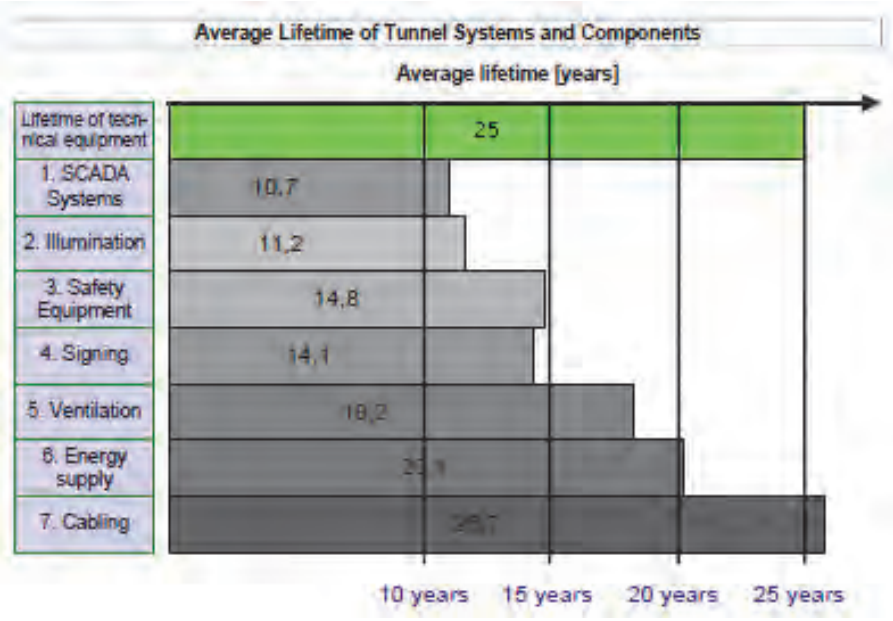

Figure 5: Average lifetime of different tunnel systems

The range here is between about 25 years for wiring and ten years for tunnel control systems. ASFINAG has prepared a lifetime table on the basis of data obtained by PIARC and slightly adapted it for better applicability to the ASFINAG network. The condition or forecast value is based on values from real world experience regarding the average achievable age of the plant. As a result, ASFINAG aims at implementing the following 30-year refurbishment cycle for tunnel structures:

- 10 years after opening: first refurbishment – small scale
- 20 years after opening: second refurbishment – medium scale
- 30 years after opening: overall refurbishment

When mechanical and electrical systems show a reduction in functionality, then the maintenance cycles are made more intensive as part of electro-mechanical risk management, or if required intermediate repairs can be carried out to maintain the required safety and quality standards (Figure 6).

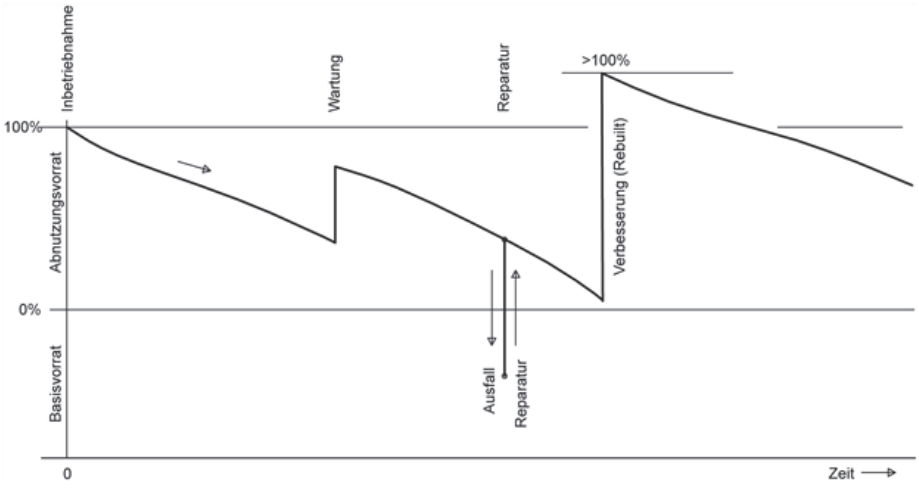

Figure 6: Time-dependent condition of tunnel electrical equipment

3.4. Influencing factors: IT systems and software

Both the increasing requirements related to the implementation of EU Directive 2016/1148 from the European Parliament of 6 July 2016 concerning measures for a unified high level of security of network and information systems throughout the EU and the life cycles of IT systems becoming ever shorter represent a problem, in that spare parts become no longer available after relatively short time periods. As an example, this can make the servicing of software impossible. In this time of worldwide interconnectedness, timely service and updates are still relevant in terms of safety.

In this regard, measures have to be taken in order to comply with the respective EU directive. This involves both road transportation authorities, who are responsible for traffic management and control, and operators/providers of intelligent road transportation systems in the sense of Article 4 No. 1 of the directive 2010/40/EU of the European Parliament and of the Council (12).

4. OPERATIONAL ASPECTS

The lifecycle of technical tunnel equipment and the related replacement of tunnel equipment components can lead to traffic impediments and limitations for roadway users. In the following sections, several aspects are described in order to illustrate in which ways the transportation management is influenced by the interplay of system design, maintenance and repair as well as various methods of refurbishment management.

4.1. Refurbishment requirements versus route availability

Time slots with low traffic volumes that can be used for carrying out refurbishment activities are becoming more and more scarce due to the overall increase in traffic volumes. As both partial refurbishments and overall refurbishments, which have to be carried out during the life cycle of tunnel structures, inevitably lead to restrictions in terms of route availability, in 2017 ASFINAG aptly adapted and advanced the customer criteria for refurbishment projects to be carried out from 2018 onwards. As a result, the following additional criteria have been defined - they are determining factors when it comes to the realisation of construction projects (Figure 7):

- Holiday criterion (concerning summer holidays)
  No obstructions on holiday traffic routes: for example on the routes A8/A9, A10/A11/A2 (Villach-Arnoldstein), A12/A13 (Kufstein-Brenner) no closures of carriageways are allowed and minimum carriageway widths of 3.25m and 3.0m must be respectively provided for heavy load vehicles and passenger cars
- Commuter criterion (i.e. “rush hour”)
  No obstructions for commuter traffic: road works have to be carried out in time slots that do not include rush hour traffic, for example during the night, on weekends or in flexible time bands

Figure 7: ASFINAG customer criteria for the carrying out of road works

These regulations have an influence on the technical tunnel equipment with respect to requirements in terms of traffic guidance systems, e.g. partial operation or bidirectional traffic in one tube. The tunnel must therefore be sufficiently equipped, in order to allow for safe operation of the tunnel during such special operational modes. A risk analysis according to the Austrian guideline RVS 09.03.11 (tunnel risk analysis model) has to be carried out. An example is the refurbishment of the Plabutsch Tunnel on the A09 motorway, which is currently being carried out. This tunnel was closed for construction work only during the night between 8 p.m. and 5 a.m. with bidirectional traffic in the other tube. On weekends with high traffic volumes (summer travelling) no construction works are carried out and the tunnel is not closed.

4.2. Tunnel structures allowing for bidirectional traffic

One of the most important factors with regard to the carrying out of tunnel refurbishments is the upkeep of traffic flow. Thus, according to ASFINAG's own targets, overall tunnel closures are generally to be avoided and are allowed only in very exceptional cases. Normally one tunnel tube is refurbished with bidirectional traffic in the other tube.

The upkeep of traffic flow is an especially great challenge in urban areas in terms of technical systems, in particular concerning route availability. As a consequence, refurbishment works can either be carried out only during very short time periods at night (e.g. refurbishment of the Plabutsch Tunnel on the A09 motorway near Graz) or by maintaining both travel directions (e.g. the Kaisermühlen Tunnel on the A22 motorway in Vienna).

Moreover, several tunnel structures have been identified as being strategically important in terms of maximal route availability. These structures should permanently allow for a short-term change from unidirectional to bidirectional traffic in one tube within one hour in cases of both events that can be planned (maintenance, repair, cleaning, refurbishment works, etc.) and unplanned events (accidents, interruptions, etc.), which means that a complete closure of one driving direction is no longer required.

In order to make possible short-term mode changes, appropriate requirements for technical facilities must be taken into consideration when planning a tunnel structure, while for existing tunnels appropriate upgrades have to be carried out. This concerns facilities such as traffic guidance systems, traffic control systems, ventilation systems, detection systems, traffic mode systems, speed monitoring systems and equipment for changing to bidirectional traffic.

The two main criteria for tunnels to be equipped with such high-tech facilities were an annual average daily traffic load of more than 25,000 vehicles and the existence of two carriageways for each travel direction. As a result of this evaluation, three tunnel structures have already been equipped in this way, i.e. the Pfänder Tunnel on A14 motorway, the Amras Tunnel on the A12 motorway and the Plabutsch Tunnel on the A09 motorway. The evaluation with regard to other tunnel structures has been completed with the result that several future refurbishment and structural upgrade projects to be carried out after 2020 will include appropriate upgrades with additional equipment.

4.3. System design as influencing factor

In order to keep the number of tunnel and carriageway closures in cases of maintenance and repair works as low as possible or to completely avoid them, tunnel equipment such as jet fans, illumination systems, video cameras (CCTV) and illuminated traffic signals have to be positioned in the tunnel traffic zone in such a way that safe access is available for the maintenance personnel, even in case of a closure of a carriageway.

An example of an optimisation of the system design carried out by ASFINAG is the LED lighting system in the tunnel traffic zone. The quality requirements as set out in the Austrian guideline RVS 09.02.41 (tunnel equipment - illumination) include a minimum useful lifespan

of 80,000 hours (which corresponds to about nine years). Those power supply components with possibly shorter useful lifespans are placed in central plant rooms in order to allow for maintenance and repair without requiring the closure of a lane in the tunnel.

Another example for the optimisation of the system design is the designing of the visibility and gas measurement systems (CO^2 / NOx / particulates), which ASFINAG prefers to design as extractive measurement systems that extract air from the tunnel and move it to the particulate sensor and the gas analysing system. The advantage is that no electronic components are located in the tunnel traffic zone, which allows for the carrying out of maintenance and repair works without closing a carriageway in the tunnel.

4.4. New methods using virtual initiation of operation (?)

Virtual engineering allows for checks, and a simulation of functions can be carried out in an early stage of required equipment replacement. The benefit is that the virtual establishment of operation can be completely carried out in the factory of the manufacturer or in the office, for example by means of a tunnel ventilation simulator. The above described Kaisermühlen Tunnel refurbishment project on the A22 in Vienna requires the replacement of the entire ventilation system with the tunnel being open to traffic. The carrying out of virtual tests of the tunnel ventilation control system, which started in April 2018, should help to minimise the number of required tests to be carried out on the real tunnel facility. This means that in the end, many tunnel closures and traffic obstructions can be avoided while at the same time normal tunnel operation is maintained.

5. SUMMARY AND CONCLUSION

The aim is to optimally harmonise the repair cycles of structural elements of the tunnel with those of the mechanical and technical elements. In this regard, the mid-term and long-term planning of refurbishment measures is required.

The life cycles of various elements are evolving. The best examples to be referred to in this regard are the continuously increasing demands in terms of IT security, which is essential for both software updates and the replacement of hardware elements. When designing technical tunnel equipment, it is important to consider overall environmental factors along with other influencing factors such as current temperature, humidity, and mechanical loads as well as the specific surroundings.

The regular carrying out of both cleaning and repair work has a significant influence on the life cycle of technical facilities. Preventative servicing and regular inspections, as prescribed by the manufacturer of the system, are thus essential and must be carried out. In this way the useful lifespan of the tunnel facilities can be guaranteed or even significantly improved. Issues regarding both servicing strategies and measures to extend the duration of life cycles will have to be addressed even more intensively in the future.

As far as the system design is concerned, requirements in terms of servicing and repair have to be taken into account. With regard to the possible necessity for closures of single tunnel tubes, the installation of specific equipment allowing for short-term switches from unidirectional traffic to bidirectional traffic, for a limited duration, should be taken into consideration and realised where necessary. The focus however is more and more on route availability as traffic volumes continue to grow. Partially or even completely barring use of tunnel facilities and the consequential tunnel closure is therefore no longer an option.

WHERE TO FROM HERE
- HOPES FOR THE FUTURE OF TUNNEL SAFETY

Conrad Stacey
Stacey Agnew Pty Ltd, Australia

ABSTRACT

Aspects of tunnel safety are discussed in the context of identifying scope for improvement, followed by organisational or cultural issues that work against such continuous improvement.

Keywords: tunnel safety, future, deluge, misting, critical velocity, emergency preparedness, innovation

1. INTRODUCTION

This paper offers opinion based on experience. I have left out the words "in my experience" for fear of repeating them too often, but the whole paper should be read in that context.

I try to add to the discussion on where tunnel safety is heading by expanding on five areas where innovation seems possible and then look at the reasons holding us back from such innovation.

In responses on a recent tunnel tender, our team was asked to provide:

> *"Examples where the proposed technical innovation has been used successfully in similar applications"*

It is a challenge to rise above such strong and official discouragement of real innovation.

2. WATER-BASED FIXED FIRE FIGHTING SYSTEMS

First some background. Appetite for risk depends a lot on the age in which a technology was first developed. Europe in particular has had major road tunnels for much longer than younger countries like Australia. When an approach becomes established and the risks accepted, the techniques tend to stay the same regardless of the decreasing acceptance of risk through the decades. So it happened that Europeans who were comfortable with tunnels were not so concerned about fire suppression, whereas Australia, developing major tunnels first in the late 1900s, did not have that cultural acceptance of them and approached them in a much more risk averse way. I see that as the primary reason in the difference of approach, between regions (taking Europe and Australia just as examples).

In some jurisdictions, particularly younger tunnelling ones, water-based suppression is seen as a life safety measure. This is odd, as culturally 'younger' tunnelling authorities have been more inclined to throw generous safety features into projects, such that the egress and smoke control provisions mean that there is rarely much motorist safety benefit left to be had by suppressing the fire. In bidirectional tunnels without separate egress, suppression may well have significant life safety benefit, but risk-averse jurisdictions no longer build such tunnels, except perhaps for very low traffic. It seems likely that water-based suppression could have reduced smoke production and hence saved some lives in the Mont Blanc Tunnel fire of 1999.

In some areas, the confusion on safety benefit in fully provisioned tunnels comes from the thinking around building fire safety. In buildings, suppression in a fire room protects the occupants of other spaces in the building from the spread of fire. In tunnels, the other tube or escape passage is protected by metres of rock or thick concrete. There is no propagation of fire through to other spaces that suppression can prevent. The thinking in most areas now is that fire suppression in tunnels is about fire fighter safety, asset protection and hence the time for

recovery to service. The suggestion is that; with a suppression system in Mont Blanc Tunnel in 1999, the tunnel closure of the order of 3 years might have been more like the 3-day closure following the 2007 truck fire in Melbourne's Burnley Tunnel.

One more piece of background is important, on the difference between water misting systems and deluge (large water droplet) systems. All water spray systems will have a spread of droplet sizes. Deluge system droplet median sizes are mostly of the order of 1 mm, with a range from perhaps 20 μm to 3 mm or so (Sæbø & Wighus, 2015). Misting system droplets range from 10 μm to 0.5 mm, with a median size around 100 μm. The aim of large droplet systems is to wet and cool the pyrolyzing surfaces, while the aim with finer droplets in mist is to cool the flame region and dilute oxygen via vaporization of the mist to steam.

Both misting systems and deluge systems are effective at suppression, albeit perhaps to different degrees for different fuels and fire geometries. They are also both effective at cooling the tunnel. So why then do some jurisdictions favour mist and others deluge? The answer came to me when visiting Felbertauern Tunnel in western Austria to see their installed misting system. Besides the misting system, I noticed that the signs, brackets, fittings and everything else fixed inside the tunnel were made from stainless steel.

I use again Australia and Europe as examples of young and mature tunnelling regions respectively. I understand that with the many older tunnels in Europe, the very large costs of tunnel downtime for renewal of tunnel fitouts are well understood. It is also the case that older European tunnels are, for the most part, mountain tunnels for which the alternative route is unattractive at any time. In contrast, the Australian tunnels are urban tunnels, which can more readily close at night for refurbishment without severe traffic effects. Being younger, the tunnel re-fit costs have been seen less often. Further, the construction contracting approaches, despite good intentions in the words, generally favour capital minimisation over whole-of-life cost minimisation. With larger diameter galvanized steel deluge piping systems being cheaper than misting systems that are always offered with smaller stainless steel pipework and expensive pumps, the choice on initial capital cost is clear. That is; the apparent jurisdictional technical preference for one over the other is really nothing to do with performance but is an economic outcome, with different cost structures being optimized.

What does that very long background lead to in a discussion of the future for water-based suppression in road tunnels? On face value, the discussion above is suggesting that the decision to include water-based suppression is an economic one, and that the choice of system is also made on economics, leaning perhaps more towards misting as the full lifecycle costs with tunnel renewal are fully appreciated. However, I think that the future opportunity is different again.

Deluge droplet size covers a wide range, with the median size being a function primarily of nozzle design and supply pressure. Standing 40 m downwind of a 10 mm/min deluge system is a good way to understand that there is an appreciable fraction of very fine droplets that carry with the breeze. So is seeing the suppression effect of a supposedly large droplet system on a well shielded fire. The choice between misting and deluge is generally presented as a binary one, but just as both have a distribution of droplet sizes, so also there is a continuum of droplet sizes between traditional deluge and mist. Why are there no systems in the enormous droplet size range between deluge and misting?

The answer is again economic, but also related to 'technical inertia'. Deluge systems have long been standard in the buildings fire industry for warehouses etc., and so they are well known and importantly, well accepted by fire brigades and insurers. Misting systems came originally from the marine industry and are still all proprietary in nature. The system suppliers, by their corporate backgrounds, are interested in supplying high pressure systems. Their testing is done to prove efficacy and hence commercially support particular proprietary systems, not to generically establish, say, trends with droplet size.

The opportunity I propose is to apply water with as much pressure as can be conveniently be arranged at the site. This will generally be more than the 2.5 bar or so of deluge systems, but will certainly be lower than the 140 bar that is typical of misting systems. It is likely that such a system will be built in stainless steel, but it may not be for tunnels where future refitting is easier. If 20 bar or even 5 bar is available from putting water storage on a local hill, or from relatively low cost centrifugal pumps, then let's use that to see how small we can get the droplets and how far we can pull back the flowrate still retaining the cooling and suppression we want. The problem of course is the lack of referenceable performance tests in between misting and deluge regimes.

My hope for the future on water-based suppression is to see testing done and systems built taking advantage of the economically available water head to get the best suppression value out of limited water, and hence reduce the total cost, including pumping and storage as well as pipework and valves. This is a call to fire research and testing centres to look at the suppression and cooling available from the full spectrum of droplet sizes, not just the high and low extremes examined carefully to date. Lithium batteries and hydrogen may also need to be considered as fuels. The change may also come from a project where the economics favour such an intermediate approach, with funds being found to do the necessary testing. It also needs an involved client seeking an economic optimum early in the project conceptual development.

3. NOT SO CRITICAL VELOCITY

A recent paper by my colleagues took a close look at the so-called 'critical velocity' (Agnew & Tuckwell, 2017). Our practice has maintained for some time that a little back-layering does no harm and this has support elsewhere (Mos, 2015), and further, that back-layering grows very slowly as velocity falls (Rojas Alva, Jomaas, & Dederichs, 2015).

Yet in many project specifications, achievement of critical velocity is non-negotiable. Were it not such a burden on projects and designs, it would simply have been entertaining to see how the immutable NFPA502 critical velocity formula suddenly mutated in 2017, then instantly became immutable again. It is the inertia behind code following that leads some astray in this area. So what if the formula has changed? Does it really matter anyway for the outcome you are seeking?

It is my hope that the tunnel safety community can evolve to universally look at smoke control rationally, chasing outcomes informed by the data and latest numerical tools, rather than by the critical velocity dogma. That may not seem radical enough to be 'innovative' but like a lot of change, after it is made, it was always clearly just common sense.

4. TRAFFIC AUTOMATION

As the technology of vehicle to infrastructure communications develops, it is certain to revolutionise traffic monitoring. Instead of measuring vehicle speed and flow every 500 m or so with traffic loops or similar, we expect that cars could be telling the tunnel systems what their speed is in real time, with special alerts when they have to brake unusually. The infrastructure (traffic management system) can make use of this to alter the signage and avoid further problems, but, better still, it might pre-emptively suggest behaviours back to the vehicles to defuse a developing hazard.

If an incident does occur, instructions to motorists might come through the dashboard rather than radio re-broadcast, public address, or variable message signs.

The effect of traffic semi-automation, along with self driving cars, should be both to increase network capacity and reduce the accident rate (and hence the fire rate). The response to any incidents should also be improved. None of this is new, but a paper with this title needs at least to record it. Exactly how the tunnel safety community takes advantage of the possibilities is still open.

5. DELUGE AND MISTING NOISE

Many jurisdictions place limits on the in-tunnel noise from ventilation plant, with the aim of allowing emergency messages to be heard clearly. It is often given as 85 dBA (or sometimes NR85) at any point 1.5 m above the roadway. Together with particular space constraints, it is that noise limit that determines the maximum jet fan thrust at any location, and the maximum thrust per kilometre of tunnel.

Our experience in running tunnel emergency exercises gave us a different perspective. In trying to generate loud fire noises, and in trying to communicate by radio from the incident site, it was deluge noise that 'drowned us out'. A paper given last year (Stacey, 2017) resulted from interest in putting numbers to the deluge noise. The summary data, with tunnel identities obscured, are tabulated below.

Table 1: A-weighted SPL data for several deluge systems and one jet fan installation, copied from (Stacey, 2017).

Noise source	Deluge rate (mm/min)	A-weighted SPL
WA deluge	6	75.5 dBA
NZ deluge 1	6.5	77.1 dBA
NZ jet fans 1	---	88.9 dBA
NZ deluge 2	6.5	76.0 dBA
NSW deluge	10	96 dBA
QLD deluge	10	85.6 dBA
QLD deluge measured in a car	10	82 dBA
QLD jet fans	---	84.4 dBA

Missing from the table are any measurements of noise from misting systems. It is hoped to add such information in later work.

With deluge pushing the noise limit applied to jet fans, and with jet fans near the incident preferably not used, the focus on PA intelligibility needs to be in the context of deluge (or mist system) noise, rather than jet fan noise. In longer tunnels where not all jet fans need to run, the noise away from the incident could be allowed to be louder, reducing the number of jet fans installed, with implications for capital and maintenance cost. I hope to see such changes.

6. EMERGENCY PREPAREDNESS

Those countries with a recent history of terrorist attacks generally pay a lot of attention to this, but it is applicable whether or not there are such threats. Incidents caused by those with nefarious intent are still only part of the risk.

All the conceivable safety features may not be sufficient if there is not the training and preparedness to operate them correctly, or if the systems are not tolerant to damage or sub-optimal application. In this aspect there is a wide variation in what preparedness means. Some road tunnels, particularly older tunnels, tunnels with very low traffic, and those where response protocols were developed some time ago, do not have manned supervision. If the first response to an incident is by the local police or fire brigade, the nature of preparedness is very different. The focus here is on supervised facilities, which includes most major road tunnels and metro type rail networks.

In the emergency operation of supervised facilities, there is a spectrum of philosophy on the role of the operators. At one end of the spectrum, the response mode is automatic, with the operator as a witness able to talk to the fire brigade but trusting that everything will work as

planned. At the other end is the view that the operators should know the plant and tunnel behaviour in detail and be able to 'drive' the controls manually, to 'play any tune' necessary to respond optimally. Of course, the best answer is a combination. It is always good if the operator understands their systems and how to make it run differently. With the high workload on operators in an emergency, it is also good if the system offers options of pre-configured responses capable of rapid acceptance by the operator. In my view it is a given that an operator observing an incident should have the ability to beneficially alter the response if they can see how.

So, talking of systems with capable operators as above, we now have a human element in the loop (which the fully automated approach recoiled from in fright). How then do we make sure that the two (or so) operators on duty are going to assist the response? With a staff retention period of perhaps 5 to 7 years, only two of 15 to 20 staff operators running the tunnel during a major exercise in any two-year period, and real incidents being uncommon, how do we give staff the operational confidence required? And how do we check procedures for real?

Our answer to these questions is to run unannounced exercises. In the typical emergency exercise, the operator on shift at least knows there is an exercise and has a week or more to brush up on procedures. The only surprise is what part of the tunnel it is in, and how the other responders might behave. The element of surprise is largely gone, such that it is not a realistic test of emergency response. There is no test of the human-machine interface, as the rehearsal week has made that largely redundant. In an unannounced exercise, the operator does not even know there is going to be an exercise. At the start of the action, they may not even recognize that it is not for real. The responses then are far more real, and the true state of preparedness can be understood.

There are challenges for this approach in facilities open to the public, but opportunities can generally be found in each facility (tunnel, station etc) by looking creatively at the operations and maintenance practices. Rail tunnels are obviously easier than road tunnels for organizing surprise tests. Sometimes the more significant challenge is overcoming management reluctance to know the truth about the state of preparedness, with a rehearsed exercise managed by the team being tested looking like the easier option to say that an exercise has been done.

7. INNOVATION AND CONTRACT FORM

Tunnel safety could move ahead by government regulation, through industry conferences, by good volunteer work on standards committees, by research on fundamentals or new techniques, or by a combination of these. It can also move ahead by innovation on individual projects, and I see that as potentially the most powerful driver, although it will often also need at least one of the others in assistance.

The thoughts here are more general than the tunnel safety aspects of projects, but apply in my experience to tunnel safety.

7.1. D&C (Design and Construct) Contracting

Time is of the essence. That is true in almost every contractual setting and lack of time is probably the single biggest brake on innovation. In design and construct contracts, clients are often reluctant to search for better ways of doing things in the very early project stages. There are several reasons put forward:

- that's the D&C's role;
- we don't have the budget to look at it;
- we don't have time to get all parties to buy in given the pressure for progress, and;
- there will be time for that later.

In Australia recently, by the time a project goes to D&C tender, the chance for innovation is often largely gone. That may sound heretical, as the whole idea of D&C tendering is to bring the good ideas from the contracting and consulting worlds to add value and hence make the bid competitive. And sometimes value does get added that way. We have seen some clever thought in ventilation, but more commonly different tunnel alignments to save cost or improve functionality. Quite commonly, good ideas, if raised at all during tender, are frozen out by the immense pressure to complete the design so that costing can be robust and the tender leaders can look their board in the eye and promise them that they have produced a safe construction plan and price. With single tenders of several billions of dollars, chasing ideas that may not have time to be proven will always give way to certainty and security. Better to have a solid price than a better value but still rubbery offer in the time available. There will always be the tension at tender, between exploring an idea, and just getting on with progressing the design as it is. With shorter tender periods, there has to be less exploring and more just getting on with it, such that innovation is stifled.

My impression is that tender designs seem to have become more and more time-challenged over the last decade and a half, significantly reducing the value that can be achieved by innovation at that stage of the project. The idea that a D&C tenderer will innovate to be competitive and hence benefit the client, while correct at face value, is often completely reversed by not only the time frame, but sometimes also the clarity of the request for tender.

The projects that go most smoothly, on time, budget, quality and dispute avoidance, are those where the client really knows what they want and why, producing clear information. On major infrastructure, knowing what you want can be as hard as designing it after you know that. That is; without a significant investment of time, money and serious focused thought, the client will still often still be fuzzy about some parts of: what they want; why they want it, or; how it should be specified. When this happens, the tenderer's effort is tied up trying to answer those questions definitively. Further innovation is harder when those objectives, and perhaps the basic specification, are uncertain. When the client has done a lot of pre-work, tender time is spent more efficiently, leading to better offers.

To spend time and money right at the front end of a D&C project, to better define it when it goes to tender, requires a clear understanding of the benefits of doing so, and the strength of will to make it happen when time and budget are always under pressure. Projects are more often now structured first to fit with finance requirements, and then structured legally, to allow contracts to be issued. In that framework, engineering is seen as a commodity that forms part of the necessary costs, not as a source of wisdom about how to drive the best value for the financiers, government members and everyone else ("It's just a railway, right?). This is a significant brake on advancing all design aspects, not just tunnel safety.

So, if a single machine gets contracted in three or more parts, to suit the financial packaging, would underperformance be accepted on the basis that only the financing made it possible at all? Or would it give cause to more closely examine the staging and financing? I don't have an answer for those questions. The truth is that financiers and political imperatives are both here to stay. I can only then express the hope that the pendulum swings back (as they do) and that the big difference in value that early engineering can bring is not always buried by focus on the 0.5% (for example) advantage of tricky finance packaging.

7.2. Client's design

In Australia, there has been, I think, no major underground infrastructure in the last decade that was designed ready-for-construction by the government client or their consultants. In the US market, it is still very common for clients to commission a large part of the design work, with much less, or zero, design development done by the contractor. This would appear to be the complete answer to a time-poor D&C process stifling innovation. The client is free to chase

value for themselves. Unfortunately, there are other drivers of behaviour that come into play to stifle innovation to a similar, or even greater extent.

The first of these is the incentive for the consultant. Again pointing the finger at accounting types, most US jurisdictions essentially demand an open book, right back to salaries, and cap the profit that can be made. Worse, they generally also further cap the charge out rates of those on upper salaries. You cannot earn a high income as a brilliant engineer, except through the ability to help win work that then feeds lots of junior people and so allows your company to stay afloat. In this way, an accountant's view of driving value in buying the commodity of engineering on government design tasks becomes a powerful disincentive to the involvement of those most capable of adding value.

In addition to this false accounting measure, once appointed to a task, a consultant often has zero incentive, besides their own drive, to innovate or indeed to drive value. Anything new brings risk to them and their client, and as long as they don't go backwards they will be safe. Making a sweeping generalization; everyone then stays just where they are, without moving forward.

Not to be forgotten in the US market is the high status of codes. I have seen designs which are just silly and that could easily and inexpensively be fixed up in the interest of reducing risk so far as is reasonably practicable, yet they are not, because the CFD shows it already "meets code". We see some of that in Australia also. It is interesting that engineers can be so ready to suspend critical thought as to whether just "meeting code" is the responsible thing to do. It is little wonder in that context that innovation to do something that might be better, but is not as foreseen by the code, is often just too difficult. See also (Dix, 2016).

7.3. Alliancing

Alliancing, or relationship contracting, offers a mechanism for facilitating innovation, provided always that the client partner actually wants to add value. Alliances were popular in Australia in the first decade of the 21st century and to my mind made it much easier to achieve the best value that we could see available. In tunnel safety terms, it meant that there could be dialogue about the best outcome through the whole project structure, with parties contributing properly. It also means that the sometimes difficult discussions with external stakeholders are not hobbled by project politics. In client design, the best information may not be available, and in D&C contracts, barriers can go up surprisingly quickly. Alliance contracting comes under pressure always to prove that similar value could not have been achieved through a D&C contract, in which everyone can transparently see the evidence of price competition. It also comes under pressure because the final cost (for whatever value) cannot be known until close to the end.

7.4. Contracting hopes

There are opportunities for innovation, and perhaps advancing some of the ideas above, in all forms of contract. Mostly they involve the addition of time to the decision processes, with the extra time taken as early as possible. On the client's side, the best time is in the earliest concept stages. On the contractor's side, it is before tenders are called, when there is still time for calm reasoning.

I have been on D&C projects that were more collaborative than some alliances, but whatever the contract form, my advice if you wish to add value by advancing the art of tunnel safety, is to seek the time at the earliest opportunity to ask what could be done better or more economically.

8. SUMMARY AND CONCLUSIONS

The starting point for making beneficial changes to the way things are done is to ask why it is currently done the way it is. If the answers aren't technically satisfying, if they refer just to 'custom and practice', or even relate to bureaucratic or contract inertia, then there is a signal that you may be on to something. Of course, it takes time and advocacy to get changes accepted, but if we are serious about reducing risks and costs so far as is reasonably practicable, we accept that challenge.

Several areas are suggested for innovation:

- Water-based fire suppression with pressures and droplet sizes between those of deluge and misting systems, using naturally available pressure sources where possible.
- Breaking the dogma around achieving critical velocity in longitudinal ventilation, with the focus on the real safety outcome.
- For further in the future; being alert to the tunnel safety opportunities that will come with vehicle to infrastructure communications and greater autonomy in vehicle control.
- Jet fan and public address joint optimization, in the context of the noise environment already created by water-based suppression.
- Reassigning the emergency exercise budget away from the major all-party exercises to smaller but more frequent impromptu tests of the most critical response activities.

The political and organisational 'handbrakes' on innovation are seen to relate mostly to time pressures at each stage of project development. The key then to capturing the value that may be offered to a project is to allow time at the earliest opportunity to identify, investigate and develop new ideas. Once the contracting schedule is set, the chance of beneficial innovation shrinks rapidly.

9. REFERENCES

Agnew, N., & Tuckwell, B. (2017). Not so 'Critical Velocity'. *16th Australasian Tunnelling Conference.* Sydney: Australasian Tunnelling Society.

Dix, A. (2016). Doing the best with the resources available: Tunnel safety and security in a severely resources limited world. *7th International Symposium on Tunnel Safety and Security.* Marseilles: SP.

Mos, A. (2015). Evaluation of the radiative hazard in tunnel fires. *16th International Symposium on Aerpdynamics, Ventilation and Fire in Tunnels.* Seattle: BHR Group.

Rojas Alva, W. U., Jomaas, G., & Dederichs, A. S. (2015). Scaled experiments using the helium technique to study the vehicular blockage effect on longitudinal ventilation control in tunnels. *16th International Symposium on Aerodynamics, Ventilation & Fire in Tunnels.* Seattle: BHR Group.

Sæbø, A. O., & Wighus, R. (2015). *Droplet sizes from deluge nozzles.* Trondheim: SP Fire Research AS.

Stacey, C. (2017). Hearing the message - emergency announcements in tunnel noise. *16th Australasian Tunnelling Conference 2017.* Sydney: Australasian Tunnelling Society.

10. ACKNOWLEDGEMENTS

I thank many industry colleagues for erudite thoughts over the years, and in the context of this paper; Jean Marc Berthier, Nick Agnew, Michael Meissner and Ben Tuckwell for suggestions on the text, and Peter Sturm for suggesting the topic.

RESEARCH@ZAB – THE NEW RESEARCH AND DEVELOPMENT AS WELL AS TRAINING AND EDUCATION CENTER ZAB – ZENTRUM AM BERG

Robert Galler,
Montanuniversitaet Leoben, Leoben, Austria

ABSTRACT

The creation of sustainable infrastructure is increasingly being provided in underground facilities. In terms of construction and maintenance, this leads to greater challenges for construction, transport and energy-provider companies. This also applies for emergency services organisations, as well as to ensure the safety for the users of the infrastructure. The project "Research@ZaB - Zentrum am Berg" will establish an underground facility for research and development, education and training purposes. On the one hand, the centre should meet the requirements of public institutions; on the other hand it represents a "development factory" for private companies as well as concerned universities.

1. INTRODUCTION

Due to the high worldwide demand for tunnelling engineers, the Montanuniversität Leoben together with the Graz University of Technology started a special professional training scheme for NATM (New Austrian Tunnelling Method) engineers in 2009, which currently has students from Columbia, Mexico, Chile, Brazil, Georgia, Spain, Germany, USA, Egypt, Israel, India, Bhutan, Greece, Turkey and Italy. This method of tunnel construction is however just one little part of the extensive professional area of underground construction. After the tragic tunnel fires around the turn of the millennium, it must now be clear that much more knowledge from other viewpoints is necessary in order to control such situations better.

There are currently about 6.600 km of tunnels in the European Union, with a further 2,100 km under construction or at the design stage. Outside Europe, there are gigantic projects such as the planned tunnel under the Bering Strait, with individual tunnel lengths of more than 200 km. In Asia, which will represent much the strongest market for tunnelling in the future, many further projects for underground railways and tunnels are currently at the design stage.

Testing under realistic conditions has scarcely been possible until now for the further development of construction methods, and also of materials and fittings, from tunnel ventilation to the entire field of safety technology including extinguishing systems integrated in the tunnel. Investigation in the laboratory is only of restricted reliability and even tests in existing tunnels cannot offer a scenario for an actual catastrophe. Tests in existing tunnels are also laborious and expensive since the tunnel has to be closed for the tests and traffic has to be diverted. It is only possible, for example, to carry out tests with a restricted fire load in existing tunnels in order to avoid damage to the structure.

An underground tunnel system for research purposes, called the Zentrum am Berg, should be of assistance here. The Zentrum am Berg is situated in a disused part of the Erzberg in Styria and will be a unique research location in the world, offering ideal conditions not only for researchers but also for the most varied areas of emergency services organisations and the industry (Figure 1).

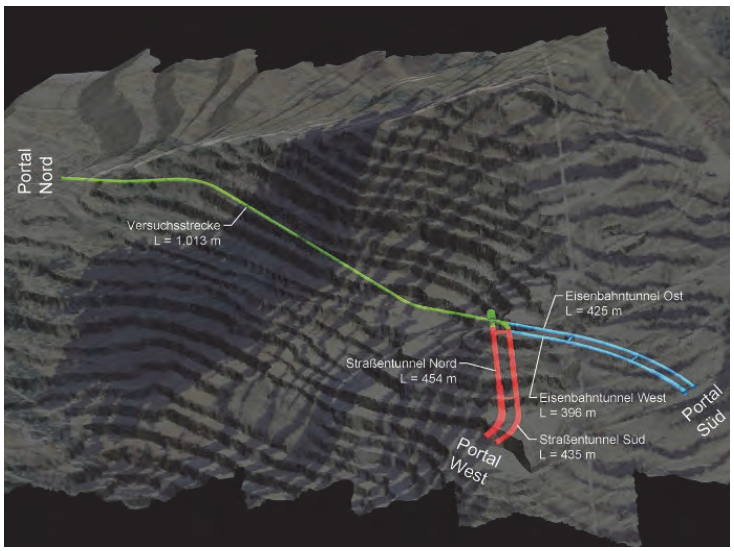

Figure 1: Zentrum am Berg – facilities under design and construction

The altogether almost 3 km of tunnels cross beneath the highest point of the Erzberg, the Erzbergspitz; although there are also sections with little overburden, which should ensure that tunnel sections can be investigated under various conditions.

Students are to be involved with the work from the start. To experience in practice what happens when a tunnel is built offers the ideal basis for the understanding of methods. Practical work at the Zentrum am Berg is already intended to become part of the courses at the Montanuniversität.

Scientists from other institutions have already shown interest in using the tunnel. Researchers from the TU Graz, for example, intend to test existing and new ventilation concepts. The propagation of gases and the necessary safety equipment can be ideally investigated in the Zentrum am Berg. The effects of climate change on tunnels, for example the consequences of heavy precipitation or mudflows, can also be measured. In this regard, rockfall protection systems can also be further developed. Geothermal energy can be used to keep tunnel portals free of ice in winter. 50 companies have already expressed interest in researching in the mountain, with project ideas ranging from civil engineering to IT.

At the start of consideration of the project, a feasibility study into the development of the Zentrum am Berg was undertaken with the support of the VA Erzberg, the ÖBB-Infrastruktur AG, the Asfinag, the Wiener Linien, the European agricultural fund for the development of rural areas and department 16 of the state government of Styria and concluded positively. According to the report, the centre will offer a facility for research and training in the following fields:

- scientific and commercial geotechnics as well as mining and tunnelling, for research work at the highest level in an in-situ environment,
- academic and business partners in metrology from geophysics to geotechnics, as well as aerodynamics and thermodynamics,
- emergency services organisations from the fire service to ambulance organisations, also for staff and civil protection,
- numerous business partners among mining and construction suppliers, as well as equipment and safety technology,
- repair and maintenance personnel for training purposes,
- and even future tunnel users, for example new drivers

The Erzberg in the Austrian state of Styria offers an excellent location for this underground test facility, above all due to its already existing tunnel system and connection to the road and rail networks.

The tunnelling work at the Zentrum am Berg will be based on two different cross-sections, a two-lane autobahn tunnel and a single-track rail tunnel. In order to be able to offer the most realistic possible training conditions underground for emergency services, a second tunnel will also be driven parallel to each of these and with the same cross-section. The parallel tunnels will be connected with cross-passages. In order to be able to investigate problems in tunnel refurbishment, and also other relevant research objects under realistic conditions, the Pressler tunnel will also be enlarged from its current cross-section of about 8 m^2 to a rail tunnel cross-section. Parallel to this enlargement, an underground test field with dimensions of about 200 m × 1,000 m will be available. The necessary operating buildings and seminar rooms will be provided near the underground facilities.

With the implementation of this project for the future, Austria will gain a unique selling point, which will be of use for all Central Europe. International trade fairs, at which companies from the most varied sectors can take part, can also lead to the making of new contacts and long-term cooperation and ensure the position of Austria on the world market. With the construction of the Zentrum am Berg, Austria is signalling a forward strategy, which should lead to positive effects both in science and business. The Research@ZaB opens up widely spread possibilities for use and thus creates space to combine the research and development work of various professions (Figure 2).

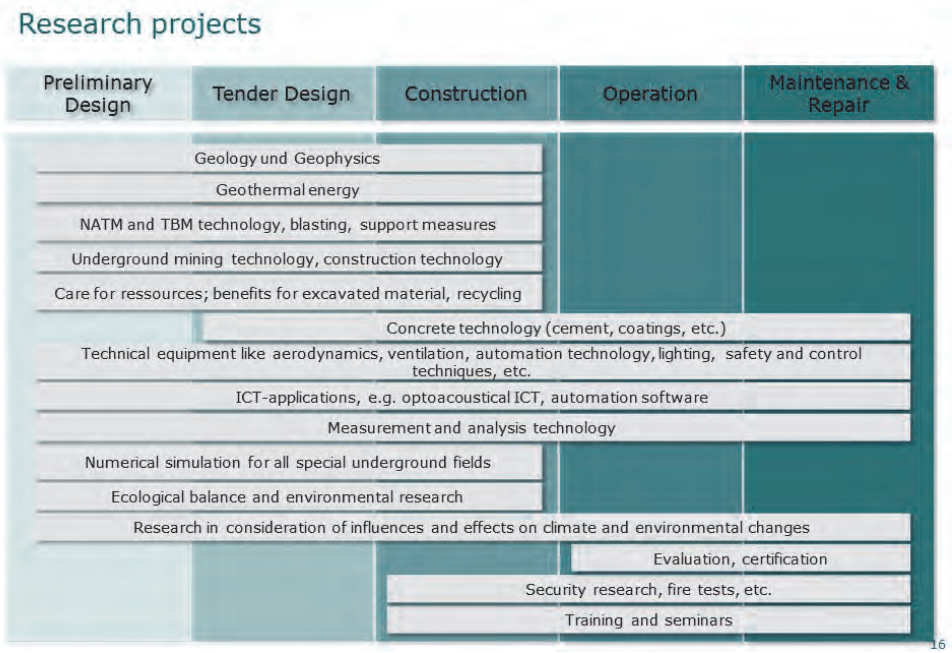

Figure 2: Current research themes in the Zentrum am Berg based on answers to surveys from industry

2. LOCATION

The location of the planned research centre is the Erzberg in Styria (Figure 3). The existing tunnel system on the Höhe Dreikönig offers an optimal space for this project.

Figure 3: View of the styrian Erzberg

3. GEOLOGY

The town of Eisenerz lies at the north edge of the northern greywacke zone. The Styrian Erzberg south-east of the town contains the entire sequence of strata, which belong to the north zone of the Norische Nappe, which according to the large-scale tectonic structure represents the western flat part in the east part of the greywacke zone.

Since most of the existing tunnel is lined with brickwork and part with concrete, it was not possible to map the lithography in the tunnel. Therefore an attempt was made to read the distribution of the lithology from the geological horizontal sections made available by the VA-Erzberg GmbH. The lithology is essentially:

- limestone,
- siderite, Rohwand (massive dolomite and ankerite),
- Blasseneck porphyroid,
- Eisenerzer beds (shale, phyllite).

The areas of the northern tunnel, which are already lined, could be lithologically well de-lineated. Eisenerzer beds and porphyroid were accordingly already categorised as problematic during the construction of the tunnel and supported, whereas the Sauberger limestone and the orebearing limestones were stable without further support and only show rupturing due to jointing. The existing tunnels are predominantly damp with some dripping and isolated running water ingress.

4. DESIGN OF THE TUNNEL CROSS-SECTIONS

4.1. Road tunnel

The road tunnel is only lined in the north tube over the first 200 m from the west portal and near the electrical room at the cavern in the extension of the north axis with an inner lining according to RVS. The excavation geometry of the standard cross-sections (RQ) “Road tunnel with inner lining” and the RQ “Road tunnel without inner lining” are identical. The tunnel cross-section is designed ac-cording to RVS 09.01.22. The carriageway width is laid down for single-directional traffic without trucks, no over-taking and a design speed of 100 km/h. The footpaths are reduced by 15 to 55 cm at the sides although the walkway width required by the RVS of 0.70 m is maintained at a height of 1.0 m. The clear height of the traffic space above

the carriageway, measured perpendicular to the road sur-face, is 4.70 m. Above the raised side strip, the structure gauge has a height of 2.25 m. On this project, the described structure gauge was rotated with the transverse fall of the carriageway.
Most new autobahn tunnels are provided with concrete surfacing. In order achieve the most realistic conditions possible, the following carriageway surfacing with a total thickness of 57 cm is provided in the areas with an inner lining:

- 22 cm concrete slab according to RVS 08.17.02
- 5 cm bituminous base layer AC16 trag T3, G4, according to RVS 08.16.01
- >30 cm unbound lower base layer according to RVS 08.15.01

For the areas without inner lining, asphalt surfacing of load class V, construction type T1 according to RVS 03.08.63 is provided to save costs. The standard cross-section in the mined areas was generally carried out with an open invert. The formation of the standard section with an invert arch is only used in zones of poor rock mass. The outer lining essentially consists of shotcrete and support measures, which are varied depending on the ground conditions encountered.

The waterproofing system consists of a double-welded synthetic waterproofing membrane and an external protective geotextile. The ground water is collected and drained through external side drains installed in the invert.

The inner lining normally consists of an unreinforced 25 cm thick in-situ concrete ring. The length of the inner lining block is specified at 12.5 m. The inner lining is founded on a strip-shaped abutment. In addition to the selected structure gauge, the duct necessary for the extraction of smoke from fire is decisive for the design of the cross-section. This is separated from the traffic space by a reinforced concrete intermediate slab supported at the sides on corbels in the inner lining. The excavated area for RQ “Tunnel without invert arch” is about 85 m^2, RQ “Tunnel with invert arch” is 102 m^2 plus overcut u_m and overprofile u_p.

4.2. Rail tunnel

The rail tunnel is only constructed with an inner lining in the section of the west tube over the first 100 m from the south portal. The excavation geometry of the RQ “Rail tunnel with inner lining” is identical to that of RQ “Rail tunnel without inner lining” and the RQ “Test tunnel” (Figure 4).

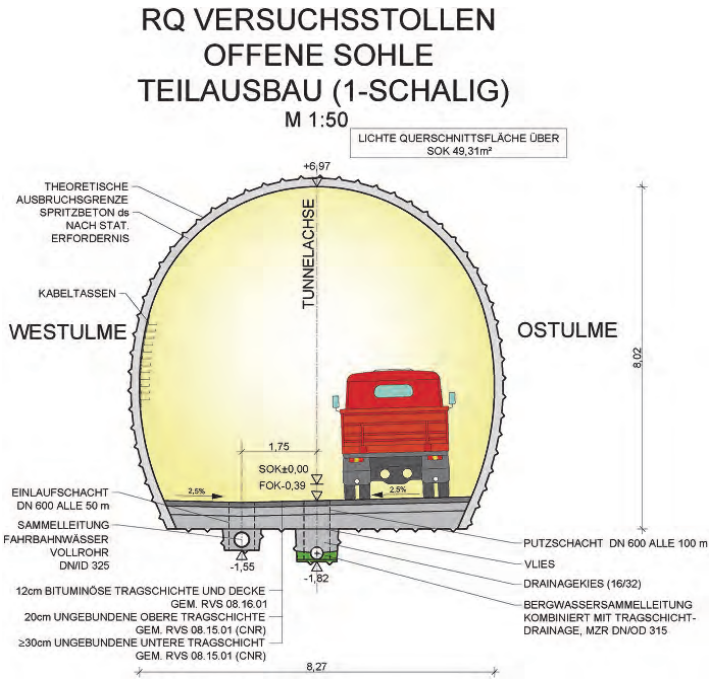

Figure 4:
Standard cross-section of the rail and test tunnel sections

For this project, the rail tunnel section is specified with an inner lining and structure gauge LPR 1 (Tunnel with slab track and R ≥ 3,000 m). This also enables investigations using ÖBB double-decker cars. The walkway with a clear height of 2.25 m and a width of 1.20 m is on the cross-passage side of the standard cross-section. In or-der to reduce cost, the slab track is omitted. Instead, a ballasted track is specified although the dimensions re-main unaltered from the design documents for "Slab track", which ensures that a change can be made to a slab track at a later time. The construction of the side walk-ways is according to the design documents for the Semmering Base Tunnel, with an additional extinguishing water line being installed in the cable duct in the east side wall and connected to the line of the road tunnel.

The standard cross-section in the area of mined tunnel has an open invert. The standard section with an in-vert arch is used in zones of poor rock mass. The standard section consists of an outer support layer of shotcrete and support measures like the road tunnel, an applied water-proofing layer and an inner lining. The excavated area for the RQ "Tunnel without invert arch" is about 62 m^2 and for RQ "Tunnel with invert arch" is 67 m^2, each with an additional overcut um and overprofile up. The walkway is constructed by extending the carriageway to the side wall and delineated by markings on the road. For the section of rail tunnel without inner lining and for the test tunnel, the same carriageway construction is selected as for the road tunnel without inner lining, load class V, construction type T1 according to RVS 03.08.63.

5. BUILDING FACILITIES FOR OPERATIONS AND SAFETY

At this point, only the building facilities for operations and safety are described in detail; the electro-mechanical tunnel equipment like hazard alarm systems is not dealt with. For the building facilities, cross-passages are provided connecting the parallel tubes to each other. The cross-passages are designed to be accessible for vehicles (EQ) or for pedestrian access (GQ). The cross passages are about 30 m long. Die to their short length, the cross-section required for the junctions is maintained along the entire length, which gives a larger cross-section than is specified in the RVS. This gives construction operational and above all safety advantages.

In the north tube of the road tunnel, two emergency call niches will be provided, although no emergency call system will be installed. The spacing of the emergency call niches is 125 m and the distance of the first emergency call niche from the portal is about 94 m. In the same road tunnel tube, the fire extinguisher niches are placed opposite the emergency call niches, with an additional hydrant at the west portal. The fire extinguisher niches in the tunnel are each equipped with a tunnel hydrant and two B (75 Ø) connections. In the west tube of the rail tunnel, three wall hydrants are provided. According to the HL guideline 2002, the extinguishing water line is run in the edge walkway and brought up at the appropriate locations on the tunnel sidewall.

For the maintenance and cleaning of the drainage, maintenance niches are provided at a maximum spacing of 100 m on both sides. All other areas are drained by an invert drain and cleaned from manholes every 100 m in the middle of the profile. Manholes are also provided at the intersections with cross-passages or other tunnel centrelines.
For escape routes, the following tunnel sections are separated by bulkheads:

- road tunnel north tube,
- rail tunnel east tube,
- rail tunnel west tube,
- test tunnel.

The escape route is marked by escape route signs, escape route orientation lighting and escape route orientation boards.

6. CONSTRUCTION METHODS

The mined section of the Zentrum am Berg will be driven under the principles of the New Austrian Tunnelling Method (NATM). The principle of this construction method is that excavation and support works are matched to each other so that the rock mass can be stabilised with the least possible extent of support measures. The support measures are adapted and optimised to suit the local conditions. The stability of the tunnel tubes is verified by geotechnical measurements. The excavation of the rock from the face is primarily by blasting, although a roadheader or excavator can be used depending on the rock mass strength.
The excavation of the face is carried out in partial faces due to the prevailing geological conditions. The crosssection is normally divided into an advanced top heading followed by bench excavation. The longitudinal spacing of these advances from each other is generally based on the geotechnical and/or construction operational requirements.

7. RESEARCH FIELDS – SOME EXAMPLES

7.1. Fire in the tunnel

Fires in enclosed spaces are characterised by rapid propagation in the room and sudden development of smoke gases. Air currents create an additional negative effect on the fire behaviour. The efforts of emergency services are made extremely difficult and often seriously dangerous by the incandescent flame front, poisonous clouds of smoke and the poor visibility conditions. The fire tunnel is intended as a training location for emergency services personnel, train and control centre staff under realistic conditions.

Figure 5:
Underground fire test

It should provide training under real fire loads, which is impossible in existing tunnels at the moment. Escape concepts can be tried out, evaluated and incorrect reactions in a real case can be avoided. The fire tunnel sections can also be used for the further development of smoke detection systems, fire alarm and extinguishing systems and fire-resistant materials for underground con-struction (Figure 5).

7.2. Aerodynamic questions

The test tunnel will be provided with extensive ventilation equipment. The installed ventilation components can realistically represent the function of various ventilation systems. Extract fans for the removal of exhaust gases and jet fans to influence the longitudinal air flow in the tunnel are intended. This means that both longitudinal ventilation and semi-transverse ventilation can be simulated in the test tunnel. In this way, the most com-mon ventilation systems used in Europe for road tunnels will be available.

7.3. Material development – long-term consideration

Tunnels are designed for a lifetime of 100 years. In order to ensure serviceability until the end of the planned period of use, knowledge about the long-term behaviour of the rock mass and the support materials used is essential. Laboratory investigations mostly only permit a coarse estimation of rock mass behaviour and are often uneconomic. The performance of long-term tests under realistic conditions can not only considerably improve design precision but at the same time lead to further development of the calculation approaches currently used in underground construction (Figure 6).

The same naturally also applies for the operational and safety equipment, which is essential for the safe operation of a tunnel.

Figure 6:
Slot compensation measurement to determine tunnel lining loading

8. ACKNOWLEDGEMENT

The construction costs for the Zentrum am Berg in the sum of EUR 30 million have been shared by the BMVIT with EUR 6 million, the BMWFW with EUR 6 million, the state of Styria with EUR 12 million and the Montanuniversitaet Leoben with EUR 6 million. In addition to these grants, we wish to thank all those who have contributed in an extremely constructive and positive way to bringing the project ZaB – Zentrum am Berg to life!

9. REFERENCES

RVS 09.01.22 Tunnelquerschnitte (März 2010)

RVS 08.17.02 Deckenherstellung (April 2011)

RVS 08.16.01 Anforderungen an Asphaltschichten (Februar 2010)

RVS 08.15.01 Ungebundene Tragschichten (Juli 2010)

RVS 03.08.63 Oberbaubemessung (April 2008)

HL-Richtlinie 2002, Anlage 3 Richtlinien für das Entwerfen von Bahnanlagen, Hochleistungsstrecken, Tunnel- und Wannenquerschnitte (Mai 2002)

NEWLY ESTABLISHED RESIDUAL RISK REDUCTION MEASURE OF THE SAFEGUARDING SUPPORTIVE SYSTEM (SSS) FOR TUNNEL CONSTRUCTION SITE - EXAMINATION OF RELIABILIBTY AND CONVENIENCE OF THE SSS

[1]S. Shimizu, [1]S. Umezaki, [1]K. Hamajima, [2]M Tsuchiya, [1]R. Hojo
[1] Japan Organization of Occupational Health and Safety, National Institute of Occupational Safety and Health, Japan
[2]ADVANTAGE Risk Management Co., Ltd., Japan

ABSTRACT

In workplaces of tunnels, everybody tries to prevent accidents with individual protection devices for each machine. However, even if all individual protections simultaneously operate, it would be difficult to cover all areas. So it could be difficult to identify every single person entering the work area. Usually, workers who operate machines in the tunnel should have access authority and should be well-trained. But as individual protection devices do not have functions to check operators' licenses and authorities, some accidents by workers, who do not have any skills and access authority as operators in the tunnel, have happened. In other words, because it is not possible to prevent severe accidents sufficiently only by individual protection devices of single machines, unacceptable residual risks still exist in construction areas in tunnels. Although safety at such workplaces currently depend on attentiveness of workers, uncertain factors of workers such as human error or intentional unsafe behavior, sometimes affect results of risk assessment. We newly established a risk reduction system, named "Safeguarding Supportive System (SSS)", to prevent human error and intentional unsafe behavior from the mechanical side (hardware side). The SSS should reduce residual errors with an appropriate Information and Communication Technology (ITC) combination. In the present study, we aimed to evaluate the reliability and convenience of the SSS. We carried out the experiment using a tunnel workplace of a company A. The SSS consisted of a RF-tag, an UWB-active-RFID system, and a monitor system. The RF-tag system confirmed workers' qualifications for entering a work zone and gave permissions to work there. The UWB-active-RFID system monitored the operational processes of workers and confirmed the location of the workers in real time. The gateway monitoring system consisted of a camera and an accurance-tag was installed. We examined 1) whether the RF-tag system was adequately operated by workers, 2) whether the UWB-active-RFID system precisely monitored and captured workers movements and locations in real time, and 3) whether the gateway monitor system appropriately monitored entering and leaving the work zone. We found that the qualification and the authority of workers were confirmed precisely with RF-tag. Though the UWB-active-RFID system monitored and captured the workers movements and locations in real time, a clear trace of movements of workers was interfered with a reflected wave derived from metal materials surrounding the antenna. Also, the gateway monitor system monitored entering and leaving the work zone appropriately. For more precise track record of workers' movements, we are planning to use radio wave absorbents to adjust the location of the antenna and to improve the software. The present situation or problems of the equipment and the work in detail can be clarified by analyzing data in the SSS. We concluded that the introduction of the SSS contributed to build up a safer work space. In addition to safety-related information, the SSS would be able to make daily work reports automatically, because mechanical operations and work circumstances are recorded in the SSS. We would like to apply the risk reduction plan to the next generation product lines such as Man-machine cooperative working systems and unguarded factories using the SSS.

Keywords: Safeguarding Supportive System (SSS), residual risk, Information and Communication Technology (ITC), RF-tag, UWB-active- Radio Frequency Identification (RFID), work-zone

INTRODUCTION

Today, the safety of workers is often secured by introducing the internet of things (IoT) technology and/or the information and communication technology (ICT) to many workplaces such as construction sites. The technology ensures safety of workers more certainly than methods of risk reduction using workers' attentiveness. On the other hand, many uncertain factors of risk reduction still exist in tunnel work sites, because many risk-reduction methods depend on the workers' attentiveness. If human errors happen and if the expected effect of risk reduction methods cannot be obtained as a result, severe accidents might occur.

In workplaces of tunnel construction, multiple machineries such as tunnel boring machines (TBMe), boring machines for blasting and rock crushers, and workers exist simultaneously. Machinery manufacturers try to prevent work accidents by equipped individual protection devices for each machine. However, even if all individual protections operate simultaneously, it would be difficult to cover all work sites of the tunnel. For example, it might be difficult for a third person entering the work area, to detect other workers standing behind the machines. The person might restart the machine even if some workers are still in dangerous positions. In other words, because it is impossible to prevent severe accidents sufficiently only by individual protection devices of single machines, unacceptable residual risks still exist at construction sites of tunnels. Some available safety strategies, not depending on human attentiveness, would be needed to prevent work accidents. For example, an entrance and exit management system, and a monitoring for location information of workers at the whole work site of the tunnel would be useful tools.

We newly established a risk reduction system, named "Safeguarding Supportive System (SSS)", to prevent human error and intentional unsafe behavior from the mechanical side (hardware side). The SSS should reduce residual errors with the usage of an appropriate ITC combination. The SSS focuses on the residual risk after implementing the 3-step method of ISO 12100/JIS B 9700 in machinery safety. The aim of the SSS is to provide an effective residual risk-reduction method using a combination of appropriate ICT equipment without depending on workers' attentiveness. Workers' qualifications (licenses) and rights (provided by ability and skill), the target machine, the work content, the place of the work and the operation time would become clear by introducing the SSS. Under the SSS, work will only be allowed when the ID information and the target machine of the tag held by a worker are matched with the information from the control machine located in the work area. Therefore, it is possible to prevent dangerous side errors caused by human error. Nevertheless, the SSS should be used simultaneously with the "protection plan" — the education and training management already introduced in Japan. The SSS is not a substitute for the protection plan.

In the present study, we tried to apply the SSS to a tunnel construction site. The SSS consisted of a RF-tag, a safety light curtain (SLC), an accurance tag system, an UWB-active-RFID system and a monitoring system. The RF-tag system confirmed worker's qualifications for entering work zones and gave permissions to work there. The UWB-active-RFID system monitored the operational processes of workers and confirmed the location of workers in real time. In the present study, we focused on workers entering and leaving check systems of the SSS at the entrance of the work-space. Different kinds of "entering and leaving detection systems" were introduced as a part of the SSS at the entrances of two washing lines. One was the SLC, and the other was a combination of an accurance tag system and access detection sensors. In the present study, we examined the accuracy of these systems. The SSS was experimentally introduced in the work sites of a workbench rental. We examined the accuracy of the SSS by counting access to the workspaces and by checking the location information of workers. As a preliminary experiment we used two washing lanes (workbench cleaning work) in a workbench rental company for examining the effectiveness of the SSS. One washing lane consisted of 4 items. One automatic washing machine was installed in the middle of two belt conveyors and two

transportation robots were situated before and after the washing lane. We assumed that a robot puts rocks derived from the face of the tunnel on a conveyor before the washing machine (rock crusher), and that rocks broken by an automatic rock crusher were carried by another conveyor, and another robot transferred the rocks to a truck.

MATERIALS AND METHODS

A work-space of a rental company named the GOP (Chiba, Japan), was used for our experiment for 3 days. Nine workers of the GOP participated in this study. The GOP Company, which is a rental company for portable construction workbenches, owned two automatic washing lanes for workbenches in the work space (Figure 1). We introduced the SSS to two lanes, lanes A and B. Each lane was virtually divided into three zones: zone 1, zone 2 and zone 3 in the SSS. Zone 1 was a compartment, where worker carried workbenches before washing. In zone 2, there were two conveyors and one automatic washing machine, which was installed between those conveyors. Zone 3 had another compartment, where workers carried workbenches after washing. Dividing the workplace into zones for the SSS, contributes to increase safety and productivity. For example, during non-routine cleaning work for the rewinding machine, the whole workplace's power supply often had to be shut down during the cleaning work, because the workplace was not separated into zones. However, under the SSS, only the power supply at zone 1 was turned off when working at zone 1, while the machines at zones 2 and 3 still worked.

Before washing one transport robot, which was located between lane A and lane B, carried workbenches from zones A1 and B1 to belt conveyors in lanes A and B alternately. Another transport robot grabbed workbenches from belt conveyors and carried them to carts in zones A3 and B3 alternately after washing.

The SSS, introduced to the workspace, consisted of an IMS control panel, a zone terminal, safety light curtains (SLC), safety beam sensors (SLSs), an accurance tag system, and access detection sensors (Figure 1). In addition, for worker's position confirmation, 23 fixed UWB readers were distributed in the whole workspace (see black dots in Figure 1) and 7 mobile active

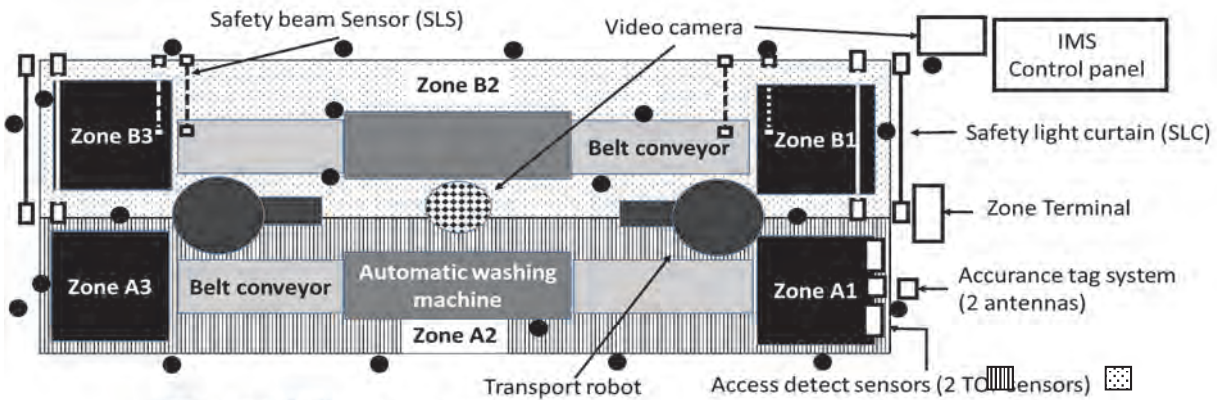

Figure 1:
Outline of the work-space at the GOP Company. The work-space had two automatic wash lanes, lane A ( ) and B ( ). Lane A (zone A1) had an accurance tag and an access detection sensor system at the entrance for counting numbers of entering and leaving workers. Lane B (zone B1) had a safety light curtain (SLC) at the entrance. Each zone 2 contained one automatic washing machine and two belt conveyers before and after the washing machines. Zones 3 were compartment for taking workbenches out from the work-space. Twenty-three UWB fixed readers ( ) were distributed in the work-space.

tags were prepared for workers. The specification of each device of the SSS were as follows;
IMS control panel: It was the main switch of the SSS. After the main control panel was turned on, all experimental procedures started, and all equipment units were shifted to working mode. The operation touch panel (OMRON, NS8-TV model) and the operation controller (OMRON,

NJ series) were installed on the IMS control panel. In addition, the safety PLC (OMRON, NX-SL&NX-SI/SO model), which took the output signal from each protective device into the main controller and sent the safety PLC's judgment to a signal tower and other external units, was also implemented to the IMS control panel. The IMS control panel, zone terminal and detection sensors for the zone B1 access were connected by Ethernet/IP and EtherCAT, which are based on a global standard of Open Devicenet Vendors Association, Inc. ***Zone terminal:*** The zone terminal was installed in the middle of the entrances of zones A1 and B1. The zone terminals contained a signal tower, a touch panel and an RFID reader/writer. The worker let the RFID reader/writer read a RF tag for the registration. Then, the worker operated the zone terminal's touch panel to select a target-task in the zone. After these processes were completed, the target-task at the zone became available. ***RF tag:*** The RF tag was used to confirm each worker's qualifications and abilities at the zone terminal. In the present study, information about each worker's licenses and abilities was stored on RF tags. Information about the workable zones was loaded on the zone terminal. We instructed workers to keep their RF tags with them during working. In the present study, RF tags with wristband shape were adopted. ***Safety light curtains (SLCs) and safety beam sensors (SBSs):*** Two pairs of safety curtains and 2 pairs of safety beam sensors were installed in the lane B. Two pairs of transmission type of photoelectric SLCs (OMRON, E3FS model) were set at the entrance of zone B1 and at the exit of zone B3, respectively. Two pairs of SBSs were set at the entrance and the exit of zone B2, respectively. When a worker mistakenly or intentionally invaded another zone besides the target zone, the power supply of all zones was shut down. ***Access detection sensors:*** Two detection sensors were installed at the entrance of zone A1. A time-of-flight (TOF) system was adopted as the detect sensor for the zone A1. The TOF sensor projected near-infrared light with an 850 nm wavelength into an object and then measured the distance using reflected lights from the objects with a special image sensor. Therefore, the TOF sensor was hardly affected by extraneous light. ***Accurance tag system:*** The accurance tag system was introduced for improving access detection of worker using concurrently the access detection sensors at zone A1. The TOF sensor judged shapes to determine whether the object entering the main gate was human or nonhuman. If the TOF judged that the object was human, then the TOF additionally judged whether the human shape was one person (without companions) or more than two people (with companions). ***UWB active RFID system:*** The UWB active RFID system was used to specify the location of workers in the target zone. Twenty-three fixed container (reader) were arranged in the whole work space. It was possible to detect the precise position specification of the worker, if the worker has an active tag with him/herself.

Table 1:
Count conditions and results of workers' entering and leaving at zones 1 in both A and B lanes

Entering			Leaving				
Actual number of worker(s)	Digital count	Counter displayed	Actual number of worker(s)	Digital count	Counter displayed	Number of actual remaining worker(s)	Result
1	1	1	1	1	1	0	Correct count
1	0	0	1	1	-1	0	Safe failure
1	1	1	1	0	1	0	
1	0	0	1	1	-1	0	
1	1	1	1	0	1	0	
2	2	2	2	2	2	0	Correct count
2	1	1	2	2	-1	0	Safe failure
2	1	1	1	1	0	1	Dangerous failure
2	2	2	1	1	1	1	Correct count

The procedure of the SSS was as follows: The experiment started when the IMS control panel was activated. Each worker held his or her RF tag over the RFID reader/writer for ID registration. Then, the screen changed to the machine selection. If the target machine was chosen, its icon was lighted up in yellow. Choosing the "Select" button on the side the work choice window opened up. In the work select window, workable and unworkable machines were shown in black and white text, respectively. If the worker pushed the “Pick” button after selecting the machine and work, the screen image was changed to “Monitor”. The operation mode of the selected machine and the selected work were indicated with colours on the monitor screen. If the worker selected an ID that was not consistent with his/her ID registered in advance, an “Invalid ID” window would come up and he/she could not select anything on the screen. In this case, the worker had to return to the previous screen by pushing the “Close” button and select the correct ID. When a worker completed the task at the target zone, the worker would register the task’s end by holding an RF tag to the zone terminal. After that, the worker moved out of the zone.

Originally, if a worker without an RF tag entered the work space, an emergency condition would have been emitted from the SSS. In this condition, all machines would be turned off. However, the emergency did not actually appear in the present study because the SSS was experimentally introduced into an actual product line. Thus, only the signal tower expressed a “pseudo-emergency” with a flickering red signal. ***Recording camera:*** Besides the SSS, we introduced two video cameras for recording the whole experiment. A recording camera was installed near the entrance of zone A1. We checked workers' access by visual recognition with pictures from the camera and compared them with data from the terminals and the worker detection sensors. All of the pictures were stored in 4ch digital recorder with an LCD monitor (OPTEX, WT-3000J). Another 360degree camera (OPTEX, UWC-1) was equipped on the roof of the workspace for recording all movements of workers and to check the experiment through visual recognition.

In the present study, data from SLCs in zone B1, and data from access detection sensors and accurance tag system at zone A1 were collected and compared.

RESULTS

In the present study, entering and leaving workers were counted at zone 1 in each lane. We categorized counting conditions and results as following (Table 1); if the actual numbers of workers, digital counts and the counter displayed at the entering of the line (zone 1) were identical, and those numbers of the leaving (zone 1) were identical, we defined results as “correct count”. If those numbers were not identical and the number of actual remaining workers was less than equal 0, this condition was thought as “safe failure”. On the other hand, when those numbers were not identical, and the number of actual remaining workers was more than 1, this condition was defined as “dangerous failure”.

The relative ratio of correct counts, safe failures and dangerous failures of zone A1, in which counting system was the safety light curtain (SLC), were categorized (Table 2). Correct counts were 27 times out of 58 times of total entry and exit. The relative ratio of correct counts was 46.6%. Safe failure and dangerous failure occurred 19 and 12 times, respectively. Relative ratios of safe failure and dangerous failure were 32.7% and 20.7%, relatively.

The relative ratio of correct counts, safe failures and dangerous failures of zone B1, in which counting system was a combination of an accurance tag system and access detection sensors, were categorized (Table 3). Correct counts were 9 times out of 15 times of total entry and exit. Th relative ratio of correct counts was 60.0%. Safe failures and dangerous failures were 3 times each.

Table 2:
Relative ratio of correct count, safe failure and dangerous failure of zone A1, in which counting system was the safety light curtain (SLC)

Correct count		27 (46.6%)
Wrong count	Safe failure	19 (32.7%)
	Dangerous failure	12 (20.7%)
Total amount of entering		58

Table 3:
Relative ratio of correct count, safe failure and dangerous failure of zone B1, in which counting systems were an accrance tag system and access detection sensors.

Correct count		9 (60.0%)
Wrong count	Safe failure	3 (20.0%)
	Dangerous failure	3 (20.0%)
Total amount of entering		15

Both relative ratios of safe failures and dangerous failures were 20.0%. The calculation of the t-test showed that correct counts, safe failures and dangerous failures between zone A1 and B1 was not statistically significant at the $p = 0.05$ level.

DISCUSSION

In the present study, there were no differences in relative ratios of correct counts, safe failures and dangerous failures in zone A1 and those of B1. These results suggest that preciseness of SLC counting system and a combination of the accurance tag system and the access detection sensors were the same.

We expected that a combination of the accurance tag system and the access detection sensors was more precise than the SLC counting system. While the accurance tag system has a camera inside, we thought that the camera would catch and count two workers as two if two workers enter the workspace at the same time. Unfortunately, the ratio of work accidents derived from so-called “tailgating” has happened frequently in Japan. However, we concluded that both 46.6 % and 60% of relative ratios of correct counts in both, A1 and B1, were not enough as the supporting protective system for prevent work accidents. Therefore, we are planning to change to the camera with higher spec in the further study. We think that the counting precision will be increased.

On the other hand, the camera detection system such as the accurance tag system might have limits. If workers intended hiding another person, it might be difficult to distinguish the number of workers even if the camera is high spec. For solving this problem, we are also planning to establish a direct monitoring system for worker in the workspace.

It was clarified that the entrance detection systems did not function for precise monitoring of workers. In the present study, we employed the UWB-active tag-RFID system for monitoring and scanning workers’ movements and positions. For the precise monitoring, both entrance detection and positioning information should be confirmed. Also, we will analyze data of the UWB-active tag-RFID system. Furthermore, another position scanning system, such as the Beacon sensor system will be examined in the near future.

CONCLUSION

The present situation or problems of equipment and work in detail can be clarified by analyzing data in the SSS. We concluded that the introduction of the SSS contributed to build up safer work space.
In the future, we'd like to apply risk reduction plans to the next generation product lines such as Man-machine cooperative working systems and unguarded factories using the SSS.

REFERENCES

1. EN ISO12100: 2010, Safety of machinery –Basic concepts of general principles for design (2003), (in Japanese).
2. International Organization for Standardization, ISO11161, Safety of machinery – Safety of integrated manufacturing systems – Basic requirements (2007).
3. Japanese Industrial Standard, Safety of machinery-General principles for design-Risk assessment and risk reduction −Part 2, JIS B 9700-2 (2004), pp.4-15, (in Japanese).
4. Massimi P and Van Gheluwe JP, Community legislation on machinery comments on directive 89/392/EEC and directive 91/368/EEC, Nikkei Mechanical, Nikkei Business Publication Inc. (1994).
5. Ministry of Health, Labor and Welfare, Ordinance of Industrial Safety and Health (Revision), Article24-3 (2014). <http://www.mhlw.go.jp/bunya/roudoukijun/anzeneisei14/dl/120521_01.pdf>, (accessed on 20 September, 2017).
6. Ministry of Health, Labor and Welfare, Sekkei Gijutsusha, Seisan Gijutsukanrisha ni taisuru Kikaianzen ni kakawaru kyouiku ni kannshi chuisubeki jikou ni tsuite (2014), <https://www.jaish.gr.jp/anzen/hor/hombun/hor1-55/hor1-55-32-1-0.htm>. (Accessed on 20 September, 2017), (in Japanese).
7. Ministry of Health, Labor and Welfare, Section 9 Industrial Robot (Articles 150-3 to 151) (2015), <http://www.japaneselawtranslation.go.jp/law/detail/?id=1984&vm=04&re=01>, (accessed on 20 September 2017).
8. Ministry of Health, Labor and Welfare, Guidelines for comprehensive safety standards of machinery (Overview), revision (2007), <https://www.jaish.gr.jp/anzen/hor/hombun/hor1-48/hor1-48-36-1-0.htm>, (accessed on 20 September, 2017).
9. NihonKantokushiKyokai, Human Error Taisaku Book (2011).
10. Rodo Shinbun Sha (2017), <https://www.rodo.co.jp/column/10133/>, (accessed on 21 September, 2017), (in Japanese).
11. The Japan Machinery Federation, Subcommittee report 2014, Supporting Protective System under Integrated Manufacturing System (2014), (in Japanese).
12. The Japan Machinery Federation, Subcommittee report 2015, Supporting Protective System under Integrated Manufacturing System (2015), (in Japanese).
13. The Japan Machinery Federation, Subcommittee report 2016, Supporting Protective System under Integrated Manufacturing System (2016), (in Japanese).

INTRODUCTION OF FIRE ACCIDENT RISK ASSESSMENT METHOD FOR JAPANESE EXPRESSWAY TUNNELS USING STATISTICAL APPROACH

Tetsuya YAMAZAKI[1], Masahiro YOKOTA[2] and Nobuyoshi KAWABATA[3]

[1] Central Nippon Expressway Company Limited, Japan
[2] Central Nippon Highway Engineering Tokyo Company Limited, Japan;
[3] Kanazawa University, Japan

ABSTRACT

Based on the European Directive 2004/54/EC, issued in 2004, safety assessment is conducted by means of risk assessment of road tunnels, and measures for risk improvement are being implemented in European countries. In order to grasp this situation, we visited European countries for several years since 2007 and a lot of useful advices about tunnel risk assessments and safety improvements are obtained through many workshops with road tunnel authorities, tunnel managers, consultants and others.

Table 1: Institutions visited and purposes of visits since 2007

Year	Visited Institution	Purpose	Achievement
2007	BASt, BMVIT, Cofiroute, CETu, ANAS, EuroTAP	To collect reports on trends in research on risk analysis, plus the Directive issued by the EU, state of improvement of emergency use equipment in tunnels before and after the Directive and other related research, and to survey specific improvement plans, countermeasure periods, safety inspection methods etc. in various countries since the Directive was issued.	Risk analysis: Workshop, TuRisMo, Linee Guida per la progettazione della sicurezza nelle Gallerie Stradali, ANAS S.p.A Tunnel inspection: Engerbert Tunnel, Felbertauern Tunnel, A86 Duplex Tunnel, Frejus Tunnel, Colle Giardino Tunnel
2008	Calle M30, TST/ AITEMIN, Iberpistas	To survey safety improvement countermeasures and risk evaluations of tunnels on urban belt expressways and survey specialized tunnel fire experiment facilities.	Risk analysis: Workshop Tunnel inspection: Calle M30 Tunnel, TST, Guadarrama Tunnel
2009	Mersey Tunnel, UK Highway Agency, ARUP, RWS, TNO	To conduct a fact-finding survey of European trends in specific tunnel fire risk reduction measures, and the state of performance of risk analysis. To survey state of reporting of risk analysis methods to the EU.	Risk analysis: Workshop, RWS QRA Tunnel inspection: Mersey Tunnel, Leidsche Rijn tunnel, Bell Common Tunnel(M 25)
2010	The Norwegian Public Roads Administratio , SP	To survey the state of planning and implementation of specific tunnel safety improvement projects.	Risk analysis: Workshop
2014	The Norwegian Public Roads Administration, ASTRA, ASFiNAG	To survey large scale fires that have occurred in recent years, responses of road managers to these fires, and causes of resulting damage, and to collect information about large scale fires that prompted the EU to issue Directive 2004/54/EC and the state of later improvement of safety.	Risk analysis: Workshop Tunnel inspection: Gudvanga Tunnel, Lardal Tunnel, Lungern Tunnel, St Gotthard Tunnel, Tauern Tunnel

Based on these valuable opinions and suggestions, the priorities for both risk assessments and detailed improvement measures for the expressway tunnels are being evaluated in Japan. For risk assessment methods for expressway tunnels, a statistical evaluation method of tunnel fire risk was developed from the fire accident database, which allows a relative evaluation for each tunnel.
This paper outlines the activities conducted by us and introduces the unique tunnel fire risk assessments/statistical risks, which are statistically estimated from expressway tunnel fire accident cases. It also summarizes the prioritization of risk improvement projects using the statistical risk as well as the selecting method of the detailed risk improvement means.

(1) Number of tunnels and fire accidents

By grade, most tunnels are B grade and fewest are AA grade, as shown in Figure 1. Figure 2 shows changes in the number of tunnel fire accidents in expressway tunnels since 1989. Fire accidents have occurred between 4 and 21 times/year and at an average of 12.3 times/year, or about once a month.

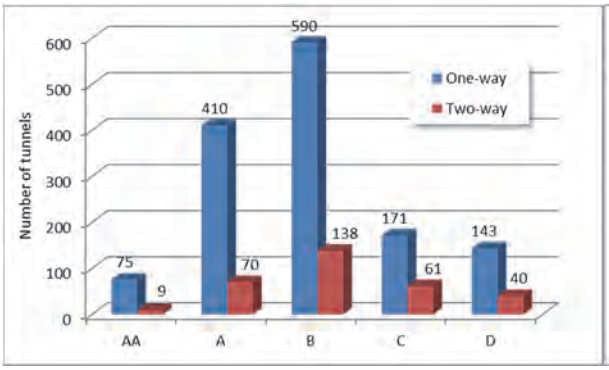

Figure 1: Number of tunnels by grade

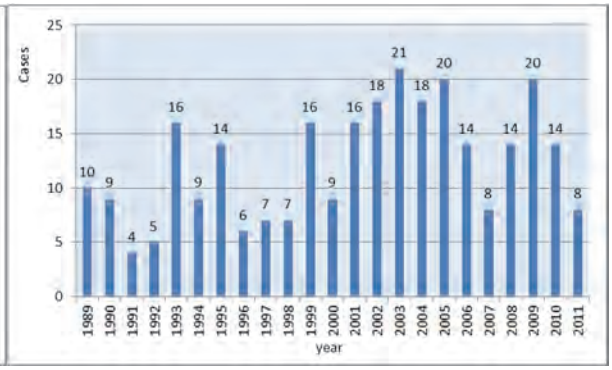

Figure 2: Number of fire accidents in tunnels

Table 2 shows trends by grade. Fire accidents occur most often in AA grade tunnels, which is the least common grade of both one-way and two-way tunnels, and never occur in grade D tunnels.

Table 2: Number of fires by tunnel grade

Equipment grade	Cases	One-way	Two-way
AA	132	117	15
A	102	84	18
B	34	33	1
C	15	11	4
Totals	283	245	38

(2) State of damage

Table 3 shows the number of deaths and injuries caused by expressway tunnel fire accidents. The cause of the outbreak of fires often is a vehicle failure, but more people are killed or injured by traffic accident fires. However, the database does not clearly show the causes of deaths and injuries (by accidents or fires), so this paper treats them as results of fires. Next, Table 4 summarizes the average data concerning the damage by traffic type. If the average values are compared, parameters as length, traffic volume, probability of a fire accident, traffic stop time and fire scale are all higher in one-way tunnels, whereas fire accidents in two-way tunnels result in more deaths and injuries. This shows that fire accidents are less likely to occur in two-way traffic tunnels than in one-way tunnels, but if there is a fire, it tends to cause greater harm.

Table 3: Deaths and injuries caused by tunnel fire accidents since 1989

Type	Tunnel type	Deaths	Injuries
Vehicle failure fire	One-way	2	10
	Two-way	1	1
Traffic accident fire	One-way	26	64
	Two-way	9	14
Totals		38	89

Table 4: Average damage data by traffic type

Items	Unit	All	One-way traffic	Two-way traffic
Tunnel length	m	3,298	3,372	2,799
Traffic volume	Vehicles/day	21,658	23,191	11,588
Probability of fire accident	Cases/100 million vehicle-km	30.7	32.3	20.1
Arrival of firefighters	Minutes	23.5	23.1	27.2
Traffic stop time	Minutes	131.6	132.6	124.8
Deaths	People killed	0.131	0.111	0.263
Injuries	People injured	0.306	0.292	0.395

(3) Concept of tunnel fire risk

The risk evaluation method is studied as a method of comparing and evaluating the relative safety from the state of damage revealed by analysis of expressway tunnel fire accident data. The general risk is obtained by combining the frequency of occurrence of damages (probability) and the extent of damages (impact) and solving equations.

Risk calculated in this way is visualized in the form of a risk matrix, permitting the state of risk ranking of the facilities, which are subjects of the risk management.

This study evaluates the present tunnel risk by analyzing data of the above-mentioned tunnel fire accident data base to calculate the "statistical risk".

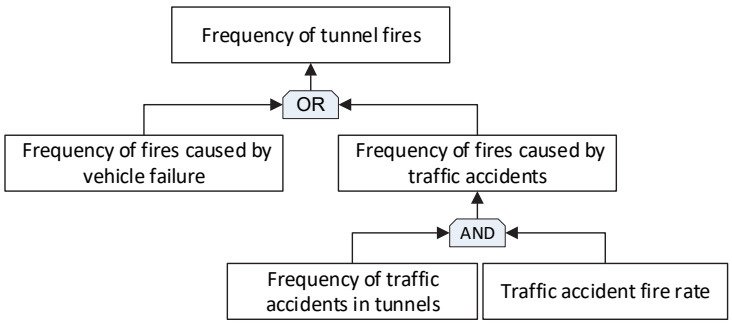

Figure 3: Configuration of frequency of occurrence of fire accidents in tunnels

$$R_s = P_t \times I_t$$

Where,

R_s: statistical fire risk (yen/year)

P_t: frequency of occurrence of tunnel fires (probability) (cases/year)

$P_t = P_b + P_f$

P_b: frequency of occurrence of vehicle failure type fire accident (cases/year)

P_f: frequency of occurrence of traffic accident fires by tunnel (cases/year)

I_t: damage by tunnel fires (impacts) (yen/case)

$I_t = I_H + I_P + I_s$

$I_H = I_{Hu} + I_{Hf}$: Human loss = human loss from vehicle failure fire + traffic accident fire

$I_p = \sum_i \sum_C R_i \times E_{i,C}$: Material loss per fire accident

$I_s = \sum_i T_i \times P_i \times V \times U_w \times U_{travel}$: social loss per fire accident

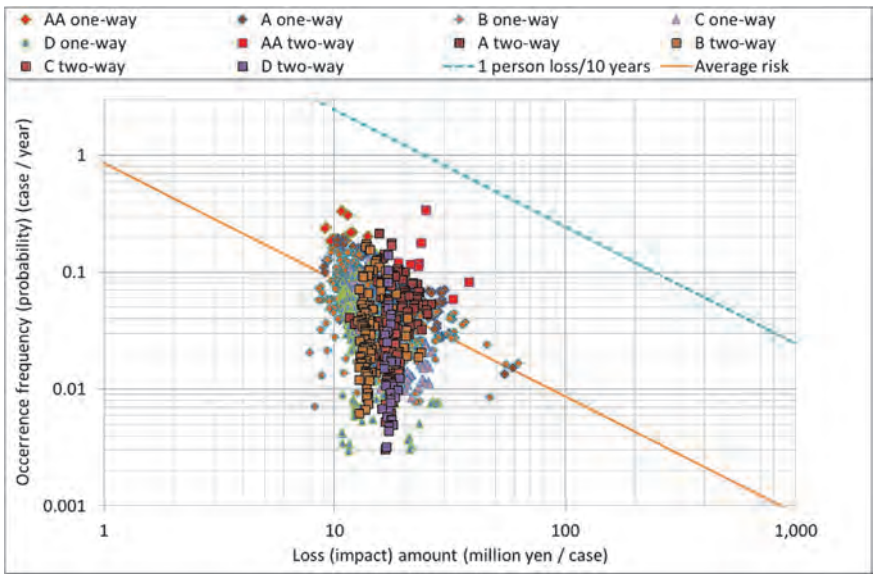

Figure 4: Expressway tunnel fire accident risk matrix

Table 5: Average values in trial calculation results by tunnel category

Category	Number of tunnels	Occurrence frequency: *P* (Cases/year)	Loss (impact): *I* (Yen/case)	Risk: *R* (Yen/year)
AA one-way	63	1.44×10^{-1}	12,891,637	1,853,310
A one-way	367	6.50×10^{-2}	17,566,033	1,141,037
B one-way	556	4.71×10^{-2}	15,912,747	749,896
C one-way	163	4.01×10^{-2}	16,027,201	642,472
D one-way	143	4.06×10^{-2}	13,581,370	551,441
AA two-way	8	1.41×10^{-1}	25,696,812	3,634,536
A two-way	62	6.51×10^{-2}	19,224,308	1,251,921
B Two-way	131	4.03×10^{-2}	14,904,028	600,139
B two-way	52	3.15×10^{-2}	17,203,914	542,010
D two-way	39	2.68×10^{-2}	17,303,313	463,536

Conclusions

The following has been learned by the analysis of expressway tunnel fire accident data performed in this study.

1) The tunnel fire accident database was analyzed to propose a fire accident occurrence probability estimation model, and to clarify parameters that are causes of fire accidents based on limiting conditions.

2) The cost of damage by the occurrence of tunnel fires was categorized as human, material and social, and a method of calculating each category was proposed based on the state of damage recorded in the tunnel fire accident database.

3) It is now possible to prioritize safety improvement projects based on quantitative tunnel fire accident risk ranks that were obtained.

But the proposed statistical risk estimates the probability of occurrence of tunnel fires and resulting damage based on past statistical data. So it is impossible to evaluate the improvement effects of specific risk reduction measures.

Therefore, regarding concrete risk improvement measures and their effectiveness evaluation, it is considered as necessary to establish an evaluation method that connects fire simulations and evaluation simulations, and to set an allowable risk threshold for tunnel fires.

Acknowledgments

Japan's risk survey group proposed this unique method while visiting countries of Europe and exchanging information almost annually since 2007. The authors wish to express their gratitude to everybody in the European countries they visited for their cooperation.

Reports of the
Institute of Internal Combustion Engines and Thermodynamics

HEFT NR.	VERFASSER	TITEL	ERSCHIENEN	PREIS in €
80	STURM P.J.	Sicherheit und Belüftung von Tunnelanlagen Tunnel Safety and Ventilation Tagung/Symposium 8.-10. April 2002	2002	50,--
81	STURM P.J.	Verkehr und Umwelt Transport and Air Pollution Tagung/Symposium 19.-21. June 2002	2002	50,--
82	HAUSBERGER St.	Simulation of Real World Vehicle Exhaust Emissions Transport and Air Pollution	2003	40,--
83		Der Arbeitsprozess des Verbrennungsmotors The Working Process of the Internal Combustion Engine Tagung / Symposium 25. und 26. September 2003	2003	70,--
84	STURM P.J.	Sicherheit und Belüftung von Tunnelanlagen Tunnel Safety and Ventilation Tagung/Symposium 19.-21. April 2004	2004	50,--
85	STURM P.J.	Verkehr und Umwelt Transport and Air Pollution Tagung/Symposium 1.-3. June 2005	2005	50,--
86		Der Arbeitsprozess des Verbrennungsmotors The Working Process of the Internal Combustion Engine Tagung / Symposium 22. und 23. September 2005	2005	70,--
87	STURM P.J.	Sicherheit und Belüftung von Tunnelanlagen Tunnel Safety and Ventilation Tagung/Symposium 15.-17. Mai 2006	2006	50,--
88		1st International Symposium on Hydrogen Internal Combustion Engines 28. und 29. September 2006	2006	50,--
89		Der Arbeitsprozess des Verbrennungsmotors The Working Process of the Internal Combustion Engine Tagung / Symposium 20. und 21. September 2007	2007	70,--
90	STURM P.J.	Sicherheit und Belüftung von Tunnelanlagen Tunnel Safety and Ventilation Tagung/Symposium 21.-23. April 2008	2008	60,--
91		Verkehr und Umwelt Transport and Air Pollution Tagung/Symposium 16.-17. June 2008	2008	60,--

92		Der Arbeitsprozess des Verbrennungsmotors The Working Process of the Internal Combustion Engine Tagung / Symposium 24. und 25. September 2009	2009	70,--
93	STURM P.J.	Sicherheit und Belüftung von Tunnelanlagen Tunnel Safety and Ventilation Tagung/Symposium 3.-4. Mai 2010	2010	70,--
94		Der Arbeitsprozess des Verbrennungsmotors The Working Process of the Internal Combustion Engine Tagung / Symposium 22. und 23. September 2011	2011	100,--
95	STURM P.J.	Sicherheit und Belüftung von Tunnelanlagen Tunnel Safety and Ventilation Tagung/Symposium 23.-25. April 2012	2012	70,--
96		Der Arbeitsprozess des Verbrennungsmotors The Working Process of the Internal Combustion Engine Tagung / Symposium 24. und 25. September 2013	2013	100,--
97	STURM P.J.	Sicherheit und Belüftung von Tunnelanlagen Tunnel Safety and Ventilation Tagung/Symposium 12.-13. Mai 2014	2014	100,--
98		Inter-Regional Air Quality Assessment Bridging the Gap between Regional and Kerbside PM Pollution Results of the PMinter Project Authors: U. Uhrner, B.C. Lackner, R. Reifeltshammer, M. Steiner, R. Forkel, P.J. Sturms	2014	30,--
99		Der Arbeitsprozess des Verbrennungsmotors The Working Process of the Internal Combustion Engine Tagung / Symposium 24. und 25. September 2015	2015	100,--
100	STURM P.J.	Sicherheit und Belüftung von Tunnelanlagen Tunnel Safety and Ventilation Tagung/Symposium 25.-26. April 2016	2016	100,--
101		Der Arbeitsprozess des Verbrennungsmotors The Working Process of the Internal Combustion Engine Tagung / Symposium 28. und 29. September 2017	2017	100,--
102	STURM P.J.	Sicherheit und Belüftung von Tunnelanlagen Tunnel Safety and Ventilation Tagung/Symposium 12.-14. Juni 2018	2018	100,--